WSRC-MS-2000-00606

CAROLINA GEOLOGICAL SOCIETY 2000 FIELD TRIP GUIDEBOOK

Savannah River Site
Environmental Remediation Systems In Unconsolidated Upper Coastal Plain Sediments - Stratigraphic and Structural Considerations

Edited by:
D. E. Wyatt and M. K. Harris

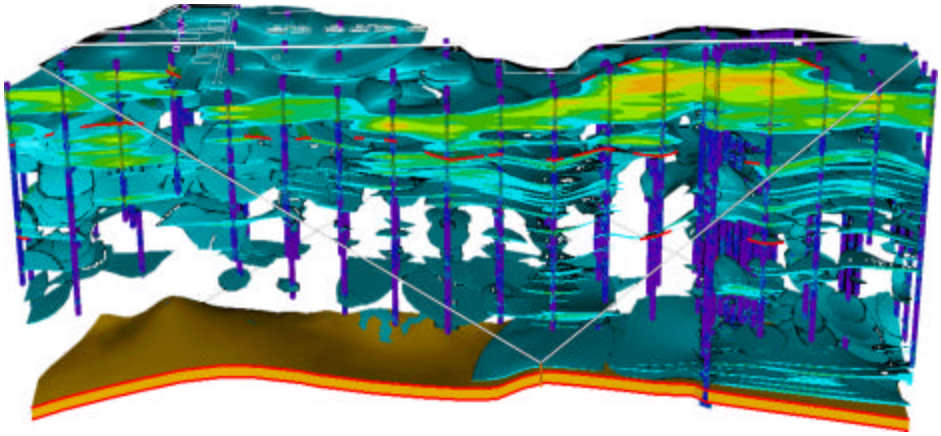

savannah river site
where excellence is achieved

Carolina Geological Society

Contributing Sponsors
(at press time)

RCS Corporation, Aiken, SC

Science Applications International Corporation (SAIC), Augusta, GA

Exploration Resources, (EXR), Augusta, GA

Kubal-Furr & Associates, Simpsonville, SC

Blue Ridge Environmental, Shelby, NC

CSRA Geological Society, Aiken, SC

napLogic, Princeton, NJ

Arcadis Geraghty and Miller, Aiken, SC

Bunnell-Lammons Engineering, Inc., Greenville, SC

CAROLINA GEOLOGICAL SOCIETY
2000 FIELD TRIP GUIDEBOOK

Aiken, South Carolina
November 4th, 2000

Savannah River Site
Environmental Remediation Systems
In Unconsolidated Upper Coastal Plain Sediments
Stratigraphic and Structural Considerations

Edited by:
Douglas E. Wyatt
and
Mary K. Harris

Co-sponsored by:

This document was prepared in conjunction with work accomplished under Contract No. DE-AC09-96SR18500 with the U.S. Department of Energy.

DISCLAIMER

Table of Contents

Table of Contents (Continued)

DESCRIPTION OF FIELD STOPS

Stop #1 - H-Area Seepage Basin Extraction, Treat and Re-Injection Project

(Coffee, juice and doughnuts provided at this stop. Please follow all instructions and watch for barricade ropes and warning signs.)

Until 1988, unlined seepage basins were used to dispose of wastewater from the Savannah River Site's (SRS) separations facilities. Six were placed in operation in 1955, and a seventh was constructed and became operational in 1962 to replace a basin that had stopped seeping. The wastewater was transported approximately 3,000 feet from each processing area through underground vitrified clay pipes to the basins. The wastewater was allowed to evaporate and to seep into the underlying soil.

Use of all the basins was discontinued on Nov. 7, 1988, when the F and H Effluent Treatment Facility replaced them. The F and H Effluent Treatment Facility continues to fulfill this function through chemical/mechanical treatment at the surface. Annually, an average of about 80 million gallons of wastewater was disposed in the basins. The three F Area basins cover about 6.5 acres, and the four H Area basins cover about 15.5acres.

A groundwater monitoring well network was installed in the 1950s. The monitoring network has been continually expanded. Approximately 234 monitoring wells, covering approximately 275 acres in these areas, are currently sampled for a variety of chemical and radioactive parameters. Groundwater monitoring results show tritium and nitrate contamination, with elevated levels of some heavy metals and radionuclides. Some of the heavy metals are classified as hazardous waste as defined under the Resource Conservation and Recovery Act (RCRA).

In 1986, it was determined that the units should be regulated under RCRA as mixed waste (waste containing hazardous and radioactive components) disposal facilities, and closure plans were initiated. Closure activities began in June 1989, immediately after the South Carolina Department of Health and Environmental Control (SCDHEC) approved the closure plans. Closure activities were completed in 1991, with SCDHEC certifying the F and H basin closures. The total cost of closing the basins was $17 million. The overall basin closure plan included:

- draining each basin;
- placing granite aggregate on the basin bottoms to stabilize the sludge and prevent airborne releases of radionuclides during construction;
- installing limestone and blast furnace slag on the aggregate to chemically stabilize contaminants in the bottom of the basin;
- backfilling the basin with compacted soil;
- placing a 2-foot thick clay cap over the basins to minimize precipitation reaching the contaminants; and
- covering the clay cap with topsoil, then sodding and/or seeding.

Groundwater remediation activities to reduce heavy metals, nitrates and some radionuclides and hydraulically control tritium are on-going.

Major components of each remediation system include:

- groundwater extraction and collection system;
- modular groundwater and secondary waste treatment systems;
- secondary waste collection and packaging system;
- treated water distribution and injection system.

Additional activities currently underway to further enhance contaminant removal include:

- modeling, fate and transport, chemical interaction and estimates to achieve groundwater clean up goals.
- Waste Minimization with a pilot demonstration of the Disc Tube Nanofiltration Unit.
- Source reduction through Hot Spot Wells.

Stop #2 - Radioactive Burial Grounds, E-Area Vadose Zone Modeling Project

(No eating, drinking or smoking is allowed during this stop. Please follow all instructions and watch for barricade ropes and warning signs.)

The Burial Ground Complex occupies approximately 194 acres in the central section of the Savannah River Site (SRS) between the F and H Separations Area. The complex consists of several former or present disposal sites for

hazardous and radioactive wastes from SRS activities. It is divided into two areas:

1. The southern area, making up 76 acres, is called the Old Radioactive Waste Burial Ground. In 1952, it began receiving wastes until it reached its full storage capacity in 1972. The area contains 22 underground tanks where used radioactive solvents were once stored. Wastes are buried in slit trenches.

2. The northern area, called the Low-Level Radioactive Waste Disposal Facility, occupies 119 acres. It includes underground tanks for radioactive solvent storage, transuranic waste storage pads and engineered and slit trenches. The facility began receiving wastes in 1970, and disposal continues there today. The 58-acre Mixed Waste Management Facility (MWMF), which is one of three separate areas of the 119-acre Low-Level Radioactive Waste Disposal Facility (LLRWDF), was closed in accordance with RCRA regulations in 1991. Five additional areas, totaling 24 acres, of the LLRWDF were closed in accordance with RCRA regulations in the 1996-99 time frame. The remaining 37 acres of the LLRWDF are active operations areas. Most of the 76-acre Old Radioactive Waste Burial Ground is being covered by a low permeability soil in 1996-98, in accordance with CERCLA Interim Action Record of Decision.

The degree of soil contamination in the complex is unknown. However, potential contaminants include chlorinated and organic solvents and toluene and benzene, both components of degreasing agents used to clean metal parts. Metals of concern are lead, cadmium and mercury. Potential radioactive materials in the soil include alpha, beta and gamma ray emitting materials.

Preliminary groundwater analyses in the complex show contamination from tritium, cadmium, lead, mercury and chlorinated organic compounds. Tritium plumes are tracked originating from the western end of the Old Radioactive Waste Burial Ground and the northern areas of the MWMF.

Radioactive operational and construction wastes are currently being disposed of in engineered slit trenches within the operational portion of the facility. As part of the modeling and performance assessment for the trenches, a vadose zone characterization program was initiated. Numerous vadose zone soil borings with sediment sampling for hydraulic parameters were obtained for instrumnt calibration and to sablish baseline conditions. CPT's, neutron probe access wells, vertical and angled lysimeters, Vapor wells, Time Domain Reflectometers, and Advanced Tensiometers have been installed in selected horizons to monitor moisture amount and flux. The lysimeters are sampled for potential contaminant concentrations. Using the CPT and boring data, a three dimensional model of the vadose zone has been completed.

Lunch Stop - The Proposed Areas for the DOE Plutonium Disposition Facilities

(A quick brown bag lunch will include sandwich, chips, apple, cookie and drink. A restroom facility is available.)

The DOE Plutonium Disposition mission includes the construction of three facilities proposed for surplus plutonium disposition. These facilities involve pit conversion, immobilization, and mixed oxide (MOX) fuel fabrication. Each process would be carried out within its own specific facility. Pit conversion would be done in the Pit Disassembly and Conversion Facility (PDCF), immobilization would be conducted in the Plutonium Immobilization Project (PIP) facility, and the MOX Fuel Fabrication Facility (MFFF) would produce MOX fuel assemblies for domestic commercial power reactors. Several subsurface investigations have been completed in support of site selection and preliminary design. Currently, structure specific investigations are underway.

Stop 3 - TNX, Geo-Siphon and Vadose Zone Remediation Project, TNX Groundwater Operable Unit

The TNX Area is an industrial facility where pilot-scale testing and evaluation of chemical processes in support for activities such as the Defense Waste Processing Facility (DWPF), Separations Area, and fuel and target manufacturing areas took place. Groundwater contamination at TNX resulted from the use of unlined seepage basins to dispose of wastewater, leakage from a network of process sewers, and leachate from various activities in the area.

The TNX Groundwater has been found to be contaminated with chlorinated volatile organic compounds (VOCs), primarily trichloroethylene

(TCE), and to a lesser extent tetrachloroethylene (PCE), and carbon tetrachloride. The VOC plume underlies eight acres, and has a maximum thickness of 20 feet. Groundwater characterization activities indicate that contamination is limited to the shallow water table aquifer, and the contaminant plume is outcropping in the TNX swamp, before it reaches the Savannah River.

An Interim Action Record of Decision (IROD) for the TNX Groundwater Operable Unit (GWOU) was authorized by EPA, SCDHEC, and DOE on November 16, 1994. The objectives of the interim action are: 1) reduce potential risk to human health and the environment, 2) maintain risk at acceptable levels to the onsite worker at the seepline, 3) mass removal of VOC contamination in the groundwater near the plume core, 4) plume stabilization by inhibiting migration of elevated levels of VOCs (500 ppb TCE) to the swamp and 5) prevent further aquifer degradation.

The selected remedy for accomplishing the Interim Remedial Action goals was designated the Hybrid Groundwater Corrective Action (HGCA) system. The system has two components: 1) traditional pump and treat technology to treat and inhibit further migration of the 500 ppb dissolved VOC plume, and 2) an innovative in-situ technology, airlift re-circulation well, located at the heart of the plume to expedite remediation.

Pump and treat is proven technology for groundwater remediation. The airlift re-circulation well is an emerging technology that could potentially reduce the contamination in the aquifer reducing remediation operation time frames for the pump and treat system. Based on testing performed in late FY 1996, it was determined that the re-circulation well was not effective in removing contaminants at this location due to site specific conditions. Furthermore, it was determined that the pump and treat system would adequately meet the remedial objectives of the Interim Record of Decision. Consequently, it was decided to discontinue further operation of the re-circulation well at TNX.

Other technological approaches are being considered and/or evaluated, in the event that the Interim Remedial Action does not suffice for a final remedy. These include: the Intrinsic Remediation Investigation, the GeoSiphon Cell Pilot Study, and the Soil Vapor Extraction Investigation.

The Intrinsic Remediation Investigation is a United States Geological Survey (USGS) project to assess natural attenuation as a remedial strategy for the chlorinated volatile organic compound contamination in the groundwater of the TNX Area. The potential intrinsic remediation pathways to be evaluated include bioremediation, sorption, and phytoremediation.

A field trial of a GeoSiphon Cell is being pursued in the TNX Area flood plain. The GeoSiphon Cell is essentially a large diameter well containing granular cast iron, which reduces the COVCs in the groundwater to ethane, methane, and chloride ions. The flow of groundwater through the treatment cell will be passively induced by the natural hydraulic head difference between the cell and the Savannah River, where the treated groundwater will ultimately be discharged.

Soil vapor analysis at TNX show that CVOCs are present in the soil at concentrations up to 55 ppmv. The residual CVOCs will continue to be a source of groundwater contamination as long as they are present in the subsurface. A pilot-study has been proposed to evaluate the applicability of soil vapor extraction at TNX utilizing existing infrastructure. Removal of residual contaminants from the unsaturated zone would significantly reduce the operating time frame of the air stripping system.

Stop 4 - C-Area Burning Rubble Pit, CPT Geo-Modeling and Air Sparging Remediation

The C Area Burning/Rubble Pit is west of C Area at the Savannah River Site (SRS). It is a shallow, unlined, earthen pit SRS excavated in 1951 to receive used organic solvents, waste oils, paper, plastics and rubber materials. The pit is 350 feet long, 25 feet wide and 10 feet deep.

Although the practice was discontinued in 1973, SRS periodically burned the pit debris. From 1973 on, the pit continued to receive construction and debris and empty, non- returnable drums. When the pit was full, workers backfilled it with soil and sediments to ground level.

SRS took preliminary soil gas surveys in and around the pit in 1985 and 1986. These show chlorinated solvents in the soil. Further investigations took place in 1989, when SRS took soil samples and used ground-penetrating radar to define the pit boundaries and locate buried objects.

In addition to chlorinated solvents, metal contaminants of concern include antimony, lead, arsenic, vanadium, chromium, cadmium, nickel, barium, copper, tin and zinc. Also of concern are cyanide, xylene and phenolic constituents.

Preliminary groundwater monitoring conducted from 1984 through 1990 shows groundwater beneath the pit contains chlorinated solvents. The history of solvent disposal at the CBRP and the persistence of high VOC concentrations 25 years after operations ceased suggests the presence of VOC in non-aqueous phase liquid (NAPL) within the vadose zone beneath the CBRP. A Soil Vapor Extraction and Air-Sparging (SVE/AS) remediation system are currently in operation for cleaning up the solvents in the soil and groundwater at this site.

Extensive CPTU data were acquired as part of the overall subsurface characterization for the CBRP. These data were calibrated to borings and core data to create a three dimensional model of the subsurface.

Stop 5 - A/M Area Horizontal Wells, Baro-Balls, Vadose Zone Extraction, Modeling, Groundwater Pump and Treat, DNAPL, High Resolution Seismic Imaging for Environmental Characterization, A/M Area Groundwater Cleanup

(Soft drinks and snacks will be available at this stop.)

In 1983, the SRS initiated one of the largest and most successful remediation programs aimed at cleaning up organic solvents from the soils and groundwater. Located in the northern portion of the SRS, the 350 acre A/M Area contained facilities for reactor fuel and target assemblies, support facilities, laboratories, and administration buildings. At several stages in the fabrication process, fuel assemblies were degreased using industrial solvents, primarily trichloroethylene (TCE) and tetrachloroethylene (PCE).

From the 1950s into the early 1980s, wastewater from fuel and target manufacturing operations was disposed in a settling basin. The basin, used from 1958 to 1985, was an 8-million-gallon earthen basin that received fluids from the M Area manufacturing facilities. Waste entered the M Area Settling Basin through an underground process sewer line from a manufacturing facility approximately 2,500 feet north of the basin. The basin periodically overflowed to a natural seepage area and shallow depression, known as Lost Lake, a Carolina Bay, via a drainage ditch. This combined area is the M Area Hazardous Waste Management Facility (HWMF).

The effluent contained heavy metals and chlorinated solvents, primarily trichloroethylene and tetrachloroethylene similar to the chemicals used in the dry cleaning industry. Most of the heavy metals were effectively captured by the soil. About half of the solvents released evaporated. Monitoring wells installed in 1981, however, showed that the remainder had seeped into the water table, contaminating the groundwater.

After discovering groundwater contamination below the M Area Settling Basin in June 1981, SRS established an interim groundwater monitoring program. Multiple groundwater zone monitoring wells were installed surrounding the basin, the principal source of groundwater contamination in the A/M Areas.

Groundwater cleanup was instituted voluntarily in February 1983, using an experimental air-stripping system. This pilot testing project included a single groundwater pumping well and a prototype 70-gallon-per-minute air stripper unit. Later, a full-scale pump-and-treat system was constructed to remediate contaminated groundwater in M Area. The system, comprised of 11 groundwater recovery wells and an air stripper column, treats contaminated groundwater from the shallow aquifer at a rate of approximately 550 gallons per minute. This system has been operating almost continuously since 1985, the year SRS submitted the M Area Part B Permit corrective action plan to the South Carolina Department of Health and Environmental Control (SCDHEC). The plan, one of the first designed at a DOE facility, was approved in 1987 and requires operation and monitoring for 30 years.

Today an extensive monitoring well network consisting of more than 400 wells and extends throughout the A/M Areas. Groundwater quality and hazardous constituents defined by regulators are analyzed regularly at the wells. These activities have been conducted in compliance with the M Area Resource Conservation and Recovery Act Part B Permit.

The M Area air stripper has removed more than 350,000 pounds of solvent from over 2.3 billion gallons of groundwater. Combined with the contaminated groundwater treated by experimental and prototype remediation units and the 5 soil vapor extraction units, more than 500,000 pounds of solvents have been removed from the subsurface. These groundwater remediation activities have been conducted in compliance with approved wastewater and air quality control permits.

Air stripping systems work by pumping contaminated groundwater to the top of an air stripping column. As groundwater cascades downward through the column, pumped air is forced upward from the bottom of the column. When the water mixes with air, solvents in the groundwater move from a liquid phase into a vapor phase, and volatile contaminants are stripped, and treated prior to release to the atmosphere. When the system first came into use, the inlet solvent concentration of untreated groundwater was approximately 40,000 parts per billion. The concentration has now dropped to approximately 9,000 parts per billion. Solvent concentration after the water has been treated in the air stripper is almost always less than one part per billion. The cleaned water is discharged through a permitted outfall to a nearby stream.

A program was initiated in 1992 to remove solvents from the vadose zone, the layer of unsaturated soils above the groundwater. Remediation of the vadose zone will further reduce the potential for more groundwater contamination. Five remediation systems, that use vacuum extraction to remove the solvents, have been installed and are operating at known contamination areas throughout the A/M area. Each unit is equipped with an offgas treatment system. This technique will reduce cost and time of remediation while increasing remediation efficiency and public and regulatory acceptability.

SRS researchers are continuing to develop new strategies for treating solvent contamination. This work includes geological modeling and geochemical studies. In addition, a process utilizing horizontal wells, called in-situ air stripping, has been developed at SRS to remove contaminants in the groundwater and the vadose zone. During pilot program operation of the in-situ air stripping system, 16,000 pounds of solvents were removed. This method is shown to be five times as effective as traditional pump-and-treat technology. In-situ bioremediation also tested with success. SRS has proposed using in-situ bioremediation at the Non Radiological Waste Disposal Facility.

Concentrated Contaminants, DNAPLs

DNAPLs are contaminants in an oil-like state that are derived from chlorinated solvents, creosote and coal tar used in industries ranging from dry cleaners to electronic instrument makers. DNAPLs at SRS contain the contaminants tetrachloroethylene and trichloroethylene, and are difficult to remediate.

SRS is looking at innovative ways to address the DNAPLs found under A/M Area. Although there is yet no known technology to clean up DNAPLs, scientists are researching several possible alternatives. One technique would include injection into the groundwater of solutions that would destroy the DNAPLs underground allowing them to breakdown into harmless components.

Vadose Zone Remediation Units

Contamination to the vadose zone occurs as contaminants seep downward from sources like wastewater basins, pipe-line breaks or surface spills of chemicals. During the production and processing years at SRS, chemical solvents used by the industry were released to wastewater discharge basins or to surface drainage facilities. This was a typical and accepted practice by industry in the past that is not allowed today without strict regulatory controls.

The Vadose Zone Remediation Process

SRS has recently added five vadose zone units to the environmental cleanup program in A/M Area. These units remove solvent vapors at the rate of about 200 pounds per day from the vadose zone. Addition of vadose zone treatment increases the cleanup rate at the A/M Area by 500 percent. Here is how it works:

- Vacuum units, connected to either horizontal or vertical wells placed into contaminated sources like basins or spill areas, withdraw contaminant vapors from the subsurface.
- The contaminated vapors pulled from the subsurface flow to a thermal treatment unit, mounted near the vapor extraction well, which

destroys the contaminants via catalytic oxidation.

Extraction of these contaminants from the vadose zone prevents their downward movement into the water table.

Cost Effectiveness

The soil vapor extraction technology is proven to be cost effective, compared to other methods of clean-up, including the removal of contaminated soil. The total project cost for the vadose zone remediation project is approximately $4 million, compared to approximately $14 million for alternative methods of soil cleanup.

CORE AND GIS WORKSHOPS

Biology and Geology Department, USC-Aiken
(Parking is available in the lot behind, west, of the science building. Please park in the white-lined spaces. The workshops will be on the 2nd. floor of the Science Bldg., down the steps)

8:30 - 10:00 ..... Core Workshop 1
8:30 - 10:00 ..... GIS Geology Database Presentation 1
10:00 ..... Refreshments
10:30 - Noon ..... Core Workshop 2
10:30 - Noon ..... GIS Geology Database Presentation 2

Core Workshop

The core workshop will consist of a hands-on viewing of representative sediments from the SRS. A presentation with an open discussion will be the format.

GIS Geology Database Presentation

The GIS presentation will demonstrate the utilization of GIS and geological data to aid in characterization and remediation. Data utilization, availability, and accessibility will be discussed.

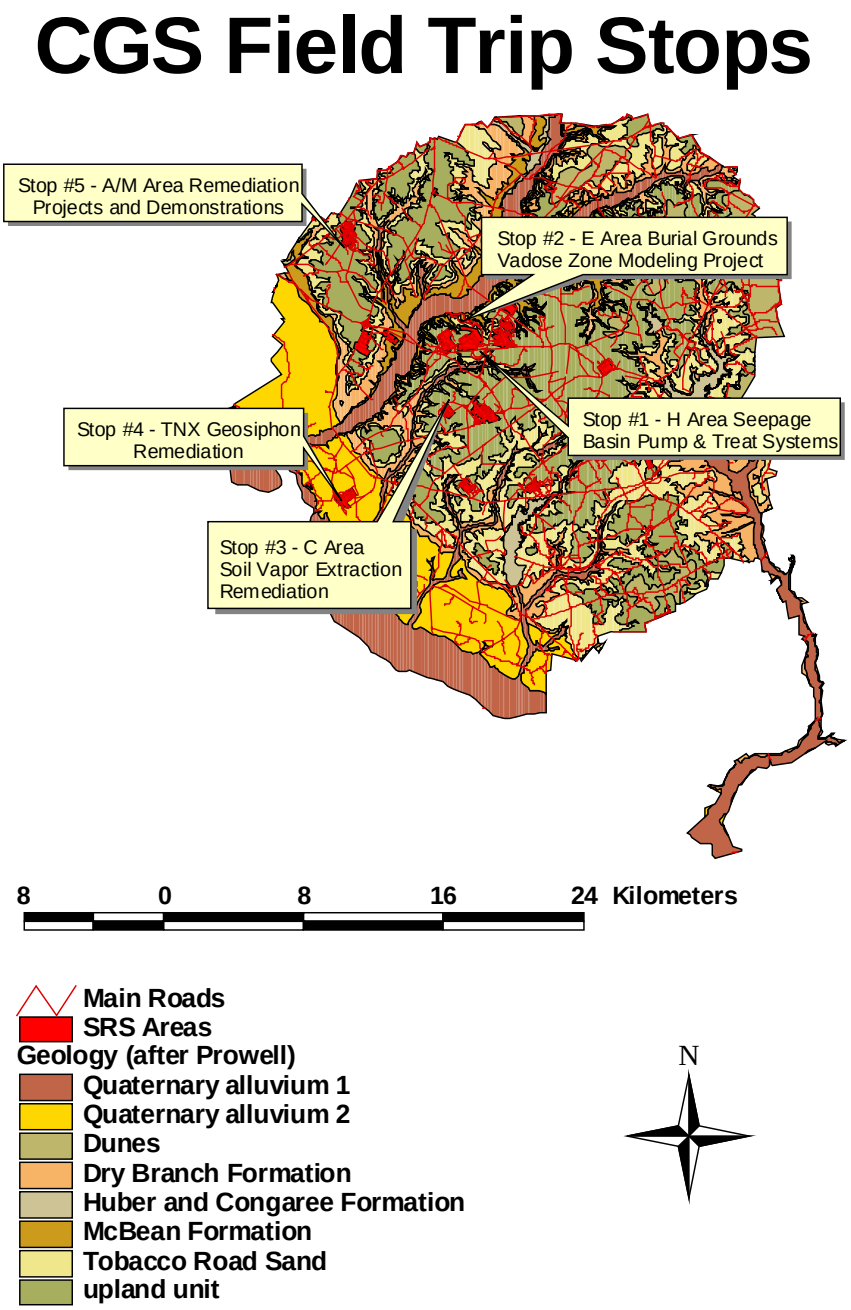

Figure 1. SRS tour stop locations. Geology is from Prowell (1994).

Sunday Workshops

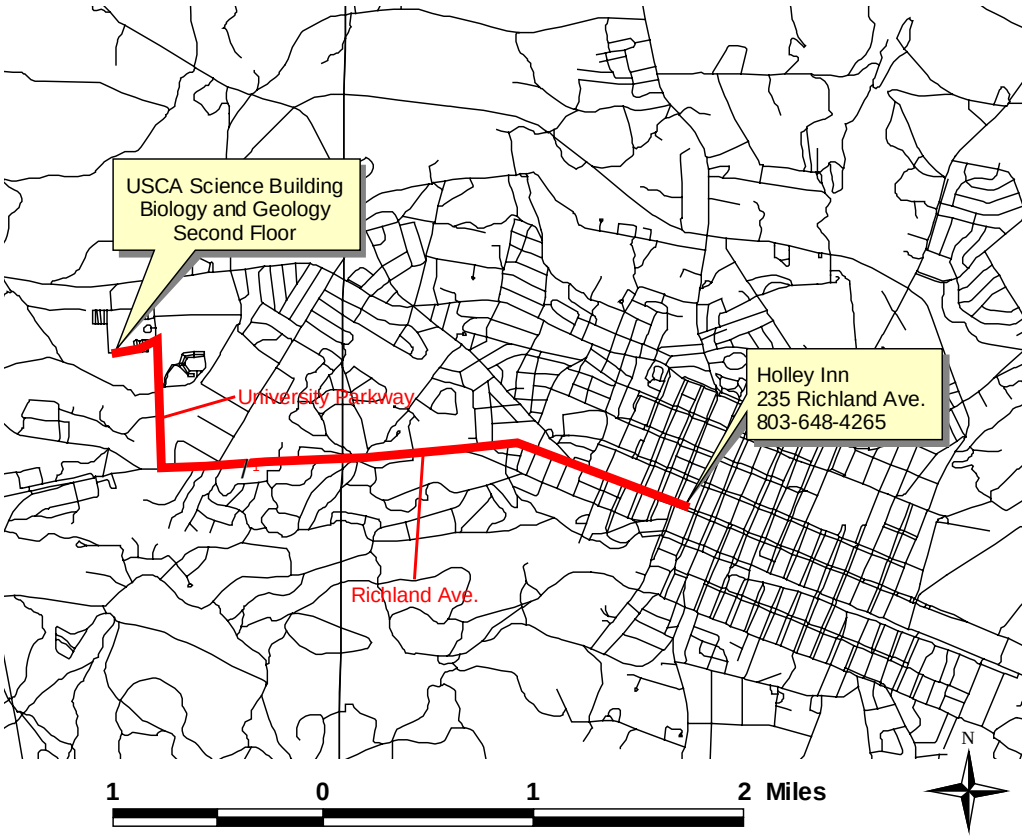

Figure 2. Route from the Holley Inn to USCA.

Savannah River Site Overview and General Site Information

Compiled from various sources, edited by Doug Wyatt

INTRODUCTION

The Savannah River Site (SRS) is a key Department of Energy industrial complex dedicated to the stewardship of the environment, the enduring nuclear weapons stockpile and nuclear materials. More specifically, the SRS processes and stores nuclear materials in support of the national defense and U.S. nuclear non-proliferation efforts. The site also develops and deploys technologies to improve the environment and treat nuclear and hazardous wastes left from the Cold War.

The SRS complex covers 198,344 acres, or 310 square miles encompassing parts of Aiken, Barnwell and Allendale counties in South Carolina, bordering the Savannah River.

The site is owned by DOE and operated by an integrated team led by Westinghouse Savannah River Company (WSRC). Under the contract that went into effect Oct. 1, 1996, WSRC is responsible for the site's nuclear facility operations; Savannah River Technology Center; environment, safety, health and quality assurance; and all of the site's administrative functions. The team also includes Bechtel Savannah River Inc. (parent company: Bechtel National Inc.), which is responsible for environmental restoration, project management, engineering and construction activities; BWXT Savannah River Company (parent company: BWX Technologies), which is responsible for facility decontamination and decommissioning; and British Nuclear Fuels, Limited (BNFL) Savannah River Corporation (parent company: BNFL Inc.), which is responsible for the site's solid waste program.

SAVANNAH RIVER SITE FOCUS

The Savannah River Site is committed to our people, missions and the future. SRS has a long track record of being the safest site in the DOE complex and one of the safest major industrial sites in the world. Protecting workers, the public, the environment, and national security interests is our highest goal. SRS will continue to maintain needed facilities and infrastructure while training and retaining a skilled and motivated workforce to insure our technical capability and performance. The SRS team has made commitments to its regulatory organizations, to the two states of the Central Savannah River Area, and to the community. Recognizing the imperative of open communication and trust, SRS will strive to accomplish regulatory milestones and community-driven obligations among the site's various neighbors and stakeholders. We also focus on cost effectiveness in contract and project management and a cross-cutting corporate perspective that will best serve SRS, other Department of Energy sites and national labs, and the U.S. Government.

SRS BUSINESS APPROACH

SRS is positioned for continued success by our commitment to a business approach focused on four cornerstones of success: technical and safety excellence, a DOE mission-supportive infrastructure, cost effectiveness and community support.

While the changing world has caused a downsizing of the site's original defense mission, the future of SRS lies in several areas: reducing the nuclear danger, transferring applied environmental technology to government and non-government entities, cleaning up the site and managing the waste SRS has produced, and forming economic and industrial alliances.

HISTORY

During the early 1950s SRS began to produce materials used in nuclear weapons, primarily tritium and plutonium-239. Five reactors were built to produce nuclear materials. Also built were support facilities including two chemical separations plants, a heavy water extraction plant, a nuclear fuel and target fabrication facility, a tritium extraction facility and waste management facilities.

Irradiated materials were moved from the reactors to one of the two chemical separations plants. In these facilities, known as "canyons," the irradiated fuel and target assemblies were chemically processed to separate useful products from waste. After refinement, nuclear materials were shipped to other DOE sites for final application. SRS produced about 36 metric tons of plutonium from 1953 to 1988.

NEW MISSIONS

SRS is one of the primary DOE sites with missions to address issues of national security and non-proliferation, including legacy material disposition.

SRS has been designated to continue as DOE's center for the supply of tritium to the enduring nuclear weapons stockpile. DOE has announced that its primary new source of tritium will be an existing commercial reactor in the Tennessee Valley Authority system. Tritium extraction from targets and loading into containers for shipment to the Defense Department will continue to be a site mission.

SRS has been selected to "blend down" highly enriched uranium from retired weapons components and reactor fuel to low-enriched uranium that can be converted to commercial reactor fuel in a privatized venture.

Plutonium stabilization now being conducted at SRS will be expanded to include materials from dismantled weapons and surpluses from other DOE sites. In early January 2000, the Secretary of Energy announced that SRS was to be the location for the Department's plutonium pit disassembly and conversion, mixed oxide fuel fabrication and plutonium immobilization facilities. These missions establish SRS's vital role in plutonium management for DOE.

ON-GOING MISSIONS

Tritium

Tritium, with a half-life of 12.5 years, must be replenished, and SRS is the nation's only facility for recycling and reloading tritium from nuclear weapons reservoirs returned from service. Recycling tritium allows the United States to stretch its tritium supplies.

All tritium unloading, mixing and loading is performed in a facility that went into operation in 1994. It replaces older facilities that processed the nation's tritium for 35 years. A new tritium extraction facility is to be built in the next few years to extract tritium created in the Tennessee Valley Authority's light-water reactors.

Spent Fuel

Spent nuclear fuel currently stored at SRS is from the site's production reactors, and from domestic and foreign research reactor programs. All of this fuel is stored in water-filled concrete storage basins, which were intended originally for interim storage while spent fuel awaited processing in a chemical separations facility.

Until 1988, it was routine for foreign researchers to return U.S.-origin spent fuel to this country. At the urging of the U.S. Department of State and the International Atomic Energy Agency, DOE renewed that policy in 1996. The first shipment of foreign-research-reactor, spent nuclear fuel under the renewed policy arrived at SRS that September.

For three decades, the SRS Receiving Basin for Offsite Fuels (RBOF) has provided safe receipt and interim storage of this fuel. Planning is under way to deinventory RBOF,

transferring spent fuel to SRS's L Area Disassembly Basin, a much larger, water-filled, reinforced-concrete facility. The basin was modified and received its first shipment of foreign spent fuel in January 1997. In addition, studies are underway to find alternative technologies, such as dry cask storage, for the spent fuel.

Canyon Operations

SRS has its two primary separations facilities — called canyons — located in F and H areas. F Canyon and H Canyon — together with the FB Line and HB Line, which are located atop the canyons — are where nuclear materials historically have been chemically recovered and purified.

HB Line has produced plutonium-238 for NASA. In 1995, SRS completed a five-year campaign to supply plutonium-238 for NASA's Cassini mission, an unmanned expedition to the planet Saturn, which was launched October 13, 1997.

Currently, both canyons continue to stabilize and manage most of the remaining inventory of plutonium-bearing materials at SRS. F Canyon is scheduled to operate until about 2002 to stabilize SRS materials. In addition, in July 1996, DOE determined that H Canyon, scheduled to operate until 2006, should be used to convert a large quantity of weapons-usable HEU to low-enriched material. No longer weapons-usable, the material will be suitable as fuel in commercial power reactors.

Waste Management

Weapons material production produced unusable byproducts, such as radioactive waste. About 34 million gallons of high-level radioactive liquid waste are stored in tanks. The Defense Waste Processing Facility (DWPF) is processing the highly radioactive waste, bonding radioactive elements in borosilicate glass, a stable storage form. DWPF began operations in March 1996. Much of the volume in the tanks can be separated as relatively low-level radioactive salt solution, which is mixed with cement, ash, and furnace slag and poured into permanent concrete monoliths for disposal at a facility called Saltstone.

In addition to high-level waste, other radioactive wastes at the site are: low-level solid and liquid waste; and transuranic waste, which contains alpha-emitting heavy isotopes that have decay rates and concentrations exceeding specified levels. Other wastes include hazardous waste, which is any toxic, corrosive, reactive or ignitable material that could affect human health or the environment; mixed waste, which contains both hazardous and radioactive components; and sanitary waste, which, like ordinary municipal waste, is neither radioactive nor hazardous.

The site's solid, low-level radioactive waste includes items such as protective clothing, tools and equipment that have become contaminated with small amounts of radioactive material. In October 1994, SRS opened engineered, concrete vaults for permanent disposal of solid low-level waste. The nation's first state-of-the-art waste vaults, they provide significantly better isolation from the environment than previous in-ground disposal methods.

Waste that contains transuranic (TRU) nuclides (radioactive elements with an atomic number greater than uranium 92) is stored temporarily at SRS. The site is developing characterization and treatment capabilities, pending eventual shipment to the Waste Isolation Pilot Plant in New Mexico. Hazardous wastes and mixed wastes are being stored on site in Resource Conservation and Recovery Act-permitted facilities until the appropriate treatment facilities are operational.

Environmental Restoration

In 1981, SRS began inventorying waste units. There are now 515 inactive waste and groundwater units included in the environmental restoration program. Waste sites range in size from a few feet to tens of acres and include basins, pits, piles, burial

grounds, landfills, tanks and groundwater contamination. Remediation of the waste sites is regulated under the Resource Conservation and Recovery Act and the Comprehensive Environmental Response, Compensation, and Liability Act.

The Resource Conservation and Recovery Act (RCRA) establishes a system for tracking and managing hazardous wastes from generation to disposal. This act also requires corrective action for releases of hazardous waste at active or inactive waste units and treatment, storage, or disposal facilities.

The Comprehensive Environmental Response, Compensation, and Liability Act (CERCLA - also known as Superfund) addresses the protection and cleanup of the environment. This act establishes a National Priorities List of sites targeted for assessment and, if necessary, restoration. SRS was placed on this list December 21, 1989.

In addition, the DOE has entered the Federal Facility Agreement (FFA) with the U.S. Environmental Protection Agency (EPA) Region IV and the South Carolina Department of Health and Environmental Control (SCDHEC). The FFA, effective August 16, 1993, specifies how SRS will address contamination or potential contamination at waste units to meet RCRA and CERCLA requirements. This agreement is required under CERCLA.

SRS works closely with state and federal regulators to determine which waste units require cleanup. If preliminary evaluations show that a waste unit may be a candidate for cleanup, it undergoes investigation and characterization. The investigation phase begins with looking at existing unit data, then developing a work plan that prescribes how to characterize the unit.

This investigation may find that a waste unit does not pose a risk to human health or the environment. If EPA and SCDHEC agree with this finding, with acceptance by the public, no further action is needed on that waste unit.

To date, 340 acres of land have been remediated. Also, almost four billion gallons of groundwater have been treated, with over 925,000 pounds of solvents removed. Even though the site has had success, this cleanup process is expected to take decades.

SRS seeks public participation in prioritizing the Environmental Management program. One way this is accomplished is through the SRS Citizens Advisory Board (CAB), formed in February 1994. This group of 25 individuals with diverse viewpoints provides advice to DOE, the U.S. Environmental Protection Agency and the South Carolina Department of Health and Environmental Control.

Research and Development

The Savannah River Technology Center – the site's applied research and development laboratory – creates, tests and deploys solutions to the site's technological challenges. SRTC researchers have made significant advances in glass technology, hydrogen technology, nonproliferation technology, environmental characterization and cleanup, sensors and probes, and other fields.

The laboratory's 750-person staff includes several internationally recognized experts; one-fourth of the research staff holds Ph.D's. SRTC's unique facilities include biotechnology laboratories, laboratories for the safe study and handling of radioactive materials, a field demonstration site for testing and evaluating environmental cleanup technologies and laboratories for ultra-sensitive measurement and analysis of radioactive materials.

Today, while the laboratory continues to solve the site's technological challenges, half of its work now comes from non-SRS customers, including DOE-Headquarters, other DOE sites and other federal agencies. The laboratory's largest work-for-others contract to date is a $31 million, multi-year contract to

demonstrate and evaluate the processes that will be used at the Hanford Site to treat and dispose of the waste in Hanford's waste tanks.

Economic Development

Because of the increased emphasis on sharing the site's expertise with the nation that, for more than four decades, has invested in its work, SRTC now forms strategic partnerships with private industry, academia and other government agencies to apply the laboratory's unique expertise to challenges of mutual interest. For example, SRTC, working with a broad-based consortium, applied its extensive hydrogen expertise to the development of a hydrogen-fueled bus that became part of the City of Augusta's public transit fleet before being shipped to another DOE site for further development.

The laboratory also shares its expertise by licensing private companies to manufacture and/or market technologies created at SRTC, a move that helps American businesses sharpen their competitive edge and provides taxpayers a second return on their investment.

Environment

Originally farmland, SRS now encompasses a timber and forestry research center managed by the U.S. Forest Service. The site also houses the Savannah River Ecology Laboratory, an environmental research center operated for DOE by the University of Georgia.

In 1972, DOE's predecessor agency, the Atomic Energy Commission, designated SRS as the first National Environmental Research Park. The site is home to the bald eagle and the red-cockaded woodpecker, an endangered species. Other endangered species, including the shortnose sturgeon, peregrine falcon and wood stork, visit the site from time to time. Other wildlife commonly found on the site includes alligators, whitetailed deer, wild turkeys and otters.

Employment

Today, about 13,900 people are employed at SRS, making it one of the largest employers in South Carolina. About 89 percent are employees of WSRC and its major subcontractors. DOE employees represent about 3.6 percent of the SRS population. The rest are other Westinghouse subcontractors and DOE contractors; the site's security contractor, Wackenhut Services Inc.; Savannah River Ecology Laboratory; and U.S. Forest Service.

Economic Impact

The site's economic impact ripples across a two-state area. Currently, the site's overall budget is about $1.5 billion. Of that, more than $900 million is payroll. In Fiscal Year 1999, which ended Sept. 30, 1999, the site purchased about $215 million in goods and services in South Carolina and Georgia combined. Of that, about $110 million was spent in the local area.

Overview of the Savannah River Site Stratigraphy, Hydrostratigraphy and Structure

Compiled from various sources, edited by D. E. Wyatt, R. K. Aadland and F. H. Syms

INTRODUCTION

This paper provides a brief overview of the stratigraphy, hydrostratigraphy and structure associated with the Savannah River Site. The information contained in this summary was abstracted from a variety of authors and sources, the majority of whom are cited in the various papers in this field guide. Additional (and many of the same) references are included as a bibliography in this guidebook.

REGIONAL PHYSIOGRAPHY

The site region, defined as the area within a 320-km (200-mile) radius of the center of SRS, includes parts of the Atlantic Coastal Plain, Piedmont and Blue Ridge physiographic provinces. SRS is located on the upper Atlantic Coastal Plain, about 50 km (30 miles) southeast of the Fall Line (Figure 1).

COASTAL PLAIN STRATIGRAPHY

The information in this section is based largely on the work of Aadland et al., (1995) and his references.

The sediments of the Atlantic Coastal Plain in South Carolina are stratified sand, clay, limestone, and gravel that dip gently seaward and range in age from Late Cretaceous to Recent. The sedimentary sequence thickens from essentially zero at the Fall Line to more than 1,219 meters (4,000 feet) at the coast. Regional dip is to the southeast, although beds dip and thicken locally in other directions because of locally variable depositional regimes and differential subsidence of basement features such as the Cape Fear Arch and the South Georgia Embayment. A cross-section depicting these strata is presented in Figure 2.

.

The Coastal Plain sedimentary sequence near the center of the region (i.e., SRS) consists of about 213 meters (700 feet) of Late Cretaceous quartz sand, pebbly sand, and kaolinitic clay, overlain by about 18 meters (60 feet) of Paleocene clayey and silty quartz sand, glauconitic sand, and silt. The Paleocene beds are in turn overlain by about 107 meters (350 feet) of Eocene quartz sand, glauconitic quartz sand, clay, and limestone grading into calcareous sand, silt, and clay. The calcareous strata are common in the upper part of the Eocene section in downdip parts of the study area. In places, especially at higher elevations, the sequence is capped by deposits of pebbly, clayey sand, conglomerate, and clay of Miocene or Oligocene age. Lateral and vertical facies changes are characteristic of most of the Coastal Plain sequence, and the lithologic descriptions below are therefore generalized. A surface geologic map for SRS is presented in the “Descriptions of Field Stops” Figure 1 in this guide book. The stratigraphic section (see Figure 2), which delineates the coastal plain lithology (see Figure 3) is divided into several formations and groups based principally on age and lithology. A reference geophysical log is shown on Figure 4.

Geology of the Coastal Plain Sediments - General

The following sections describe regional stratigraphy and lithologies, with emphasis on variations near the SRS. The data presented are based upon direct observations of surface outcrops; geologic core obtained during drilling of bore holes; microfossil age dating; and borehole geophysical logs. Several key boring locations within the SRS boundaries and in the adjacent regions (presented in Figure 5) are referenced throughout the following discussions.

Rocks of Paleozoic and Triassic ages have been leveled by erosion and are unconformably overlain by unconsolidated to poorly consolidated Coastal Plain. This erosional surface dips approximately 7 m/km (37 ft/mile) toward the southeast. The Atlantic Coastal Plain sediments in South Carolina are stratified sand, clay, limestone, and gravel that dip gently seaward and range in age from Late Cretaceous to Recent. Near the coast, the wedge is approximately 1,219 meters (4,000 feet) thick.

Upper Cretaceous Sediments

Upper Cretaceous sediments overlie Paleozoic crystalline rocks or lower Mesozoic sedimentary rocks throughout most of the study area. The Upper Cretaceous sequence includes the basal Cape Fear Formation and the overlying Lumbee Group, which is divided into three formations. The sediments in this region consist predominantly of poorly consolidated, clay-rich, fine- to medium-grained, micaceous sand, sandy clay, and gravel, and is about 213 meters (700 feet) thick near the center of the study area. Thin clay layers are common. In parts of the section, clay beds and lenses up to 21 meters (70 feet) thick are present. Depositional environments were fluvial to prodeltaic.

Cape Fear Formation

The Cape Fear Formation rests directly on a thin veneer of saprolitic bedrock and is the basal unit of the Coastal Plain stratigraphic section at SRS. The saprolite ranges from less than 3 meters (10 feet) to more than 12 meters (40 feet) in thickness and defines the surface of the crystalline basement rocks and sedimentary rocks of the Newark Supergroup (Middle to Upper Triassic age). The thickness of the saprolite reflects the degree of weathering of the basement prior to deposition of the Cape Fear Formation. The Cape Fear is encountered at about 61 meters (200 feet) msl just south of well C-3 in the north and at about 366 meters (1,200 feet) msl at well C-10 in the south. The Cape Fear does not crop out in the study area, and its northern limit is north of the C-1 and P-16 wells and south of wells C-2 and C-3. The unit thickens to more than 70 meters (230 feet) at well C-10 and has a maximum known thickness of about 213 meters (700 feet) in Georgia. The top of the Cape Fear Formation dips approximately 5 m/km (30 ft/mile) to the southeast across the study area.

The Cape Fear Formation consists of firm to indurated, variably colored, poorly sorted, silty, clayey sand and sandy silt and clay. Bedding thickness of the sand, silt and clay ranges from about 1.5 meters (5 feet) to 6 meters (20 feet), with the sand beds generally thicker than the clay beds. The sand grains are typically coarse-grained with common granule and pebble. The sand is arkosic with rock fragments common in the pebbly zones.

The Cape Fear Formation is more indurated than other Cretaceous units because of the abundance of cristobalite cement in the matrix. The degree of induration decreases from north to south across the area. In the northern part of the area, the formation is represented on geophysical logs as a zone of low resistivity. In the southern part of the study area, the unit is more sandy, and is noted on geophysical logs by increased electrical resistivity (wells ALL-324 and C-10). The transition from the more indurated clayey sand in the north to the poorly consolidated cleaner sand in the south may be due to deeper fluvial incisement and erosion of the Cape Fear section to the north. This may bring the deeper, more cristobalite-rich part of the section into proximity with the overlying unconformity that caps the formation. Clark et al. attribute the differences between updip and downdip lithologies to changes in source material during deposition or to the southern limit of the cristobalite cementation process.

The lithologic characteristics and the paucity of marine fossils are indicative of a high-energy environment close to a sediment source area. Thus, these sediments may represent deposition in fluvial-deltaic environments on the upper parts of a delta

plain, grading downdip to marginal marine. The Cape Fear Formation was erosionally truncated prior to deposition of the overlying Middendorf Formation, resulting in a disconformity between the two formations.

Lumbee Group

Three formations of the Late Cretaceous Lumbee Group are present in the study area. These are, from oldest to youngest, the Middendorf, Black Creek, and Steel Creek Formations.

The Lumbee Group consists of fluvial and deltaic quartz sand, pebbly sand, and clay in the study area. The sedimentary sequence is more clayey and fine-grained downdip from the study area, reflecting shallow to deep marine shelf sedimentary environments. Thickness ranges from about 122 meters (400 feet) at well C-3 in the north, to about 238 meters (780 feet) near well C-10 in the south. At least part of the group crops out in the northern part of the study area but it is difficult to distinguish the individual formations. Consequently, the Lumbee Group was mapped as undifferentiated Upper Cretaceous by Nystrom and Willoughby. The dip of the upper surface of the Lumbee Group is to the southeast at approximately 4 m/km (20 ft/mile) across the study area.

The Middendorf Formation (now in question) unconformably overlies the Cape Fear Formation with a distinct contact. The contact is marked by an abrupt change from the moderately indurated clay and clayey sand of the underlying Cape Fear to the slightly indurated sand and lesser clayey sand of the Middendorf. The basal zone is often pebbly. The contact is unconformable and is marked by a sudden increase in electrical resistivity on geophysical logs. Thickness of the formation ranges from approximately 37 meters (120 feet) in well C-2 in the north, to 73 meters (240 feet) in well C-10 in the south. It has a maximum known thickness of about 158 meters (520 feet) in Georgia. The top of the formation dips to the southeast at about 4.9 m/km (26 ft/mile) across the study area. Fossil data for the Middendorf are sparse and the formation is not well dated in the study area.

The sand of the Middendorf Formation is medium to very coarse grained, typically angular, slightly silty, tan, light gray, and yellow in color. It is much cleaner and less indurated than the underlying Cape Fear sediments. Sorting is generally moderate to poor. Pebble and granule zones are common in updip parts of the study area, whereas clay layers up to 3 meters (10 feet) thick are more common downdip. Clay clasts are abundant in places. Some parts of the unit are feldspathic and micaceous, but not as micaceous as in the overlying Black Creek Formation. Lignitic zones are also common.

Over much of the study area, a zone of interbedded sand and variegated clay up to 18 meters (60 feet) thick is present at or near the top of the Middendorf Formation. The interbedded sand is upward fining in places. This lithology and the marine microfauna found in core samples indicate that the unit was deposited in lower delta plain and delta front environments under some marine influence. In the northern part of the study area, the formation is variably colored, composed of tan, red, and purple sand. Here, the sediments have the characteristics of fluvial and upper delta plain deposits.

The Black Creek Formation is penetrated at virtually all well-cluster sites in the study area. The unit ranges in thickness from approximately 46 meters (150 feet) at well C-2 in the north to 91 meters (300 feet) near the center of the study area in well PBF-3 and to 113 meters (370 feet) at well C-10 in the south. The unit dips approximately 4 m/km (22 ft/mile) to the southeast.

The Black Creek is distinguished from the overlying and underlying Cretaceous units by its better sorted sand, fine-grained texture, and relatively high clay content. It is generally darker, more lignitic, and more micaceous, especially in the updip part of the section, than the other Cretaceous units. In much of the

study area, the lower one-third of the formation is mostly sand that is separated from the upper two-thirds of the unit by clay beds. These beds are 6 meters (20 feet) to 12 meters (40 feet) thick in the northern part of the region and more than 46 meters (150 feet) at well C-10 in the south. In general, the top of the Black Creek Formation is picked at the top of a clay bed that ranges from 3 meters (10 feet) to 8 meters (25 feet) in thickness. The clay bed is exceptionally thick but not laterally extensive. For example, it is essentially absent in wells P-21, CPC-1, P-26, and P-29. This suggests lagoonal back barrier bay deposition associated with nearby shorelines. Often the thick clay beds flank the areas where shoaling is suggested owing to uplift along the Pen Branch and Steel Creek Faults, which was contemporaneous with deposition. Overall, the Black Creek consists of two thick, fining-upward sequences, each capped by thick clay beds. The lower sequence is predominantly silty, micaceous sand in the area of SRS, while the upper sequence is mostly clay and silt.

Where the Black Creek Formation is present north of SRS, it consists of clayey, micaceous, poorly to moderately well sorted, fine to medium-grained, subangular to subrounded quartz sand beds and silty clay beds. Pebbly beds are present throughout the unit. This sandy lithology is indicative of fluvial to upper delta-plain environments; the clay beds that cap the upward-fining sandy sequences are typical of lower delta plain depositional environments. Near Millet, SC, the basal beds of the Black Creek consist of sand and silty clay and are similar to underlying Middendorf sediments. Here, deposition occurred on a lower delta plain. Fossils recovered from the unit suggest marine influences during deposition of the sediments, especially the clay.

In the central and downdip part of the study area (wells P-22, ALL-324, C-6, C-10), the unit grades into gray-green clayey silt, micritic clay, and fine- to medium-grained, upward fining sand that is moderately well sorted, micaceous, carbonaceous, and locally glauconitic. The sequence suggests deposition in a delta front or shallow shelf environment, as indicated by the lithology and an abundance of marine macrofauna and microfauna. The transition from fine-grained, prodelta or delta front deposits in the southern part of the study area to coarser-grained, more landward deltaic deposits in the northern part of the area is reflected in the general increase in electrical resistivity noted on geophysical logs in the wells in the north, especially in the upper part of the Black Creek section.

The Peedee Formation was previously considered by some investigators to be absent in the study area; however, recent paleontological evidence provides dates of Peedee age from sediment samples in the southern part of SRS. Because there is a considerable difference in lithology between the type Peedee and the sediments in the SRS region, Peedee-equivalent sediments in the vicinity of SRS were referred to as the "Steel Creek Member" of the Peedee Formation (Ref. 115). Raising the Steel Creek Member to formational status was recommended by Aadland et al., and it is so used in this document. The type well for the Steel Creek Formation is P-21, located near Steel Creek. The top of the Steel Creek is picked at the top of a massive clay bed that ranges from 1 meter (3 feet) to more than 9 meters (30 feet) in thickness. The formation dips approximately 4 m/km (20 ft/mile) to the southeast.

The unit ranges in thickness from approximately 18 meters (60 feet) at well P-30 to 53 meters (175 feet) at well C-10 in the south. It has a maximum known thickness of 116 meters (380 feet) in Georgia. The Steel Creek section thins dramatically between the ALL-324 and the P-22 wells due to truncation by erosion at the Cretaceous-Tertiary unconformity. The Steel Creek Formation overlies the Black Creek Formation and is distinguished from it by a higher percentage of sand, which is represented on geophysical logs by a generally higher electrical resistivity and lower natural gamma radiation count.

The formation consists of yellow, tan, and gray, medium to coarse, moderately sorted sand interbedded with variegated clay. The lower part of the unit consists of medium- to coarse-grained, poorly to well-sorted, quartz sand, silty sand, and off-white to buff clay that contains thin beds of micaceous and carbonaceous clay. Pebbly zones are common, as are layers with clay clasts. Fining-upward sand is interbedded with the clay and silty clay beds in some areas. It is difficult to differentiate the Steel Creek from the underlying Black Creek in the northwestern part of the study area. The unit appears to have been deposited in fluvial environments in updip areas and upper to lower delta plain environments in the south. The massive clay that caps the unit suggests lower delta plain to shallow shelf depositional environments. The presence of certain microfossils indicates some marine influence in parts of the Steel Creek. A pebble-rich zone at the base of the unit suggests a basal unconformity.

Tertiary Sediments

Tertiary sediments range in age from Early Paleocene to Miocene and were deposited in fluvial to marine shelf environments. The Tertiary sequence of sand, silt, and clay generally grades into highly permeable platform carbonates in the southern part of the study area and these continue southward to the coast. The Tertiary sequence is divided into three groups, the Black Mingo Group, Orangeburg Group, and Barnwell Group, which are further subdivided into formations and members. These groups are overlain by the ubiquitous Upland unit.

The Tertiary sedimentary sequence deposited in west-central South Carolina has been punctuated by numerous sea level low stands and/or affected by subsidence in the source areas (which reduced or eliminated sediment availability) resulting in a series of regional unconformities. Four such regionally significant unconformities are defined in the Tertiary stratigraphic section and include the “Cretaceous-Tertiary” unconformity, the “Lang Syne/Sawdust Landing” unconformity, the “Santee” unconformity and the “Upland” unconformity. Based on these unconformities, four sequence stratigraphic units (unconformity bounded sedimentary units) have been delineated. Work is currently underway to place the units in the global sequence stratigraphic framework.

Black Mingo Group

The Black Mingo Group consists of quartz sand, silty clay, and clay that suggest upper and lower delta plain environments of deposition generally under marine influences. In the southern part of the study area, massive clay beds, often more than 50 feet (15 meters) thick, predominate. Downdip from the study area, thin red to brown sandy clay beds, gray to black clay beds and laminated shale dominate the Black Mingo Group and suggest deposition in clastic shelf environments. At the South Carolina coast, carbonate platform facies-equivalents of the updip Black Mingo clastic sediments first appear. The carbonate units are all referred to as "unnamed limestones" by Colquhoun et al. These are equivalent to the thick beds of anhydrite and dolomite of the Paleocene Cedar Keys Formation and the lower Eocene glauconitic limestone and dolomite of the Oldsmar Formation. Both carbonate units are delineated and mapped in coastal Georgia and northeastern Florida.

Basal Black Mingo sediments were deposited on the regional “Cretaceous-Tertiary” unconformity of Aadland that defines the base of Sequence Stratigraphic unit I. There is no apparent structural control of this unconformity. Above the unconformity, the clay and clayey sand beds of the Black Mingo Group thin and often pinch out along the traces of the Pen Branch and Crackerneck Faults. This suggests that coarser-grained materials were deposited preferentially along the fault traces, perhaps due to shoaling of the depositional surface. This, in turn, suggests movement (reactivation) along the faults. This reactivation would have occurred during Black

Mingo deposition, that is, in Paleocene and lower Eocene time.

The upper surface of the Black Mingo Group dips to the southeast at 3 m/km (16 ft/mi.), and the group thickens from 18 meters (60 feet) at well C-2 in the north, to about 52 meters (170 feet) near well C-10 in the south. The group is about 213 meters (700 feet) thick at the South Carolina coast. Throughout the downdip part of the South Carolina Coastal Plain, the Black Mingo Group consists of the Rhems Formation and the overlying Williamsburg Formation.

The Rhems Formation contains four members, each representing a depositional facies. They are the Sawdust Landing Member, an upper delta plain fluvial deposit which unconformably overlies the Cretaceous Peedee Formation; the Lang Syne Member, a lower delta-plain deposit of estuarine and littoral origin; the Perkins Bluff Member, a shallow shelf deposit; and the Browns Ferry Member, a deep-water shelf deposit. Additionally, an unnamed unit represents the carbonate-shelf facies.

In the updip part of the South Carolina Coastal Plain, the Black Mingo Group consists of the Sawdust Landing and Lang Syne Formations, which are equivalent to the Ellenton Formation of Siple; the Snapp Formation, which is the updip equivalent of the Williamsburg Formation of Colquhoun et al.; and the Fourmile Formation, which is the updip equivalent of the Fishburne Formation of Gohn et al.

Lang Syne/Sawdust Landing Formations. Siple proposed the name Ellenton Formation for a subsurface lithologic unit in the SRS area consisting of beds of dark, lignitic clay and coarse sand, which are equivalent to the Sawdust Landing and Lang Syne Members of the Rhems Formation of Colquhoun et al. Fallaw and Price suggested that the Sawdust Landing Member and the overlying Lang Syne Member of the Rhems Formation be raised to formational status and replace the term Ellenton in the study area

In the absence of detailed paleontological control, the Sawdust Landing Formation and the overlying Lang Syne Formation could not be systematically separated for mapping in this region. Thus, they are treated as a single unit; the Lang Syne/Sawdust Landing undifferentiated, on all sections and maps. This is consistent with the approach taken by Fallaw and Price. The sediments of the unit generally consist of two fining-upward sand-to-clay sequences, which range from about 12 meters (40 feet) in thickness at the northwestern boundary of SRS to about 30 meters (100 feet), near the southeastern boundary. The unit is mostly dark gray to black, moderately to poorly sorted, fine to coarse-grained, micaceous, lignitic, silty and clayey quartz sand interbedded with dark gray clay and clayey silt. Pebbly zones, muscovite, feldspar, and iron sulfide are common. Individual clay beds up to 6 meters (20 feet) thick are present in the unit. Clay and silt beds make up approximately one-third of the unit in the study area. The dark, fine-grained sediments represent lower delta plain, bay-dominated environments. Tan, light gray, yellow, brown, purple, and orange sand, pebbly sand, and clay represent upper delta plain, channel-dominated environments.

In the southern part of the study area, dark, poorly sorted, micaceous, lignitic sand and silty sand containing a diverse assemblage of pollen and microfauna of early and middle Paleocene (Midwayan) age are present. This is the Perkins Bluff Member of the Rhems Formation, which was deposited in lower delta plain or shallow marine shelf environments.

Toward the coast, the Rhems Formation includes shallow to increasingly deeper water clastic shelf facies sediments (Browns Ferry Member) that ultimately pass into a shallow carbonate platform facies at the South Carolina coastline. Colquhoun et al., referred to the carbonate platform facies equivalent as “unnamed limestone." The carbonate platform sequence is correlative with the anhydrite- and gypsum-bearing dolomitized limestone and finely crystalline dolomite of the lower part of

the Cedar Keys Formation that is mapped in coastal Georgia and northeastern Florida. The carbonate sequence is about 76 meters (250 feet) thick at the South Carolina coastline. The Cedar Keys Formation has a maximum thickness of 130 meters (425 feet) in coastal areas of Georgia. The carbonate platform sediments of the Cedar Keys Formation are generally impermeable, and the unit acts as the underlying confining unit of the Floridan Aquifer System in the coastal areas of South Carolina and Georgia.

Snapp Formation (Williamsburg Formation). Sediments in the study area that are time equivalent to the Williamsburg Formation differ from the type Williamsburg and have been designated the "Snapp Member of the Williamsburg Formation". Fallaw and Price have suggested that the "Snapp Member" of the Williamsburg be raised to formational status. The Snapp Formation is used in this report. The unit is encountered in well P-22 in the southeastern part of SRS near Snapp Station. The basal contact with the underlying Lang Syne/Sawdust Landing undifferentiated is probably unconformable. The Snapp Formation appears to pinch out in the northwestern part of SRS and thickens to about 15 meters (50 feet) near the southeastern boundary of the site.

The Snapp Formation (Williamsburg Formation) crops out in Calhoun County. The sediments in the upper part of the unit consist of low-density, fissile, dark-gray to black siltstone and thin layers of black clay interbedded with sand in the lower part. These and similar sediments in Aiken and Orangeburg Counties were probably deposited in lagoonal or estuarine environments. Within and near SRS, the Snapp sediments typically are silty, medium- to coarse-grained quartz sand interbedded with clay. Dark, micaceous, lignitic sand also occurs, and all are suggestive of lower delta plain environments. In Georgia, the unit consists of thinly laminated, silty clay locally containing layers of medium- to dark-gray carbonaceous clay. This lithology is indicative of marginal marine (lagoonal to shallow shelf) depositional environments. Clayey parts of the unit are characterized on geophysical logs as zones of low electrical resistivity and a relatively high-gamma ray response. In the southernmost part of the study area, the Snapp consists of gray-green, fine to medium, well-rounded, calcareous quartz sand and interbedded micritic limestone and limey clay that is highly fossiliferous and glauconitic. This lithology suggests deposition in shallow shelf environments somewhat removed from clastic sediment sources

The upper surface of the Williamsburg Formation is defined by the "Lang Syne/Sawdust Landing" unconformity.

Fourmile Formation. Early Eocene ages, derived from paleontological assemblages, indicate that the sand immediately overlying the Snapp Formation in the study area is equivalent to the Fishburne. These sediments were deposited on the "Lang Syne/Sawdust Landing" unconformity and constitute the basel unit of Sequence Stratigraphic Unit II. The Fishburne is a calcareous unit that occurs downdip near the coast. The sand was initially designated the Fourmile Member of the Fishburne Formation. Owing to the distinctive difference in lithology between the type, Fishburne Formation and the time-equivalent sediments observed in the study area, Fallaw and Price have recommended that the Fourmile Member of the Fishburne be raised to formational rank. The term Fourmile Formation is used in this report.

The Fourmile Formation averages 9 meters (30 feet) in thickness, is mostly tan, yellow-orange, brown, and white, moderately to well-sorted sand, with clay beds a few feet thick near the middle and at the top of the unit. The sand is very coarse to fine grained, with pebbly zones common, especially near the base. Glauconite, up to about 5%, is present in places, as is weathered feldspar. In the center and southeastern parts of SRS, the unit can be distinguished from the underlying Paleocene strata by its lighter color and lower content of silt and clay. Glauconite and

microfossil assemblages indicate that the Fourmile is a shallow marine deposit.

Overlying the Fourmile Formation in the study area is 9 meters (30 feet) or less of sand similar to the Fourmile. This sand is better sorted, contains fewer pebbly zones, less muscovite and glauconite, and in many wells is lighter in color. Microfossil assemblages indicate that the sand is correlative with the early middle Eocene Congaree Formation. In some wells a thin clay occurs at the top of the Fourmile, separating the two units; however, the difficulty in distinguishing the Fourmile Formation from the overlying Congaree Formation has led many workers at SRS to include the entire 293 meters (960 feet) section in the Congaree Formation.

Orangeburg Group

The Orangeburg Group consists of the lower middle Eocene Congaree Formation (Tallahatta equivalent) and the upper middle Eocene Warley Hill Formation and Santee Limestone (Lisbon equivalent). Over most of the study area, these post-Paleocene units are more marine in character than the underlying Cretaceous and Paleocene units; they consist of alternating layers of sand, limestone, marl, and clay.

The group crops out at lower elevations in many places within and near SRS. The sediments thicken from about 26 meters (85 feet) at well P-30 near the northwestern SRS boundary to 61 meters (200 feet) at well C-10 in the south. Dip of the upper surface is 2 m/km (12 ft/mile) to the southeast. Downdip at the coast, the Orangeburg Group is about 99 meters (325 feet) thick and is composed of shallow carbonate platform deposits of the Santee Limestone.

In the extreme northern part of the study area, the entire middle Eocene Orangeburg Group is mapped as the Huber Formation. The micaceous, poorly sorted sand, abundant channel fill deposits and cross bedding, and carbonaceous kaolin clay in the Huber is indicative of fluvial, upper delta plain environments.

In the central part of the study area the group includes, in ascending order, the Congaree, Warley Hill, and Tinker/Santee Formations. The units consist of alternating layers of sand, limestone, marl, and clay that are indicative of deposition in shoreline to shallow shelf environments. From the base upward, the Orangeburg Group passes from clean shoreline sand characteristic of the Congaree Formation to shelf marl, clay, sand, and limestone typical of the Warley Hill and Santee Limestone. Near the center of the study area, the Santee sediments consist of up to 30 vol% carbonate. The sequence is transgressive, with the middle Eocene Sea reaching its most northerly position during Tinker/Santee deposition.

Toward the south, near wells P-21, ALL-324, and C-10, the carbonate content of all three formations increases dramatically. The shoreline sand of the Congaree undergoes a facies change to interbedded glauconitic sand and shale, grading to glauconitic argillaceous, fossiliferous, sandy limestone. Downdip, the fine-grained, glauconitic sand, and clay of the Warley Hill become increasingly calcareous and grades imperceptibly into carbonate-rich facies comparable to both the overlying and underlying units. Carbonate content in the glauconitic marl, calcareous sand, and sandy limestone of the Santee increases towards the south. Carbonate sediments constitute the vast majority of the Santee from well P-21 southward.

Congaree Formation. The early middle Eocene Congaree Formation has been traced from the Congaree valley in east central South Carolina into the study area. It has been paleontologically correlated with the early and middle Eocene Tallahatta Formation in neighboring southeastern Georgia by Fallaw et al.

The Congaree is about 9 meters (30 feet) thick near the center of the study area and consists of yellow, orange, tan, gray, green, and

greenish gray, well-sorted, fine to coarse quartz sand, with granule and small pebble zones common. Thin clay laminae occur throughout the section. The quartz grains tend to be better rounded than those in the rest of the stratigraphic column are. The sand is glauconitic in places suggesting deposition in shoreline or shallow shelf environments. To the south, near well ALL-324, the Congaree Formation consists of interbedded glauconitic sand and shale, grading to glauconitic, argillaceous, fossiliferous sandy limestone suggestive of shallow to deeper shelf environments of deposition. Farther south, beyond well C-10, the Congaree grades into platform carbonate facies of the lower Santee Limestone.

The equivalent of the Congaree northwest of SRS has been mapped as the Huber Formation. At these locations it becomes more micaceous and poorly sorted, indicating deposition in fluvial and upper delta plain environments. On geophysical logs, the Congaree has a distinctive low gamma ray count and high electrical resistivity.

Warley Hill Formation**.** Unconformably overlying the Congaree Formation are 3 meters (10 feet) to 6 meters (20 feet) of fine-grained, often glauconitic sand and green clay beds that have been referred to respectively as the Warley Hill and Caw Caw Members of the Santee Limestone. The green sand and clay beds are referred to informally as the "green clay" in previous SRS reports. Both the glauconitic sand and the clay at the top of the Congaree are assigned to the Warley Hill Formation. In the updip parts of the study area, the Warley Hill apparently is missing or very thin, and the overlying Tinker/Santee Formation rests unconformably on the Congaree Formation.

The Warley Hill sediments indicate shallow to deeper clastic shelf environments of deposition in the study area, representing deeper water than the underlying Congaree Formation. This suggests a continuation of a transgressive pulse during upper middle Eocene time. To the south, beyond well P-21, the green silty sand, and clay of the Warley Hill undergo a facies change to the clayey micritic limestone and limey clay typical of the overlying Santee Limestone. The Warley Hill blends imperceptibly into a thick clayey micritic limestone that divides the Floridan Aquifer System south of the study area. The Warley Hill is correlative with the lower part of the Avon Park Limestone in southern Georgia and the lower part of the Lisbon Formation in western Georgia.

In the study area, the thickness of the Warley Hill Formation is generally less than 6 meters (20 feet). In a part of Bamberg County, South Carolina, the Congaree Formation is not present, and the Warley Hill rests directly on the Williamsburg Formation.

Tinker/Santee Formation**.** The late middle Eocene deposits overlying the Warley Hill Formation consist of moderately sorted yellow and tan sand, calcareous sand and clay, limestone, and marl. Calcareous sediments dominate downdip, are sporadic in the middle of the study area, and are missing in the northwest. The limestone represents the farthest advance to the northwest of the transgressing carbonate platform first developed in early Paleocene time near the South Carolina and Georgia coasts.

Fallaw et al., divided the Santee into three members in the study area: the McBean, Blue Bluff, and Tims Branch Members. The McBean Member consists of tan to white, calcilutite, calcarenite, shelly limestone, and calcareous sand and clay. It dominates the Santee in the central part of the study area and represents the transitional lithologies between clastics in the north and northwest (Tims Branch Member), and fine-grained carbonates in the south (Blue Bluff Member).

The carbonates and carbonate-rich clastics are restricted essentially to three horizons in the central part of, the Griffins Landing Member of the Dry Branch Formation, the McBean Member of the Tinker/Santee Formation and the Utley Limestone member of the Clinchfield Formation. The uppermost horizon

includes the carbonates of the Griffins Landing Member of the Dry Branch Formation found below the “tan clay” interval that occurs near the middle of the Dry Branch. The isolated carbonate patches of the Griffins Landing are the oyster banks that formed in the back barrier marsh zone behind the barrier island system. Underlying the Dry Branch, directly below the regionally significant Santee Unconformity, is the Utley Limestone Member of the Clinch Field Formation. Without the benefit of detailed petrographic and paleontological analysis, the Utley carbonates cannot be systematically distinguished from the carbonates of the underlying Tinker/Santee Formation. Thus the carbonate-rich sediments between the Santee Unconformity, and the Warley Hill Formation are referred to as the Tinker/Santee (Utley) sequence in this report.

The Blue Bluff Member consists of gray to green, laminated micritic limestone. The unit includes gray, fissile, calcareous clay and clayey micritic limestone and very thinly layered to laminated, clayey, calcareous, silty, fine sand, with shells and hard, calcareous nodules, lenses, and layers. Cores of Blue Bluff sediments are glauconitic, up to 30% in places. The Blue Bluff lithology suggests deposition in offshore shelf environments. Blue Bluff sediments tend to dominate the formation in the southern part of the study area and constitute the major part of the “middle confining unit" that separates the Upper and Lower Floridan aquifers south of the study area.

Fallaw et al., described the Tims Branch Member of the Santee as the siliciclastic part of the unit, consisting of fine- and medium-grained, tan, orange, and yellow, poorly to well sorted, and slightly to moderately indurated sand. The clastic lithologies of the Tims Branch Member dominate the Santee in the northern part of the study area. Because the clastic lithologies differ so markedly from the type Santee, Fallaw and Price raised the Tims Branch Member of the Santee to formational rank, namely the Tinker Formation. Because the clastic and carbonate lithologies that constitute the Tinker/Santee sequence in the upper and middle parts of the study area are hydrologically undifferentiated, the units are not systematically separated, and they are designated Tinker/Santee Formation on maps and sections. The thickness of the Tinker/Santee Formation is variable due in part to displacement of the sediments, but more commonly to dissolution of the carbonate resulting in consolidation of the interval and slumping of the overlying sediments of the Tobacco Road and Dry Branch Formations into the resulting lows.

The Tinker/Santee (Utley) interval is about 21 meters (70 feet) thick near the center of SRS, and the sediments indicate deposition in shallow marine environments. The top of the unit is picked on geophysical logs where Tinker/Santee (Utley) sediments with lower electrical resistivity are overlain by the more resistive sediments of the Dry Branch Formation. In general, the gamma-ray count is higher than in surrounding stratigraphic units.

Often found within the Tinker/Santee (Utley) sediments, particularly in the upper third of the interval, are weak zones interspersed in stronger carbonate-rich matrix materials. The weak zones, which vary in apparent thickness and lateral extent, were noted where rod drops and/or lost circulation occurred during drilling, low blow counts occurred during SPT pushes, etc. The weak zones have variously been termed as “soft zones”, the “critical layer”, “underconsolidated zones”, “bad ground”, and “void”. For this report, the preferred term used to describe these zones will be “soft zones.”

Barnwell Group

Upper Eocene sediments of the Barnwell Group represent the Upper Coastal Plain of western South Carolina and eastern Georgia. Sediments of the Barnwell Group are chronostratigraphically equivalent to the lower Cooper Group (late Eocene) of Colquhoun et al. The Cooper Group includes sediments of

both late Eocene and early Oligocene age and appears downdip in the Lower Coastal Plain of eastern South Carolina.

Sediments of the Barnwell Group overlie the Tinker/Santee Formation and consist mostly of shallow marine quartz sand containing sporadic clay layers. Huddleston and Hetrick recently revised the upper Eocene stratigraphy of the Georgia Coastal Plain, and their approach has been extended into South Carolina by Nystrom and Nystrom and Willoughby. These authors elevated the Eocene "Barnwell Formation" to the "Barnwell Group." In Burke County, Georgia, the group includes (from oldest to youngest) the Clinchfield Formation, and Dry Branch Formation, and the Tobacco Road Formation. The group is about 21 meters (70 feet) thick near the northwestern boundary of SRS and 52 meters (170 feet) near its southeastern boundary. The regionally significant Santee Unconformity that defines of boundary between Sequence Stratigtraphic units II and III (Figure 1.4-18) separates the Clinchfield Formation from the overlying Dry Branch Formation. The Santee Unconformity is a pronounced erosional surface observable throughout the SRS region.

In the northern part of the study area, the Barnwell Group consists of red or brown, fine to coarse-grained, well-sorted, massive sandy clay and clayey sand, calcareous sand and clay, as well as scattered thin layers of silicified fossiliferous limestone. All are suggestive of lower delta plain and/or shallow shelf environments. Downdip, the Barnwell undergoes a facies change to the phosphatic clayey limestone that constitutes the lower Cooper Group. The lower Cooper Group limestone beds indicate deeper shelf environments.

Clinchfield Formation. The basal late Eocene Clinchfield Formation consists of light colored quartz sand and glauconitic, biomoldic limestone, calcareous sand, and clay. Sand beds of the formation constitute the Riggins Mill Member of the Clinchfield Formation and are composed of medium to coarse, poorly to well sorted, loose and slightly indurated, tan, clay, and green quartz. The sand is difficult to identify unless it occurs between the overlying carbonate layers of the Griffins Landing Member and the underlying carbonate layers of the Santee Limestone. The Clinchfield is about 8 meters (25 feet) thick in the southeastern part of SRS and pinches out or becomes unrecognizable at the center of the site.

The carbonate sequence of the Clinchfield Formation is designated the Utley Limestone Member. It is composed of sandy, glauconitic limestone and calcareous sand, with an indurated, biomoldic facies developed in places. In cores, the sediments are tan and white and slightly to well indurated. Without the benefit of detailed petrographic and paleontological analysis, the Utley carbonates cannot be systematically distinguished from the carbonates of the underlying Tinker/Santee Formation. Thus the carbonate-rich sediments between the Santee Unconformity, and the Warley Hill Formation are referred to as the Tinker/Santee (Utley) sequence in this report.

Dry Branch Formation. The late Eocene Dry Branch Formation is divided into the Irwinton Sand Member, the Twiggs Clay Member, and the Griffins Landing Member. The unit is about 18 meters (60 feet) thick near the center of the study area. The top of the Dry Branch is picked on geophysical logs where a low gamma-ray count in the relatively clean Dry Branch sand increases sharply in the more argillaceous sediments of the overlying Tobacco Road Sand.

The Dry Branch sediments overlying the Tinker/Santee (Utley) interval in the central portion of SRS were deposited in shoreline/lagoonal/tidal marsh environments. The shoreline retreated from its position in northern SRS during Tinker/Santee (Utley) time to the central part of SRS in Dry Branch time. Progradation of the shoreline environments to the south resulted in the sands and muddy sands of the Dry Branch being deposited over the shelf carbonates and clastics of the Tinker/Santee (Utley) sequence.

The Twiggs Clay Member does not seem to be mappable in the study area. Lithologically similar clay is present at various stratigraphic levels in the Dry Branch Formation. The tan, light-gray, and brown clay is as thick as 4 meters (12 feet) in SRS wells but is not continuous over long distances. This has been referred to in the past as the "tan clay" in SRS reports. The Twiggs Clay Member, that predominates west of the Ocmulgee River in Georgia, is not observed as a separate unit in the study area.

The Griffins Landing Member is composed mostly of tan or green, slightly to well indurated, quartzose calcareous micrite and sparite, calcareous quartz sand and slightly calcareous clay. Oyster beds are common in the sparry carbonate facies. The unit seems to be widespread in the southeastern part of SRS, where it is about 15 meters (50 feet) thick, but becomes sporadic in the center and pinches out. Carbonate content is highly variable. In places, the unit lies unconformably on the Utley Limestone Member, which contains much more indurated, moldic limestone. In other areas, it lies on the noncalcareous quartz sand of the Clinchfield. Updip, the underlying Clinchfield is difficult to identify or is missing, and the unit may lie unconformably on the sand and clay facies of the Tinker/Santee Formation. The Griffins Landing Member appears to have formed in lagoonal/marsh environments.

The Irwinton Sand Member is composed of tan, yellow and orange, moderately sorted quartz sand, with interlaminated and interbedded clay abundant in places. Pebbly layers are present, as are clay clast-rich zones (Twiggs Clay lithology). Clay beds, which are not continuous over long distances, are tan, light gray, and brown in color, and can be several feet thick in places. These are the "tan clay" beds of various SRS reports. Irwinton Sand beds have the characteristics of shoreline to shallow marine sediments. The Irwinton Sand crops out in SRS. Thickness is variable, but is about 12 meters (40 feet) near the northwestern site boundary and 21 meters (70 feet) near the southeastern boundary.

Tobacco Road Formation. The Late Eocene Tobacco Road Formation consists of moderately to poorly sorted, red, brown, tan, purple, and orange, fine to coarse, clayey quartz sand. Pebble layers are common, as are clay laminae and beds. Ophiomorpha burrows are abundant in parts of the formation. Sediments have the characteristics of lower Delta plain to shallow marine deposits. The top of the Tobacco Road is characterized by the change from a comparatively well-sorted sand to the more poorly sorted sand, pebbly sand, and clay of the "Upland unit." Contact between the units constitutes the "Upland" unconformity. The unconformity is very irregular due to fluvial incision that accompanied deposition of the overlying "Upland unit" and later erosion. As stated previously, the lower part of the Cooper Group (upper Eocene) is the probable downdip equivalent of the Tobacco Road Formation.

"Upland Unit"/Hawthorn/Chandler Bridge Formations. Deposits of poorly sorted silty, clayey sand, pebbly sand, and conglomerate of the "Upland unit" cap many of the hills at higher elevations over much of the study area. Weathered feldspar is abundant in places. The color is variable, and facies changes are abrupt. Siple assigned these sediments to the Hawthorn Formation. Nystrom et al.., who mapped it as the "Upland unit", discuss evidence for a Miocene age. The unit is up to 18 meters (60 feet) thick. The environment of deposition appears to be fluvial, and the thickness changes abruptly owing to channeling of the underlying Tobacco Road Formation during "Upland" deposition and subsequent erosion of the "Upland" unit itself. This erosion formed the "Upland" unconformity. The unit is up to 18 meters (60 feet) thick.

Lithologic types comparable to the "Upland" unit but assigned to the Hawthorn Formation overlie the Barnwell Group and the Cooper Group in the southern part of the study area.

In this area, the Hawthorn Formation consists of very poorly sorted, sandy clay, and clayey sand, with lenses of gravel and thin beds of sand very similar to the "Upland unit". Farther downdip, the Hawthorn overlies the equivalent of the Suwanee Limestone and acts as the confining layer overlying the Floridan Aquifer System. It consists of phosphatic, sandy clay and phosphatic, clayey sand and sandy, dolomitic limestone interbedded with layers of hard, brittle clay resembling stratified fuller's earth.

Colquhoun et al., suggest that the “Upland unit”, Tobacco Road Formation, and Dry Branch Formation are similar in granularity and composition, indicating that they might be similar genetically, that is that they are part of the same transgressive/regressive depositional cycle. The "Upland unit" represents the most continental end member (lithofacies) and the Dry Branch Formation represents the most marine end member. Thus, the “Upland unit” is the result of a major regressive pulse that closed out deposition of the Barnwell Group/Cooper Group depositional cycle. Colquhoun et al., suggested that the "Upland unit" is correlative with the Chandler Bridge Formation downdip toward the coast. This hypothesis is significant because it implies that there was no major hiatus between the "Upland unit" and the underlying Tobacco Road and Dry Branch Formations. The existence of a hiatus between the units has been reported by numerous studies of the South Carolina Coastal Plain.

Quaternary Surfaces and Deposits

SRS lies within the interfluve area between the Savannah and the Salkahatchie Rivers. The drainage systems within the site consist entirely of streams that are tributary to the Savannah River. A series of nested fluvial terraces are preserved along the river and major tributaries. Fluvial terraces are the primary geomorphic surface that can be used to evaluate Quaternary deformation within SRS. However, there is limited data available for the estimation of ages of river terraces in both the Atlantic and Gulf Coastal Plains.

Major stream terraces form by sequential erosional and depositional events in response to tectonism, isostasy, and climate variation. Streams respond to uplift by cutting down into the underlying substrate in order to achieve a smooth longitudinal profile that grades to the regional base level. Aggradation or deposition occurs when down-cutting is reversed by a rise in base level. The stream channel is elevated and isolated from the underlying marine strata by layers of newly deposited fluvial sediments. Down-cutting may resume and the aggraded surface is abandoned. The result is a landform referred to as a fill terrace.

At the SRS there are two prominent terraces above the modern floodplain (Qal). These designations are based on morphology and relative height above local base level. Local base level is the present elevation of the Savannah River channel. In addition, there are other minor terraces: one lower and several higher, older terrace remnants.

Carbonate and Soft Zones

Often found within the Tinker/Santee (Utley) sediments, particularly in the upper third of this section, are weak zones interspersed in stronger carbonate-rich matrix materials. These weak zones, which vary in apparent thickness and lateral extent, were recorded where rod drops and/or lost circulation occurred during drilling, low blow counts occurred during SPT pushes, etc. They have variously been termed as “soft zones”, “the critical layer”, “underconsolidated zones”, “bad ground”, and “void”. The preferred term used to describe these zones is “soft zones”. Aadland et al. discuss these features in their paper in this guide book.

Deeper Sediments

Beneath the Coastal Plain sedimentary sequence and below a pre-Cretaceous unconformity are two geologic terranes: (1) the Dunbarton basin, a Triassic-Jurassic Rift basin, filled with lithified terrigenous and

lacustrine sediments with possible minor amounts of mafic volcanic and intrusive rock; and (2) a crystalline terrane of metamorphosed sedimentary and igneous rock that may range in age from Precambrian to late Paleozoic (reference Figure 6). The Paleozoic rocks and the Triassic sediments were leveled by erosion, forming the base for Coastal Plain sediment deposition.

The lithologies and structures in the crystalline terrane are basically similar to that seen in the eastern Piedmont province as exposed in other parts of the southeastern United States. The crystalline rocks form a volcanic – intrusive sequence of calc-alkaline composition, portions of which record both ductile and brittle deformational events. These relationships indicate that these rocks are the metamorphosed and deformed remnants of an ancient volcanic arc that are interpreted to be Carolina Terrane equivalents.

Ten core borings into the basin penetrated sedimentary rocks. Fanglomerate, sandstone, siltstone, and mudstone are the dominant lithologies. These rocks are similar to the clastic facies in other Newark Supergroup basins

HYDROSTRATIGRAPHY
INTRODUCTION

Two hydrogeologic provinces are recognized in the subsurface beneath the SRS region (reference Figures 6 and7). The uppermost province, which consists of the wedge of unconsolidated Coastal Plain sediments of Late Cretaceous and Tertiary ages, is referred to as the Southeastern Coastal Plain hydrogeologic province. It is further subdivided into aquifer or confining systems, units, and zones. The underlying province, referred to as the Piedmont hydrogeologic province, includes Paleozoic metamorphic and igneous basement rocks and Upper Triassic lithified mudstone, sandstone, and conglomerate in the Dunbarton basin.

The following hydrogeological characteristics are of particular interest:

- The layered structure of the coastal plain sediments effectively controls migration of contaminants in the subsurface, limiting vertical migration to deeper aquifers.
- Between the ground surface and the primary drinking water aquifer(s) are several low permeability zones which restrict vertical migration from a given point source.
- The abundance of clay size material and clay minerals in the aquifer and aquitard zones affects groundwater composition and vertical migration. The concentration of some potential contaminants, especially metals and radionuclides, may be attenuated by exchange and fixation of dissolved constituents on clay surfaces.
- The recharge area(s) for the deeper drinking water aquifers used are updip of SRS, near the fall line. Some recharge areas are located at the northern-most fringe of the site.
- Recharge for the water-table aquifers, namely the Upper Three Runs and Gordon Aquifers, is primarily from local precipitation.
- Discharge of groundwater from the Upper Three Runs and Gordon aquifers is typically to the local streams on the SRS.
- Groundwater at the SRS is typically of low ionic, low dissolved solids and moderate pH (typically ranging from 4.4 to 6.0). Other constituents such as dissolved oxygen and alkalinity are more closely associated with recharge and aquifer material. Dissolved oxygen is typically higher in the updip and near-surface recharge areas, and alkalinity, pH and dissolved solids are typically higher in those portions of the aquifers regions containing significant carbonate materials.

- The presence of an upward vertical gradient or "head reversal" between the Upper Three Runs and Gordon aquifers and the Crouch Branch aquifer is significant in that it prevents downward vertical migration of contaminants into deeper aquifers over much of central SRS.

Hydrogeology

The method for establishing a nomenclature for the hydrogeologic units in the following discussion is based on Aadland et al., and generally follows the guidelines set forth by the South Carolina Hydrostratigraphic Subcommittee. Hydrogeologic units are shown on Figure 2.

A hydrogeologic unit is defined by its hydraulic properties (hydraulic conductivity, hydraulic head relationships, porosity, leakance coefficients, vertical flow velocity and transmissivity) relative to those properties measured in the overlying and underlying units. The properties are measured at a type well or type well cluster location. Aquifer and confining units are mapped on the basis of the hydrogeologic continuity, potentiometric conditions, and leakance-coefficient estimates for the units. These properties are largely dependent on the thickness, areal distribution, and continuity of the lithology of the particular unit. However, a hydrogeologic unit may traverse lithologic unit boundaries if there is not a significant change in hydrogeologic properties corresponding to the change in lithology.

Upper Three Runs Aquifer Unit

The Upper Three Runs Aquifer Unit occurs between the water-table and the Gordon Confining Unit and includes all strata above the Warley Hill Formation (in updip areas) and the Blue Bluff Member of the Santee Limestone. It includes the sandy and sometimes calcareous sediments of the Tinker/Santee Formation and all the heterogeneous sediments in the overlying Barnwell Group. The Upper Three Runs aquifer is the updip clastic facies equivalent of the Upper Floridan aquifer in the carbonate phase of the Floridan Aquifer System.

The Upper Three Runs aquifer is defined by the hydrogeologic properties of the sediments penetrated in well P-27 located near Upper Three Runs Creek in the center of SRS. Here, the aquifer is 40 meters (132 feet) thick and consists mainly of quartz sand and clayey sand of the Tinker/Santee Formation; sand with interbedded tan to gray clay of the Dry Branch Formation; and sand, pebbly sand, and minor clay beds of the Tobacco Road Formation. Calcareous sand, clay, and limestone, although not observed in the P-27 well, are present in the Tinker/Santee Formation throughout the General Separations Area near well P-27
.
Downdip, at the C-10 reference well, the Upper Three Runs aquifer is 116 meters (380 feet) thick and consists of clayey sand and sand of the upper Cooper Group; sandy, shelly limestone, and calcareous sand of the lower Cooper Group/Barnwell Group; and sandy, shelly, limestone and micritic limestone of the Santee Limestone.

Water-level data are sparse for the Upper Three Runs aquifer unit except within SRS. The hydraulic-head distribution of the aquifer is controlled by the location and depth of incisement of creeks that dissect the area. The incisement of these streams and their tributaries has divided the interstream areas of the water-table aquifer into "groundwater islands." Each "groundwater island" behaves as an independent hydrogeologic subset of the water-table aquifer with unique recharge and discharge areas. The stream acts as the groundwater discharge boundary for the interstream area. The head distribution pattern in these groundwater islands tends to follow topography and is characterized by higher heads in the interstream area with gradually declining heads toward the bounding streams. Groundwater divides are present near the center of the interstream areas. Water-table elevations reach a maximum of 76 meters (250 feet) msl in the northwest corner of the study

area and decline to approximately 30 meters (100 feet) msl near the Savannah River.

Porosity and permeability of the Upper Three Runs aquifer are variable across the study area. In the northern and central regions, the aquifer yields only small quantities of water, owing to the presence of interstitial silt and clay and poorly sorted sediments that combine to significantly reduce permeability. Local lenses of relatively clean, permeable sand however, may, yield sufficient quantities for domestic use. Such high-permeability zones have been observed in the General Separations Area near the center of the study area and may locally influence the movement of groundwater .

Porosity and permeability were determined for Upper Three Runs aquifer sand samples containing less than 25 percent mud, using the Beard and Weyl method. Porosity averages 35.3 percent; the distribution is approximately normal, but skewed slightly toward higher values. Geometric mean permeability is 31.5 Darcies (23 m/day [76.7 ft/day]) with about 60 percent of the values between 16 and 64 Darcies (12 and 48 m/day [39 and 156 ft/day]).

Recharge to the Upper Three Runs aquifer occurs at the water-table by infiltration downward from the land surface. In the “upper" aquifer zone, part of this groundwater moves laterally toward the bounding streams while part moves vertically downward. The generally low vertical hydraulic conductivities of the “upper" aquifer zone and the intermittent occurrence of the “tan clay" confining zone retard the downward flow of water, producing vertical hydraulic-head gradients in the "upper" aquifer zone and across the "tan clay” confining zone.

Downward hydraulic-head differences in the “upper” aquifer zone vary from 1.4 to 1.64 meters (4.5 to 5.4 feet), and differences across the “tan clay” are as much as 6.5 meters (15.8 feet) in H Area. At other locations in the General Separations Area, the head difference across the “tan clay” confining zone is only 0.3 to 1 meter (0.1 to 3.2 feet), essentially what might be expected due simply to low vertical flow in a clayey sand aquifer. Therefore, the ability of the "tan clay” confining zone to impede water flow varies greatly over the General Separations Area.

Groundwater leaking downward across the "tan clay” confining zone recharges the "lower" aquifer zone of the Upper Three Runs aquifer. Most of this water moves laterally toward the bounding streams; the remainder flows vertically downward across the Gordon confining unit into the Gordon aquifer. All groundwater moving toward Upper Three Runs Creek leaks through the Gordon confining unit or enters small streams. Vertical hydraulic-head differences in the "lower" aquifer zone range from 0.5 to 1 meter (1.5 to 3.2 feet) in H Area and indicate some vertical resistance to flow.

Gordon Confining Unit

Clayey sand and clay of the Warley Hill Formation and clayey, micritic limestone of the Blue Bluff Member of the Santee Limestone constitute the Gordon confining unit. The Gordon confining unit separates the Gordon aquifer from the overlying Upper Three Runs aquifer. The unit has been informally termed the "green clay" in previous SRS reports.

In the study area, the thickness of the Gordon confining unit ranges from about 1.5 to 26 meters (5 to 85 feet). The unit thickens to the southeast. From Upper Three Runs Creek to the vicinity of L Lake and Par Pond, the confining unit generally consists of one or more thin clay beds, sandy mud beds, and sandy clay beds intercalated with subordinate layers and lenses of quartz sand, gravelly sand, gravelly muddy sand, and calcareous mud. Southward from L Lake and Par Pond, however, the unit undergoes a stratigraphic facies change to clayey micritic limestone and limey clay typical of the Blue Bluff Member. The fine-grained carbonates and carbonate-rich muds constitute the farthest updip extent of the "middle confining unit" of

the Floridan Aquifer System (the hydrostratigraphic equivalent of the Gordon confining unit), which dominates in coastal areas of South Carolina and Georgia.

North of the updip limit of the Gordon confining unit, the fine-grained clastics of the Warley Hill Formation are thin, intermittent, and no longer effective in regionally separating groundwater flow. Here, the Steed Pond aquifer is defined. Although thin and intermittent, the clay, sandy clay, and clayey sand beds of the Warley Hill Formation can be significant at the site-specific level and often divide the Steed Pond aquifer into aquifer zones.

Gordon Aquifer Unit

The Gordon aquifer consists of all the saturated strata that occur between the Gordon confining unit and the Crouch Branch confining unit in both the Floridan - Midville Aquifer System and the Meyers Branch confining system. The aquifer is semiconfined, with a downward potential from the overlying Upper Three Runs aquifer observed in interfluvial areas, and an upward potential observed along the tributaries of the Savannah River where the Upper Three Runs aquifer is incised. The thickness of the Gordon aquifer ranges from 12 meters (38 feet) at well P-4A to 56 meters (185 feet) at well C-6 and generally thickens to the east and southeast. Thickness variations in the confining lithologies near the Pen Branch Fault suggest depositional effects owing to movements on the fault in early Eocene time. The Gordon aquifer is partially eroded near the Savannah River and Upper Three Runs Creek. The regional potentiometric map of the Gordon aquifer indicates that major deviations in the flow direction are present where the aquifer is deeply incised by streams that drain water from the aquifers.

The Gordon aquifer is characterized by the hydraulic properties of the sediments penetrated in reference well P-27 located near the center of SRS. The unit is 23 meters (75.5 feet) thick in well P-27 and occurs from 38 to 15 meters (125 to 48 feet) msl. The aquifer consists of the sandy parts of the Snapp Formation and the overlying Fourmile and Congaree Formations. Clay beds and stringers are present in the aquifer, but they are too thin and discontinuous to be more than local confining beds. The aquifer in wells P-21 and P-22 includes a clay bed that separates the Congaree and Fourmile Formations. The clay bed appears sufficiently thick and continuous to justify splitting the Gordon aquifer into zones in the southeastern quadrant of SRS.

Downdip, the quartz sand of the Gordon aquifer grades into quartz-rich, fossiliferous lime grainstone, packstone, and wackestone, which contain considerably more glauconite than the updip equivalents. Porosity of the limestone as measured in thin-section ranges from 5 to 30 percent and is mostly moldic and vuggy.

South of SRS, near well ALL-324, the Gordon aquifer consists of interbedded glauconitic sand and shale, grading to sandy limestone. Farther south, beyond well C-10, the aquifer grades into platform limestone of the Lower Floridan aquifer of the carbonate phase of the Floridan Aquifer System.

The Gordon aquifer is recharged directly by precipitation in the outcrop area and in interstream drainage divides in and near the outcrop area. South of the outcrop area, the Gordon is recharged by leakage from overlying and underlying aquifers. Because streams such as the Savannah River and Upper Three Runs Creek cut through the aquifers of the Floridan Aquifer System, they represent no-flow boundaries. As such, water availability or flow patterns on one side of the boundary (stream) will not change appreciably due to water on the other side. In the central part of SRS, where the Gordon confining unit is breached by faulting, recharge to the Gordon aquifer is locally increased.

Most of the Gordon aquifer is under confined conditions, except along the fringes of Upper Three Runs Creek (i.e., near the updip limit of the Gordon Confining Unit) and the Savannah

River. The potentiometric-surface map of the aquifer shows that the natural discharge areas of the Gordon aquifer at SRS are the swamps and marshes along Upper Three Runs Creek and the Savannah River. These streams dissect the Floridan Aquifer System, resulting in unconfined conditions in the stream valleys and probably in semiconfined (leaky) conditions near the valley walls. Reduced head near Upper Three Runs Creek induces upward flow from the Crouch Branch aquifer and develops the "head reversal" that is an important aspect of the SRS hydrogeological system. The northeast-southwest oriented hydraulic gradient across SRS is consistent and averages 0.9 m/km (4.8 ft/mi). The northeastward deflection of the contours along the Upper Three Runs Creek indicates incisement of the sediments that constitute the aquifer by the creek.

Hydraulic characteristics of the Gordon are less variable than those noted in the Upper Three Runs aquifer. Hydraulic conductivity decreases downdip near well C-10 owing to poor sorting, finer grain size, and an increase in clay content.

Steed Pond Aquifer Unit

North of Upper Three Runs Creek where the Floridan - Midville Aquifer System is defined, the permeable beds that correspond to the Gordon and Upper Three Runs aquifers of the Floridan Aquifer System are only locally separated, owing to the thin and intermittent character of the intervening clay beds of the Gordon confining unit (Warley Hill Formation) and to erosion by the local stream systems that dissect the interval. Here, the aquifers coalesce to form the Steed Pond aquifer of the Floridan-Midville Aquifer System.

The Steed Pond aquifer is defined by hydrogeologic characteristics of sediments penetrated in well MSB-42 located in A/M Area in the northwest corner of SRS. The aquifer is 29.6 meters (97 feet) thick. Permeable beds consist mainly of subangular, coarse- and medium-grained, slightly gravelly, submature quartz sand and clayey sand. Locally, the Steed Pond aquifer can be divided into zones. In A/M Area three zones are delineated, the "Lost Lake" zone, and the overlying "M Area" aquifer zones, separated by clay and clayey sand beds of the "green clay" confining zone.

In A/M Area, water enters the subsurface through precipitation, and recharge into the "M-Area" aquifer zone occurs at the water-table by infiltration downward from the land surface. A groundwater divide exists in the A/M Area in which lateral groundwater flow is to the southeast towards Tims Branch and southwest towards Upper Three Runs Creek and the Savannah River floodplain. Groundwater also migrates downward and leaks through the "green clay" confining zone into the "Lost Lake" aquifer. The "green clay" confining zone that underlies the "M-Area" aquifer zone is correlative with the Gordon confining unit south of Upper Three Runs Creek.

Meyers Branch Confining System. The Meyers Branch confining system separates the Floridan Aquifer System from the underlying Dublin and Dublin-Midville Aquifer Systems. North of the updip limit of the confining system, the Floridan and Dublin-Midville Aquifer Systems are in hydraulic communication and the aquifer systems coalesce to form the Floridan-Midville Aquifer System.

Sediments of the Meyers Branch confining system correspond to clay and interbedded sand of the uppermost Steel Creek Formation, and to clay and laminated shale of the Sawdust Landing/Lang Syne and Snapp Formations. In the northwestern part of the study area, the sediments that form the Meyers Branch confining system are better sorted and less silty, with thinner clay interbeds. This is the updip limit of the Meyers Branch confining system .

Crouch Branch Confining Unit

In the SRS area, the Meyers Branch confining system consists of a single hydrostratigraphic unit, the Crouch Branch confining unit, which includes several thick and relatively continuous (over several kilometers) clay beds. The Crouch Branch confining unit extends north of the updip limit of the Meyers Branch confining system where the clay thins and is locally absent and faulting observed in the region locally breaches the unit. Here, the Crouch Branch confining unit separates the Steed Pond aquifer unit from the underlying Crouch Branch aquifer unit. Downdip, generally south of the study area, the Meyers Branch confining system could be further subdivided into aquifer and confining units if this should prove useful for hydrogeologic characterization.

As indicated earlier, a hydraulic-head difference persists across the Crouch Branch confining unit near SRS. Owing to deep incisement by the Savannah River and Upper Three Runs Creek into the sediments of the overlying Gordon aquifer, an upward hydraulic gradient (vertical-head reversal) persists across the Crouch Branch confining unit over a large area adjacent to the Savannah River floodplain and the Upper Three Runs Creek drainage system. This "head reversal" is an important aspect of the groundwater flow system near SRS and provides a natural means of protection from contamination of the lower aquifers.

The total thickness of the Crouch Branch confining unit where it constitutes the Meyers Branch confining system ranges from 17.4 to 56.1 meters (57 to 184 feet). Updip, the thickness of the Crouch Branch confining unit ranges from < 1 to 31.7 meters (3.3 to 104 feet). The confining unit dips approximately 5 m/km (16 ft/mi) to the southeast. The confining unit is comprised of the “upper” and “lower” confining zones, which are separated by a “middle sand” zone.

In general, the Crouch Branch confining unit contains two to seven clay to sandy clay beds separated by clayey sand and sand beds that are relatively continuous over distances of several kilometers. The clay beds in the confining unit are anomalously thin and fewer in number along a line that parallels the southwest-northeast trend of the Pen Branch and Steel Creek Faults and the northeast southwest trending Crackerneck Fault. The reduced clay content near the faults suggests shoaling due to uplift along the faults during deposition of the Paleocene Black Mingo Group sediments.

In A/M Area, the Crouch Branch confining unit can often be divided into three zones: an “upper clay” confining zone is separated from the underlying “lower clay” confining zone by the “middle sand” aquifer zone. The "middle sand" aquifer zone consists of very poorly sorted sand and clayey silt of the Lang Syne/Sawdust Landing Formations. The "middle sand" aquifer zone has a flow direction that is predominantly south/southwest toward Upper Three Runs Creek.

In places, especially in the northern part of A/M Area, "upper clay" confining zone is very thin or absent. Here, only the “lower clay” confining zone is capable of acting as a confining unit and the "middle sand" zone is considered part of the Steed Pond aquifer. Similarly, when the clay beds of the "lower clay" confining zone are very thin or absent, the "middle sand" aquifer zone is considered part of the Crouch Branch aquifer unit. This is the case in the far northeastern part of the study area.

The "lower clay" confining zone has been referred to as the lower Ellenton clay, the Ellenton clay, the Peedee clay, and the Ellenton/Peedee clay in previous SRS reports. It consists of the massive clay bed that caps the Steel Creek Formation. The zone is variable in total thickness and, based on 31 wells that penetrate the unit, ranges from 1.5 to 19 meters (5 to 62 feet) and averages 7.3 meters (24 feet) thick.

Dublin Aquifer System. The Dublin Aquifer System is present in the southeastern half of SRS and consists of one aquifer, the Crouch Branch aquifer. It is underlain by the Allendale confining system and overlain by the Meyers Branch confining system. The updip limit of the Dublin Aquifer System in the study area corresponds to the updip limit of the Allendale confining system. North of this line, the Dublin-Midville Aquifer System is defined.

The thickness of the Dublin Aquifer System generally increases toward the south and ranges from approximately 53 to 88 meters (175 to 290 feet). The top of the unit dips 3.79 m/km (20 ft/mi) to the southeast. The unit thins to the east toward the Salkehatchie River and to the west toward Georgia. Near the updip limit of the system, thicknesses are variable and probably reflect the effects of movement along the Pen Branch Fault during deposition of the middle Black Creek clay.

The Dublin Aquifer System was defined and named by Clarke et al., for sediments penetrated by well 21-U4 drilled near the town of Dublin in Laurens County, Georgia. The upper part of the Dublin Aquifer System consists of fine to coarse sand and limestone of the lower Huber-Ellenton unit. Comparable stratigraphic units serve as confining beds in the SRS area and are considered part of the overlying Meyers Branch confining system. Clarke et al.., noted that to the east near the Savannah River, clay in the upper part of the lower Huber-Ellenton unit forms a confining unit that separates an upper aquifer of Paleocene age from a lower aquifer of Late Cretaceous age. The upper aquifer of Clarke et al., is the Gordon aquifer as defined in the study, and their confining unit constitutes the Meyers Branch confining system of the SRS region. The lower part of the Dublin Aquifer System consists of alternating layers of clayey sand and clay of the Peedee-Providence unit.

Sediments typical of the Dublin Aquifer System are penetrated in the reference well P-22. The system consists of the well-sorted sand and clayey sand of the Black Creek Formation and the moderately sorted sand and interbedded sand and clay of the Steel Creek Formation. The aquifer is overlain by the clay beds that cap the Steel Creek Formation. These clay beds constitute the base of the Meyers Branch confining system.

The Dublin Aquifer System is 65 meters (213 ft) thick in well P-22; the top is at an elevation of -68 meters (-223 feet) msl and the bottom at -133 meters (-436 feet) msl. The Dublin includes five clay beds in this well.

In the southern part of the study area and farther south and east, the Dublin shows much lower values for hydraulic conductivity and transmissivity, probably due to the increase of fine-grained sediments toward the coast.

Dublin - Midville Aquifer System. The Dublin-Midville Aquifer System underlies the central part of SRS. The system includes all the sediments in the Cretaceous Lumbee Group from the Middendorf Formation up to the sand beds in the lower part of the Steel Creek Formation. The system is overlain by the Meyers Branch confining system and underlain by the indurated clayey silty sand and silty clay of the Appleton confining system. The updip limit of the system is established at the updip pinchout of the overlying Meyers Branch confining system (see Figure 1.4-22). The downdip limit of the Dublin-Midville is where the Allendale becomes an effective confining system (see Figure 1.4-22). The Dublin-Midville and the updip Floridan-Midville Aquifer Systems were referred to as the Tuscaloosa aquifer by Siple.

The thickness of the Dublin-Midville Aquifer System ranges from approximately 76 to 168 meters (250 to 550 feet). The dip of the upper surface of the system is about 3.8 m/km (20 ft/mi) to the southeast. Near the downdip limit of the system, thicknesses are variable and probably reflect the effects of movement along the Pen Branch Fault. Shoaling along the fault trace resulted in a relative increase in the

thickness of the aquifers at the expense of the intervening confining unit.

The Dublin-Midville Aquifer System includes two aquifer units, the McQueen Branch aquifer, and the Crouch Branch aquifer, separated by the McQueen Branch confining unit. The two aquifers can be traced northward, where they continue to be an integral part of the Floridan-Midville Aquifer System and southward where they constitute the aquifer units of the Midville and Dublin Aquifer Systems, respectively.

The Dublin-Midville Aquifer System is defined at the type well P-27. Here, the system is 153 meters (505 feet) thick and occurs from -25 meters (-82 feet) msl to -179 meters (-587 feet) msl. It consists of medium- to very coarse-grained, silty sand of the Middendorf Formation and clayey, fine to medium sand and silty clay beds of the Black Creek Formation (Ref. 118). The system includes a thick clay bed, occurring from -100 meters (-329 feet) msl to -117 meters (-384 feet) msl, which constitutes the McQueen Branch confining unit.

A regional potentiometric surface map prepared by Siple for his "Tuscaloosa aquifer," indicates that the Savannah River has breached the Cretaceous sediments and is a regional discharge area for the Floridan-Midville Aquifer System, the Dublin-Midville Aquifer System, and the updip part of both the Dublin and Midville Aquifer Systems. The Savannah River, therefore, represents a no-flow boundary preventing the groundwater in these aquifer systems from flowing southward into Georgia.

Crouch Branch Aquifer Unit

The Crouch Branch aquifer constitutes the Dublin Aquifer System in the southern part of the study area. Farther south, the Dublin can be subdivided into several aquifers and confining units. In the central part of the study area, the Crouch Branch aquifer is the uppermost of the two aquifers that constitute the Dublin-Midville Aquifer System. Farther north in the northwestern part of SRS and north of the site, the Crouch Branch aquifer is the middle aquifer of the three aquifers that constitute the Floridan-Midville Aquifer System.

The Crouch Branch aquifer is overlain by the Crouch Branch confining unit and is underlain by the McQueen Branch confining unit. It persists throughout the northern part of the study area, but near the updip limit of the Coastal Plain sedimentary clastic wedge, the Crouch Branch confining unit ceases to be effective and the Crouch Branch aquifer coalesces with the Steed Pond aquifer.

The Crouch Branch aquifer ranges in thickness from about 30 to 107 meters (100 to 350 feet). Thickness of the unit is variable near the updip limit of the Dublin Aquifer System where sedimentation was affected by movement along the Pen Branch Fault. The reduced clay content in this vicinity suggests shoaling due to uplift along the fault during Late Cretaceous and Paleocene time, resulting in the deposition of increased quantities of shallow-water, coarse-grained clastics along the crest of the fault trace. The sandy beds act hydrogeologically as part of the Crouch Branch aquifer, resulting in fewer and thinner, less persistent clay beds in the overlying and underlying confining units.

The Crouch Branch aquifer thins dramatically in the eastern part of the study area at the same general location where the underlying McQueen Branch confining unit and the overlying Crouch Branch confining unit thicken at the expense of Crouch Branch sand. Clay beds in the Crouch Branch aquifer generally thicken in the same area and constitute as much as 33 percent of the unit at the well C-6.

Sediments of the Crouch Branch aquifer are chiefly sand, muddy sand, and slightly gravelly sand intercalated with thin, discontinuous layers of sandy clay and sandy mud. Hydraulic conductivity of the Crouch Branch aquifer, determined from eleven pumping tests by Siple and from analyses

made by GeoTrans, ranges from 8.5 to 69 m/day (28 to 227 ft/day). Comparatively high hydraulic conductivity occurs in a northeast-southwest trending region connecting D Area, Central Shops, and R Area and defines a "high permeability" zone in the aquifer. Here, hydraulic conductivities range from 36 to 69 m/day (117 to 227 ft/day). The "high permeability" zone parallels the trace of the Pen Branch Fault, and reflects changing depositional environments in response to movement along the fault as described above. South of the trace of the Pen Branch Fault, hydraulic conductivity for the aquifer reflects the return to a deeper water shelf/deltaic depositional regime.

Allendale Confining System. The Allendale confining system is present in the southeastern half of the study area and separates the Midville Aquifer System from the overlying Dublin Aquifer System. In the study area, the Allendale confining system consists of a single unit, the McQueen Branch confining unit. The confining system is correlative with the unnamed confining unit that separates the Middendorf and Black Creek aquifers of Aucott et al., and with the Black Creek-Cusseta confining unit of Clark et al. The system dips approximately 6.7 m/km (27 ft/mi) to the southeast and thickens uniformly from about 15.2 meters (50 feet) at the updip limit to about 61 meters near the eastern boundary of the study area. The rate of thickening is greater in the east than in the west. The updip limit of this confining system is established where pronounced thinning occurs parallel to the Pen Branch Fault.

Sediments of the Allendale confining system are fine grained and consist of clayey, silty sand, clay, and silty clay and micritic clay beds that constitute the middle third of the Black Creek Formation. North of the updip limit of the confining system, where the McQueen Branch confining unit is part of the Dublin-Midville Aquifer System, the section consists of coarser-grained, clayey, silty sand and clay beds.

McQueen Branch Confining Unit

The McQueen Branch confining unit is defined by the hydrogeologic properties of the sediments penetrated in well P-27. At its type-well location, the McQueen Branch confining unit is 17 meters (55 feet) thick, and is present from -100 to -117 meters (-329 to –384 feet) msl. Total clay thickness is 14 meters (45 feet) in three beds, which is 82% of the total thickness of the unit, with a leakance coefficient of 3.14×10^{-6} m/day (1.03×10^{-5} ft/day). The confining unit in well P-27 consists of the interbedded, silty, often sandy clay and sand beds that constitute the middle third of the Black Creek Formation.

The clay beds tend to be anomalously thin along a line that parallels the southwest-northeast trend of the Pen Branch Fault and the north-south trend of the Atta Fault. The reduced clay content in these areas suggests shoaling due to uplift along the faults during Upper Black Creek-Steel Creek time.

Midville Aquifer System. The Midville Aquifer System is present in the southern half of the study area; it overlies the Appleton confining system and is succeeded by the Allendale confining system. In the study area, the Midville Aquifer System consists of one aquifer, the McQueen Branch aquifer unit. South of well C-10 (see Figure 1.4-21), the system may warrant further subdivision into several aquifers and confining units. Thickness of the unit ranges from 71 meters (232 feet) at well P-21 to 103 meters (339 feet) at well C-10. Variation in the thickness of the unit, as well as the updip limit of the system, results from variation in the thickness and persistence of clay beds in the overlying Allendale confining system. Near the Pen Branch Fault, contemporaneous movement on the fault may have resulted in shoaling in the depositional environment, which is manifested in a thickening of the sands associated with the Midville Aquifer System. The upper surface of the aquifer system dips approximately 4.73 m/km (25 ft/mi) to the southeast across the study area.

The Midville Aquifer System was defined and named by Clarke et al. (Ref. 121) for the hydrogeologic properties of the sediments penetrated in well 28-X1, near the town of Midville in Burke County, Georgia. Here, the upper part of the aquifer system consists of fine to medium sand of the lower part of the Black Creek-Cusseta unit. The Midville is comparable to the lower portion of the Chattahoochee River aquifer of Miller and Renken (Ref. 104) and correlative with the Middendorf aquifer of Aucott and Sperian.

McQueen Branch Aquifer Unit

The McQueen Branch aquifer unit occurs beneath the entire study area. It thickens from the northwest to the southeast and ranges from 36 meters (118 feet) at well AIK-858 to 103 meters (339 feet) at well C-10 to the south. Locally, thicknesses are greater along the trace of the Pen Branch Fault because of the absence and/or thinning of clay beds that compose the overlying McQueen Branch confining unit. The upper surface of the McQueen Branch dips approximately 4.7 m/km (25 ft/mi) to the southeast.

The McQueen Branch aquifer unit is defined for the hydrogeologic properties of sediments penetrated by well P-27 near the center of the study area. Here, it is 62 meters (203 feet) thick and occurs from -117 to -180 meters (-384 to –587 feet) msl. It contains 56 meters (183 feet) of sand in four beds, (which is 90% of the total thickness of the unit). The aquifer consists of silty sand of the Middendorf Formation and clayey sand and silty clay of the lower one-third of the Black Creek Formation. Typically, a clay bed or several clay beds that cap the Middendorf Formation are present in the aquifer. These clay beds locally divide the aquifer into two aquifer zones.

Appleton Confining System

The Appleton confining system is the lowermost confining system of the Southeastern Coastal Plain hydrogeologic province and separates the province from the underlying Piedmont hydrogeologic province. It is equivalent to the Black Warrior River aquifer of Miller and Renken and to the basal unnamed confining unit of Aucott et al. (Ref. 122). The confining system is essentially saprolite of the Paleozoic and Mesozoic basement rocks and indurated, silty and sandy clay beds, silty clayey sand and sand beds of the Cretaceous Cape Fear Formation. Thickness of saprolite ranges from 2 to 14 meters (6 to 47 feet), reflecting the degree of weathering on the basement unconformity prior to deposition of the Cape Fear terrigenous clastics. Thickness of saprolite determined from the Deep Rock Borings study (DRB wells) ranges from 9 to 30 meters (30 to 97 feet) and averages 12 meters (40 feet) in wells DRB-1 to DRB-7. In the northern part of the study area, the Cape Fear Formation pinches out and the Appleton consists solely of saprolite.

Some variability in thickness is noted along the trace of the Pen Branch Fault. It dips at about 5.9 m/km (31 ft/mi) to the southeast and thickens from 4.6 meters (15 feet) in well C-2 near the north end of the study area to 22 meters (72.2 feet) in well C-10 in the south. Sediments of the confining system do not crop out in the study area. Thinning of the Appleton confining system in well PBF-2 is probably a result of truncation of the section by the Pen Branch Fault.

The confining system consists of a single confining unit throughout the study area. Toward the coast, however, the Appleton confining system thickens considerably and includes several aquifers. The aquifers included in the confining system in the downdip region are poorly defined because few wells penetrate them. They are potentially water producing but the depth and generally poor quality of water in the aquifers probably precludes their utilization in the foreseeable future. The Appleton confining system includes no aquifer units or zones in the northern and central parts of the study area.

Fine- to coarse-grained sand beds, often very silty and clayey, occur in the upper part of the Cape Fear Formation in the southern part of the study area. The sand appears to be in communication with sand of the overlying McQueen Branch Aquifer System and is included with that unit.

Hydrogeology of the Piedmont Province

The basement complex, designated the Piedmont hydrogeologic province in this report, consists of Paleozoic crystalline rocks, and consolidated to semiconsolidated Upper Triassic sedimentary rocks of the Dunbarton basin. All have low permeability. The hydrogeology of the province was studied intensively at SRS to assess the safety and feasibility of storing radioactive waste in these rocks. The upper surface of the province dips approximately 11 m/km (36 ft/mi) to the southeast. Origins of the crystalline and sedimentary basement rocks are different, but their hydraulic properties are similar. The rocks are massive, dense, and practically impermeable except where fracture openings are encountered. Water quality in these units is also similar. Both contain water with high alkalinity and high levels of calcium, sodium, sulfate, and chloride. The low aquifer permeability and poor water quality in the Paleozoic and Triassic rocks render them undesirable for water supply in the study area.

TECTONIC STRUCTURES: FAULTING, FOLDING, AND RIFT BASINS

Paleozoic Basement Beneath SRS

Information concerning structural features in the basement beneath Savannah River Site is mainly derived from analysis of structural fabrics recorded in core samples from deep borings and at larger scales from geophysical techniques such as gravity and magnetic surveys and seismic reflection profiles (see Dennis, this field guide).

An integrated analysis of the structural fabric in the basement core in addition to the geophysical data concluded that at least two regional scale ductile faults are present in the basement beneath Savannah River Site and vicinity, the Upper Three Runs fault and the Tinker Creek Fault. These faults are expressed in the aeromagnetic data as lineaments and are interpreted to be associated with a thrust duplex that emplaces the rocks of the PBF Formation (Tinker Creek Nappe) over the DRB formation . The age of the faulting is constrained by a radiometric age on biotite that dates the movement at about 300 Ma, which would indicate that these faults are part of the Paleozoic Eastern Piedmont Fault System.

In order to resolve faulting that deform Coastal Plain sediments, the topography of the basement surface was mapped utilizing the data listed above along with more recently acquired seismic reflection profiles. The map of basement topography indicates that offsets of the basement surface that range from approximately 30 meters (100 ft) in magnitude down to the resolution limits of the data are present on the basement surface. However most of these offsets are of relatively small magnitude and have limited lateral extents.. The Crackerneck and Pen Branch Faults are relatively well constrained with borings. The other faults are projected from geophysical data only and their parameters are less well known. Of these faults the Pen Branch fault has been extensively studied.

Post-Rift and Cenozoic Structures. These structures include offshore sedimentary basins, such as the Carolina trough and the Blake Plateau basin; transverse arches and embayments, such as the Cape Fear arch and the Southeast Georgia Embayment; Coastal Plain faulting; and paleoliquefaction features that provide information on the recurrence of the Charleston earthquake.

Folding and Faulting

The most definitive evidence of crustal deformation in the Late Cretaceous through Cenozoic is the reverse sense faulting found in the Coastal Plain section of the eastern U.S. Under the auspices of the Reactor Hazards

Program of the late 1970s and early 1980s, USGS conducted a field mapping effort to identify and compile data on all young tectonic faults in the Atlantic Coastal Plain. Consequently, many large, previously unrecognized Cretaceous and Cenozoic fault zones were found (Prowell, 1983). Of 131 fault localities cited, 26 were within North and South Carolina. The identification of Cretaceous and younger faults in the eastern United States is greatly affected by distribution of geologic units of that age. Many of the faults reported by Prowell are located in proximity to the Coastal Plain onlap over the crystalline basement. This may be due to the ease of identifying basement lithologies in fault contact with Coastal sediments.

Prowell and Obermeier characterized the faults as mostly northeast trending reverse slip fault zones with up to 100 km (62 miles) lateral extent and up to 76 meters (250 feet) vertical displacement in the Cretaceous. The faults dip 40° to 85°. Offsets were observed to be progressively smaller in younger sediments. This may be due to an extended movement history from Cretaceous through Cenozoic .

Offset of Coastal Plain sediments at SRS includes all four Tertiary unconformities. Following deposition of the Snapp Formation some evidence indicates oblique-slip movement on the existing faults. The offsets involve the entire Cretaceous to Paleocene sedimentary section. In A/M Area, this faulting formed a serious of horsts and grabens bounded by subparallel faults that truncate at the fault intersections. The strike orientations of the individual fault segments vary from N 11°E to N 42°E, averaging about N 30°E. Apparent vertical offset varies from 4.5 to 18 meters (15 to 60 feet), but throws of 9 to 12 meters (30 to 40 feet) are most common.

This faulting was followed by erosion and truncation of the Paleocene section at the Lang Syne/Sawdust Landing unconformity. Subsequent sediments were normal faulted following deposition of the Santee Formation. Typically, the offset is truncated at the Santee unconformity, and the overlying Tobacco Road/Dry Branch formations are not offset. Locally, however, offset of the overlying section indicates renewed movement on new or existing faults after deposition of Tobacco Road/Dry Branch sediments.

In conjunction with these observations of Coastal Plain faults, modern stress measurements provide an indication of the likelihood of Holocene movement. Moos and Zoback report a consistent northeast-southwest direction of maximum horizontal compressive stress (N 55-70°E) in the southeast U.S. Their determination is based on direct in situ stress measurements, focal mechanisms of recent earthquakes (see Stevenson this guide book), and young geologic indicators. Shallow seismicity in the area, within crystalline terranes, is predominantly reverse character. Moos and Zoback conclude that the northeast directed stress would not induce damaging reverse and strike-slip faulting earthquakes on the Pen Branch fault, a northeast striking Tertiary fault in the area. These same conclusions may be implied for the other northeast trending faults mapped by Prowell.

In A/M Area at SRS, faulting appears to have been episodic and to have varied in style during the Tertiary. Oblique-slip faulting dominated the Cretaceous/Paleocene events, with a local north-south stress orientation. Subsequently, left-lateral shear on the pre-existing faulting and normal faulting occurred, with a corresponding shift in the direction of maximum compressional stress oriented N 20°E to N 30°E.

Pen Branch Fault

The Pen Branch fault has been regarded as the primary structural feature at SRS that has the characteristics necessary to pose a potential seismic risk. As stated below, studies have indicated that, despite this potential, the fault is not capable.

The Pen Branch fault is an upward propagation of the northern boundary fault of the Triassic Dunbarton basin that was reactivated in Cretaceous/Tertiary time. The fault dips steeply to the southeast. In the crystalline basement, slip was originally down to the southeast, resulting in the formation of the Dunbarton rift basin. However, movement during Cretaceous into Tertiary time was reverse movement, that is, up to the southeast. There could also be a component of strike-slip movement.

Joints

Joints are common on the SRS and vicinity. Though their mechanism of formation is not well understood, their age was determined to be constrained by interpretation that cutans often developed along pre-existing joints. The joints, therefore, pre-dated the pedogenic processes that formed the cutans. Highly variable orientations of cutans suggested that the orientation of joints on the SRS was also highly variable. A gradual and consistent change in orientation of cutans over 30 to 60 meters (100 to 200 feet) at some outcrops suggested the orientation of joints also locally changed gradually and consistently. A lack of consistent preferred orientations of joints across the SRS did not favor a tectonic origin for these features. Furthermore, no clear relationship existed between the joint-controlled cutans and the local topography. The joints, therefore, were probably not related to slope mass wasting. A local, gradual change in orientation over several hundred feet, and the common occurrence of closed depressions on the SRS, are consistent with differential settling from subsurface dissolution.

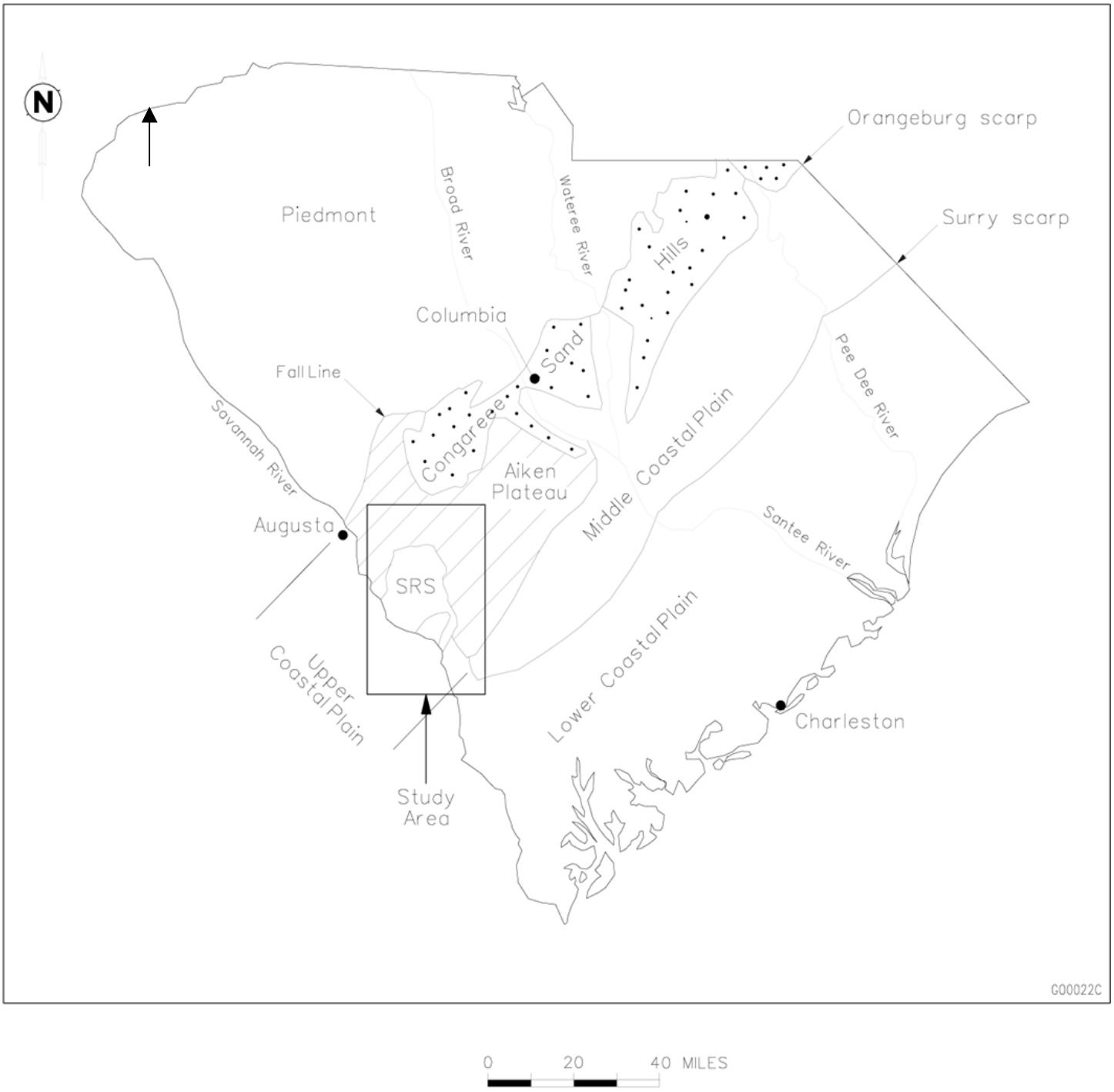

Figure 1. Generalized phyisiography for the SRS.

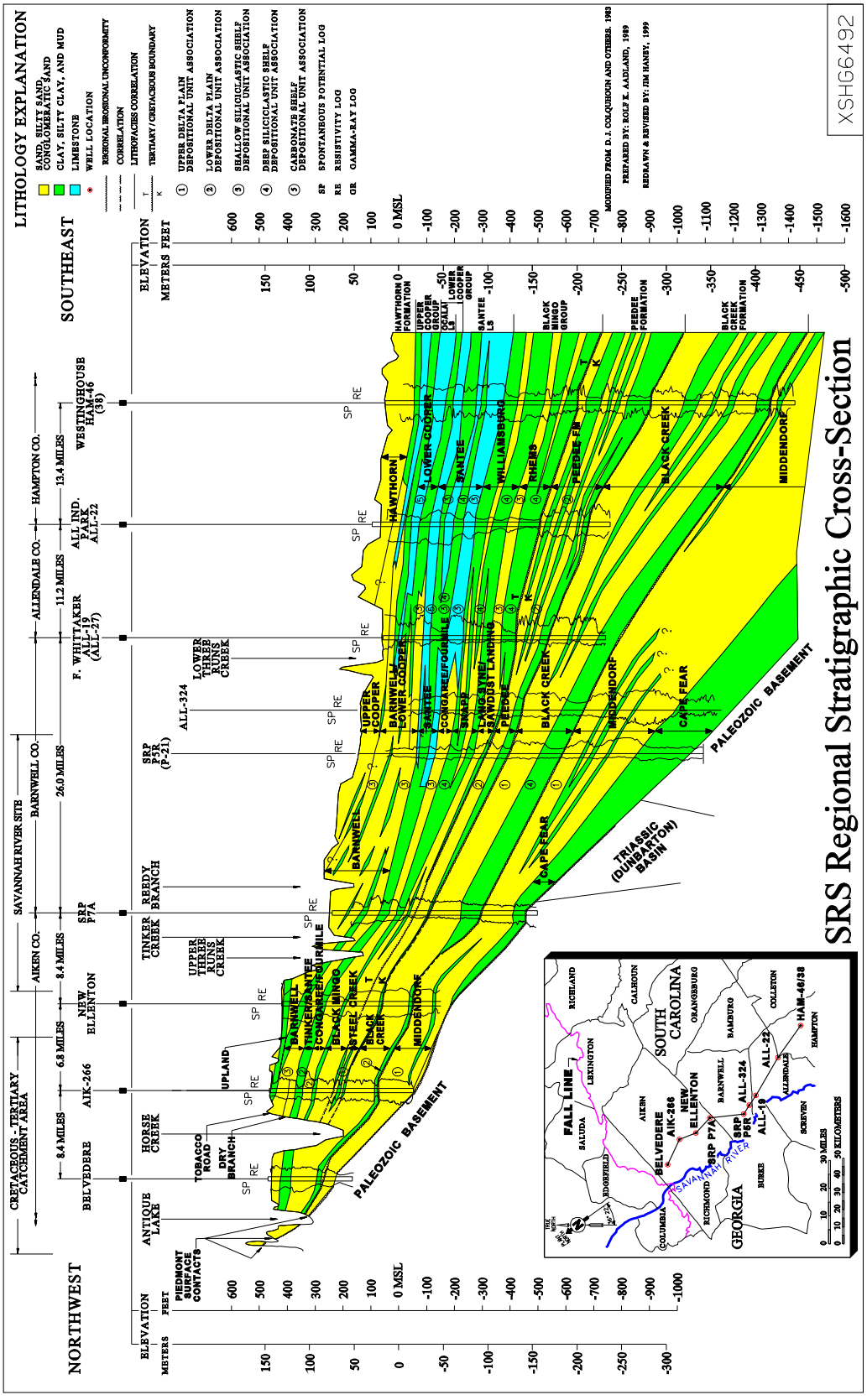

Figure 2. Regional stratigraphy.

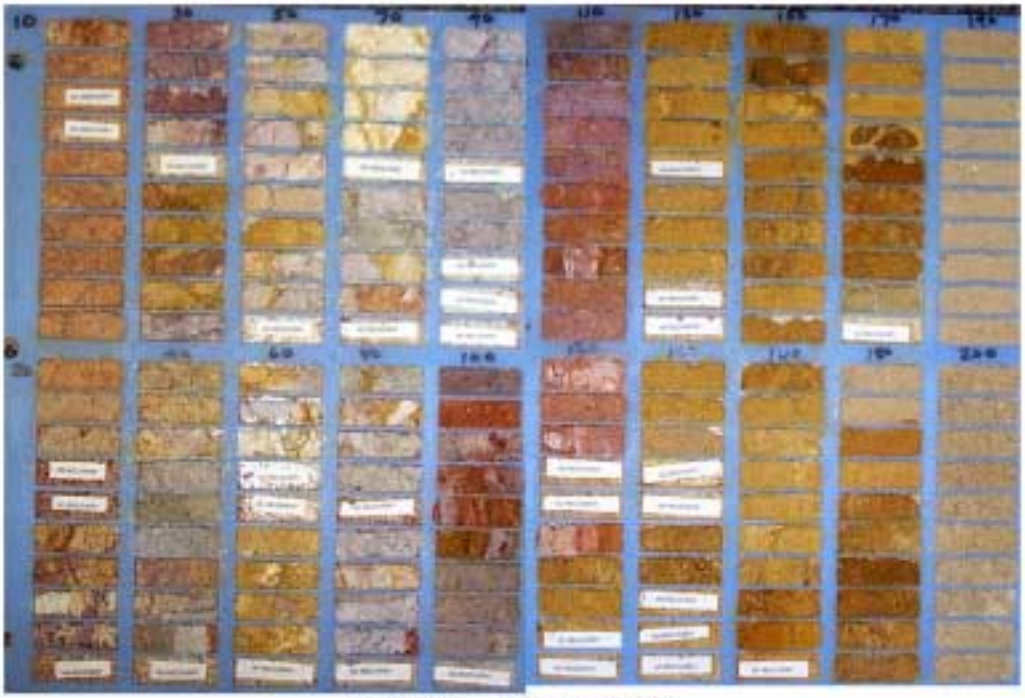

GCB-5 10' -- 210'

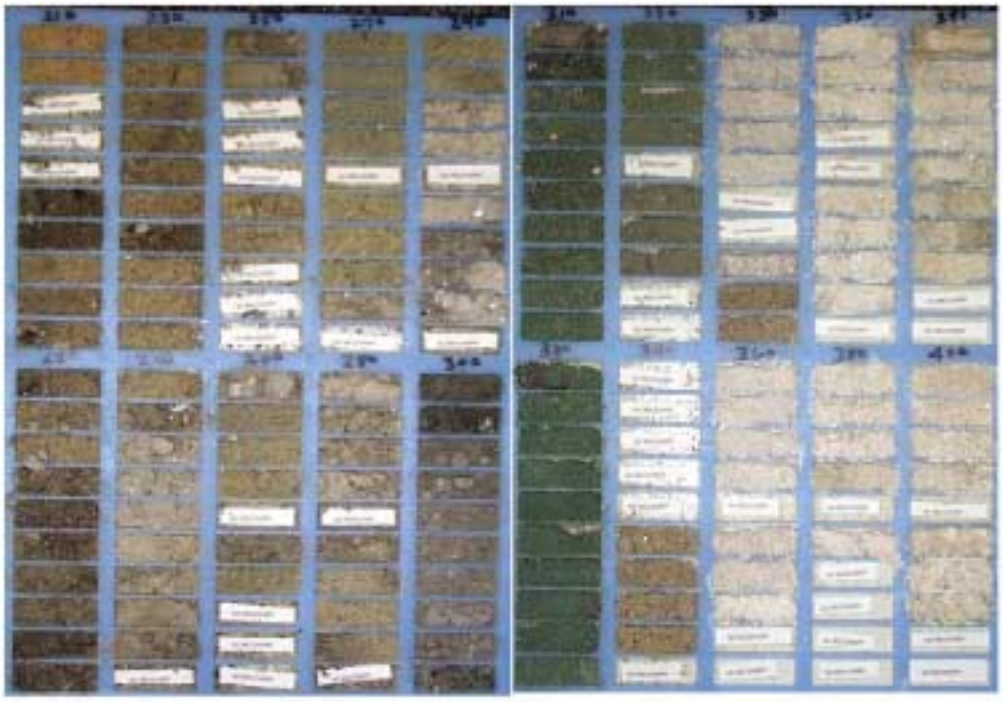

GCB-5 210' -- 410'

Figure 3. Foot by foot sediment samples from well GCB-5. White strip indicates missing data.

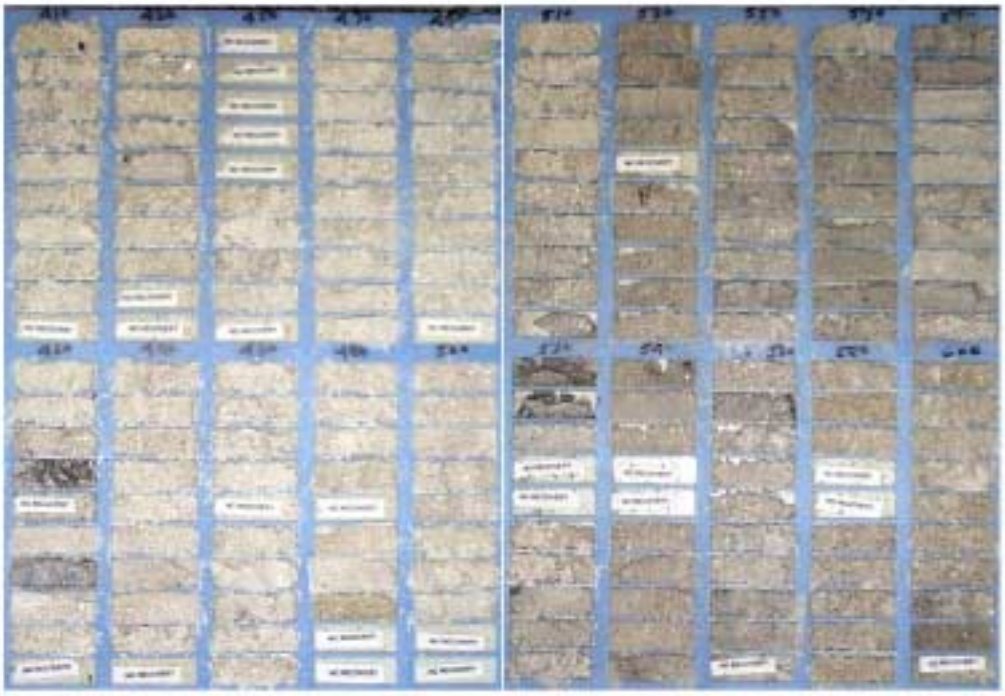

GCB-5 410' -- 610'

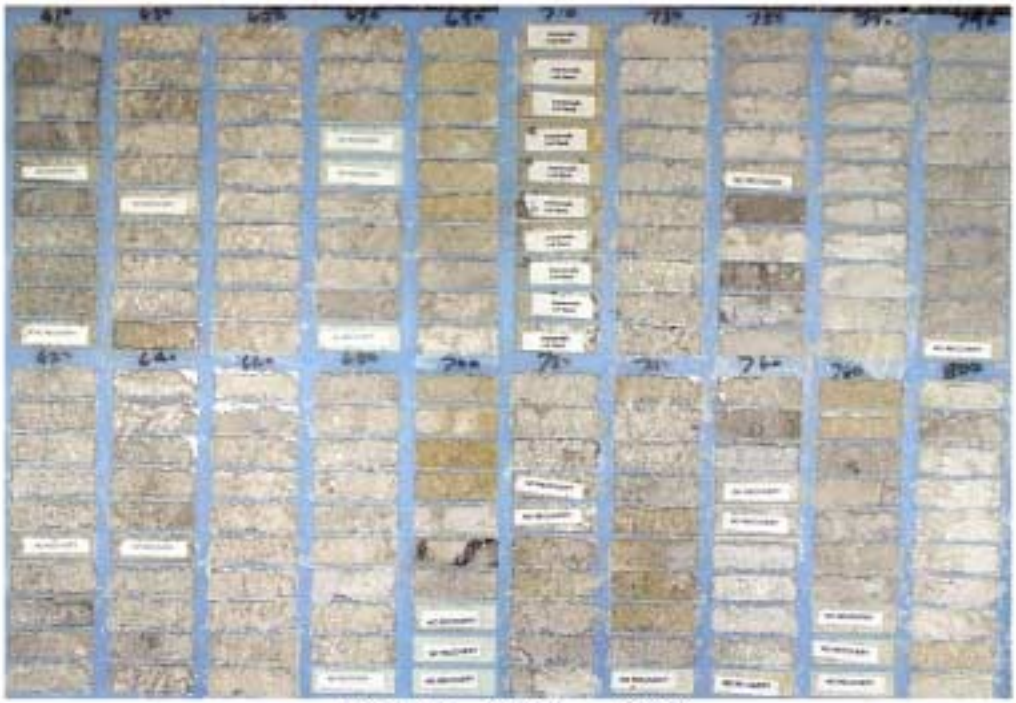

GCB-5 610' -- 810'

Figure 3. continued.

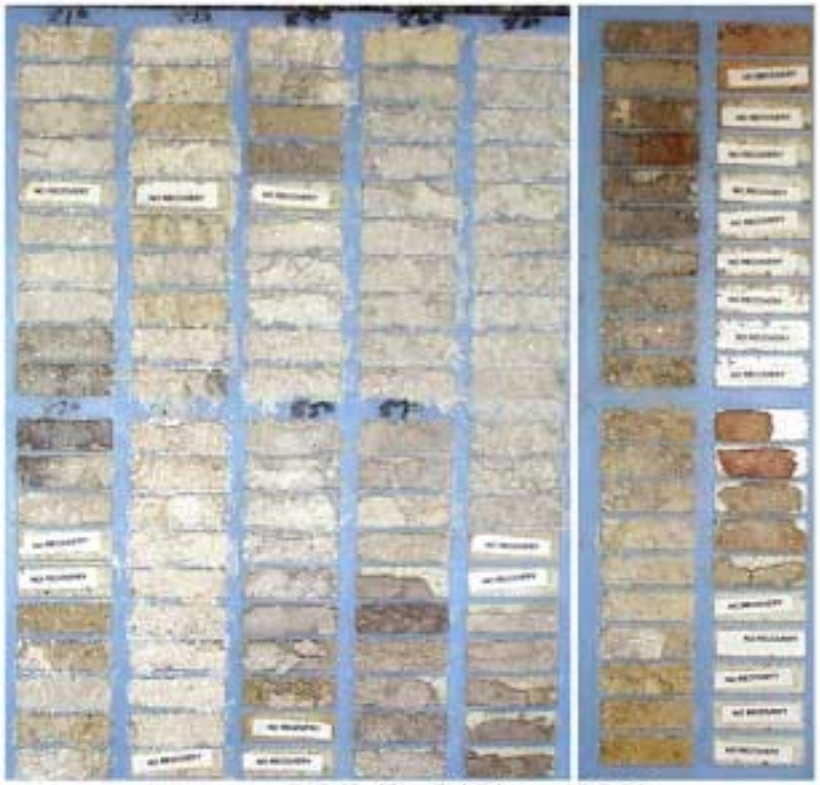

Figure 3. continued.

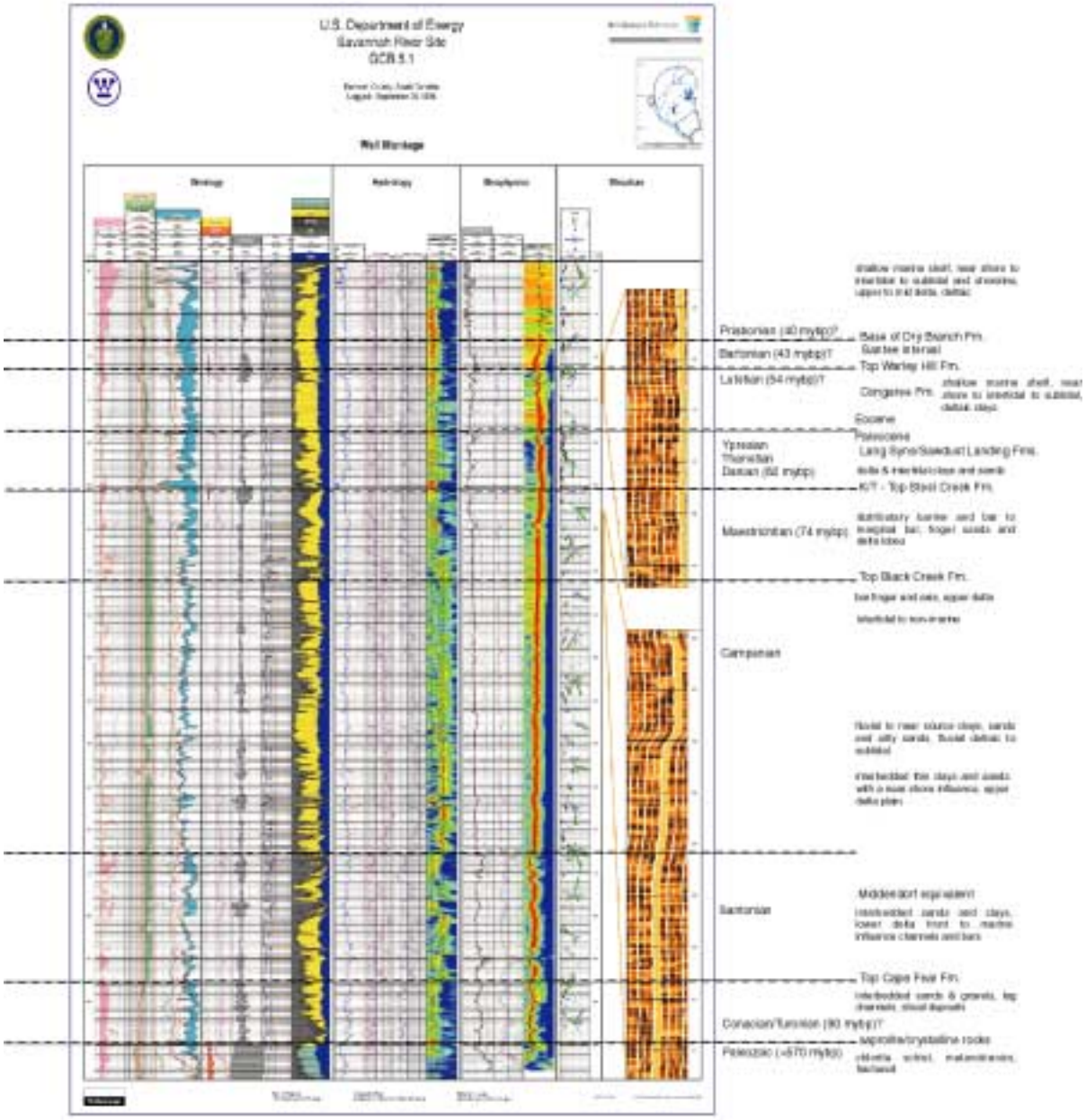

Figure 4. Geophysical log signature with stratigraphic markers.

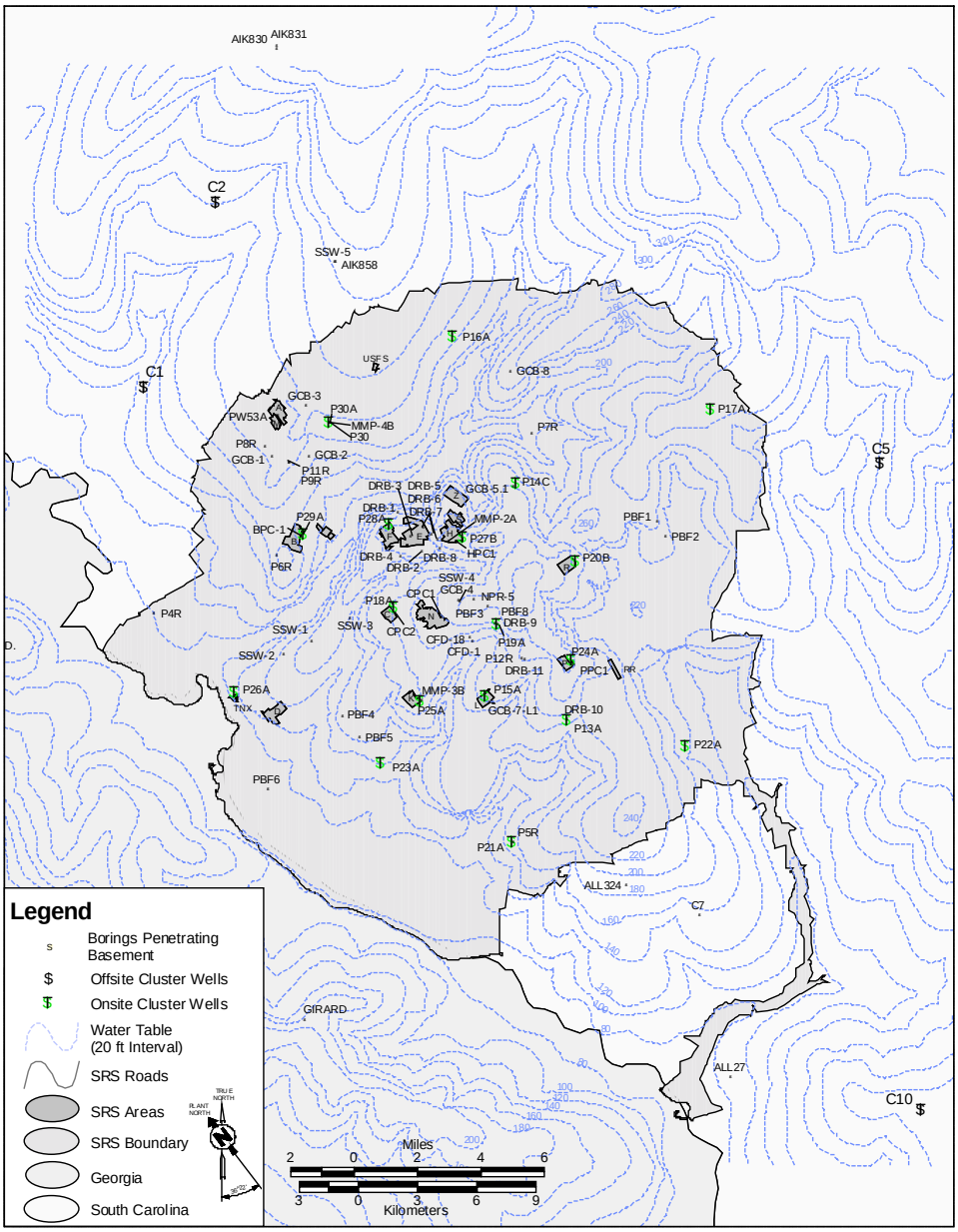

Figure 5. Location of type and reference wells for hydrostratigraphic units at SRS.

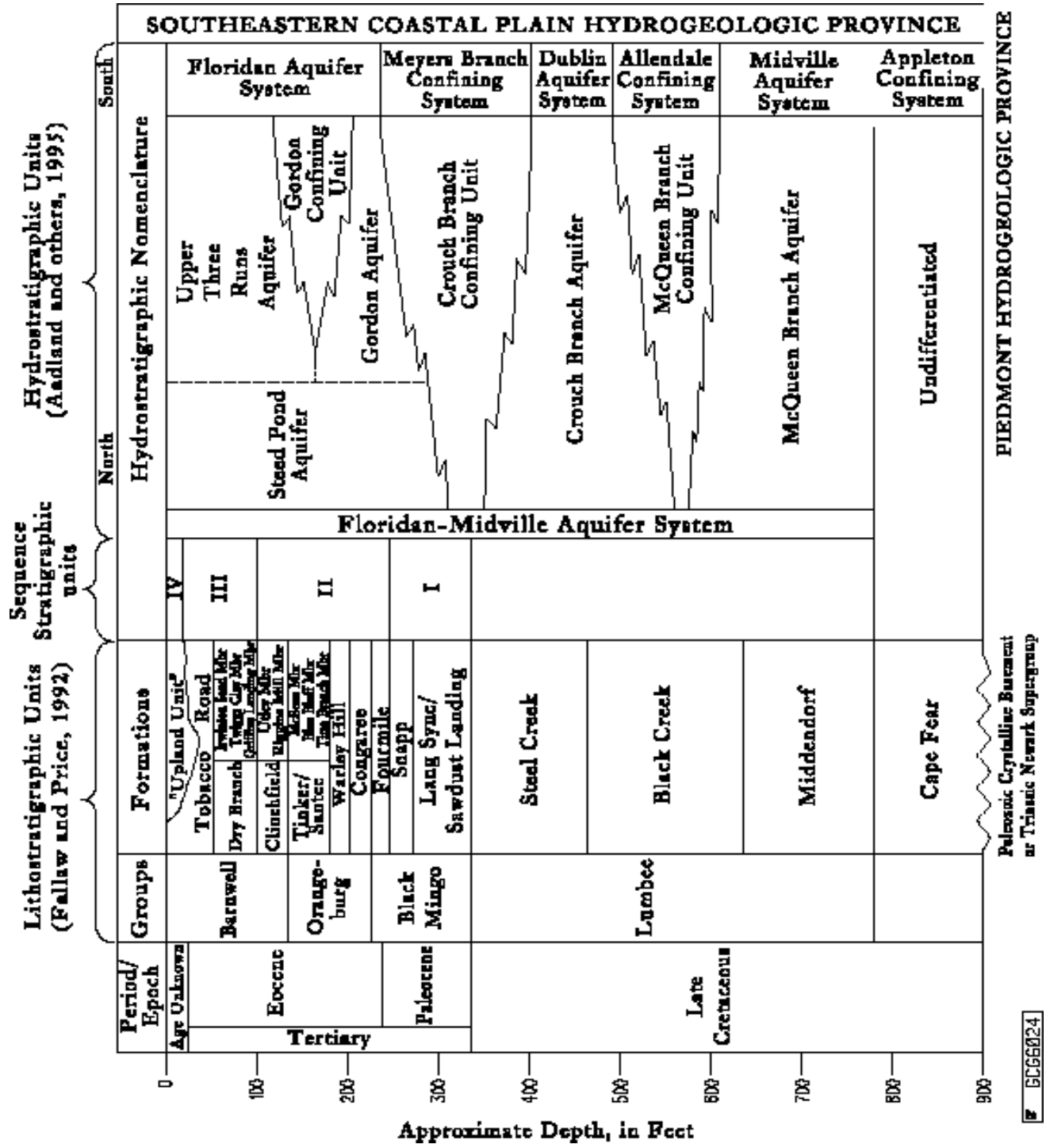

Figure 6. Comparison of chronostratigraphic, lithostratigraphic, and hydrostratigraphc units in the SRS region.

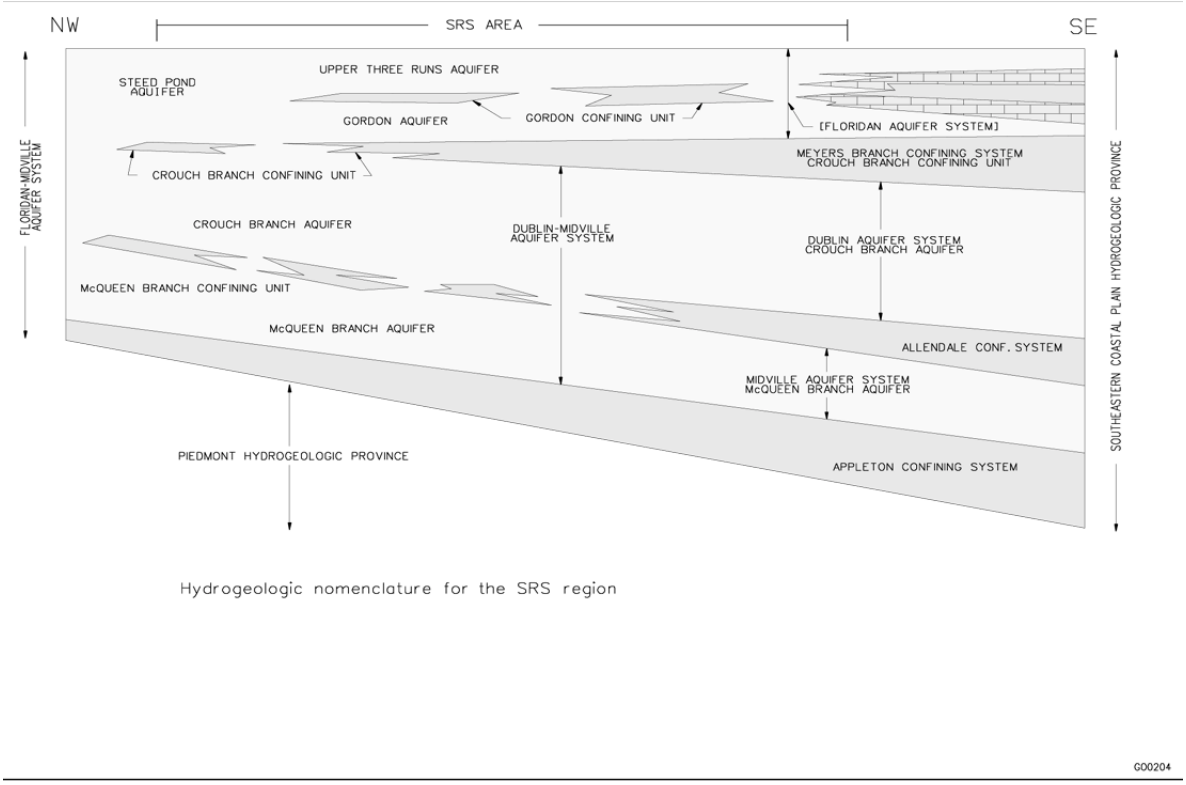

Hydrogeologic nomenclature for the SRS region

Figure 7. Hydrogeologic nomenclature for the SRS region.

Establishing a Hydrostratigraphic Framework using Palynology: An Example from the Savannah River Site, South Carolina, U.S.A.

Robert S. Van Pelt, Bechtel Savannah River Inc., Savannah River Site, Aiken South Carolina
Donald W. Engelhardt (deceased), Earth Sciences Resources Institute, University of South Carolina, Columbia, South Carolina
Raymond A. Christopher, Dept. of Geological Sciences, Clemson University, Clemson, South Carolina
Joyce Lucas-Clark, Clark Geological Services, 1023 Old Canyon Road, Fremont, California

INTRODUCTION

The primary mission of the Savannah River Site (SRS) is to produce nuclear materials for national defense. In the 1980's concern about environmental issues precipitated studies of the hydrogeology of the SRS. Since 1990, the mission has expanded to include environmental restoration following more than 40 years of waste-producing activities. Numerous waste-sites at SRS are currently undergoing environmental assessments and/or remediation under state and federal regulations.

An essential part of the environmental assessments is the characterization of the subsurface hydrogeology. Hydrogeological characterization involves establishing the hydrologic and geologic conditions (including the hydrostratigraphy), and incorporating this information into groundwater flow and contaminant transport models. Results from the hydrogeology and groundwater models are then applied in the selection of remediation strategies for a waste site. At the SRS, palynology has played a critical role in establishing the hydrogeologic framework, including the identification and characterization of hydrogeologic units and their relationships.

Differentiating among the sedimentary units that comprise the hydraulic system at SRS can be difficult when based solely on lithology. Most of the units consist of sediments of near shore and deltaic origin, regardless of age, such that similar depositional origins mask lithostratigraphic distinctions. Many sedimentary units are lenticular, comprise several depositional facies, and transgress time. Palynology has been applied to the various sedimentary units for age determination and paleoenvironmental interpretation.

Palynology also plays an important role in the detection of groundwater preferential pathways, such as facies changes and structural elements (e.g., faults). Prediction of such pathways is essential for developing accurate models of ground water contaminant flow and transport. The subsurface investigation at the SRS represents one of the frontier applications of palynology to hydrogeology and environmental restoration.

PREVIOUS PALYNOLOGICAL WORK AT SRS

As early as the middle of the 1970's, the need for accurate interpretation of the hydrostratigraphy beneath the SRS became apparent to those concerned with potential contamination problems (Cahil, 1982; Faye and Prowell, 1982; Marine and Root, 1975). Palynology has been used from the middle of the 1960's to the present as a basis for revising the formal stratigraphy (Siple 1967; Prowell et al., 1985a, 1985b; Gohn and Campbell, 1992; Nystrom et al., 1991; Fallaw and Price, 1992, 1995). For example, the Sawdust Landing Formation (hydrostratigraphically equivalent to the middle part of the Crouch Branch Confining Unit in the northern part of the SRS; see Text-Figure 2) was determined to be Paleocene rather than Cretaceous in age by dinoflagellate and pollen analysis (Lucas-

Clark, 1992a). Subsequently, this confining unit was separated into three distinct unconformity-bound units based on palynological age interpretations (Aadland et al., 1992). In general, age interpretations based on palynology allow for more accurate correlation with other stratigraphic units in the southeastern Coastal Plain, in what has come to be considered the Floridan Aquifer System. The revised lithostratigraphy and study of groundwater transport led to a complete formal hydrostratigrapic nomenclature for the SRS and surrounding vicinity (Aadland, 1990; Aadland and Bledsoe, 1992, Aadland et al., 1992; 1995) (Text-Figure 2).

Studies in the middle of the 1980's focused on Tertiary carbonate units which were considered as conduits for contaminants, and which were difficult to correlate due to their discontinuous, lenticular, reef-like nature. Although palynomorphs are usually sparse in the carbonates themselves, they are abundant in the interbedded and encapsulating clays and mud. Determining the age and identifying reliable palynological datums in these otherwise unfossiliferous fine-grained detrital units was determined to be more critical to the correlation of the carbonates than were the fossils in the carbonates themselves.

More recent emphasis on environmental restoration has required compliance with state and federal regulations, (e.g. Resource Conservation and Recovery Act (RCRA)/ Comprehensive Environmental Response Compensation and Liability Act (CERCLA)), which require a complete subsurface hydrogeologic/geologic characterization of waste sites, such as landfills, settling basins, storage tank areas, etc. (Van Pelt et. al., 1993; Lucas-Clark and Van Pelt, 1993; Van Pelt and Lucas-Clark, 1996). In nearly all cases, palynology has been utilized to aid in identifying hydrostratigraphic units and improving and confirming well log correlation.

Certain hydrostratigraphic units, specifically confining units, have characteristic dinoflagellate and pollen assemblages that can provide age and paleoenvironment interpretations. The interpretations allow for accurate correlation as well as prediction of pinch outs and leaks in the confining units. Some confining units, such as the lower part of the Crouch Branch Confining Unit, were deposited under marine conditions and represent a major transgressive sequence. Others units, such as the late Paleocene upper part of the Crouch Branch Confining Unit, are characterized by dinoflagellates that are abundant in deltaic and possibly brackish water environments. Overall, shelfal dinoflagellate assemblages appear to dominate confining units that are more reliable as continuous barriers to hydrologic flow except where breached by unconformities; shallow water (e.g., estuarine, lagoonal) dinoflagellate assemblages generally comprise confining units that are not reliable barriers to vertical groundwater flow. This relationship is illustrated by the upper part of the Crouch Branch Confining Unit, which grades into coarser grained non-marine sediments on the southeastern side of the Savannah River, and is absent on the northwest side of the Savannah River. This conclusion was particularly significant to the Trans-River Flow study conducted in the middle of the 1990's by the United States Geological Survey and the Georgia State Geological Survey. The focus of the Trans-River Flow study was to determine the possibility of contaminated groundwater migrating from the Savannah River Site under the Savannah River and into the aquifers in Georgia (Clarke et al.,1994; Clarke et al., 1996; Leeth et al., 1996; Falls et al., 1997a and b; Huddlestun and Summerour, 1996; and Clarke and West, 1997).

SAVANNAH RIVER SITE HYDRO-GEOLOGY AND PALYNOLOGICAL STRATIGRAPHY

The hydrology beneath the SRS and surrounding area is controlled by the pre-Cretaceous Paleozoic metamorphic and Triassic clastic rocks and overlying Coastal

Plain sediments. Poor water quality and low permeability prevent usage of ground water from within the pre-Cretaceous units. Overlying these units, however, the Coastal Plain sediments comprise a multi-layer hydrologic system in which retarding clay and marl beds are inter-layered with sands and limestone beds that transmit water more readily (Aadland and Bledsoe, 1992). In ascending stratigraphic order, the hydrologic system is divided into four aquifers (McQueen Branch, Crouch Branch, Gordon, and Upper Three Runs Aquifers), each separated by intervening confining units (Text-Figure 3). The Gordon and Upper Three Runs Aquifers coalesce in the northern part of the area to form the Steed Pond Aquifer (Lewis and Aadland, 1992).

The relation between the palynology and the hydrogeology is presented below. Selected palynomorphs that are useful in hydrostratigraphic correlation are presented in Text-Figures 4 through 8. The hydrogeology is presented in ascending order.

Appleton Confining System

Separating the aquifers of the Coastal Plain sequence from basement is the Appleton Confining System, which consists of saprolite overlying crystalline basement rock, and the sedimentary unit referred to as the Cape Fear Formation. The Cape Fear Formation is mainly non-marine and dated by pollen and spores as middle Turonian to Santonian (Late Cretaceous) in age (Lucas-Clark, 1992a). The Appleton Confining System/Cape Fear Formation is characterized by the presence of a distinctive pollen type that has been referred to as aff. *Porocolpopollenites* spp. by Doyle and Robbins (1977) (Text-Figure 6A). In addition, the unit contains diverse and abundant representatives of the genus *Complexiopollis*, including *C. abditus* Tschudy 1973 (Text-Figure 6B), as well as other described and undescribed forms. All species of *Complexiopollis* that occur in the unit are of the "newer" variety as characterized by Christopher (1979). Representatives of the genus *Pseudoplicapollis* (Text-Figure 6C) also occur throughout the unit, but they are not so abundant as are the *Complexiopollis* forms. Other genera that are present in assemblages from the Appleton Confining System/Cape Fear Formation are *Praecursipollis (*Text-Figure 6D), *Osculapollis* (Text-Figure 6E), *Trudopollis* (Text-Figure 6F), *Plicapollis* (Text-Figure 6G), *Labrapollis* (Text-Figure 6H), and numerous undescribed forms.

McQueen Branch Aquifer

The McQueen Branch Aquifer overlies the Appleton Confining System and is the lower of two Cretaceous aquifers at SRS. This aquifer represents the principal source for domestic use at SRS. Domestic wells in these sands commonly yield more than 1000 gallons per minute of high quality water.

The McQueen Branch Aquifer corresponds to the sands that are referred to as the Middendorf Formation as well as these in the lower part of the Black Creek Formation at SRS. The Middendorf Formation is considered non-marine to shallow marine in origin, and correlates with the lower (but not basal) part of the Tar Heel Formation in North Carolina. Dinoflagellates and pollen in the shallow marine facies have yielded mainly early Campanian (Late Cretaceous) ages. In most marine samples from the Middendorf Formation, dinoflagellates are sparse and assemblages consist mainly of spiny cysts and a few peridiniacean genera such as *Subtilisphaera* Jain & Millepied, *Spinidinium* Cookson & Eisenack, and *Palaeocystodinium* Alberti. Pollen assemblages from units mapped as the Middendorf Formation at SRS are distinctly different from those in the underlying Appleton Confining System/Cape Fear Formation, which reflects the unconformity that separates these units. Occurring in the Middendorf assemblages are *Plicapollis usitatus* Tschudy 1975 (Text-Figure 6I), representatives of the genus *Proteacidites* (Text-Figure 6J), two undescribed species with monocolpate

apertures and echinate surface ornamentation, and a variety of undescribed taxa. In addition, the lowest stratigraphic occurrence of *Holkopollenites chemardensis* Fairchild in Stover et al., 1966 (Text-Figure 6M, N) occurs within this unit (Text-Figure 4). The pollen data suggest an early Campanian age for the unit.

The lower part of the Black Creek Formation is marine to non marine in origin, and contains pollen assemblages similar to those in the underlying Middendorf Formation. Dinoflagellates in the shallow marine facies have yielded mainly Campanian ages. In most of the marine samples, dinoflagellates are abundant, and assemblages consist of abundant small peridiniacean species of *Subtilisphaera*, *Spinidinium*, *Palaeohystrichophora* Deflandre, and larger peridiniacean species of *Andalusiella* (Riegel) Riegel & Sarjeant, *Xenascus* Cookson & Eisenack, *Palaeocystodinium* Alberti, *Cerodinium* Vozzennikova, and *Trithyrodinium* Drugg. Gonyaulacacean dinoflagellates other than ceratioid types are sparse (Lucas-Clark, 1992a). Age diagnostic dinoflagellate species in the McQueen Branch Aquifer/Black Creek Formation include *Andalusiella spicata* (May) Lentin and Williams, *Xenascus sarjeantii* (Corradini) Stover & Evitt, and *Palaeohystrichophora infusorioides* Deflandre.

McQueen Branch Confining Unit

The McQueen Branch Confining Unit separates the two Cretaceous (McQueen Branch and Crouch Branch) aquifers. The unit thins and pinches out in the vicinity of the well cluster P 19 (Text-Figure 1) near the center of the SRS (where the two Cretaceous aquifers are in communication) but it persists throughout the remainder of the site region. The unit corresponds to the clays of the middle part of the Black Creek Formation.

Dinoflagellates from this unit have yielded mainly late Campanian ages. Characteristics of the dinoflagellate assemblages vary. Some assemblages are dominated by spiny cysts; others by *Areoligera coronata* (Wetzel) Lejeune-Carpenter/*senonensis*; others by small peridiniacean cysts; and others by *Xenascus ceratioides* (Deflandre) Lentin & Williams/*sarjeantii* complex. Useful species of dinoflagellates include *Dinogymnium euclaense* Cookson & Eisenack, *D. digitus* (Deflandre) Evitt et al., and *Palaeohystrichophora infusorioides* var. A and B of Aurisano (1989). Resedimentation of early Cretaceous dinoflagellates is not uncommon (Lucas-Clark, 1992a).

Pollen assemblages from the McQueen Branch Confining Unit include a variety of triporate forms that can be assigned to the genera *Momipites* (Text-Figure 7Q, Z), *Caryapollenites* (Text-Figure 7R), and *Betulaceoipollenites* (Text-Figure 7S) In addition, representatives of the genus *Holkopollenites* (Text-Figure 7V) are diverse and, at times, common elements in these assemblages. A late Campanian age is suggested by the pollen data (Text-Figure 4).

Crouch Branch Aquifer

The Crouch Branch Aquifer represents the upper of the two Cretaceous aquifers at SRS. It consists of the sand layers at the uppermost part of the Black Creek Formation and the majority of the overlying Steel Creek Formation. Dinoflagellates from the fine-grained marine portions of this aquifer suggest ages of late Campanian and Maastrichtian. Unfortunately, the clean sands and highly altered kaolinitic clays comprising the upper part of this aquifer often do not contain well-preserved fossil material. However, generic level identification of dinoflagellates such as *Dinogymnium* spp. and species of *Rugubivesiculites* (Text-Figure 7BB) pollen are useful in distinguishing Cretaceous from overlying Tertiary units (Lucas-Clark and Van Pelt, 1993). Diagnostic dinoflagellate species include: *Dinogymnium acuminatum* Evitt et al, *Palaeocystodinium benjaminii* Drugg, and *Cerodinium striatum* (Drugg) Lentin & Williams.

Pollen data from the Crouch Branch Aquifer suggest the presence of an unconformity within the unit; this unconformity corresponds to the contact between the Black Creek and Steel Creek Formations, and represents the uppermost part of the Campanian and most of the lower Maastrichtian. *Osculapollis aequalis* Tschudy 1975 (Text-Figure 7W) is restricted to the units below the unconformity, as are several morphotypes of the genus *Holkopollenites* (Text-Figure 7O,V). Restricted to the units above the unconformity are *Libopollis jarzenii* (Text-Figure 7X) and a thin-walled species of *Baculostephanocolpites* (MPH-1 of Wolfe, 1976) (Text-Figure 7Y). In the SRS and surrounding vicinity, the Steel Creek Formation is primarily non-marine to marginal marine, whereas the underlying Black Creek Formation is near shore to open marine in origin.

Crouch Branch Confining Unit

The confining system that overlies the Crouch Branch Aquifer represents the principal confining unit for the SRS and vicinity. This confining unit prevents migration of contaminated water from the Steed Pond and Gordon Aquifers of Tertiary age into the underlying Cretaceous Crouch Branch Aquifer. However, in some areas within the SRS, the confining unit is discontinuous resulting in local communication of the Tertiary and Cretaceous aquifers. It is thus critical to identify the confining unit where it is present, and important to understand its relation to other units.

The Crouch Branch Confining Unit corresponds to lower and upper Paleocene and lower Eocene lithologic units, which correspond to the Lang Syne, Sawdust Landing, the Snapp, and the Fourmile Branch Formations. The base of the Crouch Branch Confining Unit/Sawdust Landing Formation is characterized by the first appearance datum (FAD) of several Danian (Paleocene) dinoflagellate species: *Carpatella cornuta* Grigorovich (Text-Figure 8A), *Damassadinium californicum* (Drugg) Fensome et al. (Text-Figure 8R) *Spiniferites septatus* (Cookson & Eisenack) McLean, *Senegalinium ?dilwynense* (Cookson & Eisenack) Stover & Evitt (Text-Figure 8B), and *Spinidinium pulchrum* (Bensen) Lentin & Williams.

The upper part of the Crouch Branch Confining Unit (equivalent to the upper part of the Lang Syne, Snapp and Fourmile Branch Formations) is characterized by dinoflagellate assemblages that are dominated by one or at most, a few species. These assemblages may comprise small peridiniacean species along with *Areoligera* Lejeune-Carpenter spp. and/or *Cordosphaeridium* Eisenack spp. *Apectodinium homomorphum* (Deflandre & Cookson) Lentin & Williams (Text-Figure 8H), *A. quinquelatum* (Williams & Downie) Lentin & Williams, and *Eocladopyxis peniculata* Morgenroth make their first stratigraphic appearance in the upper part of the confining unit (Edwards, 1990; Lucas-Clark, 1992b).

There are several pollen species that have their bases or first appearances (FAD) in the Crouch Branch Confining Unit/ Sawdust Landing Formation (Text-Figure 5A,B). These include *Choanopollenites conspicuus* (Groot & Groot 1962) Tschudy 1973, *Choanopollenites discipulus* Tschudy 1973 (Text-Figure7G), *Favitricolporites baculoferus* (Pflug in Thompson and Pflug 1953) Srivastrava 1972 (Text-Figure 7E), *Nudopollis terminalis* (Pflug & Thompson in Thompson & Pflug, 1953) Pflug 1953 (Text-Figure 7D), *Nudopollis thiergarti* (Thompson & Pflug 1953) Pflug 1953 (Text-Figure 7I), *Momipites dilatus* Fairchild in Stover et al. (1966), *Pseudoplicapollis limitata* Frederiksen 1978, *Tricolpites asper* Frederiksen 1978, and *Trudopollis plenus* Tschudy 1975 (Text-Figure 7J). All of these taxa have tops or last appearances (LADs) higher in the stratigraphic section but the assemblage is characteristic of early Paleocene age. The range top of *Pseudoplicapollis serenus* Tschudy 1975

(Text-Figure 7O,P) that is within the Sawdust Landing Formation is considered by Frederiksen (1991) to mark the top of the Danian or early Paleocene.

In the upper part of the Crouch Branch Confining Unit which includes the upper Lang Syne and Snapp Formations, there are several pollen and spore species that have their last appearances. These include taxa which had their first appearances in the lower part of the Crouch Branch Confining Unit: *Choanopollenites conspicuus*, *Favitricolporites baculoferus* (Text-Figure 7E), *Interpollis paleocenicus* (Elsik 1968) Frederiksen 1980, *Lusatisporis indistincta* Frederiksen 1979 (Text-Figure 7H), *Momipites dilatus* (Text-Figure 6Z), *Nudopollis thiergartii* (Text-Figure 7I), *Pseudoplicapollis limitata* (Text-Figure 7b), *Tricolpites asper* (Text-Figure 7K), *and Trudopollis plenus* (Text-Figure 7J). *Holkopollenites chemardensis* Fairchild in Stover et al. (1966) Text-Figure 6M,N), which first appears in the Upper Cretaceous has a top in this interval. *Corsinipollenites? verrucatus* Frederiksen 1988 has a first and last appearance within the Snapp Formation. Frederiksen (1998) reports this species from the lower Eocene. Taxa such as *Subtriporopollenites nanus* (Pflug & Thompson in Thompson and Pflug 1953) Frederiksen 1980 (Text-Figure 7F), *Pseudolaesopollis ventosus* (Potonie' 1931) Frederiksen 1979, and *Milfordia hungarica* (Kedves 1965) Krutzsch & Vanhoorne 1977 (Text-Figure 7R) have their first appearances or bases within the Snapp Formation or equivalents in the southeastern United States (Frederiksen 1980a and b, 1988 and 1998).

Gordon/Steed Pond Aquifer and Gordon Confining Unit

The middle to upper Eocene aquifer (Steed Pond/Gordon) and confining unit (Gordon) that overlies the Crouch Branch Confining Unit is a complex set of strata consisting, in part, of carbonates (limestone) that are lenticular and discontinuous, as well as alternating clay and sand layers that act as confining units. Understanding the potential complexity of groundwater flow requires considerable accuracy in the identification and correlation of the lithologic units.

Lithologic units that correspond to the Steed Pond and equivalent aquifers include the Congaree Formation, Warley Hill Formation, Santee Formation, Clinchfield Formation, Irwinton Sand and Griffins Landing Members of the Dry Branch Formation, and the Tobacco Road Formation. Sediments comprising the Tobacco Road Formation are consistently barren of organic-walled microfossils. The other lithologic units have yielded dinoflagellate and pollen assemblages, usually from the clay- and silt-rich intervals.

Dinoflagellates useful in correlating the complex of middle to upper Eocene units include: *Pentadinium favatum* Edwards, *P. goniferum* Edwards (Text-Figure 8I), *Glaphrocysta* Stover & Evitt spp. (Text-Figure 8F), *Wetzelliella articulata* Eisenack group (Text-Figure 8E), *Membranophoridium aspinatum* Gerlach, *M. bilobatum* Michoux and *Charlesdowniea variabilis* (Bujak) Lentin & Vozzhennikova (Text-Figure 8Q).

Throughout most of the SRS, confining conditions (Gordon Confining Unit) exist to separate the Steed Pond Aquifer into two distinct aquifer zones, the Upper Three Runs and underlying Gordon Aquifer zones. The Gordon Confining Unit consists of sandy clays to clayey sands which represent parts of the Warley Hill and Tinker Formations, and the Blue Bluff Unit. Dinoflagellates first appearing within this confining unit include *Pentadinium laticinctum* Gerlach (Text-Figure 8N), *Cordosphaeridium cantharellus* (Brosius) Gocht, and *Charlesdowniea variabilis* (Text-Figure 8Q) *Pentadinium goniferum* (Text-Figure 8I) last appears within the upper part of this confining unit.

There are not as many extinctions or tops for pollen taxa in the middle and late Eocene Gordon Confining Unit as in the Crouch Branch Confining Unit. The most distinctive species are *Bombacacidites aff. B. reticulatus*

Krutzsch 1961, *Subtriporopollenites nanus* (Text-Figure 7F), *Malvacipollis tschudyi* (Frederiksen 1973) Frederiksen 1980 (Text-Figure 7W), *Brosipollis striata* Frederiksen 1988 (Text-Figure 7M), *Milfordia* hungarica (Text-Figure 7R), *Lanagiopollis hadrodictya* Frederiksen 1988, *Plicatopollis triradiata* (Nichols 1973) Frederiksen and Christopher 1978 (Text-Figure 7T), *Ulmipollenites krempii* (Anderson 1960) Frederiksen 1979 and *Retibrevitricolpites simplex* Frederiksen 1988 (Text-Figure 7X). *Dicolpopollis* spp. and *Proxapertites* spp. are reported by Tschudy (1973a and b) and Frederiksen (1988) to have their last appearances in the middle and late Eocene.

In addition to the tops observed in the Gordon Confining Unit several species have first occurrences within this unit. *Retibrevitricolpites simplex* (Text-Figure 7X) first appears in the Congaree Formation. Other species that have bases in the Congaree and Warley Hill and Santee formations are *Juglans nigripites* Wodehouse 1933, *Ulmipollenites undulosus* Wolff 1934, *Lymingtonia cf. L. rhetor* Erdtman 1960 (Text-Figure 7Q) in Frederiksen (1988), *Symplocos? jacksoniana* Traverse 1955, *Gothanipollis cockfieldensis* Engelhardt 1964, and *Boehlensipollis hohlii* Krutzsch 1962 (Text-Figure 7A). *Graminidites* spp. is reported by Tschudy (1973) and Frederiksen (1988) to have a first appearance in the late Eocene.

Many of the first appearance datums or bases (FAD) and last appearance datums (LADs) or tops are shown in Text-Figures 5A and B. These figures summarize the results of observations of palynomorph taxa in the cores from the Savannah River Site and published data. The principal publications on pollen and spores that were utilized in the study include: Elsik, 1974, Elsik and Dilcher, 1974, Frederiksen, 1978, 1979,1980a, 1980b, 1988, 1991,1998, in press, Frederiksen and Christopher, 1978, and Tschudy 1973a, 1975.

CONCLUSIONS

Dinoflagellate and pollen biostratigraphy has been applied successfully as a geologic tool for helping establish the subsurface hydrogeologic framework beneath the SRS. Because of the rapid vertical and lateral changes in updip coastal plain setting, dinoflagellate, and pollen and spore biostratigraphy, and to some extent dinoflagellate paleoenvironmental interpretations, have been critical in the correlation of aquifers and confining units and in the identification of facies changes and structural elements (e.g., Pen Branch Fault, Aadland et al., 1995). Recognition of these features is important as they serve as preferential pathways for groundwater movement and contaminant transport.

REFERENCES

Aadland, R.K., 1990, Hydrogeologic Characterization of the Cretaceous-Tertiary Coastal Plain Sequence at the Savannah River Site, South Carolina. *In*: Zullo, V.A., Harris, W.B., Price, V., (eds.) 1990, Savannah River Region: Transition between the Gulf and Atlantic Coastal Plains, *Proceedings of the Second Bald Head Island Conference on Coastal Plains Geology* p. 57-60.

Aadland, R.K. And Bledsoe, H.W., 1992, Hydrogeologic Classification of the Cretaceous-Tertiary Coastal Plain Sequence at the Savannah River Site. *Geological Society of America Abstracts with Programs*, Vol. 24, No.2, p.1.

Aadland, R.K., Thayer, P.A., And Smits, A.D., 1992, The Hydrogeological Atlas of West-Central South Carolina. *Westinghouse Savannah River Company, Westinghouse Savannah River Company Technical Report* 90-987.

Aadland, R.K., Gellici, J.A., And Thayer, P.A.,1995, Hydrogeologic Framework of West-Central South Carolina. *South Carolina Department of Natural Resources, Water Resources Division Report* No. 5, 200 p.

Aurisano, R.W., 1989, Upper Cretaceous dinoflagellate biostratigraphy of the

subsurface Atlantic Coastal Plain of New Jersey and Delaware, U.S.A. *Palynology*, v.13, p.143-180.

Berggren, W.A., Kent, D.V., Swisher, C.C. Iii, and Aubry, M.-P., 1995, Arevised Cenozoic geochronology and chronostratigraphy: in Berggren, W. A., Kent, D.V., Aubry, M.-P., Hardenbol, Jan (eds.), Geochronology, Time Scales andGlobal Stratigraphic Correlation: *Society of Economic Paleontologists and Mineralogists, Special Publication* No. 54, P. 129-212.

Cahil, J.M., 1982, Hydrology of the low-level radioactive solid-waste burial site and vicinity near Barnwell, South Carolina. *U.S. Geological Survey Open File Report* 82-863, 101 p.

Christopher, R.A., 1979, Normapolles and triporate pollen assemblages from the Raritan and Magothy Formations (Upper Cretceous) of New Jersey: *Palynology*, v.3, p. 73-121, 15 text-figs., 1 table, 9 pls.

Clarke, J.S., Falls, W.F., Edwards, L.E., Frederiksen, N.O., Bybell, L.M., Gibson, T.G., And Litwin, R.J., 1994, Geologic, Hydrologic, and Water Quality Data for a Multi-Aquifer System in Coastal Plain Sediments Near Millers Pond, Burke County, Georgia, 1992-93, *Georgia Department of Natural Resources Information Circular* 96, 34p.

Clarke, J.S., And West, C.T., 1997, Ground-Water Levels, Predevelopment Groundwater Flow, and Stream-Aquifer Relations in the Vicinity of the Savannah River Site, Georgia and South Carolina, *United States Geological Survey, Water-Resources Investigations Report* 97-4197, 120p.

Doyle, J.A., And Robbins, E.I., 1977, Angiosperm pollen zonation of the continental Cretaceous of the Atlantic Coastal Plain and its application to deep wells in the Salisbury embayment: *Palynology*, v. 1, p. 43-78.

Edwards, L. E., 1990, Dinocysts from the Lower Tertiary Units in the Savannah River area, South Carolina and Georgia. *In*: Zullo, V.A., Harris, W.B., Price, V., (eds.) 1990, Savannah River Region: Transition between the Gulf and Atlantic Coastal Plains, *Proceedings of the Second Bald Head Island Conference on Coastal Plains Geology*, p.89-90.

Elsik, W.C., 1974, Characteristic Eocene palynomorphs in the Gulf Coast, U.S.A.: *Palaeontographica*, Abt. B, v. 149, p.90-111.

Elsik, W.C., and Dilcher, D.L., 1974, Palynology and age of clays exposed in Lawrence clay pit, Henry County, Tennessee: *Palaeontographica*, Abt. B, v. 146, p.65-87.

Engelhardt, D.W., 1964, A new species of Gothanipollis Krutzsch from the Cockfield Formation (middle Eocene) of Mississippi: *Pollen et Spores*, v.6 no. 2, p.597-600.

Erdtman, G., 1960, On three new genera from the Lower Headon Beds, Berkshire: *Botaniska Notiser*, v. 113, p. 46-48.

Fallaw, W.C. And Price, V., 1992, Outline of stratigraphy at the Savannah River Site. *In*: Fallaw, W.C., and Price, V., (eds.), 1992, *Carolina Geological Society Field Trip Guide Book, Nov. 13-15, 1992*, Geological Investigations of the central Savannah River area, South Carolina and Georgia: U.S. Department of Energy and S.C. Geological Survey, p. CGS-92-B-11-1-33.

Fallaw, W.C. And Price, V., 1995, Stratigraphy of the Savannah River Site and Vicinity. *Southeastern Geology*, V.35, No.1, p.21-58.

Falla, W.F., Baum, J.S., And Prowell, D.C., 1997, Physical Stratigraphy and Hydrostratigraphy of Upper Cretaceous and Paleocene sediments, Burke and Screven Counties, Georgia, *Southeastern Geology*, v.36, no. 4, p. 153-176.

Faye, R.E. And Prowell, D.C., 1982, Effects of Late Cretaceous and Cenozoic faulting on the geology and hydrology of the Coastal Plain near the Savannah River, Georgia, and South Carolina. *U.S. Geological Survey Open File Report* 82-156.

Frederiksen, N.O., 1978, New Paleogene pollen species from the Gulf Coast and Atlantic Coastal Plains: *U.S. Geol. Survey Journ. Research*, 6: 691-696.

1979, Paleogene sporomorph biostratigraphy, northeastern Virginia: *Palynology*, v. 3, p. 129-167.

1980a, Sporomorphs from the Jackson Group (upper Eocene) and adjacent strata of Mississippi and western Alabama: *U.S. Geol. Survey Professional Paper* 1084, 75p.

1980b, Paleogene sporomorphs from South Carolina and quantitative

correlations with the Gulf Coast: *Palynology*, v. 4, 125-179.

1988, Sporomorph biostratigraphy, floral changes, and paleoclimatology, Eocene and earliest Oligocene of the eastern Gulf Coast: *U.S. Geol. Survey Professional Paper* 1448, 68p.

1991, Midwayan (Paleocene) pollen correlations in the eastern United States: *Micropaleontology*, v. 37,no. 2, p. 101-123.

1998, Upper Paleocene and lowermost Eocene angiosperm pollen biostratigraphy of the eastern Gulf Coast and Virginia: *Micropaleontology*, v. 44, no.1, p. 45-68.

In Press, Lower Tertiary pollen biostratigraphy of testholes in Georgia near the Savannah River Site: *U.S. Geol. Survey Professional Paper*.

Frederiksen, N.O. And Christopher, R.A., 1978, Taxonomy and biostratigraphy of Late Cretaceous and Paleogene triatriate pollen from South Carolina: *Palynology*, v. 2, p. 113-145.

Gohn, G.S. And Campbell, B.G., 1992, Recent revisions to the stratigraphy of subsurface Cretaceous sediments in the Charleston, South Carolina area. *South Carolina Geology*, v.34, p.25-38.

Huddlestun, P.F. And Summerour, J.H., 1996, The Lithostratigraphic framework of the uppermost Cretaceous and lower Tertiary of Eastern Burke County, Georgia, *Georgia Geologic Survey Bulletin* 127, 94p.

Krutzsch, W., 1960, Ueber Thomsonipollis magnificus (Th. and Pf. 1953) n.f. gen. n. comb. und Bemerkungen zur regionalen Verbreitung einiger Pollengruppen im aelteren Palaeogen: *Freiberger Forschungshefte*, v. C86, p. 54-65.

1961, Beitrag zur Sporenpalaeontologie der praaoberoligozaenen kontinentalen und marinen Tertiaerablagerungen Brandenburgs: *Berichte der Geologischen Gesellchaft in der Deutschen Demokratischen Republik*, v. 5, p.290-343.

1962, Stratigraphisch bzw. botanisch wichtige neue Sporen -und Pollenformen aus dem deutschen Tertiaer: *Geologie*, v. 11, no. 3, p.265-307.

Krutzsch, W. And Vanhoorne, R., 1977, Die Pollenflora von Epinois und Loksbergen in Belgien: *Palaeontographica*, Abt. B, v. 163,p. 1-110.

Lewis, S. And Aadland, R.K.,1992, Hydrogeologic Setting of the A/M Area: Framework for Groundwater Transport. *Westinghouse Savannah River Company Technical Report* 92-355, 80 p.

Leeth, D.C. And Nagle, D.D., 1996, Shallow subsurface geology of part of the Savannah River alluvial valley in the upper Coastal Plain of Georgia and South Carolina, *Southeastern Geology*, v.36, no.1, p. 1-14.

Lucas-Clark, J., 1992a, Problems in Cretaceous palynostratigraphy (dinoflagellates and pollen) of the Savannah River Site Area. *In*: Zullo, V.A., Harris, W.B., Price, V., (eds.) 1992, Savannah River Region: Transition between the Gulf and Atlantic Coastal Plains, *Proceedings of the Second Bald Head Island Conference on Coastal Plains Geology*, p.74.

Lucas-Clark, J., 1992b, Some Characteristic fossil Dinoflagellate cysts of Eocene Strata, Savannah River Site, South Carolina. *In*: Fallaw, W. and Price, V. 1992, Geological Investigations of the Central Savannah River Area, South Carolina and Georgia. *Carolina Geological Society Field Trip Guidebook 1992*, p. 58-60.

Lucas-Clark, J. And Van Pelt, R.S., 1993, Application of Dinoflagellate Biostratigraphy to Environmental Restoration Activities at the Savannah River Site, South Carolina, U.S.A., (abst.) *Abstracts with Programs: Fifth International Conference on Modern and Fossil Dinoflagellates, Zeist, The Netherlands, April 1993*.

Marine, I.W. And Root, K.R., 1975, A ground water model of the Tuscaloosa aquifer at the Savannah River Plant. *In*: Crawford, T.V. (ed.) *Savannah River Laboratory Environmental Transport and Effects Research Annual Report*, USERDA Report DP-1374, E.I. duPont de Nemours & Co., Savannah River Laboratory, Aiken, South Carolina.

Martini, E., 1971, Standard tertiary and Quaternary Calcareous Nannoplankton Zonation, *Proceedings of the II Planktonic Conference*, Rome, 1970, p.739-785.

Nystrom, P.G., Jr., Willoughby, R.H. And Price, L.K., 1991, The Cretaceous and Tertiary stratigraphy of the South Carolina upper

Coastal Plain. *In*: Horton, J.W., Jr., and Zullo, V.A., (eds.), *Geology of the Carolinas*. University of Tennessee Press, Knoxville, Tennessee, p.221-240.

Prowell, D.C., Christopher, R.A., Edwards, L.E., Bybell, L.M., And Gill, H.E.,1985a, Geologic section of the updip Coastal Plain from central Georgia to western South Carolina. *U.S. Geological Survey Miscellaneous Field Studies*, Map MF-1737.

Prowell, D.C., Edwards, L.E., And Frederiksen, N.O., 1985b, The Ellenton Formation in South Carolina-A revised age designation from Cretaceous to Paleocene. *U.S. Geological Survey Bulletin*, 1605-A, p.A63-A69.

Siple, G.E., 1967, Geology and ground water of the Savannah River Plant and vicinity, South Carolina. *U.S. Geological Survey Water-Supply Paper* 1841, 113 p.

Sissingh, W.,1977, Biostratigraphy of Cretaceous Calcareous Nannoplankton, *Geologic en Mijnbow*, v.56, no.1, p.37-65.

Srivastava, S.K.,1972, Some spores and pollen from the Paleocene Oak Hill Member of the Naheola Formation, Alabama (U.S.A.): *Rev. of Palaebot. and Palyn*. v.14, p. 217-285.

Stover, L.E., Elsik, W.C. And Fairchild, W.W.,1966, New genera and species of Early Tertiary palynomorphs from the Gulf Coast: Kansas Univ. *Paleontological Contrib. Paper* 5, p.10.

Thomson, P.W. And Pflug, Hans,1953, Pollen and sporen des mitteleuropaEischen TertiaErs: *Palaeontographica*, Abt. B, v. 94, p.1-138.

Traverse, A.F.,Jr.,1955, Pollen analysis of the Brandon lignite of Vermont: *U.S. Bur. Mines Rept. Inv*. 5151, p. 107.

Tschudy, R.H.,1973a, Stratigraphic distribution of significant Eocene palynomorphs of the Mississippi embayment: *U.S. Geol. Survey Professional Paper* 743-B, p. 24.

1973b *Complexiopollis* pollen lineage in Mississippi Embayment rocks: *U.S. Geological Survey Professional Paper* 743-C, p. C1-C15.

1975 Normapolles pollen from the Mississippi Embayment: *U.S. Geological Survey Professional Paper* 865, 42 p.

Van Pelt, R.S., Waanders, G.L., Lucas-Clark, J., And Harris, M.K., 1993, The Application of Palynology to Waste-Site Characterization: An Example from the Savannah River Site, South Carolina, (Abst.) *American Association of Stratigraphic Palynologists 1993 Annual Meeting Programs and Abstracts*, p.82.

Van Pelt, R.S., And Lucas-Clark, J., 1996, The Application of Palynology to Environmental Restoration Activities: An Example from the Savannah River Site, South Carolina, (Abst.) *Ninth International Palynological Congress Programs and Abstracts*, June 1996, p.82.

Wodehouse, R.P., 1933, Tertiary pollen. II The oil shales of the Eocene Green River formation: *Torrey Bot. Club Bull*., v.60, p.479-524.

Wolfe, J.A., 1976, Stratigraphic distribution of some pollen types from the Campanian and lower Maastrichtian rocks (Upper Cretaceous) of the Middle Alantic States: *U.S. Geological Survey Professional Paper* 977, p. 1-18.

Wolff, H., 1934, Mikrofossilien des pliocaenen Humodils der Grube Freigericht bei Dettingen a.M. und Vergleich mit alteren Schichten des Tertiaers sowie posttertiaeren Ablagerungen: *Preuss. Geol. Landesanstalt, Inst. Palaeobotanik und Petrographie Brennsteine Arb*., v.5, p.55-86.

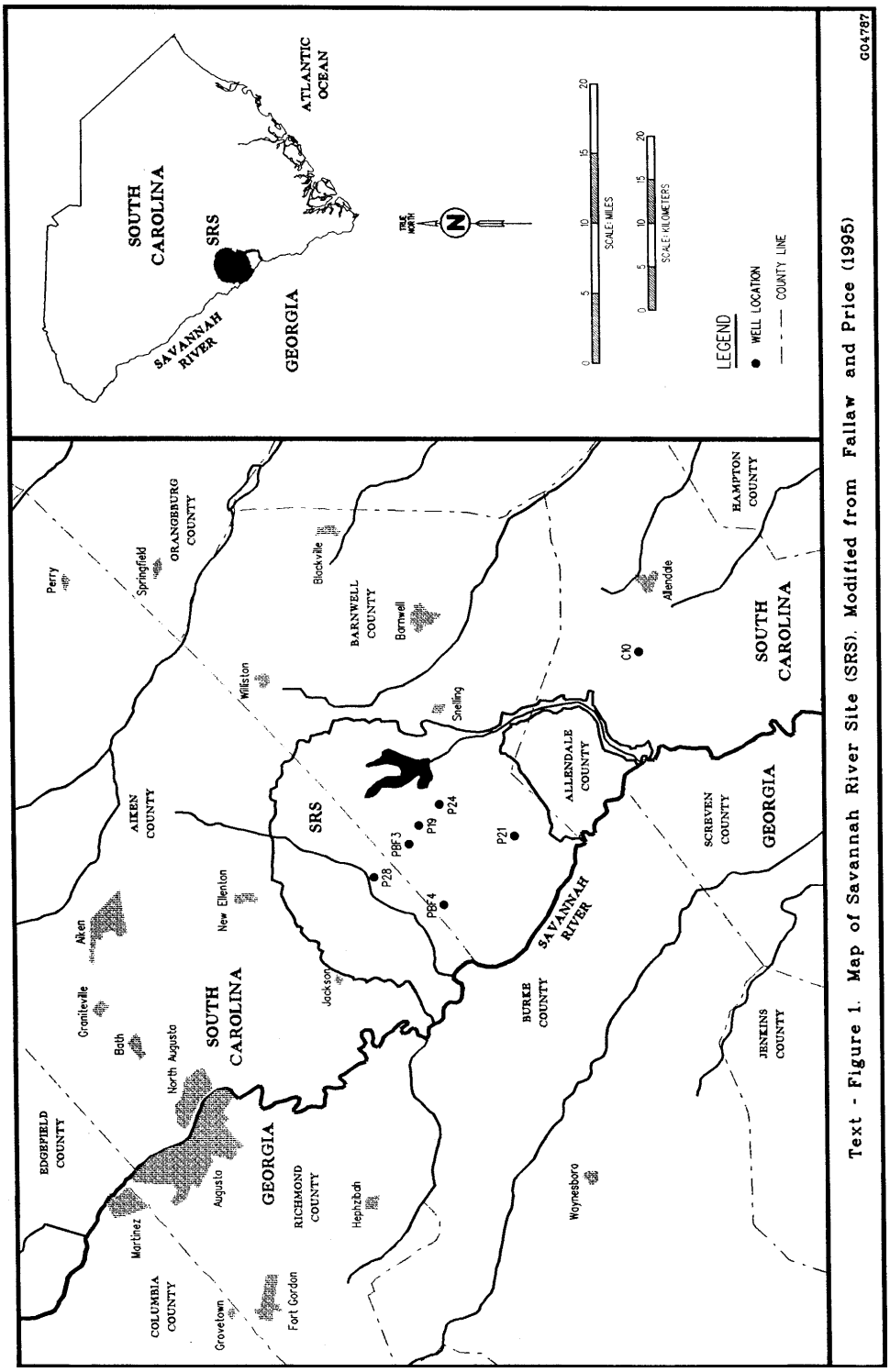

Figure 1. Location of the study area, Savannah River Site (SRS). Palynological data have been obtained for all or part of the wells shown on the map (modified from Fallaw and Price, 1995).

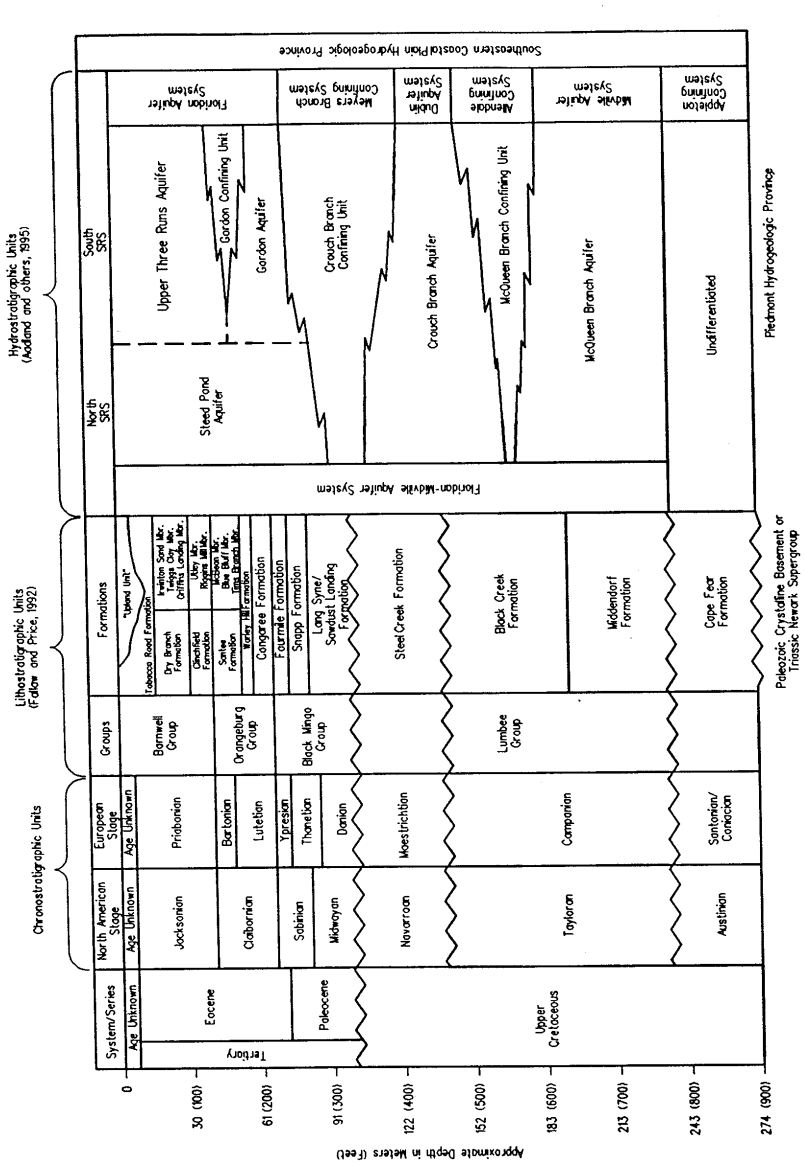

Text - Figure 2.
Comparison of chronostratigraphic, lithostratigraphic and hydrostratigraphic units in the SRS region

Figure 2. Comparison of chronostratigraphic, lithostratigraphic, and hydrostratigrahpic units in the SRS region: IRM=Irwinton Sand member; CF=Clinchfield Formation; RMM=Riggins Mill member; BBU=Blue Bluff unt; UM=Utley member; GLM=Griffins Landing member; ODB=Orangeburg District bed.

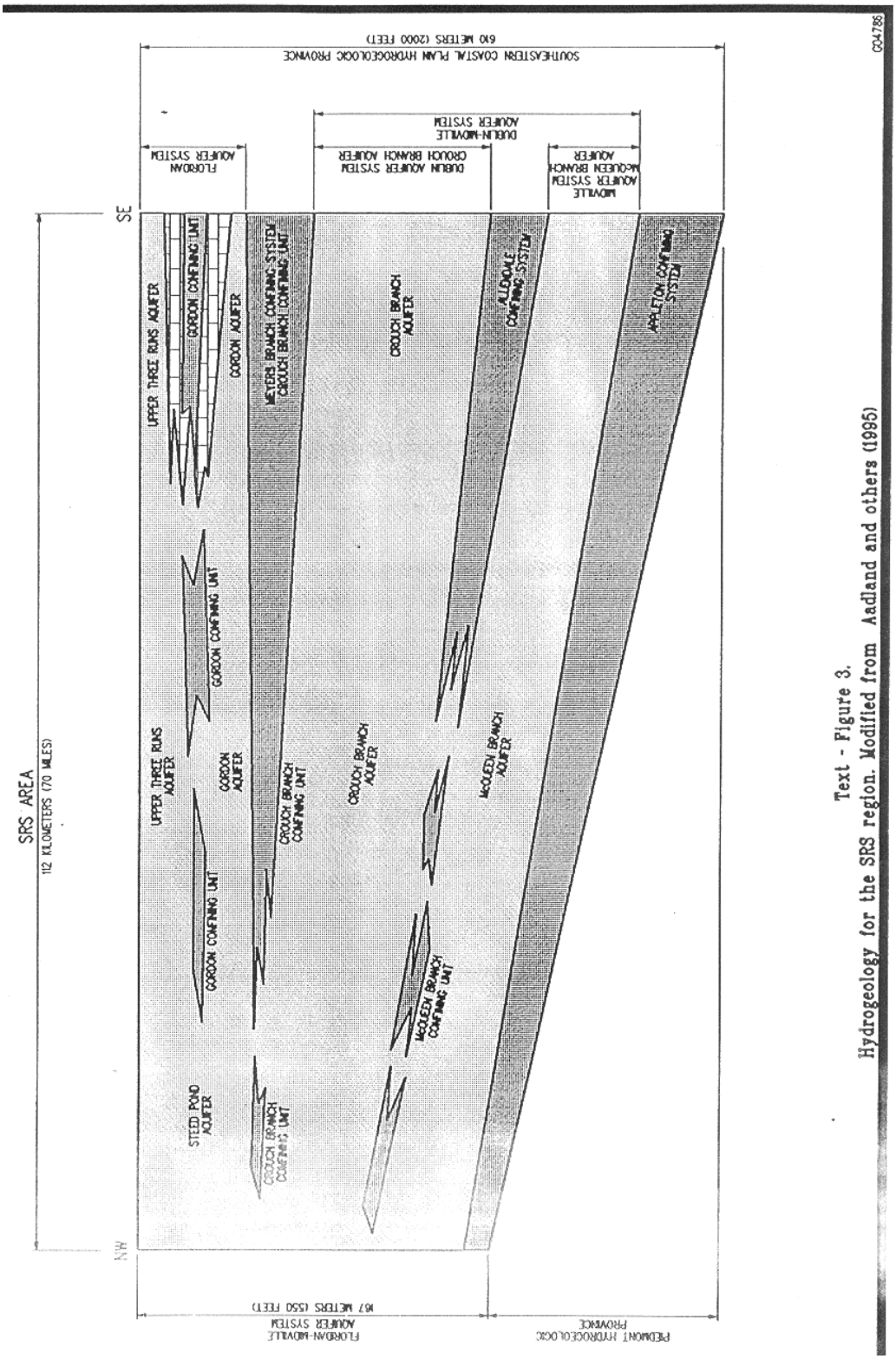

Figure 3. Cross section of the Uper Cretaceous and Tertiary hydrostratigraphic sequence beneath the SRS (modified from Aadland *et al*., 1995).

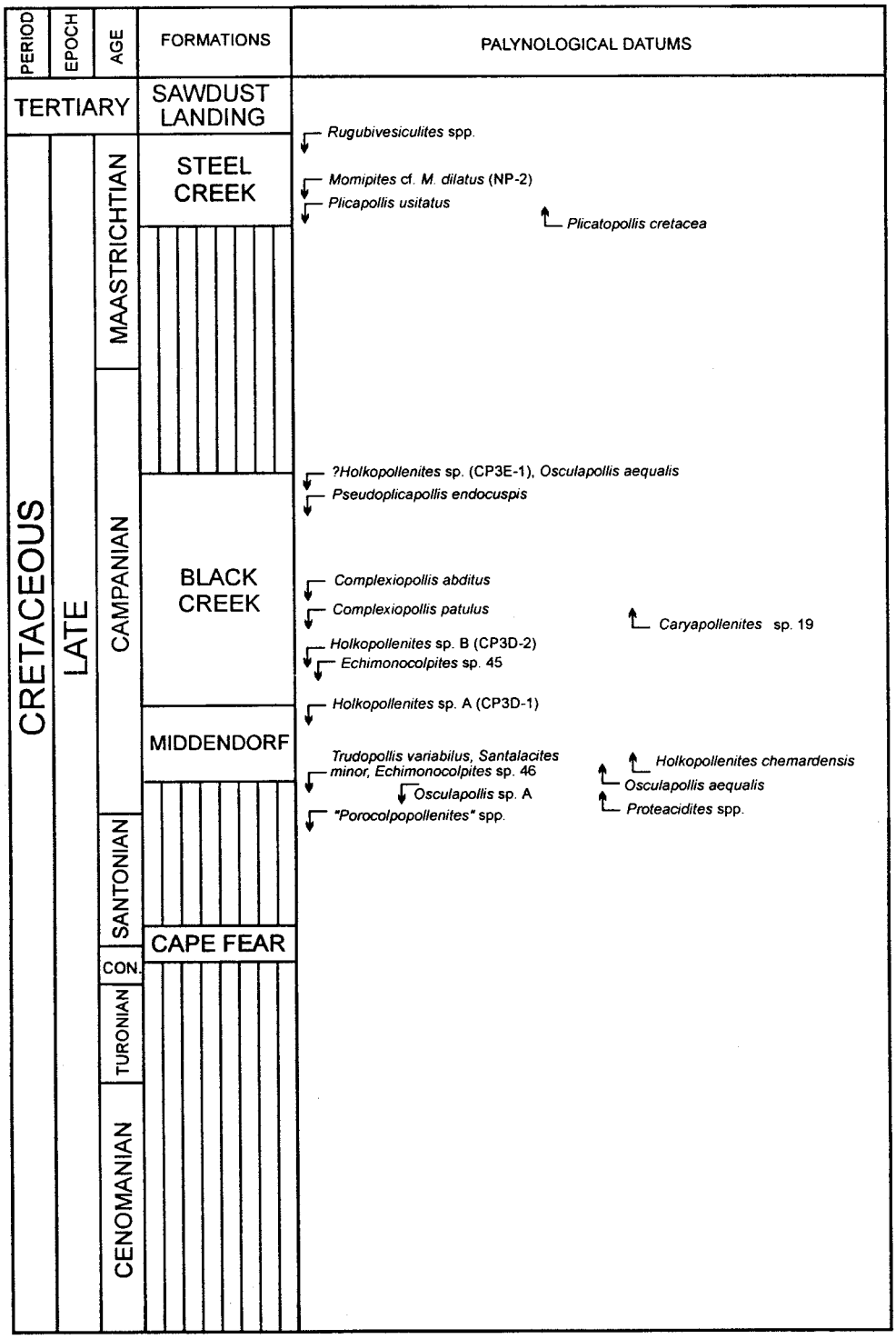

Figure 4. Selected Cretaceous palynomorph datums. The relatonship of formational boundaries to stage boundaries is modified following Berggren *et al.*, 1996.

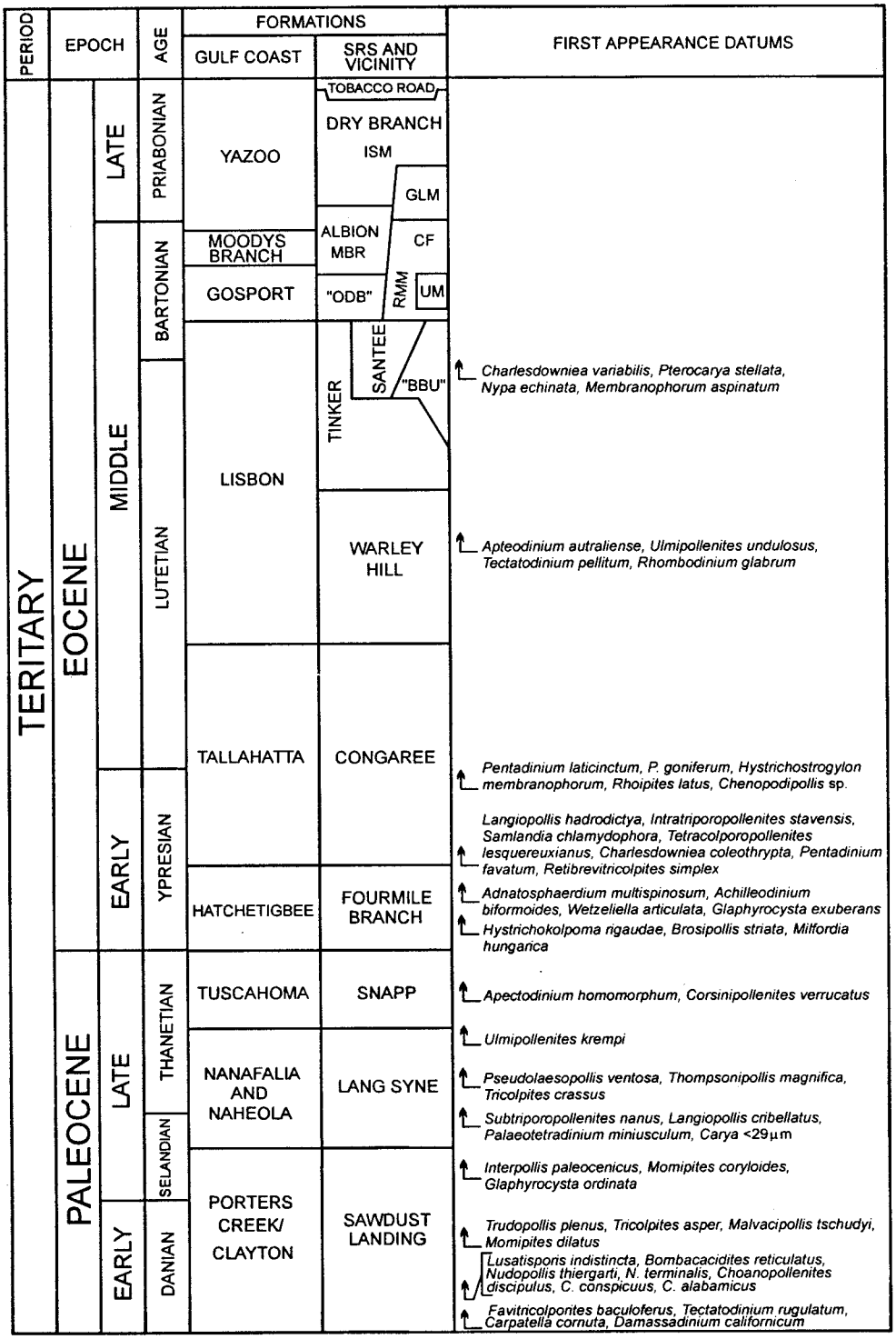

Figure 5A. Selected Tertiary palynomorph (first appearance) datums. The relationshp of formational boundaries to stage boundaries is modified following Berggren et al., 1996: IRM=Irwinton Sand Member; CF=Clinchfield Formation; RMM=Riggins Mill Member; BBU=Blue Bluff Unit; UM=Utley Member; GLM=Griffins landing Member; ODB=Orangeburg District Beds.

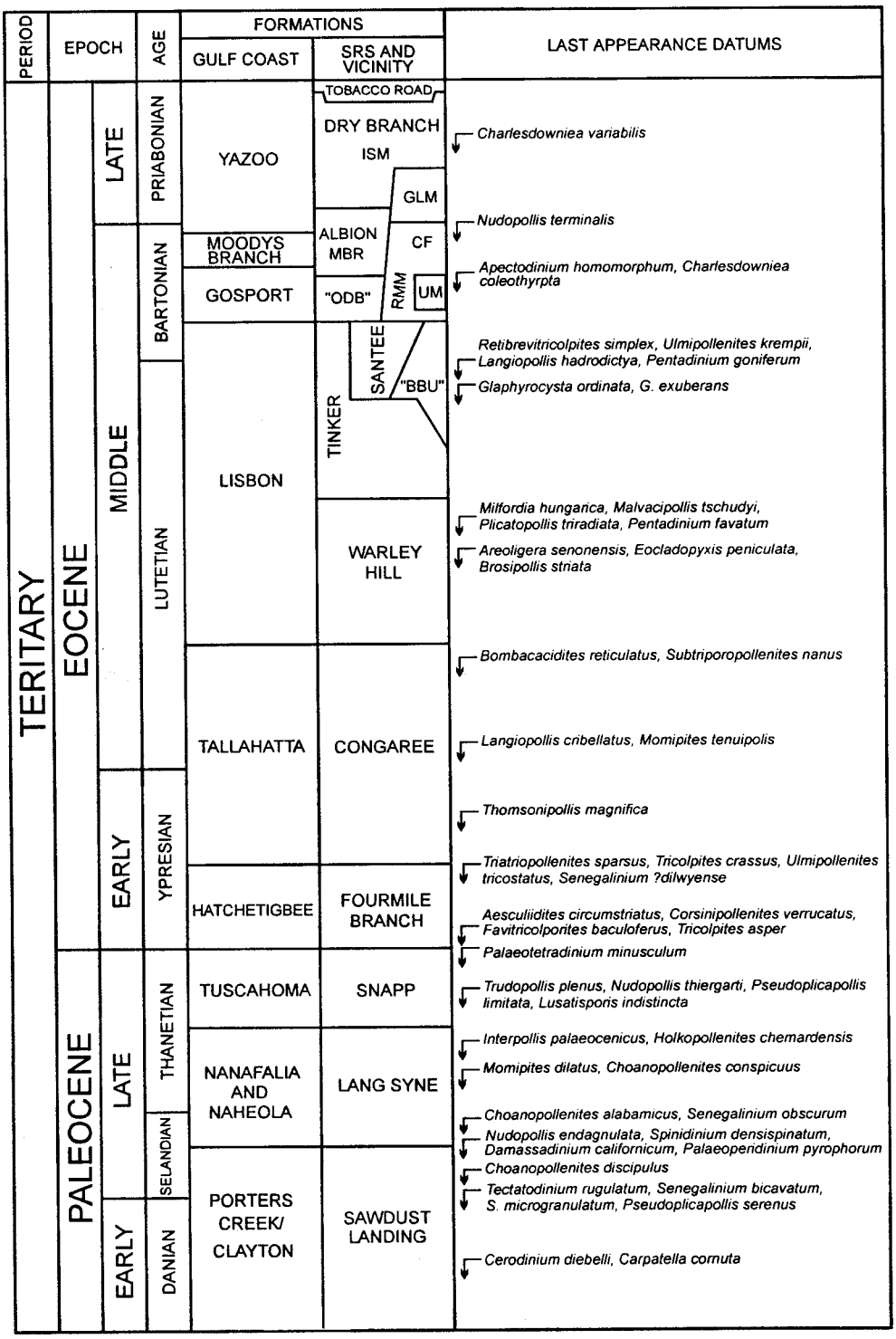

Figure 5B. Selected Tertiary palynomorph (last appearance) datums. The relationshp of formational boundaries to stage boundaries is modified following Berggren et al., 1996: IRM=Irwinton Sand Member; CF=Clinchfield Formation; RMM=Riggins Mill Member; BBU=Blue Bluff Unit; UM=Utley Member; GLM=Griffins landing Member; ODB=Orangeburg District Beds.

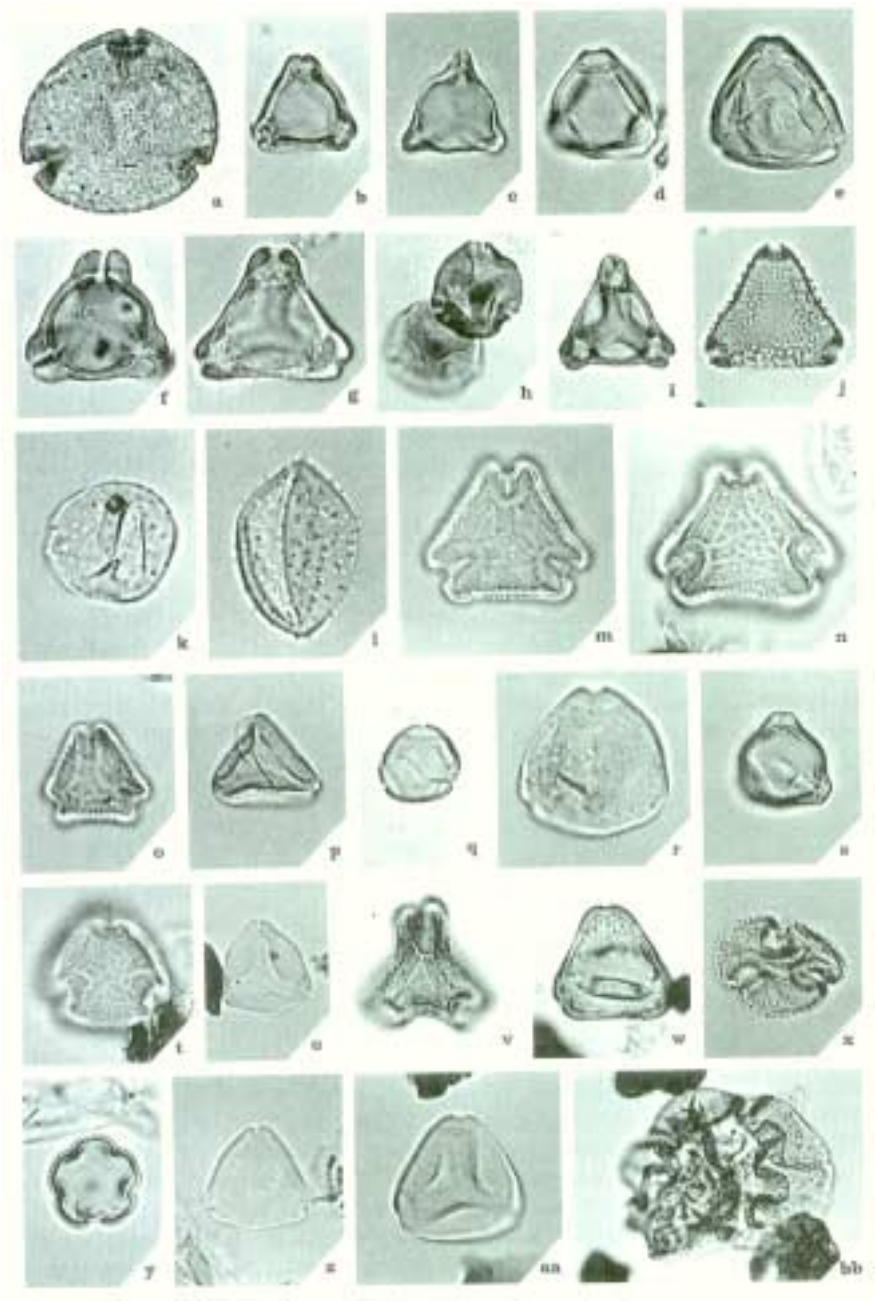

Figure 6. Selected Cretaceous pollen used in hydrostratigraphic correlation. All figures are 800 x, except BB, which is 400 x (reduced 25% for reproduction): (a) *Porocolpopollenites* sp.*(sensu* Doyle, 1969); (b) *Complexiopollis abditus* Tschudy 1973; (c) *Pseudoplicapollis longion-* nulata Christopher 1979; (d) *Praecursipollis plebus* Tschudy 1975; (e) *Osculapollis Sp.; (f) Trudopollis* sp.; (g) *Plicapollis* sp.; (h) *Labrapollis* sp.; (i) *Plicapollis usitatus* Tschudy 1975; (j) Proteacidites sp.; (k) *Echimonocolpites* sp. 45 (Cl-45); (1) Echimonocolpites sp. 46 (Cl-46); *(m,n) Holkopollenites chemardensis* Fairchild in Stover, Elsik and Fairchild 1966; *(o) Holkopol- lenites* sp. A (=CP3d-1 of Wolfe, 1976); (p) *Santalacites minor* Christopher 1979; (q) *Momipites* sp.; (r) *Caryapollenites sp.; (s) Betulaceoipollenites* sp. (=NO-3 of Wolfe, 1976); (t) *?Holkopol- lenites* sp. (CP3E-1 of Wolfe, 1976); (u) *Pseudoplicapollis endocuspis* Tschudy 1975; (v) *Holkopol- lenites* sp. B (=CP3D-2 of Wolfe, 1976); (w) *Osculapollis aequalis* Tschudy 1975; (x) *Libopollis* jarzenii Farabee, Daghlian, Canright and Oftedabi 1984; (y) *Baculostephanocolpites* sp. B (= MPH-2 of Wolfe, 1976); (z) *Mornipites dilatus* group (=NP-2 of Wolfe, 1976); (aa) *Plicatopollis cretacea* Frederiksen and Christopher 1979; (bb) *Rugubivesiculites sp.*

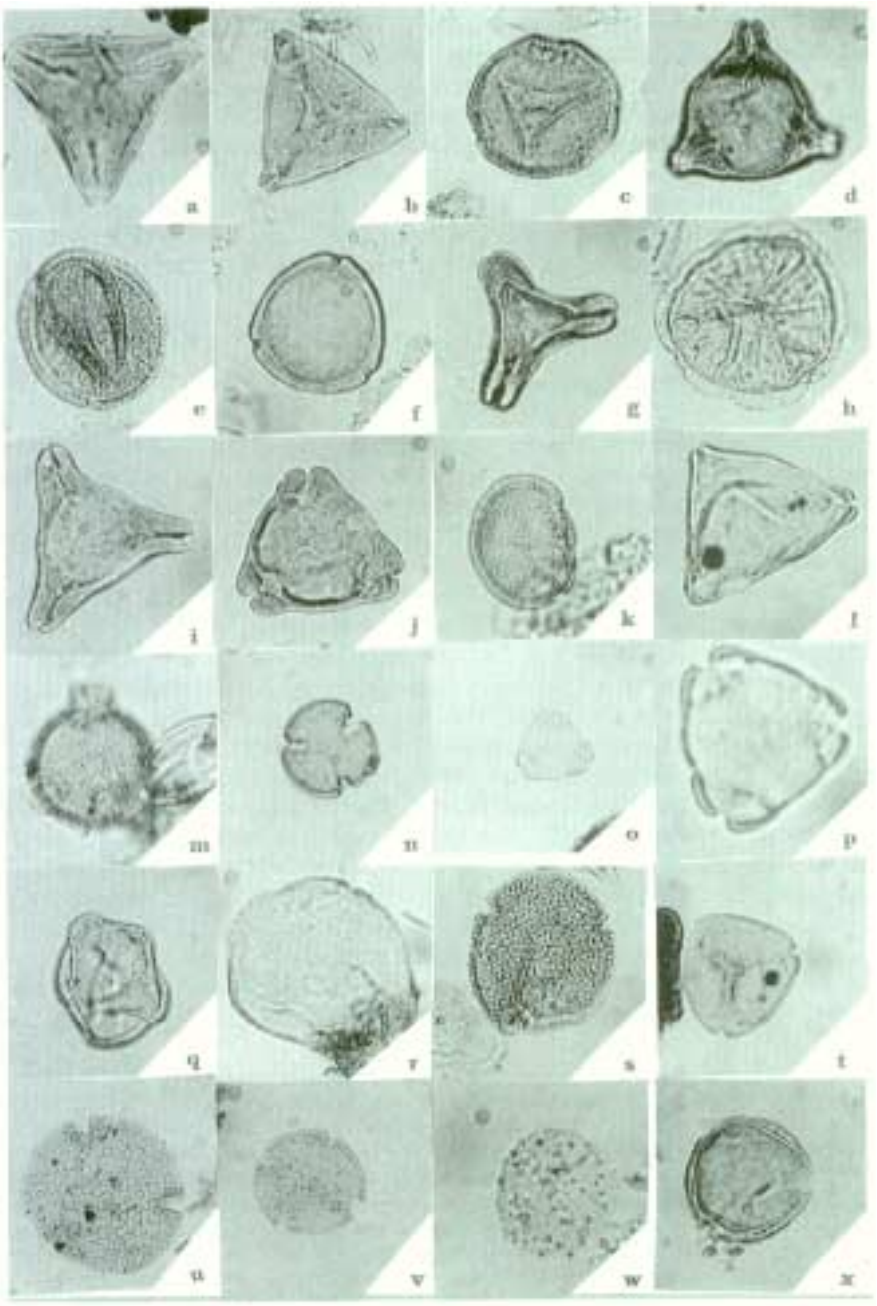

Figure 7. Selected Tertiary pollen used in hydrostratigraphic corrlation. All figures are 625 x, except fotr (p), which is 1500 x (reduced 25% for reproduction: (a) *Boehlensipollis holii* Krutzsch 1962; (b) *Pseudoplicapollis limitata* Froderiksen 1978; *(e) Thomsonipollis magnificus* (Pflug in Thomson and Pflug) Krutzsch 1960; (d) *Nudopollis terminals* (Thomson and Pflug in Thomson and Pflug, 1953); *(e) Favitticolpozites baculoferous* (Thomson and Pflug) Pflug 1953; (f) *Sub- tziporopollenites nanus* (Thomson and Pflug in Thomson and Pflug, 1953); (g) *Choanopollenites discipulus* Tschudy 1973; (h) *Lusatispozis indistincta* Froderikson 1979; (i) *Nudopollis thiergartii* (Thomson and Pflug) Pflug 1953; (j) *Trudopollis plenus* Tschudy 1975; (k) *Tilcolpites asper* Froderiksen 1978; *(1) Piolencipollis endocuspoides* Froderikson 1979; (m) *Bz-osipollis striata* Froderiksen 1988; (n) *Tricolpites crossus* Froderiksen 1979, (o) *Pseudoplicapollis serenus* Tschudy 1975; (p) *Pseudoplicapollis serenus* Tschudy 1975 1500 x; (q) *Lymingtonia* cf. L. *rhetor* Erdtman 1960 in Froderiksen 1988; (r) *Milfordia hungarica* (Kedves, 1965) Krutzsch and Vanhoome 1977; *(s) Intratziporopollenites stavensis* Froderiksen 1980; *(t) Plicatopollis tdradiata* (Nichols 1973) Frederiksen and Christopher 1978; (u) *Bombacacidites reticulatus* Krutzsch 1961; (v) *Quadmpol- lenites vagus* Stover in Stover et a]., 1966; (w) *Malvacipollis tschud@di* (Frederikson 1973) Frederiksen 1980; *(x) RetibzvWtricolpites simplex* Froderikson 1988.

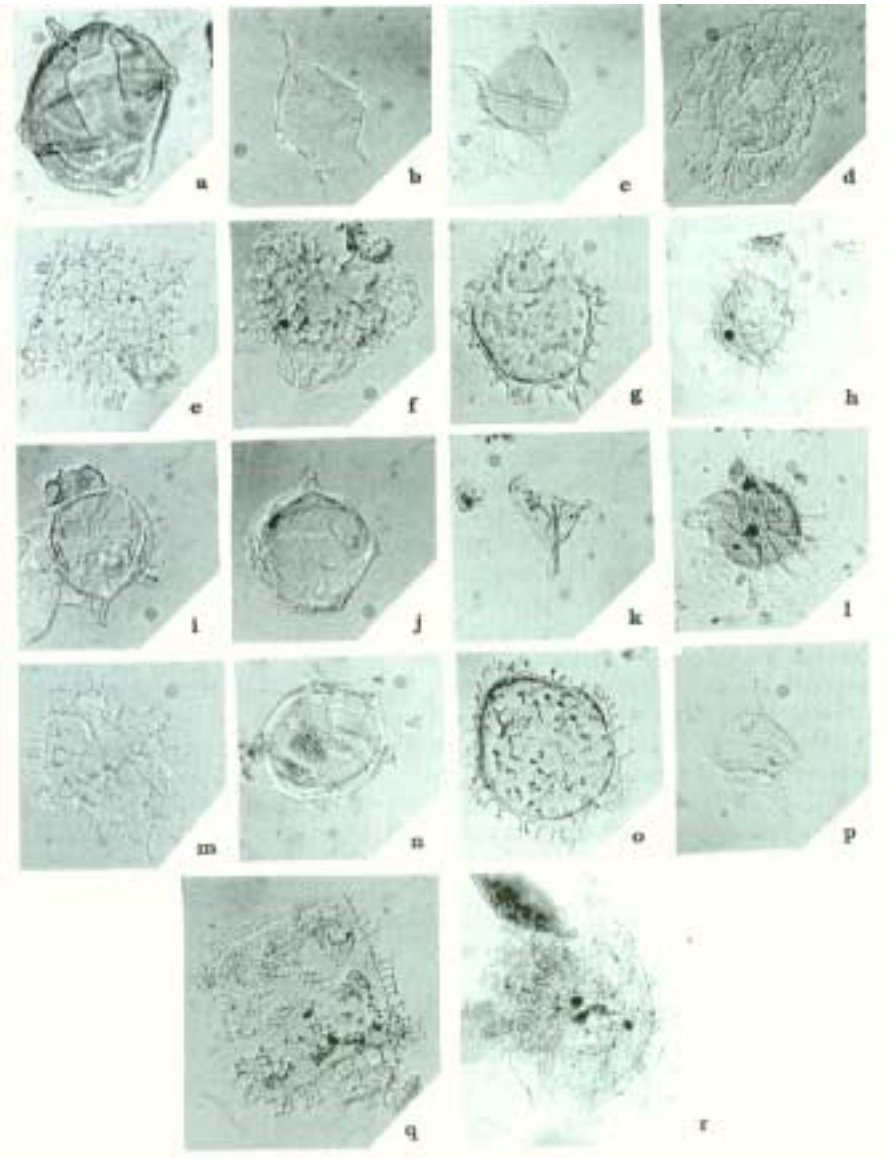

Figure 8. Selected Tertiary dinoflagellates used in hydrostratigraphic correlation. All figures are 500 x. (reduced 25% for reproduction): (a) *Carpatelia cornuta* Grigorovich 1969; (b) *Senegalinium ?dil"nense* (Cookson and Eisenack) Stover and Evitt 1978; (c) *Senegaliniurn bicavaturn* Jain and Millepied 1973; (d) *Adnatosphaeridium multispinosum* Willianis and Downie 1966; (e) *Wet- zelialia articulate* Eisenack 1938; (f) *Glaphyrocysta ?vicina* (Eaton) Stover and Evitt 1978; (g) *Dracodinium* sp.; (h) *Apectodinium homomorphum* (Deflandre and Cookson) Harland 1979; (i) *Pentadinium goniferum* Edwards 1982; *(i) Samlandia chlamydophora* Eisenack 1954; (k) Palaeotetradinium minusculum (Alberti) Stover and Evitt 1978; *(1) Hafniasphaera septata* (Cook- son and Eisenack) Hansen 1977; (m) *Wetzelielia cf. W. aiticulata* Eisenack 1938; (n) *Pentadinium laticinctum* Gerlach 1961; (c)) *Wetzelielia* sp.; (p) *Lentinia sp.; (q) Chariesdowniea variabilus* (Bujak) Lentin and Vozzhennikova 1989; (r) *Damassadinium californicurn* (Drugg) Fensome et al., 1993.

Notes

Methodology and Interpretation of the Piezocone Penetrometer Test Sounding for Estimating Soil Character and Stratigraphy at the Savannah River Site

Frank H. Syms, Bechtel Savannah River, Inc.
Douglas E. Wyatt, Westinghouse Savannah River Company
Greg P. Flach, Westinghouse Savannah River Company

PREFACE

Experience with the Piezocone Penetration Test (CPT) technology, and site-specific correlations developed at the Savannah River Site (SRS), have resulted in a methodology that makes the CPT a viable tool for geologic mapping. This methodology has evolved through the collective interest and contributions of numerous investigators. This paper will review the test equipment as well as present ongoing research for interpretation of upper Coastal Plain sediments at the SRS using the CPT.

INTRODUCTION

The piezocone penetration test (CPT) has become a common tool for subsurface characterization at the Savannah River Site (SRS) due to the cost and quality benefits of the technology. In the last 8 years, over 800 CPT soundings have been pushed for various geotechnical, environmental and geologic investigations (Figure 1). Many of these soundings reach depths greater than 60 meters providing a vast amount of data for the middle and upper Eocene (and younger) sediments. Use of the CPT for geologic mapping has evolved from gained experience, proven reliability and correlation capabilities of the technique. Because the CPT was originally developed for engineering applications, the technology was not broadly exposed to geologists until its use became more common on environmental projects in the late 1980's. The increased use and popularity of the CPT can be attributed to several qualities including:

- Standard equipment and test procedure
- Depth control on the scale of centimeters
- Multiple measurement parameters
- Highly repeatable, nearly continuous, electronic data
- Depth of penetration
- Cost effectiveness

Direct correlation of CPT measurements to stratigraphic units within the upper 60 meters at the SRS has been demonstrated on numerous investigations (Ref WSRC, 1994, WSRC, 1995, Wyatt, et al, 1997). Several investigations at the SRS beginning in the early 1990's, used closely spaced CPT soundings and soil borings for local stratigraphic correlation. From this data, it became evident that CPT measurements can be used not only for determining local

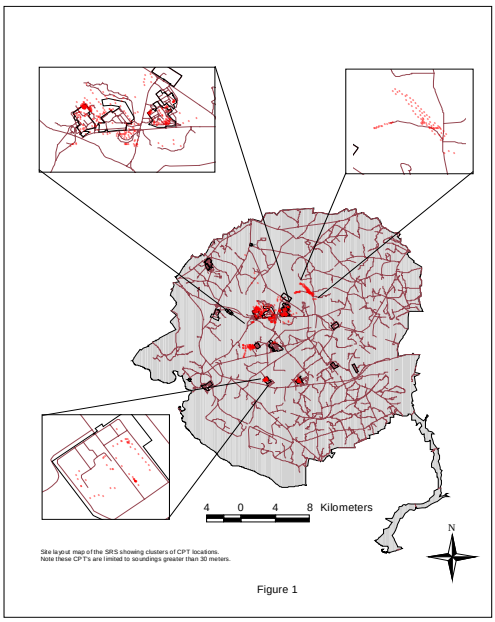

Figure 1. Distribution of CPT soundings around the SRS.

subsurface layering, but also to describe other geologic characteristics of the sediments such as vertical sedimentation sequences and facies distribution. This paper discusses the standard

CPT equipment in use at the SRS as well as proposed methods of geologic interpretation.

TEST METHOD AND EQUIPMENT

The first generation CPT's were developed in the 1930's for investigating the bearing strength of fairly shallow, loose, sensitive soils native to Holland. These early mechanical tools eventually evolved into the electro-mechanical devices in use today. The test equipment and procedures in use at the SRS are controlled by American Standard Test Method (ASTM) D5778, Standard Test Method for Performing Electronic Friction Cone and Piezocone Penetration Testing of Soils.

The CPT discussed here is a quasi-static, electro-mechanical probe that measures three separate parameters with depth (see Figure 2). These include tip resistance (q_c), sleeve resistance (f_s) and pore pressure (u). A fourth parameter, friction ratio (R_f) is computed by dividing the sleeve friction by the tip resistance and multiplying by 100. Measurements are acquired at roughly 1 second intervals. At a penetration rate of about 2cm per second, a vertical resolution of about 2cm is achieved. Forces are sensed by load cells and a pressure transducer. Data are transmitted from the probe assembly via a cable running through the push rods to the data acquisition system at the surface. The analog data are digitized and recorded by computer in the penetrometer truck. The typical CPT test rig used at the SRS consists of a hydraulic load frame mounted on a heavy truck with the weight of the truck providing the necessary reaction mass (see Figure 3).

INTERPRETATION OF CPT DATA

Interpretation of CPT data is similar to methods used for down-hole geophysical logs i.e., measurements can be related to some characteristic of the sediment. For the SRS, the relative amount of fine grained soils (fines content) is the most useful for engineering and hydrogeologic mapping. The vertical resolution of CPT provides well defined boundaries where changes in lithology may be inferred. Discrete sedimentation sequences such as fining or coarsening sequences may also be defined.

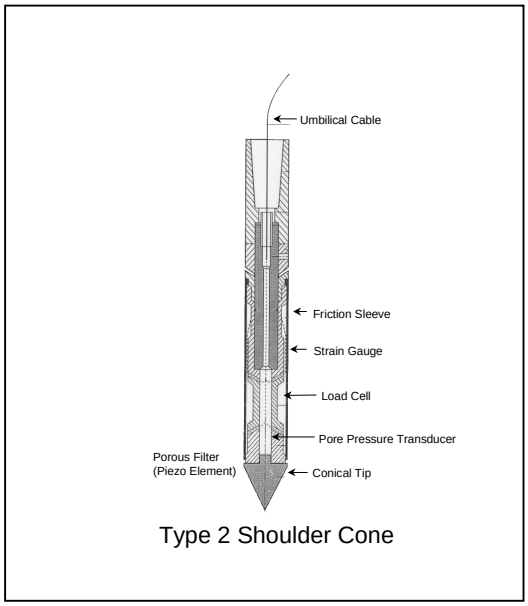

Figure 2. Type 2 Shoulder Cone CPT probe.

Basic CPT Response Characteristics

Each sensor on the CPT probe provides a separate measurement of the soil properties as the probe is being advanced. In general, tip resistances are relatively higher in sands and decrease as the fines content increases. The tip resistance is considered to be one of the most reliable CPT parameters. Inversely, sleeve resistances are relatively lower in sands and increase as the fines content increases. Sleeve resistances are acquired over larger surface areas behind the tip and are considered to be less reliable and of lower resolution. Pore pressures are lower in sands and higher in finer grained soils due the higher transmissivity of sands. The pore pressure element measures an induced pressure as the probe is advanced and is referred to as a dynamic pore pressure. Therefore, in finer grained sediment, the induced pressures will tend to be higher and dissipate slower than a

more porous (sandy) sediment. These relationships have shown that as a general rule, friction ratio increases as fines content and plasticity increase (Lunne, et al, 1997). As shown in Figure 4, fines content results from sieve analysis plotted against friction ratio values support this general trend, however there is significant scatter in the data. These CPT characteristics are general but provide a fundamental basis for data interpretation although numerous exceptions can be demonstrated for SRS soils.

Several published CPT soil classification charts have been developed based on theoretical relationships as well as empirical data. However, many factors influence CPT measurements resulting in inconsistent performance of these charts for SRS soils. An understanding of the influences that can affect the measurements is required for proper interpretation.

Factors Affecting CPT Measurements

Several factors can affect CPT measurements and should be considered before interpreting the data. Several of these

Figure 3. Typical CPT rig used at the SRS.

factors have been mitigated at SRS by standardizing the type of CPT probe used, calibration requirements, and data acquisition and processing parameters. However, other affects from geologic conditions such as layer transition, aging, cementation, weathering, consolidation and in-situ state of stress, may result in variations in the CPT measurements that if not corrected for, will result in misleading

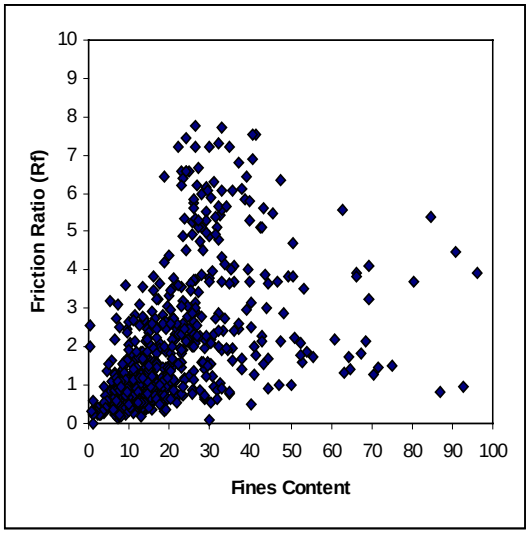

Figure 4. Friction ratio versus measured percent fines.

interpretations. Experience and familiarity with the CPT, as well as understanding the subsurface conditions of the site, is paramount to assessing data quality. One selected reference which discusses these affects as well as methods of interpretation is Lunne, et al, (1997).

Applicability of Soil Classification Charts

The most common classification chart parameters use the relationship of tip resistance (q_t) and friction ratio (R_f) to predict a soil type. The most recent charts use these parameters normalized for stress effects (Q_t and F_r) as well as normalized pore pressure (B_q).

An evaluation of 11 published CPT soil classification charts using high quality CPT soundings paired with adjacent soil borings demonstrated inconsistent predictions of soil type for SRS sediments. Figures 5 and 6 show the distribution of sieve test results correlated to adjacent non-normalized and normalized CPT measurements, respectively. Indicated on these charts, however, is the tendency of quite different fines contents to co-populate areas on the charts. This demonstrates that the

relationship of these CPT parameters for predicting a soil type is not unique. This is likely due to various subsurface conditions as discussed previously. The degree of this issue varies for all classification charts but is most prominent for soils that have moderate to significant ratios of fines to sand-sized constituents.

Soil type alone does not provide adequate resolution of sediment gradation to be useful for interpreting sedimentation sequences and sequence boundaries. Therefore, a method to predict gradation (sand versus fines content) directly from CPT measurements has been developed from site-specific correlations at the SRS.

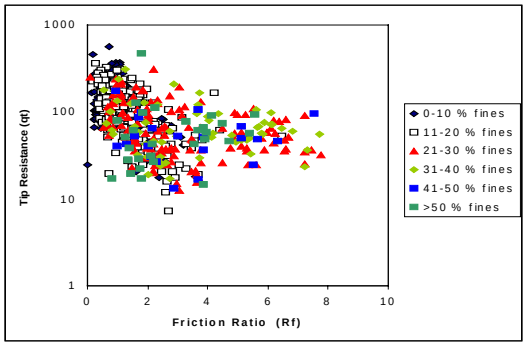

Figure 5. Fines content distribution plotted against correlating non-normalized CPT measurements.

RESULTS

Proposed Method for Estimating Gradation Changes from the CPT

To interpret sedimentation sequences from CPT measurements requires a method to relate the CPT measurements to changes in gradation. Closely spaced (nominal 10 feet) CPT soundings combined with soil borings have been used to develop a site-specific relationship between fines content (defined as the combined percent by weight of silt and clay passing a No. 200 mesh sieve) and CPT measurements (Q_t and F_r). This allows resolution vertical gradation trends for SRS sediments.

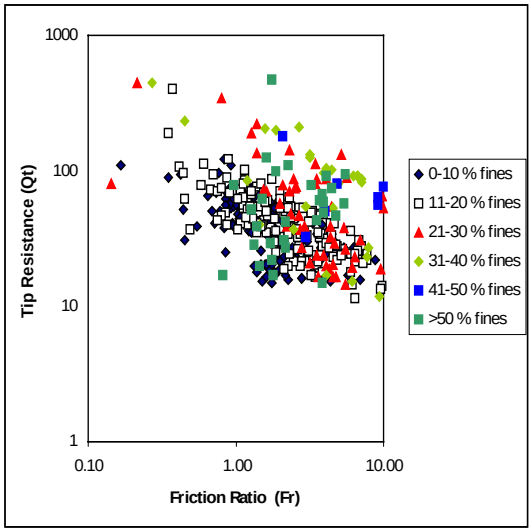

Figure 6. Fines content distribution plotted against correlating normalized CPT measurements.

The basis for this approach follows a methodology suggested by Robertson and Fear (1995). Two baseline equations, presented below, for estimating a Classification Index (Ic) and ultimately fines content (FC) (Jefferies and Davies, 1993 and Robertson and Fear, 1995, respectively) were modified using data acquired from the CPT and soil boring pairs.

$$Ic=[(3.47-\log Qt)^2+(\log Fr+1.22)^2]^{0.5}$$

From Ic:

$$FC\%=1.75Ic^3-3$$

Where: $Q_t=(q_t-\sigma_{vo})/\sigma'_{vo}$
$F_r=[f_s/(q_t-\sigma_{vo})]X100\%$
σ_{vo} - Total overburden stress
σ'_{vo} - Effective stress

Significant improvement was achieved by developing stratigraphic specific relationships. Currently, three modified equations are proposed for each layer and are discussed below. However, these equations are currently being re-evaluated based on additional data and analytical techniques.

Stratigraphic Interpretation and Prediction of Gradation Trends

The high vertical resolution, repeatability and multi-parameter measurements of the CPT make it an ideal stratigraphic mapping tool for unconsolidated sediments. One of the primary uses and advantages of the CPT is defining subsurface layering of the investigation site (Schmertmann, 1978 and Robertson and Campanella, 1988). Figure 7 shows a cross-section developed from CPT soundings. The high vertical resolution of the CPT is obvious but more importantly the continuity of measurements (repeatability) between penetrations is what makes the technique useful for subsurface mapping.

Figure 8 represents a CPT sounding and adjacent soil boring. Also shown on this figure is a fines content profile produced from the stratigraphic Ic and FC equations. Measured fines content values determined from sieve test results from the adjacent soil boring are plotted for comparison.

SRS Stratigraphy

Altamaha

As shown on Figure 8, the upper portion of the profile represents the Altamaha Formation. This unit consists of massive clayey sands with varying amounts of fine and coarse-grained sediments, but typically contains a moderate to high amount of fines (greater than 30 percent).

The CPT response can be described as moderate to high tip (50-300 tsf) and sleeve (2-5 tsf) resistances and a resulting high friction ratio (3 percent or greater). High pore pressures are noted as well even though the groundwater table is much deeper. These CPT responses are typical for overconsolidated soils, a known condition of the Altamaha (Ref WSRC, 1995). The overconsolidated state tends to yield higher sleeve friction values than would be expected for corresponding high tip resistances. This can also account for the high pore pressures as well.

The proposed equations for the Altamaha are as follows:

$$Ic_A=[(3-\log Qt)^2+(\log Fr+1.5)^2]^{0.5}$$
$$FC_A=(1.75(Ic)^{3.5})-6$$

Tobacco Road/Dry Branch

As shown on Figure 8, the middle portion of the profile corresponds to the Tobacco Road and Dry Branch. These units consist of normally to slightly overconsolidated clayey/silty sands with most of the clay bound as matrix material. Fines content of the Tobacco Road typically range from low to moderate (5-25 percent). The Dry Branch fines content is generally less than the overlying Tobacco Road Formation yet the occurrence of clayey beds are more massive and can form confining units locally.

This unit can be distinguished from the overlying Altamaha by the reduced sleeve resistance and pore pressure measurements. CPT measurements can be described as moderate tip resistances (100-300 tsf) where increasing resistance with depth can be noted. Sleeve resistance is generally low to moderate (1-2 tsf). Friction ratios are uniform and relatively low except where higher values result from decreases in tip resistances. Pore pressure response is generally moderate (at, or slightly above, hydrostatic pressure) with higher measurements noted in zones with higher friction ratios.

The proposed equations for the Tobacco Road/Dry Branch are as follows:

$$Ic_{TD}=[(2-\log Qt)^2+(\log Fr+1.7)^2]^{0.5}$$
$$FC_{TD}=(1.75(Ic)^{3.5})$$

Santee/Tinker

The lower portion of the profile consists of the Santee/Tinker as shown on Figure 8. This portion of the section represents one of the most lithologically complex units in the shallow subsurface of the SRS. These sediments were deposited under near shore

marine environments resulting in varying amounts of carbonate bearing sediments. Cementation and/or dissolution have occurred irregularly throughout this unit. The Santee can be described as silty to clayey fine sands.

CPT measurements can be described as low to high tip resistances (20-300 tsf) and moderate to high sleeve resistances (2- 4 tsf). Friction ratios are moderate to high (2-4 percent) in low tip resistance intervals and low (1-1.5 percent) in high tip resistance intervals. Pore pressure measurements are generally erratic but are high in the high friction ratio intervals and around or slightly below hydrostatic in the high tip resistance intervals.

Proposed equations for the Santee/Tinker are as follows:

$$Ic_S=[(1.5-\log Qt)^2+(\log Fr+1.7)^2]^{0.5}$$

$$FC_S=(1.75(Ic)^{3.5})-1$$

Recommended Approach to Estimating Fines Content

1. Care must be taken to assure the CPT measurements are consistent for a given site. This requires a subjective review of the data to assess the reported q_t, f_s, R_f and u measurements.

2. The CPT data must consist of piezocone measurements with proper input for the groundwater table. The data must be normalized as specified in the I_c equations.

3. Specific stratigraphic layers (Altamaha, Tobacco Road, Dry Branch, Santee) must be defined where CPT measurements show similar characteristics (refer to the discussion of shallow stratigraphy and CPT measurements). Different relationships should be expected in different parts of the SRS.

4. The application of the proposed Ic equations are for guidance and must be adjusted based on site specific sieve data.

5. For a given site, the continuity of stratigraphic CPT layers must be assessed and used as guidance to determine reasonable sample intervals and locations to verify the Ic equations.

SUMMARY AND APPLICATION

The CPT provides many advantages for subsurface mapping. However, interpreta-tion of the data requires an initial understanding of the subsurface conditions and testing parameters. Correlation with adjacent soil borings has provided a means to estimate gradational trends directly from CPT data. This is a significant advancement for engineering and hydrogeologic applica-tion.

The ability to better predict the amount of fines can be used to quantitatively describe subsurface units. In the case of hydrogeologic mapping, units can be mapped definitively as more fine grained (less transmissive) or more sandy (more transmissive). For engineering application, more compressible (fine grained) units can be distinguished from more less compressible (sandy) units. Also, the ability to estimate a fines content allows a Unified Soil Classification System (USCS) soil type be assigned.

ADVANCEMENTS AND FUTURE TRENDS

One recent advancement in CPT technology used at the SRS is the CPT sampler. In soft intervals where traditional drilling techniques have generally failed in recovery of such soft materials, the CPT sampler has proved repeatedly to have a nearly perfect recovery rate. Another advancement being tested for application is down-push video. Several soundings on site have been pushed using cameras with various focal lengths providing magnified images with on-screen scales. Down-push geophysical logs (resistivity and natural gamma) coupled with the standard CPT measurements are becoming standard test suites. Environmental probes are numerous and include water and gas samplers as well as

in-situ characterization/detection systems. Use of the CPT will continue to grow not only for environmental and engineering characterization and will become an additional tool for geologic mapping in unconsolidated sediments.

REFERENCES AND SELECTED BIBLIOGRAPHY

Jefferies, M.G., Davies, M.P., 1993, "Use of the CPTu to Estimate Equivalent SPT N_{60}", Geotechnical Testing Journal, GTJODJ, Vol. 16, No. 4, December, pp 458-468.

Lunne, T., Robertson, P.K., and Powell, J.J.M.,(1997) "Cone Penetration Testing in Geotechnical Practice", Blackie Academic and Professional, U.K.

Robertson, P.K., Fear, C.E., 1995, "Liquefaction of Sands and it's Evaluation", IS TOKYO 95, First International Conference on Earthquake Geotechnical Engineering, Keynote Lecture, November.

Robertson, P.K., and Campanella, R.G., (1983a) "Interpretation of the Cone Penetrometer Test; Part I: Sand." Canadian Geotechnical Journal, 20(4). 718-733.

Robertson, P.K., and Campanella, R.G., (1983b) "Interpretation of the Cone Penetrometer Test; Part II: Clay." Canadian Geotechnical Journal, 20(4). 734-745.

Robertson, P.K., and Campanella, R.G., (1988) "Guidelines for Geotechnical Design using the CPT and CPTU." University of British Columbia, Vancouver, Dept. of Civil Engineering, Soil Mechanics Series 120.

Schmertmann and Crapps, Inc. (1988) "Guidelines for using the CPT, CPTU and Marchetti DMT for Geotechnical Design. Volume II – Using CPT and CPTU Data." PB88-211644.

U.S. Dept. of Transportation, (1992) "The Cone Penetrometer Test", Pub. No. FHWA-SA-91-043.

WSRC (1994), "Geological Characterization in the Vicinity of the In-Tank Precipitation Facility," WSRC-TR-94-0373, Rev. A, October.

WSRC (1995) "In-Tank Precipitation (ITP) and H-Tank Farm (HTF) Geotechnical Report," WSRC-TR-95-0057, Rev. 0, September.

Wyatt, D.E., Cumbest, R.J., Aadland, R.K., Syms, F.H., Stephenson, J.C., and Sherrill, J.C., 1997, Investigation on the Combined Use of Ground Penetrating Radar, Cone Penetrometer and High Resolution Seismic Data for Near Surface and Vadose Zone Characterization in the A/M Area of the Savannah River Site, WSRC-RP-97-0184.

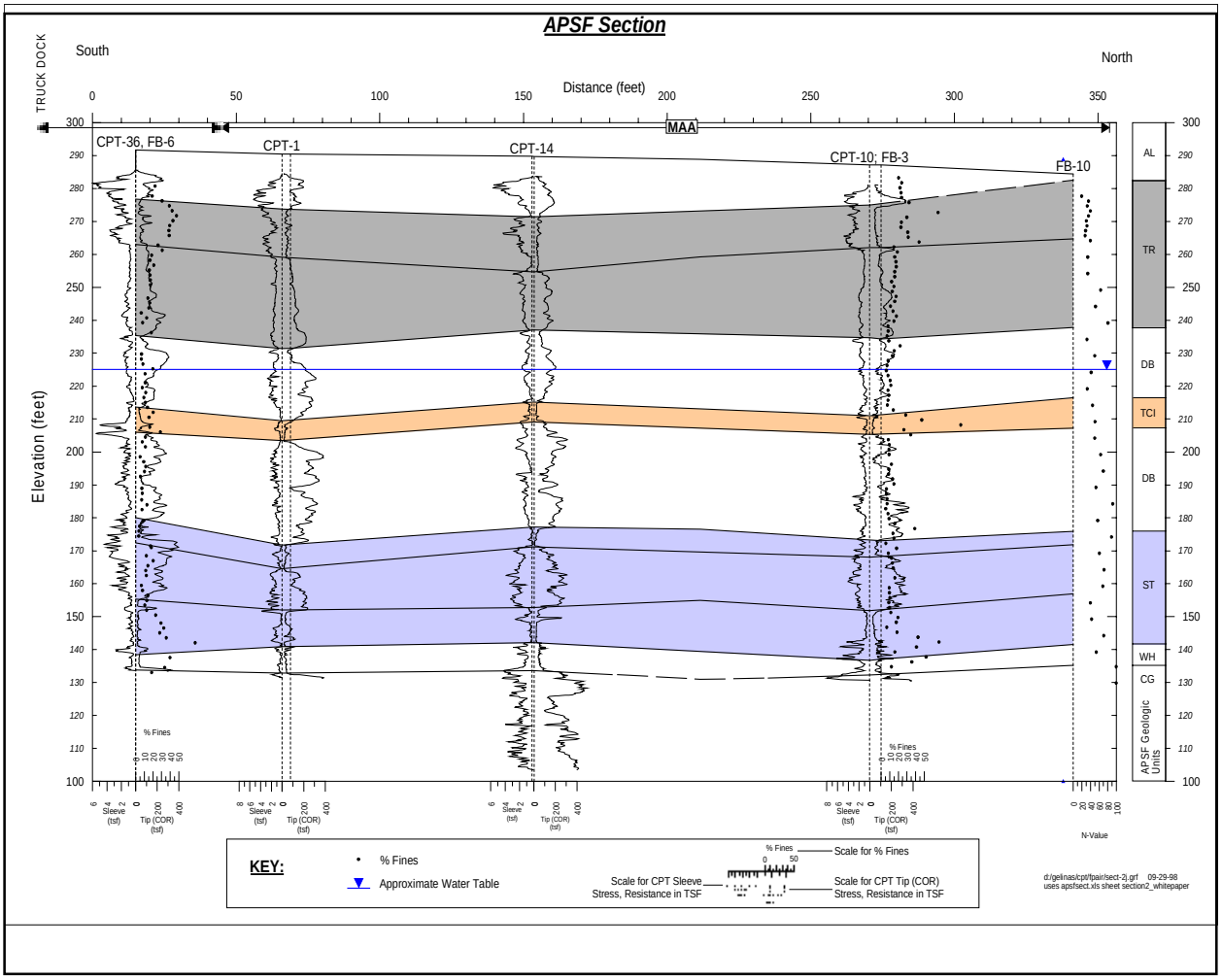

Figure 7. Cross-section constructed from CPT soundings. Note the continuity and repeatability of measurements. The plotted parameters include CPT tip resistances to the right of the axis with sleeve resistances plotted inversely to the left. Also, fines content values determined from sieve tests from adjacent borings are plotted along the tip resistances. The stratigraphic column on the right denotes the Altamaha (AL), Tobacco Road (TR), Dry Branch (DB) including the Tan Clay Interval (TCI) and Santee (ST).

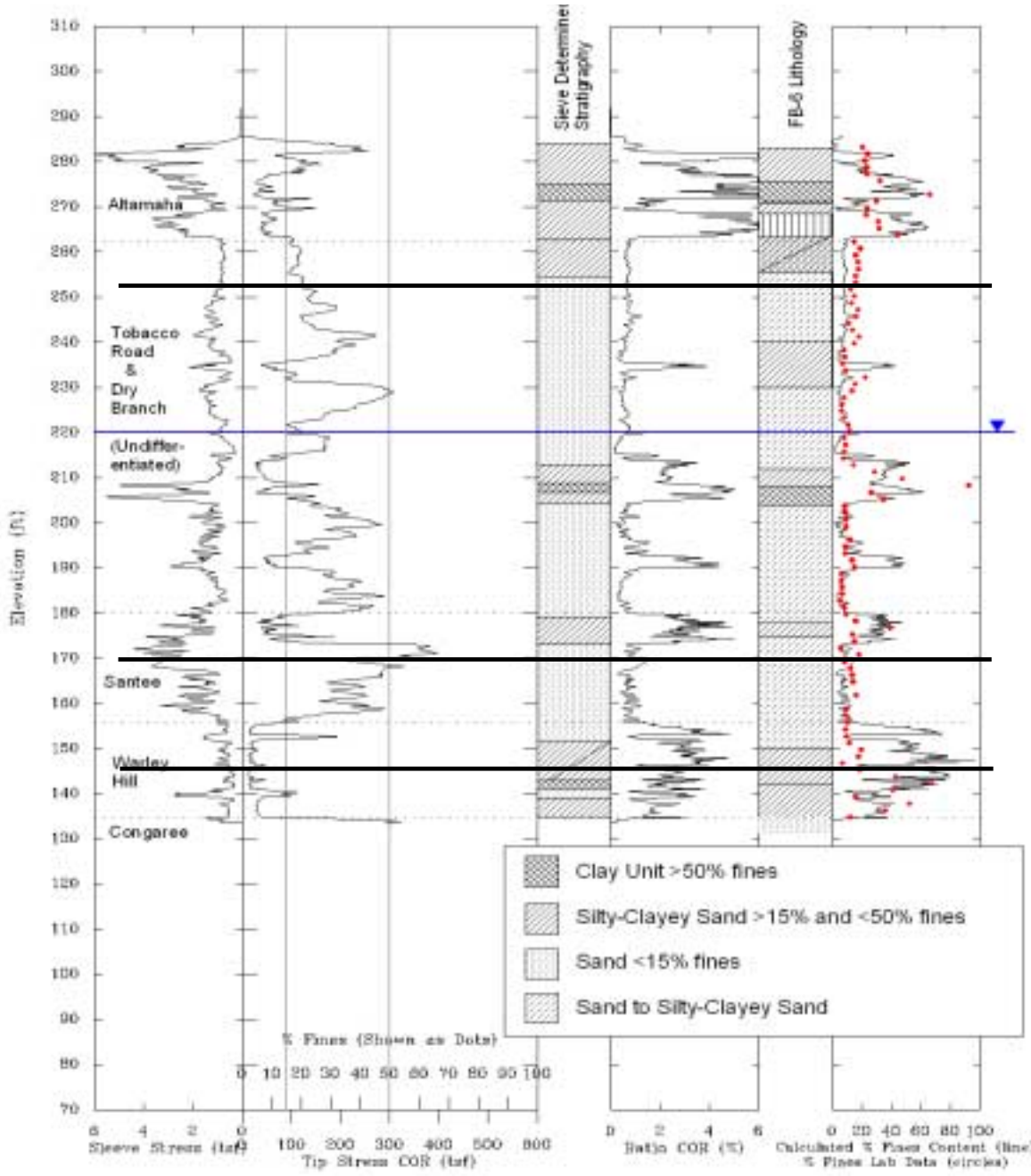

Figure 8. CPT sounding profile with adjacent boring data. Note the sharp breaks at stratigraphic boundaries. Fines content values determined from sieve tests are plotted as red dots. A calculated fines content curve was generated from applying the proposed Ic and FC equations.

Notes

Contaminant Transport and Hydrologic Properties of Fault-Propagation Folds in Poorly Consolidated Coastal Plain Sediments

R. J. Cumbest and D. E. Wyatt, Westinghouse Savannah River Co., Aiken, SC 29808

INTRODUCTION

The Atlantic margin Coastal Plain at regional scales is commonly characterized as a thin, seaward thickening wedge of poorly consolidated sediments that overly rigid crystalline, and indurated sedimentary rocks. Primary structure in the Coastal Plain sedimentary cover is characterized by a gentle (a few degrees) seaward dip. In many cases and certainly at regional scales this is an accurate and useful approximation. However, it has previously been recognized that locally the sediments of the Coastal Plain record secondary structure due to tectonic deformations that are primarily shallow expressions of high angle faulting in the underlying rigid basement rocks (Howell and Zupan, 1974; Prowell and O'Connor, 1978; Prowell, 1983, York and Oliver, 1976; Cramer and Arden, 1978; Bramlett and others, 1982, Mixon and Newell, 1982; Prowell, 1988, Domoracki, 1995). Because of the way the basement deformation is partitioned in the poorly consolidated Coastal Plain sedimentary sequence, recognition of this deformation in the near surface is difficult and in some cases may be so subtle as to require high resolution techniques that image most of the cover sequence and possibly the basement surface itself. This is because the high angle faulting in the rigid basement rocks is propagated as a discrete offset only in the lower parts of the sedimentary package. Above this the structural deformation is accommodated by fault-propagation folding, which by the time it reaches the surface may result in dip anomalies of only a few degrees. These relatively minor deformations in the shallow section would be extremely difficult to recognize in near surface geologic characterizations such as those commonly performed in most environmentally related studies. However, these relatively small deformations may have significant effects on both hydrologic behavior and contaminant migration properties of Coastal Plain sediments. In consequence, recognition and careful characterization of these near surface expressions of Coastal Plain faulting may be extremely useful in designing effective and efficient remediation efforts in settings where these types of structures are present.

Fault Propagation Folding in Loosely Consolidated Cover above High Angle Basement Reverse Faults

Fault-propagation folding has been analyzed and discussed by Mitra, 1993, Narr and Suppe, 1994, and McConnell, 1994. McConnell, 1994, described several general characteristics (Fig. 1) of fault-propagation folds based on extensive field observations:

(1) Fold axial surfaces intersect faults at or near the basement cover contact and diverge up-section.

(2) Fold hinges are typically narrow and angular but may become more open up-section.

(3) Heterogeneous thickness changes result in thickening in syncline hinge zones and thinning of forelimbs adjacent to anticline axial planes.

(4) Foot wall synclines are typically preserved so that faults cut steep fold forelimbs or are located near anticline axial planes.

McConnell (1994) also developed a kinematic model for the geometry and evolution of these structures that gives quantitative relationships for the major geometric elements. In particular, McConnell (1994) gives the

following relationships, which are important to this discussion:

$$\gamma_s=\tan^{-1}[1/(2\cot \alpha - \cot \gamma_a)] \quad (1),$$

relates the exterior angle of the foot wall syncline axial surface (γ_s) to the exterior angle of the hanging wall anticline axial surface (γ_a) and the dip of the fault (α).

$$\beta =\tan^{-1}[H/(u \cot \gamma_s - u \cot \gamma_a - H \cot \alpha)] \quad (2),$$

gives the angle of inclination of any un-faulted bed as a function of the structural relief on the basement surface (H), the distance above the basement surface (u), and the exterior angles of the axial surfaces and the fault.

$$T_h/T_o = \sin \gamma_{a'}/\sin \gamma_a \quad (3)$$

$$T_f/T_o = \sin \gamma_{s'}/\sin \gamma_s \quad (4)$$

relate the relative thickness changes of faulted units in the hanging wall (T_h/T_o) and foot wall (T_f/T_o) to the interior and exterior inter-limb axial angles (γ_a), ($\gamma_{a'}$), (γ_s), and (γ_s'). These equations can be powerful tools for predicting specific geometric elements of fault-propagation folds based on their inter-limb angles or other easily measured parameters. In addition, McConnell (1994) gives the following relationship between the length to displacement ratio for the fault, defined as relative stretch (ε_r), and the inter-limb angles:

$$\varepsilon_r = (\sin \gamma_{a'} \sin \gamma_s)/(\sin \gamma_a \sin \gamma_{s'}) \quad (5).$$

Small values of relative stretch indicate that the fault tip has migrated a relatively small distance up-section relative to the total amount of basement offset and that most of the total strain is being accommodated by folding ahead of the fault tip. This type of behavior would be expected from loosely or unconsolidated material. In contrast, large values of relative stretch would indicate significantly larger fault tip migration relative to total offset and would be indicative of stronger materials that could not accommodate significant strain by folding before failure by faulting.

Examination of the above equation (5) shows that values of relative stretch are minimized, as the divergence of the axial surfaces is maximized, that is as ($\gamma_{a'}$) and (γ_s) are made smaller as (γ_a) and ($\gamma_{s'}$) are forced to 90 degrees. This in effect forces open the angle between the hanging wall anticline and foot wall syncline axial surfaces and allows deformation to be spread over larger horizontal distances with consequent smaller strain gradients and minimization of energy. However, this effect is mitigated by the thickening of the fold limbs. Note from equation (4) that minimizing (γ_s) causes severe thickening in the foot wall syncline. This means that the angle of divergence of the axial surfaces will be a competition between minimization of the relative stretch and resistance to thickness changes of the fold limbs. In effect the angle between the hanging wall anticline and foot wall syncline axial surfaces are indicative of the material strength. Stronger materials will resist thickness changes of the fold limbs and show little axial surface divergence. In contrast, weak materials, such as loosely or unconsolidated sediments, will allow thickness changes easily and will seek to minimize energy by exhibiting relatively open axial surfaces.

Note that equation (1) may be rearranged to give:

$$\alpha = \tan^{-1}[2/(\cot \gamma_s + \cot \gamma_a)] \quad (6)$$

which relates the dip of the basement fault to the exterior angles of the axial surfaces. For the special case of a vertical basement fault (γ=90 degrees) the exterior angles of the axial surfaces are constrained to be complementary angles resulting in a symmetrical structure. This indicates that for relatively steep basement faults (γ_a) may become greater than

90 degrees particularly in weak materials such as unconsolidated sediments.
Seismic reflection imaging of Coastal Plain sediments located above steeply dipping reverse basement faults (Fig.2) often show characteristics that closely approximate those discussed above (see Fig. 1). Distinct offset is typically observed at the basement surface but dies out up section. Above the fault tip deformations in the shallower parts of the section are accommodated, at least at larger scales, by fault propagation folding. This folding can be characterized as a monocline with steeply dipping limbs directly above the fault tip that progressively show less dip up section. The axial surfaces of the hanging wall anticline and foot wall syncline diverge upward and are relatively open resulting in deformation occurring over a large horizontal area. In addition the exterior angles observed for the hanging wall axial surfaces of these structures are typically near vertical or greater than 90 degrees with very open folding. These characteristics are all indicative of fault-propagation folding in unconsolidated to loosely consolidated sediments.

Potential Hydrologic and Contaminant Transport Properties of Fault-Propagation Folds

The addition of regional dip to the relatively simple geometry exhibited by a typical fault-propagation fold (Fig. 4) has potentially significant consequences for the hydrologic and contaminant transport properties exhibited by the local stratigraphy. These consequences are critically dependant on the way that the faulting and folding is accommodated at small scales. Below the fault tip in the lower part of the section where significant offset of stratigraphic units may occur potential hydrogeologic effects include, damming resulting from juxtaposition of impermeable confining layers against more permeable units (Fig. 4) or connection of previously isolated aquifers by moving one opposite the other. The potential for both of these situations is enhanced by the heterogeneous strains experienced by the hydrogeologic units in the forelimbs of the foot wall syncline and hanging wall anticline as expressed in equations (3) and (4).

In the shallower section, above the fault tip potential hydrogeologic effects are more complicated and dependent on the failure properties of the confining units (i.e. clays). If the confining lithologies respond to the folding in a completely plastic mode then it is feasible that the confining units will retain their competency and no connection will occur between the aquifers. However, if the confining units exhibit some component of brittle failure and develop open fractures to a significant degree then it is likely that their confining properties will be compromised.

The interaction between the elevation changes in confining units resulting from fault-propagation folding and potentiometric surfaces may also result in subtle localized hydrologic effects. Areas where the potentiometric surface is below a particular confining unit will exhibit “downward head” relative to the confining unit. However, in the vicinity of the foot wall syncline, where the confining unit is lower in elevation due to folding, the confining unit will drop below the potentiometric surface and locally an “upward head” condition will be observed. In the shallow parts of the stratigraphic section where inter-limb fold angles of only a few degrees are present this local “head reversal” condition could be very enigmatic if the fault-propagation folding were not recognized.

The localized dip anomalies resulting from fault-propagation folding may also have profound effects on the migration behavior of dense non-aqueous phase liquids (DNAPL, Fig. 5) since the migration of these materials is to a significant degree gravity controlled. If the DNAPL source is up regional dip these materials will have a tendency to migrate down dip and pool in the trough formed by the foot wall syncline. Again, however, the subsequent migration behavior will depend in large part on the failure mode exhibited by the

material comprising the confining units. If the folding is accommodated completely by plastic deformation the confining units probably will fully retain their confining properties and the DNAPL will remain above the confining unit. In this case as long as the DNAPL does not fill the synclinal trough and spill over the lip formed by the hanging wall anticline it will remain localized or at least channeled down the trough. However, if the folding of the confining units results in open transmissive fractures, particularly in the hinge zone of the synclinal trough then it is likely that the DNAPL will migrate through the confining unit below and into the lower aquifers. In this scenario since the strains experienced by the confining units in the lower parts of the section due to the fault-propagation folding are larger it is likely that the DNAPL will migrate down section through the hinge zones of the foot wall syncline to the first competent unit. , probably the basement. Note however that at this point the dam formed by the high angle reverse offset will effectively stop any continued down dip movement.

More complicated scenarios may be envisioned when the hydrologic effects and migration properties of fault-propagation structures are combined. It may be entirely feasible in hanging wall synclines in which open fracturing has compromised confining units to have DNAPL contaminants migrating down section while at the same time groundwater migrates up-section due to the localized “head reversal” effect. This could lead to a plume of dissolved component significantly down hydrologic gradient from the structure in spite of the fact that the free phase is effectively localized by the fault-propagation fold structure.

DISCUSSION AND CONCLUSIONS

Deformation of poorly to unconsolidated Coastal Plain sediments resulting from non-vertical high angle reverse faulting in rigid basement rocks typically is expressed as fault-propagation folding in the shallower part of the stratigraphic section. The local dip anomalies associated with this type of structure and the behavior of confining units may have significant effects on local hydrologic behavior and contaminant transport properties depending upon the details on the failure mode that accommodates the folding in the confining lithologies. In the deeper section below the fault tip where significant offsets are recorded by geohydrologic units, damming may occur where less permeable units are juxtaposed against more permeable units. Or connection between aquifers may occur due to the offset. These phenomena will be amplified due to the thickening and thinning of geohydrologic units in the forelimb of the structure.

In the shallower section above the fault tip where deformation of the section is accommodated by fault-propagation folding more subtle effects may be observed. If the folding is accompanied by open fracturing of the confining units then connection between aquifers may occur. However, even if the confining units fail completely in a plastic mode and retain their integrity localized “head reversals” may occur due to the interaction of local dip anomalies and potentiometric surfaces.

Localized dip anomalies will also affect the migration of contaminants such as DNAPL, which move primarily down gravitational gradients. For a scenario in which confining units retain their integrity DNAPL will migrate down regional dip and pool in the trough formed by the footwall syncline. In scenarios in which the confining units are compromised by open fracturing DNAPL will likely migrate down section along the axial surface of the footwall syncline to the lowest uncompromised confining unit which in the most extreme case will be the rigid basement. However at this location migration will be arrested by the dam formed by the up-thrown side of the high angle reverse fault. In both cases migration pathways and pooling areas may be predicted based on the locations of the

axial surfaces of the fault-propagation fold. Since these pooling areas will be areas of DNAPL concentration knowledge of this behavior in detail may lead to extraction points that result in highly effective and efficient remediation system design. Also, since groundwater could migrate up-section while at the same time DNAPL is flowing down section plumes of dissolved component may be present at large distances from the free phase in spite of the fact that the free phase is localized by the structure.

It should be noted that for typical basement offsets recorded for the Atlantic Coastal Plain (i.e. < 100ft.) shallow section dip anomalies will be very subtle (on the order of a few degrees) and difficult to recognize especially by conventional borehole techniques. For instance shallow boreholes that sample only the upper part of the fault-propagation fold will show the enigmatic effect that the closer the boreholes are together the less apparent offset that they record. The shallow section is also very difficult to image with high resolution geophysical techniques such as reflection seismic profiling. However reflection profiling in most cases can image the intermediate and deeper parts of the section in addition to the basement surface offset to indicate the presence of fault propagation folding. If the geometry of the structure can be determined in the deeper section the geometries of shallow stratigraphic units may be effectively calculated using previously determined kinematic models for these structures. This interpretation technique may be used to explain unusual “head reversals” or used to design efficient contaminant remediation systems.

REFERENCES

Bramlett, K.W., Secor, D.T. Jr., and Prowell, D.C. (1982) The Belair fault: A Cenozoic reactivation structure in the eastern Piedmont. Geological Society of America Bulletin, v.93, p.1117.

Cramer, H.R., Arden, D.D Jr. (1978) Faults in Oligocene rocks of the Georgia Coastal Plain. Geological Society of America Abstracts with Programs, v.10 p.166.

Domoracki, W.J. (1995) A geophysical investigation of geologic structure and regional tectonic setting at the Savannah River Site, South Carolina. Ph.D. Dissertation, Virginia Polytechnic Institute and State University, Blacksburg, Va. 236pp.

Howell, B. B., Zupan, A.W. (1974) Evidence for post-Cretaceous tectonic activity in the Westfield Creek area, North of Cheraw, South Carolina. Geologic Notes, South Carolina State Development Board, v.18, p.98-105.

McConnell, D. A., (1994) Fixed-hinge, basement involved fault-propagation folds, Wyoming. Geological Society of America Bulletin, v.106 (12), pp. 1583-1593.

Mitra, S. (1993) Geometry and kinematic evolution of inversion structures. The American Association of Petroleum Geologists Bulletin, v.77 (7), p.1159-1191.

Mixon, R.B., Newell, W.L. (1982) Mesozoic and Cenozoic compressional faulting along the Atlantic Coastal Plain Margin, Virginia. In Central Appalachian Geology NE - SE Geological Society of America Field Trip Guide Books, P.T. Lyttle (ed) American Geological Institute.

Narr, W., Suppe, J. (1994) Kinematics of basement-involved compressive structures. American Journal of Science, v.294, p802-860.

Prowell, D.C., O’Connor, B.J. (1978) Belair fault zone: Evidence of Tertiary fault displacement in eastern Georgia. Geology, v.6, p.681-684.

Prowell, D.C. (1983) Index of faults of Cretaceous and Cenozoic age in the eastern U.S. U.S. Geological Survey Miscellaneous Field Studies Map, MF-1269.

Prowell, D. C. (1988) Cretaceous and Cenozoic tectonism on the Atlantic Coastal Margin. in The Geology of North America, v. I-2 The Atlantic Continental Margin: US. Geological Society of America.

York, J.E., Oliver, J.E., (1976) Cretaceous and Cenozoic faulting in Eastern North America. Geological Society of America Bulletin, v.87, p.1105-1114.

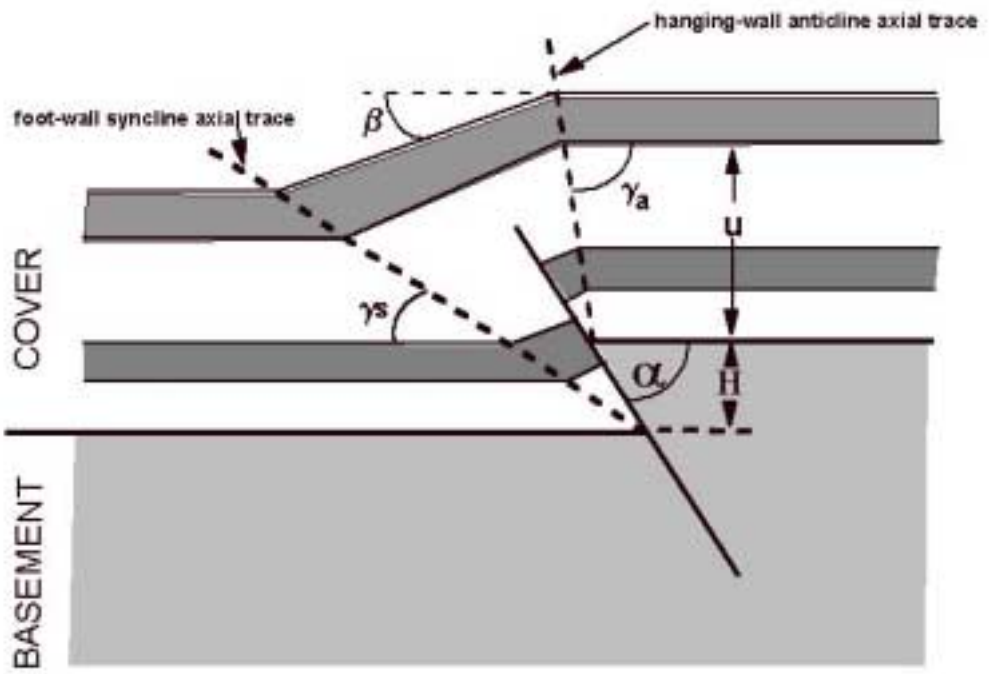

Figure 1. Geometric elements of fault-propagation fold kinematic model (after McConnell, 1994). (a & β dip of fault surface; ($\gamma_a + \gamma_{a'}$): anticline inter-limb angles; ($\gamma_s + \gamma_{s'}$): syncline inter-limb angles; (U): dip of unfaulted bed; (H): structural relief on basement surface; (u): elevation above basement surface; (T_o): thickness of undeformed beds; (T_f): thickness of faulted bed in syncline forelimb; (T_h) thickness of faulted bed in anticline forelimb.

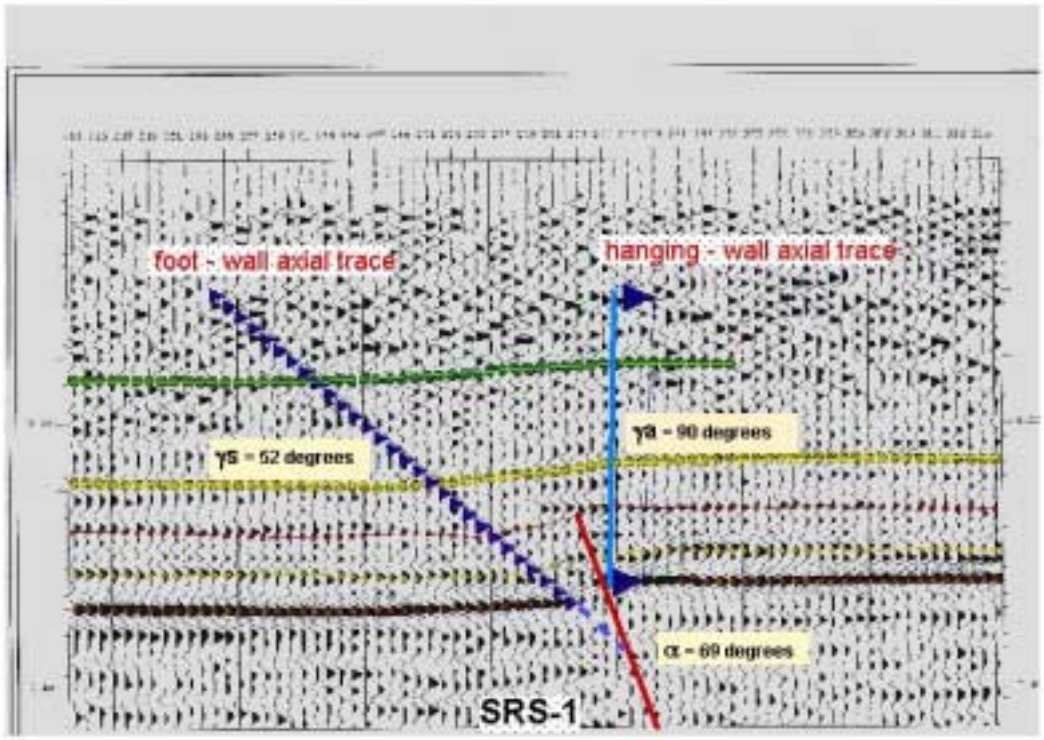

Figure 2. Seismic reflection profiles across the Crackerneck fault (a) in the Coastal Plain of South Carolina (Domoracki, 1995). Events corresponding to basement surface and other geologic units in cover sequence annotated in addition to the axial surfaces of the foot wall syncline and hanging wall anticline.

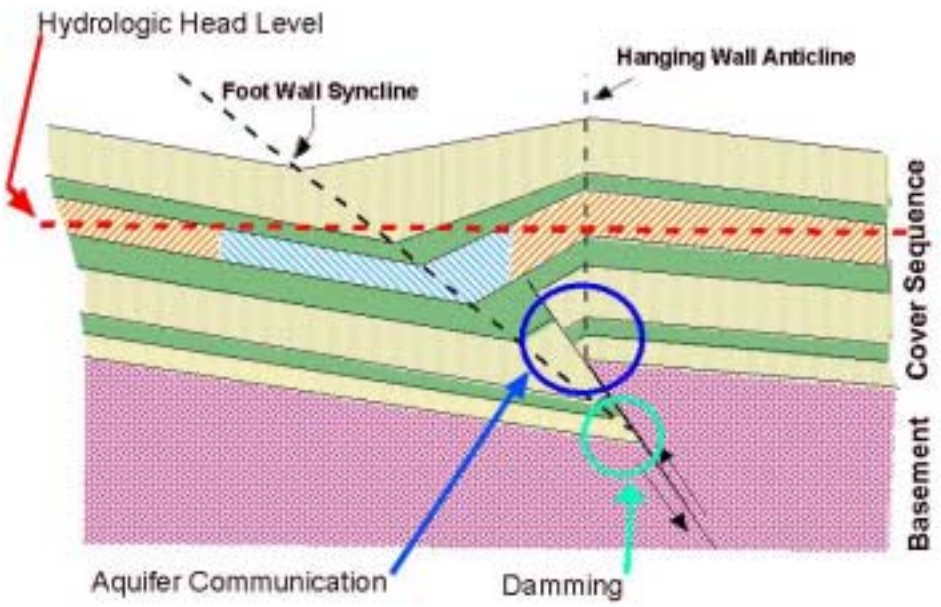

Figure 3. Fault-propagation fold with regional dip. Potential hydrogeologic effects illustrated. A local condition of "upward head" may occur relative to the confining unit above the cross hatched area.

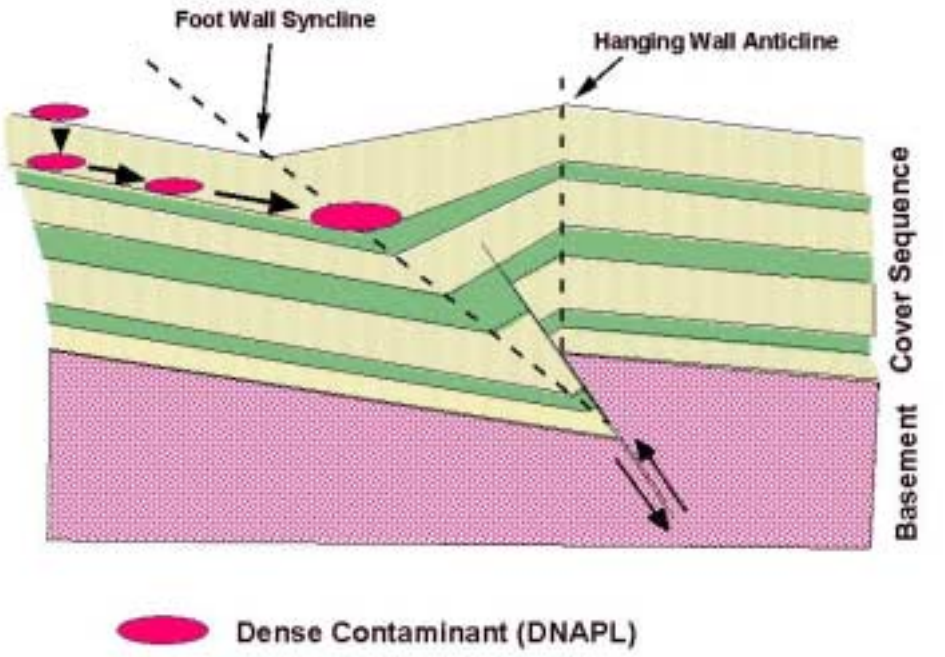

Figure 4. Fault-propagation fold with regional dip illustrating the probable behavior of DNAPL when confining unit integrity is not compromised.

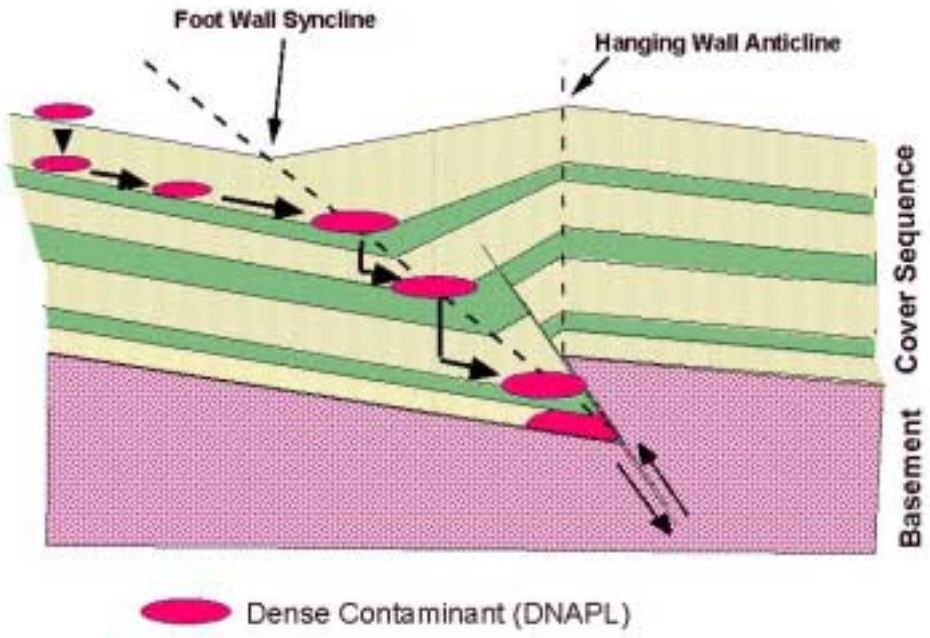

Figure 5. Fault-propagation fold with regional dip illustrating probable behavior of DNAPL if confining units are compromised.

Outline of the Geology of Appalachian Basement Rocks Underlying the Savannah River Site, Aiken, SC

Allen J. Dennis, Biology and Geology, University of South Carolina Aiken, Aiken SC 29801-6309
John W. Shervais, Department of Geology, Utah State University, Logan, UT 84322 and
Harmon D. Maher, Jr., Geology and Geography, University of Nebraska Omaha, Omaha, NE 68182-0199

INTRODUCTION

Basement core collected over a forty year campaign at the Savannah River Site and surrounding environs affords an unparalleled opportunity to observe Appalachian basement rock and its alteration during Mesozoic rifting and subsequent Tertiary tectonism. The structures that are preserved would surely not survive long at the earth's surface, and have the potential to change how we think about the history of Piedmont rock exposures we use for detailed bedrock geologic mapping. Remarkably no less than 5000m of core sample fault zones that have been intermittently active throughout the Phanerozoic. These fault zones acted as conduits for fluids throughout the Mesozoic and Cenozoic. Additionally, evidence presented here and elsewhere in this volume indicates that syn- and post-depositional faulting of the Tertiary section is fundamentally controlled by long-lived Appalachian structures.

The following short paper draws on our in press or submitted manuscripts for Geological Society of America Bulletin, American Journal of Science, and Geological Society of London treating the geochemistry and petrology of metamorphosed Neoproterozoic arc rocks underlying SRS, the Paleozoic structure of those rocks, and evidence for Mesozoic and younger fluid flow and pseudotachylyte generation. This work was supported by South Carolina Universities Research and Education Foundation contract 170.

We are grateful to Randy Cumbest, Sharon Lewis, Van Price, Doug Wyatt (all at Site Geotechnical Services for all or some fraction of the time this work was done), Tom Temples (at DOE during the time this work was done) for their assistance and support during the study. Josh Mauldin, Hampton Uzzelle, Lynda Bolton, John Harper, and Tom Creech assisted in this work.

Lithology

Greenschist to granulite facies metamorphosed volcanic arc rocks that underlie the Savannah River Site are divided, from northwest to southeast, by metamorphic grade, into the **Crackerneck Metavolcanic Complex**, **Deep Rock Metaigneous Complex**, and **Pen Branch Metaigneous Complex** (Fig. 1; Dennis and others, 2000, Shervais and others, 2000). The Crackerneck Metavolcanic Complex are the lowest grade rocks and comprise very weakly metamorphosed mafic and felsic tuffs, with relict lapilli. These are best observed in wells P30 and P6R (Fig. 2). Deep Rock Metaigneous Complex is made up of the Deep Rock Metavolcanic Suite and the DRB Metaplutonic Suite. Rocks of the Deep Rock Metavolcanic Suite are generally dark grey-green mafic metavolcanic rocks, "well-exposed" in DRB wells 2-7 at depths from ca. 1100' to ca. 1900'. These metavolcanic rocks are locally garnet-bearing, indicating amphibolite facies conditions. These rocks are cut by metamorphosed mafic and felsic dikes that locally preserve good primary textures. The DRB Metaplutonic Suite comprises metadiorite and (locally mylonitic) quartz diorite gneiss. In the DRB-1 where this rock is observed, a serrated contact between the diorite and well-foliated mafic metavolcanic rock is observed. Furthermore, deformation in the diorite is very heterogeneous and may be best described as thin, late stage anastomosing shear zones. The Pen Branch Metaignous Complex is

likewise made up of The Pen Branch Metavolcanic Suite and PBF Metaplutonic Suite. The Pen Branch Metavolcanic Suite is made up of distinctive layered (transposed) intermediate to mafic orthogneisses. These rocks are observed in PBF-7 between 2500-3500 where they are screens within the PBF Metaplutonic Suite, and between 3600-3648' (TD) in that well. Pen Branch Metavolcanic Suite is also observed in the Seismic Attenuation (SA) Core in spot cores between 1959' and 4002'. The PBF Metaplutonic Suite is best observed in PBF-7 and is a garnet-bearing granodiorite to granodiorite gneiss, locally with hornblende megacrysts. In that well it is heterogeneously deformed, with a locally intense K-metasomatic overprint. The variety of deformation and metamorphic textures in this unit, as well as the variability of the metasomatic overprint is displayed in PBF-7 2550'-3600'.

A schematic interpretation of the temporal or stratigraphic relations between these units is presented in Figure 3.

Dennis and others (1997) report U-Pb zircon ages and Sr and Nd isotopic data for the DRB Metaplutonic Suite and PBF Metaplutonic Suite. Dennis and others (1997) report U-Pb zircon crystallization ages of 625.1± 1.4 Ma (weighted mean $^{207}Pb/^{206}Pb$ dates of four size fractions) and 619.2 ± 3.4 Ma (average of $^{207}Pb/^{206}Pb$ dates from only two size fractions analyzed) for the PBF-7 granodiorite and DRB-1 diorite respectively. Neither sample showed evidence of inheritance. ε_{Nd} values for PBF-7 and DRB-1 rocks are 2.0 and 3.5 respectively (Dennis and others, 1997). DRB-1 tonalite yields a $^{87}Sr/^{86}Sr$ ratio of 0.701939. Sr isotopic systematics of PBF-7 granodiorite are significantly complicated by the addition of Rb during the pinking event discussed below, but a primary initial ratio of 0.703 may be estimated.

Based on the differences between Nd isotopes in PBF Metaplutonic Suite and DRB metaplutonic suite and *similarities* in REE chemistry (unpublished data, Dennis and others, 2000, Shervais and others, 2000) *between Pen Branch Metaigneous Complex, Deep Rock Metavolcanic Suite* and *differences* in REE patterns *between those two "units" and DRB Metaplutonic Suite* we interpret that The DRB Metaplutonic Suite may be faulted into a Pen Branch Metaigneous Complex-Deep Rock Metavolcanic Suite intrusive-extrusive complex. We interpret that this faulting may have occurred in Neoproterozoic time, and may have served to initially localize the Tinker Creek nappe.

Alleghanian (Pennsylvanian) Structure

A body of evidence supports a faulted overturned nappe limb as the likely contact between the Pen Branch Metaigneous Complex and Deep Rock Metaigneous Complex. The overturned nappe limb is called the Tinker Creek nappe, and the shear zone that "decapitates" the Tinker Creek nappe is called the Four Mile Branch fault. The name Four Mile Branch fault has been used previously in the SRS region to describe offsets of Tertiary strata by Wyatt and others (1996) and Harris and others (1997). We interpret the Tinker Creek nappe and Four Mile Branch fault to be Carboniferous in age based on the similarity of structural style with that observed in the exposed eastern Piedmont of South Carolina (e.g., Maher , 1987, Secor and others, 1986), supplemented by a single $^{40}Ar/^{39}Ar$ age (305±5 Ma) of a hornblende neoblast from these rocks reported by Roden and others (1996).

The evidence supporting the interpretation that the structure underlying the DRB (1-7) well array is an overturned nappe limb includes parasitic folds, chloritic slip surfaces and shear bands, and evidence of extensive transposition (Fig. 4). These data have been supplemented by P-T calculations based on garnet-biotite thermometry that support inferences based on map-scale petrology, and the seismic reflection processing of Domoracki (1995). These structures (Tinker Creek nappe - Four Mile Branch fault) controlled the location of the Triassic Dunbarton basin border fault. An

Andersonian (1951) analysis supports this interpretation. Tinker Creek nappe mesoscopic structures such as the chloritic slip surfaces were later reactivated as conduits for fluid flow (pinking event), gouge zones, and ultimately pseudotachylyte.

Mesoscopic structures that indicate nappe emplacement from southeast to northwest are abundant in DRB formation and include parasitic folds, chloritic slip surfaces and shear bands (Fig. 5). These structures are best represented in DRB well series, particularly in DRB-6. Mesoscopic folds interpreted to be parasitic have a down dip vergence that indicates an overturned limb geometry. The trailing limb of these mesoscopic folds has a dip of 50-60° typically (assuming that the core is vertical), and an overturned limb that is nearly horizontal. Interlimb angles are usually in the range of 30-60°. It can be shown that the axes of these folds are nearly horizontal. Most foliation dips are in the range of 40-60° in DRB formation; rarely are dips subhorizontal. There are also "floating" isoclinal fold hinges, intact isoclinal folds, and evidence for transposition within the DRB formation. Probably most of this isoclinal-transposed fabric records nappe deformation but some may record a Late Precambrian orogenic event.

Chloritic slip surfaces cross-cut parasitic, mesoscopic folds and transposed layering, and show hanging wall up offset. Chloritic slip surfaces have the same strike as foliation and almost always dip in the direction of foliation, but with a shallower dip, ca. 30-50° (Fig. 5g). A small fraction have the opposite dip. The surfaces range in thickness from less than 1 mm thick to 4 mm thick. Sense of offset across these features is consistently hangingwall up. The amount of offset can be up to several cm. Chloritic slip surfaces are separated by 2-10 cm. In DRB-6 are spectacular examples of down-dip vergent (overturned limb) parasitic folds cross cut by hangingwall up chloritic slip surfaces. The precise origins of the geometry of these surfaces and the chlorite along them are unclear, but are of considerable interest.

Mesocopic shear bands are present in both vertical and horizontal sections of core, and indicate hangingwall up, and dextral motion respectively. Horizontal sections of a few samples showed sinistral shear sense. It was not possible to discern overprinting relations of dip-slip and strike-slip shear bands. It may be simplest to intepret these structures as having formed during dextral tranpression that has not been partitioned spatially as it seems to be the case of the Irmo shear zone and Augusta fault (Secor and others, 1986; Maher and others, 1991).

Norian (Late Triassic) Metasomatism – "The Big Pink"

The Dunbarton Triassic basin (Marine, 1974; Marine and Siple, 1974) is one of a well studied array of basins described by Olsen and others (1991) related to opening of the present day Atlantic. The border fault rocks and fanglomerates of the northwestern margin of the basin are well exposed in coreholes PBF-7 and 8. Mesozoic and younger veining and alteration paragenesis are generally best expressed in these wells.

Pinking Event

The effects of a hydrothermal alteration ("pinking") event are widespread and heterogeneous in Pen Branch Metaigneous Complex and Deep Rock Metaigneous Complex. Hot waters with abundant dissolved silica, K and Al were responsible for metasomatic alteration along fracture surfaces and foliation planes. Hydrolysis of groundmass biotite in the PBF-7 granodiorite is interpreted to be the source of K^+; this phase is consistently altered to chlorite in the unpinked granodiorite. In DRB rocks, pinking is observed as zones typically less than 1 cm thick that reactivate chloritic fractures or quartz veining.

Pinking of the PBF granodiorite occurs as limited alteration proceeding along foliation planes with grain size reduction and nucleation of quartz and potassium feldspar

grains along the faces of potassium feldspar megacrysts parallel and adjacent to foliation planes. It is also observed as veins of alteration cross-cutting foliation. In pinked rocks, sericitization of plagioclase feldspars is observed, and these crystals appear to have a dusty coating in thin section. Microprobe analysis indicates that the An content of plagioclase is $\leq An_5$.

Pinking may occur along fractures in as a band less than 5mm thick, or as broad zones that affect ten's of meters of core (Fig. 6). The most spectacular location that this effect may be observed covers the range 3496' (box 167) - 3602' (box 173) in PBF-7, over which the rocks are completely pinked with less than 5% mafic minerals. The presence of garnet and altered hornblende megacrysts (altered to magnetite and pyroxene) in a felsic gneiss affirms that the protolith of these rocks was the PBF-7 granodiorite. These rocks are very hard and recrystallized as befits the silicification accompanying their alteration. Few later fractures crosscut this zone. Below this zone, there is no evidence of pinking, and the rock is a garnet amphibolite. Biotite and amphibole have not been chloritized.

An isocon diagram (Fig. 7; O'Hara, 1988, 1990; O'Hara and Blackburn, 1989; Grant, 1986, after Gresens, 1964) was prepared for the PBF-7 granodiorite. The construction of this diagram requires the ratio of major and trace element analyses for altered rock (pinked) and protolith (unpinked) be calculated, and scaled such that all ratios may be observed on a single plot. If a metamorphic or hydrothermal event is isochemical the ratios of analysed elements or oxides in the altered rock and protolith will equal 1 and lie along a line with a slope of 1. Deviations from a slope of 1 may suggest relative enrichment (>1) or leaching (<1). However if certain trace elements are immobile (e.g., Ni, Sc, Zr, Cr, Ti, V), then the line that passes through those elements' ratios on the isocon diagram may demark the boundary between leaching and enrichment in other elements. Using this logic, it is concluded that MnO, MgO, and to a lesser extent CaO are relatively depleted in the pinked rocks and K_2O, Na_2O, SiO_2, Rb, and to a lesser extent Al_2O_3 are enriched in the pinked rocks.

Pinking is observed to cross-cut different deformation-metamorphic facies of the PBF Metaplutonic Suite granodiorite and thus must postdate the event responsible for fabric differences. Kish (1992) reports a 2 point Rb-Sr isochron of 220±5 Ma (Norian) for a granite recovered from the C-10 borehole. Petrography and chemistry of this sample confirm that it has been pinked, and that it is similar to the PBF-7 granodiorite. The isochron is interpreted to date the pinking event in this area. That the pinking is most intensive in the PBF-7 well, and that the biotite (interpreted to be source of the K^+) is ubiquitously altered to chlorite in the PBF-7 granodiorite suggests that the Dunbarton Basin border fault was the conduit for the pinking event hydrothermal fluids. It is estimated that the temperature of the waters was low enough to allow chlorite and oligoclase to form.

Greening Event

A "greening" event postdates the pinking event. In crystalline rocks (particularly of the PBF-7 core) this event is recognized by epidote (and rare pyrite) veining that may cause local brecciation as the vein is injected. Epidote veins are generally 1 mm- 1 cm thick and fine-grained. The veins typically have the same strike as foliation, and dip steeply in the same direction (concordant), or in the opposite direction (discordant). The effects of the greening are, however, most spectacularly developed in Triassic fanglomerates of PBF-7 (Fig. 8; boxes 10-21, footage 1150-1330). The matrix of these conglomerates is no longer brick red but instead is a pale green, and an irregular white and grey rind (5mm to 1 cm thick) appears on oxidized gneiss clasts greater than 2-3 cm in diameter (Fig. 8). The alternating white and grey bands correspond to gneissosity in the oxidized clast, and interpreted to represent partially resorbed edges and the penetration of reducing fluids

along gneissosity. In box 10 it is apparent that shallowly dipping fractures (≤ 25° dip) control greening, and greening extends 1-10 cm away from these fractures. In boxes 13-18 this greening of conglomerate matrix is complete. Microprobe analyses of fibrous intergranular material (cement?) in the (PBF-7-16) matrix indicate that this is green muscovite. Locally this material contains fine disseminated pyrite.

Similar relations are observed in GCB-2-648' (Fig. 8). Here saprolitized Triassic fanglomerate is observed. The matrix comprises coarser grained white to creamy green material, while the clasts are finer grained (clayey) and brick red. The margins of these clasts are discernible as reduced ghosts in the matrix, while the clasts' reddish interiors have very highly irregular shaped that are again interpreted as the delimiting the extent of penetration of reducing fluids along foliation. In poorly sorted Cretaceous (?) sediments 30' above (GCB-2-615') the reduced fanglomerate, a clot of euhedral chalcopyrite grains 2.5 cm x 5 cm (long axis) parallel to bedding plane is recognized. It is unlikely that this (≥ 10 cm^3) euhedral sulfide clot is a detrital clast (in sand), and it is interpreted to record the greening event in Coastal Plain rocks.

The "greening" event indicates a flushing of reducing waters along Triassic basin border faults, that may be related to migration of hydrocarbons derived from Triassic sedimentary rocks (e.g., D. Richers, pers. comm.) The presence of chalcopyrite in rocks tentatively identified as Cape Fear, approximately 10 m above reduced clasts and matrix of a thin zone of preserved Triassic fanglomerate in GCB-2-648, suggests that this event postdates Cape Fear deposition (Coniacian). Differences in oxidation state between Cape Fear rocks and overlying red and yellow Middendorf Formation (?) sands indicate that the greening event occurred prior to Middendorf deposition in the Santonian (86.6-83.0 Ma). Furthermore the presence of reduced fanglomerate in GCB-2 suggests that a border fault of another Triassic sub-basin may lie in the the vicinity of the GCB-2 well.

Quartz Veining and Vuggy Quartz

Quartz veining, locally quite vuggy, cuts epidote veins in PBF-7 core. These veins are subparallel to epidote veins when crosscutting relations are observed. The veins generally have the same strike as foliation, and usually dip parallel to foliation or less commonly in the opposite direction. The veins can be irregular and not simple planar features. They are typically not more than 2 cm thick, but thick veins may present open vugs up to 7 mm lined with well terminated crystals. These vuggy veins are most notable below PBF-7-(box) 111-2662, and occur with irregular increasing frequency through box 163-3452', and then less frequently in completely pinked mylonite through 173-3602'. Thick veins may also contain cm-scale clasts of the variably pinked granodiorite gneiss they cut. Both these observations strongly suggest high fluid pressures in the vicinity of the Dunbarton Basin border fault during Late Mesozoic through Paleogene time.

Zeolite ± calcite

Zeolite ± calcite, locally euhedral, veins cut and locally fill vuggy quartz veins throughout DRB and PBF formations. These veins are subparallel to foliation as the epidote and quartz veining events, but may crosscut foliation. The zeolite is typically pinkish orange or less commonly white. Very commonly it forms radiating sprays, less than 2 cm in diameter, of euhedral crystals, less than 1 cm in length, on the fracture surface. Calcite is typically colorless and rarely forms euhedral blocky crystals.

Strike normal zeolite

Nearly vertical (75-90°), nearly "strike-normal" zeolite-filled fractures are very common in DRB and PBF formation rocks. Map view of individual core segments indicates that often the strike of veins is 15-20° clockwise of foliation dip direction rather than precisely strike-normal. The veins are typically less than 1 cm thick, and are filled with pinkish orange to white crystals. Some

veins show evidence of (considerable) indeterminate amounts of offset, but this offset must predate filling of fractures by large well-formed crystals.

Approximately strike-normal joint sets have been recognized in the eastern Piedmont of South Carolina during the course of detailed bedrock mapping by the authors (unpublished data; Bartholomew and others, 1997, Brodie and Bartholomew, 1997, Heath and Bartholomew, 1997). Assuming a regional strike of 065 it is estimated that the orientation of the "strike-normal" zeolite filled fracture set is 350-355°, and probably indicates an episode of approximately E-W extension, accompanied by minor strike-slip motion.

Understanding the timing of this motion is important for an understanding of Teritary regional kinematics; Dennis and others (2000) report an attempt was made to date these mineralized veins. These efforts were encouraged by the report of Secor *et al.* (1982, p. 6952) of the successful K-Ar dating of a strike-parallel (060) set of zeolites in the Carboniferous Winnsboro (SC) granite near the Virgil Summer nuclear station. The age reported is 45±5 Ma (South Carolina Electric & Gas Company 1977). This set is post-dated by a second zeolite array oriented 332 (approximately "strike normal" to regional strike, Secor *et al.* 1982, their fig 5c.) that shows several cm of oblique slip. Both sets are reported to be steeply dipping. Based on microprobe analysis, PBF-7 strike-normal zeolite crystals are laumontite-chabazite and have K in the range of 0.2 weight percent. A single 3 gram sample (PBF-7-139-3089) of handpicked (2mmx7mm) zeolite grains yielded a conventional K-Ar age of 22.9±1.5 Ma. This is considered to be a minimum age, because radiogenic Ar may have been lost from the system continuously or episodically since the crystals formed. Other strike normal zeolites from the SRS basement should be dated in an effort to push this minimum age back.

Pseudotachylyte

Over two dozen pseudotachylytes have been recognized in core (Fig. 9). The common characterstics of these features are 1) formation in a fine-grained intermediate to mafic protolith; 2) nucleation along pre-existing, thin chloritic slip surfaces; 3) evidence that suggests K-metasomatism along chloritic slip surfaces influenced pseudotachlyte generation, perhaps by reducing the melting temperature of chloritic gouge; 4) evidence for multiple events within a single pseudotachylyte vein; different events are recognized based on discrete banding of hydrated or devitrified vs. glassy or simply aphanitic matrix; 5) preservation of angular clasts at all scales; 6) mm scale teepee or injection structures that may penetrate the adjacent rock from 3 mm to 2 cm. It has generally not been possible to recognize the magnitude or sense of offset across the pseudotachylytes. Locally it has been recognized that presence of felsic layering within several cm of the chloritic slip surfaces may influence pseudotachylyte development; perhaps through a very local increase in differential shear stress.

Pen Branch fault

The Pen Branch fault has been described by Snipes and others (1993) and Stieve and Stephenson (1995, based on Domoracki, 1995). These authors recognized the Pen Branch fault as a surface across which the basement-coastal plain unconformity has been offset as much as 50 m (southeast side up) with offset of middle Eocene units decreasing to as little as 3-4 meters. The extent of control of the Pen Branch fault on outcrop patterns of the Upland unit, or surface drainages and the relative importance of strike slip motion along this fault system is a matter of some controversy (R.J. Cumbest, T.J. Temples, pers. comms.). Domoracki (his fig. 23, 1995) plots two recent hypocenters (6/1985 and 8/1988) on SRS line 1 on the basement fault above the Tinker Creek nappe, in the vicinity of the Pen Branch fault, at depths of .96 and 2.86 km respectively.

In our observations the Pen Branch fault cuts crystalline basement in PBF-7 between boxes 25 (1375') and 78 (2183'). Over this interval at least two intrusive units of granodioritic composition are hydrated and retrogressed so that they appear as chlorite schists. Deformation is highly heterogeneous, and several less completely retrogressed slices or lenses are preserved. The largest slice occurs between boxes 38-48, with a much smaller example at about 2078'. None of the previously described vein sets appear to crosscut the sheared, hydrated schists, while at least some are observed in the protolith. Evidence of the orthogneiss protolith is demonstrated by preservation of pink granitic vein arrays that maintain orientation in the retrogressed rock, and the presence of relict feldspar grains (porphyroclasts), up to 1 cm long. within the chloritic matrix. Gouge, breccia zones and chloritic fractures typically occur with 15-20° dips, parallel to foliation (ca. 45°) and steeply dipping (ca. 75°). Breccia zones, up to 10's of cm thick, and gouge zones, up to 2 cm thick, appear to nucleate on chloritic fractures Within 15 m of the fault zone, chloritic fracture surfaces are oxidized to a black hematite. At some locations these oxidized coatings are striated.

Pseudotachylyte and the Pen Branch fault are both interpreted to largely postdate strike-normal zeolite though both may extend back through the Mesozoic. That pseudotachylyte postdates the pinking event (220±4 Ma, Kish, 1990; Norian) is evinced by the observation of pseudotachylyte crosscutting rocks that have been visibly pinked. Microprobe analyses of pseudotachylyte glass and devitrified glass/chlorite grains show that in DRB formation mafic metavolcanic rocks with a bulk composition that is typically well below 4 weight % K_2O (Shervais and others, 2000), glass and devitrified glass compositions are typically in the range 8-12 weight % K_2O. This indicates the likelihood of pinking fluids altering chloritic vein material and adjacent mafic metavolcanic and subsequent reactivation of these chloritic slip surfaces as sites of pseudotachylyte generation.

In over two dozen observations there are only a couple instances of any crosscutting mineralized veins cutting pseudotachylyte. In one very thin (<1 mm) calcite vein cuts pseudotachylyte at an oblique angle (DRB-7-9-1419). In the second, it is clear that pseudotachylyte predates at least one zeolite mineralized fracture event. The pseudotachlyte (Fig. 9; PBF-7-89-3089) is an irregular brick red, oxidized, devitrified zone, greater than 1 cm thick that is subparallel to and crosscuts epidote and calcite + zeolite veins and includes clasts of mineralized veins within it. These clasts are less than 1 cm and and are visible at all microscope scales. The brick red, cherty appearance of the feature strongly suggests oxidizing fluids passed through a cryptocrystalline or glassy material. The relative timing of this event can only be said to be post-zeolite + calcite veining. The oxidizing fluids appear to predate the cross-cutting zeolite-filled fracture that is subparallel to the margin of the pseudotachylyte and "decapitates" (oxidized) teepees.

In the case of basement expression of the Pen Branch fault (250 m (800') over PBF-7- 25 through 78) it can be shown that this feature cross-cuts all mineralized veins including strike-normal zeolite. Intact mineralized fractures are not preserved in the interval PBF-7-25 through 78. Given the relative decrease in offset of Tertiary units in the Atlantic Coastal Plain cover (Snipes and others, 1993) above the expression of Pen Branch fault motion in the crystalline rocks, the retrogression of fault rock protolith and disruption of mineralized fractures and veins in bedrock is interpreted to have occurred from the Late Cretaceous through the Neogene.

CONCLUSIONS

Repeated episodic Phanerozoic reactivations of basement fault zones are documented in more than 5000m of basement core recovered from beneath the updip coastal underlying the US Department of Energy Savannah River

Site, near Aiken, South Carolina. Neoproterozoic (ca. 619 and 624 Ma) metadiorite and metagranodiorite rocks contain a heterogeneously developed, anastomosing mylonitic fabric and intrude foliated mafic metavolcanic rocks. At approximately 305 Ma, granulite facies orthogneisses were thrust over amphibolite facies metaigneous rocks on (northwest-vergent? and dextral) structures called the Tinker Creek nappe and Four Mile Branch fault. The overturned limb of the Tinker Creek nappe and Four Mile Branch fault control the location the border fault of the Dunbarton Triassic basin. The Dunbarton basin border fault region acted as a conduit for fluids in Mesozoic and Cenozoic time. Ca. 220±5 Ma, a potash and silica metasomatic event ("pinking" event) affected crystalline rocks throughout the SRS basement region. A "greening" event flushed highly reducing fluids through crystalline rocks, Triassic fanglomerates and affected rocks interpreted to be as young as Santonian (Cape Fear Fm.). Based on the occurrence of saprolite of fanglomerates affected by greening in core, the remains of a subbasin of the Dunbarton basin were identified in the northwest part of the site (GCB-2 well). A consistent vein paragenesis interpreted to to be Cretaceous and younger overprints the previous events and includes 1) locally vuggy quartz veins with the same strike as foliation, 2) zeolite ± calcite with the same strike as foliation, and 3) a near vertical strike-normal zeolite set. A conventional K-Ar age of a separate of euhedral, 2mm x 7mm zeolite grains from the last set yields an age of 22.9 ± 1.5 Ma, interpreted to be a minimium age. More than 30 pseudotachylytes are found throughout the metavolcanic terrane and are preferentially localized along Alleghanian age chloritic fractures dipping less steeply than foliation that have been “pinked.” In virtually every case, pseudotachylyte can be shown to post-date mineralized fractures. Thus, pseudotachylytes beneath SRS are likely no older than Mesozoic, and many are probably Tertiary in age. The Pen Branch fault is "exposed" in approximately 250 m of basement core between PBF-7-(box) 25-(footage) 1375 and PBF-7-78-2168. Most recent motion on this fault must postdate strike-normal zeolites, because the zone cross-cuts all mineralized fractures.

REFERENCES

ANDERSON, E.M. 1951. *The dynamics of faulting*. Oliver & Boyd, Edinburgh, 206p.

BARTHOLOMEW, M.J., HEATH, R.D., BRODIE, B.M., & LEWIS, S.E. 1997. Post-Alleghanian deformation of Alleghanian granites (Appalachian Piedmont) and the Atlantic Coastal Plain: *Geologic Society of America Abstracts with Programs*, **29/3**, 4.

BRODIE, B.M. & BARTHOLOMEW, M.J. 1997. Late Cretaceous-Paleogene phase of deformation in the Upper Atlantic Coastal Plain. *Geologic Society of America Abstracts with Programs*, **29/3**, 7.

CUMBEST, R.J., PRICE, V. & ANDERSON, E.E. 1992. Gravity and magnetic modelling of the Dunbarton Triassic basin, South Carolina. *Southeastern Geology*, **33**, 37-51.

DANIELS, D.L. 1974. *Geologic interpretation of geophysical maps, central Savannah River area, South Carolina and Georgia*. US Geological Survey, Geophysical Investigations Map, **GP-893**.

DENNIS, A.J. , WRIGHT, J.E. , MAHER, H.D., MAULDIN, J.C. & SHERVAIS, J.W. 1997. Repeated Phanerozoic reactivation of a Southern Appalachian fault zone beneath the up-dip coastal plain of South Carolina. *Geological Society of America Abstracts with Programs*, **29/6**, 223.

DENNIS, A.J., MAHER, H.D, SHERVAIS, J.W.,MAULDIN, J.C, & UZZELLE, G.H. 2000a. The role of fluid flow in basin-bounding faults and metasomatic transformation of basement: An example from the Mesozoic and Cenozoic deformation of a Neoproterozoic volcanic arc beneath the Atlantic Coastal Plain, Savannah River Site, South Carolina, USA, In: HOLDSWORTH, R.E. (ed) *Nature and tectonic significance of fault zone weakening*, *Geological Society of London Special Volume*, in press.

DENNIS, A.J. , WRIGHT, J.E. , MAHER, H.D., & SHERVAIS, J.W. 2000b. Neoproterozoic and Late Paleozoic deformation and metamorphism of a volcanic arc beneath the Atlantic Coastal Plain, Savannah River Site, South Carolina.*ms.*

DOMORACKI, W. J. 1995. *Geophysical Investigation of geologic structure and regional tectonic setting at the Savannah River Site*. Ph.D. thesis, Virginia Polytechnic and State University.

GRANT, J.A. 1986. The isocon diagram - A simple solution to Gresens' equation for metasomatic alteration. *Economic Geology*, **81**, 1976-1982.

GRESENS, R.L. 1967. Compostion-volume relationships of metasomatism. *Chemical Geology*, **2**, 47-55.

HARRIS, M.K., THAYER, P.A., & AMIDON, M.B., 1997, Sedimentology and depositional environments of middle Eocene terrigenous-carbonate strata, southeastern Atlantic Coastal Plain, USA. Sedimentary Geology, 108: 141-161.

HEATH, R.D. & BARTHOLOMEW, M.J. 1997. Mesozoic phase of post-Alleghanian deformation in the Appalachian Piedmont. *Geologic Society of America Abstracts with Programs*, **29/3**, 23.

KISH, S.A. 1992. An initial geochemical and isotopic study of granite from core C-10. *In:* FALLAW, W.C. & PRICE, V. (eds) *Geological Investigations of the central Savannah river Area, South Carolina and Georgia: Carolina Geological Society Guidebook*. South Carolina Geological Survey, Columbia, B-IV-1 - B-IV-4.

MAHER, H.D. 1987a. Kinematic history of mylonitic rocks from the Augusta fault zone, South Carolina and Georgia. *American Journal of Science*, **287**, 795-816.

MARINE, I.W. 1974. Geohydrology of buried Triassic basin at Savannah River Plant, South Carolina. *American Association of Petroleum Geologists Bulletin*, **58**, 1825-1837.

MARINE, I.W. & SIPLE, G.E. 1974. Buried Triassic basin in the Central Savannah River Area, South Carolina and Georgia. *Geological Society of America Bulletin*, **85**, 311-320.

O'HARA, K. 1988. Fluid flow and volume loss during mylonitization: An origin for phyllonite in an overthrust setting, North Carolina, U.S.A.. *Tectonophysics*, **156**, 21-36.

O'HARA, K. 1990. State of strain in mylonites form the western Blue Ridge Province, southern Appalachians: The role of volume loss. *Journal of Structural Geology*, **12**, 419-430.

O'HARA, K. & BLACKBURN, W.H. 1989. Volume-loss for trace-element enrichments in mylonites. *Geology*, **17**, 524-527.

OLSEN, P.E., FROELICH, A.J., DANIELS, D.L., SMOOT, J.P. & GORE, P.J.W. 1991. Rift basins of early Mesozoic age. *In:* HORTON, J.W., & ZULLO, V.A. (eds*) The Geology of the Carolinas*. University of Tennessee Press, Knoxville, 142-170.

PETTY, A.J., PETRAFESO, F.A. & MOORE, F.C. 1965. *Aeromagnetic map of Savannah River Plant area, South Carolina and Georgia.* US Geological Survey, Geophysical Investigations Map, **GP-489**.

RODEN, M.F., LATOUR, T.E., CAPPS, C., & WHITNEY, J.A. 1997. Incomplete metamorphic reequilibration in a metadiorite from the crystalline basement of Savannah River Site. *Geological Society of America Abstracts with Programs*, **29/3**, 65.

SECOR, D.T., JR. , PECK, L.S., PITCHER, D.M., PROWELL, D.C., SIMPSON, D.H., SMITH, W.A. & SNOKE, A.W. 1982. Geology of the area of induced seismic activity at Monticello Reservoir, South Carolina. *Journal of Geophysical Research*, **87**, 6945-6957.

SECOR, D.T., JR., SNOKE, A.W., BRAMLETT, K.W., COSTELLO, O.P. & KIMBRELL, O.P. 1986. Character of the Alleghanian orogeny in the southern Appalachians. Part I. Alleghanian deformation in the eastern Piedmont of South Carolina . *Geological Society of America Bulletin*, **97**, 1314-1328.

SHERVAIS, J.W., DENNIS, A.J. & MAULDIN, J.C. 2000. Petrology and geochemistry of a volcanic arc beneath the Atlantic Coastal Plain, Savannah River Site, South Carolina. *ms.*

SHERVAIS, J.W., SHELLEY, S.A., & SECOR, D.T. 1996. Geochemistry of volcanic rocks of the Carolina and Augusta terranes in central South Carolina. *In:* NANCE, R.D. & THOMPSON, M.D. (eds) *Avalonian and related peri-Gondwanan terranes of the circum-North Atlantic*. Geological Society of America, Boulder, Special Paper, **304**, 219-236.

SNIPES, D.S., FALLAW, W.C., PRICE, V., JR. & CUMBEST, R.J. 1993a, The Pen Branch fault: Documentation of Late Cretaceous-Tertiary faulting in the Coastal Plain of South Carolina. *Southeastern Geology*, **33**, 195-218.

SOUTH CAROLINA ELECTRIC & GAS COMPANY 1977. *Virgil C. Summer Nuclear Station Final Safety Analysis Report*, **2**. South Carolina Electric & Gas Company, Columbia.

SPEER, J.A. 1982. Description of granitoid rocks associated with two gravity minima in Aiken and Barnwell counties, South Carolina. *South Carolina Geology*, **26**, 15-24.

STIEVE, A. & STEPHENSON, D. 1995. Geophysical evidence for post-Late Cretaceous reactivation of basement structures in the central Savannah River area. *Southeastern Geology*, **35**, 1-20.

WYATT, D.E., WADDELL, M.G., and SEXTON, G.B. 1996. Geophysics and shallow faults in unconsolidated sediments. *Groundwater*, **34**, 236-334.

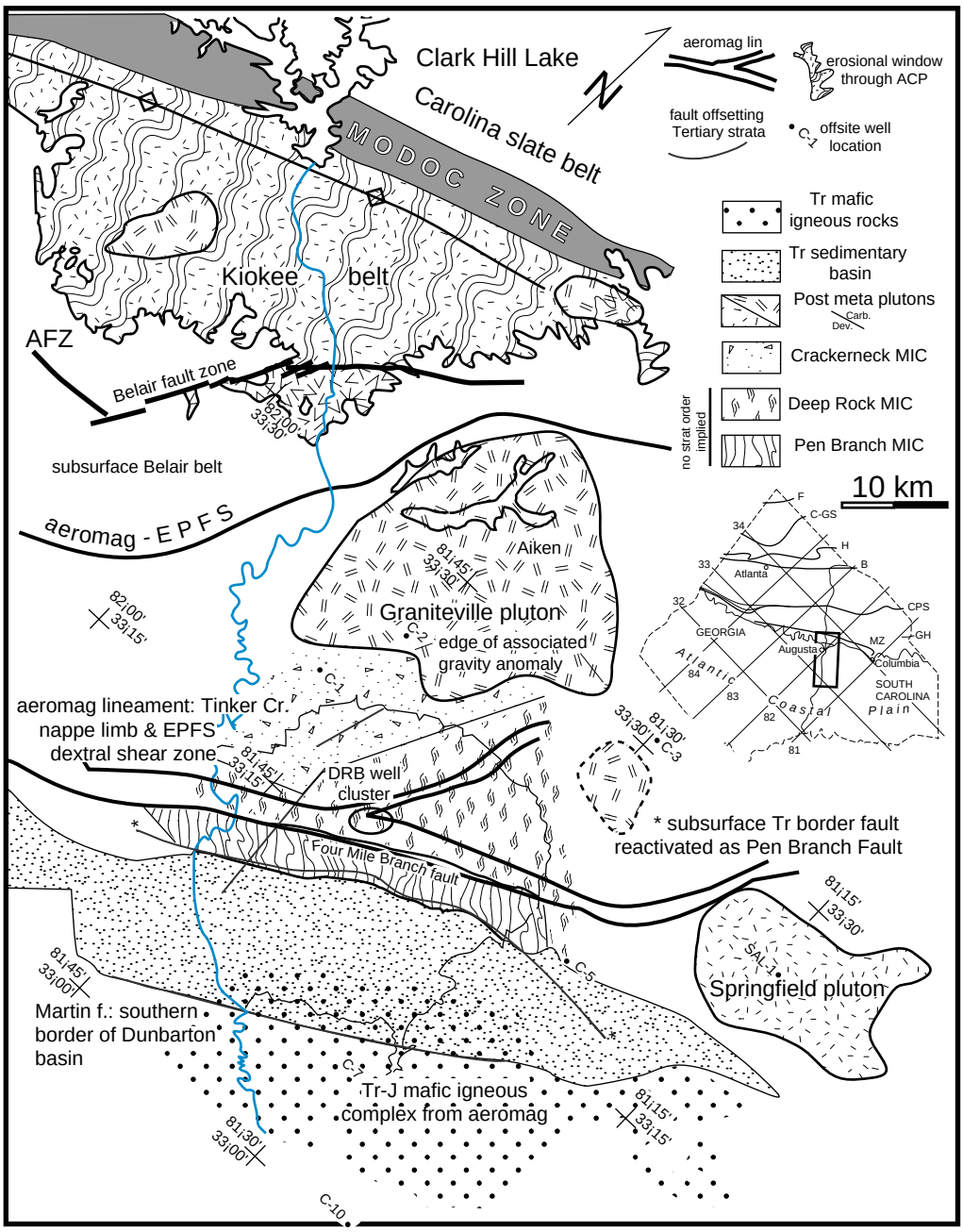

Figure 1. Eastern Piedmont of Georg-olina. Compiled from our work and interpreted from Petty *et al.* 1965, Daniels 1974, Speer 1982, Cumbest *et al.* 1992, and Snipes, pers. comm. Off-site C-wells and SAL-10 located on this map.

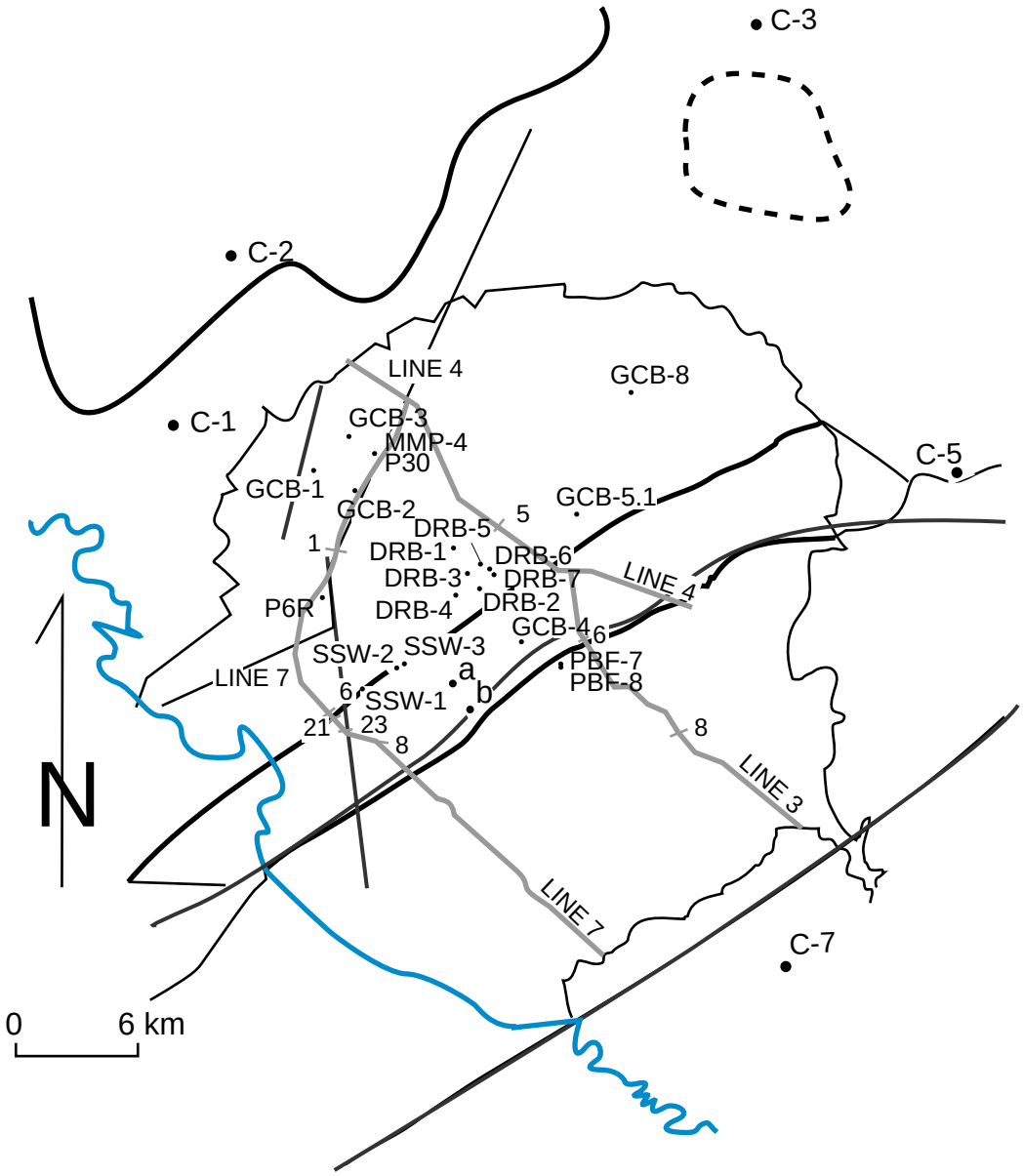

Figure 2. Index map showing location of cores used in this study, as well as location of Domoracki's (1995) seismic lines 3, 4, 7, and epicenters (a, 6/9/1985; b, 8/4/1988) plotted by Domoracki (his p. 23). Locations where other seismic lines cross Lines 3, 4, 7 are indicated: 1, 21, 8 cross line 7; 5 crosses line 4; and 6 and 8 cross line 3).

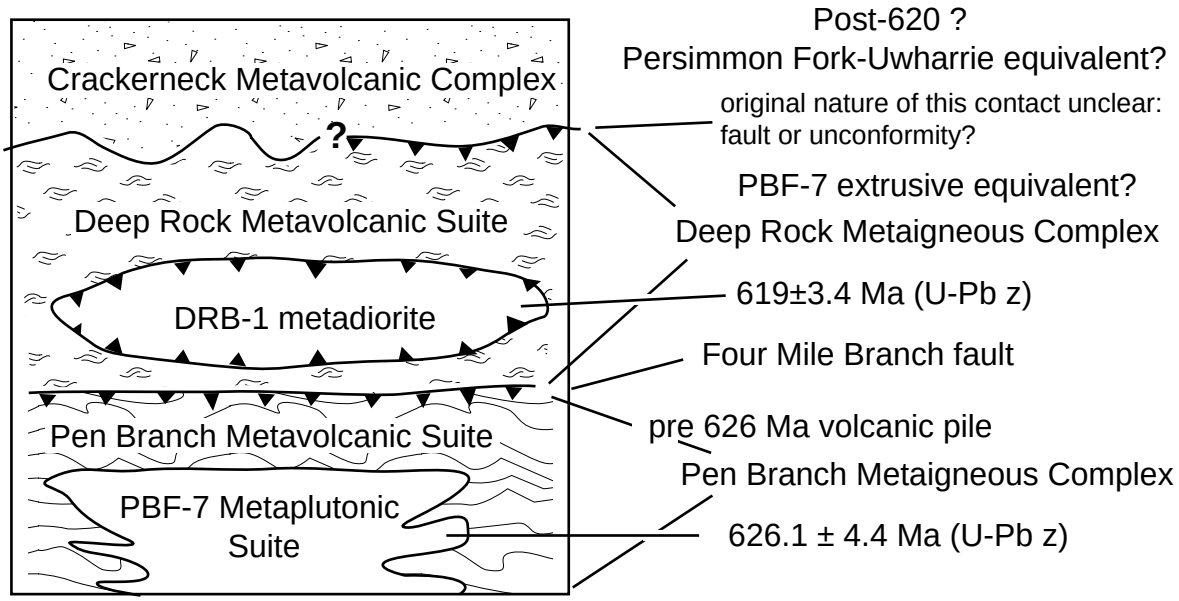

Figure 3. Schematic column of Appalachian litho-"stratigraphic" units beneath the US DOE Savannah River Site.

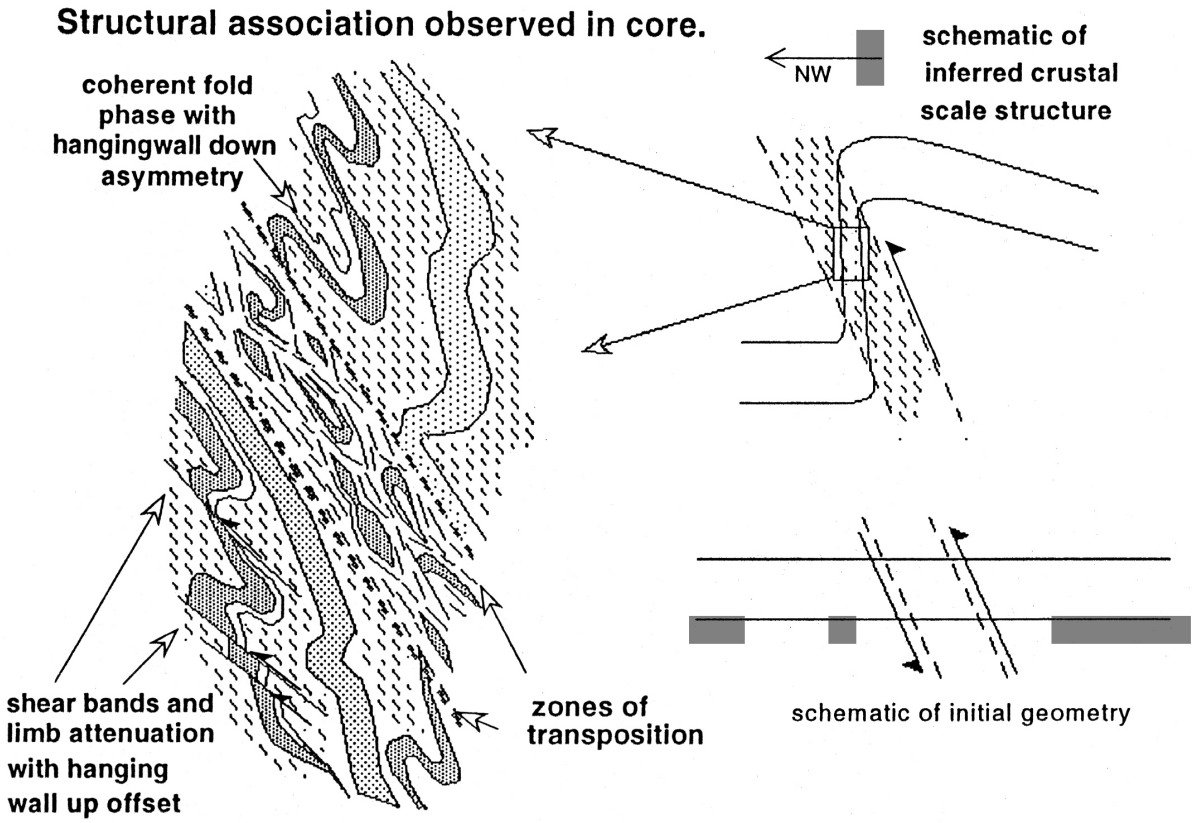

Figure 4. Overturned limb structure of the Tinker Creek nappe from structural analysis of over 3000m of basement core in the DRB well cluster.

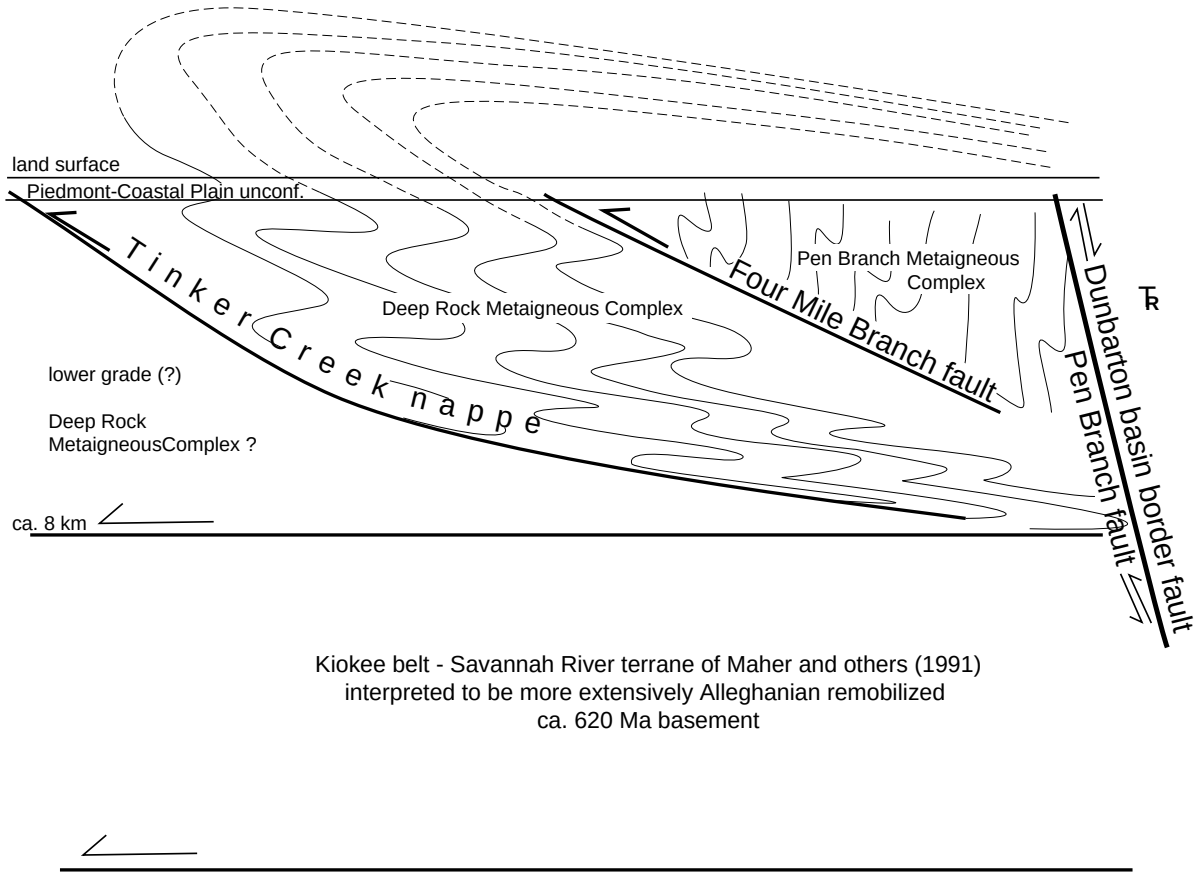

Figure 5. Schematic cross-section of Appalachian structure underlying the middle third of the Savannah River Site.

Figure 6. Comparison of the relative amounts of pinking or K-metasomatic alteration of PBF Metaplutonic Suite observed in PBF-7. Second and third numbers refer to box # and footage (depth from surface). XRF analysis of whole rock powders from this set was used to construct the isocon diagram (Fig 8).

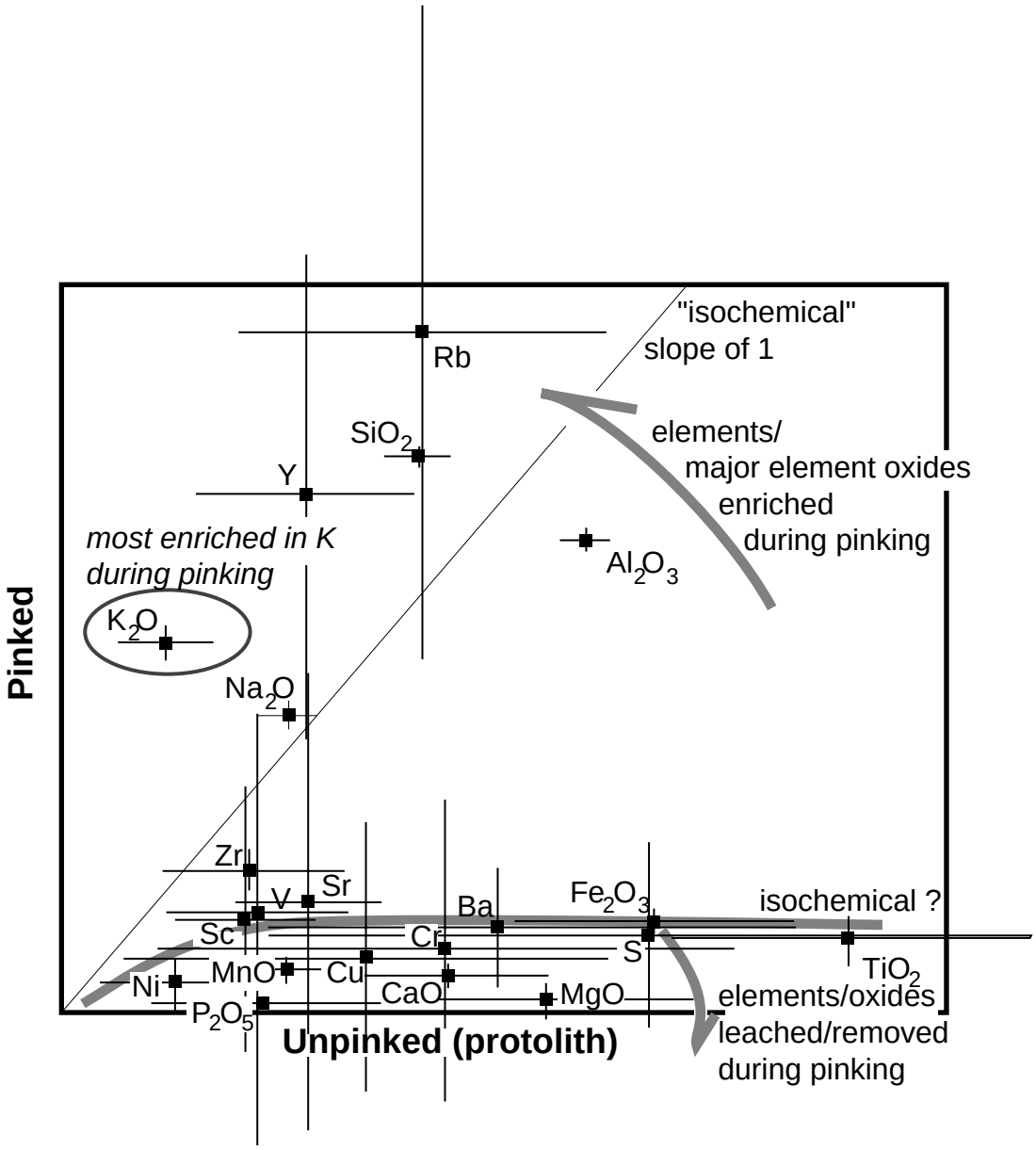

Figure 7. Isocon diagram showing changes in ratios of major and trace elements as a result of pinking in PBF-7 gneisses of PBF Metaplutonic Suite. Discussed in text. Standard deviations are shown. Slope of "1" represents isochemical conditions in theory; ratio of elements/major oxides before/after pinking equals 1. Perhaps a line that drives through Ni, Zr, Sc, V, TiO_2 supposedly immobile elements really represents isochemical conditions – ratios that have not been changed by metasomatism. Elements/major oxides that appear below this line have been leached or depleted during the pinking event, elements/major oxides that appear above the line represent increasing additions of certain elements during pinking, in particular K_2O, Y, Rb, SiO_2, Na_2O and (to a somewhat lesser extent) Al_2O_3. 15 unpinked protolith (boxes 103, 107, 108, 139, 143, 145, 149, 157, 159, 161, 165, 171, 173, 175, 177) and 8 pinked (101, 115, 115t, 167, 171, 171-3568, 175, 176-3541) samples. Compare Figure 6.

Figure 8. PBF-7-16-1249' (and PBF-7-13) and GCB-2-648' illustrate the "greening" event. A brick-red arkose (DRB-11-2741') from within the Dunbarton basin is included to compare color. The matrix of the PBF-7 sample on a wet surface is grayish yellow green (5GY 7/2) on the Munsell rock color chart. Microprobe analyses of a fibrous mineral that defines the matrix indicates that it is muscovite. Irregular margins of oxidized fanglomerate clasts have been reduced and now appear cream colored. Reducing fluids penetrated along gneissosity. The GCB-2 sample is saprolite, but shows a very similar texture. Coarser grained matrix is completely reduced. The ragged irregular margins of (brick-red) fine-grained clayey clasts show incomplete penetration of reducing fluids parallel to foliation.

Figure 9. Pseudotachylyte hand specimens: a) DRB 3-13-1038, b) DRB 7-6-1394, c) DRB-7-1419'. Inspection of pseudotachylyte samples commonly shows that these features reactivate thin chlorite shear surfaces that dip less steeply than foliation, and show hangingwall up sense of displacement. It can be shown that most pseudotachylytes must post-date Alleghanian time because the rock they cut has been pinked, and pinking is a Triassic event. Some pseudotachylytes seem to form near felsic mafic contacts, and may reflect local shear stress accumulations at these sites. PBF-7-89-2344: pseudotachylyte clearly postdates pinking, the "greening" as observed in crystalline rocks , and zeolite ±calcite veining (pale pinkish orange).

Notes

Significance of Soft Zone Sediments at the Savannah River Site

R. K. Aadland, Westinghouse Savannah River Co., Aiken, SC 29808
W. H. Parker, Science Applications International Corp., Augusta, GA 30901
R. J. Cumbest, Westinghouse Savannah River Co., Aiken, SC 29808

ABSTRACT

Rod drops and lost circulation during drilling, commonly occur in the middle Eocene marine carbonates and clastics of the Santee Formation, the Clinchfield Formation and to a lesser extent the Dry Branch Formation. Historically the rod drop (including low blow counts in SPT borings) was assumed to indicate the presence of "soft zones." Until recently, sediment from soft zones as defined by SPT N-values, rod drops and lost circulation was never recovered. Conventional coring methods was unable to recover sediment from the intervals. Therefore, soft zone sediment, and certainly the precursor sediment to the final soft zone sediment was unknown. Nearby sediments to the soft zones, whether they are carbonate-bearing to carbonate-rich clastics or limestones have been observed to have undergone minor to extensive carbonate dissolution. Silicification was commonly noted where the precipitation of silica was minor to extensive, replacing and cementing much of the original sediment. It has generally been assumed that the carbonate in the sediment in the soft zones has undergone extensive if not complete carbonate dissolution leaving behind vugular, moldy clastic debris. Thus a soft zone occurs in the "end member" sediment where the carbonate dissolution noted in varying degrees in the nearby non-soft zone sediments was complete.

Core recovered from a soft zone in the Santee/Clinchfield section in F-Area (GSA) using CPT technology, indicates that the sediment had not undergone extensive carbonate dissolution. Instead, the precursor carbonate sediment underwent extensive opal-CT (amorphous silica) replacement much like the silica replacement/cementation that commonly occurs in overlying and nearby competent sediments.The silica was precipitated as 2-5 μm opal-CT lepispheres that replaced carbonate mud (micrite) matrix, and precipitated as linings within molds and vugs and in micropores in the lime mud matrix. Thus, opal-CT replacement of the original carbonate sediment in the soft zone interval, is the crucial event in the formation of the soft zone. Where carbonate has been replaced by silica the soil properties of the resulting sediment is such that it has neither cohesion nor very much compressive strength. Here the tip resistance to the CPT push would be low, rod drops would be encountered during conventional drilling and the surrounding relatively unaltered carbonate sediment supports the overburden.

The extent and distribution of soft zones in the GSA was mapped. Soft zones are generally thicker and more concentrated where carbonate is thickest and most concentrated (has the highest average percentages).

[1]Information developed under Contract DE-AC09-89SR19015 with the U.S. Dept. of Energy

INTRODUCTION

The purpose of this paper is to provide information on the origin and extent of "soft zones" encountered in the carbonate bearing strata at the Savannah River Site (SRS). (see Figure 1, in Aadland and others, 2000, this volume). Near the center of the SRS, middle Eocene marine carbonates and clastics of the McBean member of the Santee Formation, the Utley limestone member of the Clinchfield

Formation and to a lesser extent the Griffins Landing member of the Dry Branch Formation (Fallaw and Price, 1995 and Aadland and others, 1995), occur at depths between 100 and 250 feet below the ground surface (see Figure 2, in Aadland and others, 2000, this volume). Often found within the carbonate rich to carbonate bearing sediments, particularly in the upper third of this section, are "weak zones" interspersed in stronger matrix materials. These weak zones, which vary in apparent thickness and lateral extent, have been variously termed "soft zones," "the critical layer," "underconsolidated zones," "bad ground," and "void." The preferred term used here is "soft zones".

Rod drops, during drilling, commonly occur in the carbonate-rich sediments in the Santee/Clinchfield and Dry Branch section (see Figures 2 and 4, in Aadland and others, 2000, this volume). Historically the rod drop (including low blow counts in SPT borings) was assumed to indicate the presence of a "soft zone." Due to the depth at which soft zones occur (typically greater than 100 ft below the ground surface) there has been no opportunity for direct visual observations of their nature and geometry. Conclusions that have been drawn on soft zone size are based on the limited penetrations of geotechnical/geophysical borings and Cone Penetrometer Tests (CPT).

The prevailing assumption of the causal mechanism for the rod drops in the soft zones has been dissolution of the carbonate-rich sediments in the zone, resulting in vugular porosity where the drill rod meets little or no resistance to penetration. An alternative hypothesis for this phenomenon is that the drill rod was pushed into uncemented sands where the overburden is supported by dense or semi-cemented beds that overly the uncemented sands. A third alternative hypothesis from data accumulated in this study (Parker, 1999 and 2000) is that soft zones form where carbonate has been largely replaced by opal-CT (amorphous silica). The uncertainty of the origin and extent of soft zones has lead to very conservative engineering analyses of this subsurface condition.

Historically, it was assumed the soft zones observed in neighboring borings were interconnected to varying degrees, thus they were grouted as an expedient way of resolving any potential foundation stability issues (Corps of Engineers, 1952). This method continued through the restart of the K-reactor (see Figure 1, in Aadland and others, 2000, this volume), where the project chose to grout "soft zones" in the Santee/Clinchfield carbonate interval beneath the cooling water lines to resolve potential foundation stability issues (WSRC, 1992a, b; Geotechnical Engineers Inc., 1991). The results of that effort were carefully studied and it was found that the grout was not having the desired effect on the subsurface soft zones as was previously thought. The results showed that soft zones in adjacent wells were poorly interconnected. The grout traveled in thin sheets along preferential pathways often bypassing "soft zones" in adjacent wells. Soft zones that existed prior to grouting still existed after grouting was completed. The grouting provided only limited benefit in reducing the potential settlement from the soft zones.

A grout assessment study was conducted at the In Tank Precipitation Facility (ITP) in H Area (Aadland and others, 1994; Syms, 1995 and WSRC, 1995) (see Figure 1, in Aadland and others, 2000, this volume). CPT and SPT borings identified locations and intervals in the Santee/Clinchfield section where soft zones were identified. Grout was injected into the soft zone intervals. Wells were drilled and cored at distances from 5 to 40 feet from the grout injection wells and the sediment analyzed to determine where the grout traveled. It was observed that the grout resided in and mixed with the clastic sediments of the

overlying Dry Branch Formation. Indeed the grout not only did not reside in nearby interconnected soft zones, it did not even remain within the Santee/Clinchfield interval.

Soft Zone Identification Criteria

1. SPT N-values of 5 and less (including weight of rods and weight of hammer) are considered to be primary indicators of soft zones. Also, when these criteria are met during SPT sampling, continuous SPT sampling is required until the soft zone interval is passed.

2. The CPT has none of the limitations associated with sampler mass or fluid injection into the formation. Because of its high data sampling frequency and array of test parameters and reliability of the measurements, it is the primary tool for detecting and locating soft zone intervals. The primary criterion is a tip resistance of 15 tsf or less over a continuous 2 feet thick interval. Further, the sleeve resistance, pore pressure and shear wave velocity measurements should be acquired and evaluated.

3. The loss of drilling fluids is not a reasonable indicator that soft materials have been intercepted by the borehole. Also, it is not a reliable indicator of soft zone size or extent. Fluid losses are a routine occurrence in sediments below 100 feet depth, and likely indicate hydrofracturing has occurred. In addition, identifying the location of leakage into the formation is notoriously difficult. Typically the only definitive information that can be obtained from fluid loss is the depth to its first occurrence and the depth of any marked increases in loss (or total loss of circulation).

4. During grouting programs it has been found that while significant quantities of grout were injected into the sediments, a substantial quantity of the grout resides probably in thin seams. Thus, the volume of grout-take in a boring is not a reliable indicator of the location or extent of a soft zone.

5. Rod drops recorded from historical drilling accounts require some knowledge of the drilling rig, type of bit and pump pressure. Therefore, rod drops during drilling operations are not considered primary indicators of soft zones

6. Depending on the type of investigation, field conditions and other circumstances, other techniques including cross-hole seismic tomography or other geophysical techniques may be used. These techniques must, however, be calibrated to more standard soft zone identification criteria such as the CPT and SPT measurements.

Origin and Delineation of Soft Zones

Until recently, sediment from soft zones as defined by SPT N-values, rod drops and lost circulation was never recovered. Conventional coring methods were unable to recover sediment from the intervals. Therefore, soft zone sediment, and certainly the precursor sediment to the final soft zone sediment was unknown.

Nearby sediments (often fossiliferous) to the soft zones, whether they are carbonate-bearing to carbonate-rich clastics or limestones have been observed to have undergone minor to extensive carbonate dissolution (see Figure 12, in Aadland and others, 2000, this volume) (Thayer and others, 1994; Rine and Engelhardt, 1999). Silicification was commonly noted where the precipitation of silica was minor to extensive (replacing and cementing much of the original sediment) (see Figures 11, 15, 16 and 17, in Aadland and others, 2000, this volume), (Thayer and others, 1994; Rine and Engelhardt, 1999 and

Parker, 1999 and 2000). Only minor carbonate cementation has been noted in near-by sediments (see Figure 14, in Aadland and others, 2000, this volume). It has generally been assumed that the carbonate in the sediment in the soft zones has undergone extensive if not complete carbonate dissolution leaving behind vugular, moldy clastic debris. Thus a soft zone occurs in the "end member" sediment where the carbonate dissolution noted in varying degrees in the nearby non-soft zone sediments was complete.

Soft Zone Study at APSF

Evidence from the soft zone study at the APSF suggests that the sediment in the rod drop/no recovery zone had not undergone extensive carbonate dissolution. Instead, the precursor carbonate sediment underwent extensive opal-CT (amorphous silica) replacement much like the silica replacement/cementation that commonly occurs in overlying and nearby competent sediments (Figure 1; see Figure 11, in Aadland and others, 2000, this volume).

A series of closely spaced CPT's were pushed at the APSF Site (Figure 2) (WSRC, 1998) in the northern portion of F Area (see Figure 1, in Aadland and others, 2000, this volume). One purpose of the investigation program was to aid in establishing the stratigraphic and lateral distribution of soft zones in the area. Using the defining criteria of tip stress values less than 15 tsf to define the presence of soft zones, it was determined that soft zones vs. non-soft zones occurred at comparable stratigraphic horizons in CPT pushes spaced less than 10 feet apart (Figure 2). An 8 feet thick soft zone occurred in the Santee/Clinchfield section immediately beneath the Santee unconformity. The soft zone was not observed in the surrounding CPT's that were pushed only a few feet away. The soft zone was continuously cored (using the newly available CPT coring tool) and three lithologies were delineated (Parker, 1999); sandy, biomoldic chert (see Figures 11 and 15, in Aadland and others, 2000, this volume); siliceous sandy mud (see Figure 16, in Aadland and others, 2000, this volume) and terrigenous sand (Figure 17, in Aadland and others, 2000, this volume).

The sandy, biomoldic chert and the siliceous, sandy mudstone were originally sandy lime mud (micrite) supported fossiliferous wackestone and sandy, lime mudstones (Parker, 1999). The carbonate mud was replaced molecule for molecule with authigenic opal-CT lepispheres and chalcedony without any loss in sediment volume (Figure 1; see Figure 11, in Aadland and others, 2000, this volume). The original sandy fossiliferous wackestone suggests deposition in clear, open-marine water of normal salinity on the inner to middle shelf (Parker, 1999). The opal-CT matrix was originally lime mud (micrite) matrix, and its abundance indicates deposition in quiet water below normal marine wave base. In short the precursor soft zone sediment was typical of the Santee/Clinchfield carbonate sediment deposited in the GSA.

The sediment in the soft zone is not a distinct microfacies separate and distinct from the sediments that comprise the surrounding carbonate, but is diagenetically altered where the initial carbonate matrix was completely replaced with opal-CT (Figures 1 and 3; see Figure 11, in Aadland and others, 2000, this volume). The silica was precipitated as 2-5 μm opal-CT lepispheres that replaced carbonate mud (micrite) matrix, and precipitated as linings within molds and vugs and in micropores in the lime mud matrix. The opal-CT formation postdates solution of the fossil shells because the opal-CT and chalcedony line the interiors of some molds.

Since the original carbonate sediment in the soft zone interval underwent complete opal-CT replacement, the working hypothesis is

that opal-CT silica replacement of carbonate sediments, not carbonate dissolution is the crucial event in the formation of the soft zones. Where carbonate has been replaced by silica the soil properties of the resulting diagenetically altered sediment is such that it has neither cohesion nor very much compressive strength. Here the tip resistance to the CPT push would be low (less than 15 tsf), rod drops would be encountered during conventional drilling and the surrounding relatively unaltered carbonate sediment supports the overburden.

Soft Zone Study R Area

Sediment from a 6 foot thick soft zone encountered in the Santee/Clinchfield section in R Area (see Figure 1, in Aadland and others, 2000, this volume) was continuously sampled using CPT technology and petrographically analyzed to corroborate the findings at the APSF site in the GSA, (Parker, 2000). The lithologies described were sandy, biomoldic chert and siliceous sandy mud very similar to the silica replaced sediments noted at the APSF site. Here, as at the APSF site, precursor calcareous wackestone and mudstone (micrite) was replaced by opal-CT, and supports the assertion that opal-CT replacement of carbonate is the primary mechanism for soft zone development.

If replacement of carbonate by amorphous silica is the controlling factor in the development of soft zones, then the controlling mechanisms for soft zone development would include (Folk and Pitman, 1971; Meliva and Siever, 1988):

- Adequate supply of amorphous silica in the form of sponge spicules and diatoms for the continued precipitation of the opal-CT.
- Adequate permeability to flush the sediment with the volumes of silica saturated pore waters needed to maintain the precipitation of the silica.
- Chemistry and mineralogy of the host sediment.
- Bulk pore-water ph.
- Presence of organic matter.
- Concentration of silica and certain other ions, such as sulfate.

Assuming the above mentioned controls are available for silica replacement/cementation to occur; the spatial geometry of the silicified “areas” would be very irregular (Figure 2). The silicification of the enclosing sediment would follow and spread along bedding planes, along microfractures of varied orientations, along corridors of locally enhanced permeability etc. The resulting “soft zone” could be in the form of irregular isolated pods, extended thin ribbons or stacked thin ribbons separated by intervening unsilicified parent sediment. Soft zones encountered in one CPT could be absent in the neighboring CPT only a few feet away. Only where silicification has spread far enough away from the bedding planes and/or fractures along which the silica replacement has taken place, where all the intervening sediment is replaced, would the soft zones be large enough and coherent enough to pose a question for the siting of new facilities. In all likelihood this would be a most uncommon event.

Delineation of the Extent of Carbonate Zones/Soft Zones

CPT logs were the primary data source queried to determine the presence, geographic distribution and stratigraphic position of the soft zones in the GSA. Where the tip stress was less than 15 tsf, a soft zone was defined. In addition, a search of the data from the field logs from the SPT boring reports was conducted for indications of "soft zones" encountered during drilling in the GSA. These data included blow count N values, where N values less than 5 are considered evidence of

soft zones. In addition, rod drop intervals, lost circulation zones were considered to further delineate the areal extent of the soft zones. These last two, rod drop intervals and lost circulation zones proved of little value in delineating soft zones and were not included in the final data base queries. The blow count data from the SPT boring logs were queried as backup to the primary data source, namely the tip stress measurements from the CPT pushes.

Three D profiles were created in EARTH VISION to illustrate the extent (stratigraphic and geographic distribution) of soft zones and carbonate zones in the GSA. The geographic distribution, and concentration of carbonate sediment in the Santee/Clinchfield section the GSA was analyzed by querying the footage of carbonate greater than or equal to 5% found in the cored wells and borings (see Figure 20, in Aadland and others, 2000, in this volume). Three areas stand out where several cored wells indicated appreciable thickness of carbonate. From east to west they include the ITP area (#1 on Figure 1, in Aadland and others, 2000, in this volume), the "H" Basin area (#2 on Figure 1, in Aadland and others, 2000, in this volume) and the Burial Grounds area (#3 on Figure 1, in Aadland and others, 2000, in this volume). Variable density and uneven distribution of the core and CPT boring data precludes defining these locations as the only areas of carbonate concentration in the GSA since the areal extent of each area is not well constrained nor are other areas where data is sparse. The areas outlined are however, considered typical of the carbonate-rich terrain in the GSA.

Query Results

Three D profiles were generated at the H Area Seepage Basin (Figures 4 and 5) and the Burial Grounds (Figures 6 and 7) illustrating the thickness and percentage of carbonate, and the thickness and distribution of soft zones. In general where the carbonate is thickest, the average carbonate percentage is greatest. Comparing the extent and lateral distribution of the soft zone "hits" with the distribution of carbonate indicates that soft zones are generally thicker and more concentrated where carbonate is thickest and most concentrated (highest average percentages). Indeed, throughout the GSA it is observed that the carbonate thickness and concentration is directly related to the isopach thickness of the Santee/Clinchfield interval. Where the Santee/Clinchfield interval is thick, carbonate is more concentrated, however, where the interval is thin, carbonate thickness and concentration is reduced. Since the thickness and distribution of soft zones is closely linked to the thickness and distribution of carbonate; those areas where the Santee/Clinchfield section is thin and where a great deal of carbonate has been removed would be areas where soft zones are less likely to be present.

REFERENCES

Aadland, R. K., Gellici, J. A. and P. A. Thayer, 1995, Hydrogeologic Framework of West-Central South Carolina. State of South Carolina Department of Natural Resources, Water Resources Division Report 5, 200p.

Aadland, R. K., Cumbest, R. J., Howe, K., Lewis, S. E., Price, v. Jr., Richers, D. E., Wyatt, D. E. and K. S. Sargent, 1994, Geological Characterization in the Vicinity of the In-Tank Precipitation Facility (U). Westinghouse Savannah River Co., Site Geotechnical Services Dept., U. S. Department Of Energy Report, WSRC-TR-94-0373, Rev. 0, 88p.

Geotechnical Engineers, Inc. 1991, "K-Reactor Area, Geotechnical Investigation for Seismic Issues, Savannah River Site (U), Volume 1: Seismic Structural Engineering," WSRC-TR-91-47, March 1991.

Fallaw, W. C., and Price, V., 1995, Stratigraphy of the Savannah River Site and vicinity: Southeastern Geology, v. 35, p. 21-58.

Folk, R. L., and J. S. Pittman, 1971, Length-slow chalcedony: a new testament for vanished evaporates: Journal of Sedimentary Petrology, v. 41, p. 1045-1058.

Maliva, R. G., and R. Siever, 1988, Mechanisms and controls of silicification of fossils in limestones: Journal of Geology, v. 96, p. 387-398.

Parker, W. H., 1999, Petrographic Analysis and Microfacies Delineation for a Soft Zone Interval Beneath F-Area, Savannah River Site, Aiken, South Carolina. Report prepared by SAIC under subcontract AB6029N to DOE. 24p.

Parker, W. H., 2000, Petrographic Analysis and Microfacies Delineation for a Soft zone Interval Beneath R-Area, Savannah River Site, Aiken, South Carolina. Report prepared by SAIC under subcontract AB6029N to DOE. 12p.

Rine, J. M. and D. W. Engelhardt, 1999, Geologic Characterization of Core from Borings HBOR-34 and HBOR-50, In Tank Processing (ITP) Area, Savannah River site, South Carolina. Report prepared for DOE by the Earth Sciences and Resources Institute, University of South Carolina, Columbia South Carolina. ESRI-USC Technical Report 99-3-F143. 16p.

Syms, F. H., 1995, In Tank Precipitation Facility (ITP) Grout assessment Final Report (U), Report prepared for DOE by Site Geotechnical Services (SGS), Westinghouse Savannah River Co., Savannah River Site, Aiken, South Carolina. Report No. WSRC-TR-950127, Rev.0

Thayer, P.A., Smits, A. D., Parker, W. H., Conner, K. R., Harris, M. K., and M. B. Amidon, 1994, Petrographic Analysis of Mixed Carbonate-Clastic Hydrostratigraphic Units in the General Separations Area (GSA); Savannah River Site (SRS), Aiken, South Carolina, Westinghouse Savannah River Company, U. S. Department of Energy Report, WSRC-RP-94-54, 83p.

Westinghouse Savannah River Company, 1992a, "Integrated Geologic Analysis of the K-Reactor Area (U)," Reactor Engineering Department, Document No. WSRC-TR-92-42-004, January, 1992.

Westinghouse Savannah River Company 1992b, "K-Area Soil Stabilization Program (KASS)," Summary Overview and

Volume I, Systems Engineering Department, Document No. WSRC-TR-92-299, Rev. 0, July, 1992.

Westinghouse Savannah River Company, 1995, “In-Tank Precipitation Facility (ITP) and H-Tank Farm (HTF) Geotechnical Report”, Site Geotechnical Services Department, Document WSRC-TR-95-0057, Rev. 0, September, 1995).

Westinghouse Savannah River Company, 1998, “APSF Packaging and Storage Facility Soft Zone Settlement Analysis (U)”, Site Geotechnical Services Department, Calculation No. K-CLC-F-00034

US Army Corps of Engineers (COE), Charleston District, 1952, "Geologic Engineering Investigations, Savannah River Plant", Volumes I and 2, Waterways Experiment Station, Vicksburg, MS.

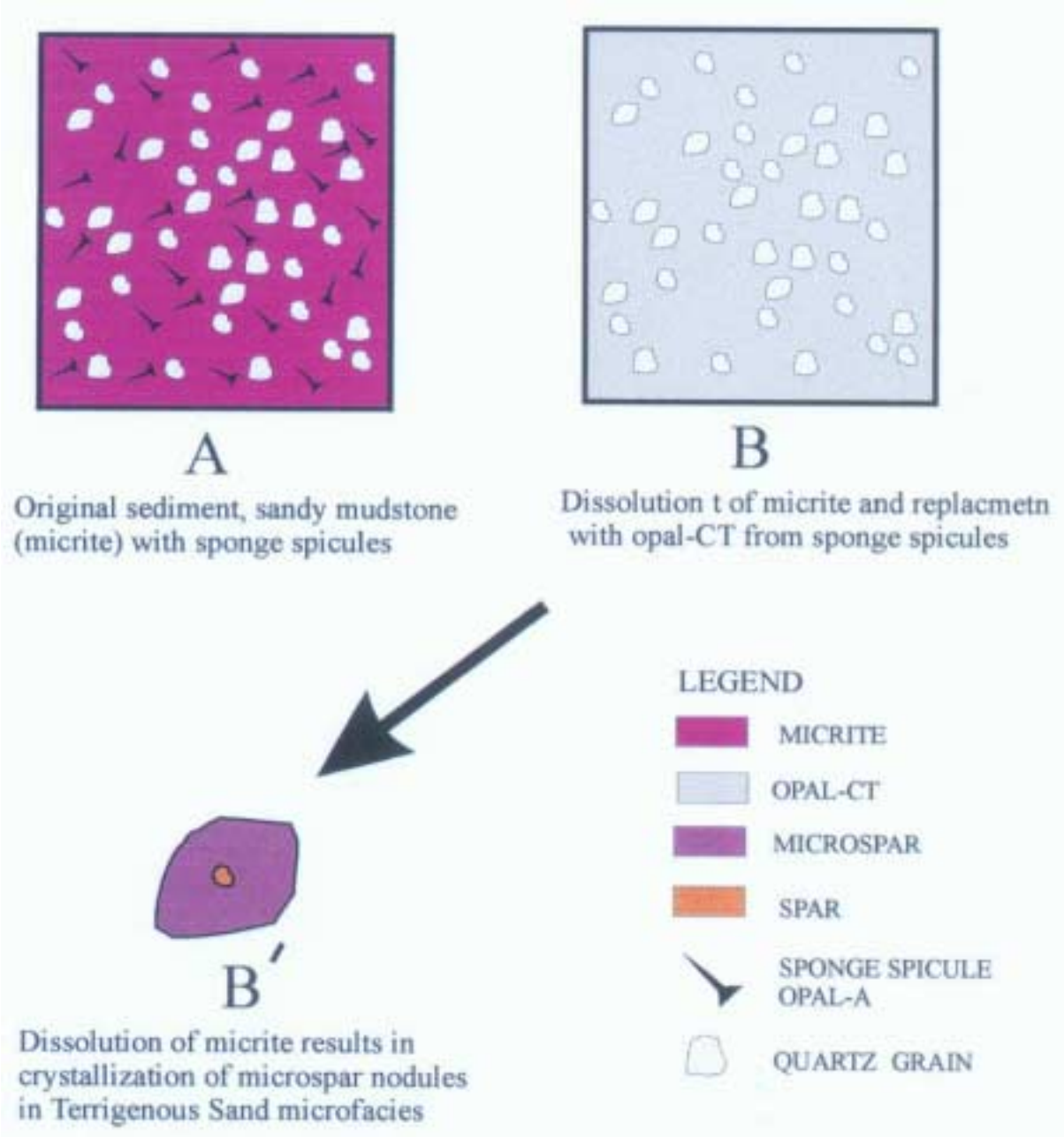

Figure 1. Diagrammatic representation of the interpreted diagenetic history of the siliceous sandy mudstone microfacies.

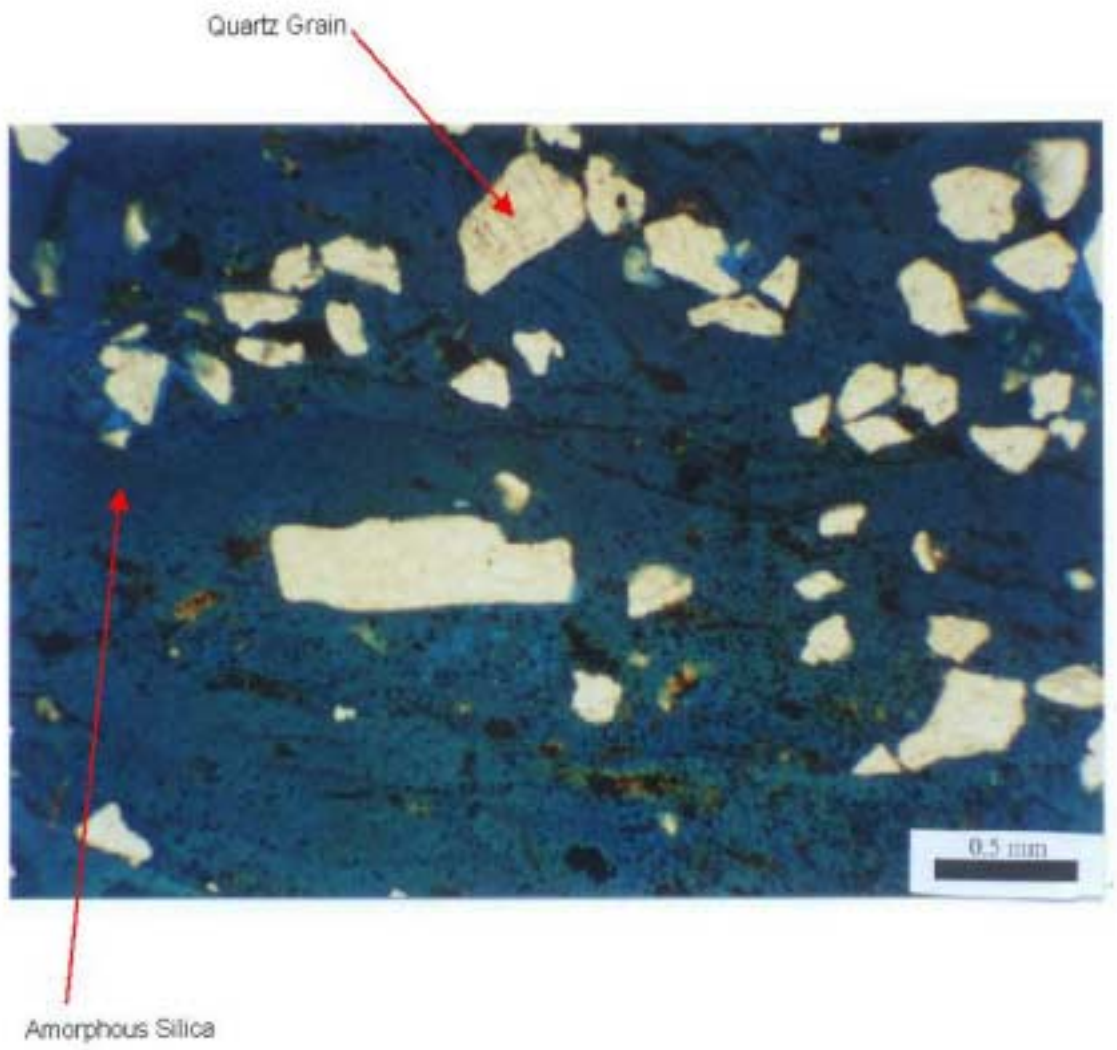

Figure 2. Photomicrograph of siliceous sandy mud microfacies, Santee/Clinchfield section from Core CPT-157S3 @ 108.35 ft. below land surface, APSF Site, F Area, General Separations Area, Savannah River Site. Plane-polarized light. Amorphous (Opal—CT) silica replaced calcite micrite (mud) matrix.

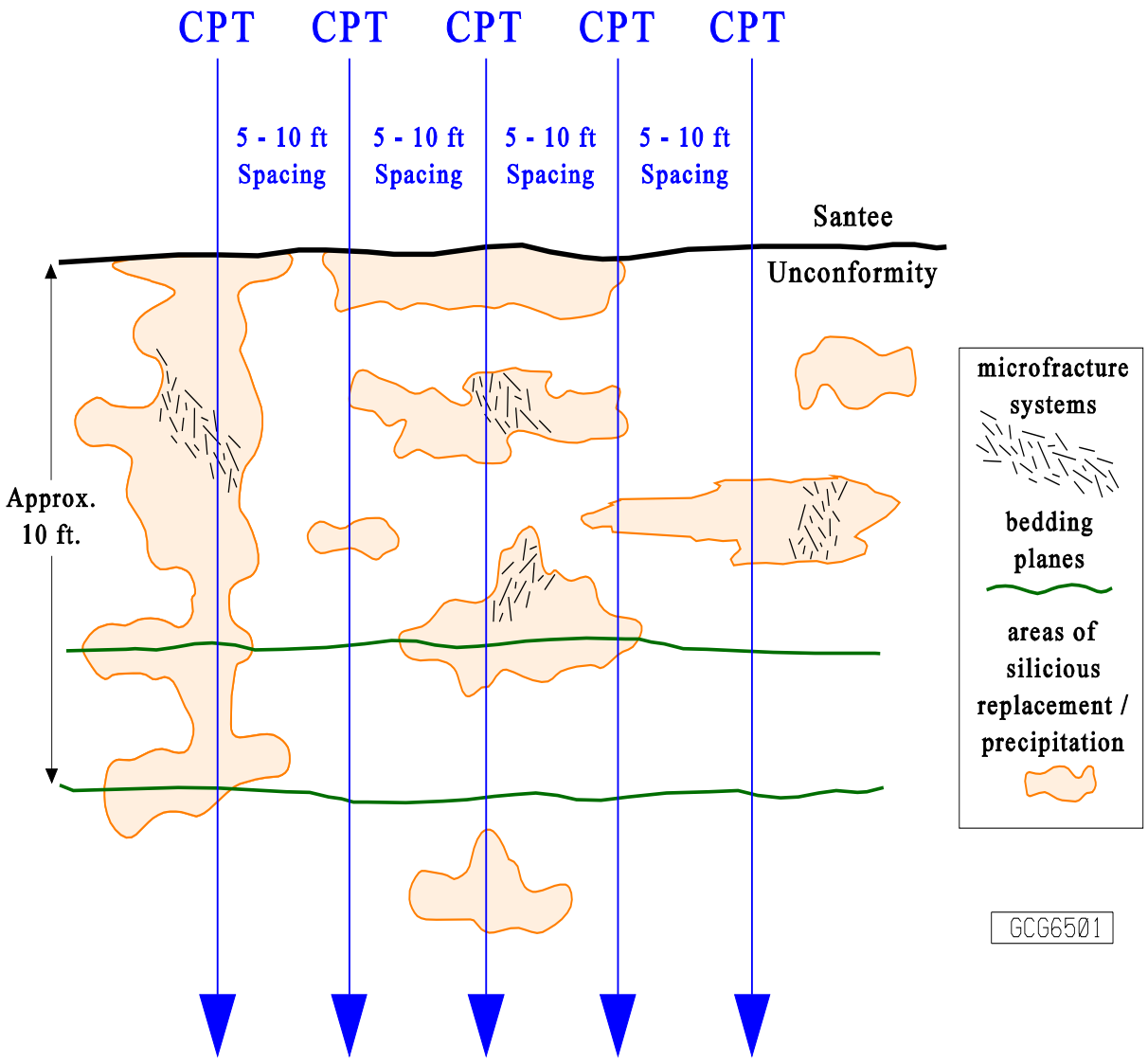

Figure 3. This diagram is illustrating the stratigraphic and lateral distribution of soft zones due to silica replacement of carbonate in the GSA. Replacement/precipitation of silica occurs along bedding planes, microfracture systems, and zones of enhanced permeability resulting in highly irregular pods, stringers and sheets of silica replaced carbonate (i.e., soft zones).

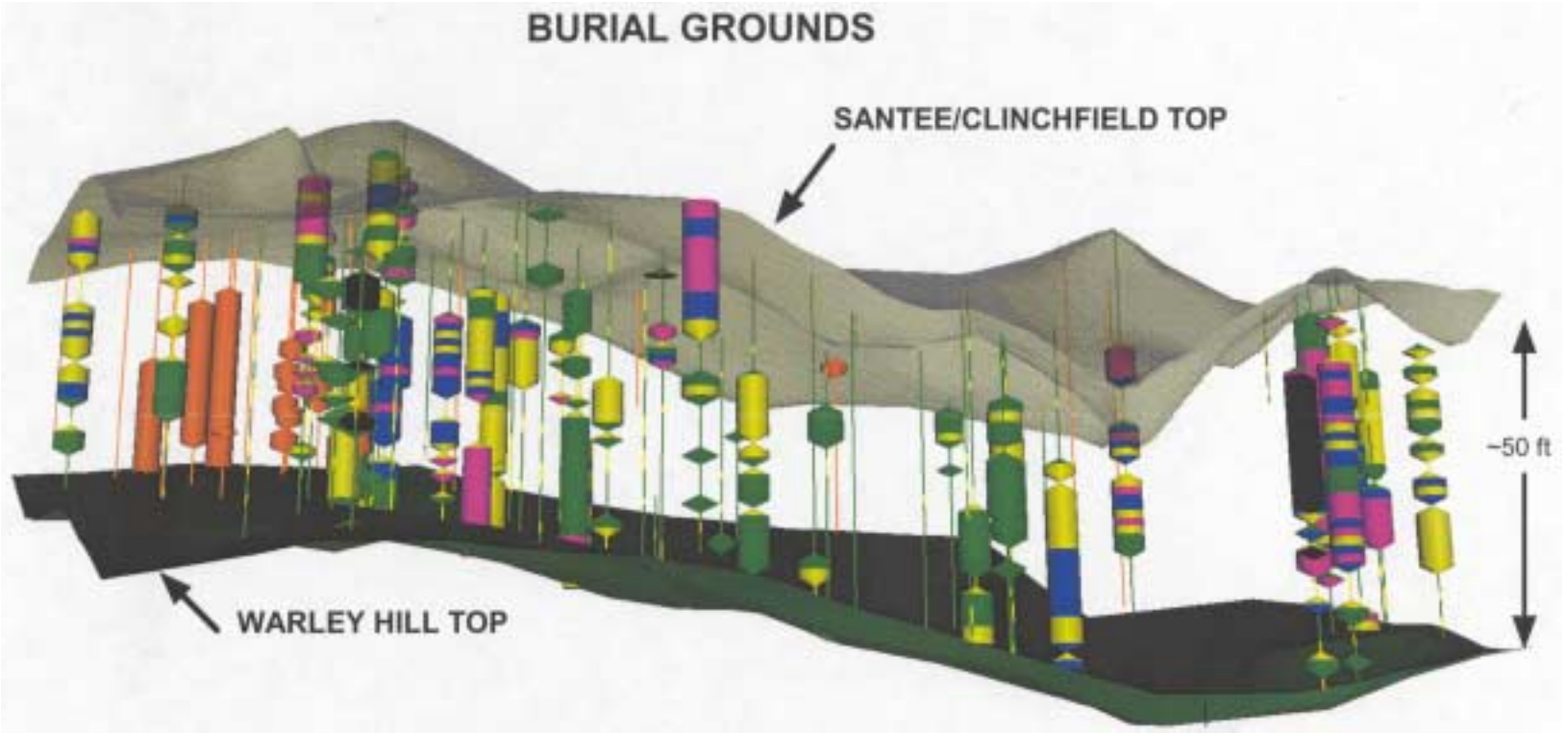

Figure 4. This figure is a 3D profile illustrating the relative thickness and percentage of carbonate from core and SPT borings at the Burial Grounds. The location of the Burial Grounds is outlined in Figure 1, in Aadland and others, 2000, in this volume. The upper bounding surface is the top Santee Unconformity surface and the lower bounding surface is the top Warley Hill surface. The tan colored "sticks" indicate carbonate "hits" occurring in the SPT borings without regard to carbonate content other than its presence at that particular depth in the boring. The percentage carbonate in the cored wells is color coded as follows: Purple >65%; Blue 45-65%; Yellow 25-45%; Green 5-25%.

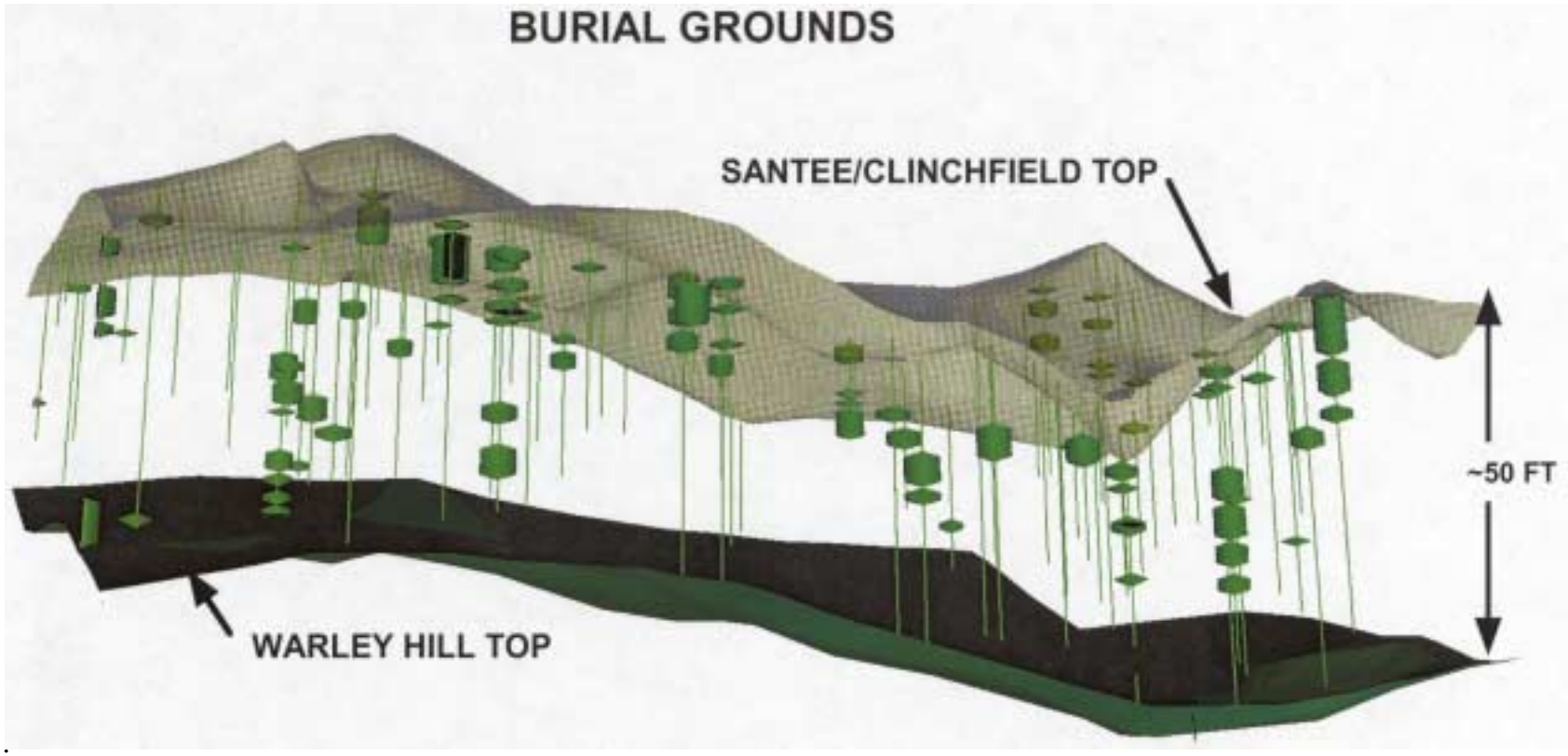

Figure 5. This figure is a 3D profile illustrating soft zones at the Burial Grounds. The location of the Burial Grounds is outlined in Figure 1, in Aadland and others, 2000, in this volume. The upper bounding surface of the query is the top Santee Unconformity surface and the lower bounding surface is the top Warley Hill surface. CPT logs were the primary source queried to determine the presence, geographic distribution and stratigraphic position of the soft zones in the GSA. Where the tip stress was <15 tsf, a soft zone was defined. Blow count N values from SPT logs were queried. N values <5 were considered evidence of soft zones. The blow count data was queried as back up to the primary data source, namely the tip stress measurements from the CPT pushes.

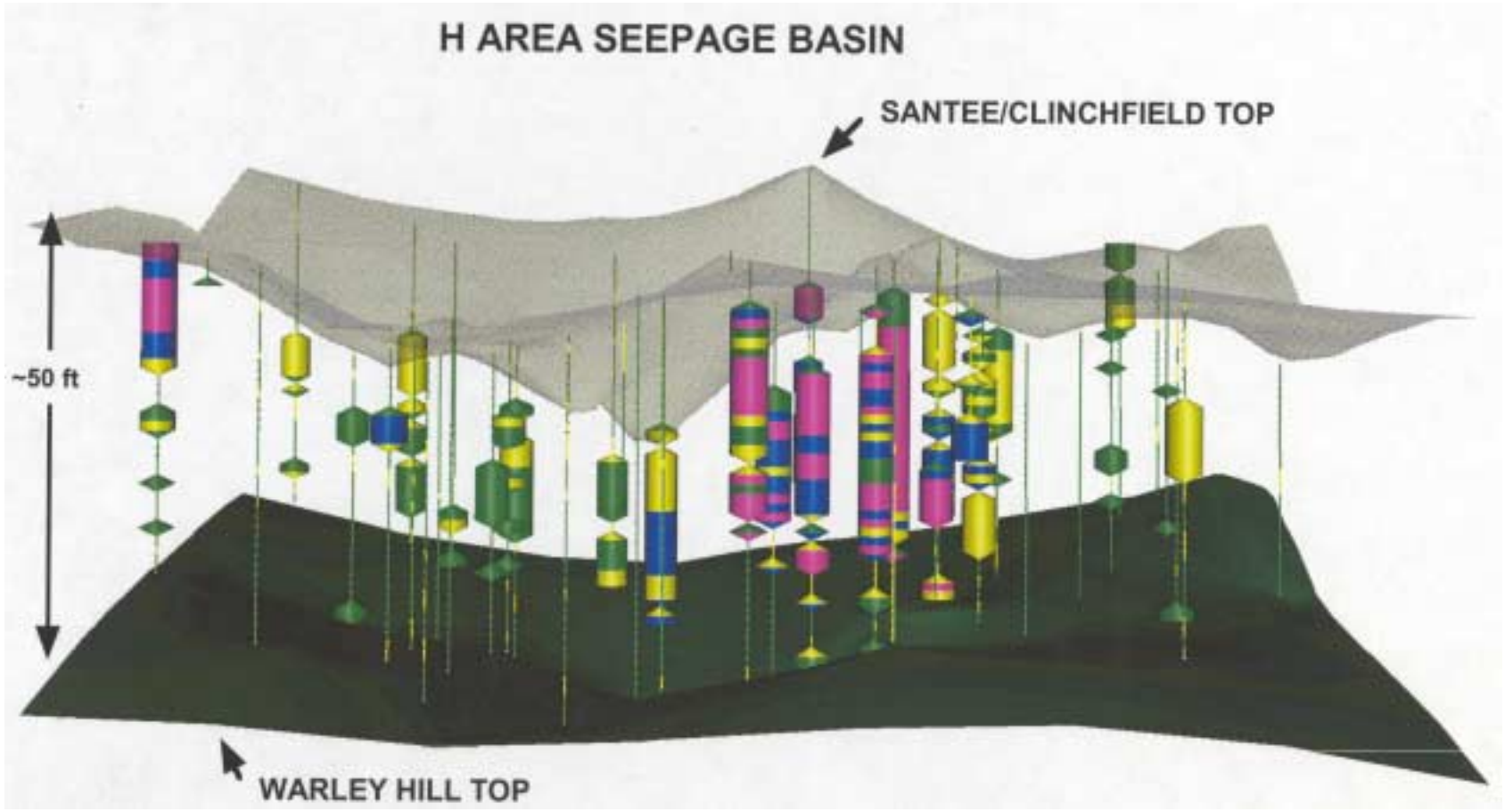

Figure 6. This figure is a 3D profile illustrating the relative thickness and percentage of carbonate from core and SPT borings at the H Area Seepage Basin. The location of the Seepage Basin is outlined in Figure 1, in Aadland and others, 2000, in this volume. The upper bounding surface is the top Santee Unconformity surface and the lower bounding surface is the top Warley Hill surface. The tan colored "sticks" indicate carbonate "hits" occurring in the SPT borings without regard to carbonate content other than its presence at that particular depth in the boring. The percentage carbonate in the cored wells is color coded as follows: Purple >65%; Blue 45-65%; Yellow 25-45%; Green 5-25%.

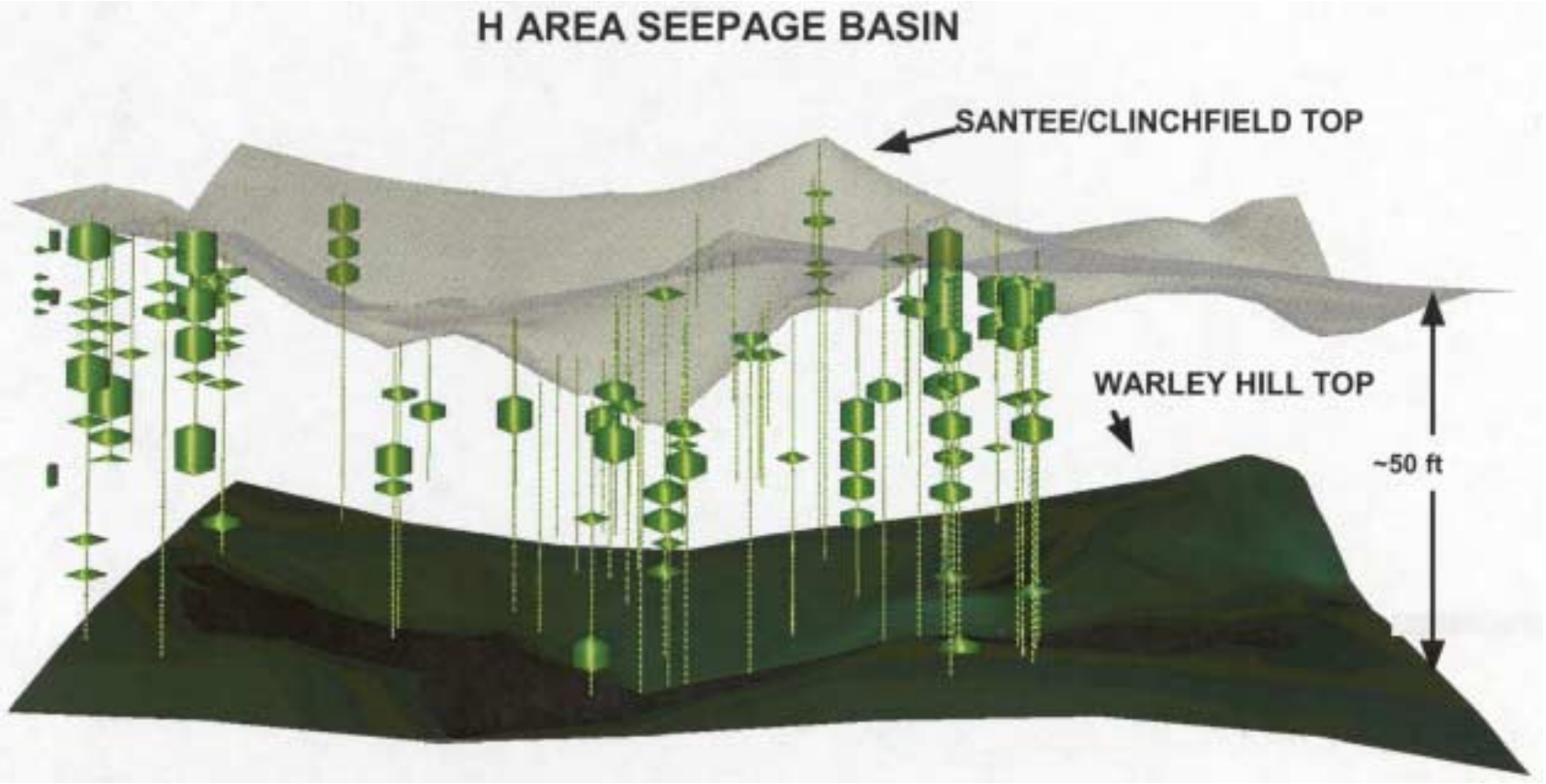

Figure 7. This figure is a 3D profile illustrating soft zones at the H Area Seepage Basin. The location of the seepage Basin is outlined in Figure 1, in Aadland and others, 2000, in this volume. The upper bounding surface of the query is the top Santee Unconformity surface and the lower bounding surface is the top Warley Hill surface. CPT logs were the primary source queried to determine the presence, geographic distribution and stratigraphic position of the soft zones in the GSA. Where the tip stress was <15 tsf, a soft zone was defined. Blow count N values from SPT logs were queried. N values <5 were considered evidence of soft zones. The blow count data was queried as back up to the primary data source, namely the tip stress measurements from the CPT pushes.

Notes

Carbonate Sediments in the General Separations Area, Savannah River Site, South Carolina

R. K. Aadland, Westinghouse Savannah River Co., Aiken, SC 29808
P. A. Thayer, University of North Carolina at Wilmington, Wilmington, NC 28403-3297
W. H. Parker, Science Applications International Corp., Augusta, GA 30901
J. M. Rine, Earth Sciences and Resources Institute, University of South Carolina, Columbia, SC 29208
D. W. Engelhardt, Earth Sciences and Resources Institute, University of South Carolina, Columbia, SC 29208
R. J. Cumbest, Westinghouse Savannah River Co., Aiken, S.C. 29808

ABSTRACT

Carbonates and carbonate-rich clastics in the General Separations Area (GSA) are restricted to the middle Eocene Warley Hill Formation, Santee and Clinchfield Formations and Griffins Landing member of the Dry Branch Formation. The preponderance of carbonate occurs in the Santee/Clinchfield section. The calcareous sediment consists of calcareous sand, calcareous mud, limestone, sandy limestone, muddy limestone, and sandy muddy limestone. They were deposited in shallow generally subtidal marine environments with the exception of the Dry Branch oyster beds that were deposited in a back barrier marsh/lagoonal environment.

The carbonates and limey sands of the Santee/Clinchfield sequence underwent a complex combination of deposition of diverse lithologies, post-depositional dissolution-precipitation-replacement of calcite, silica and other minerals. The result is sediment often far removed from its initial depositional fabric and mineralogy. Local dissolution is sometimes so pervasive that the precursor sediment is no longer identifiable.

The thickness and concentration of carbonate in the GSA is directly related to the overall thickness of the Santee/Clinchfield interval. In general where the Santee/Clinchfield interval is thickest the footage of carbonate is greatest and the average carbonate content (percentage) in the cores is greatest. Where the interval is thin the thickness and percentage of carbonate in the core is reduced.

Where the Santee/Clinchfield section is thick and where carbonate is concentrated, the overlying “upland unit” and the Tobacco Road/Dry Branch section is generally structurally high. Where the section is thin and the carbonate content is reduced or absent, the overlying “upland unit” and Tobacco Road/Dry Branch section is structurally low. Since the Dry Branch/Tobacco Road/”upland unit” section is relatively uniform in thickness over both the structurally high and low areas and not draped over the features, the removal of carbonate and the thinning (collapse) of the Santee/Clinchfield interval occurred in post Tobacco Road/”upland unit” time.

[1]Information developed under Contract DE-AC09-89SR19015 with the U.S. Dept. of Energy

Geologic Setting

Sediment underlying the Savannah River Site (SRS) (Figure 1) forms a wedge of strata that thickens from about 700 ft in the northwest to almost 1400 ft at the southeastern boundary of the site (see Figure 2, in Introduction to this volume, Wyatt, ed.). measuring on average 900 ft in thickness in the GSA (Figure 2). Regional dip is to the southeast and decreases upward from about 48 ft/mi at the base of the Cretaceous-aged strata to about 15 ft/mi at the top of middle Eocene-aged strata.

Late Cretaceous sediments of possible Coniacian/Turonian (?) to Santonian through Maastrichtian age (91 to 66 Ma) (Fallow and Price, 1995; Aadland and others, 1995) average

550 feet in thickness in the GSA (Figure 2). The sequence consists of quartz sand; pebbly sand and sandy clay generally deposited in lower to upper delta plain environments (Figure 3). Following a period of erosion of the Cretaceous section, Tertiary sediments were deposited when seas transgressed onto the Cretaceous-Tertiary unconformity surface. Tertiary sediments average about 350 feet in thickness in the GSA (Figure 2), range in age from Early Paleocene to Miocene (?)/Oligocene (?) and were deposited in fluvial to marine shelf environments (Figure 3).

Four regionally significant unconformities are defined in the Tertiary section (Figure 4). From base upward, they include the "Cretaceous-Tertiary" unconformity, the "Lang Syne/Sawdust Landing" unconformity, the "Santee" unconformity, and the "Upland" unconformity). Four sequence stratigraphic units (labeled Sequence I, II, III and IV) that are bounded by the unconformities have been delineated (Figures 2 and 4).

The "calcareous zone" in the GSA includes calcareous strata belonging to the Warley Hill Formation, Santee and Clinchfield Formations and Griffins Landing member of the Dry Branch Formation (Figure 4). The preponderance of carbonate occurs in the Santee/Clinchfield section (Thayer and others, 1994), and consists of calcareous sand, calcareous mud, limestone, sandy limestone, muddy limestone, and sandy muddy limestone.

Chronology of Tertiary Geologic Events in the GSA

The chronology of events and the depositional setting that characterized deposition of the Tertiary sequence in the GSA is presented here.

Oldest

- The Snapp Formation (Figures 2 and 4) and older Paleocene sediments (Sequence Stratigraphic unit I) were deposited in shallow clastic shelf and delta plain environments (Figure 3). Shallow shelf (platform) carbonate deposition was restricted to coastal areas of South Carolina at this time.
- Sequence I deposition was followed by erosion of the section (Lang Syne/Sawdust Landing unconformity) (Figure 4).
- A rise in sea level initiated deposition of the Congaree/Fourmile sands (Sequence Stratigraphic unit II) in shoreline to shallow shelf depositional environments (Figure 3). Shallow shelf (platform) carbonate deposition rapidly expanded landward and reached the southern boundary of SRS, but remained to the south and east of the GSA (see Figure 2, in Introduction to this volume, Wyatt ed.).
- Sea level continued to rise resulting in deposition of the Warley Hill clays (Sequence Stratigraphic unit II) in deeper shelf depositional environments (Figures 3 and 4).
- A lowering of sea level and/or an increased rate of sediment supply resulted in deposition of the Santee and Clinchfield carbonates and clastics in shallow shelf depositional environments in the GSA (Figure 5). This completed deposition of the Sequence Stratigraphic unit II sedimentary package (Figures 2 and 4).
- A retreat of the sea resulted in substantial erosion of the Santee/Clinchfield (Sequence II) sediments (Santee unconformity).
- Deposition of the Dry Branch Formation (Sequence III), including the Griffins Landing limestone member, was deposited over the Santee/Clinchfield section in shoreline to lagoonal/marsh depositional environments (Figure 5). The shoreline retreated from its position in the northern part of SRS, where it was located during Santee/Clinchfield time,

to the central part of SRS in Dry Branch time. Progradation of the shoreline environments to the south resulted in the sands and muddy sands and locally the oyster banks of the Griffins Landing member of the Dry Branch being deposited over the shelf carbonates and clastics of the Santee/Clinchfield sequence (Figure 5). The shallow shelf (platform) carbonates that had reached their most northwesterly updip position in Santee/Clinchfield time, reaching the GSA, retreated far to the south and east of SRS in Dry Branch time (see Figure 2, in Introduction to this volume, Wyatt ed.).

- Deposition of the Dry Branch clastics was followed by deposition of the Tobacco Road Formation (Sequence III) probably in moderate to high-energy lagoonal/open bay environments (Figures 4 and 5).
- A dramatic increase in sediment supply and a retreat of the shoreline towards the southeast, resulted in deposition of the "upland unit" sand and gravel (Sequence IV) in fluvial to upper delta plain environments (Figure 3).

Youngest

In conclusion, the deposition of shallow shelf carbonates generally remained to the south and east of the Savannah River Site during the Tertiary (see Figure 2, in Introduction to this volume, Wyatt ed.). Only during middle Eocene Santee/Clinchfield time did deposition of the carbonates extended as far inland as the GSA (Figures 4 and 5).

Stratigraphy of the Carbonate Sediments in the GSA

The carbonates and carbonate-rich clastics are essentially restricted to two intervals in the Tertiary section in the GSA; the Dry Branch Formation and the underlying Santee and Clinchfield formations. The upper most interval includes the carbonates of the Griffins Landing member of the Dry Branch Formation found below the "tan clay" beds that occur near the middle of the Dry Branch (Figures 2 and 4). The isolated carbonate patches of the Griffins Landing are the oyster banks that typically form in the back barrier marsh zone behind a barrier island system (Figures 4 and 5). Underlying the Dry Branch, directly below the regionally significant Santee unconformity, is the Utley Limestone member of the Clinchfield Formation. Without the benefit of detailed petrographic and paleontological analysis, the Utley carbonates cannot be systematically distinguished from the carbonates of the McBean member of the underlying Santee Formation. Thus the carbonate-rich sediments deposited in shallow shelf environments found between the Santee unconformity (Figure 4), and the Warley Hill Formation are referred to as the Santee/Clinchfield sequence in this report. The preponderance of the carbonate observed in the GSA occurs in the Santee/Clinchfield interval. Upon occasion carbonate mud and wackestone deposited in deeper shelf environments is observed in the underlying Warley Hill Formation (Figure 4).

Distribution and Depositional Environments of Carbonates at SRS

The regional distribution of the Santee/Clinchfield carbonate-rich sequence is illustrated in Figure 6. Carbonate content in the sequence is minimal in northwestern SRS and predominates near the southeast boundary of the site. The GSA is in that part of the mixed clastics/carbonate zone where the clastic sediments generally constitute a greater percentage of the section than the carbonates. In northern SRS the depositional equivalent of the Santee/Clinchfield sediments are mostly sands and muddy sands deposited in shoreline to lesser lagoonal and tidal marsh environments (Figure 5). The sands and muddy sands constitute the Tinker Formation (Fallaw and Price, 1995). In the central SRS the mixed carbonates and

clastics of the McBean member of the Santee Formation and the Utley member of the Clinchfield Formation (Figure 2) were deposited in middle marine shelf environments. The result is a varied mix of lithologies ranging from carbonate-rich sands and mud to sandy and muddy limestone (mostly micrites and wackestones, and to a lesser extent packstones and grainstones) (Thayer and others, 1994) (Figure 7). In southern SRS the Blue Bluff member of the Santee/Clinchfield sequence was deposited further offshore, further removed from riverine clastic input into the shelf environment resulting in deposition of carbonate mud (micrite) (Figure 5).

Approximately 40-50% of the wells that drilled through the Santee/Clinchfield interval in the GSA penetrated quantities of carbonate ranging from 5-78% of the sediment sampled. Thayer and others, 1994, conducted a binocular microscope and thin-section examination of core samples from the Santee/Clinchfield section and delineated five carbonate, two terrigenous, and one siliceous microfacies. The eight microfacies include: 1) lime mud (micrite); 2) skeletal wackestone; 3) skeletal packstone 4) skeletal grainstone; 5) microsparite; 6) terrigenous mud; 7) terrigenous sand and sandstone; and 8) siliceous mudstone. Skeletal wackestone is the dominant microfacies in the stratigraphic interval, and is found throughout the "calcareous zone" beneath the GSA, forming 55 percent of the sampled population. The carbonate-rich clastics and limestone in the Santee/Clinchfield-Dry Branch stratigraphic interval vary widely in thickness. Calcareous sands range from 2 feet to 33 feet in thickness, the sandy and muddy limestones range in thickness from 3 feet to 30 feet. This complex sedimentary package underlies most of the facilities in the GSA including the burial grounds, the tank farms, and the seepage basins (Figure 1).

The presence of glauconite along with a normal marine fauna including foraminifers, molluscs, bryozoans, and echinoderms, indicates that the Santee/Clinchfield limestones and limy sandstones were deposited in clear, open-marine water of normal salinity on the inner to middle shelf (Figures 3 and 5) (Thayer and others, 1994; Parker, 1999 and 2000). The abundance of carbonate mud (micrite) in the limestones suggests deposition in quiet water below normal marine wave base. The presence of abraded and well-worn skeletal grains indicates that bottom transport by currents or storm-generated waves alternated with quiet-water conditions in which the sediments accumulated.

The presence of varying percentages of fine, subangular quartz sand and terrigenous mud in the carbonate lithologies indicates the varying but ever presence proximity of the carbonates to riverine input (Figures 3 and 4). Viewing the Santee/Clinchfield sedimentary package parallel to the shoreline (Figure 5), the carbonate-rich sediments would be concentrated in the areas furthest removed from the tidal inlets at the shoreface where clastic sediments supplied by riverine input is concentrated. The clastic-rich sediments on the other hand would concentrate opposite the tidal inlet areas where clastic sediment is more readily available. The lateral facies transition of the sediments in the subtidal shelf environment from carbonate-rich to clastic-rich lithologies is therefore gradual and measures in the thousands of feet. Shifting locations of the tidal inlets at the shoreline has resulted in a complex sedimentary package (Figure 7) where facies gradually transition from one lithology to another both laterally and vertically. Therefore both vertical and lateral lithologic variability in the Santee/Clinchfield sequence is the result.

The Dry Branch Formation (Sequence III), including the Griffins Landing limestone member and the Tobacco Road Formation, were deposited over the Santee/Clinchfield section in shoreline to lagoonal/marsh depositional environments (Figure 5). The Dry Branch/Tobacco road sedimentary package in the GSA is interpreted to be upward fining low sinuosity distributary channel and over bank deposits that retain there depositional fabric and

thickness over several miles as the distributary channels swept across the lagoonal/marsh environment. Thus the primary depositional fabric (several upward fining sequences from coarse channel sand to overbank silty mud) and the uniformity in the thickness of the sequence can be traced for miles in the central part of the SRS.

Locally however, the contact between carbonate sediments and laterally comparable clastic sediments is sharply drawn, occurring over distances of only a few feet. Here the carbonate is interpreted to be the remains of more continuously deposited beds (Thayer and others, 1994: Parra and others, 1998) where post depositional dissolution and removal of carbonate left isolated remnants over time. The overlying Dry Branch/Tobacco Road (”Upland” unit ?) clastics being uniform in depositional fabric and thickness over extensive lateral distances, are interpreted to have slumped downward compensating for the removal of the carbonate (Figure 8). The slumping into the lows left by the removal of the Santee/Clinchfield carbonate did not result in the draping and thinning of the overlying Dry Branch/Tobacco Road sediments over the carbonate rich structural highs. That would have occurred if the dissolution and differential collapse of the Santee/Clinchfield section predated Dry Branch/Tobacco Road deposition. On the contrary, the Dry Branch/Tobacco Road section is uniform in thickness over both the underlying structural highs and lows. Thus the consolidation (collapse) of the Santee/Clinchfield section due to the removal of the carbonate, post-dates deposition of the Dry Branch and Tobacco Road sands and possibly the “upland unit” sands and gravel as well.

Diagenesis of the Carbonate Sediments and Formation of Soft Zones

The carbonate-bearing and carbonate-rich Santee/Clinchfield sediments underwent extensive diagenesis due to dissolution and/or precipitation of calcite, silica and other minerals. Post-depositional events affecting the limestones and limey sandstones occurred in both the marine and freshwater phreatic (saturated) environments.

The Santee/Clinchfield sediments were deposited in the subtidal “normal” marine environment where marine phreatic waters bathed the newly deposited sediment. Diagenetic events occurring in the marine phreatic environment included: 1) boring and micritization of skeletal grains to form micrite envelopes (Figures 9 and 10), mainly pelecypods, and 2) precipitation of subsea cements, including pyrite and glauconite. Glauconite precipitates under slightly reducing conditions in water depths greater than 10 m; its presence indicates slow sedimentation rates (Nystrom and others, 1989, 1991) in marine shelf environments. The pervasive presence of glauconite in the Santee/Clinchfield sediments corroborates the interpretation that the sediments were deposited in subtidal marine shelf environments based on fossil content and sediment fabric analysis. Pyrite precipitates and is associated with organic matter within the carbonate mud (micrite) matrix of the limestones indicating that it formed under localized reducing conditions in areas containing putrifying tissue where sulfate-reducing bacteria were abundant (Scoffin, 1987).

The limestones commonly underwent minor post-depositional compaction within the first few hundred feet of burial as shown by the presence of broken pelecypod and other shells (Figure 11).

The Santee/Clinchfield sediments underwent at least two episodes of fresh water flushing. The initial episode of dissolution/erosion of the middle Eocene Santee/Clinchfield sediments occurred soon after burial following the drop in sea level at the Santee unconformity (Figure 4). The diagenetic changes that occurred that materially effected the mineralogy and/or the

engineering properties of the sediments include the following:

- Skeletal grains, mostly pelecypods, dissolved to create molds (Figures 9, 10 and 11). The molds underwent solution-enlargement to form vugs (Choquette and Pray, 1970) and channels (Figure 12). This was an important porosity-creating process in the limestones and limey sandstones because pelecypods formed up to 20 percent of the original unconsolidated sediment (Thayer and others, 1994). Locally the molds and vugs collapsed due to compaction following the dissolution of the fossil debris (Figure 13).
- Some of the carbonate derived from dissolution of the fossil shell debris described above was precipitated nearby as pore-reducing or pore-filling calcite cement (Figure 14). Rine and Engelhardt, 1999, noted that at least two generations of spar cements appear to be present in the carbonates from core at the ITP site in H Area (Figure 1), both related to separate episodes of dissolution. Carbonate precipitation however was a minor process in the limestones and limey sandstones. Most of the carbonate material released from dissolution of fossil shells was exported out of the system as indicated by the small number of pores that are lined or filled with sparry calcite cement. Where it occurred however, the carbonate was often lithified (cemented) into hard limestone.
- Biogenic opal-A in the form of sponge spicules and diatom valves dissolved to create silica-rich pore water. Some of the silica was precipitated as 2-5 μm sized opal-CT lepispheres that replace carbonate mud (micrite) matrix (Figure 11), precipitated within molds and vugs and in micropores in the lime mud matrix. Opal-CT formation generally postdates solution of skeletal grains because the silica lines the interiors of some molds.

The amount and selectivity of the Opal-CT and chalcedony precipitation and replacement of carbonate is variable in the Santee/Clinchfield sediments (Parker, 1999). Precipitation of the opal-CT silica varies from rare to pervasive where the entire precursor carbonate sediment was 100 percent replaced by silica (Figures 15 and 16). The main limiting factor for silica precipitation and replacement of carbonate depends on the quantity and availability of amorphous biogenic opal-A (sponge spicules and diatom valves) that dissolved to create silica-rich pore water for mobilization and precipitation of the silica into the nearby sediment (Maliva and Seiver, 1988). The silicification process ceased when the silica supply (diatom and sponge-spicule biogenic opal-A) was exhausted.

Fibrous chalcedony precipitates locally as rim cements on detrital quartz grains (Figures 15 and 17). Cement stratigraphy indicates that chalcedony formed after precipitation of opal-CT.

Following the episode of fresh water flushing and exposure of the Santee/Clinchfield sediments at the Santee unconformity, Tobacco Road and Dry Branch sediments were deposited in shoreline environments in the GSA. Now the underlying Santee/Clinchfield section would be alternately flushed by the meteoric phreatic zone (fresh water)/marine phreatic zone (salt water) mixing zone (Figure 18). Here further dissolution of the Santee/Clinchfield carbonates occurred albeit at a reduced rate, and siliceous replacement and cementation of the clastics and carbonates progressed until the supply of silica was exhausted. Eventually, as Dry Branch and especially Tobacco Road sedimentation continued, the Santee/Clinchfield sediments were buried more deeply and the mixing zone waters could no longer reach the section (Figure 18). Here the sequence remained in the marine phreatic environment for extended lengths of time and diagenetic alteration of the sediments was reduced to a minimum or essentially ceased.

A dramatic increase in sediment supply and a retreat of the shoreline seaward to the southeast, resulted in deposition of the "upland unit" sand and gravel (Sequence IV) in fluvial to upper delta plain environments (Figure 3). This is the time frame of the further dissolution and removable of the Santee/Clinchfield carbonate due to renewed fresh water flushing of the sequence. Here the overlying Dry Branch/Tobacco Road ("Upland" unit ?) clastics are interpreted to have slumped downward compensating for the removal of the carbonate (Figure 8). Slumping into the lows left by the removal of the Santee/Clinchfield carbonate corroborates the assertion that the consolidation of the interval post-dates deposition of the Dry Branch and Tobacco Road sands and possibly the "upland unit" sand and gravel.

Rine and Engelhardt, 1999, noted vugs filled with sand and silt sized limestone fragments and quartz grains present in thin sections from the ITP site in H Area (Figures 1 and 19) and concluded that the detritus was probably derived from leaching and collapse of rock adjoining the vug. The voids not containing the detritus are probably molds of single shells and are not connected to other large pores. These limestone and quartz debris filled vugular limestones formed during the "collapse" and consolidation of the Santee/Clinchfield carbonates in "upland and/or post upland unit" time.

In conclusion, two episodes of freshwater flushing of the Santee/Clinchfield section resulting in two (or more) stages of fossil shell dissolution are hypothesized based on the multiple episodes of erosion/dissolution of the section. The first occurred at the time of the Santee unconformity, the second at the time of deposition of the "upland unit" following the Upland unconformity. During the interim period between the two primary episodes of fresh water flushing of the Santee/Clinchfield section, dissolution of carbonate and precipitation and replacement of carbonate by silica continued albeit at a slower rate during deposition of the Dry Branch and Tobacco Road sands.

The carbonates and limey sands of the Santee/Clinchfield sequence underwent a complex combination of deposition of diverse lithologies, post-depositional dissolution/precipitation/replacement of calcite, silica and other minerals. The result is sediment often far removed from its initial depositional fabric and mineralogy. Local dissolution is so pervasive that the precursor sediment is no longer identifiable.

Extent of Carbonate Zones

A database was established that cataloged all data retrieved from core, geophysical logs, CPT logs and geotechnical (SPT) borings related to the stratigraphy and the presence of carbonates in the Dry Branch-Santee/Clinchfield interval. The primary sources of data for mapping the extent (stratigraphic and geographic distribution and "concentration") of the carbonate zones were binocular and petrographic examination of core retrieved from wells drilled in the GSA, SPT boring logs and borehole geophysical logs. The percentage of carbonate was recorded on a foot by foot basis from core described in the core lab. The thickness, distribution and percentage of carbonate were mapped from the core data. Mapping the stratigraphic and lateral extent of the carbonate was augmented with lithologic data interpreted from the geophysical and SPT boring logs.

A file was assembled with stratigraphic information from core and geophysical log data that includes picks for the top of the Dry Branch Formation, top of the Santee/Clinchfield section (i.e., top surface of the Santee unconformity) and top of the Warley Hill Formation for the GSA area. The top surfaces were mapped and used to constrain the data query for the presence of calcareous sediments to the stratigraphic interval between the top of the Santee unconformity and the top of the Warley Hill Formation where the zones are located.

RESULTS

The geographic distribution, and concentration of carbonate sediment in the Santee/Clinchfield section in the GSA was analyzed by querying the footage of carbonate greater than or equal to 5% found in the cored wells and SPT borings. Figure 20 is a 3D profile illustrating the relative thickness and percentage of carbonate from core and SPT borings throughout the area.

Three areas stand out where several cored wells indicated an appreciable thickness of carbonate. From east to west they include the H Area ITP site (#1 on Figure 1), the H Area Seepage Basin (#2) and the Burial Grounds area (#3). In "F" Area at the APSF site (#4) and the F Basin area (#5) extensive SPT boring data is available indicating concentrations of carbonate. Neither area has concentrated core data that is needed to verify the SPT findings. In other areas carbonate is encountered in isolated cored wells. Here the extent of the carbonate is indeterminate. These large areas of sparse data precludes making the assumption, as was done in the past (Aadland and others, 1991; Richardson 1994; Thayer and others, 1994 and Aadland and others, 1994), that the carbonate is concentrated only in the areas indicated on the profile.

The average percentage of carbonate in each core was mapped. In general where the carbonate is thickest, the average carbonate percentage is greatest. The thickness of the Santee/Clinchfield section (interval between the Santee unconformity and the Warley Hill Formation) was mapped in the GSA. Carbonate thickness and concentration is directly related to the isopach thickness of the Santee/Clinchfield interval. Where the Santee/Clinchfield interval is thick carbonate is more concentrated, where the interval is thin carbonate thickness and concentration is reduced. It is further observed that where carbonate is concentrated in the Santee/Clinchfield section the overlying "upland unit", Tobacco Road/Dry Branch section is generally structurally high, and where the carbonate content is reduced or absent the overlying "upland unit", Tobacco Road/Dry Branch section is generally structurally low. This fact, and the uniformity in thickness of the Dry Branch/Tobacco Road section in the area mapped, indicates that the removal of carbonate and the thinning of the Santee/Clinchfield interval occurred in post Tobacco Road ("upland unit") time.

Significant Findings and Observations

- The carbonates and limey sands of the Santee/Clinchfield sequence underwent a complex combination of deposition of diverse lithologies, post-depositional dissolution/precipitation/replacement of calcite, silica and other minerals. The result is sediment often far removed from its initial depositional fabric and mineralogy. Local dissolution is sometimes so pervasive that the precursor sediment is no longer identifiable.
- The thickness of the Santee/Clinchfield interval in the GSA is variable. The thickness and concentration of carbonate is directly related to the thickness of the Santee/Clinchfield interval. In general where the Santee/Clinchfield interval is thickest the footage of carbonate is greatest and the average carbonate content (percentage) in the cores is greatest. Where the interval is thin the thickness and percentage of carbonate in the core is reduced.
- It is further observed that where the Sante/Clinchfield section in thick and where carbonate is concentrated, the overlying "upland unit" and Tobacco Road/Dry Branch section is generally structurally high (Figure 8). Where the section is thin and the carbonate content is reduced or absent, the overlying "upland unit" and Tobacco Road/Dry Branch section is structurally low but uniform in thickness with the section in the structurally high areas. This

indicates that the removal of carbonate and the thinning of the Santee/Clinchfield interval occurred in post Tobacco Road/"upland unit" time.

- All degrees of carbonate dissolution from minor to complete are observed in the Santee/Clinchfield sediments.
- Two primary episodes of freshwater flushing of the Santee/Clinchfield section resulting in two (or more) stages of fossil shell dissolution are hypothesized based on the multiple episodes of erosion/dissolution of the section. The first occurred at the time of the Santee unconformity, the second at the time of deposition of the "upland unit" following the upland unconformity. During the interim period between the two primary episodes of fresh water flushing of the Santee/Clinchfield section, dissolution of carbonate and precipitation and replacement of carbonate by silica continued albeit at a slower rate during deposition of the Dry Branch and Tobacco Road sands.
- The second episode of fresh water flushing in "upland unit" time resulted in the further dissolution and removable of the Santee/Clinchfield carbonate. Here the overlying Dry Branch/Tobacco Road ("Upland unit" ?) clastics are interpreted to have slumped downward compensating for the removal of the carbonate (Figure 8). Slumping into the lows left by the removal of the Santee/Clinchfield carbonate corroborates the assertion that the consolidation of the interval post-dates deposition of the Dry Branch and Tobacco Road sands and possibly the "upland unit" sand and gravel.

REFERENCES

Aadland, R. K., Gellici, J. A. and P. A. Thayer, 1995, Hydrogeologic Framework of West-Central South Carolina. State of South Carolina Department of Natural Resources, Water Resources Division Report 5, 200p.

Aadland, R. K., Cumbest, R. J., Howe, K., Lewis, S. E., Price, v. Jr., Richers, D. E., Wyatt, D. E. and K. S. Sargent, 1994, Geological Characterization in the Vicinity of the In-Tank Precipitation Facility (U). Westinghouse Savannah River Co., Site Geotechnical Services Dept., U. S. Department Of Energy Report, WSRC-TR-94-0373, Rev. 0, 88p.

Aadland, R. K., Harris, M. K., Lewis, C. M., Gaughan, T. F. and T. M. Westbrook, 1991, Hydrostratigraphy of the General Separations Area, Savannah River Site (SRS), South Carolina, USDOE Report WSRC-RP-91-13, Westinghouse Savannah River Company, Aiken, SC., 29808, 114 p.

Choquette, P. W. and L. C. Pray, 1970, Geological Nomenclature and Classification of Porosity in Sedimentary Carbonates. American Association of Petroleum Geologists Bull 54, p. 207-250.

Fallaw, W. C., and Price, V., 1995, Stratigraphy of the Savannah River Site and vicinity: Southeastern Geology, v. 35, p. 21-58.

Maliva, R. G., and R. Siever, 1988, Mechanisms and controls of silicification of fossils

in limestones: Journal of Geology, v. 96, p. 387-398.

Parra, J.O., Price, V., Addington, C., Zook, B.J., and Cumbest, R.J., 1998, Interwell seismic imaging at the Savannah River Site, South Carolina: Geophysics, 63: 1858-1865.

Parker, W. H., 1999, Petrographic Analysis and Microfacies Delineation for a Soft Zone Interval Beneath F-Area, Savannah River Site, Aiken, South Carolina. Report prepared by SAIC under subcontract AB6029N to DOE. 24p.

Parker, W. H., 2000, Petrographic Analysis and Microfacies Delineation for a Soft zone Interval Beneath R-Area, Savannah River Site, Aiken, South Carolina. Report prepared by SAIC under subcontract AB6029N to DOE. 10p.

Richardson, G. A., 1994, Petrographic and Hydrogeologic Characteristics of Eocene Calcareous Strata of the General Separations Area, Savannah River Site, South Carolina; Masters Thesis, University of North Carolina, Wilmington, 59p.

Rine, J. M. and D. W. Engelhardt, 1999, Geologic Characterization of Core from Borings HBOR-34 and HBOR-50, In Tank Processing (ITP) Area, Savannah River site, South Carolina. Report prepared for DOE by the Earth Sciences and Resources Institute, University of South Carolina, Columbia South Carolina. ESRI-USC Technical Report 99-3-F143. 16p.

Thayer, P.A., Smits, A. D., Parker, W. H., Conner, K. R., Harris, M. K., and M. B. Amidon, 1994, Petrographic Analysis of Mixed Carbonate-Clastic Hydrostratigraphic Units in the General Separations Area (GSA). Westinghouse Savannah River Company, Savannah River Site (SRS), Aiken, South Carolina, Report prepared for the U. S. Department of Energy, WSRC-RP-94-54, 83p.

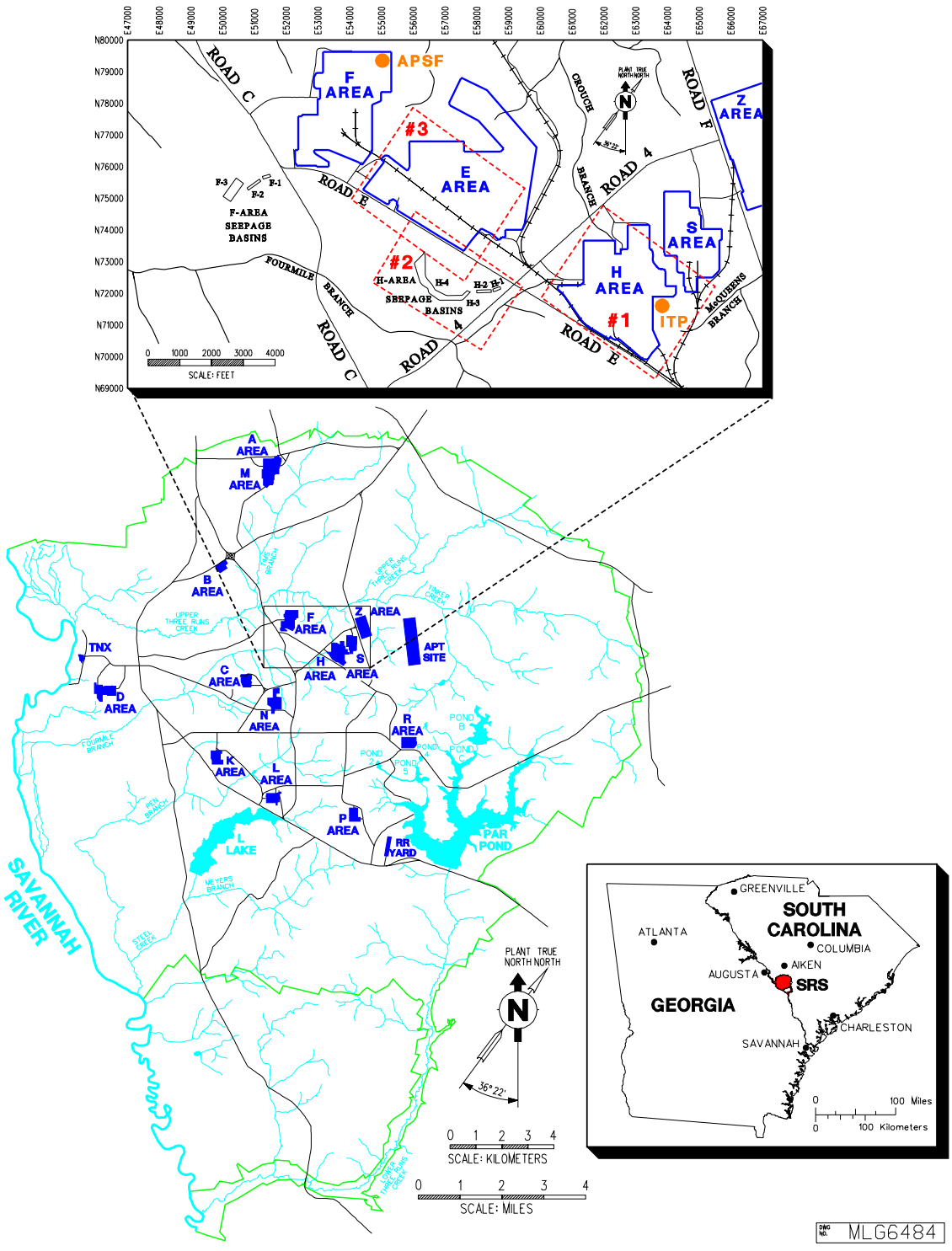

Figure 1. Location map of the General Separations area (GSA) at the Savannah River Site. The Burial Grounds, H Area Seepage Basin and the H Area ITP Site used in the Carbonate and soft zone query are outlined in red.

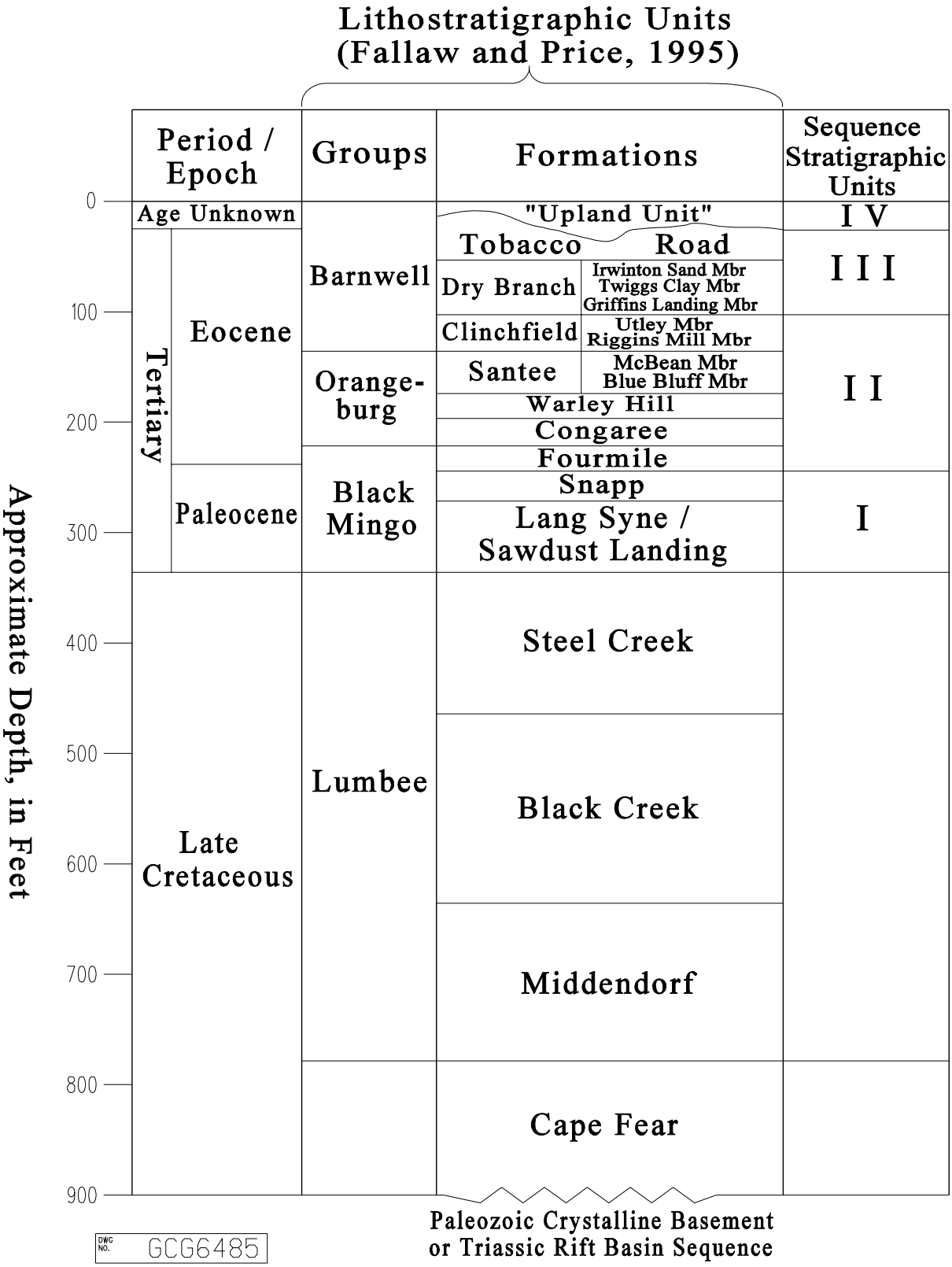

Figure 2. Lithostratigraphic and Sequence Stratigraphic Units, at the Savannah River Site.

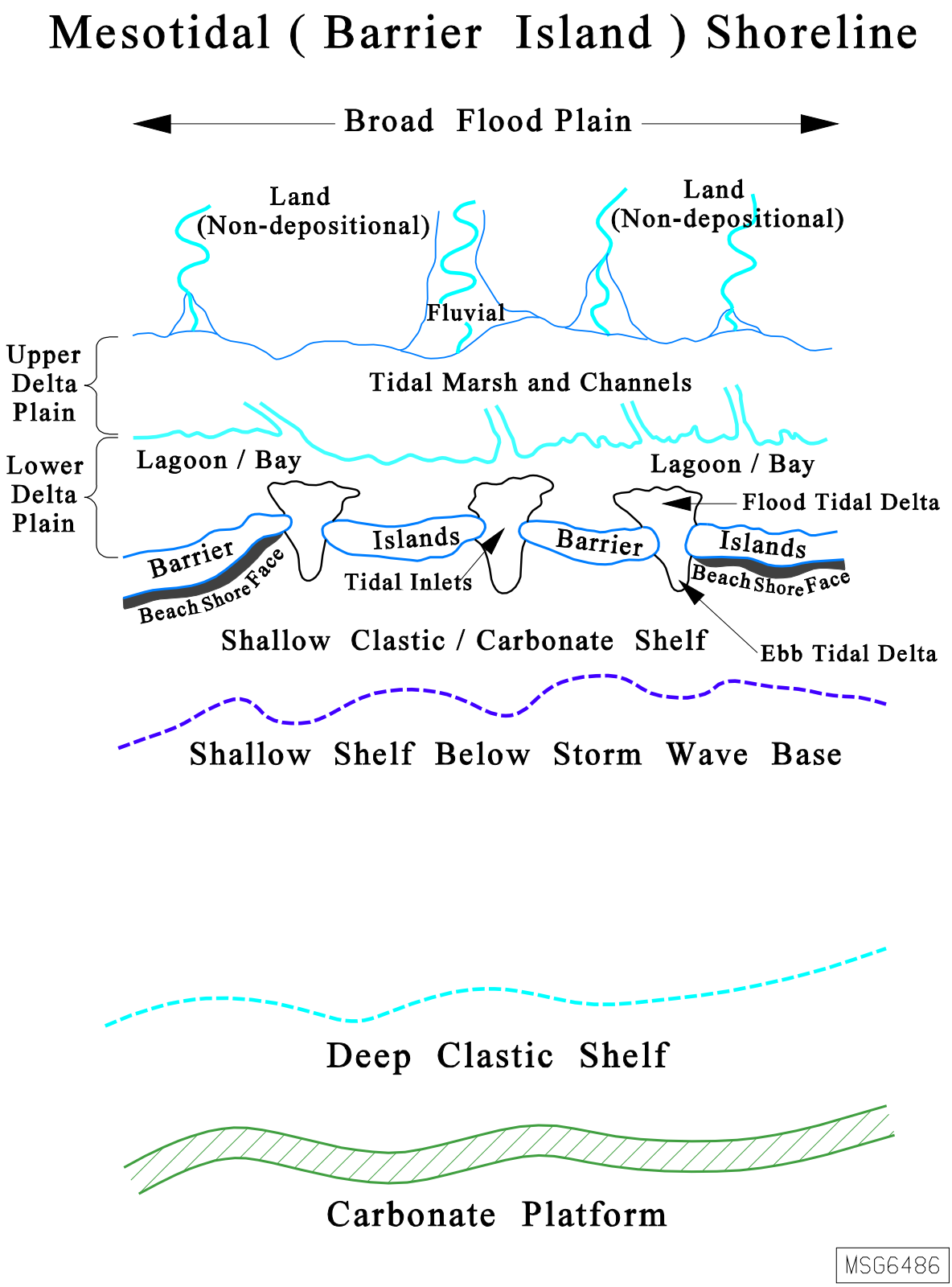

Figure 3. Spatial relationships of depositional environments typical of the Tertiary sediments at SRS.

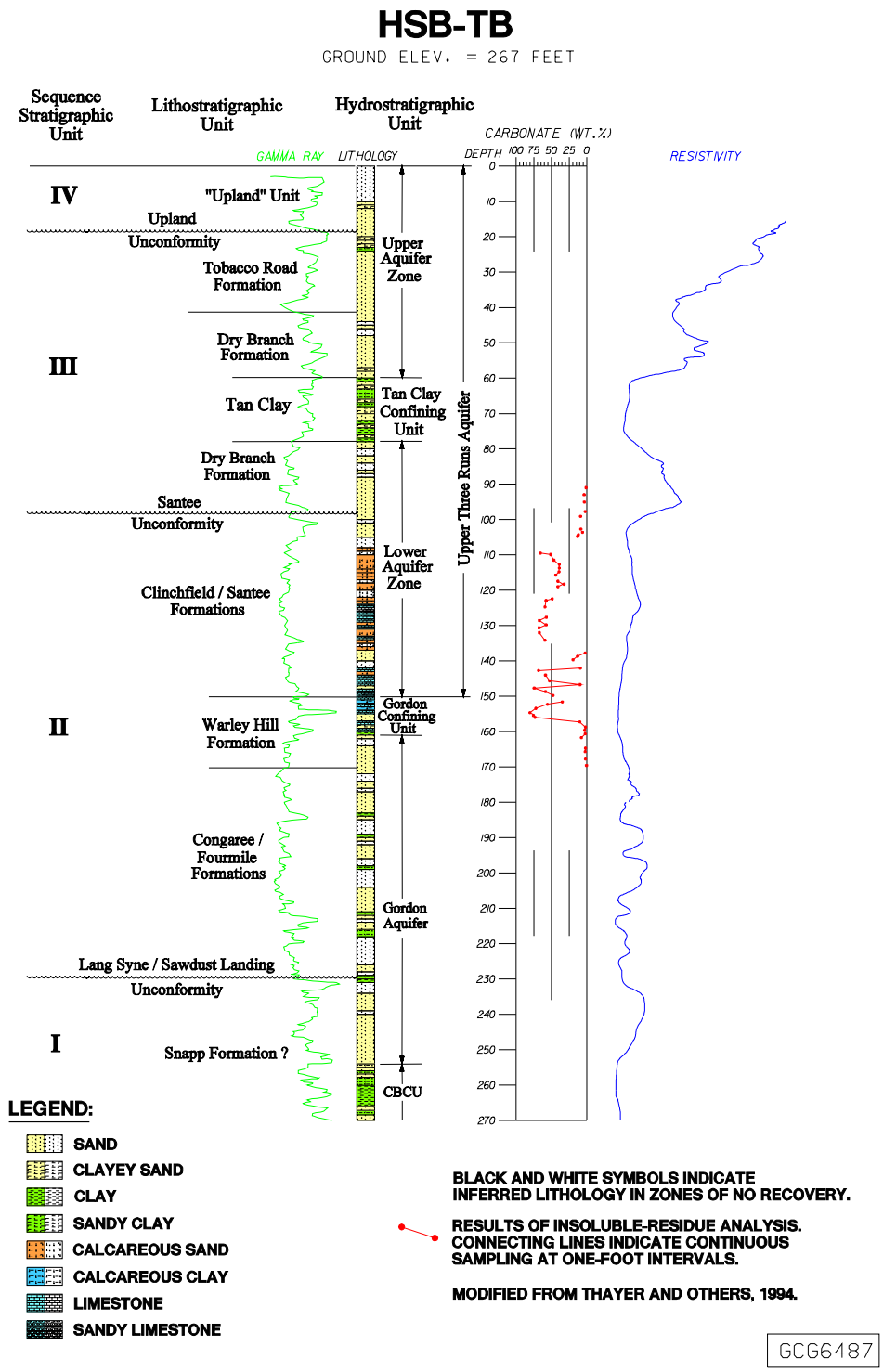

Figure 4. Lithologic data retrieved from core, and the summary of insoluble residue and carbonate WT % data, from Well HSB-TB, H Area, General Separations Area, Savannah River site.

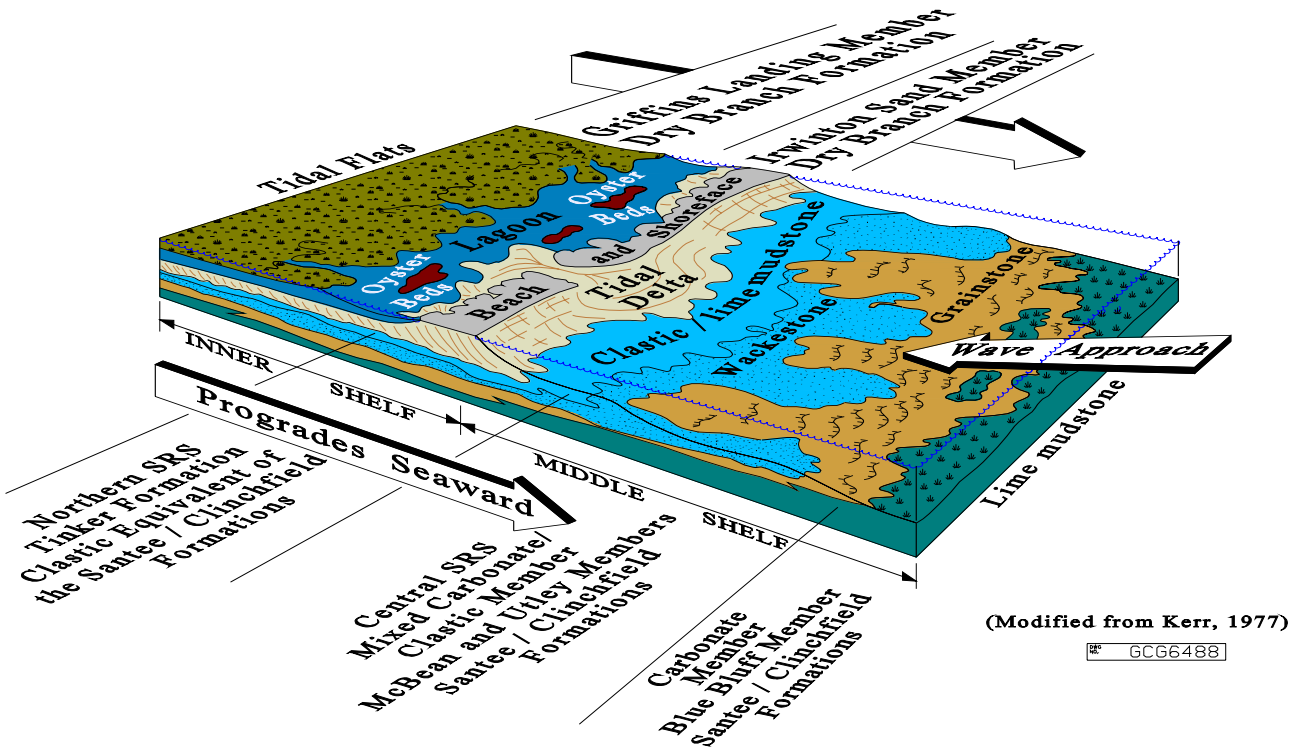

Figure 5. Spatial relationships of depositional environments typical of the Dry Branch and Santee/Clinchfield sediments at SRS. Progradation seaward puts the younger tidal flat/marsh/shoreline (inner shelf) sediments of the Dry Branch Formation over the older middle shelf sediments of the Santee/Clinchfield Formations in the General separations Area at SRS.

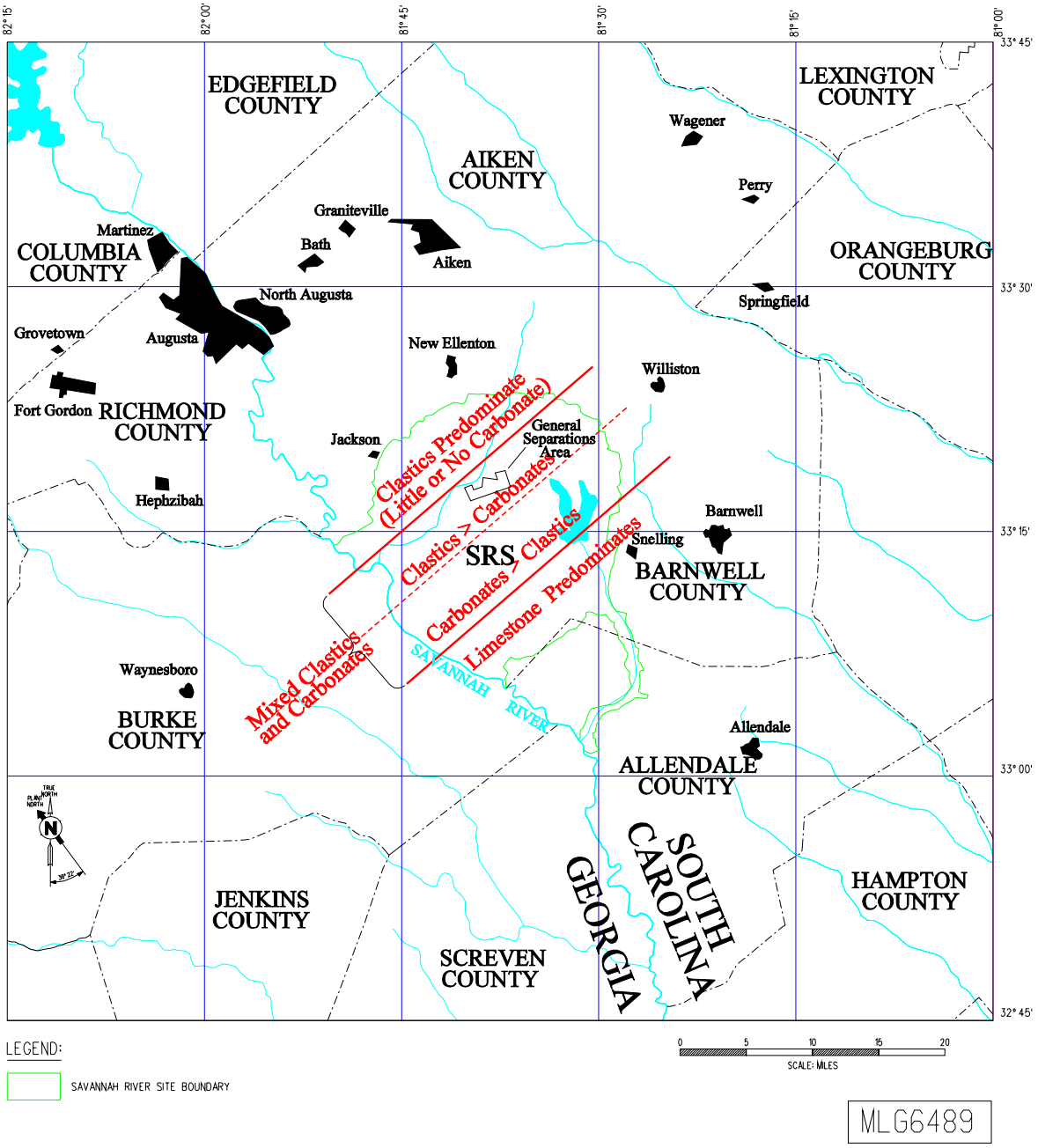

Figure 6. Regional distribution of carbonate in the Dry Branch-Santee/Clinchfield sequence at SRS.

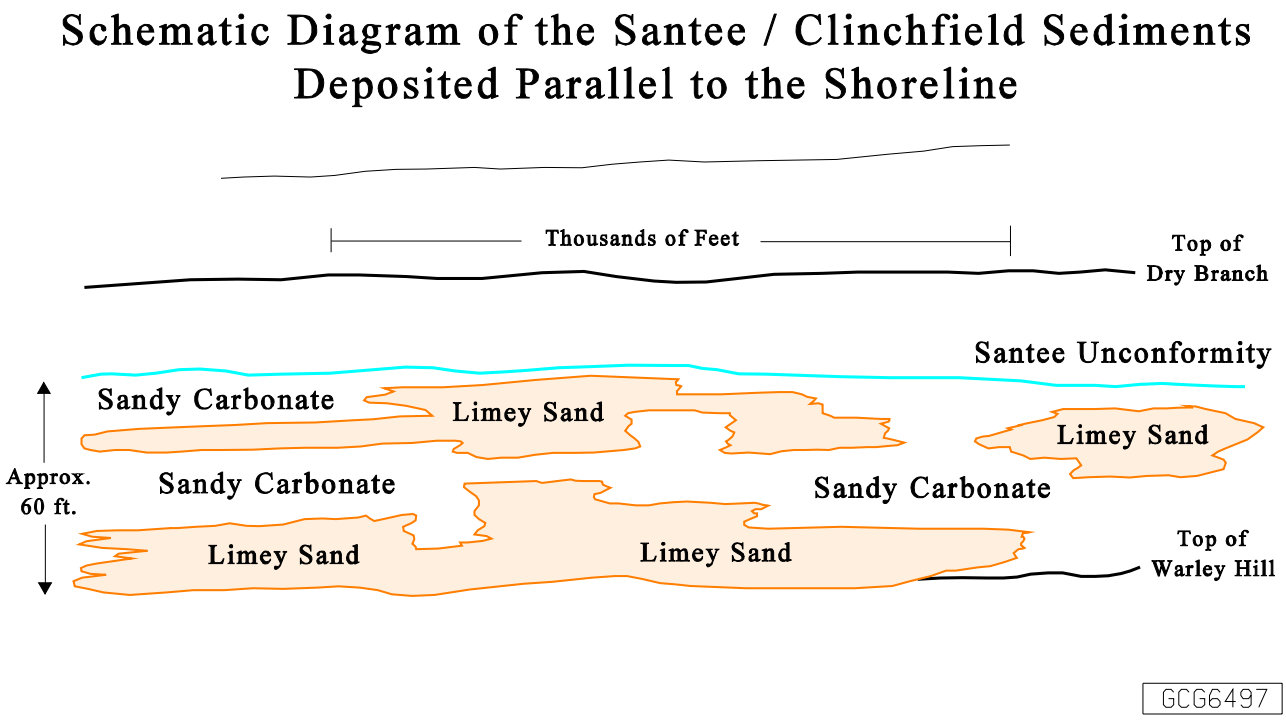

Figure 7. Shifting locations of tidal inlets at the shore face would result in shifting positions of the clastic-rich/carbonate-rich sediments deposited out on the subtidal shelf. The result is a complex mixture of sediment types that gradually transition from one lithology to another.

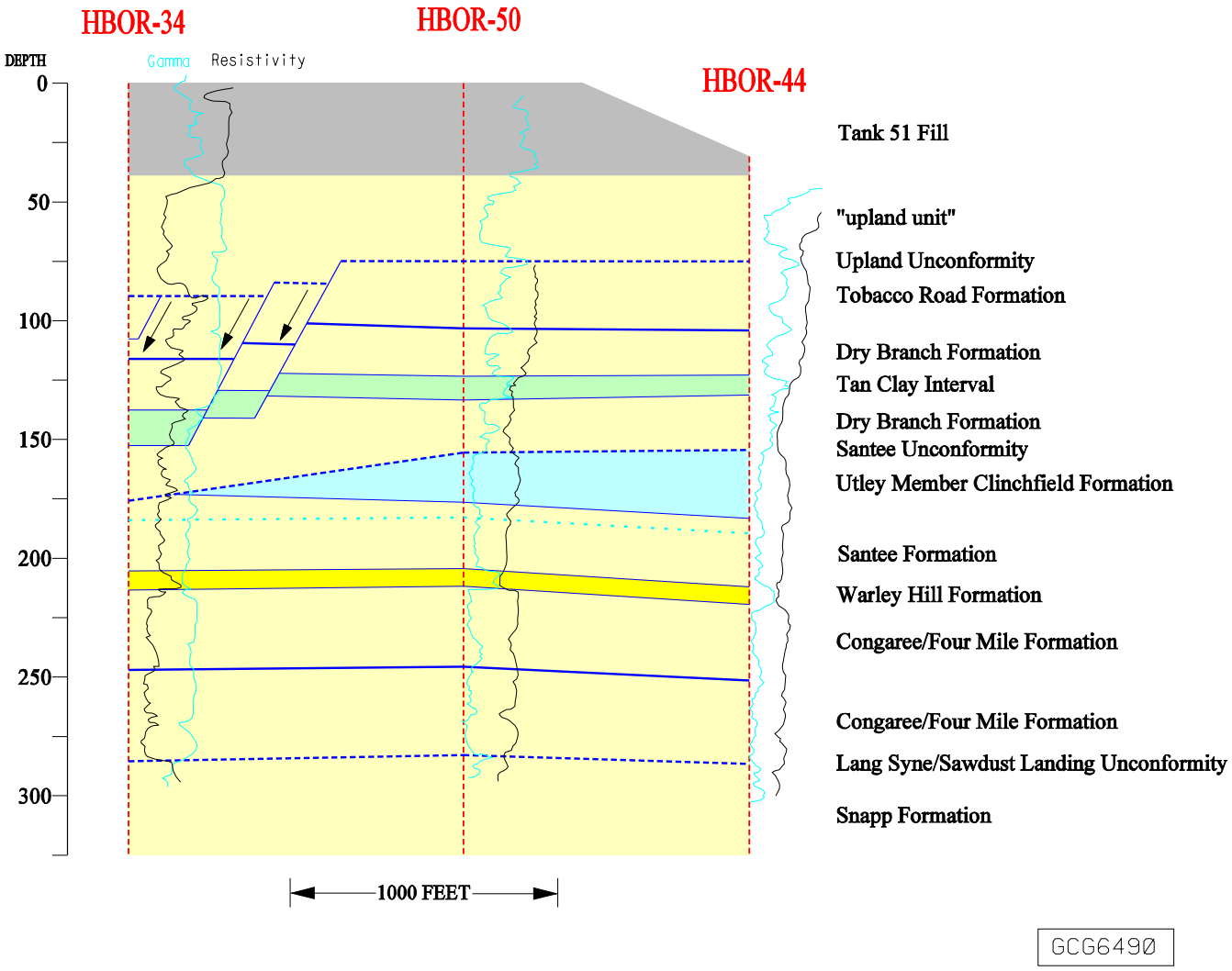

Figure 8. Slump faulting at the H Area ITP Site. Dissolution of carbonate in the Santee/Clinchfield sediments especially the Clinchfield, resulted in slumping and collapse of the section with Dry Branch, Tobacco Road and 'upland unit" sediments slumping into the resulting low areas.

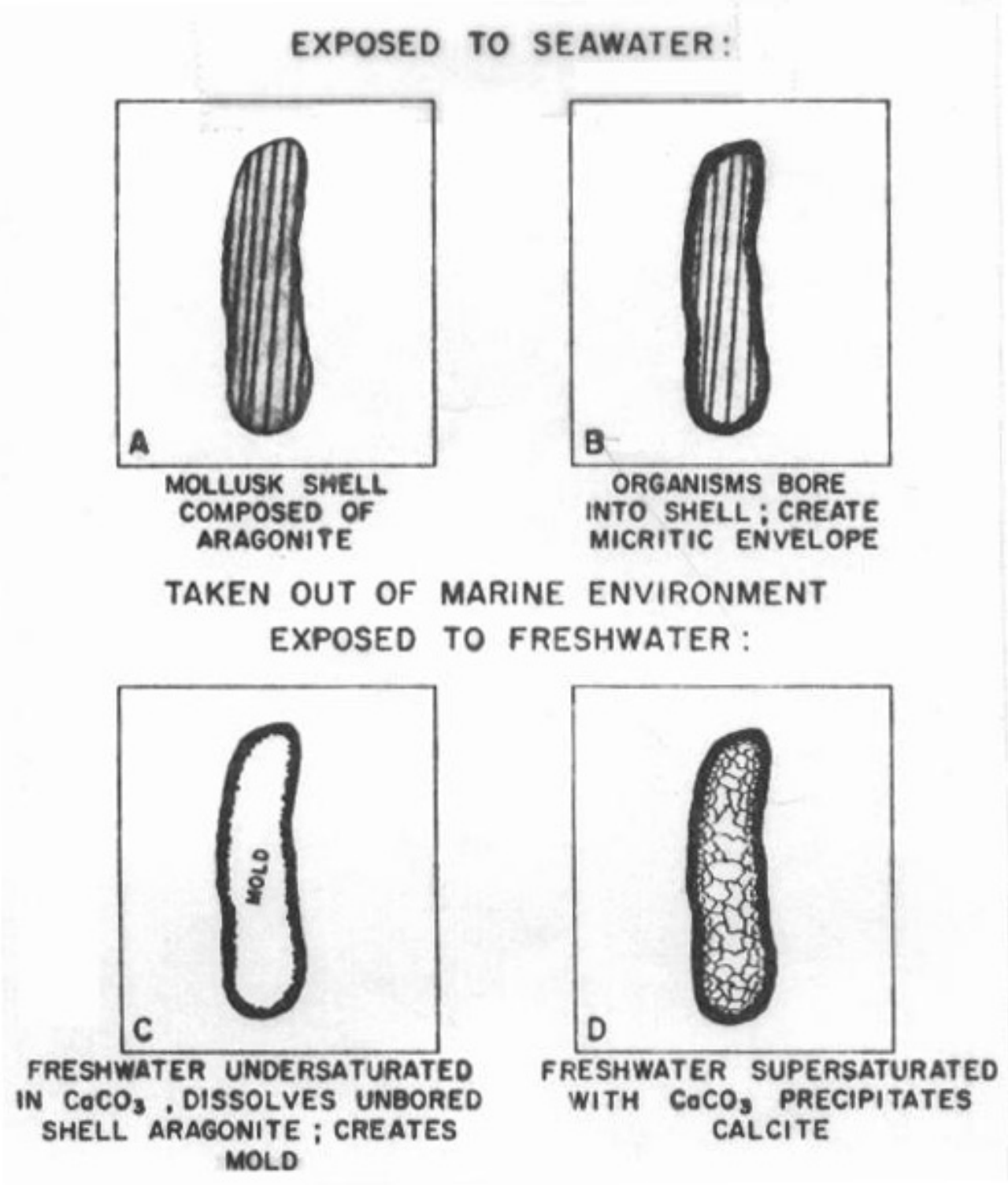

Figure 9. Diagrammatic summary showing steps in solution and precipitation of calcium carbonate by fresh water.

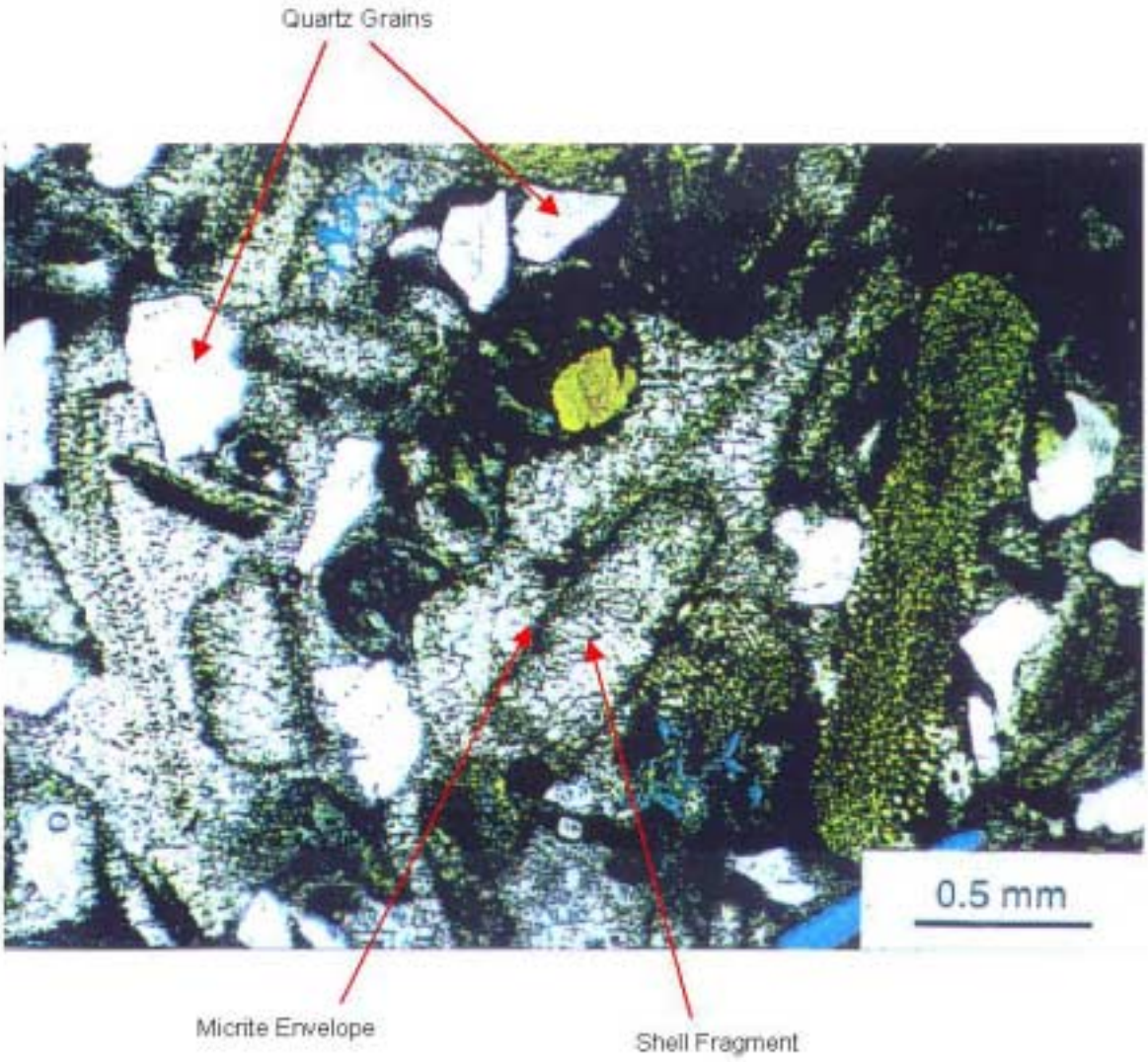

Figure 10. Photomicrograph of quartz-rich skeletal packstone from the Burial Grounds, GSA, SRS that has been diagenetically altered to sandy, molluscan-mold microsparite. From the Santee/Clinchfield section in Well BGO-14A, 122 ft. Crossed nicols. Blue area is void space filled with blue epoxy glue.

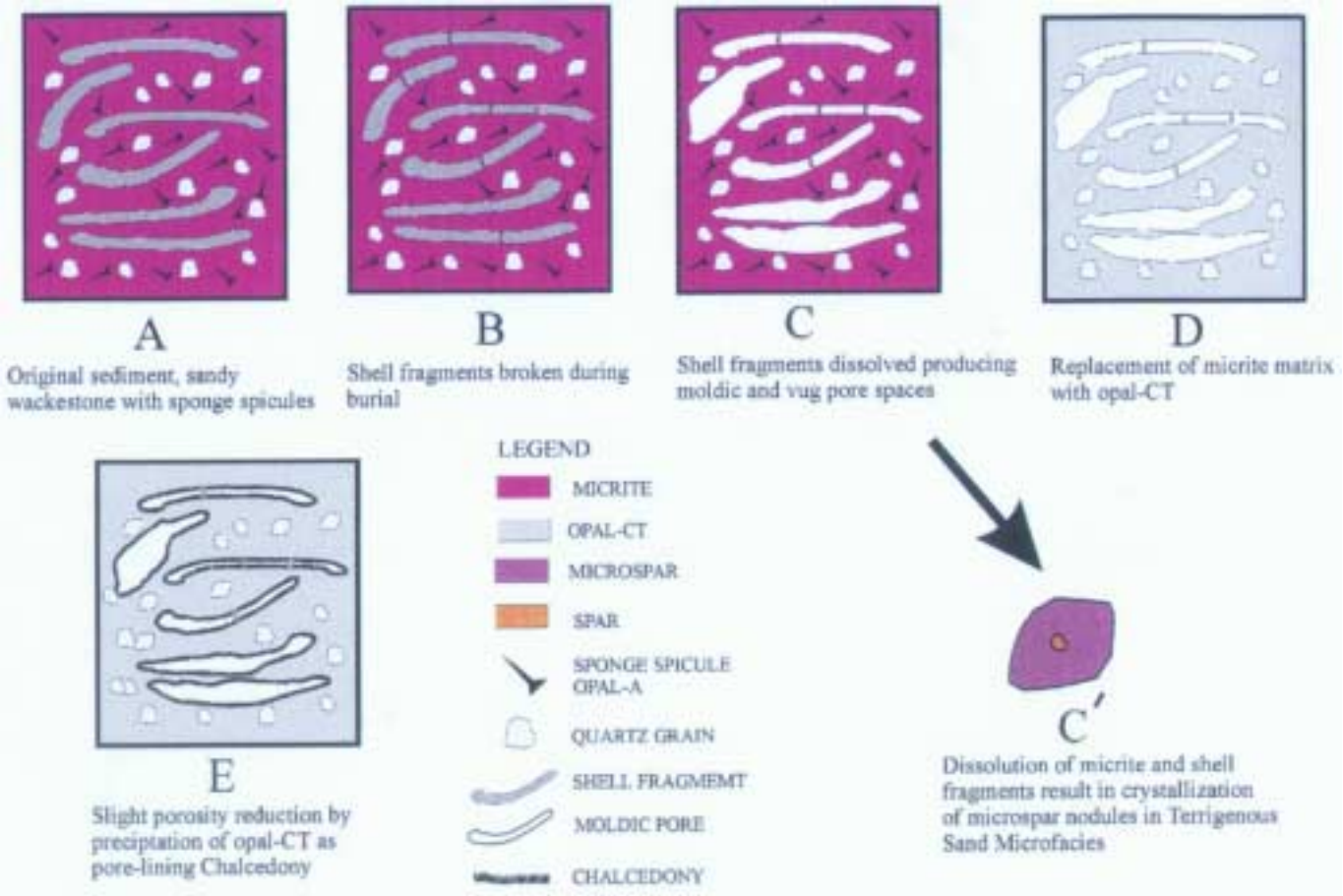

Figure 11. Diagrammatic representation of the interpreted diagenetic history of the sandy biomoldic chert microfacies.

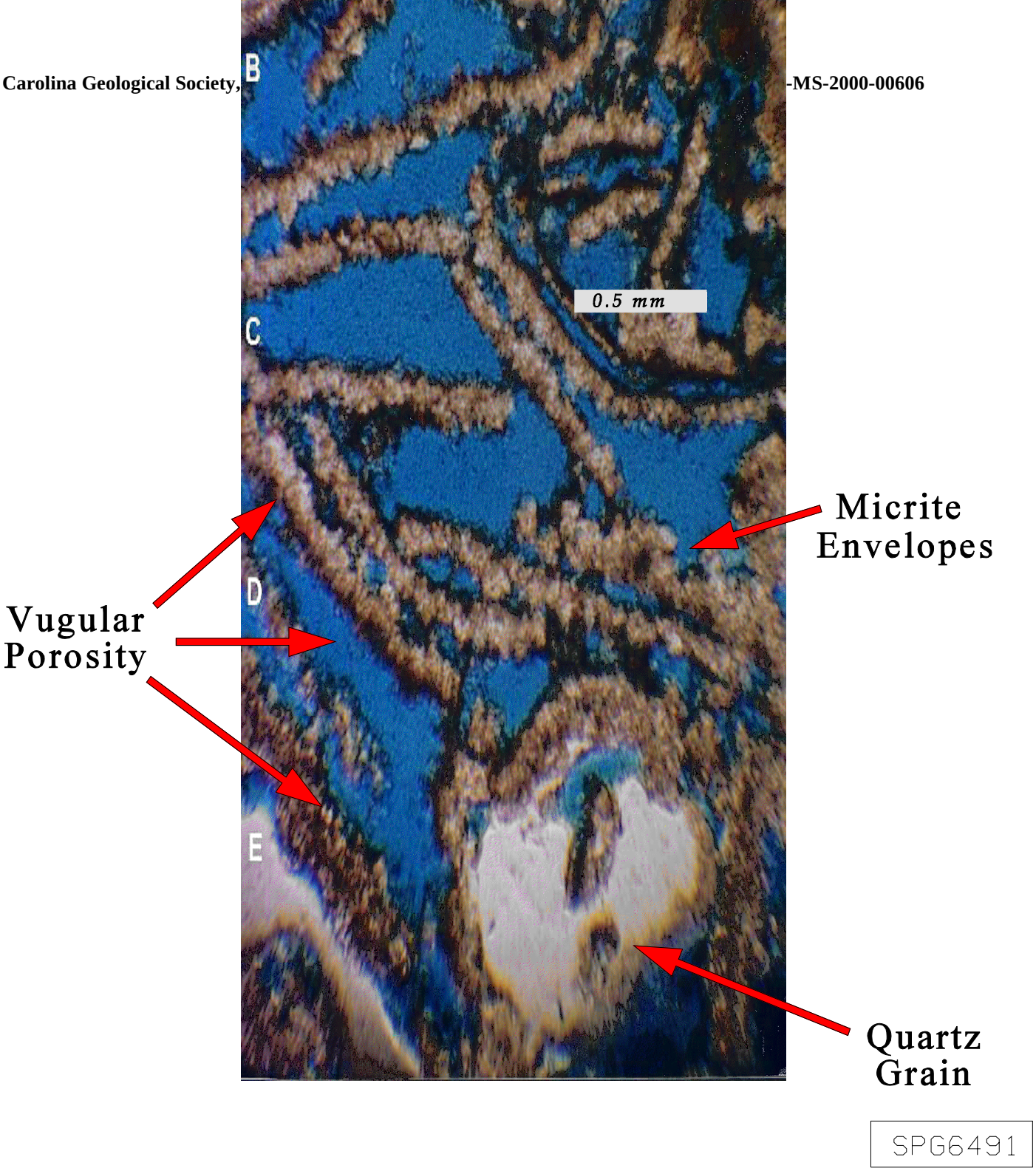

Figure 12. Extensive dissolution of fossil fragments in a skeletal grainstone (?) resulting in vugular porosity. Only micrite envelopes of the shell fragments remain. From the Santee/Clinchfield section, Well HBOR-50 @ 165 ft. H-Area ITP Site, General Separations Area, Savannah River Site. Void space filled with blue epoxy glue.

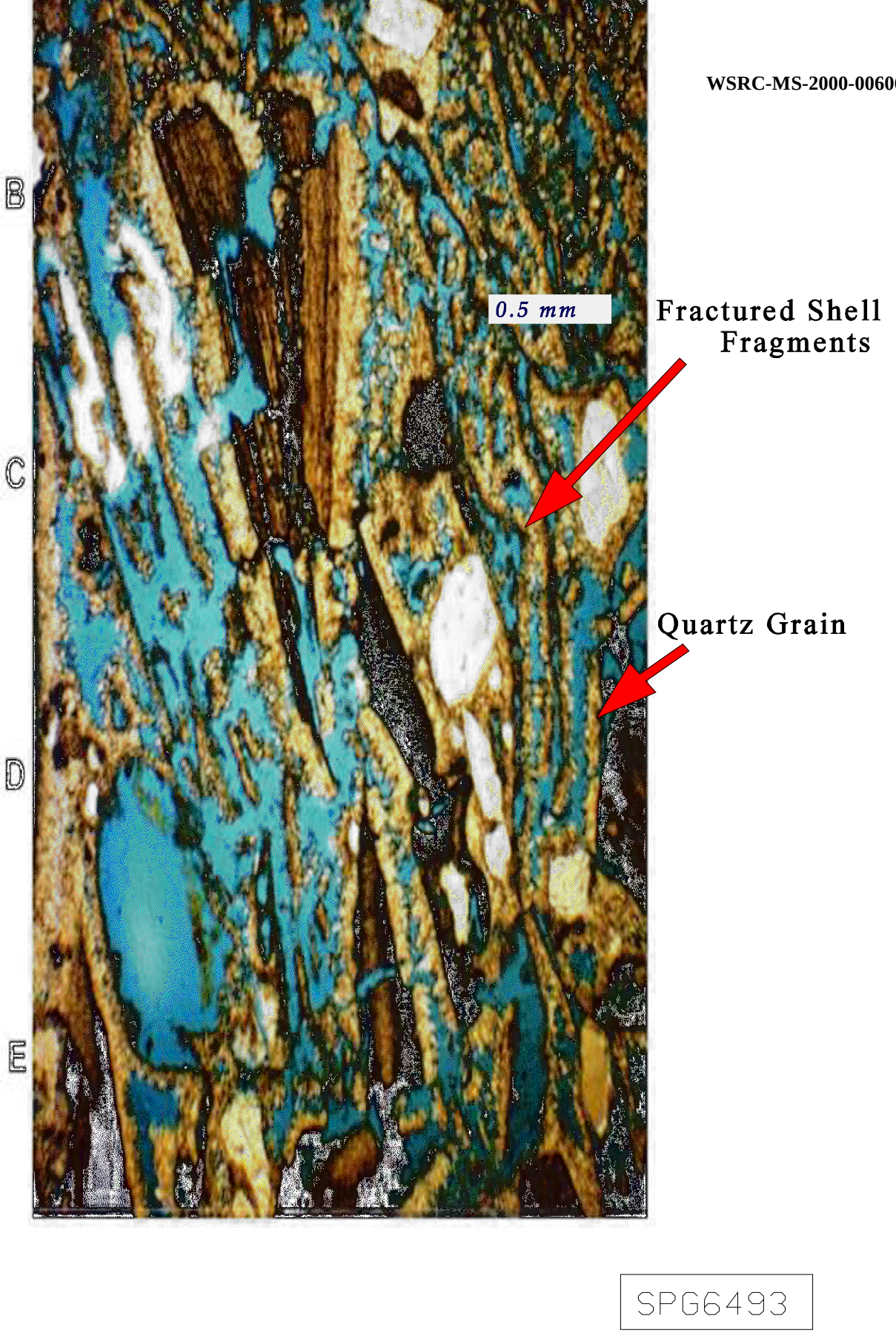

Figure 13. Collapsed and fractured shell fragments in a skeletal Grainstone (?). Well HBOR-50 @ 179 ft. in the Santee/Clinchfield section. Crossed Nicols. H-Area ITP Site, General Separations Area, Savannah River Site. Void space filled with blue epoxy glue.

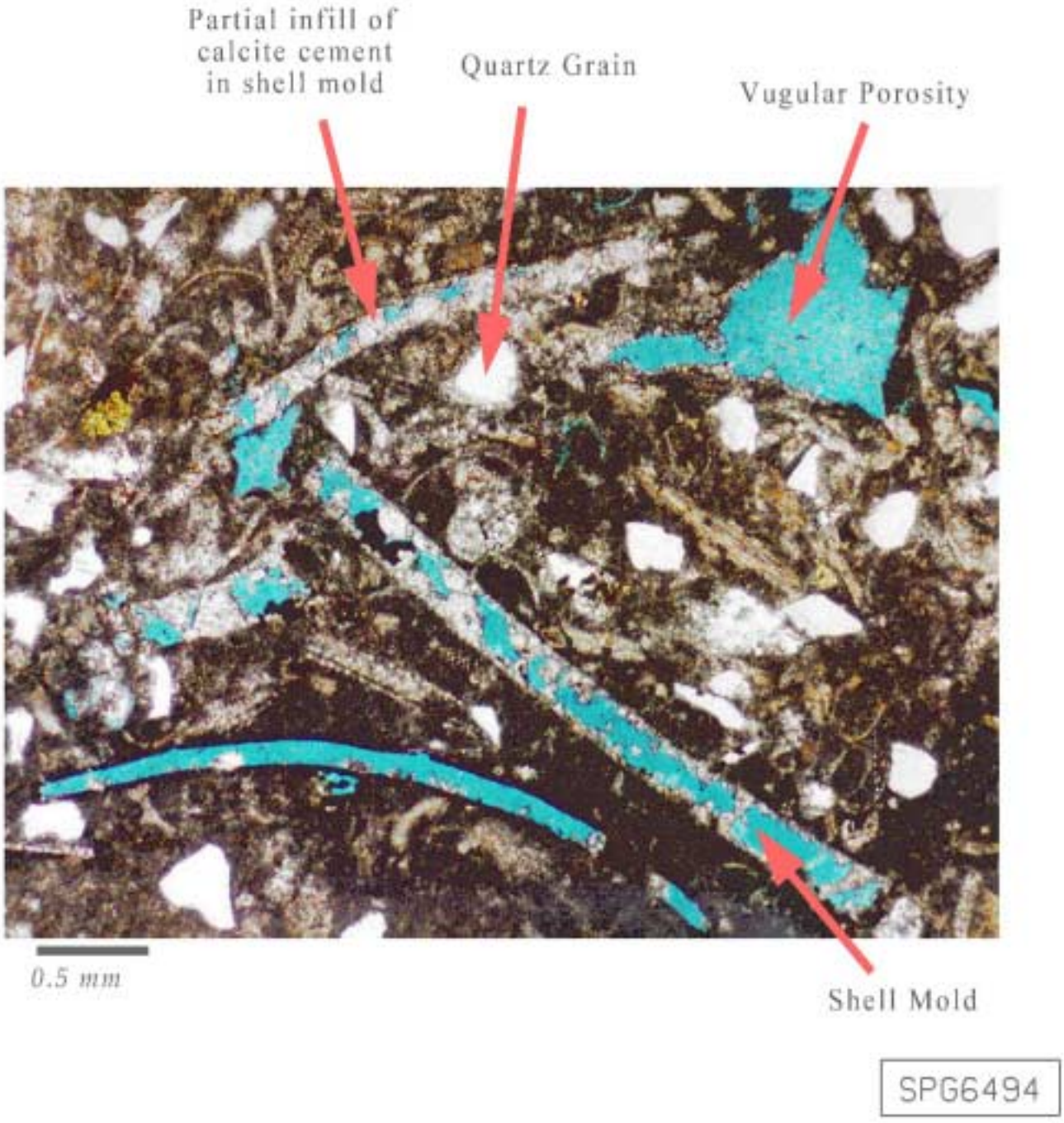

Figure 14. Sandy, pelecypod, pellet packstone. Santee/Clinchfield section, Burial Grounds, General Separations Area, Savannah River Site. Crossed nicols. Void space filled with blue epoxy glue.

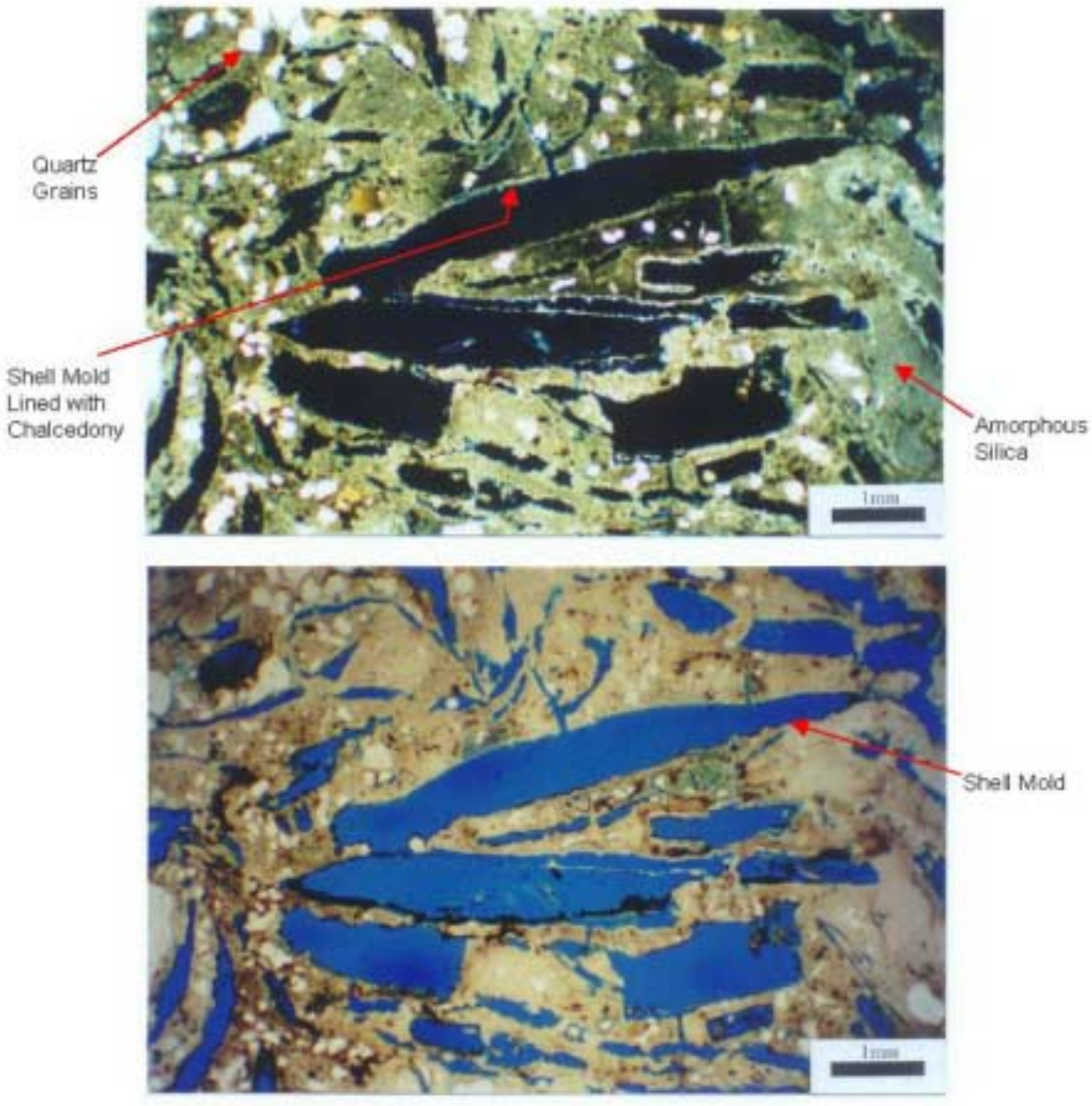

Figure 15. Photomicrographs of sandy biomoldic chert, Santee/Clinchfield section, Core CPT-157S3 @ 109.85 ft. F-Area APSF Site, General Separations Area, Savannah River Site. Bottom picture plane-polarized light. Amorphous silica (Opal-CT) replacement of calcite micrite (mud) matrix.

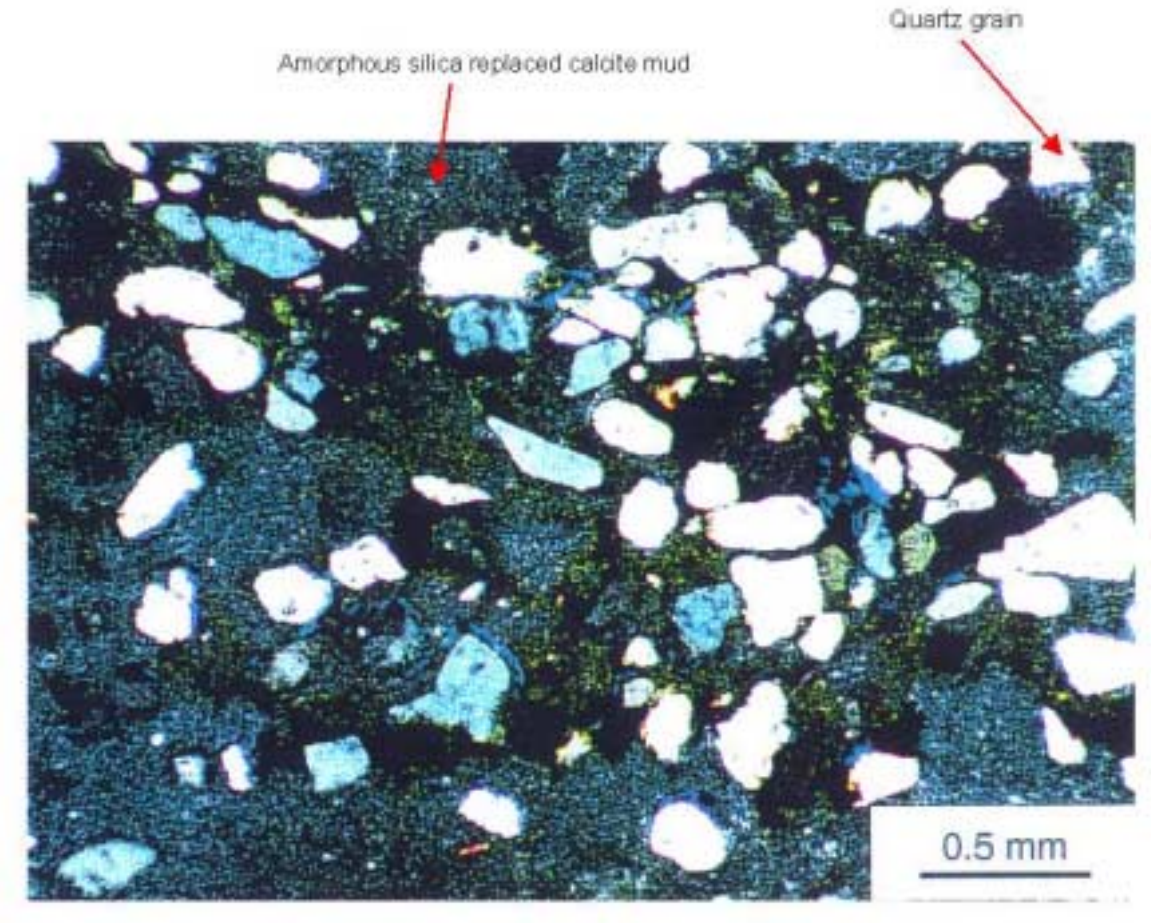

Figure 16. Photomicrograph of sandy siliceous mudstone, Santee/Clinchfield section, Burial Grounds, General Separations Area, Savannah River Site. Well BGX-2B, @ 151.2 ft. Crossed nicols. Calcite micrite (mud) matrix was replaced by amorphous (Opal-CT) silica.

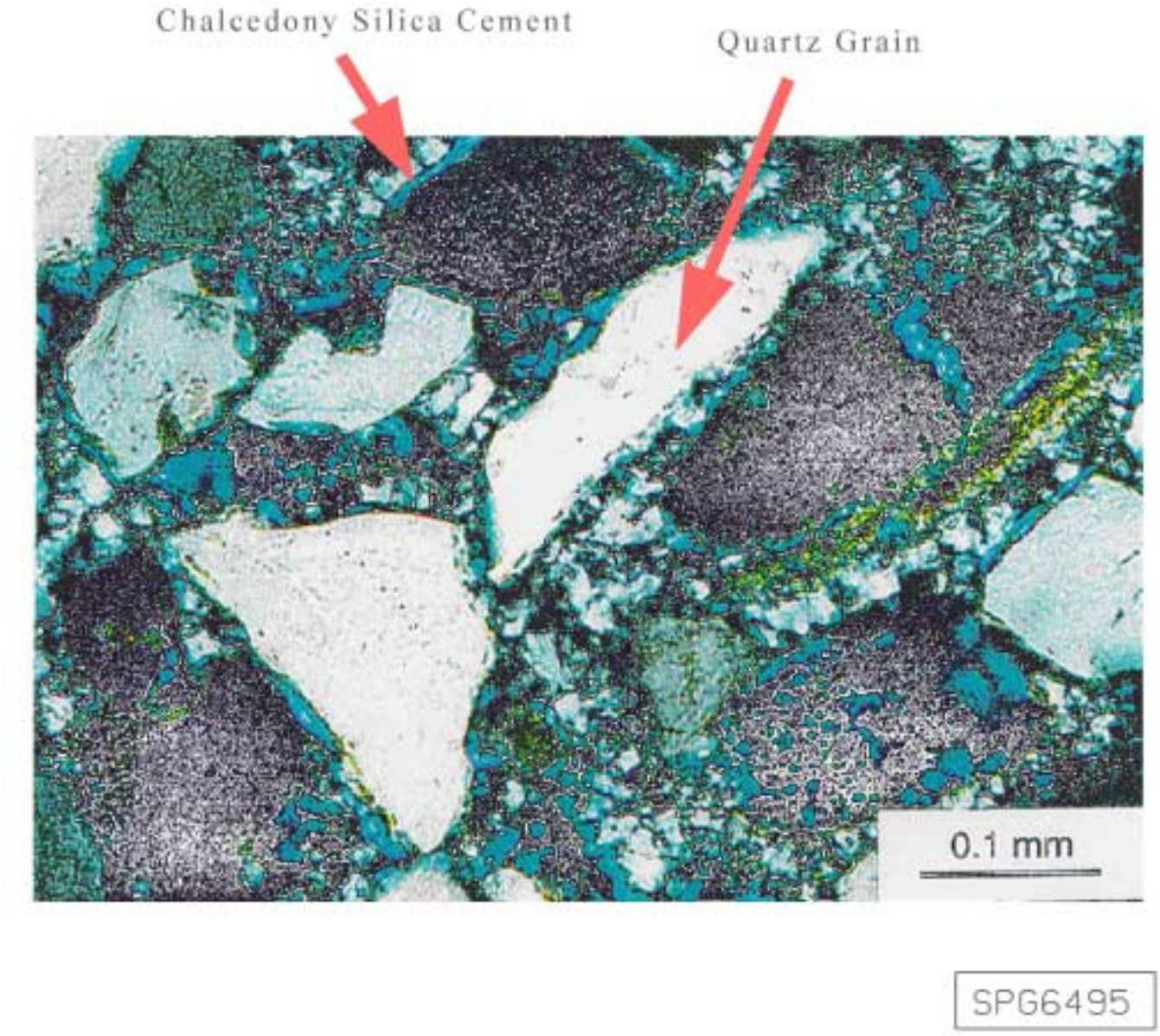

Figure 17. Chalcedony-cemented, quartz arenite, Terrigenous sand and sandstone microfacies. Santee/Clinchfield section, H Area, General Separations Area, Savannah river Site. Well YSC02A @ 109 ft. Crossed nicols.

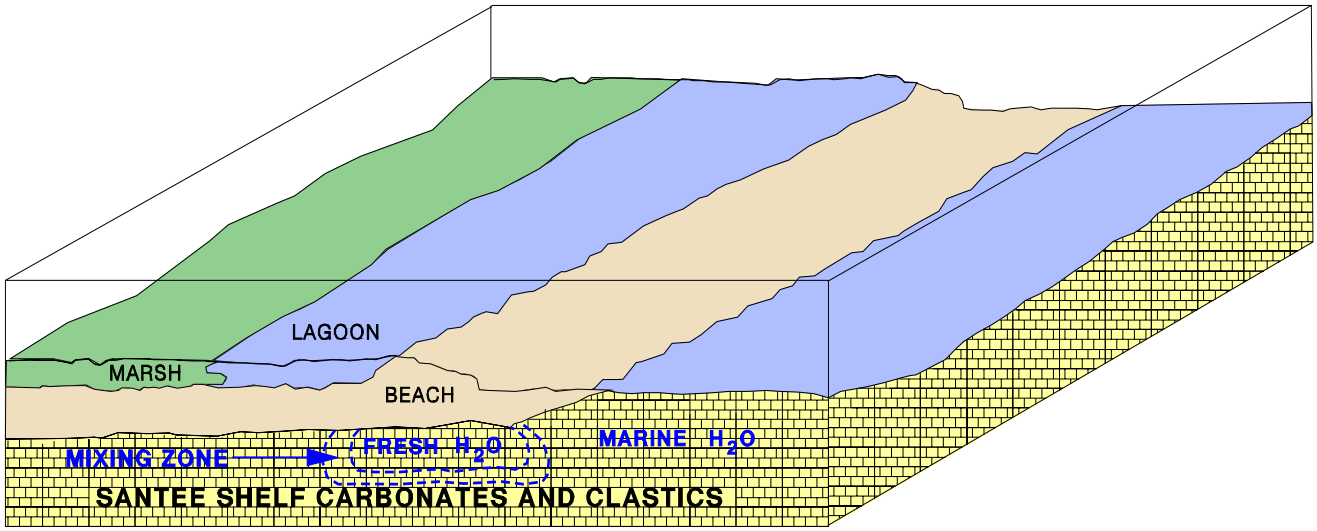

Figure 18a. Model for development of facies and soft zones in the General Separation Area, Savannah River Site.

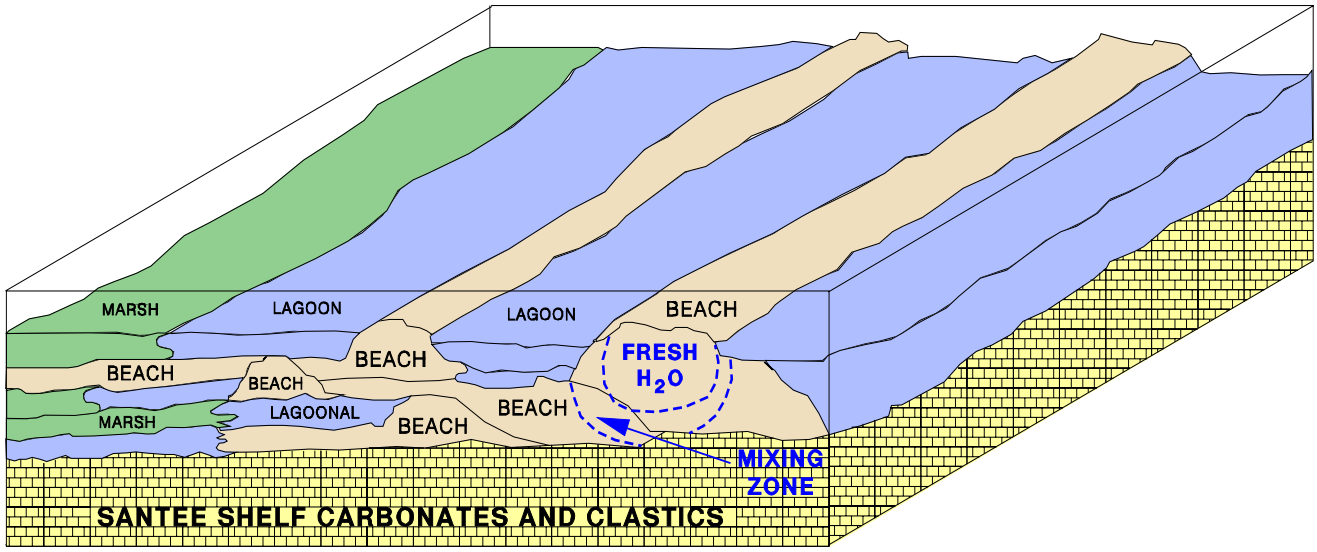

Figure 18b. Model for development of facies and soft zones in the General Separation Area, Savannah River Site.

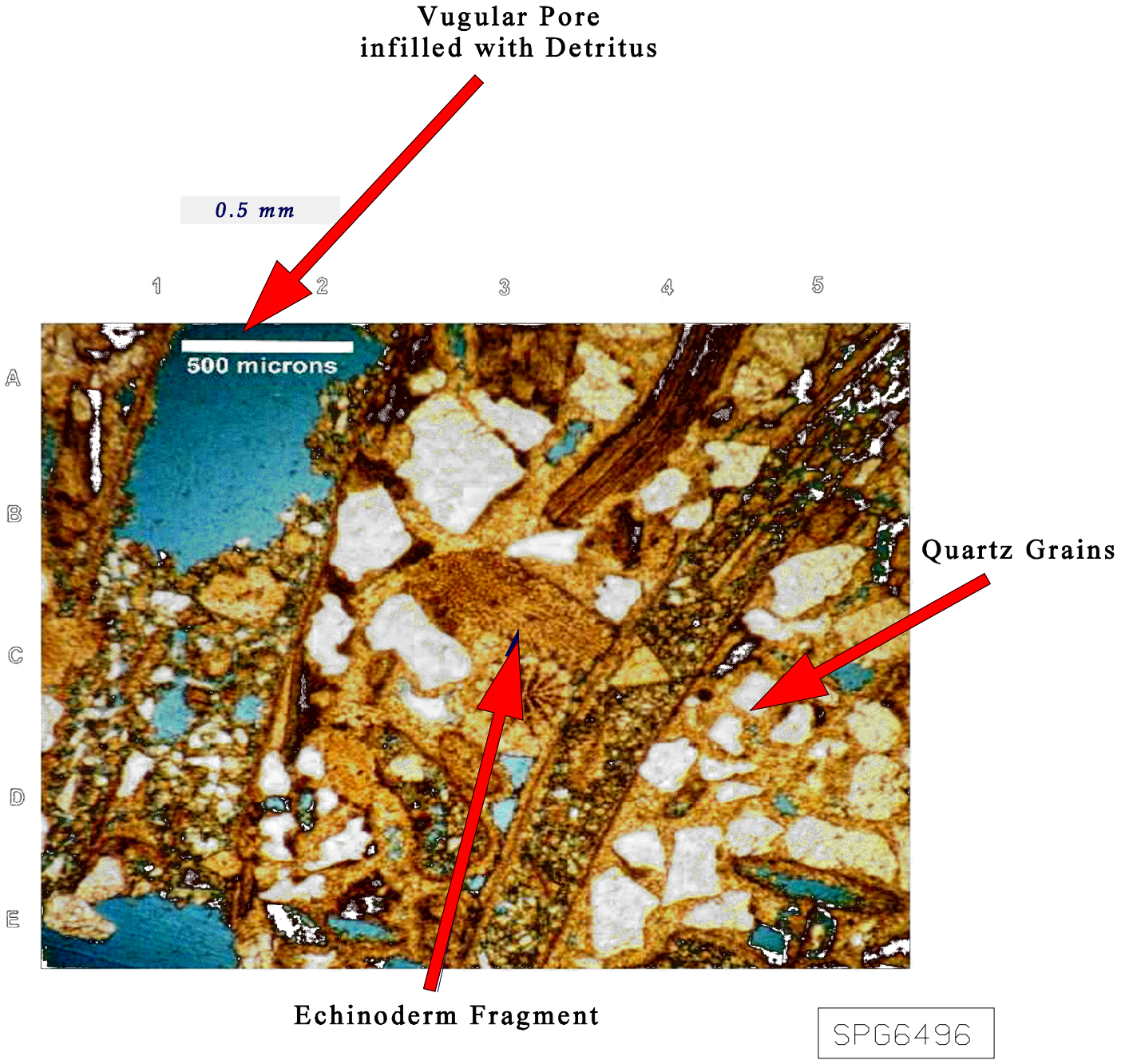

Figure 19. Quartz-rich, skeletal grainstone, with carbonate/quartz detritus present in vuggy pores. Skeletal Grainstone Microfacies, Santee/Clinchfield section, H Area ITP Site, General Separations Area, Savannah river Site. Well HBOR-50 @ 166 ft. Crossed nicols. Void space filled with blue epoxy glue.

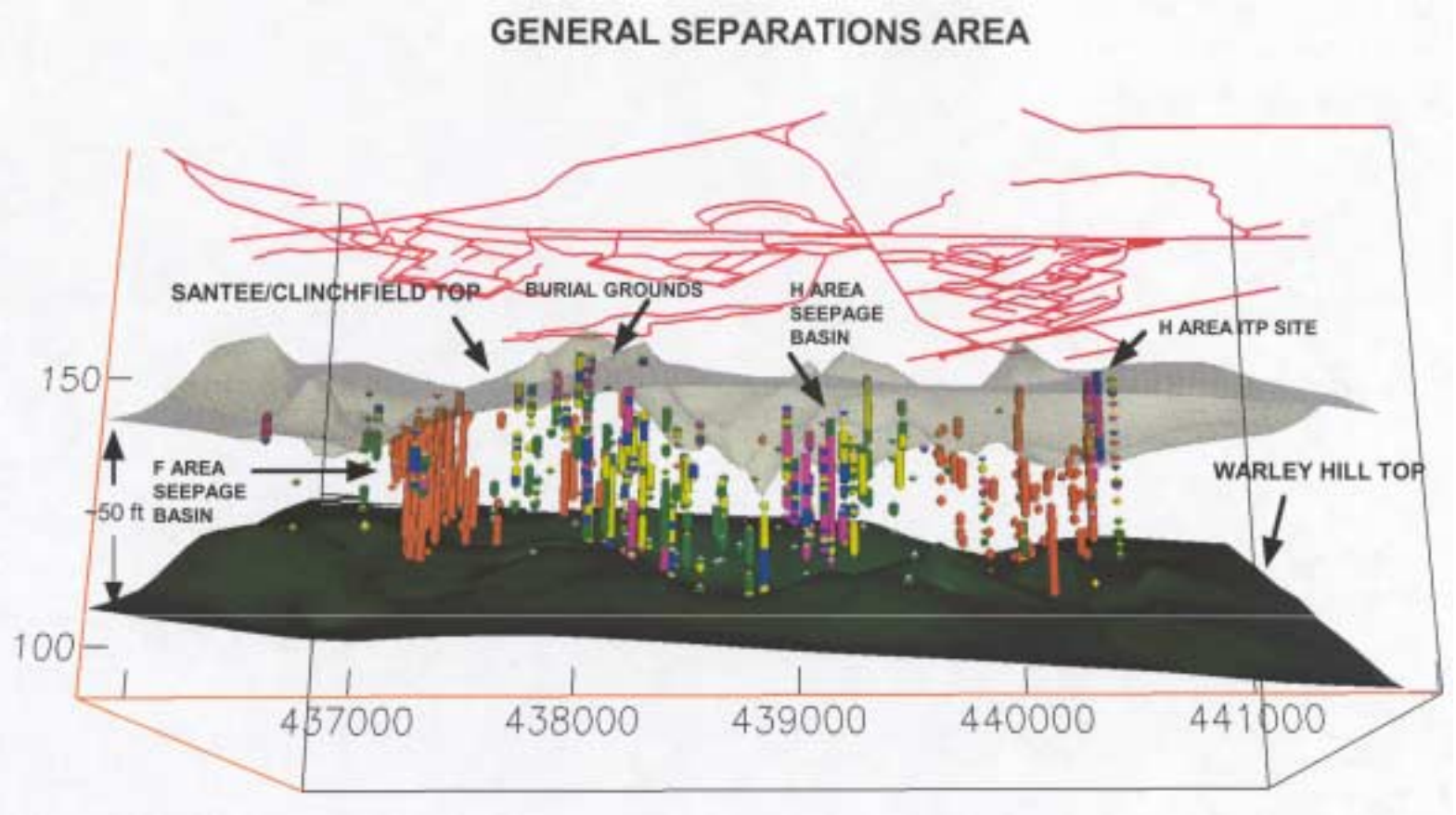

Figure 20. This figure is a 3D profile illustrating the relative thickness and percentage of carbonate from core and SPT borings throughout the GSA. The upper bounding surface is the top Santee Unconformity surface and the lower bounding surface is the top Warley Hill surface. The tan colored "sticks" indicate carbonate "hits" occurring in the SPT borings without regard to carbonate content other than its presence at that particular depth in the boring. The percentage carbonate in the cored wells is color coded as follows: Purple >65%; Blue 45-65%; Yellow 25-45%; Green 5-25%.

The Savannah River Site E-Area Vadose Zone Monitoring System

Heather Holmes Burns, Bechtel Savannah River Company, Aiken, SC 29808
Doug Wyatt, Tom Butcher, Jim Cook, Brian Looney, Joe Rossabi, WSRC, Aiken, SC 29808
Michael Young, Georgia Institute of Technology, Atlanta, GA 30332

ABSTRACT

Shallow disposal trenches located in the Savannah River Site's E-Area contain low-level radioactive waste. To help protect the groundwater below these trenches, a comprehensive vadose zone monitoring system was developed and deployed. A vadose zone-based monitoring approach was utilized since groundwater contamination from nearby facilities would limit the sensitivity and increase the cost of a traditional groundwater-based monitoring system. The E-Area Vadose Zone Monitoring System (VZMS) monitors the three soil parameters (i.e., water content, water potential or tension, and contaminant concentration) that determine how fast and in what concentration contaminants are traveling to the groundwater. Forty instruments were installed in three vertical boreholes and four angled boreholes drilled underneath the centerline of the trench. The various monitoring instruments were mounted on assemblies that were installed in each borehole. The equipment at each depth typically included: 1) a porous-cup vacuum lysimeter (i.e., solution sampler) for collecting water from the vadose zone for analysis, 2) an advanced tensiometer (AT) for measuring soil-water tension, and 3) a water content reflectometer (WCR) for measuring soil-water content. The electronic instruments were connected to data loggers with cellular telephone links to allow direct downloading of data and calibration information to both onsite and offsite computers. Thin-walled stainless steel tubes were installed near the instrument holes to allow more detailed water content logging using neutron probes. The initial data indicate that many of the instruments have equilibrated with the moisture in the surrounding backfill and environment. The data are being closely monitored to track the wetting fronts and analyze the potential movement of contaminants.

Several innovative methods for characterization, drilling and installation were utilized during implementation of the EMOP-Phase IA. Extensive characterization of the geology using a combination of cone penetrometer lithology data and conventional drilled soil core data from around the trenches enabled development of 3-D models of the lithology allowing for precise instrument placement. An innovative approach for installing the WCRs was developed to ensure instrument contact with "undisturbed" soils. The team also developed a new method for installation of the angled lysimeters that would allow removal and replacement, when required.

The number of vadose zone wells installed this fiscal year was deliberately limited to allow system evaluation. By evaluating the strengths and weaknesses of the system, future deployment of vadose zone monitoring systems could be improved. The strengths and weaknesses of the system are described in this document with respect to installation, maintenance, and operation. The results are also discussed. Preliminary results indicate that the VZMS will provide cost effective, high quality performance monitoring and a sensitive early warning of any releases from the shallow disposal trench operation.

INTRODUCTION

E-Area, located in the central portion of SRS, is the principal disposal facility for low-level radioactive wastes. Some of these wastes are disposed of in unlined trenches. Vaults are also used for disposal if additional isolation is required due to higher radionuclide content.

The trenches vary in length and width but are typically constructed within the upper eight meters of the local sediments. The vadose zone underlying the E-Area study extends to a depth of approximately 21 meters. Water from the surface must pass through the vadose zone to reach the saturated water table, and therefore, potential contaminants from the trenches must also pass through the vadose zone.

The approach prior to VZMS installation primarily relied on groundwater monitoring. This monitoring program could not meet DOE requirements because of the several tritium plumes that emanate from the Burial Ground Complex (BGC) disposal facilities located upgradient of the shallow trenches and vaults. Because of the proximity of these facilities to the E-Area Disposal Facility (EADF) units, the previous tritium contamination masks any potential contributions from the EADF. Therefore, monitoring the vadose zone was the best alternative to demonstrate compliance with DOE Order 435.1 which requires both 1) a comprehensive monitoring program that validates the performance assessment (PA) and 2) an assessment of impacts to groundwater. At SRS, this has been interpreted to mean that concentrations of radionuclides in groundwater not exceed drinking water standards (DWS).

The significant accomplishments of this program are summarized in Table 1.0. The data supplied by the monitoring program provides information about the integrity of the disposal unit, and whether or not elements of the disposal site are functioning as intended and predicted. Initial data obtained from both vadose zone characterization and monitoring demonstrates that the E-Area disposal trenches are meeting the requirements established in DOE Order 435.1. The E-Area VZMS is designed to detect and quantify the rate and volume of both water and contaminant movement released from the trenches to the undisturbed environment. The VZMS will be used to show that facilities are operating safely during waste emplacement, and also, serve as an early-warning indication of the magnitude of any releases from the shallow disposal trench operation. The early-warning measure will allow corrective actions to be conducted to prevent further degradation of the groundwater resources.

Brief Description of Monitoring Strategy

Instruments were selected that had been demonstrated in industry or by research and development efforts ready for deployment. An array of VZMS instruments installed around the perimeter of the E-Area disposal trenches was selected to provide data for determining the quantity, rate, and direction of soil-water and contaminants in the vadose zone. Three types of vadose zone monitoring devices were selected to comprise the core technology for this system:

- Advanced Tensiometers measure soil-water tension or potential. This parameter relates to how well the soil retains moisture.

- Water Content Reflectometers sense the dielectric constant of the soil to determine moisture content.

- Porous-cup lysimeters or solution samplers collect soil-water samples that will be analyzed for tritium and other contaminants.

Tritium was the contaminant of interest since the PA predicts tritium to be the contaminant first reaching the groundwater. The VZMS was to define tritium transport in two ways to meet the two primary objectives stated in this section. The first was to provide soil-water samples from the vadose zone using porous-cup lysimeters for determining the concentration of tritium. The second was to provide the flux velocity of tritium carried to the groundwater using data from the AT and WCR.

The instruments are installed in boreholes traditionally used for monitoring contaminants at depth. Data collection using tensiometers and WCRs is automated, so that site personnel

are not needed for data collection. Other monitoring points will be taken with a neutron probe which is designed to provide a continuous water content profile for the entire thickness of the vadose zone. Probes are lowered into the borehole, readings are taken, and the probe is removed. The neutron probe access tubes are located adjacent to each borehole containing the WCRs to allow redundant measurements of water content.

Brief Description of Installation Strategy

The installation strategy was dictated by the monitoring strategy as described below:

- Lysimeters were placed under the center-line of the trench using angled boreholes to monitor vertical contaminant transport.

- Instruments were placed in vertical wells at the north end of the trench to monitor the greatest tritium activity and to monitor lateral contaminant transport.

- Vadose zone monitoring wells were installed in a triangular pattern to provide data that could be used to better determine the flow direction or gradient.

The E-Area VZMS was installed on two adjacent sides of the outermost completed disposal trench. Seven boreholes were installed, including three vertical boreholes and four angled boreholes. The angled boreholes were cased with PVC pipe. Vertical boreholes were not cased but backfilled with alternating layers of silica flour and native backfill. The vertical boreholes contained each of the three instruments (i.e., ATs, WCRs, and solution samplers) emplaced at four depths, whereas, the angled boreholes contain one solution sampler that is retrievable if failure occurs.

CHARACTERIZATION OF THE SRS VADOSE ZONE

Field characterization to support the VZMS deployment was completed in January 1999. The vadose zone in E-Area was characterized by three methods: 1) split spoon sampling, 2) Shelby Tube samples and subsequent laboratory analysis on sediment samples, and 3) PiezoCone Penetrometer Testing (CPTU) to determine soil characteristics or the sand/silt/clay horizons and dielectric constant and pore pressure to determine moisture content. Geological models were developed from the characterization data. The 3-D models were utilized in determining the optimum depths for locating the instruments in the subsurface strata with the highest moisture content. Laboratory analysis of field samples collected during characterization allowed comparison of actual field data to the hydraulic parameters and the determination of coefficients required as input to the models used in the E-Area RPA. Soil hydraulic property data was also used to calculate the soil-water flux through the vadose zone that could be compared to PA mathematical model output.

The 3-D models of the vadose zone were correlated with data obtained from the Shelby Tube soil samples. The models depicted the sand/silt/clay horizons (See Figure 1.0) and soil moisture. The 3-D model indicates there are three major horizons underneath the E-Area disposal trenches that differ in ways that are important for placement of vadose zone instruments. The A-horizon dominates the upper 7 meters of the vadose zone and is a predominantly clay layer. The B-horizon begins at about the 7 meter depth and extends to 18 meters and is characterized by higher sand content than the A or C horizons. The C-horizon is at the 20 meters depth and includes the water table overlaying a clay-confining zone. Within the area of the localized model, there are apparent channels interspersed in these horizons that cause variations in the clay and sand content underlying the trenches. Because of this, there are lateral variations in the overall soil moisture throughout the vadose zone.

The approximate depths selected for placement of instruments is presented in Figure 2.0. The uppermost tensiometer was placed just below the clay surface. The

second tensiometer was placed above the clay interbedded in the sandy zone at about 14 meters depth. The next two tensiometers were installed slightly above and in the capillary fringe zone.

DEPLOYMENT OF THE SRS VADOSE ZONE MONITORING SYSTEM

The goal of deploying a vadose zone monitoring system in E-Area was to instrument the disposal trenches with a system that would meet the two primary objectives: 1) validation/calibration of the performance assessment mathematical model and 2) protection of groundwater resources. The strategy used to meet the stated objectives was to monitor the soil-water parameters that directly relate to water movement and contaminant migration from the trench disposal area. Therefore, the VZMS was designed to monitor soil-water content, tension, and contaminant concentration which are the soil-water parameters that directly relate to water movement and contaminant migration from the trench disposal area. These three primary soil parameters could be utilized to determine the contaminant flux, or how fast a given contaminant is traveling to the groundwater through the vadose zone.

SRS is the first site to utilize the AT in combination with other instruments to monitor soil parameters at up to 18 meters depth in the vadose zone at a humid site. The AT has paved the path for a permanently installed tensiometer allowing it to be utilized in long-term monitoring programs. The AT has these advantages over other tensiometers: (a) it can operate at depths exceeding 30 meters, (b) it can be checked for proper operation in the field, (c) the pressure sensor can be calibrated in the field, and (d) the pressure sensor can be replaced, if required. All of these advantages result in reduced maintenance and servicing needs for the AT.

The AT and the WCR instruments have electrical leads that are connected to data loggers. Three data loggers that are supplied with power utilizing a solar panel have been installed adjacent to each of the three vertical wells. The data loggers are equipped with cellular telephone links to allow direct downloading of data and calibration information to both offsite and onsite personal computers. The soil-water samples collected by the vacuum lysimeters are manually collected.

Methodology

Seven vadose zone wells were installed around two sides of the outermost completed disposal trench (i.e., slit trench #1). The location of each of the vadose zone wells was selected based on the following considerations:

1) to allow monitoring of the entire length of the outermost trench,
2) to determine the flow of contaminants in vertical and lateral flow patterns,
3) to facilitate the earliest detection of tritium by being placed next to the highest tritium containing waste and underneath the centerline of the trench, and
4) to monitor the water flow through the trench.

Four of the wells were angled and placed under the centerline of the trench to enable monitoring of vertical contaminant transport. Each of the angled wells were equipped with one lysimeter and were spaced approximately 30 meters apart to enable monitoring the entire length of the trench. Three vertical wells were placed at the NE and NW corners of the trench and on the eastern side of the trench to form a triangular pattern. This arrangement would allow the soil-water flux to be measured based on the gradient between the instruments and would allow monitoring of lateral contaminant transport. Instrument clusters containing one AT, one porous-cup lysimeter, and one WCR were placed at four vertical depths inside each vertical well. Neutron probe access ports were placed adjacent to each of the vertical wells. The E-Area VZMS vertical wells contain ATs at four different depths so that the rate at which a wetting-front is moving through the vadose zone can be used to determine the soil-

water velocity, the direction of water movement, and the soil-water flux. The contaminant flux that is directly comparable to that estimated in a performance assessment is obtained from both the soil-water flux and the contaminant concentration.

Innovative Installation Methods

Two instruments required innovative installation methodologies to ensure proper instrument performance and sensitivity: 1) the water content reflectometer and 2) the neutron probe access port.

1) Water Content Reflectometer

The WCR requires monitoring of undisturbed soil and can be installed via two methods: 1) insertion into the side-wall or 2) placement against the side-wall of the borehole. The WCRs were installed in boreholes by forcing the assembly against the borehole wall using a short lever-arm attached to the WCR as shown in Figure 3.0. To provide redundant measurement of water content, a neutron probe access port was installed adjacent to each vertical well to provide continuous measurement of soil-water content.

2) Neutron Probes

The neutron probe enables a continuous soil-water content measurement along the length of the vadose zone. Periodic monitoring with these probes will allow the tracking of moisture fronts traveling through the E-Area vadose zone. It has long been recognized that the nature of the access borehole can significantly affect neutron probe sensitivity (i.e., performance). Stainless steel was selected as the material of construction for the neutron access pipe. Steel tubing was preferred over PVC pipe since it does not contain chlorine to effect neutron attenuation and is commonly available. The steel tubing used in this application consisted of flush threaded well casing. The tubing was schedule 5 with a maximum thickness of schedule 40 near each threaded coupling. The stainless steel material of the access tube was selected not only because of its minimal effect on the neutron flux, but also because of its durability and its ability to be pushed in the soil by a hydraulic cone penetrometer test (CPT) rig. The access tube was installed by a CPT rig to eliminate the generation of an annular space created by conventional drilling, and therefore, to eliminate the need for backfill. The most commonly used backfill materials have different moisture contents than the actual formation. Therefore, the moisture content of the backfill, being the closest material to the neutron source, will cause the thermalization of a large fraction of the high-energy neutron flux resulting in significant attenuation of the neutron flux before it enters the formation.

PERFORMANCE OF INSTRUMENTS

In this section, the performance of all three vadose zone instruments/samplers (i.e., the AT, WCR, and solution sampler) and the analyzed results are discussed. Two soil parameters are required to calculate the contaminant flux to the groundwater: 1) the soil-water flux determined from the AT and WCR data, and 2) the contaminant concentration obtained via the solution sampler. Tritium was selected as the target constituent because: 1) it is present in the waste disposed of in the trenches, and 2) the SRS PA model indicates that it would be the fastest traveling radionuclide to the groundwater.

Water Content Reflectometer Sensor Performance

WCR data was collected and analyzed several months after installation, allowing for equilibrium of the sensor with the host soil. The data are very consistent with time showing little change in water content in the vadose zone at the depths installed. Average water contents after equilibrium with the host soil are values of 0.284, 0.181 and 0.266 m^3/m^3 for the three vertical wells. These values are consistent in time and reasonable given the soil texture.

Advanced Tensiometer Performance

The water potentials as measured by the ATs reflected expected conditions in the subsurface. The lowest water potentials reflecting dryer conditions were located in the shallower zones while the deeper zones near the wetter capillary fringe had higher potential. Figure 4.0 shows the soil-water tension data obtained from the AT sensors in vertical Boring #5 at all four depths in the vadose zone (from 7 to 17-meters depth). Data from the AT sensors in boring #5 were selected for illustration since this borehole contains the most operative solution samplers. The solution samplers, when placed under vacuum, collect soil moisture until the vacuum equilibrates with the surrounding soil tension. At that time, water from the soil is no longer drawn into the lysimeter collection chamber. In Figure 4.0, the sharp decreases in tension (days #134, #141, #182, #225, and #230) occurred on the days in which the solution samplers were placed under vacuum. The ATs performed as expected since the soil-water tension decreased as the surrounding soils become dryer when soil-water was being collected into the solution sampler. The step change seen in the instrument tension at the deepest depth (17-meters) was at the time of a heavy rainfall resulting in the water table rising. The instrument AT-5-55 indicates that saturation occurred at that time and was to be expected since boring #5 soils were wetter at a shallower depth than that of either boring #6 and boring #7).

All of the data from the ATs in Boring #5 (AT-5), Boring #6 (AT-6), and Boring #7 (AT-7) indicate that the soil tension is relatively constant ranging between -100 cm (wetter) to -200 cm (dryer) and is consistent with expected tensions for SRS soils. Water potential appeared to be unaffected by daily or yearly infiltration events at these depths. The total variation in water potential was less than 100 cm in all tensiometers over the 3.5-month period.

Solution Samplers

Sixteen vacuum solution samplers were placed in the seven boreholes around the sides of the E-Area disposal trenches. Table 2.0 lists the solution samplers and the sample volumes collected during FY99. Thirteen out of sixteen solution samplers have collected samples. Each of the solution samplers in the four angled boreholes placed under the centerline of the trench have been successfully collecting samples. Nine out of the twelve solution samplers placed in the three vertical boreholes have been able to collect samples. A sample as small as 5-10 milliliters is sufficient for obtaining the concentration of tritium, which is the primary contaminant of interest. The three solution samplers that have not collected samples on either of the two collection dates, have not yet been declared inoperative. Other methods to improve the collection performance are planned which include placing solution samplers under a constant vacuum. The first set of water analyses, as expected, shows that tritium above background levels is moving through the vadose zone beneath the trench area where debris with the highest tritium content has been buried.

DATA ANALYSIS

The SRS PA model estimates the peak groundwater concentrations based on 1) an estimated groundwater flux and 2) a maximum curie concentration in the disposal area that will not exceed the DWS. Comparison of the measured tritium concentrations with PA model results indicates that groundwater concentrations will meet the DWS as discussed in this section.

The first round of sampling from the vacuum lysimeters produced tritium concentrations ranging from about 1.0 pCi/ml to about 84 pCi/ml as shown in Table 2.0. A simple calculation was made to compare the highest concentration of 84 pCi/ml with the results of the vadose zone model used in the performance assessment. The comparison

indicated that a tritium concentration of about 400 pCi/ml migrating through the vadose zone was required to produce a tritium concentration equal to the DWS of 20 pCi/ml at a hypothetical 100-meter well. The measured vadose zone concentration of 84 pCi/ml is about 20% of the 400 pCi/ml. Therefore, this maximum tritium concentration measured by the SRS Vadose Zone Monitoring Program should result in a groundwater concentration of about 4.0 pCi/ml, or 20% of the DWS at the 100-meter well.

OVERALL ASSESSMENT: LESSONS LEARNED

This section describes the lessons learned from implementation of the first phase of the vadose zone monitoring system deployment program at SRS. The number of vadose zone wells and instruments installed during the first phase was deliberately limited to allow system evaluation. The next phase of monitoring will be designed to incorporate the "lessons learned" from the installation and operation of the first VZMS at SRS. The three largest improvement areas in subsequent monitoring designs are (1) redundancy in monitoring critical soil parameters, (2) maintenance and long-term monitoring, and (3) statistical validation of data.

Redundancy in Monitoring Critical Soil Parameters

Redundant monitoring of critical soil parameters using different instruments should improve the confidence that changes in the soil-water conditions are real and not affected by the monitoring systems themselves. The first phase of the SRS VZMS deployment included redundant monitoring of soil water content by neutron logging and by WCRs.

Maintenance and Long-Term Monitoring

The SRS VZMS deployment program utilized the borehole monitoring strategy for installation of instruments because of its use in traditional well installations and because of its primary advantage that allows placement of instruments at lower depths. However, the borehole monitoring strategy suffers from a significant disadvantage for long-term monitoring: replacement of instruments. Loss of fixed instruments in the borehole results in a loss of monitoring points. The loss of a few instruments can leave potentially large gaps of the subsurface unmonitored. Borehole instrument replacement requires re-drilling which is not feasible.

Subsequent monitoring programs should maximize access ports for multiple instrument use and easy replacement upon failure. The existence of access tubes and ports will facilitate the use of new technologies. Long-term monitoring programs (e.g., greater than 10 years) can benefit from the installation of access boreholes. Future developments in downhole instrumentation could improve the accuracy in monitoring subsurface conditions, and the presence of access tubes could facilitate the testing and use of these instruments.

Statistical Validation of Data

Data collection from the SRS VZMS has been on-going since installation in May 1999. Data collection intervals are important aspects of statistical analyses. In addition, up to three months is required for the data to equilibrate with the surrounding environment. Sampling over a longer period of time permits the quantification of seasonal variability and other time-dependent behavior. Insufficient data and inadequate methodology for representing significance and uncertainty in data can lead to faulty conclusions. Without sufficient amounts of data it is not statistically possible to conclude whether baseline conditions have changed.

Table 1. EAVZ accomplishments and lessons learned.

EVALUATION OF:	SUMMARY OF ACCOMPLISHMENTS
Vadose Zone Characterization	- Developed 3-D Models of lithology allowing for precise instrument placement.
Borehole Drilling	- Successfully utilized a mud rotary drilling rig to drill angled holes. - Vertical boreholes remained open allowing proper instrument placement. - Obtained split-spoon samples during installation to verify placement of instruments in optimum moisture zones.
Instrument Installation	- Developed innovative method for placing WCRs against the side-wall of the borehole. - Developed innovative approach to eliminate annular space around the neutron probe access port. A cone penetrometer rig pushed the stainless steel access port directly into the ground.
Instrument Performance	- Deep lysimeters (i.e., > 12-meters) are able to collect large samples for lab analyses. - ATs and WCRs have equilibrated with surrounding environment. - ATs and WCRs indicate consistent soil-water tension and content that is independent of influx events.
PA Validation	- Characterization data obtained from analyses of soil samples are comparable to performance assessment input data.
DOE Order Compliance / PA Validation	- Lysimeter data indicates tritium concentration underneath trenches will meet the Drinking Water Standard at the compliance point (i.e., 100-meter well).
Summary of Lessons Learned	- Increase redundant monitoring of critical soil parameters using different instruments to improve confidence in data. - Increase usage of access ports to facilitate the use of multiple technologies. - Increase usage of cased boreholes to allow instrument replacement in case of failure. - Design system to include all phases of monitoring: pre-operational, operational, and post-operational. - Establish baseline to definitively distinguish between background radiation and that contributed by the disposal area. - Quantify uncertainty in measurements and observations. Utilize statistical analyses to validate data.

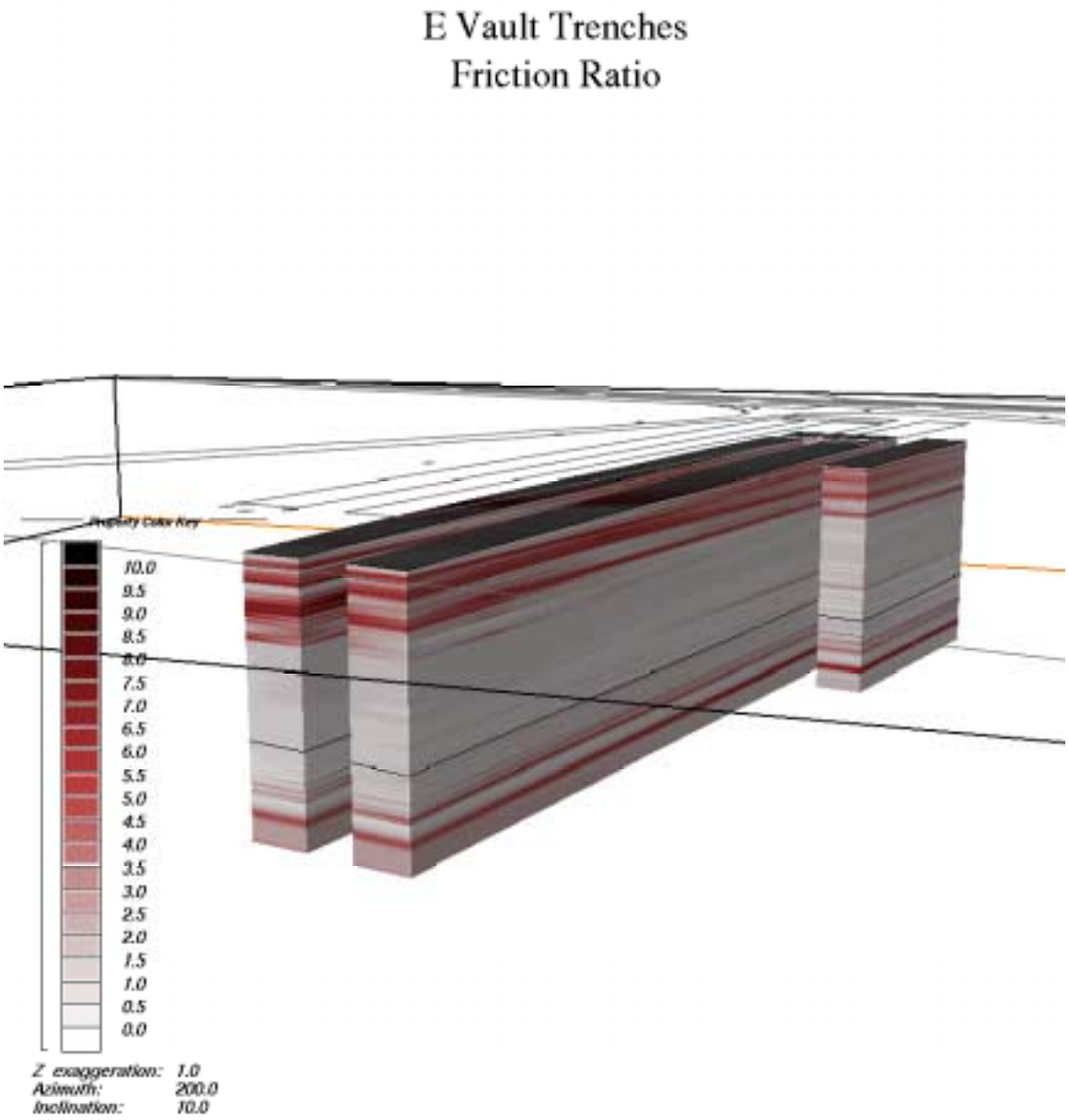

Figure 1. 3-D model depicting sand/clay horizons using CPT Friction Ratio. Brighter colors (dark reds) indicate more clay-rich sediments, and lighter colors (grays) indicate more sand-rich sediments.

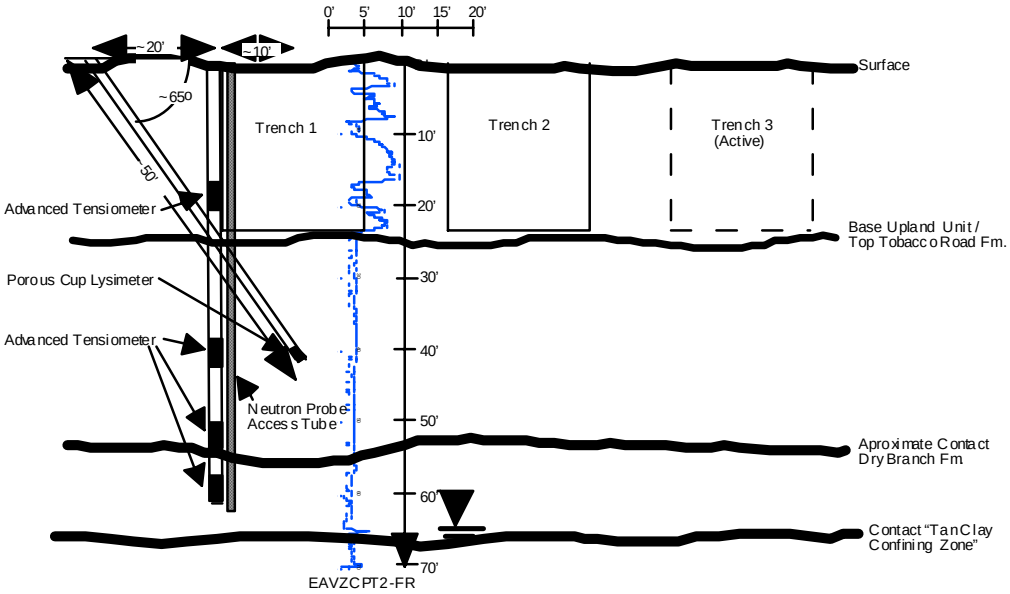

View from northern end of trenches facing southward.
(relative scale is correct)

Figure 2. Instrument depths as determined from the 3-D models.

ADVANCED TENSIOMETER (AT) SYSTEM FOR E AREA

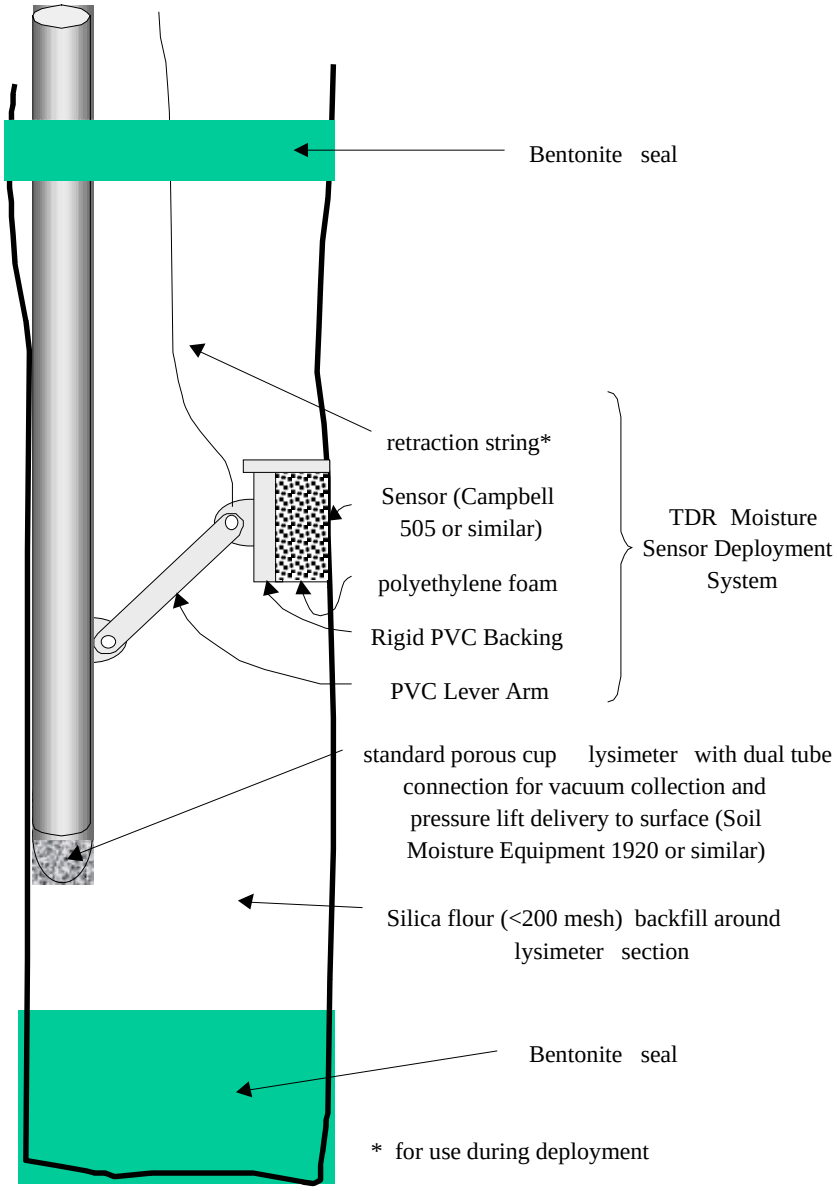

Installation steps for Advanced Tensiometer (AT) Assembly: 1) lower to depth while TDR probe is retracted, 2) release TDR and pull back to engage, 3) test TDR probe response, 4) while holding AT system, emplace silica flour

Figure 3. Conceptual diagram of the installation method for the Advanced Tensiometer and Water Content Relectometer instrument cluster.

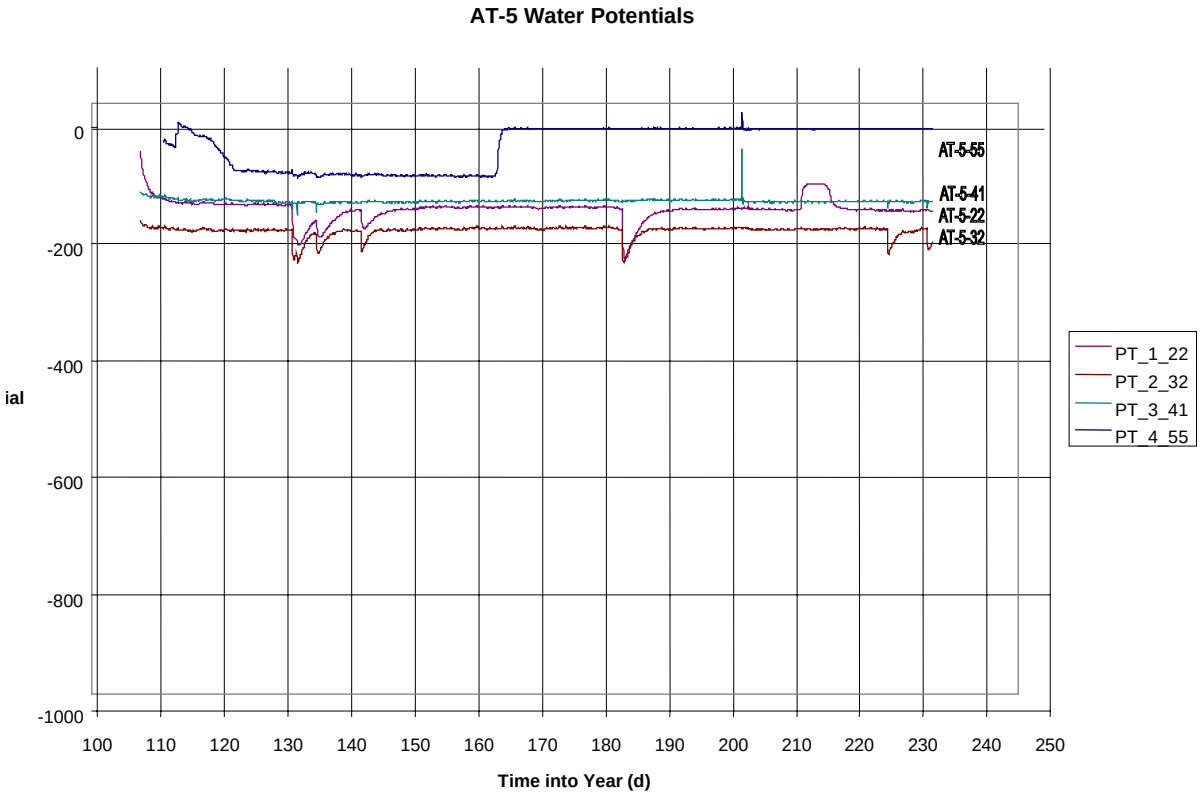

Figure 4. Advanced Tensiometer Data for Boring #5 (AT-5).

Table 2. Volumes of soil-water samples collected by the lysimeters.

Solution Sampler #	Sample Volume (mls)		Average Tritium Conc. (pCi/ml)
	July 1	Sept 13	
BORING #1 (AL-1)	800	600	4.3
BORING #2 (AL-2)	800	600	1.0
BORING #3 (AL-3)	800	700	2.5
BORING #4 (AL-4)	800	600	3.3
BORING #5			
AT-5-23	900	0*	84.0
AT-5-33	825	0*	29.7
AT-5-42	0	10	14.1
AT-5-57	775	700	21.7
BORING #6			
AT-6-24	0	0	--
AT-6-34	0	0	--
AT-6-43	400	350	13.3
AT-6-55	150	0	12.4
BORING #7			
AT-7-12	0	0	--
AT-7-23	0	5	2.2
AT-7-42	0	200	7.4
AT-7-54	5 – 10	0	--

* Tubing had leaks and could not sustain a vacuum. Tubing has been temporarily repaired as parts are being ordered for permanent replacement.

Notes

Modeling Aquifer Heterogeneity at the Savannah River Site Using Cone Penetrometer Data (CPT) and Stochastic Upscaling Methods

M. K. Harris, G.P. Flach, WSRC, Savannah River Technology Center (SRTC), Aiken, SC 29808
A.D. Smits, Science Applications International Corporation (SAIC), Augusta, GA 30901
F.H. Syms, BSRI, Site Geotechnical Services, Aiken, SC 29808

ABSTRACT

Cone penetrometer tests (CPT) have become an increasingly popular characterization method for Tertiary shallow subsurface investigations (less than 200 feet) in the Atlantic Coastal Plain of South Carolina. These sediments consist primarily of interbedded and interfingering fluvial, deltaic, and shallow marine sediments. CPT provides relatively inexpensive subsurface data without drilling fluid or cuttings. For environmental restoration applications at the Savannah River Site (SRS), CPT is typically used to obtain depth-discrete groundwater samples, small-diameter permeability samples, and to define hydrostratigraphic horizons. A recent example is the C-reactor area at the SRS, the focus of this study. At this site, 140 CPT locations were used to define contaminant plumes and hydrostratigraphy over a 3 mi^2 area, rather than conventional borehole techniques (e.g. monitoring wells, cores, electric well logs, slug and pumping tests). In this investigation, the CPT lithologic data are further used to predict hydraulic conductivity variations within hydrostratigraphic zones of the uppermost aquifer unit. The method involves correlating tip resistance, sleeve resistance and pore pressure measurements to percent fines (mud, silt, and clay) content and hydraulic conductivity. Predicted percent fines content at the scale of the CPT measurements (0.1 ft) were categorized into high, medium and low conductivity and upscaled to the flow model resolution using geostatistical methods. The resulting model conductivity field provided a realistic representation of aquifer heterogeneity in coastal plain sediments. The method significantly improved groundwater modeling flow path predictions. The resulting tritium transport simulations compared well with field data.

PURPOSE OF STUDY

A geospatial mapping and groundwater modeling case study was completed at the C-Reactor Area at the Savannah River Site (SRS) based primarily on cone penetration testing (CPT) (Figures 1 and 2). For a detailed discussion on CPT methods see Syms and others (2000). CPT was utilized for the definition of hydrostratigraphic unit boundaries and hydraulic conductivities instead of conventional hydrogeological methods (e.g. monitoring wells, cores, electric well logs, slug and pumping tests). Approximately 140 CPT tests were used to map the hydrostratigraphic unit boundaries and define hydraulic conductivities of the hydrostratigraphic units. In conjunction with the CPT tests approximately 1000 depth-discrete water samples were taken to characterize the tritium and volatile organic compound (VOC) contaminant plumes in the area. A three-dimensional geospatial model of the hydrostratigraphy was constructed based on correlation of the CPT data, while three-dimensional groundwater plume maps were constructed based on the water samples. The resulting hydrogeological framework was coupled with a groundwater flow model for particle track analysis and subsequent transport modeling. This paper concentrates on two main areas of the case study. The first illustrates CPT data for detailed hydrogeological mapping and integration of all characterization data (geological, hydrological, and contaminant) to understand the relations of groundwater and plume

movement. Secondly this study presents a method for transforming CPT data into hydraulic conductivity data for definition of hydrogeologic properties in groundwater modeling.

SITE DESCRIPTION AND HISTORY

The study area is located in the Upper Atlantic Coastal Plain physiographic province in southwestern South Carolina at the U.S. Department of Energy's Savannah River Site (SRS). The SRS occupies about 300 mi^2 and was set aside in 1950 as a controlled area for the production of nuclear material for national defense and specialized nuclear materials. This study focuses on a 3 mi^2 area in the central portion of the SRS near the C Reactor Area which is undergoing environmental characterization and remediation for RCRA and CERCLA regulatory investigations. The C-Reactor Seepage Basins (CRSBs) and the C-Area Burning/Rubble Pit (CBRP) (Figures 1 and 2) are the two principal reactor waste units associated with C-Area.

The CRSBs consist of three unlined (earthen) basins constructed in 1957 to contain radioactive water discharged from the reactor process buildings. The seepage basins were used from 1959 to 1970 to dispose of low-level radioactive process purge water from the reactor disassembly basin. In 1963, the purge water was deionized and filtered and to remove solids and sludge prior to discharge to the basins. The seepage basins were not used from 1970 to 1978. During this period, purge water was mixed with large volumes of cooling water from the heat exchanger and discharged to area streams. Discharge to the CRSBs resumed in 1978 after improvements were made to the processing of purge water from the disassembly basin. The C-Reactor was shutdown for repairs in 1985, and the CRSBs have not received wastewater since 1987. The CRSBs are currently undergoing feasibility studies to determine the regulatory path forward. Waste disposal records indicate that the main basin received aqueous radioactive waste. Radionuclides in the wastewater from the disassembly basin, sumps, tanks and drums included tritium, chromium-51, cobalt-60, cesium-134, cesium-137, and other beta-gamma fission products (WSRC, 1993). Tritium releases to CRSBs are documented in Environmental Protection Department (EPD) annual monitoring reports.

The CBRP was constructed in 1951 and used to dispose of and burn organic solvents, waste oils, paper, plastics, and rubber through 1973. After 1973, the pit was filled with inert rubble and soil (WSRC, 1994). The CBRP was a shallow, unlined excavation (approximately 25 feet wide and 350 feet long) with depths of approximately 8 to 12 feet. The history of solvent disposal at the CBRP and the persistence of high VOC concentrations 25 years after operations ceased suggests the presence of VOC in non-aqueous phase liquid (NAPL) within the vadose zone beneath the CBRP. A Soil Vapor Extraction and Air-Sparging (SVE/AS) remediation system are currently in operation for cleaning up the solvents in the soil and groundwater at this site.

Primary groundwater contaminants in C-area include tritium for the CRSBs and VOC for the CBRP. This study will only discuss the CBRP VOC groundwater contamination distribution in detail.

CHARACTERIZATION DATA

Geologic descriptions from three cores and CPT lithologic data (tip stress, sleeve stress, and pore pressure) from 139 locations were used to identify and delineate hydrostratigraphic boundaries beneath the study area (Figure 2). The CPT data were also used to infer conductivity distribution using stochastic methods. The hydrostratigraphic boundaries were compiled into a hydrogeologic model using EarthVision® geospatial analysis (Dynamic Graphics Inc., Alameda CA, www.dgi.com). Contaminant plume mapping was based on over 1000 depth-discrete water samples taken with the cone-penetrometer to characterize

tritium and VOC plumes in the area. Analytical data was compiled into three-dimensional maps utilizing EarthVision™ software.

HYDROGEOLOGY

The SRS lies within the Upper Atlantic Coastal Plain, a southeast-dipping wedge of unconsolidated and semi-consolidated sediment that extends from its contact with the Piedmont Province at the Fall Line to the edge of the continental shelf. The sediment ranges from Late Cretaceous to Miocene in age and comprises layers of sand, muddy sand, and mud with minor amounts of calcareous sediment (Fallaw and Price, 1995). The Coastal Plain sediment rests unconformably on Triassic-aged sedimentary rock of the Dunbarton Basin and Paleozoic-aged crystalline rock.

This study involves the Tertiary-age sediment, principally the Eocene to Miocene sequence. The up-dip portion of the Floridan aquifer system includes the Gordon aquifer, the Gordon confining unit and the Upper Three Runs aquifer (Aadland and others, 1995), and is considered in geospatial and groundwater analysis. The Upper Three Runs aquifer was analyzed in more detail in relation to the CPT data and will be discussed in more detail than the underlying hydrostratigraphic units. Figure 3 correlates the hydrostratigraphic nomenclature with the local lithostratigraphy as defined by Fallaw and Price (1995).

Gordon Aquifer Unit (GAU)

The Gordon aquifer constitutes the basal unit of the Floridan aquifer system at the SRS and is the lowermost unit characterized in this study. The aquifer includes loose sand and clayey sand of the Congaree Formation and, where present, the sandy parts of the underlying Fourmile Branch and Snapp Formations (Figure 3), (Harris and others, 1990; Aadland and others, 1991 and 1995). The sand within the Gordon aquifer is yellowish to grayish orange and is sub- to well rounded, moderately to poorly sorted, and medium- to coarse-grained. Pebbly layers and zones of sand cemented with iron and silica are common. The Gordon aquifer includes rare interbeds of light tan to gray clay that range up to three feet in thickness. Lenses of clay less than 6 inches in thickness are common near the base of this unit. The Gordon aquifer contains a small amount of sporadically distributed calcareous sediment. The thickness of this unit is variable, ranging from approximately 60 feet to 160 feet across the SRS (Flach and others, 1999). Multi-well pumping tests performed on Gordon aquifer wells at the SRS and vicinity produce conductivity values that average 35 ft/day (Aadland and others, 1995). Ten single-well pumping tests within the Gordon aquifer give permeability values that range from 0.82 to 143 ft/day (Flach and others, 1999).

Gordon Confining Unit (GCU)

The Gordon confining unit separates the Gordon aquifer from the Upper Three Runs aquifer. This unit is commonly referred to as the “green clay” in previous SRS literature and includes sediment of the Warley Hill Formation (Figure 3). The unit comprises interbedded silty and clayey sand, sandy clay and clay. The clay is stiff to hard and is commonly fissile. Glauconite is a common constituent and imparts a distinctive greenish cast to the sediment, hence the informal name of “green clay” given to this unit. Within the study area the GCU includes some calcareous sediment and limestone, primarily calcarenaceous sand and clayey sand with subordinate calcarenaceous clay, micritic clay, and sandy micrite and limestone.

The GCU dips toward the south-southeast, increasing in thickness downdip across the SRS from approximately 10 feet to 80 feet. Laboratory tests of undisturbed samples taken from the GCU at locations across the SRS indicate vertical permeability ranges from 1.14E-06 to 4.27E-01 ft/day and horizontal permeability ranges from 5.40E-06 to 1.22E-

01 ft/day within this unit (Flach and others, 1999).

Upper Three Runs Aquifer (UTRA) Unit

The Upper Three Runs aquifer includes the informally named "upland" unit, Tobacco Road Sand, Dry Branch Formation, Clinchfield Formation, and Santee Limestone. At SRS, the UTRA is divided into informal "lower" and "upper" aquifer zones separated by the "tan clay" confining zone (Figure 3).

"Lower" Aquifer Zone (LAZ). The "lower" aquifer zone of the UTRA consists of siliciclastic and calcareous sediments of the Santee Formation and parts of the Dry Branch Formation beneath the "tan clay" confining zone (TCCZ) (Figure 3). The zone is highly variable in thickness ranging from around 40 – 80 feet thick in the study area. The LAZ represents shallow, moderate to high-energy nearshore fluvial and marine environments (Harris and others, 1997). Core descriptions within and adjacent to the study area indicate the LAZ represents a dual facies, one that is dominated by siliciclastic components and the other dominated by carbonate components resulting in highly permeable sediments directly in contact with sediments of lower permeability. Typically, the sands and clayey sands are unconsolidated fine- to medium grained, moderate to well sorted and have good to excellent measured porosities (>30%) with permeabilities ranging from 6.8 to 40.8 ft/day (Harris and others, 1997). In contrast the carbonate sediments are unconsolidated and consolidated with excellent measured porosities (>35%) and moderate to low permeabilities ranging from .03 to 4.0 ft/day (Harris and others, 1997). The carbonate sediments are generally mud supported (wackestones and packstones). The lithified carbonates are sometimes partially silicified with biomoldic characteristics. Both lithologies exhibit good porosity but low permeability because the pores are not interconnected or are filled with micrite mud that is highly porous but not very permeable.

Based on the heterogeneity within the LAZ and for the purposes of this study, the LAZ was sub-divided into five informal hydrostratigraphic intervals. Characteristic log signatures of tip, sleeve, and pore pressure data from the CPT data were utilized to delineate permeable (dominantly siliciclastic) and non-permeable (dominantly calcareous) intervals. This sub-division was necessary to map the calcareous sub-zones which function as localized confining zones and strongly influence groundwater flow direction. From the bottom up, these intervals include the lower siliciclastic interval (lLAZ), calcareous interval 2 (CC2), middle siliciclastic interval (mLAZ), upper calcareous interval (CC1), and upper siliciclastic interval (uLAZ) of the LAZ.

"Tan Clay" Confining Zone (TCCZ). The "tan clay" confining zone is lithologically equivalent to the Twiggs Clay and Irwinton Sand Members of the Dry Branch Formation (Figure 3). The zone contains light-yellowish tan to orange clay and sandy clay interbedded with clayey sand and sand. Clay layers are dispersed vertically and horizontally throughout the zone and are probably not laterally continuous over distances greater than 100 to 200 feet (Harris and others, 1990; Aadland and others, 1991). The TCCZ consists of two sequences of interbedded mud and sand with some calcareous sediment in the study area. The lower sequence contains light green to tan, slightly fissile clay and silty sand that is commonly interbedded with sand, silty sand, and coarse-grained, carbonate gravel. The carbonate gravel consists of oysters and other shell debris that is mixed with mud, sand, and gravel. The lower sequence commonly includes interbeds of relatively dense, well-indurated layers of a matrix-supported, shelly, sandy carbonate mudstone. This material consists of siliciclastic sand, mud, and gravel, shell debris, and other carbonate fragments contained in a micrite (mud) matrix.

The upper sequence within the TCCZ consists of interbedded siliciclastic sand and mud and represents an interbedded dual facies with low

permeability sediments closely interbedded with high permeability sediments . The mud is waxy and commonly fissile, with a very high clay content. The interbedded sand is generally well-sorted and medium-grained, with good interstitial porosity. Thicknesses of the TCCZ range from approximately 2 feet to 40 feet. The TCCZ becomes very thin in the vicinity of Caster Creek and is deeply incised at Fourmile Branch. Laboratory tests of undisturbed samples taken from the TCCZ in cores across the SRS indicate vertical permeability ranges from 3.70E-08 to 2.39E-01 ft/day and horizontal permeability ranges from 1.45E-05 to 2.04E-01 ft/day within this unit (Flach and others, 1999).

"Upper"Aquifer Zone (UAZ). The "upper" aquifer zone includes the "upland" unit, Tobacco Road Sand, and part of the Dry Branch Formation (Figure 3). Massive beds of sand and clayey sand with minor interbeds of clay characterize the UAZ. The sediment within the "upland" unit is commonly very dense and clayey and often contains gravely sand.

The top of the UAZ is defined by the present-day topographic surface. The UAZ may be subdivided into four informal hydrostratigraphic intervals that are delineated by characteristic log signatures of tip, sleeve, and pore pressure data from the CPT tool. From the bottom up, these intervals include the "transmissive" zone (TZ), "AA" interval, "A" interval, and an undifferentiated soils interval ("uu" interval) (Figure 3). All the units vary greatly in thickness due to the fluvial nature of deposition. The UAZ averages around 75 feet in thickness in the study area.

Hydrostratigraphic Mapping

Geologic descriptions from three cores and CPT lithologic data from 139 locations (Figure 2) were used to identify and delineate hydrostratigraphic boundaries within the near surface sediments beneath the study area. Figure 4 is a composite log illustrating correlation between CPT, core, and geophysical data which form the basis for the correlation of the hydrostratigraphic units within the Upper Three Runs aquifer. The hydrostratigraphic boundaries were compiled into a 3-dimensional hydrogeologic model using EarthVision® geospatial analysis software. EarthVision® processes sets of spatial and property data by calculating minimum-tension grids to contour a "best fit" of the data. The grids can contour data in 3 dimensions (x,y,z), such as the top of a geologic unit, as two-dimensional grids, or contour data in 4-dimensions: x,y,z, and a "property." Figure 5 is a 3-dimensional visualization of the hydrostratigraphic model illustrating the relations of the units to stream and valley incisions.

Hydrogeological Conceptual Model

Based on the hydrogeology and knowledge of groundwater recharge and discharge zones, a hydrogeological conceptual model for the area was developed. Figure 6 presents a schematic depiction of the hydrogeologic conceptual model for groundwater flow within the study area. The figure illustrates the water table and the hydrostratigraphy previously discussed. Groundwater flow in the Upper Three Runs aquifer is driven by recharge, with Fourmile Branch and tributaries intercepting flow from higher elevation. The underlying Gordon aquifer is influenced at a regional scale by the Savannah River and Upper Three Runs. Within C-Area, the Gordon aquifer is recharged by the overlying Upper Three Runs aquifer. Except for process water outfalls, surface water bodies gain from groundwater discharge. Groundwater flow in the Gordon aquifer appears to be influenced significantly by recharge from the overlying UTR aquifer, and lateral flow within the study area boundaries. Solute groundwater contamination originating in the C-Area is expected to be confined to the Upper Three Runs and Gordon aquifers. Most surface recharge groundwater discharges to the nearest stream (e.g. Fourmile Branch), with the balance entering the Gordon aquifer. In C-Area, the flow between the

deeper coastal plain aquifers and the overlying Gordon aquifer is upward; therefore contamination is not expected to be migrate downward.

Hydrogeologic Property Mapping Using Cone Penetration Testing

CPT data were also used to define hydraulic conductivity variation within the hydrostratigraphic zones previously discussed. The method discussed herein involves correlating CPT tip resistance, sleeve friction and pore pressure measurements to fine grained (mud, silt, and clay) sediment percentages and hydraulic conductivity. The resultant small-scale conductivity estimates were upscaled and interpolated onto the groundwater model grid using stochastic methods.

Fines Correlation to CPT

Soil classification charts in the geotechnical literature typically correlate CPT tip resistance, sleeve resistance, and pore pressure to soil categories (e.g. Lunne and others, 1997), but do not predict fine-grained sediments percentages within categories. Fine-grained sediments, or fines, are defined as particle sizes passing a #200 sieve (e.g. mud, silt, clay). Techniques for prediction of fines content have been demonstrated by Jefferies and Davies (1993) and Robertson and Fear (1995). These studies were used as guidelines for the prediction of the fine-grained sediment percentages.

Data specific to the Savannah River Site (SRS) were used to develop the correlations. Sieve data from F- and H-areas of the SRS were paired with nearby CPT pushes. A total of 516 data pairs were assembled. The paired data were next segregated into 4 categories of fines content based on #200 sieve results: 0-15%, 15-30%, 30-50% and 50%-100%. The data pairs are plotted in Figures 7 and 8, color-coded by percentage fines content (%FC) category: 0-15% (group 1, blue), 15-30% (group 2, green), 30-50% (group 3, red) and 50%-100% (group 4, yellow/black). The data are plotted in terms of normalized tip (Q_{tn}), sleeve (F_{sn}) and pore pressure (B_q) parameters that, in part, account for depth effects. Normalized tip resistance, Q_{tn}, is defined by

$$Q_{tn} = \frac{q_t - \sigma}{\overline{\sigma}} \qquad (1)$$

where q_t is the corrected tip resistance, and σ and $\overline{\sigma}$ are the total and effective overburdens. Normalized tip resistance can be interpreted as the net force required to advance the cone tip (deform the medium) divided by the grain-to-grain contact stress. Normalized sleeve friction (a type of friction ratio) is defined by

$$F_{sn} = \frac{f_s}{q_t - \sigma} \times 100\% \qquad (2)$$

and represents sleeve friction relative to the net force required to advance the cone tip. Normalized pore pressure is similarly defined as

$$B_q = \frac{u - p}{q_t - \sigma} \qquad (3)$$

The numerator is net pore pressure in excess of hydrostatic conditions.

Figures 7 and 8 illustrate that although the %fines groups significantly overlap, they are separated in an average sense. "Center of mass" points are depicted in each figure, and represent the average positions of each %fines group. The first three groups (0-50% fines) follow a definite, nearly linear, trend in Figure 7. Specifically, %fines increases with friction ratio (F_{sn}) and pore pressure (B_q) on average. The sieve data show little dependence on normalized tip resistance (Q_{tn}) in Figure 8. However, the 50-100% fines group, which represents low conductivity sediments, deviates from the trend established by the 0-

50% fines data. Specifically, friction ratio decreases on average when the fines content exceeds 50%.

Because the objective of this study is to distinguish between high and low conductivity sediments, accurate prediction of fines >50% is not critical and these data were omitted in regression analysis in order to achieve a better correlation in the 0-50% range. The resulting correlation is

$$\%FC = 5.009 + 15.98 * \log_{10} F_{sn} + 24.14 * B_q + 6.869 * \log_{10} Q_{tn} \quad (4)$$

The correlation coefficient (R^2) for the regression is 0.45, meaning that the equation (4) explains about 45% of the variation in %FC. While there is large uncertainty in the predictions, the correlation is nevertheless useful given the absence of other more precise characterization data in C-area.

Hydraulic Conductivity Correlation

Hydraulic conductivity has been directly correlated to CPT measurements on SRS sediments by Parsons and ARA (1997) and Celeste (1998). Also, conductivity has been correlated to %fines (e.g. Kegley, 1993; Parsons and ARA, 1997; Celeste, 1998; Flach and others, 1998; Flach and Harris, 1999). These correlations could be used in conjunction with equation (4) to predict conductivity from CPT data. In this study, a hybrid approach was preferred, whereby conductivity is related to CPT measurements indirectly through predicted %fines from equation (4), and directly through the normalized pore pressure parameter, B_q.

The %FC ranges of 0-15%, 15-30% and >30% are considered to correspond to "high", "medium" and "low" conductivity. Based on conductivity data taken at various scales, previous flow models, and groundwater flow model calibration, reasonable values for these conductivity categories appear to be 20, 2 and 0.01 ft/d. Since B_q is good predictor of low conductivity intervals, we also use $B_q > 0.1$ to define an "extra low" conductivity category. The "extra low" conductivity zone is assigned a value of 0.0001 ft/d, irrespective of predicted %fines. The chosen hydraulic conductivity relationship is summarized in Table 1.

The conductivity settings listed in Table 1 are based partially on qualitative knowledge of how conductivity varies with lithology and support scale. As with all groundwater flow models, the specific values of conductivity assigned to a grid are ultimately based on model calibration. The settings in Table 1 are typical values for small-scale conductivity measurements on sediments ranging from clean sand (high K) to clay (extra low K) (e.g. Kegley, 1993; Parsons and ARA, 1997; Celeste, 1998; Flach and others, 1998; Flach and Harris, 1999). Example small-scale tests include the laboratory falling head permeameter and mini-permeameter. After the correlation is applied to the CPT data, the small-scale conductivity estimates are scaled up to the flow model grid (field scale) through a process described in the next section. The upscaled estimates for horizontal conductivity compare favorably with average field-scale measurement data from slug and pumping tests, and previous calibrated flow models. The predicted conductivity fields based on Table 1 are viewed as a starting point for final flow model calibration to additional targets such as water level and plume data.

Upscaling to the Groundwater Flow Model Grid

CPT measurements have a vertical resolution of 0.1 ft, and the radius of influence of the cone in the horizontal plane is similarly small. Therefore, a method for upscaling CPT measurements to the coarser resolution of the groundwater flow model mesh is required. Upscaling refers to the process of replacing a heterogeneous conductivity field within a particular finite volume with a single, "equivalent", conductivity value. The reader is referred to Sanchez-Vila and others (1995),

Wen and Gomez-Hernandez (1996), and Renard and de Marsily (1997) for a review of upscaling and related topics in the stochastic hydrology.

The stochastic upscaling approach in this study is based on combining the work of Gelhar and Axness (1983), Ababou and Wood (1990), and Desbarats (1992). Gelhar and Axness (1983) derived analytical expressions for the effective conductivity tensor of an infinite, ergodic, anisotropically-correlated medium subjected to a uniform mean flow. The three-dimensional anisotropy of the heterogeneous medium is defined in terms of an exponential autocovariance function with distinct correlation scales for each coordinate direction, $_1$, $_2$ and $_3$. Ababou and Wood (1990) pointed out that expressions of the type derived by Gelhar and Axness (1983) can alternatively be written in terms of a "power-average" defined by

$$K_p \equiv \left[\frac{1}{N} \sum_i (K_i)^p \right]^{1/p} = \left(\overline{K^p} \right)^{1/p} \quad (5)$$

where the exponent (power) p is application specific. Arithmetic, geometric and harmonic averaging are special cases of equation (5) gotten by choosing p = 1, 0 and -1. Hence, power-averaging is a generalization of common approaches to averaging. Through numerical studies, Desbarat (1992) demonstrated that the power-averages are an effective approximation to upscaled conductivity, provided an appropriate exponent is chosen. The work of Gelhar and Axness (1983) provides guidance for selecting exponents appropriate for upscaling horizontal and vertical conductivity in C-area.

The conductivity estimates inferred from CPT measurements have a vertical resolution of 0.1 ft and are considered to be "point" measurements. Atlantic Coastal Plain sediments are clearly stratified and imply anisotropic correlation scales in the horizontal and vertical directions, $_h$ and $_v$. Their ratio cannot be derived from the CPT data because none of the 139 locations are close enough in the horizontal plane (i.e. within inches). However, judgement based on knowledge of the depositional environment and visual inspection of outcrops suggests a reasonable ratio is approximately $_h$ / $_v$ = 10. Furthermore, the vertical and horizontal correlation scales within stratigraphic zones are probably on the order of a few inches and several feet, respectively. Considering that the typical model block will be a few feet thick and span on the order of 100 ft in the horizontal plane, the "equivalent" block conductivity should be close to the "effective" conductivity (Kitanidis, 1997), in the terminology of Sanchez-Vila and others (1995). Therefore, power averaging parameters derived from Gelhar and Axness (1983) can reasonably be applied to upscaling of C-area CPT data. For $_h$ / $_v$ = 10, the power-averaging exponents are p_h = +0.86 and p_v = -0.72 for horizontal and vertical conductivity, respectively. For horizontal conductivity the averaging is nearly arithmetic, and for vertical conductivity averaging is similar to harmonic.

To avoid introducing bias into the predicted conductivity fields, the following upscaling process is chosen for K_h and K_v:

1) Transform the point data K to K^p, where p = +0.86 for horizontal conductivity and p = -0.72 for vertical conductivity

2) For each CPT push, arithmetically average K^p over the thickness of each model layer

3) Interpolate $\overline{K^p}$ within each layer using two-dimensional block kriging

4) Back transform $\overline{K^p}$ block estimates by computing $(\overline{K^p})^{1/p}$, where p takes on the value used in step 1)

Vertical averaging in step 2) reduces the three-dimensional CPT data to a sequence of two-dimensional data sets, one per model layer. Model layers conform to stratigraphic units, zones or sub-zones. Kriging is chosen in step 3) because it is an exact interpolator for point estimation and can be optimized for the characteristics of individual formations through the variogram model.

For kriging, an isotropic exponential semivariogram model was chosen (e.g. de Marsily, 1986). The functional form is

$$\gamma(h) = c\left[1 - \exp\left(-\frac{3h}{a}\right)\right] \qquad (6)$$

where

$\gamma(h)$ ≡ semivariogram;
$\frac{1}{2}\mathrm{E}\left\{\left[\mathrm{K}^{\mathrm{p}}(\vec{x}+\vec{h}) - \mathrm{K}^{\mathrm{p}}(\vec{x})\right]^2\right\}$

h ≡lag distance, $\left|\vec{h}\right|$

c ≡contribution

a ≡effective range

A variogram analysis of the synthetic $\overline{\mathrm{K}^{\mathrm{p}}}$ data for each model layer in the UTRA was performed to estimate the effective range, a. As an example, the experimental variograms for horizontal and vertical conductivity for model layer #13 in the Transmissive Zone are presented in Figure 9. The variograms are based on the 139 lithologic CPT pushes in C-area, among a larger total number that included groundwater sampling. The estimated variogram ranges (a) vary from 300 to 1000 ft, confirming that the vertically-upscaled CPT estimates are relevant at field scale. Occasionally a nugget effect is observed. For convenience and consistency, a model variogram with a range of 750 ft and no nugget effect was subsequently used in the block kriging performed for each unit. The model variograms for model layer #13 are also shown in Figure 9. The contribution, c, does not affect the block conductivity estimates so its specification can be arbitrary. The contribution does affect the uncertainty of the conductivity estimates, and an estimate would be needed if an uncertainty analysis were desired.

Predicted Conductivity Fields for C-Area

Figures 10 through 13 illustrate predicted upscaled hydraulic conductivity for key model layers which represent in descending order, the TZ, the TCCZ, the uLAZ, and CC1 (Figure 3). The spatial trends observed in the predicted conductivity fields are supportive of geological interpretations based on CPT data, groundwater flow directions and plume movement. Figure 10 illustrates the predicted horizontal conductivity for the TZ of the UAZ. This zone is important hydrogeologically because it represents a sandy saturated zone overlying the TCCZ and is a controlling factor for the water table flow directions. The predicted conductivities over a large portion of the study area exceed 10 feet/day, which is consistent with field test conductivities for this aquifer zone from other areas at SRS. Figure 11 illustrates vertical conductivity for the TCCZ underlying the TZ. In the northern portion of the study area the predicted conductivities of roughly 10^{-3} ft/day are consistent with known TCCZ conductivities at SRS and are indicative of a good confining zone. In contrast, the southern portion of the study area near Caster Creek exhibits much higher conductivities (roughly 3×10^{-2}) that are more typical of aquifers at SRS. Interpretation of CPT data suggest that toward the south the zone becomes a coarse grained sandy material while the clayey sediments become very thin and discontinuous. A possible explanation is fluvial channeling which would produce coarser grained sandy sediments with higher conductivities and aquifer characteristics. Figure 12 illustrates the predicted conductivities for the uLAZ which lies directly beneath the TCCZ. Good aquifer conductivities are observed in the northern

portion of the study area and excellent aquifer conductivities are prevalent in the southern region. Figure 12 illustrates the predicted conductivities for CC1. Geologically this zone is interpreted to represent a calcareous confining sub-zone within the LAZ. In contrast to the TCCZ conductivities decrease from the northern to southern portions of the study area. Predicted values indicate that CC1 is a very competent confining zone having values of 10^{-4} ft/day or lower. The combination of the range of aquifer and confining zone conductivities of these four hydrostratigraphic intervals control shallow groundwater flow and contaminant migration.

Tritium Contaminant Migration Pathways

Prior to the detailed conductivity field predictions just presented, preliminary groundwater modeling flow predictions of groundwater flow from the CRSB indicated a westerly migration of tritium towards Twin Lakes and Fourmile Branch (Figure 13), along a path parallel to the VOC contamination from CBRP. However, this interpretation contradicted depth discrete tritium data from CPT. Tritium concentrations above 400 pCi/ml are shown in Figure 13. These data indicate that the tritium plume is moving primarily south toward Caster Creek, with smaller concentrations discharging to Fourmile Branch well south of Twin Lakes.

Based on initial hydrostratigraphic CPT interpretations, the initial groundwater model assumed that the LAZ functioned as a relatively homogenous aquifer zone, and the TCCZ as a competent confining zone. Careful re-examination of the CPT data, coupled with nearby core data, identified two low permeability calcareous intervals in the LAZ. Based on the heterogeneity within the LAZ and for the purposes of this study, the LAZ was subsequently sub-divided into five informal hydrostratigraphic intervals. Additionally, the TCCZ was recognized as becoming extremely sandy in the southern region of the study area with the clays very thin and discontinuous. Within this framework, the observed CRSB plume movement can be explained by the corresponding conductivity variations predicted in Figures 10 through 13. In the southern portion of the study area, higher horizontal conductivities in the TZ and uLAZ, coupled with the water table being supported by the deeper CC1 rather than the TCCZ, preferentially draw groundwater toward Caster Creek.

Figure 15 illustrates simulated tritium migration from CRSB based on the revised hydrostratigraphic intervals and conductivity variations. In agreement with the CPT depth discrete contaminant data the bulk of the tritium plume discharges to Caster Creek with a low concentration fringe discharging to Fourmile Branch.

CONCLUSIONS

CPT was successfully utilized in the absence of conventional borehole data for geospatial and contaminant plume mapping. The variations of hydraulic conductivity within the hydrostratigraphic zones of the UTRA were predicted by coupling CPT data and geostatistical methods. Incorporating the hydraulic conductivity variations into groundwater modeling significantly improved flow path predictions. The model conductivity field provided a realistic representation of aquifer heterogeneity in coastal plain sediments. The resulting tritium transport simulations compared well with field data. The CPT geospatial mapping is a viable method for characterization of hydrostratigraphy and sediment behavior in coastal plain depositional environments.

REFERENCES

Aadland, R. K., Gellici, J. A., and Thayer, P. A., 1995. Hydrogeologic Framework of West-Central South Carolina. Report 5, Water Resources Division, South Carolina Department of Natural Resources, Columbia, SC.

Aadland, R. K., Harris, M. K., Lewis, C. M., Gaughan, T. F., and Westbrook, T. M., 1991. Hydrostratigraphy of the General Separations Area, Savannah River Site (SRS), South Carolina. WSRC-RP-91-13, Westinghouse Savannah River Company, Aiken, SC 29808.

Ababou, R. and E. F. Wood, 1990, Comment on "Effective groundwater model parameter values: influence of spatial variability of hydraulic conductivity, leakance, and recharge" by J. J. Gomez-Hernandez and S. M. Gorelick, Water Resources Research, v26, n8, 1843-1846.

Celeste, 1998, Permeability of R-area sediments, Savannah River Site, South Carolina: Minipermeameter vs. cone penetrometer technology, M. S. Thesis, Department of Earth Sciences, University of North Carolina at Wilmington.

de Marsily, G., 1986, Quantitative hydrogeology; Groundwater hydrology for engineers, Academic Press.

Desbarats, A. J., 1992, Spatial averaging of hydraulic conductivity in three-dimensional heterogeneous porous media, Mathematical Geology, v24, n3, 249-267.

Fallaw, W. C. and V. Price, 1995, Stratigraphy of the Savannah River Site and vicinity, Southeastern Geology, v35, 21-58.

Flach, G. P., L. L. Hamm, M. K. Harris, P. A. Thayer, J. S. Haselow and A. D. Smits, 1998, A method for characterizing hydrogeologic heterogeneity using lithologic data, in G. S. Fraser and J. M. Davis, Hydrogeologic models of sedimentary aquifers, SEPM Concepts in Hydrogeology and Environmental Geology No. 1.

Flach, G. P. and M. K. Harris, 1999, Integrated hydrogeological modeling of the General Separations Area, Volume 2, Groundwater flow model, WSRC-TR-96-0399, Rev. 1.

Flach, G. P., M. K. Harris, R. A. Hiergesell, A. D. Smits and K. L. Hawkins, 1999, Regional groundwater flow model for C, K, L, and P areas, Savannah River Site, Aiken, South Carolina (U), WSRC-TR-99-00248, Rev. 0.

Harris, M. K., Aadland, R. K., and Westbrook, T. M., 1990. Lithological and Hydrological Characteristics of the Tertiary Hydrostratigraphic Systems of the General Separations Area, Savannah River Site, South Carolina. Savannah River Region: Transition Between the Gulf and Atlantic Coastal Plains, Proceedings of the Second Bald Head Island Conference on Coastal Plains Geology, University of North Carolina at Wilmington, pp 68-73.

Harris, M.K., Thayer, P.A. and Amidon, M.B., 1997, Sedimentology and depositional environments of middle Eocene terrigenous-carbonate strata, southeastern Atlantic Coastal Plain, USA, v108, nos. 1-4, February, 163-180.

Gelhar, L. W. and C. L. Axness, 1983, Three-dimensional stochastic analysis of macrodispersion in aquifers, Water Resources Research, v19, n1, 161-180.

Jefferies, M. G. and M. P. Davies, 1993, Use of the CPT to estimate equivalent SPT N_{60}, Geotechnical Testing Journal, GTJODJ, v16, n4, December, 458-468.

Kegley, W. P., 1993, Distribution of permeability at the MWD well field, Savannah River Site, Aiken, South Carolina, M. S. Thesis, Clemson University.

Kitanidis, P. K., 1997, Groundwater flow in heterogeneous formations, in G. Dagan and S. P. Neuman, eds., Subsurface flow and transport: a stochastic approach, Cambridge University Press.

Lunne, T., P. K. Robertson and J. J. M. Powell, 1997, Cone Penetration Testing in Geotechnical Practice, Blackie Academic and Professional.

Parsons Engineering Science, Inc. and Applied Research Associates, Inc., 1997, Evaluation of cone penetrometer data for permeability correlation at the Savannah River Site, WSRC-RP-97-63.

Renard, Ph. and G. de Marsily, 1997, Calculating equivalent permeability: a review, Advances in Water Resources, v20, n 5-6, 253-278.

Robertson, P. K. and C. E. Fear, 1995, Liquefaction of sands and its evaluation, IS TOKYO 95, First International Conference on Earthquake Geotechnical Engineering, Keynote Lecture, November.

Sanchez-Vila, X., J. P. Giradi and J. Carrera, 1995, A synthesis of approaches to upscaling of hydraulic conductivities, Water Resources Research, v31, n4, 867-882.

Syms, F.H., Wyatt, D.E. and Flach G.P., 2000, Methodology and Interpretation of the Piezocone Penetrometer Test Sounding (CPT) for Estimating Soil Character and Stratigraphy at the Savannah River Site, this volume.

Wen, X-H. and J. J. Gomez-Hernandez, 1996, Upscaling hydraulic conductivities in heterogeneous media: An overview, Journal of Hydrology, 183, ix-xxxii.

WSRC, 1993. Site Evaluation Report for the C-Area Reactor Seepage Basin (904-68G)(U), WSRC-RP-93-360, Westinghouse Savannah River Company, Aiken, SC, 29808.

WSRC, 1994, Phase II, Revision 2, RCRA facility investigation/remedial investigation plan for the C-Area Burning/Rubble Pit (131-C) (U), WSRC-RP-91-1122, Rev. 2.

Table 1. Hydraulic conductivity correlation.

Conductivity category	**Definition**	**Value** (ft/d)
High	0-15% fines predicted from equation (4)	20
Medium	15-30% fines predicted from equation (4)	2
Low	>30% fines predicted from equation (4)	0.01
Extra Low	$B_q > 0.1$ irrespective of predicted %fines	0.0001

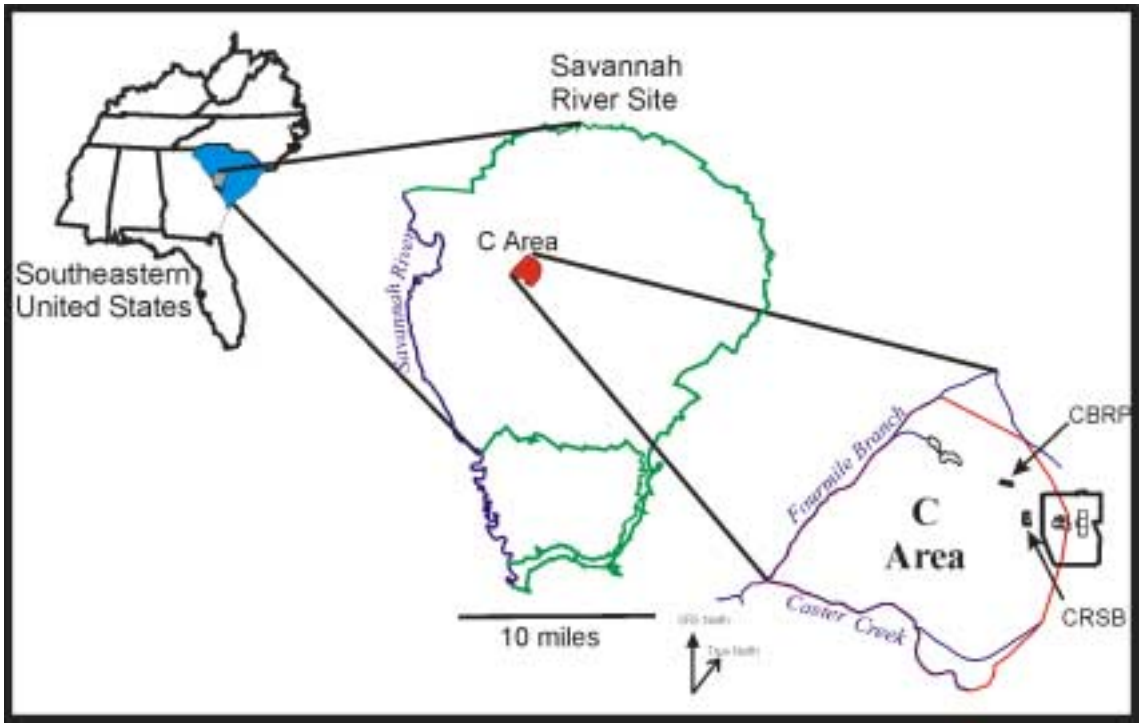

Figure 1. Location of study area.

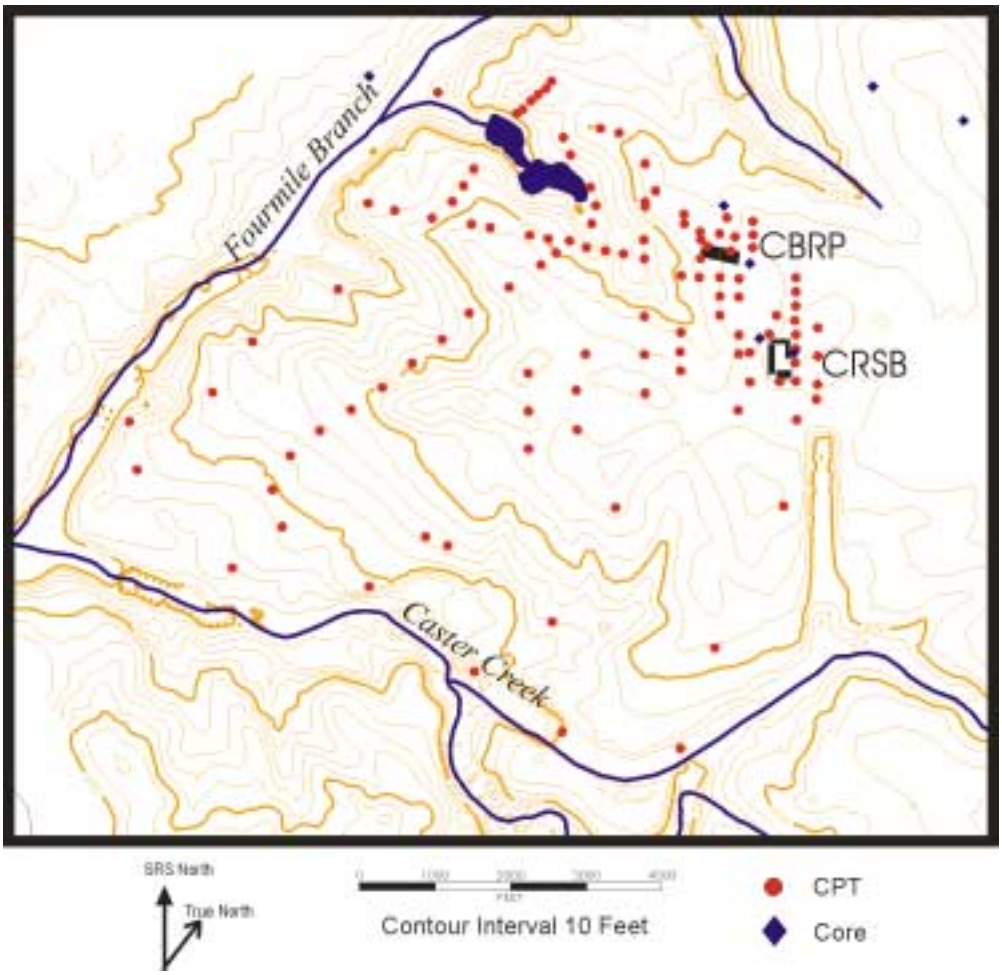

Figure 2. Locations of CPT and borehole data within C-area.

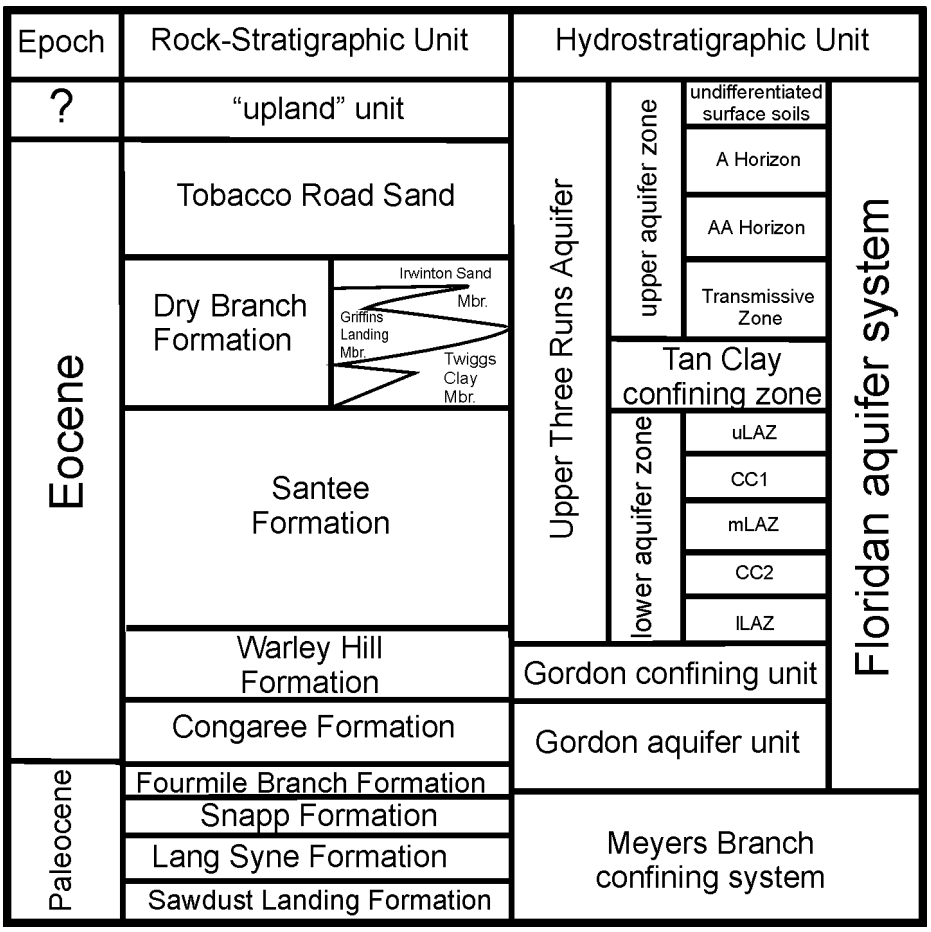

Figure 3. Lithostratigraphic and hydrostratigraphic nomenclature.

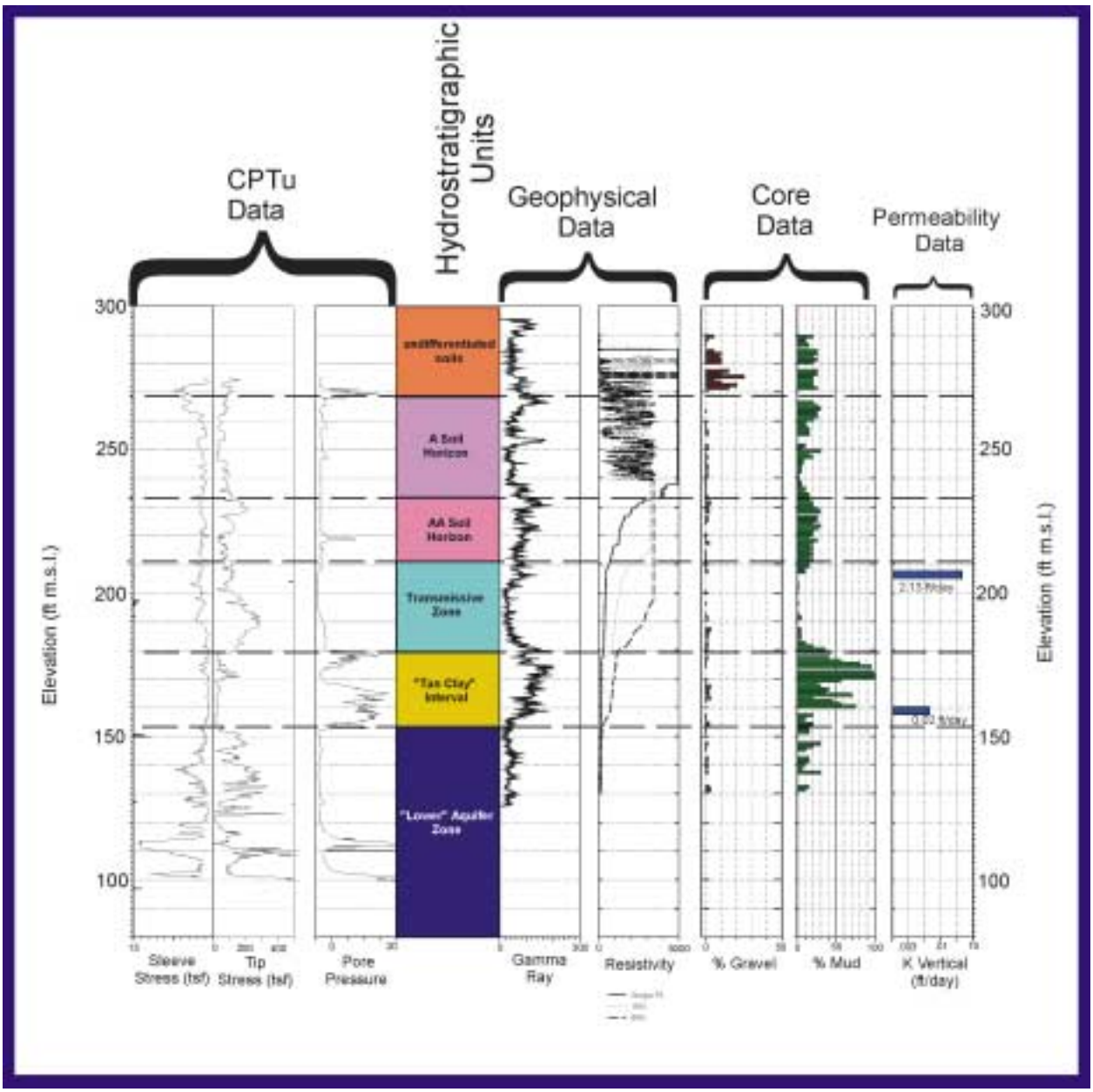

Figure 4. Composite log illustrating correlation between CPT, core and geophysical data.

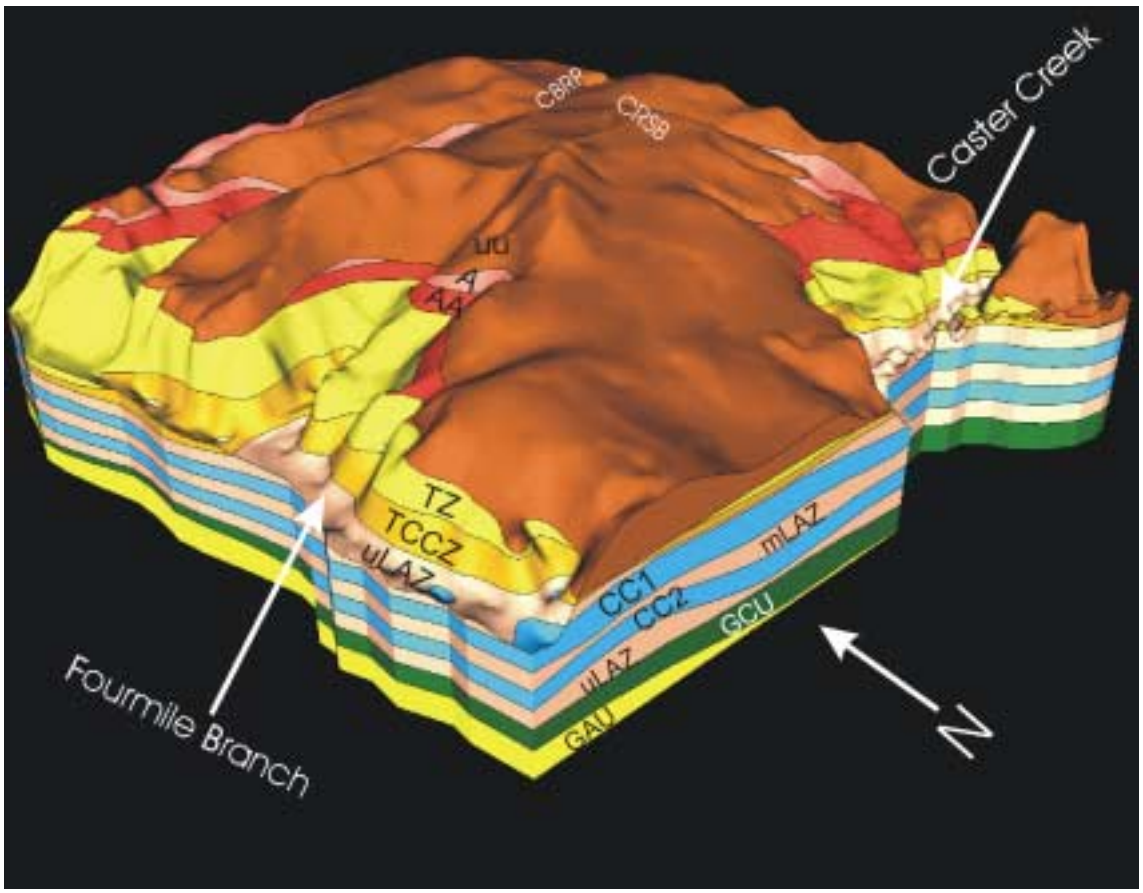

Figure 5. Three-dimensional map of hydrostratigraphic model.

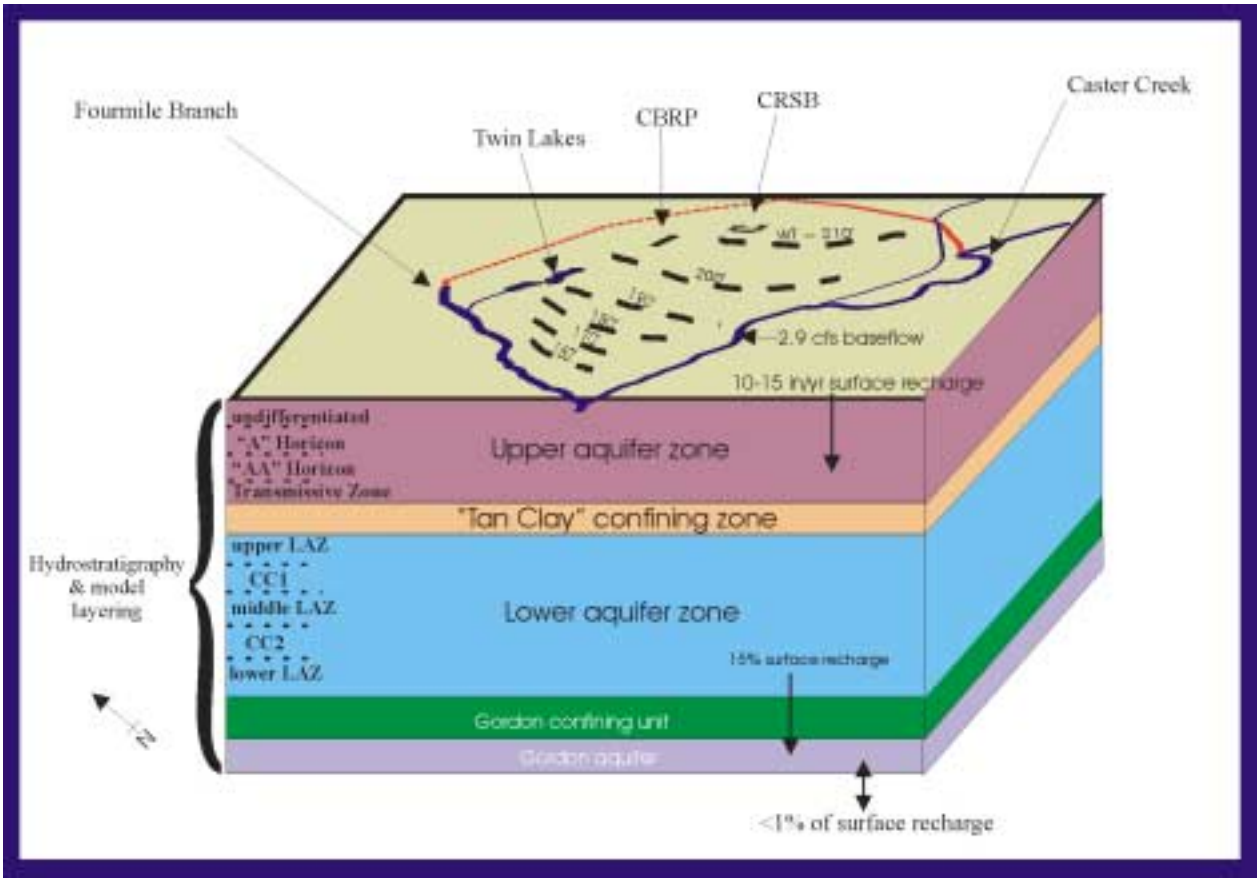

Figure 6. Conceptual model of hydrogeology and groundwater flow.

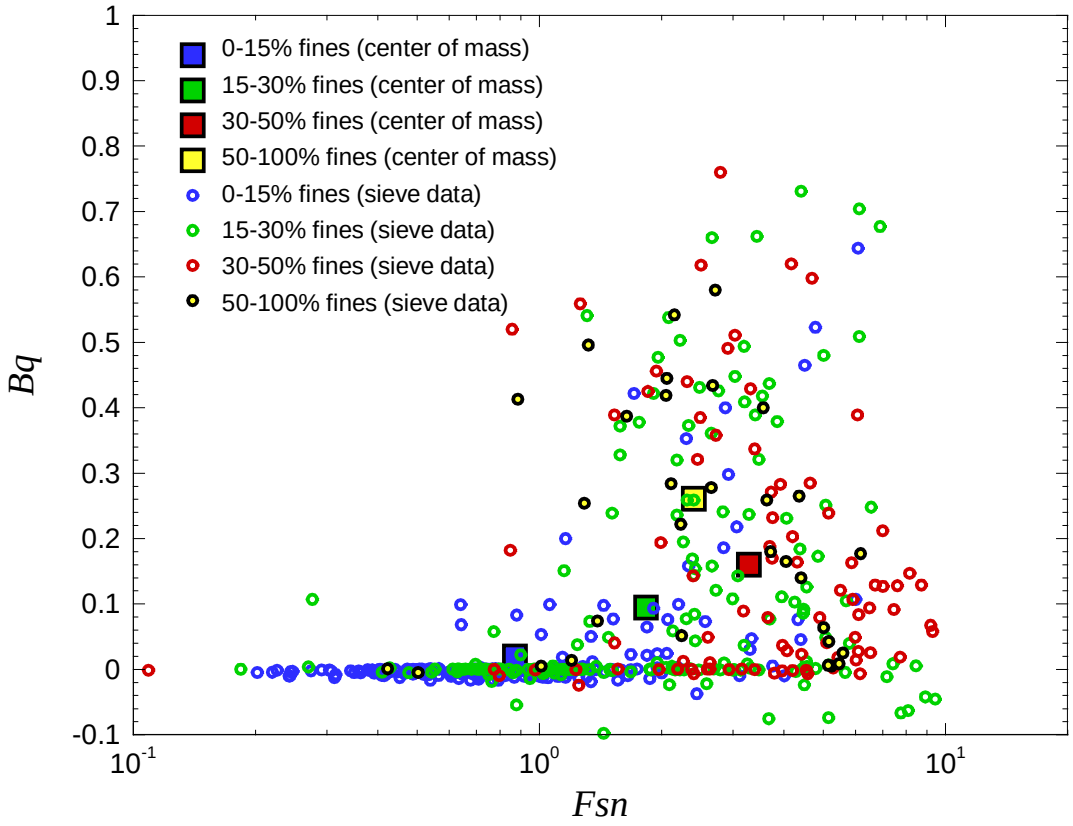

Figure 7. Normalized pore pressure (Bq) and friction ratio (Fsn) CPT data, color-coded by %fines content (group 1 / blue = 0 to 15%; group 2/green = 15 to 30%; group 3 / red = 30 to 50%; group 4 / yellow & black = 50 to 100%).

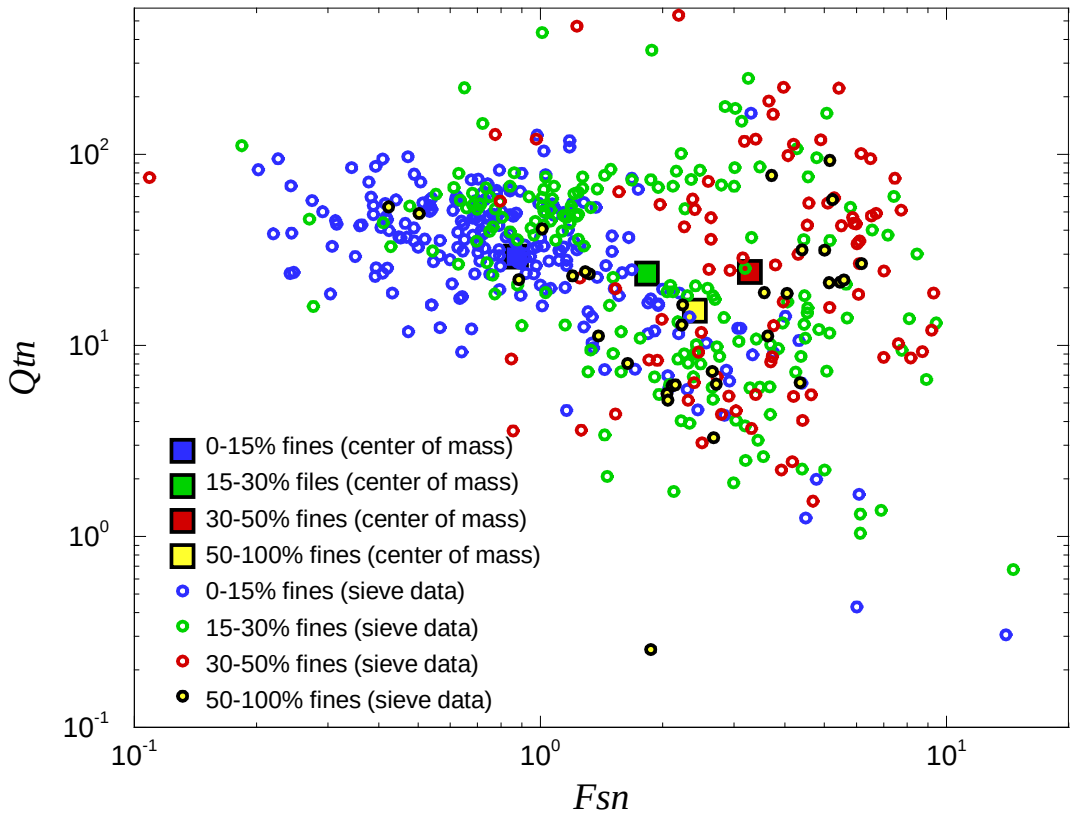

Figure 8. Normalized tip resistance (Qtn) and friction ratio (Fsn) CPT data, color-coded by %fines content (group 1 / blue = 0 to 15%; group 2/green = 15 to 30%; group 3 / red = 30 to 50%; group 4 / yellow & black = 50 to 100%).

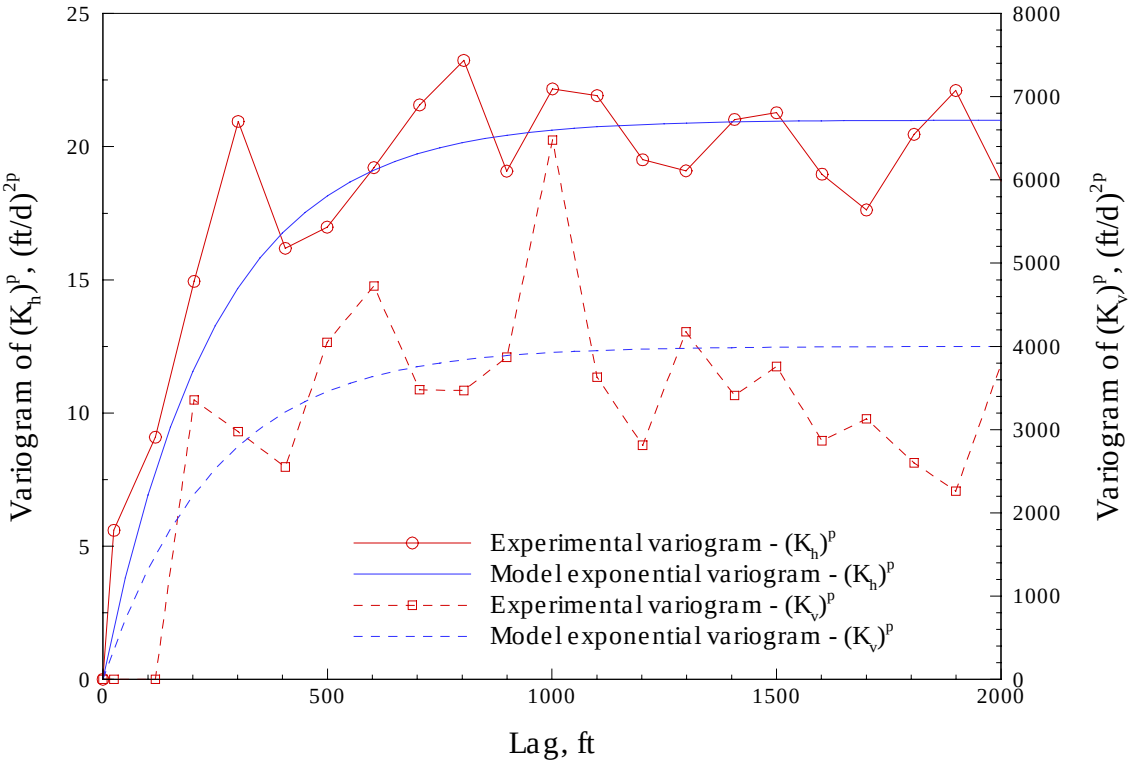

Figure 9. Variogram analysis for K^p in model layer #13 in "transmissive" zone (TZ).

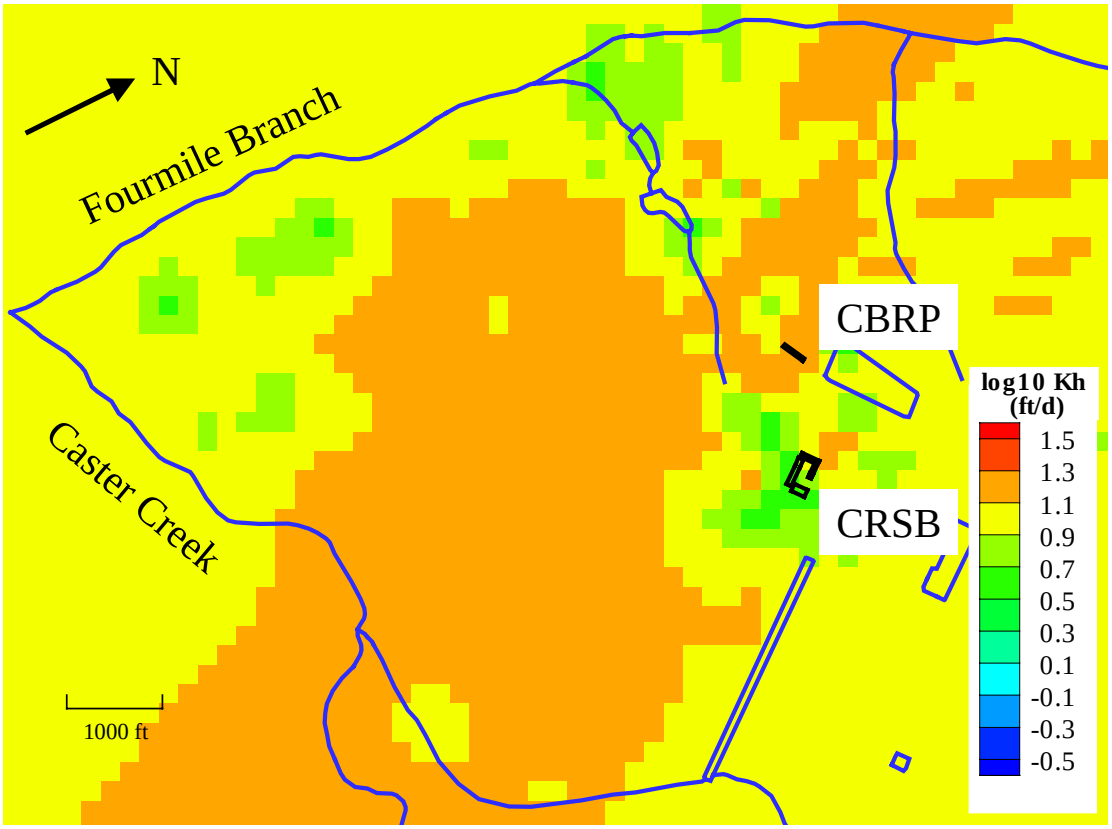

Figure 10. Block kriging estimates of K_h in model layer #12 (Transmissive Zone).

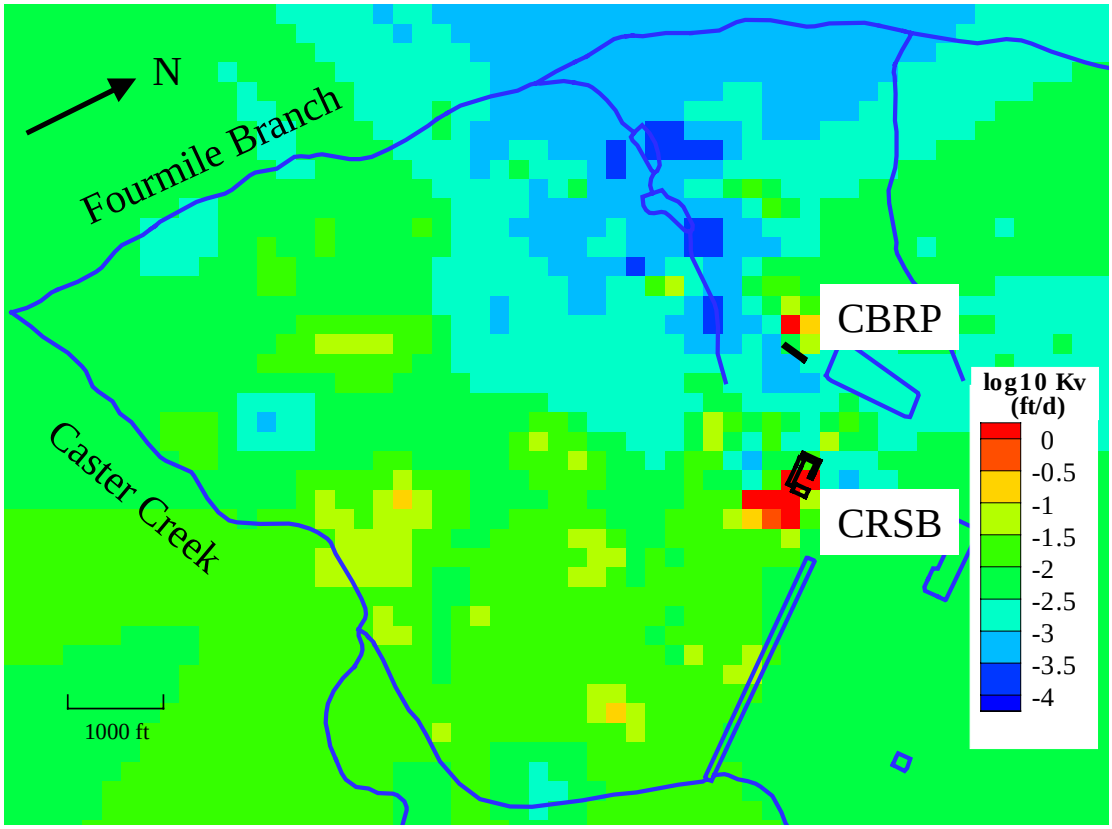

Figure 11. Block kriging estimates of K_v in model layer #11 (Tan Clay Confining Zone).

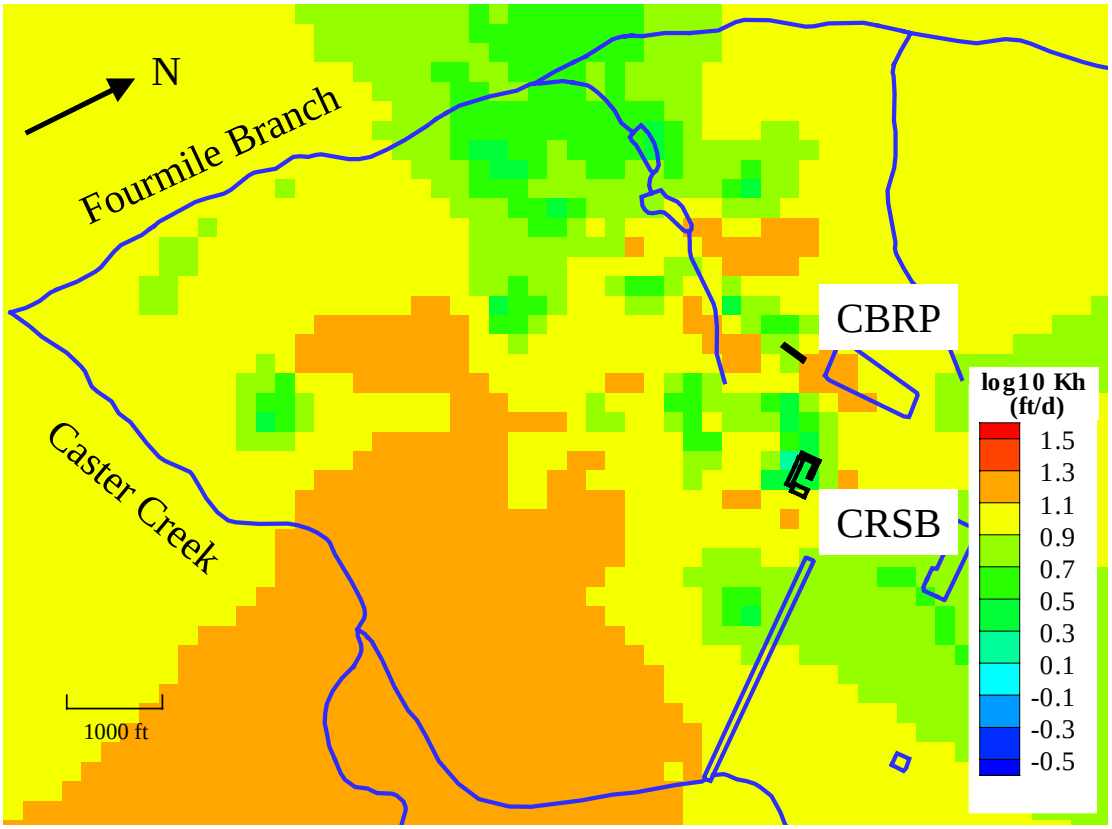

Figure 12. Block kriging estimates of K_h in model layer #9 (upper LAZ).

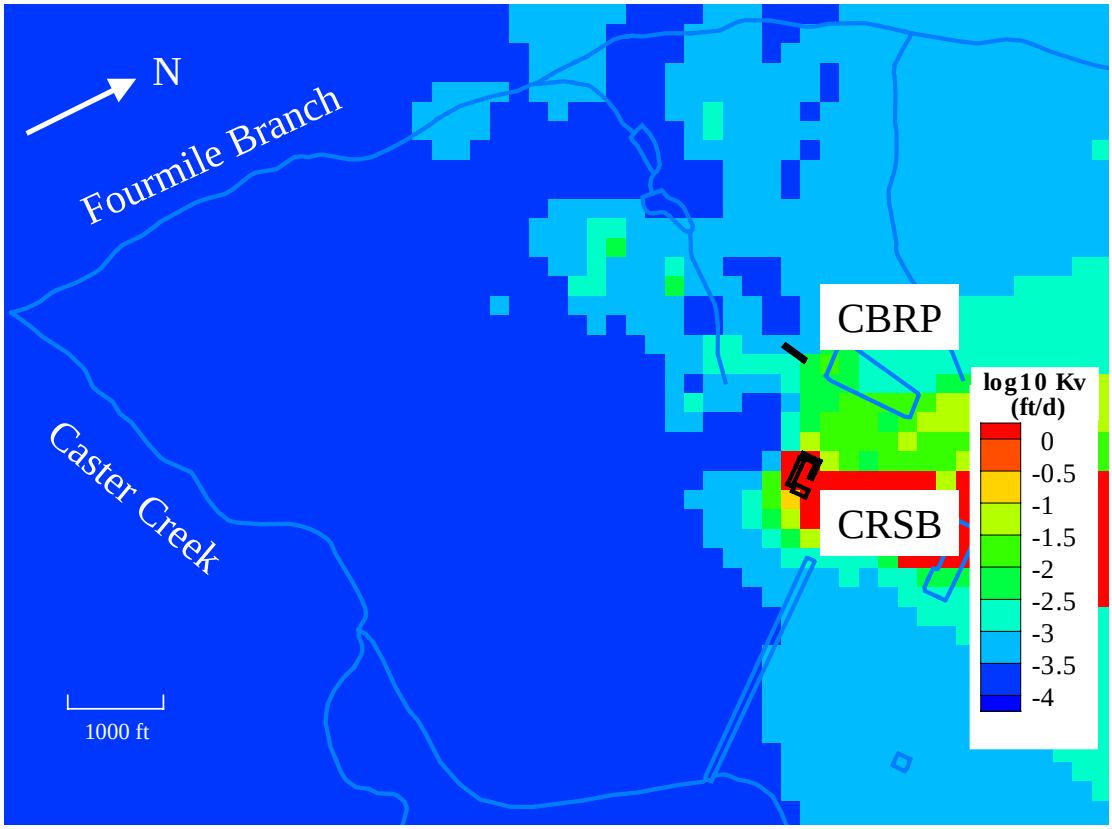

Figure 13. Block kriging estimates of K_v in model layer #8 (CC1).

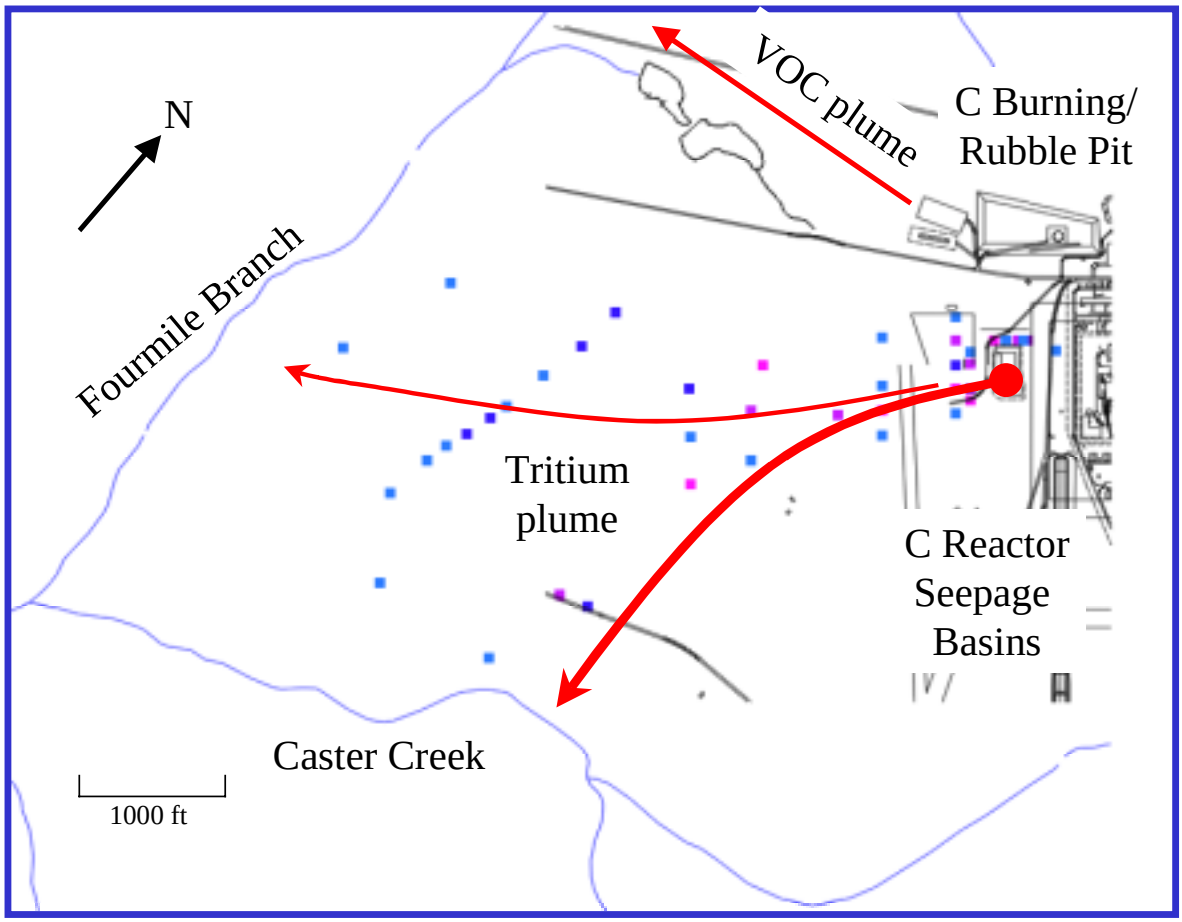

Figure 14. Plan view of CPT tritium concentration data exceeding 400 pCi/ml.

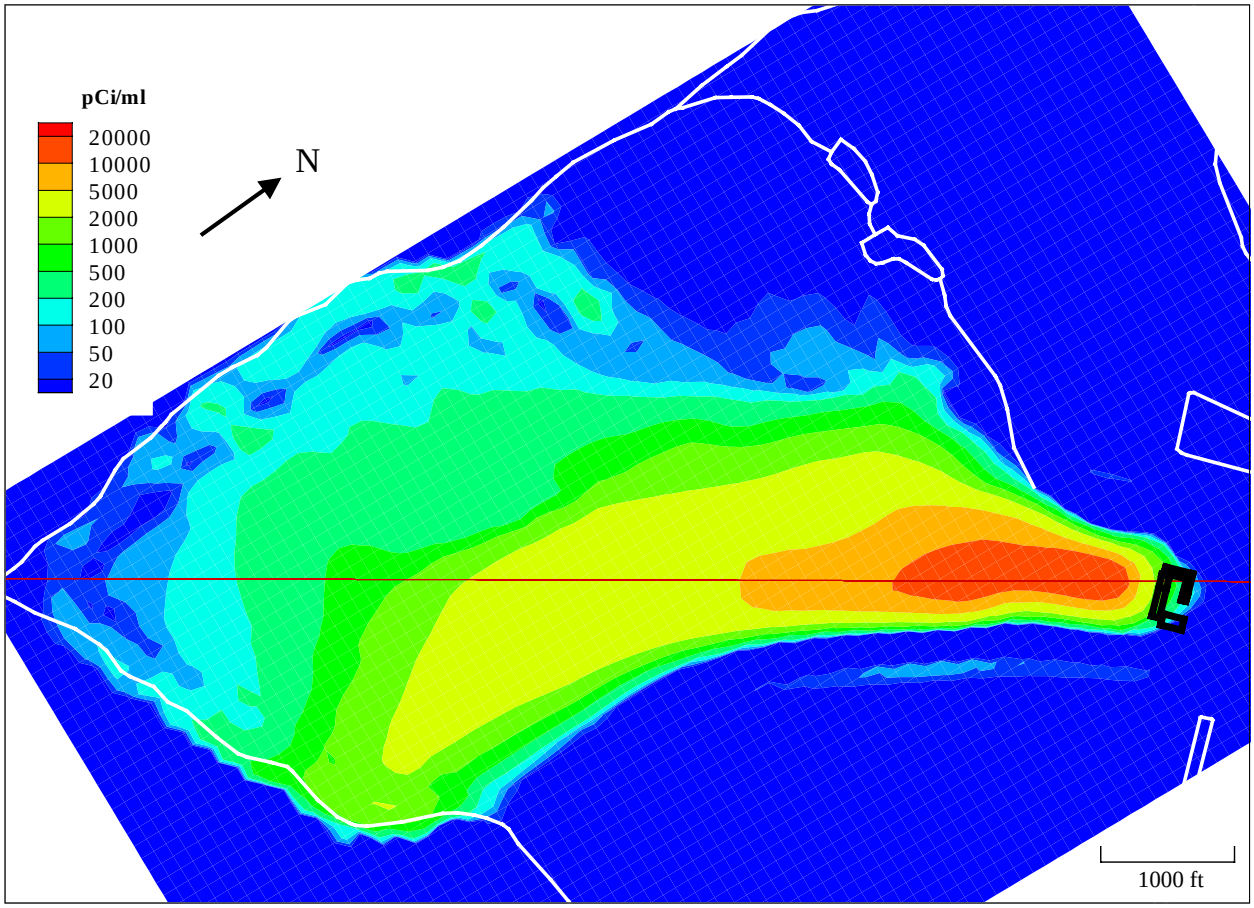

Figure 15. Simulated tritium plume originating from C-Reactor Seepage Basins.

Notes

Soil Vapor Extraction Remediation of Trichloroethylene Contamination at the Savannah River Site's C-Area Burning Rubble Pit

Christine Switzer and David Kosson, Department of Civil and Environmental Engineering, Vanderbilt University, Box 1831, Station B, Nashville, TN 37235
Joseph Rossabi, Savannah River Technology Center, Aiken, SC, 29808

ABSTRACT

Soil vapor extraction (SVE) has become the Environmental Protection Agency's (EPA) presumptive remedy for cleanup of the vadose zone when contaminated with volatile organic compounds. Air sparging (AS) has been employed to remediate shallow groundwater contamination, normally in conjunction with SVE. A SVE/AS pilot system was installed at a small waste area on the Savannah River Site to remediate trichloroethylene (TCE) contamination and evaluate the technology for application to future projects. The system has been operating since October 1999. Concentrations of TCE measured in vadose zone extraction wells and monitoring points between extraction wells have decreased since operation began. After periods of shutdown, subsurface soil gas concentrations of TCE have rebounded to high levels indicating remaining contamination, possibly in the form of dispersed non-aqueous phase liquid (NAPL) or a mass transfer limited phase in the subsurface.

INTRODUCTION

In the past ten years, soil vapor extraction (SVE) has become the presumptive remedy for the remediation of volatile organic compound (VOC) contamination in soils and sediments. Because of the unique aspects of individual waste sites and contaminant configurations, no standard approach to SVE design or modeling has been adopted, although several guidance documents have become available (USEPA, 1994).

In typical implementations of SVE, wells are screened in the vadose zone according to the geology and the contaminant distribution. Vacuum is applied to the configuration and the contaminant is drawn out of the subsurface and either treated or discharged. Treatment methods include collection on activated carbon, collection of the VOC by condensation, and thermal oxidation techniques.

During SVE operation, three phases of mass transport have been observed (Hiller and Guidermann, 1989; Johnson et al., 1990). At the beginning of SVE operation, concentrations remain approximately constant as the available gas phase contaminant is removed from the subsurface pore spaces that are in the directly accessible flow path of the vapor extraction system. The length of this period depends on the type of soil, the vapor flow achieved through the subsurface, and the extent of contamination. Operation then enters a transition period where concentrations decline drastically as the VOC in the accessible flow path is depleted. Diffusion of VOC from less accessible pores and mass transfer from the liquid or aqueous phase to the accessible pores limit VOC recovery. Eventually, a point is reached where mass removal becomes diffusion-limited. In the diffusion-limited regime, contaminant mass removal rates may decline further, even if total mass flow rates are held constant, because VOC diffusive flux may have been diluted by advective flow from clean areas. When the system is shutdown, the accessible pores in the flow path had time to re-equilibrate with the less accessible sources of contaminant. In this regime, the rebound regime, subsurface contaminant concentrations in the soil gas increase as more contaminant became available for removal.

Remediation by SVE/AS can be greatly affected by the presence of non-aqueous phase liquid (NAPL) in the subsurface. Modeling approaches have varied with respect to inclusion of a NAPL component. Some researchers neglected the NAPL phase entirely for reasons that included the age of the spill and the type of soil in which the spill occurred (Ng and Mei, 1996, Kaleris and Croise, 1999, Ng, 1999). The presence of partially saturated, low permeability material in the subsurface increases the likelihood of NAPL,

as capillary action retains the NAPL in the pore space (Massmann et al., 2000). Partially saturated conditions also diminish the effective diffusivity of the contaminant in the gas phase by the cube (approximately) of the gas phase saturation (Rossabi, 1999). Smaller effective diffusivity limits the volatilization and removal of the NAPL.

SITE BACKGROUND

The C-Area Burning Rubble Pit (CBRP) at the Department of Energy's Savannah River Site (SRS) was used for trichloroethylene (TCE) disposal during the site's Cold War activities. The pit was active from the 1950's to the 1980's. The amount of TCE disposed in the pit is not accurately known because disposal records were not kept. The site was selected as a pilot site for evaluation of soil vapor extraction and air sparging (SVE/AS) technologies.

Prior to startup of SVE/AS operation, site characterization was carried out to aid in system design. In January 1999, cone penetrometer pushes were carried out at six locations to determine subsurface stratigraphy. Thirty-nine SVE wells and seventeen AS wells were installed in the western portion of the pit in February and March (Figure 1). Some wells were installed in a clustered configuration of three depths per location. Since these three depths differed in each cluster, the deepest has been designated as the "A" well, the middle designated the "B" well and the most shallow designated the "C" well. Locations 1 through 12 and 15 through 17 have a single well installed at the equivalent "A" depth. Locations 13, 14 and 18 through 23 have the clustered configuration. The vadose zone wells were not developed before operation. The wells are manifolded together with underground piping leading to the soil vapor extraction and catalytic oxidation treatment unit. The unit was designed to operate with a vacuum of up to 24 kilopascals at each well and a flow capacity of more than 470 cm^3/s (600 scfm).

Three well locations (SVE 18, 19 and 22) were selected for extensive characterization. All three of these locations were clustered configurations. In May 1999, twenty-three soil cores were taken from locations along the triangle connecting SVE 18, 19 and 22. In June, EPA installed twenty-six concentration and pressure monitoring implants along the same triangle (Figure 1).

Operation began at CBRP in October 1999. Operation was limited to SVE 18, 19 and 22 at the B and C depths. Samples were collected at the wells and the implants at regular intervals. Operation of additional wells began in December.

In January 2000, the system was shutdown for a few days and rebound was observed based on a single sampling event. In late January, the system was shutdown for two weeks to measure the rebound effect with more detail. The system was turned on again for a few days in mid-February before it was shutdown for repairs. Many of the wells and some of the underground pipes in the manifold system had become clogged with sediments and required cleaning before operation could resume.

Operation resumed in late April using a subset of available wells. The wells that continued operating were 12, 13AB, 17, 18AC, 19AC, 21A, 22AC and 23C.

RESULTS AND DISCUSSION

Initially, data were collected daily at all operating SVE points. Monitoring transitioned gradually to semiweekly, weekly, biweekly and then monthly. Between each transition, VOC concentration and operating pressure were measured at the implants. After each long-term shutdown event, the sampling schedule was revised to capture the expected system behavior.

Operational data showed the characteristic behavior of a SVE system (Figure 2). Concentrations decreased over time and eventually reached a point where continued operation produced little mass removal. When the system was shutdown, concentrations rebounded significantly at most locations. Since operation began, TCE concentrations have decreased at the wells and implants from their initial values. The observed high rebound has indicated that residual TCE contamination must continue to be addressed.

The highly heterogeneous vadose zone with many low permeability layers (Figure 3) increased the probability of NAPL in the vadose zone, despite the age of the pit. The observed high soil gas concentration rebound at wells 18, 19 and 22 during the two monitored shutdown periods also suggested the possibility of NAPL, because TCE concentrations rebounded to levels at or near those before SVE operation began (Figure 2). Concentrations of TCE at the C series wells were as high as 5% of the TCE saturated partial pressure during the rebound events. Pressure and concentration data recorded at the EPA implants have helped provide a better understanding of contaminant distribution and behavior during operation and rebound periods (Figure 4). Implant data suggested that, although high concentrations have persisted at the wells, SVE operation has reduced concentrations of TCE in the subsurface at distances away from the wells.

Many of the wells experienced low vapor flow or a loss of flow due to clogging by sediments and water. The screened zones were selected to be in permeable materials (sandy) that were adjacent to fine grain units (silt and clay) where residual contamination was likely to reside. Because of the heterogeneity of the formation, however, screened zones often crossed some fine grain units as well as the more permeable zones. Since the wells were not developed before operation began, the initial operating period served as a well development cycle, producing an accumulation of fines and water in the wells. The wells were cleaned by bailing and brushing. Limited operation of a subset of the wells was conducted so that the remaining wells could be cleaned and fitted with filters to limit fines traveling through the pipes to the extraction unit. The limited operation at the pit area, which began in April, isolated several problem wells. Flow criteria were defined as “good flow” at wells producing 5 cfm or greater, “acceptable flow” as wells producing 3 cfm or greater and “poor flow” at wells producing less than 3 cfm. Wells 18C and 22C had poor flow and high concentrations. In contrast, well 19C had good flow and a much lower concentration. When the system was shutdown again the first few days of June, soil gas concentrations of TCE at all wells rebounded. Poor flow was observed in most of the operating wells in the limited configuration (Figure 5).

After several weeks of operation, the removal rate of TCE observed at well 19C was more than twice that observed at 18C and four times that observed at 22C (Figure 5). Possible explanations for the poor flow at 18C and 22C included well placement and sediment accumulation. Because 18C and 22C were screened mostly into the stiff clay layer, residual moisture may have decreased the permeability of the sand layers above and below, where high permeability would normally be expected. Advective flow was determined by the relative permeability of the sediments, which depended on the tortuosity of the subsurface material. This parameter also scaled with the cube of the gas saturation in subsurface pore space (Rossabi, 1999). As the relative saturation of water in a two fluid phase porous medium increased, the advective flow decreased. The remedies to the flow problem included removing the accumulated sediments from the wells, developing the wells, and injecting air in at both low and high pressures to create pathways for airflow to the wells. These repairs have been successful for many but not all of the wells. Some of the poorly performing wells may have been screened in zones that are inaccessible to permeable sediments.

Early zone of influence testing at CBRP, which used the EPA implants to measure pressure changes in the subsurface when each well in the group of SVE 18, 19 and 22 was operated individually, provided interesting insight to the flow problems. During pressure testing, a single SVE well in that group was operated and pressure was recorded at the EPA implants. Implant depth varied by location. For most locations, there were two implant depths installed. For simplicity in discussion, these were grouped as “upper” (above 30ft) and “lower” (below 30ft). These groupings corresponded with location of the stiff clay layer, which was present between 25 and 30 ft (Figure 3b). Comparison of vacuum at 19C and vacuum response at the implants, a well that that produced high flow rates, and 22C, a well that produced low flow rates, supported well placement as a significant contributing factor to well performance. Both of these wells were included in the “upper” grouping because portions of their screens were above 30ft. While 19C was operating, vacuum diminished in the corresponding “upper” implants as distance from

the well increased. Vacuum recorded at the "lower" implants was close to or at zero. While 22C was operating, vacuum at the "upper" implants was small, approaching zero while vacuum at the "lower" implants was much greater, suggesting that 22C was inducing flow below the stiff clay layer (in the clayey sand) instead of above it (Figure 6).

This same zone of influence testing at 18C also provided insight to the low flow there. When 18C was operated, a significant vacuum was measured at the nearest of the shallow implants only. Little to no vacuum was measured at all of the other implants, suggesting a small radius of influence for 18C (Figure 7).

CONCLUSIONS

Soil gas concentrations of TCE in the subsurface have decreased significantly at many locations since operation of the SVE/AS system began. The observed high rebounds in soil gas TCE concentration at several locations indicated that TCE contamination must continue to be addressed. Limited operation at the pit area, which began in April, isolated several poorly performing wells. Low flow was observed in most of the operating wells in the limited configuration. Possible explanations for the poor flow included well placement and sediment accumulation. Some of the wells were placed across lower permeability zones. The attempted remedies to the poor flow problem have been partially successful. Despite these problems, the observed decrease in soil gas TCE concentrations at the implants indicated significant removal of TCE from the subsurface by the SVE/AS system.

ACKNOWLEDGEMENTS

The authors gratefully acknowledge the financial support of the Consortium for Risk Evaluation with Stakeholder Participation (a cooperative agreement with the Department of Energy) and the assistance of Jerry Nelsen, Mary Harris, Gregory Flach, Michael Morgenstern, John Bradley, Keith Hyde and Brian Riha.

REFERENCES

USEPA (1994). EPA Soil Vapor Extraction (SVE) Treatment Technology Resource Guide. Office of Solid Waste and Emergency Response Technology Innovation Office Washington, DC, 20460, EPA/542-B-94-007.

Hiller, D., and H. Guidemann (1989). "Analysis of vapor extraction data from applications in Europe." In Proceedings of Third International Conference on New Frontiers for Hazardous Waste Management, EPA/600/8-89/072, Pittsburgh, PA, September 10-13.

Johnson, P. C., M. W, Kemblowski, J. D. Colthart (1990). "Quantitative analysis for the cleanup of hydrocarbon-contaminated soils by in situ venting." Ground Water, 28(3): 413-429.

Kaleris, V. and J. Croise (1999). "Estimation of cleanup time in layered soils by vapor extraction." Journal of Contaminant Hydrology **36**: 105-129.

Massmann, J. W., S. Shock, et al. (2000). "Uncertainties in cleanup time for soil vapor extraction." Water Resources Research **36**(3): 679-692.

Ng, C.-O. (1999). "Macroscopic equations for vapor transport in a multi-layered unsaturated zone." Advances in Water Resources **22**(6): 611-622.

Ng, C.-O. and C. C. Mei (1996). "Aggregate diffusion model applied to soil vapor extraction in unidirectional and radial flows." Water Resources Research **32**(5): 1289-1297.

Rossabi, J. (1999). "The influence of atmospheric pressure variations on subsurface soil gas and the implications for environmental characterization and remediation." Ph.D. thesis, Clemson University, University of Michigan Press.

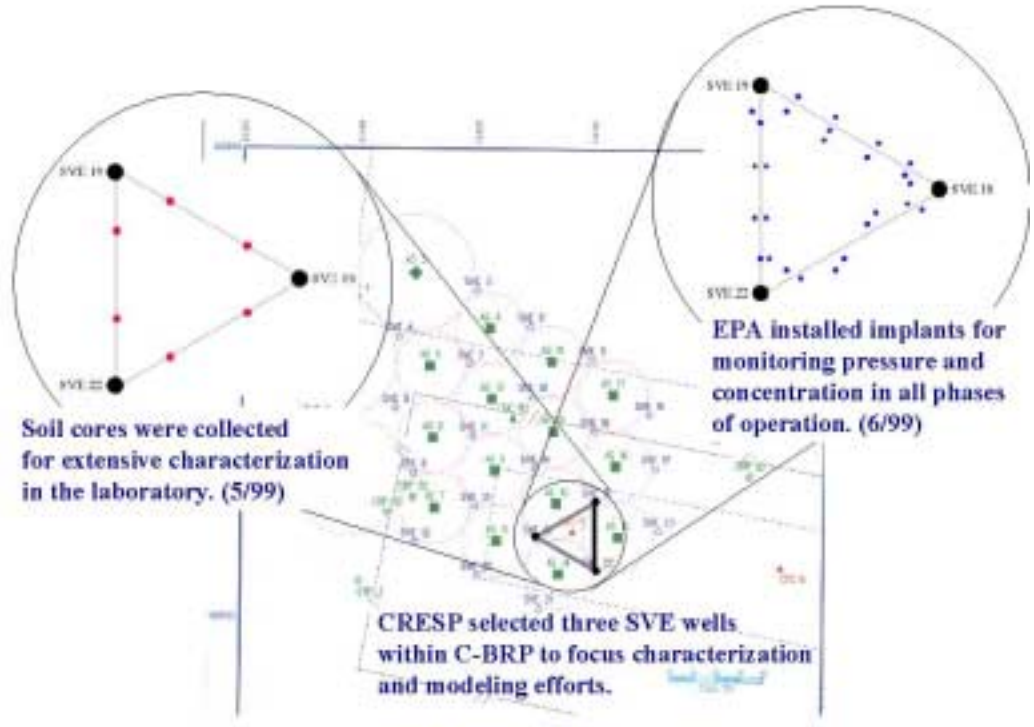

Figure 1. Diagram of SVE and AS well locations with region of study indicated.

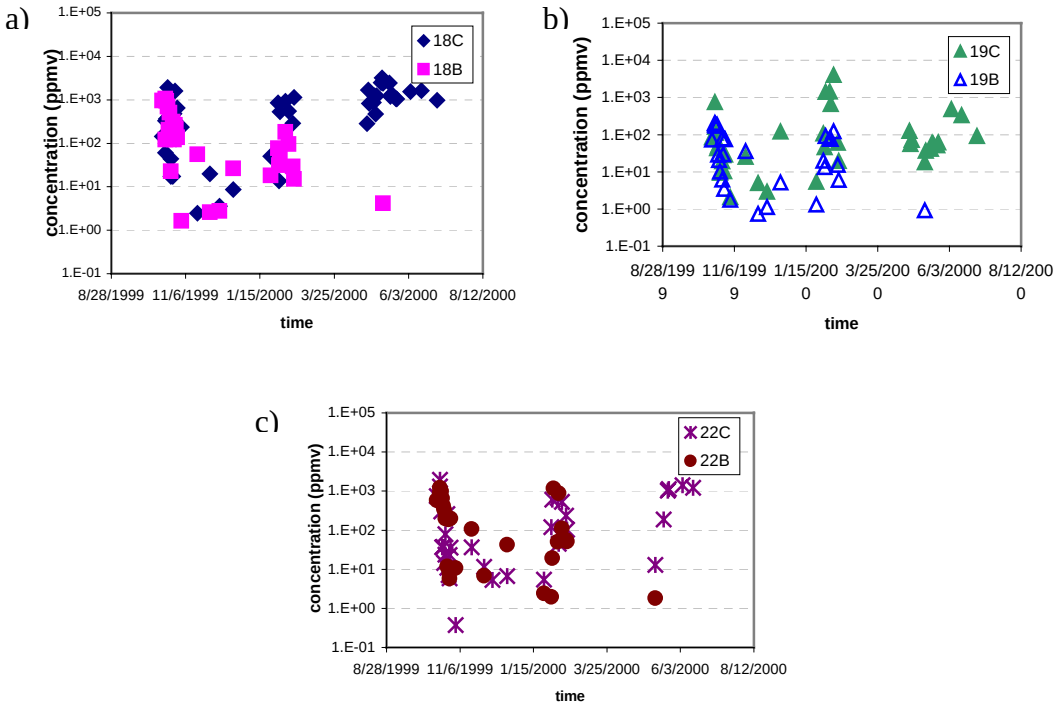

Figure 2. Concentration of TCE recorded at a) SVE18, b) SVE 19 and c) SVE 22.

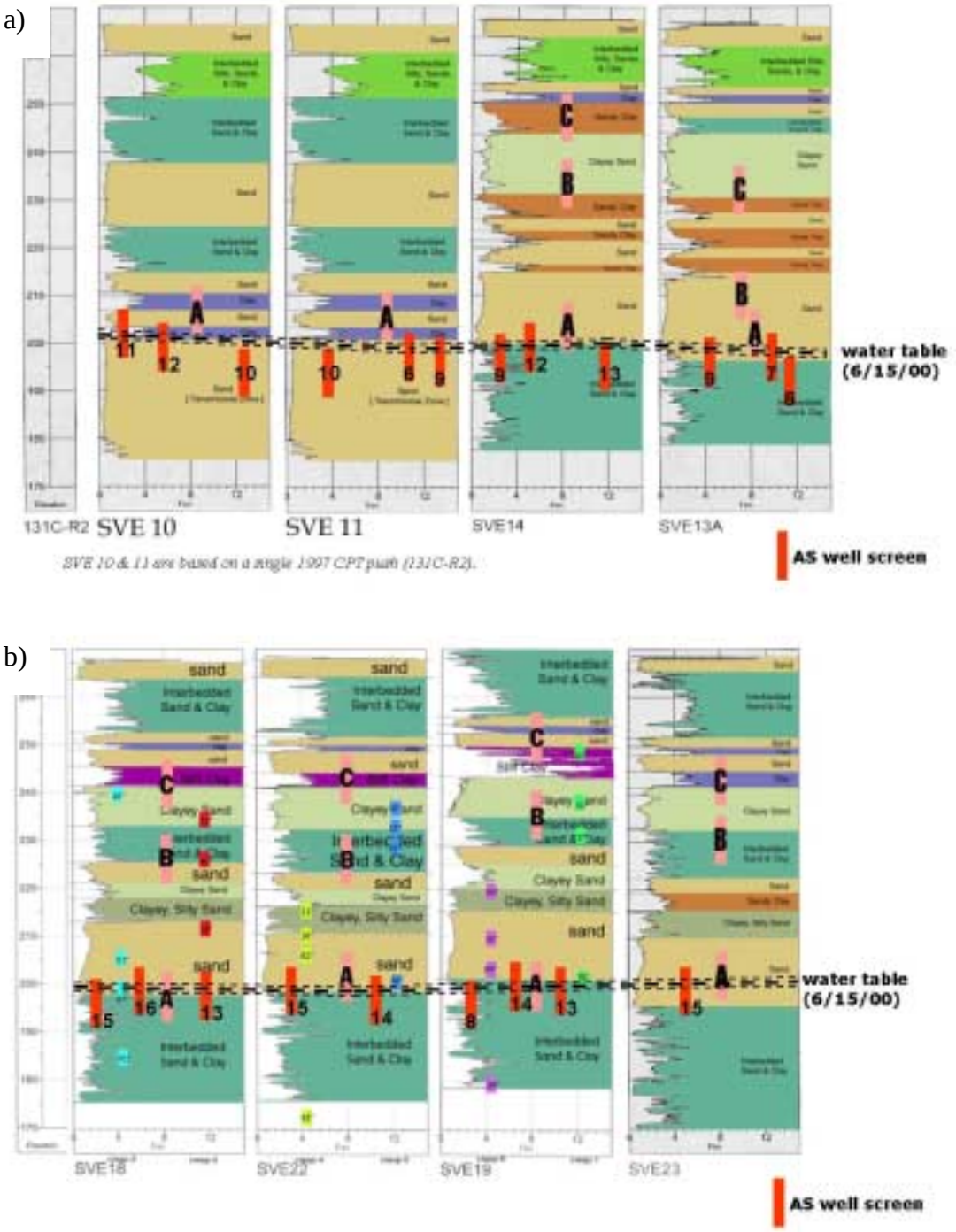

Figure 3. Detailed stratigraphy based on CPT information (courtesy of Greg Flach and Mary Harris, Savannah River Technology Center). SVE well locations are indicated by the larger blocks with screen (A, B or C) designated, and shelby tube sample locations are indicated by the smaller blocks.

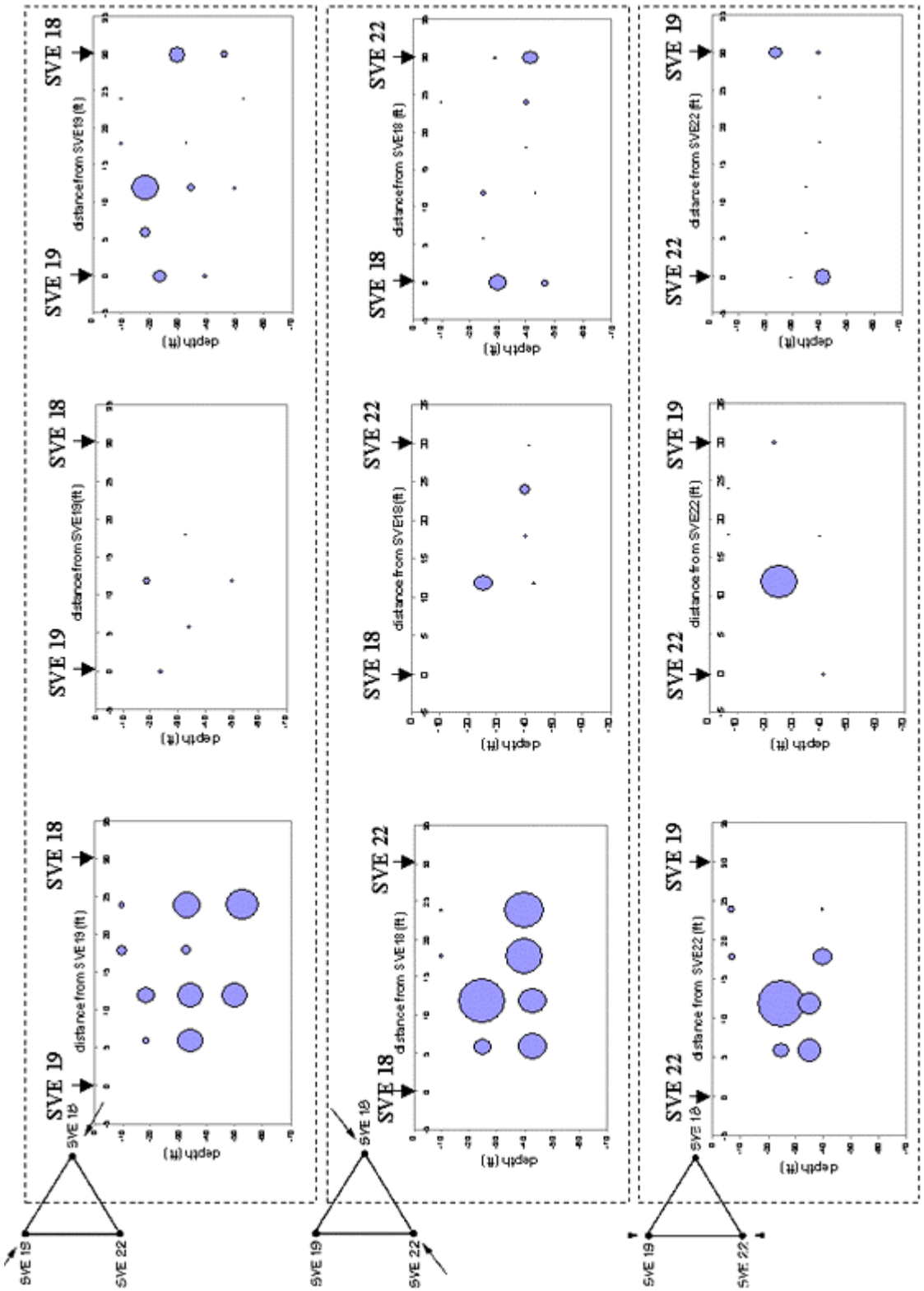

Figure 4. A two-dimensional perspective on the concentration data recorded at CBRP. Plots are two-dimensional in space, taken at three discrete time points : before operation, after three months of operation, and after two weeks of rebound. Area of the bubble is proportional to concentrations.

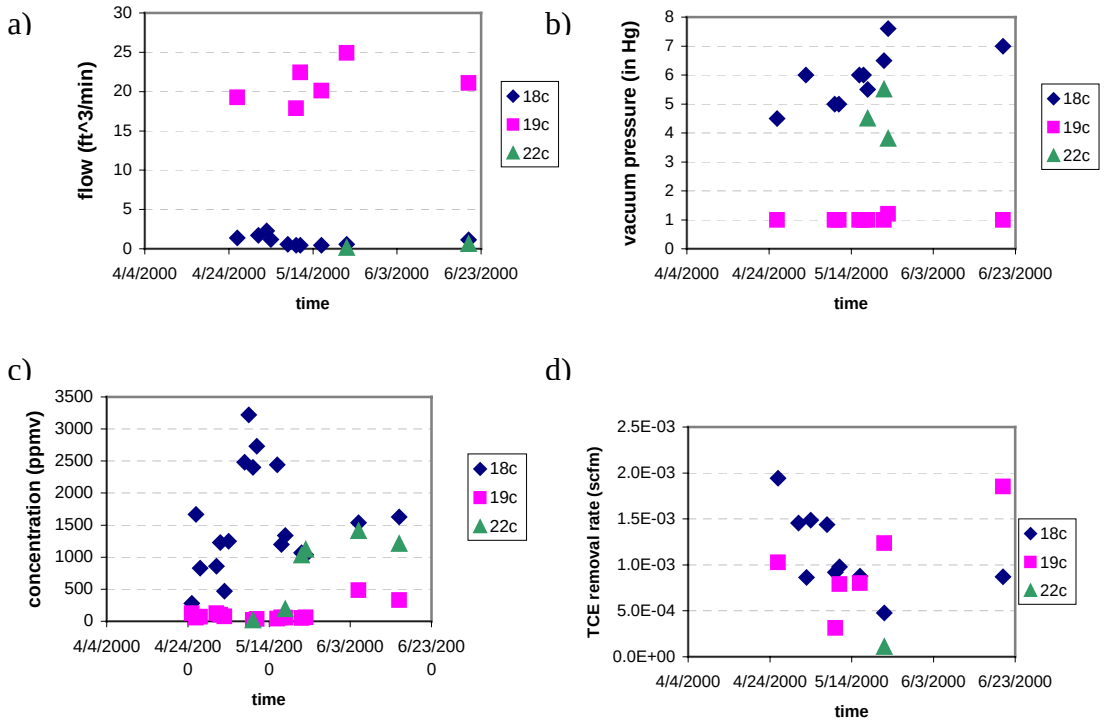

Figure 5. a) Total flow, b) vacuum pressure, c) concentration and d) removal rate of TCE recorded at SVE 18C, 19C and 22C after the system was down for one month of repairs.

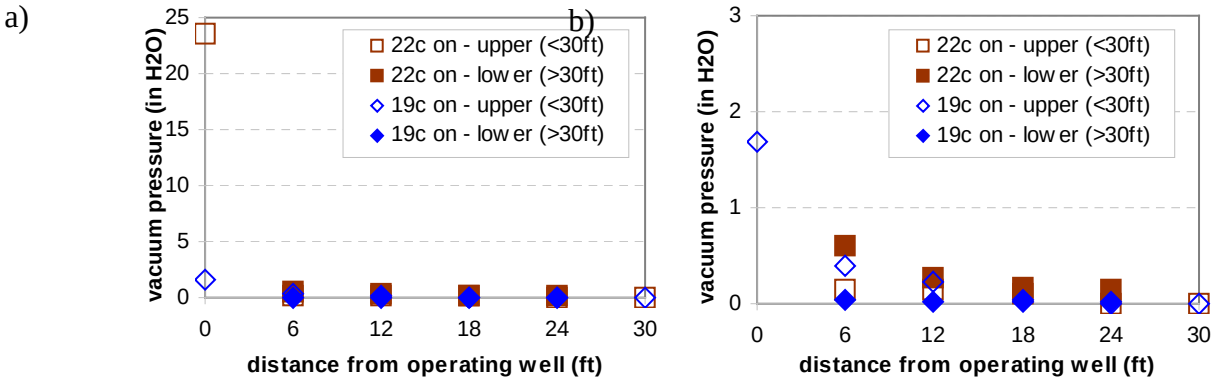

Figure 6. Vacuum pressure measured during preliminary pressure testing at the EPA implants plotted with respect to distance from the SVE well that was operating, shown at a) large scale (0-25kPa) and b) small scale (0-3kPa). Implant depth varied by position so locations were categorized as upper (above 30ft) and lower (below 30ft).

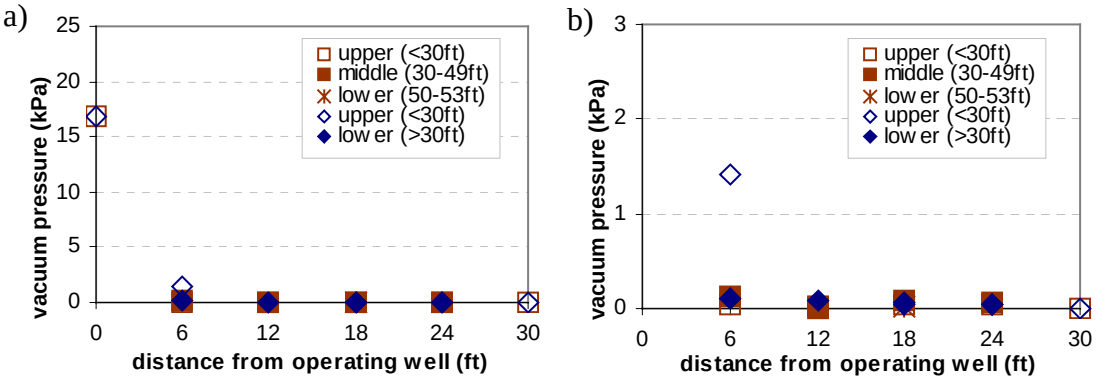

Figure 7. Vacuum pressure measured during preliminary pressure testing at the EPA implants while SVE 18C was operating, shown at a) large scale (0-25kPa) and b) small scale (0-3kPa). Data were recorded at two sets of implants near 18C.

Notes

DNAPL Penetration of Saturated Porous Media Under Conditions of Time-Dependent Surface Chemistry

David M. Tuck, Westinghouse Savannah River Company, Aiken, SC 29808[1],
Gary M. Iversen, WSRC, Aiken, SC, 29808
William A. Pirkle, University of South Carolina, Aiken, SC 29801

ABSTRACT

Two long-term experiments were run to observe the behavior of a DNAPL containing a nonvolatile, surface active dye in water-saturated porous media. The DNAPL was tetrachloroethylene (PCE), and the dye was Sudan IV, the most frequently used dye used to stain organic phases in multiphase flow visualization studies. The DNAPL penetrated the top two millimeters of the porous medium in which a PCE-dye solution with 0.508 g/L of dye was used. The results provide the first qualitative experimental evidence in support of a pore-scale model which explicitly incorporates the time-dependent surface chemistry exhibited in the water-PCE-SudanIV dye system.

INTRODUCTION

The presence of dense, non-aqueous phase liquids (DNAPLs) in the subsurface is a major environmental problem facing the Savannah River Site, as well as other commercial and industrial sites around the country. It is important to understand and attempt to predict their behavior during any enhanced remediation effort to avoid exacerbating the existing problem. Previous research (Pirkle et al. 1997a) indicated that entry pressures are considerably different for PCE/Sudan IV dye solutions than for pure PCE, due to the surface active nature of the dye. This is important since most sites contaminated with PCE or other DNAPLs involve impure solutions containing potentially surface active substances. The purpose of the current research was to experimentally examine the subsurface behavior of perchloroethylene (PCE), which is the major component of the SRS M-Area DNAPL, under conditions of time-dependent surface chemistry.

BACKGROUND AND THEORY

Capillary forces play a major role in controlling where and how DNAPLs migrate in the subsurface. DNAPL fluid saturation in an initially water-saturated porous medium is a function of the capillary pressure, i.e., the difference between the wetting and non-wetting fluid pressures. This capillary pressure-saturation relationship is important input data required for modeling multiphase fluid flow in porous media.

In previously reported research (Pirkle et.al., 1996, 1997a), the Hobson Equation, a modification of the Young-Laplace equation (HOBSON, 1954, 1975), was changed to account for the fact that, under the experimental conditions used, there was no bouyant force supporting the PCE column prior to its entry into the medium. For our experimental set-up (Figure 1) the Young-Laplace equation was expressed as:

$$P_c = L_v \rho_o g = \frac{2\sigma_{ow}\cos\theta}{r_t} \quad (1)$$

[1] Current address NAPLogic, Inc. P.O. Box 72, Princeton, NJ 08542-00722; email: dtuck@naplogic.com

Where L_v is the height of the PCE or SUDAN IV dye/PCE solution column prior to penetrating the medium (cm), σ_{ow} is the interfacial tension between SUDAN IV dyed-PCE solution and water (dynes/cm), θ is the contact angle between the PCE-water interface and a glass surface, r_t is the "effective" pore throat radius (cm), ρ_o is the density of PCE (g/cm^3), and g is the acceleration of gravity (980 cm/ sec^2).

SUDAN IV dye dissolved in PCE reduces interfacial tension between the PCE and water and changes the wetting relationship between PCE, water and glass. These changes occur relatively slowly in a roughly log-linear fashion over time spans of minutes to days (Tuck and Rulison 1998). The extent to which interfacial tension reduction and wetting changes take place depends upon the concentration and activity of the dye (Tuck and Rulison 1998). In addition to the above considerations, the addition of a dye may also affect other parameters such as the fluid density and viscosity. The effects of the SUDAN IV dye are analogous to the surface chemistry and physical changes one might expect of a weak, oil-soluble surfactant. The extent to which Sudan IV dye effects the system surface chemistry (contact angle and interfacial tension) depends on the concentration of the dye (see Figure 2 a and b).

The Hobson equation treats the surface chemistry as constant, i.e., as equilibrium values. Recent theoretical work (Tuck accepted, Tuck 1999, Tuck et al. 1998b) suggests that equilibrium values do not necessarily yield the best understanding and, therefore most accurate modeling of multiphase flow in porous media. Surface chemical kinetics, i.e., the time-dependent nature of surface chemical properties (surface or interfacial tension and contact angle), may, under certain circumstances, dominate the pore-scale processes which govern multiphase flow in porous media. The time-dependence may be represented as $\sigma = \sigma(t)$ and $\theta = \theta(t)$, where σ is the interfacial tension, θ is the contact angle, and t is time.

The conditions under which surface chemical kinetics (i.e., the time rate of change of the surface chemical properties interfacial tension and contact angle) become important are when the capillary pressure is close to the critical capillary pressure required for immiscible displacement to occur.

Tuck (accepted) postulated the age of an interface gets re-set each time it becomes unstable and advances through the subsequent pore-body during a "Haines jump." He suggested this results in a time-dependent critical capillary pressure for any given pore-throat because the surface chemistry controlling the stability of the interface is time-dependent. Thus for a given pore-throat of radius r_t and constant fluid pressure difference, P_c, a critical age (t_{crit}) at which an interface will become unstable is given when the following equation is satisfied

$$P_c - \frac{2\sigma(t_{crit})\cos\theta(t_{crit})}{r_t} = 0 \qquad (2)$$

Using this model, he showed that immiscible displacement can occur at lower hydrostatic fluid pressure differences than those normally measured in experimental work. His model was designed to approximate a fine sand, and the surface chemical kinetics were those for the water-glass-PCE-Sudan IV dye system with a dye concentration of 0.508 g/L. The modeled PCE penetration rate under these conditions decreased in log-linear fashion as the hydrostatic fluid pressure difference decreased. Penetration of the model medium continued at hydrostatic fluid pressure differences well below the entry pressure difference for pure PCE. The model results

thus predict that Sudan IV-dyed PCE should penetrate a water saturated porous media even at pressures below the normally defined "entry pressure", but the rate of penetration should be quite slow.

The objective of this research was to test the conceptual theoretical model developed by Tuck (accepted). Under the relatively slow surface chemical kinetics associated with the Sudan IV dye, PCE should penetrate a water saturated medium at hydrostatic fluid pressure differences less than measured in previous experimental work (Pirkle et al. 1997a), but the rate of penetration is expected to be very slow.

EXPERIMENTAL PROCEDURE

The experimental apparatus is illustrated in Figure 1. Two identical experimental set-ups with "uniform" diameter glass bead porous media were used. The glass beads were obtained from Potter Industries Inc. They were washed and re-sieved at the University of South Carolina Aiken. The beads were dry sieved to reduce the amount of material for further processing. Dry-sieved beads were soaked overnight in ethanol, and then thoroughly washed with ethanol to remove any hydrocarbon residues. The beads were thoroughly rinsed with deionized (DI) water to remove the ethanol. Washed beads were then wet classified on stainless steel sieves to obtain the desired size range (US 170 mesh sieve, $106\mu > d_b > 90\mu$). Finally, the beads were permitted to air dry, were homogenized, and stored in a dessicator prior to use. The experiments were set up with the same, narrow-size-range of glass beads used in previously reported work (Pirkle et al. 1997a). Both fluid reservoirs (water reservoir burette and PCE standpipe) were Schellbach burettes, which allowed fluid volume changes of 0.01 mL to be clearly detected. This corresponds to approximately 33,000 unit voids (pores) of displacement ocurring in the glass bead medium assuming orthorhombic packing of uniform spheres with a grain diameter midway between the sieve limits (Graton and Fraser 1935).

A known mass of the glass beads was loaded into each apparatus. A vacuum of 21 inches of mercury was applied. This vacuum was less than that which would cause water to boil at the prevailing range of laboratory temperatures (approximately $22^o \pm 2^o$ C). The medium of glass beads was saturated from the bottom under the vacuum conditions. Several pore volumes of DI/DA water were drained downward through the media as a final form of packing and stabilization of the media. Falling-head permeability measurements were then made on each medium (Pirkle et al. 1997a, 1997b).

For the current experiments, two solutions used in prior research were utilized except that they were equilibrated with deionized water prior to use. Table 1 contains the dye concentration data. These concentrations correspond with concentrations Tuck and Rulison (1998) used to characterize the surface chemical kinetics of the water-glass-PCE-Sudan IV-dye system (see Figure 2). Solutions C2 and C4 were chosen for the current research and were equilibrated with deionized water. Originally the second experiment was to be run with pure PCE. However it was desirable to have some dye in the solution for visualization purposes. The surface chemistry illustrated in Figure 2 and the entry pressures reported in Table 1 indicate that the C4 dye concentration solution behaves virtually identically as pure PCE. The two long-term experiments were designated "C2 170F" and "C4 170H".

The media were flushed with ten pore volumes of pre-equilibrated water following the permeability determinations for each experiment. This water had been pre-equilibrated with the SUDAN IV dye/PCE solution. The water reservoir burette was

adjusted so the water pressure was just sufficient to fully saturate the medium. Thus the top of the bead media was conveniently selected as the reference height for all fluid head measurements.

The levels in the water reservoir burette and the media were allowed to equilibrate for 15 minutes. A Schellbach burette, which had been cut off and fused to a glass bulb with an O-ring, was used as the standpipe for the PCE column. The standpipe assembly was inserted to 2mm above the media surface. Finally, a column of the PCE-Sudan IV dye solution was added to the Schellbach standpipe to a height of 9 cm above the top of the water saturated glass bead porous media. This height was well below the expected entry pressure for PCE having the 0.508 g/L dye Sudan IV dye concentration.

In prior work (Pirkle et al. 1997a). the mean entry pressure for PCE with this dye concentration was 15.45 cm of PCE with a standard deviation of 0.66 cm (n=4) (Table 1). This translates to an expected capillary entry pressure of 24,500 baryes (g/cm-sec^2). The 95% confidence interval for the entry pressure of PCE with this dye concentration in this medium was thus 13.35 to 17.55 cm of PCE (21,200 to 27,900 baryes). The run times for the previous experiments were less than eight (8) hours. Thus the surface chemical time-dependence became the primary variable governing penetration of the glass bead medium in the experiments described here since the target fluid pressure difference was less than 60% of the expected entry pressure and less than 70% of the lower 95% confidence limit for entry pressure.

Evaporation of the fluids was anticipated to be significant in these experiments since they were to be run for many weeks. Therefore separate evaporation studies were conducted in order to assess the extent of evaporation. Initial evaporation studies were conducted in ordinary Schellbach burettes. Later, the burettes were cut off and fused at the base to eliminate fluid losses through the stop-cocks.

RESULTS

Evaporation Studies

The results of the evaporation rate studies were divided into three essentially linear evaporation rate groups for both water and PCE. The groups correspond to the following evaporation burette conditions: early, unsealed burette; later, unsealed burette; and sealed burette. High rates of evaporative loss were interpreted to be the combined result of evaporation loss upward through the burette above the fluid surface and evaporative loss through the burette stopcock. The stopcocks were tightened in an effort to reduce that source of fluid loss. Stopcocks were later cut off the Schellback burettes, and the open ends were fused shut. Evaporation studies were initiated in the sealed burettes when the losses were still noted to be high. Thus evaporation was only possible upward above the top of the fluid surfaces in these sealed burettes, allowing an estimate to be made of the separate evaporative loss components. The loss rate through a stopcock was estimated assuming the early, unsealed rate represents a sum of stopcock loss plus evaporative loss out the top of the burette. The stopcock loss rates were estimated to be 0.0057 mL/day for water, 0.0561 mL/day for C2-PCE, and 0.0348 mL/day for C4-PCE.

Experiment C2 170F

The rates of fluid loss from the water reservoir burette in experiment C2 170F were noted to be high. Periodic additions of water were made to the burette to prevent the water pressure from decreasing to the point where the capillary entry pressure for the dyed-PCE solution would be reached. The water loss was essentially linear over the time intervals between additions, but the rates of fluid loss

decreased by an order of magnitude in approximately exponential fashion over the course of the experiment (Table 3). The cumulative fluid volume loss measured in the water reservoir burette over the nearly 70 days of the experiment was 9.31 mL. The cumulative fluid loss measured in the PCE standpipe was 0.34 mL.

The capillary pressure history for experiment C2 170F is shown in Figure 3. The capillary pressure followed a saw-tooth pattern with time since water was periodically added to keep the reservoir pressure difference relatively constant. It is important to note the spike in capillary pressure that occurred due to fluid loss from the water reservoir burette over the first four days of the experiment. The reservoir pressure difference, at its peak, exceeded the lower 95% confidence limit of the maximum stable pressure difference for this medium and this dye concentration.

Tiny fiber-like structures, presumably consisting of water sheathed with a PCE-film containing a significant surface excess of the dye, were noted emanating from the top of the water saturated porous medium on the second day of the experiment. PCE was visually observed to be entering the top of the medium on day four with "fingers" extending to depths of up to 1 mm. At the same time, the tiny fibrous structures appeared to be continuing to "grow" out of the medium. Examination of the fibrous structures with a magnifying glass revealed an appearance resembling a "string of pearls" with small bubbles of water connected via the fibers. The PCE fingers extended as much as 1.8 to 2 mm below the porous medium surface by day five. In addition, many of the tiny water balloons had begun to agglomerate into larger drops having an exterior texture resembling a tight cluster of grapes. PCE continued to accumulate in the top 2 mm of the porous medium leading to a noticeable darkening of that portion of the medium by day 30. There was never any visual indication that PCE had penetrated to a depth greater then the top 2 mm. While water was clearly escaping from the top of the medium, there was never any significant accumulation of water in the PCE standpipe.

Figures 4 and 5 are photographs showing early and ending conditions in experiment C2 170F. The photo in Figure 4 was taken approximately 1.7 hours after starting to add the dyed-PCE solution to the standpipe in experiment C2 170F. Figure 5 illustrates the penetration of the dye to a maximum depth of 2mm after 69 days.

The glass beads in the top 2 mm of the column were found to be stained red by Sudan IV dye upon disassembling the column. Excavation of the medium confirmed a) that penetration had occurred relatively uniformly over the top of the medium, and b) that penetration had not occurred to any detectable degree beyond approximately 2 mm below the top of the medium.

Experiment C4 170H - Control Experiment

As in experiment C2 170F, capillary pressure followed a saw-tooth pattern with time (Figure 6). The early rate of fluid loss measured in experiment C4 170H was high (0.217 mL/day), significantly exceeding the measured evaporation loss rate. This high rate lasted approximately 7 days after which it declined to a rate of 0.068 mL/day, approximating the loss rate in an unsealed burette (i.e., including a stopcock). This second rate declined further beginning on day 18 when it decreased to 0.016 mL/day. The spike in fluid reservoir pressure difference occurred when a "major" leak occurred in the apparatus. This spike (approximately 25,500 baryes), however, remained well below the expected entry pressure for the medium of 27.71 cm of PCE (44,050 baryes) (see Table 1) and the lower 95% confidence limit for the entry pressure (21.64 cm of PCE or 34,400 baryes).

There was no indication of PCE penetration into the glass bead medium throughout the course of experiment C4 170H (43 days). The contact between the water-saturated glass beads and the free dyed-PCE phase remained visually sharp throughout the course of the experiment. Figure 7 is a photo of the PCE-glass bead contact at the start of experiment C4 170H (3.5 hours after starting to add the dyed-PCE solution to the standpipe), and Figure 8 shows the contact at the end of the experiment (43 days). Excavation of the glass bead medium indicated there was no staining of the beads nor any penetration in the interior portion of the column away from the glass walls.

DISCUSSION

PCE Evaporation

The order of magnitude difference between C2 and C4 PCE solution evaporation rates is notable. It suggests that minor (<<1%), nonvolatile components dissolved in volatile solvents can greatly reduce solvent volatility. The dye concentration in C2 was about 300 ppm by weight; in C4 it was about 3 ppm. A major implication is that one of the important mechanisms for solvent depletion in the vadose zone, volatilization, may be significantly curtailed by comparable minor components in a field DNAPL. The concentration of nonvolatile components would increase as evaporative remediation progresses. This process could place a limit on the fraction of solvent contamination in the vadose zone that can be recovered by vapor extraction. At the least, it could be expected to significantly reduce the rate of solvent recovery. More detailed study is needed to confirm these results.

Time-Dependent Penetration of a Capillary Barrier

The results of experiment C2 170F are interesting, but do not as yet provide solid experimental support for the hypothesis that the time-dependent chemistry can govern the penetration of a porous medium capillary barrier. The spike in capillary pressure early in the experiment exceeds the lower 95% confidence limit for entry pressure for this medium and this dyed-PCE solution. It only exceeded that limit for less than a day, however, and likely for only a matter of hours. The correspondence of PCE penetration of the medium beginning on day 4 raises questions regarding whether the entry pressure for this medium, as defined by previous work (Pirkle et al. 1997a) was exceeded. On the other hand, the slow and limited penetration of the medium is consistent with the time-dependent pore-scale behavior modeled by Tuck (accepted). In addition, Pirkle et al. (1997a) found that if the entry pressure had been exceeded, the PCE penetrated the whole length of the medium and even drained into the open space below the screen any time an experiment was left overnight. The broad, relatively uniform penetration over the whole upper portion of the medium is also consistent with Tuck's modeling results for capillary pressures significantly below the entry pressure for pure PCE (i.e., zero dye content). An experimental apparatus specifically designed for maintaining constant capillary pressure during longer-term experiments is needed to provide a better test of Tuck's model of pore-scale behavior incorporating time-dependent surface chemistry.

There is additional anecdotal evidence supporting the role of the time-dependent surface chemistry in the behavior observed in the experiment, including the fiber-like structures emanating from the medium and the staining of the glass beads. Formation of the fiber structures was not observed until day two; at least 10 hours passed before they were observed. The best explanation for these structures is that partitioning of the dye into the water-PCE interface lowers interfacial tension sufficiently to allow tubes of water to form which rise due to the unstable density configuration. Adsorption of the dye onto the

glass bead surfaces was indicated by the fact of their having become stained. Dye adsorption explains the change in PCE-glass-water contact angles observed by Tuck and Rulison (1998) and illustrated in Figure 2.

Incorporating the role of time-dependent surface chemistry into our understanding of multiphase flow in porous media is important, presuming it is a real phenomenon and behaves comparably to the pore-scale model developed by Tuck. In the case of NAPL contamination, any separate phase penetration of finer-grained layers will be significantly harder to remediate. Relatively little penetration, such as observed in experiment C2 170F, can result in a significant amount of NAPL penetration into finer layers. DNAPL contamination at the Savannah River Site A/M-Area has been found to be distributed in multiple, relatively thin zones in the M-Area aquifer (Tuck et al. 1998a). The magnitude of this issue can be estimated by making a few simple assumptions. A total bulk volume of 40,000 L of DNAPL-containing, finer-grained layers results if we assume ten such zones each of 1000 m^2 in area and bounded above and below by finer-grained layers each of which has been penetrated to a depth of 2 mm by DNAPL. The total pore space available to contain fluids is 1,520 L assuming an average porosity of 0.38 (Eddy-Dilek, et al. 1994). If we further assume a range of DNAPL saturation between 0.10 and 0.50, the total volume of DNAPL caught in those bounding zones due to the time-dependent penetration would be 150 to 760 L. This volume of DNAPL would be expected to be more difficult to remediate.

Another important issue arises from how we model and understand DNAPL flow and distribution following its initial release into the subsurface. The result of time-dependent surface chemistry during flow of a NAPL is to increase the effective interfacial tension governing that flow (Tuck et al. 1998b). The result is that the faster a NAPL-front is advancing, the higher will be the average interfacial tension governing the capillary forces acting to resist the NAPL movement. This arises from the lower average time that NAPL-water interfaces spend in pore-throats. The influence of average interface age on the effective interfacial tension can be seen in Figure 2b. The net result in terms of modeling multiphase flow is that there will be an additional iteration loop required since interfacial tension plays an important role in the capillary pressure-saturation relationship, which in turn will effect the average rate of advance of NAPL-water interfaces through the medium.

Further research is needed to confirm or negate the validity of incorporating time-dependent surface chemistry in pore-scale models of multiphase flow as developed by Tuck (accepted) given its potential importance for better understanding of NAPL behavior in porous media. Additional research should include experimental testing under more closely maintained capillary pressure conditions and the development of a more comprehensive pore-scale model. The means for scaling-up the time-dependent pore-scale behavior into continuum scale models is also an important area requiring research and development.

ACKNOWLEGEMENTS

We are grateful to the Department of Energy at the Savannah River Site for providing funding for the experimental work reported here. The research was performed at USC Aiken under South Carolina Universities Research and Education Foundation contract AA00900T. The authors also wish to thank Westinghouse Savannah River Company and its management and colleagues for support and encouragement. In particular, we wish to thank Dr. Brian B. Looney, Dr. Richard Strom, Joette Sonnenberg, and Deb Moore-Shedrow. The authors also wish to express their appreciation to the USC Aiken administration, especially Dr. Harold Ornes, former Chair, and Dr. Allen Dennis, current

Chair, of USC Aiken's Department of Biology and Geology for their support and encouragement of the project.

REFERENCES

Eddy-Dilek, C.A., T. R. Jarosch, M. A. Keenan, W. H. Parker, S. P. Poppy, J. S. Simmons. 1994. Characterization of the Geology and Contaminant Distribution at the Six Phase Heating Demonstration Site at the Savannah River Site (U). Westinghouse Savannah River Company, Aiken, SC, WSRC-TR-93-678. .

Graton, L. C. and H. J. Fraser. 1935. "Systematic Packing of Spheres with Particular Relation to Porosity and Permeability," J. Geology, v.43, p.785-909.

Hobson, G. D. 1954. Some Fundamentals of Petroleum Geology, Oxford University Press, NY, NY.

Hobson, G. D. and E. N. Tiratsoo. 1975. Introduction to Petroleum Geology, Scientific Press, Ltd., Beaconsfield, England.

Pirkle W. A., G. M. Iversen, and D. M. Tuck. 1996. DNAPL Entry Pressure Into Water Saturated Porous Media, Final Report Submitted in Completion of SCUREF Task 185. University of South Carolina Aiken.

Pirkle W. A., G. M. Iversen, and D. M. Tuck. 1997a. The Effect of an Organic Dye on DNAPL Entry Pressures into Water Saturated Porous Media, Final Report Submitted in Completion of SCUREF Task 185, Phase II, Vols. I&II. University of South Carolina Aiken.

Pirkle W. A., G. M. Iversen, and D. M. Tuck. 1997b. DNAPL penetration of capillary barriers due to time-dependent wetting relationships. University of South Carolina-Aiken. Final Report Submitted in Completion of SCUREF Task 232. University of South Carolina Aiken.

Tuck, D. M., and C. Rulison. 1998. Interfacial effects of a hydrophobic dye in the tetrachloroethylene-water-glass system (U). Westinghouse Savannah River Company, WSRC-TR-97-0038. Aiken, SC, 23 p.

Tuck, D. M., G. G. Exner, B. B. Looney, B. Riha, J. Rossabi. 1998a. Phase I Field Test Results of an Innovative DNAPL Remediation Technology: The Hydrophobic Lance(U). Savannah River Technology Center, WSRC-TR-98-00308. Aiken, SC, 24 pp .

Tuck, D. M., G. M. Iversen, W. A. Pirkle, C. Rulison. 1998b. Time-dependent interfacial property effects on DNAPL flow and distribution. In: Wickramanayake, G.B., Hinchee, R.E. (Eds.), Nonaqueous-Phase Liquids: Remediation of Chlorinated and Recalcitrant Compounds. Battelle Press, Columbus, OH, 73-78.

Tuck, D. M. 1999. Time for a new dimension in Pc-S space. in: Seventh Annual Clemson University Hydrogeological Symposium, April 9, 1999, Clemson, SC, Clemson University, p. 13.

Tuck, D. M. accepted. Primary drainage of NAPL governed by time-dependent interfacial properties. Chemical Geology.

Table 1. Sudan IV dye concentrations in PCE used in this and previous research and resulting entry pressures for dyed PCE in glass-bead media of the same type used here (Tuck and Rulison year, Pirkle, et al. 1997a).

	Entry Pressures from Prior Research in glass-bead media				
Solution Pressure Label	Sudan IV dye Conc. (g/L)	Number of Experiments	Mean Entry Pressure (cm of PCE)	Standard Deviation (cm of PCE)	Mean Entry (baryes, g/cm-sec^2)
C0	0.00000	12	27.14	2.48	43,150
C4	0.00508	7	27.71	2.48	44,050
C2	0.508	4	15.45	0.66	24,560

Table 2. Rates of evaporative loss for the different fluids. The difference between sealed burette and unsealed burette loss rates provides an estimate of evaporative loss through a stopcock.

	Water	C2 PCE	C4 PCE	
Early, Unsealed Burette				
rate (mL/day)		0.0121	0.0598	
r2	0.9215	0.9925		
n	17	36		
Later, Unsealed Burette				
rate (mL/day)		0.0086	0.0554	0.0676
r2	0.9919	0.9929	0.9818	
n	29	14	30	
Sealed Burette				
rate (mL/day)		0.0064	0.0037	0.0328
r2	0.9933	0.9846	0.9939	
n	40	33	32	

Table 3. Fluid loss rates from the water reservoir burette in experiment C2 170F

Time Interval Midpiont (days)		Loss Rate (mL/day)	R^2	Number of Data Points, n	Average Temperature (C)
1.97	0.6114	0.9931	25	23.16	
4.41	0.8739	0.9951	5	22.93	
5.91	0.3753	0.9985	7	23.44	
8.43	0.2748	0.9854	7	23.17	
11.40	0.1947	0.9994	6	22.72	
14.58	0.1777	0.9881	5	22.20	
21.66	0.1112	0.9933	14	22.84	
35.58	0.0693	0.9966	18	22.73	

51.23	0.0516	0.9946	17	22.46
64.27	0.0460	0.9842	11	22.60

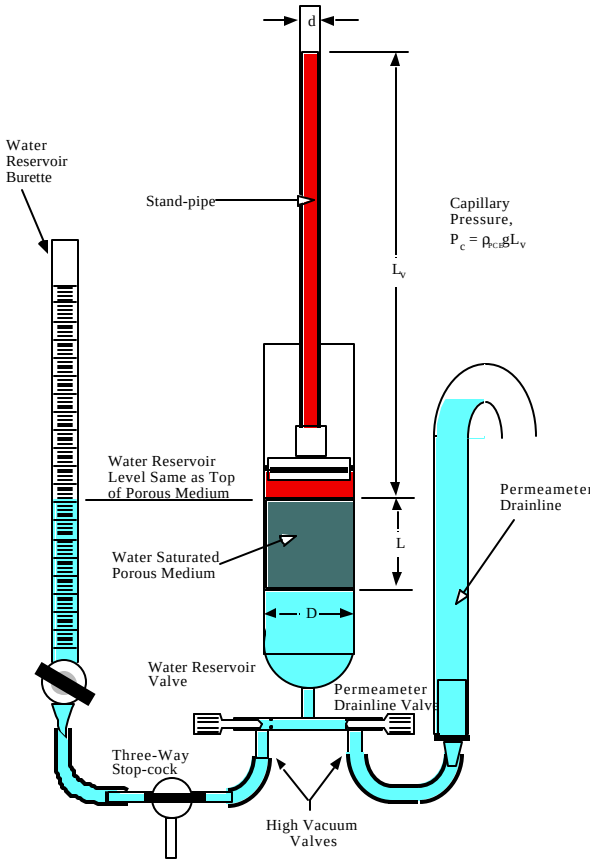

Figure 1. Experimental set-up used for PCE entry pressure in the water-glass-PCE-Sudan IV dye system.

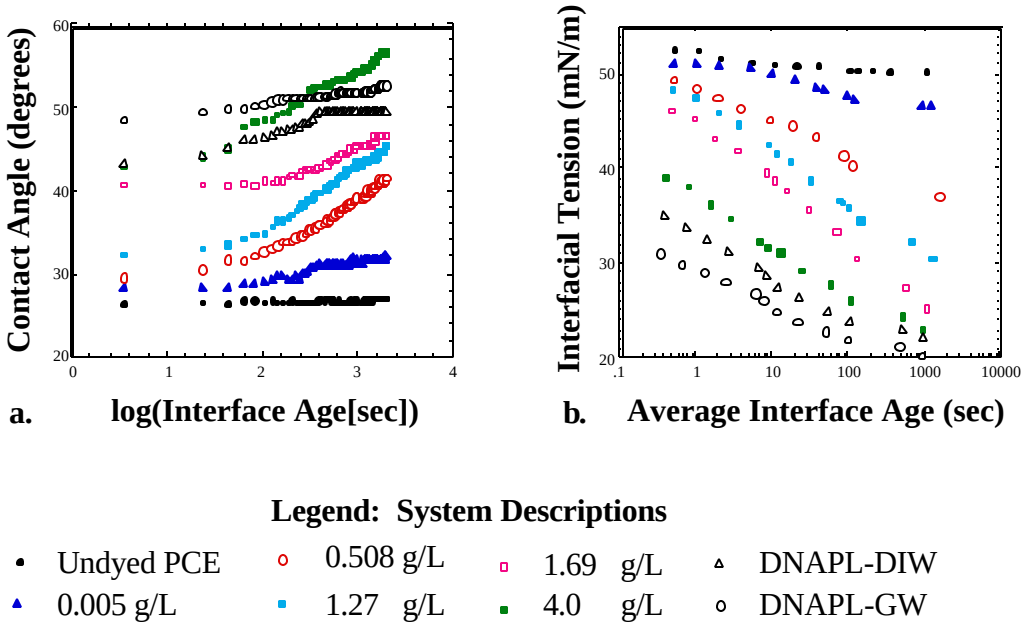

Figure 2. Time-dependence of interfacial tension and contact angle in the water-glass-PCE-Sudan IV dye system.

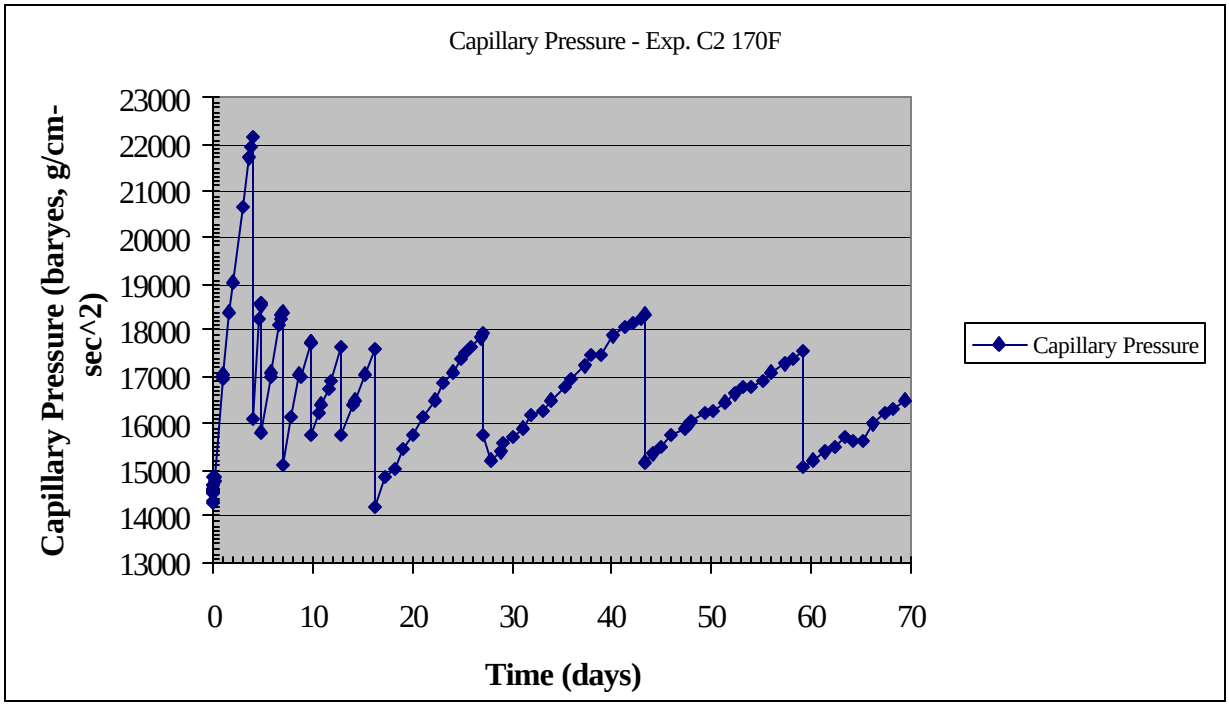

Figure 3. Capillary pressure history for experiment C2-170F. Sudan IV dye concentration in PCE was 0.5 g/L.

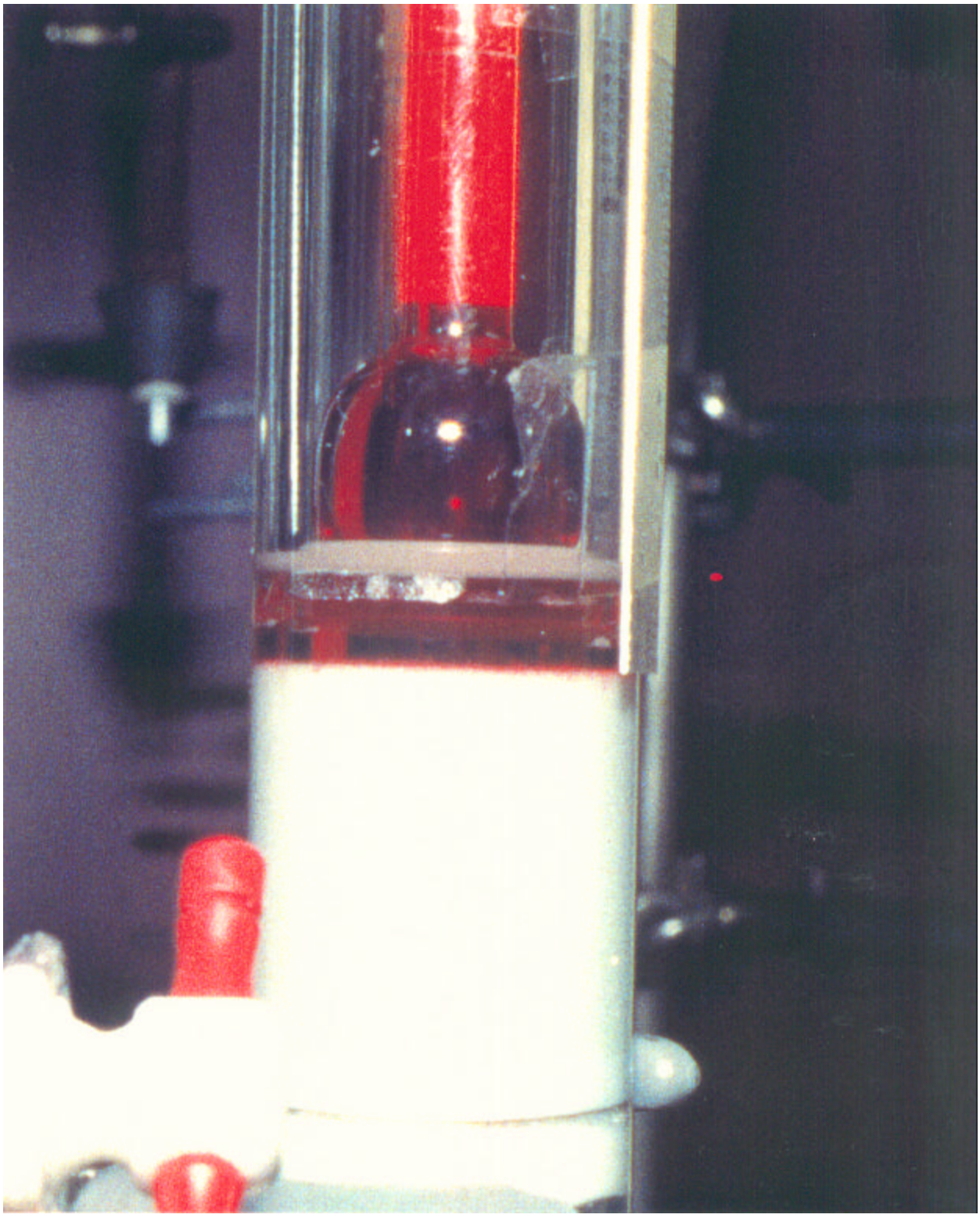

Figure 4. Beginning of experiment C2 170F. Photo was taken approximately 1.7 hours (0.069 days) after the first addition of PCE to the PCE-Standpipe.

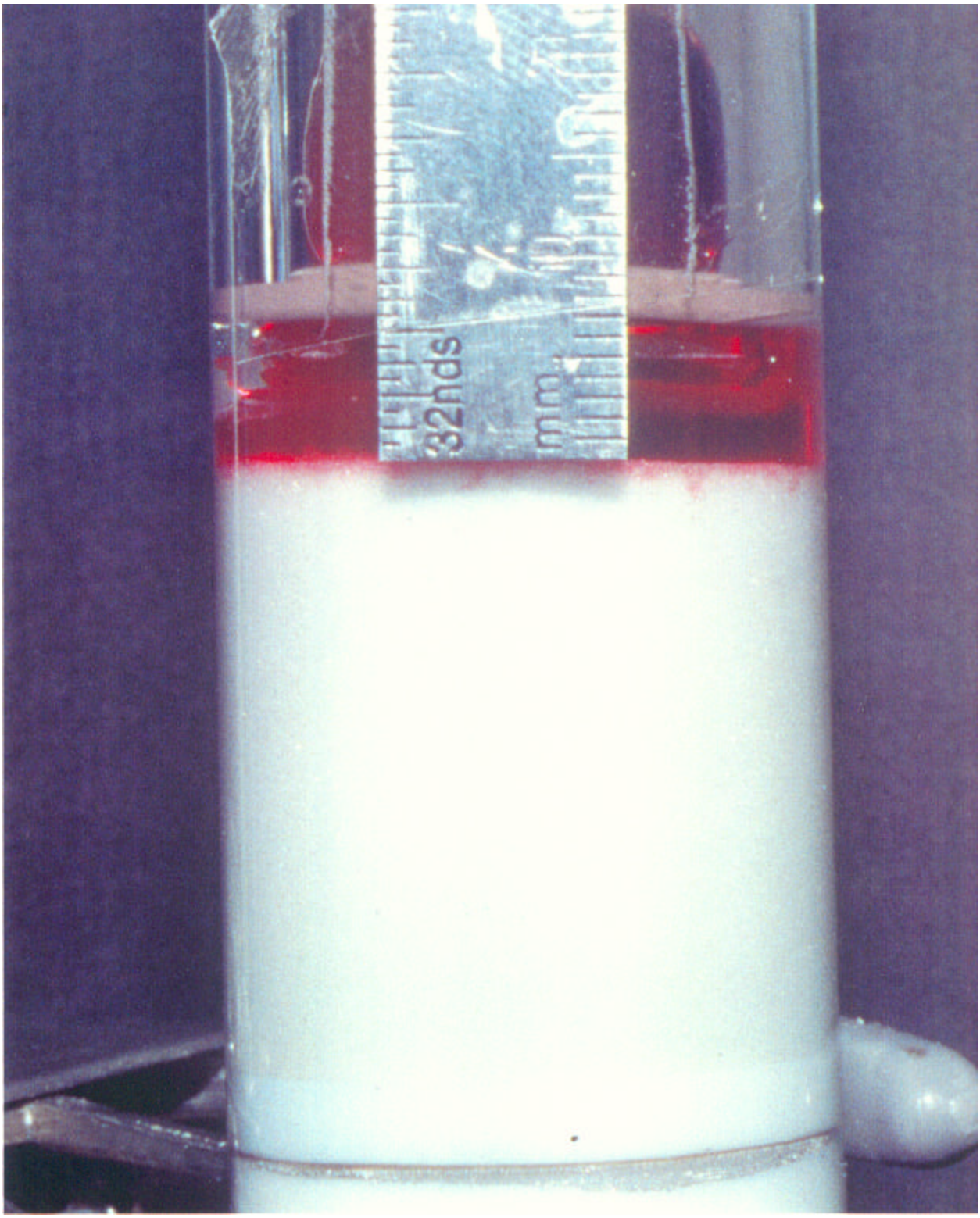

Figure 5. End of experiment C2 170F. Photo was taken on the 69th day from the start of the experiment.

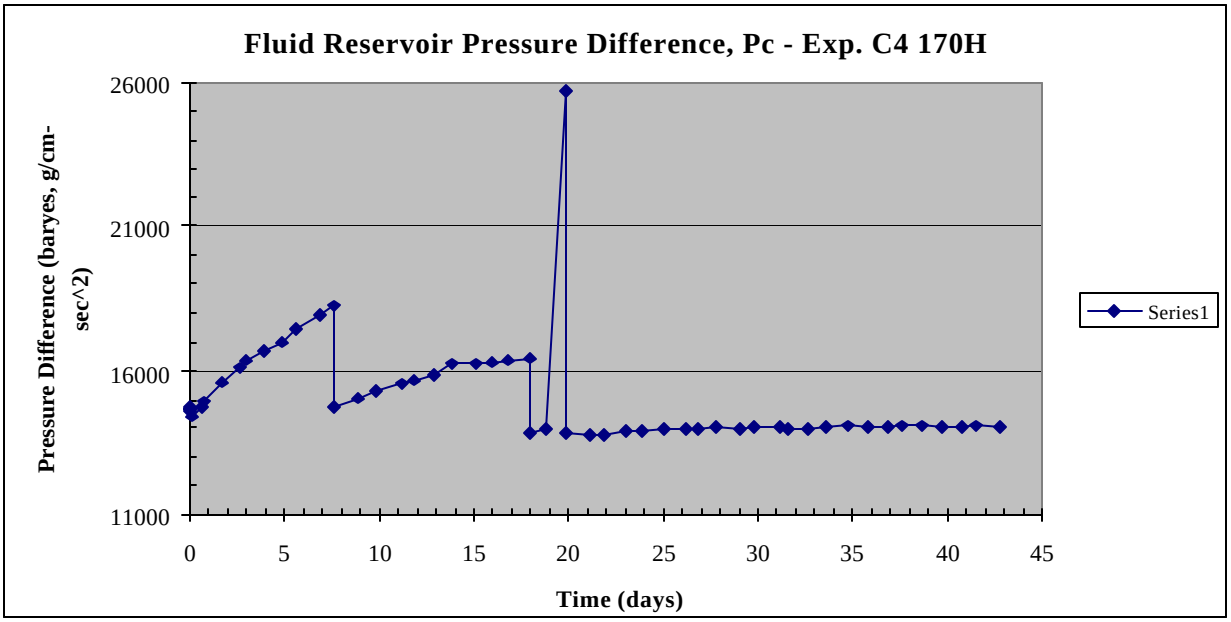

Figure 6. Capillary pressure history for experiment C4 170H. Sudan IV dye concentration was 0.005 g/L, too low to significantly change the entry pressure for PCE.

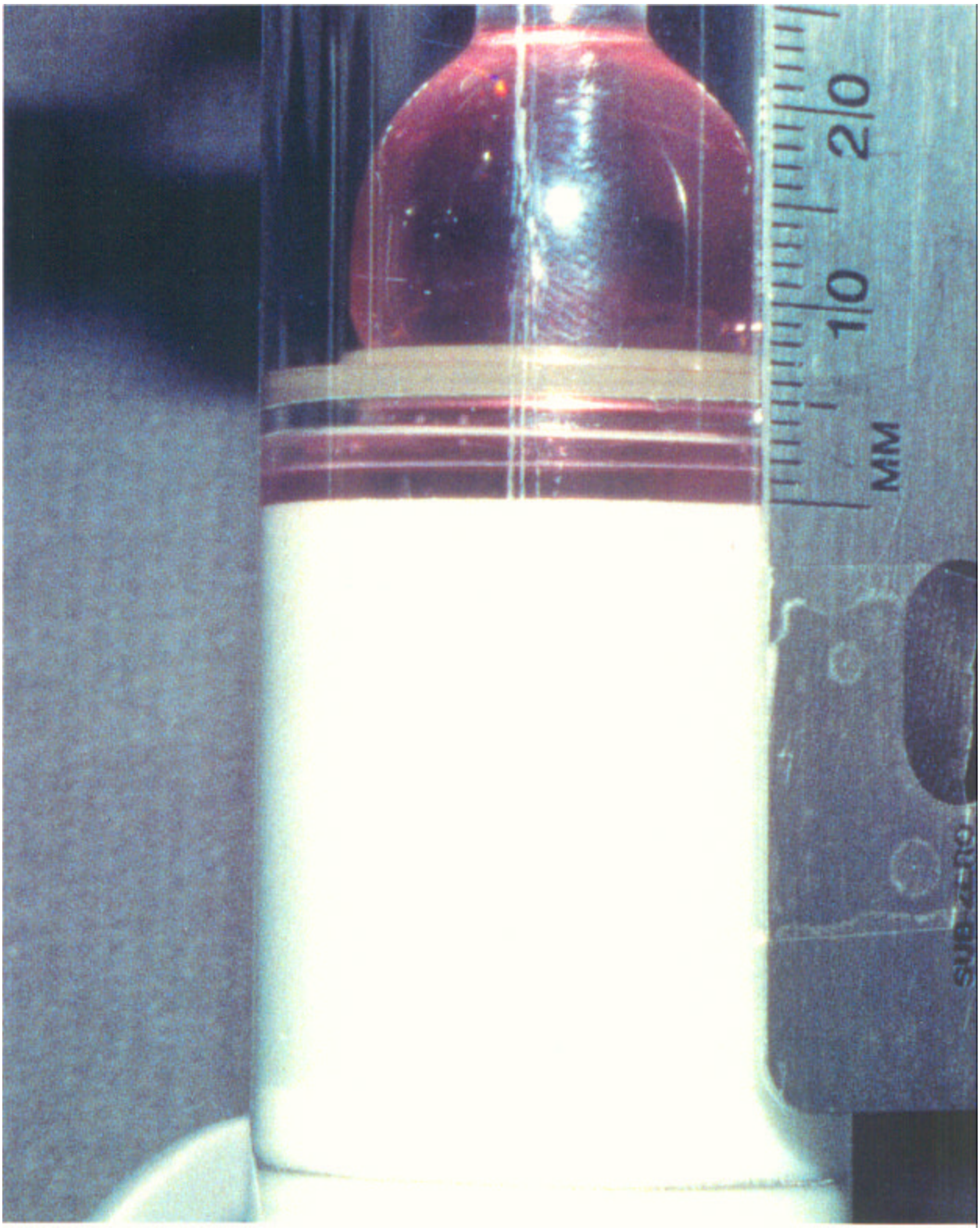

Figure 7. Beginning of experiment C4 170H. Photo was taken approximately 3.5 hours (0.15 days) after the first addition of PCE to the PCE-Standpipe.

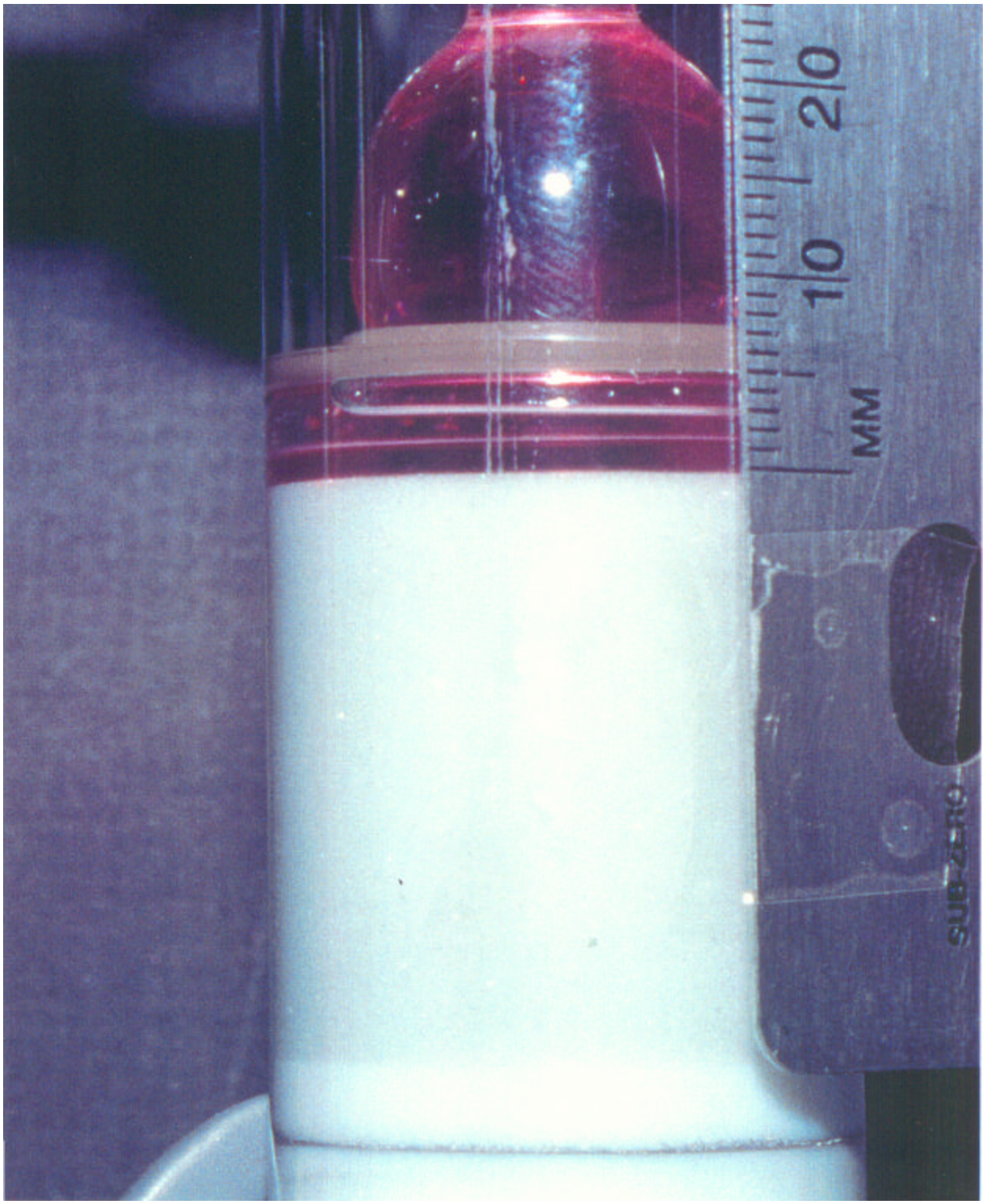

Figure 8. End of experiment C4 170H. Photo was taken on the 43rd day from the start of the experiment.

Subsurface Correlation Of Cenozoic Strata In The Updip Coastal Plain, Savannah River Site (SRS), South Carolina

R. K. Aadland, Westinghouse Savannah River Co. Aiken, S.C. 29808
P. A. Thayer, University of North Carolina at Wilmington, Wilmington N.C. 28403-3297

ABSTRACT

Difficulties with correlation and the paleogeographic reconstruction of fluvial and marginal-marine terrigenous strata near the Fall Line result from: 1) lithologic similarity throughout the section, typically coarse, poorly sorted unconsolidated sand and mud; 2) few marker beds; 3) paucity of age-diagnostic fossils due to original depositional environment and post-depositional leaching; 4) facies changes; 5) hard to recognize unconformities; and 6) structural complexity. Down-hole geophysical logs and core descriptions from 245 soil borings and monitoring wells were used to delineate the stratigraphy and structure of the Cenozoic section in the 15 square mile A/M Area at SRS. The density of subsurface data made possible the detailed correlation of stratigraphic units and the understanding of facies relationships. In addition, the importance of faulting, which has largely gone unrecognized in previous studies in the Atlantic Coastal Plain, has been demonstrated. The juxtaposition of differing lithologies in coastal plain strata has commonly been interpreted to result from facies change. This study however, indicates that fault displacement of stratigraphic units often accounts for the perceived "facies changes." In order to develop correct depositional models incorporating the relative contribution of eustacy, sediment supply and tectonics, the density of subsurface data must be sufficient to distinguish stratigraphic variations resulting from sedimentological factors versus post-depositional structural events.

[1]Information developed under Contract DE-AC09-89SR19015 with the U.S. Dept. of Energy

INTRODUCTION

The Savannah River Site (SRS) is a 300-square-mile facility located near the Fall Line in the Upper Atlantic Coastal Plain of South Carolina (Figure 1). The A/M Area, which covers approximately 15 square miles, is situated in the northwestern part of the Site (Figure 1). The sedimentary section underlying A/M Area is 700 to 800 feet thick and consists of coarse to fine, often gravely sands and interbedded clays of Late Cretaceous to Holocene age.

The purpose of this study is to describe and evaluate the stratigraphy and structure of unconsolidated coastal plain strata in the A/M Area. The study will aid in delineating hydraulic characteristics of the sediments for modeling groundwater movement and contaminant transport.

METHODS

Detailed analysis of down-hole geophysical data and core from more than 245 monitoring wells and soil borings were utilized in the study. Down-hole geophysical logs, including gamma ray, gamma ray density, neutron density, resistivity surveys, and detailed descriptions of drill core were used to delineate lithologic types and facies relationships.

Eight cross-sections were prepared and used to correlate lithologic units. Structure contour and isopachous maps were constructed to show the overall geometry, thickness, and continuity of the stratigraphic units in the study area.

STRATIGRAPHY

The SRS is underlain by Paleozoic igneous and metamorphic rocks, Mesozoic terrigenous clastics of the Dunbarton rift basin (Marine and Siple, 1974), and Late Cretaceous and Tertiary sediments of the Atlantic Coastal Plain.

Paleozoic basement and Triassic/Jurassic (?) sedimentary rocks of the Dunbarton Basin have been beveled by erosion and are unconformably overlain by unconsolidated to poorly consolidated Late Cretaceous and Tertiary coastal plain sediments (Cooke, 1936; Siple, 1967; Colquhoun and Johnson, 1968;). Coastal plain strata form a mostly clastic wedge that thickens and dips to the southeast (Colquhoun and Johnson, 1968). The sedimentary wedge is about 700 feet thick in the A/M Area, and accumulated in environments ranging from fluvial to shallow marine shelf. Fluctuating conditions of deposition account for the complex variations in sediment lithology throughout the study area.

Paleontological data is sparse in coastal plain strata of A/M Area. Further south, in the southern and central parts of SRS, coastal plain sediments were deposited in lower delta plain and shallow marine environments. It is here that age-diagnostic fossils are more plentiful; hence, age and stratigraphic relationships can be resolved with greater certainty. The stratigraphy of coastal plain sediments in A/M Area was determined by correlation to type wells located less than 10 miles to the southeast, which were established by Fallaw and Price (1995).

Cretaceous Strata

In A/M Area Upper Cretaceous strata overlie Paleozoic basement. The Upper Cretaceous sequence includes the basal Cape Fear Formation and overlying Lumbee Group. The Lumbee Group includes from the base upward (Faye and Prowell, 1982), Middendorf, Black Creek, and the Steel Creek Formations (Figure 2). The Cretaceous sequence is about 400 feet thick in A/M Area, and consists of quartz sand, pebbly sand and sandy clay, which accumulated in lower to upper delta plain environments.

Tertiary Strata

Tertiary sediments are approximately 300 feet thick in A/M Area and range from Paleocene to Miocene/Oligocene (?) in age (Figure 2). They are interpreted to have been deposited in fluvial, marginal marine, and shallow marine shelf environments. Tertiary strata consist of moderately to very poorly sorted quartz sand and pebbly quartz sand with varying amounts of mud matrix. Interbedded mud units consist mainly of quartz silt and kaolinitic clay and are commonly sandy.

Four regionally significant unconformities are recognized within the Tertiary section of A/M Area. From the base upward, they include the Cretaceous-Tertiary unconformity, Lang Syne/Sawdust Landing unconformity, Santee unconformity, and "Upland" unconformity (Figures 2, 3 and 4). Four sequence stratigraphic units, here labeled Sequence I, II, III and IV, which are bounded by the unconformities, are delineated (Figure 2). Work is currently underway to place these sequences into a global sequence stratigraphic framework.

STRUCTURE

Post Sequence I Faulting

Figure 4 is a cross-section showing faulting in A/M Area and Figures 5, 6 and 7 illustrate fault distribution in plan view. The oldest post-Sequence I oblique-slip reverse faults are labeled alphabetically, and the youngest post-Sequence II and III/IV series of normal faults are labeled numerically.

Several episodes of oblique-slip reverse faulting or renewed faulting occurred in A/M Area following the Triassic/Jurassic rifting event. The first episode began at the close of Cape Fear time and continued intermittently through Paleocene time (Aadland, 1997). The final episode of oblique-slip reverse offset involved the upper Paleocene Lang Syne Formation, and was followed by erosion and truncation of the unit at the Lang Syne/Sawdust Landing unconformity. The unconformity is the defining event in A/M Area, as it is regionally, separating Paleocene Sequence I strata and associated tectonic events from Sequence II and younger strata/tectonic events.

The pre-Sequence II oblique-slip reverse faults (Figures 4, 5 and 6) form a series of closely-spaced (< 2000 ft), high-angle reverse faults, any one of which can be traced for approximately 1 to 4 miles. The faults overlap resulting in a fault zone where several sub-parallel faults are noted. The faults form a series of horsts and grabens, some of which truncate at fault intersections. The strike of individual fault segments varies from N 17° E to N 42° E, averaging about N 30° E. Apparent vertical offset on the faults varies from 15 to 60 feet (Figures 3, 4, 5 and 6), with throws of 30 to 40 feet most common in the Cretaceous-Paleocene section.

Post Sequence II and III/IV Faulting

Faulting that offsets post-Sequence II and III/IV strata form an en echelon series of normal faults that strike from N 21° W to N 6° E, averaging N 11° W (Figures 6 and 7). The en echelon normal faults strike at an acute angle (about 41°) to the average orientation of the oblique-slip reverse faulting that offsets the underlying late Cretaceous-Paleocene sediments of Sequence I (Figure 6). The apparent throw on the normal faults usually varies from 10 to 20 feet (Figure 4).

DISCUSSION

Active tension in a direction perpendicular to the strike of faults in the post-Sequence II and III/IV section would account for the observed normal faulting. However, regional tension acting in this direction cannot account for the en echelon fault pattern. Left-lateral shear along one of the pre-existing post-Sequence I oblique-slip reverse faults beneath the passive Sequence II and III/IV strata (Figure 8), where the northwestern block moves to the southwest relative to a southeastern block, could account for the en echelon pattern of normal faults observed in the Sequence II and III/IV section. Alternately, a couple (Figure 9), caused by a northerly block moving towards the southwest relative to a southerly block moving towards the northeast, with a block wedged between the two moving blocks, could produce the type of en echelon normal faults observed in the overlying Sequence II and III/IV passive sediments.

SUMMARY AND CONCLUSIONS

1. The density of subsurface data has made possible the detailed correlation of stratigraphic units and understanding of facies relationships in the A/M Area.

2. The importance of faulting, which has gone largely unrecognized in Atlantic Coastal Plain studies, is demonstrated.

3. The juxtaposition of differing lithologies in coastal plain strata has commonly been interpreted to be the result of facies change. This study however, indicates that fault displacement of stratigraphic units often accounts for the perceived ”facies changes.”

4. The relative contribution of tectonics, versus eustacy and sediment supply, to the depositional model developed in the updip coastal plain setting of A/M Area is critical to remediation efforts of contaminants in subsurface aquifers. The density of subsurface data must be sufficient to distinguish stratigraphic variations resulting from sedimentological factors versus post-depositional structural events in determining the hydraulic characteristics of sediments for modeling groundwater movement and contaminant transport.

REFERENCES

Aadland, R. K., 1997, Tertiary geology of A/M Area, Savannah River Site, S.C. (U): U.S. Department of Energy, WSRC-RP-0505, 94 p. + 17 plates.

Billings, M.P., 1972. Structural Geology. 3d ed. Englewood Cliffs, New Jersey: Prentice-Hall, Inc.

Cooke, C. W., 1936, Geology of the Coastal Plain of South Carolina: U.S. Geological Survey Bulletin 867, 196 p.

Colquhoun, D. J., and Johnson, H. S., Jr., 1968, Tertiary sea-level fluctuation in South Carolina:

Palaeogeography, Palaeoclimatology, Palaeoecology, v. 5, p. 105-126.

Fallaw, W. C., and Price, V., 1995, Stratigraphy of the Savannah River Site and vicinity: Southeastern Geology, v. 35, p. 21-58.

Faye, R. E., and Prowell, D. C., 1982, Effects of Late Cretaceous and Cenozoic faulting on the geology and hydrology of the coastal plain near the Savannah River, Georgia, and South Carolina: U.S. Geological Survey Open-File Report 82-156, 73 p.

Marine, I. W., and Siple, G. E., 1974, Buried Triassic basin in the Central Savannah River Area, South Carolina and Georgia: Geological Society of America Bulletin, v. 85, p. 311-320.

Pascal, R. and R.W. Krantz, 1991. "Experiments on Fault Reactivation in Strike-Slip Mode," Tectonophysics. 188:p. 117-131.

Siple, G. E., 1967, Geology and groundwater of the Savannah River Plant and vicinity, South Carolina: U.S. Geological Survey Water-Supply Paper 1841, 113 p.

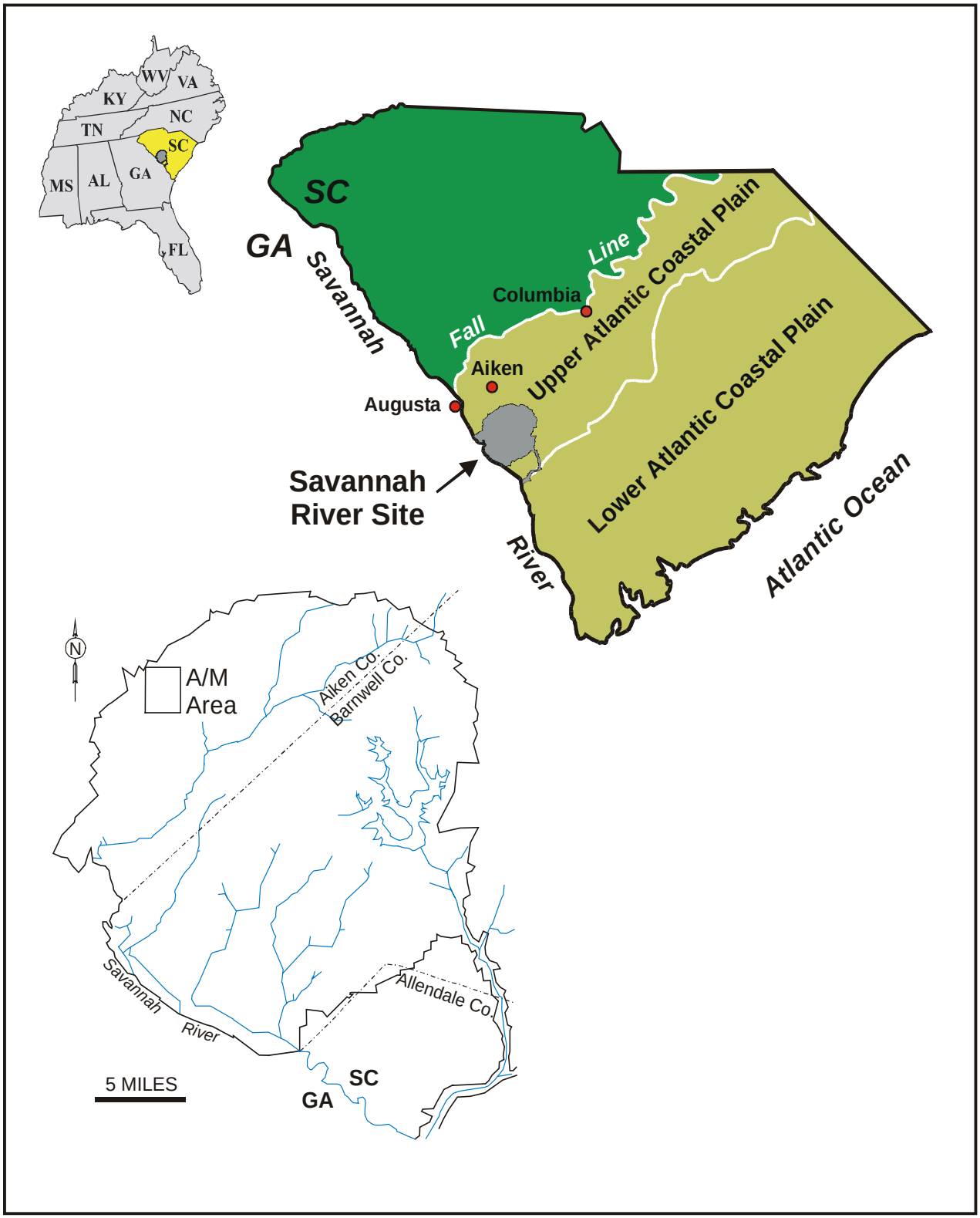

Figure 1. Location of the Savannah River Site and the A/M Area.

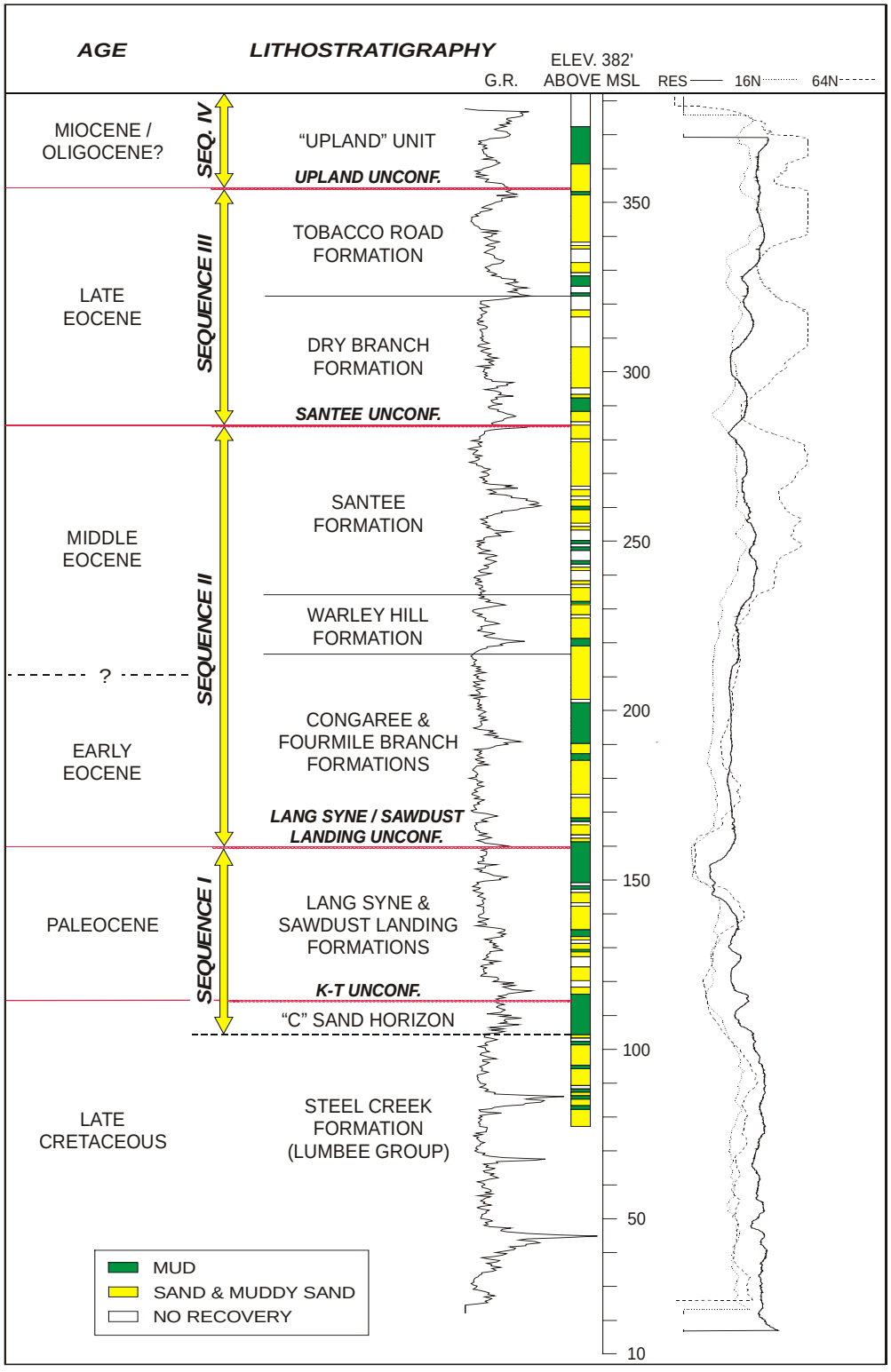

Figure 2. Stratigraphic units in A/M area at Well MSB-69. The location of MSB-69 is shown in Figure 5.

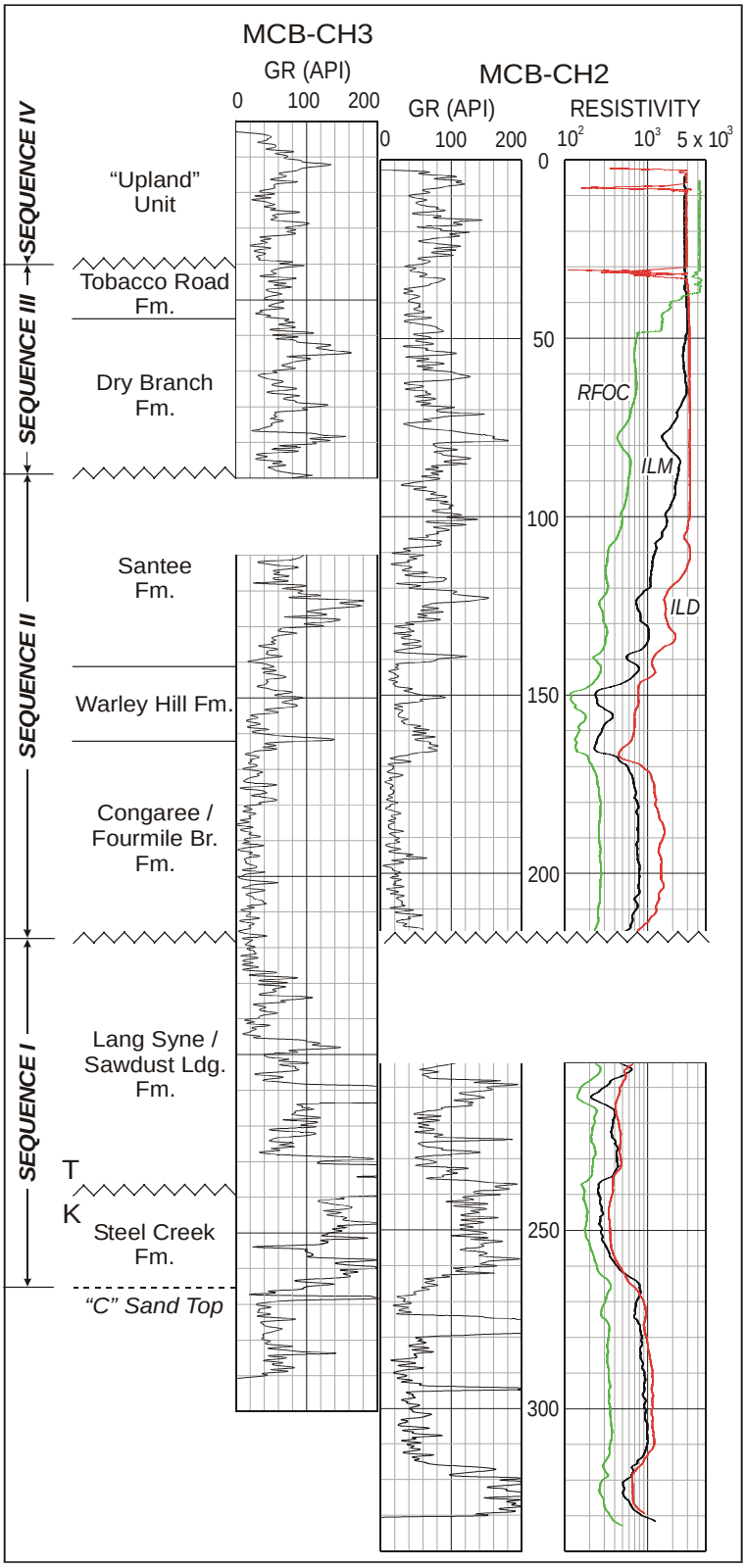

Figure 3. Stratigraphic Units in Wells MCB-CH2 and MCB-CH3. Missing Section in Both Wells is due to Greater Erosional Truncation on the Upthrown Fault Blocks.

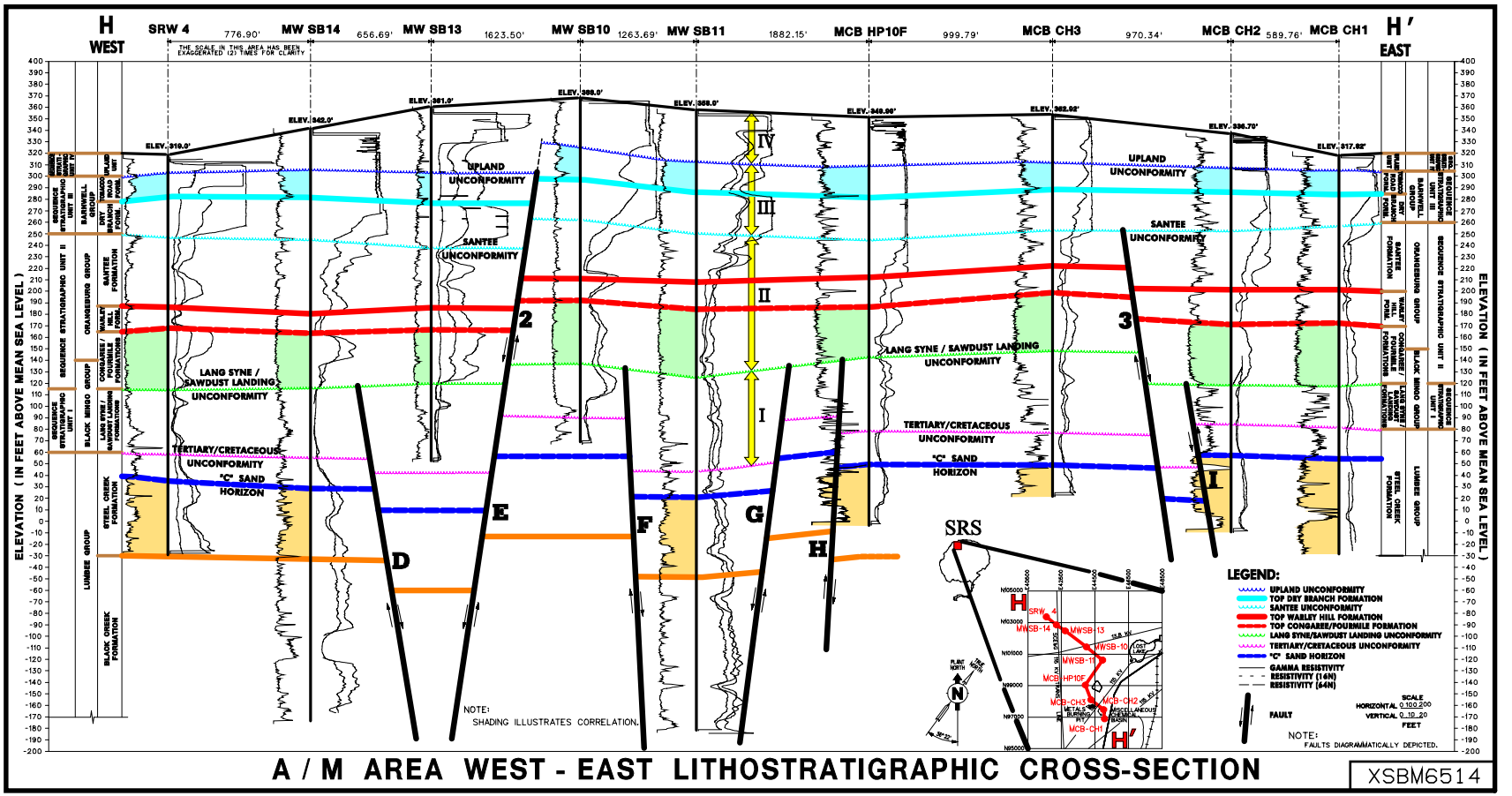

Figure 4. West-east lithostratographic cross-section A/M Area, Savannah River Site.

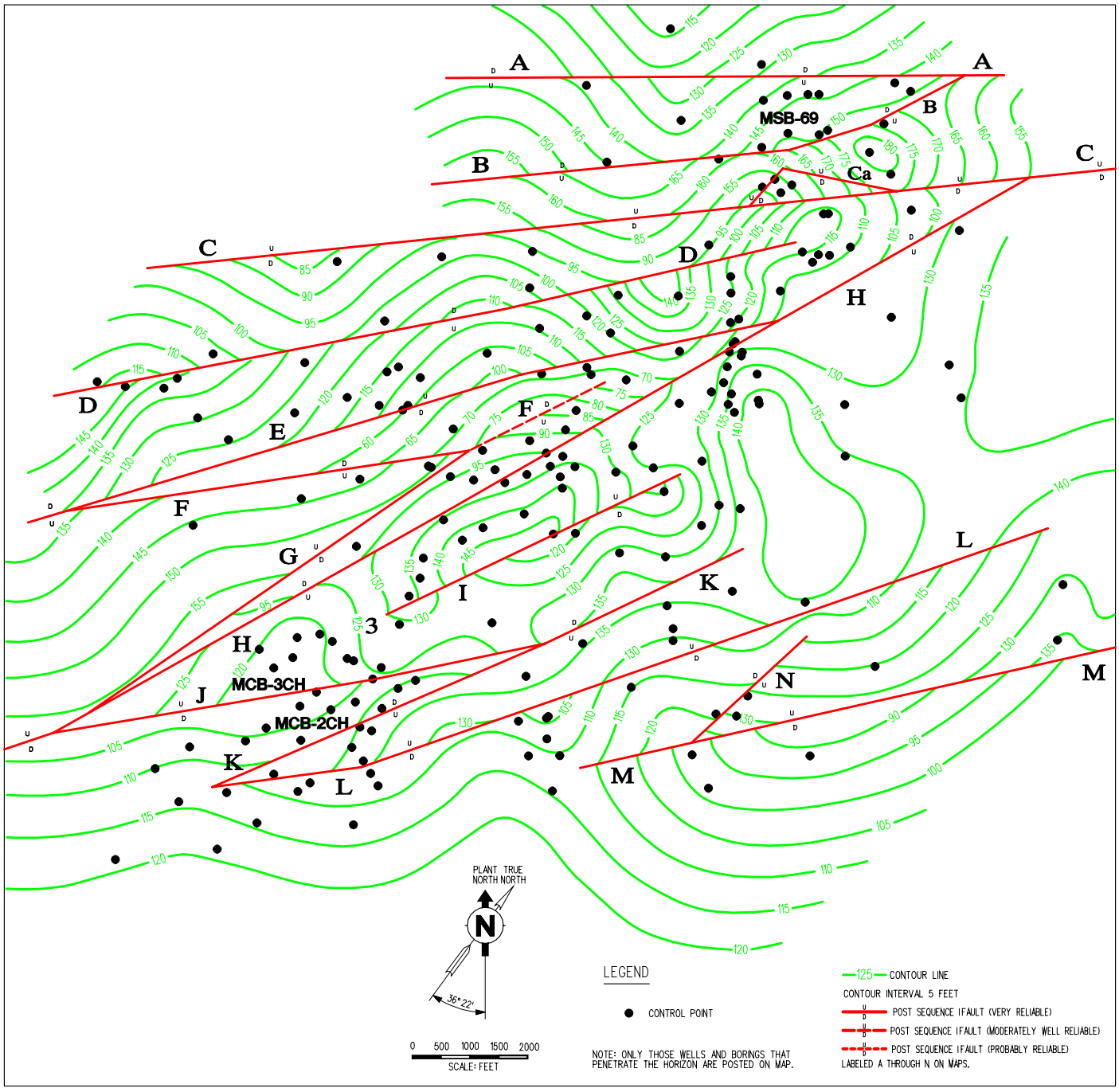

Figure 5. Middle Eocene time "C" Sand structure map. Note location of wells MSB-69, MCB-CH2 and MCB-CH3 (see Figs. 2 and 3). "C" Sand mapped from the Lang Syne/Sawdust Landing unconformity surface datum. The unconformity surface was arbitrarily assigned an elevation of 200 feet from which the "C" Sand surface was mapped. The offset noted on faults A through L predate Congaree/Fourmile deposition.

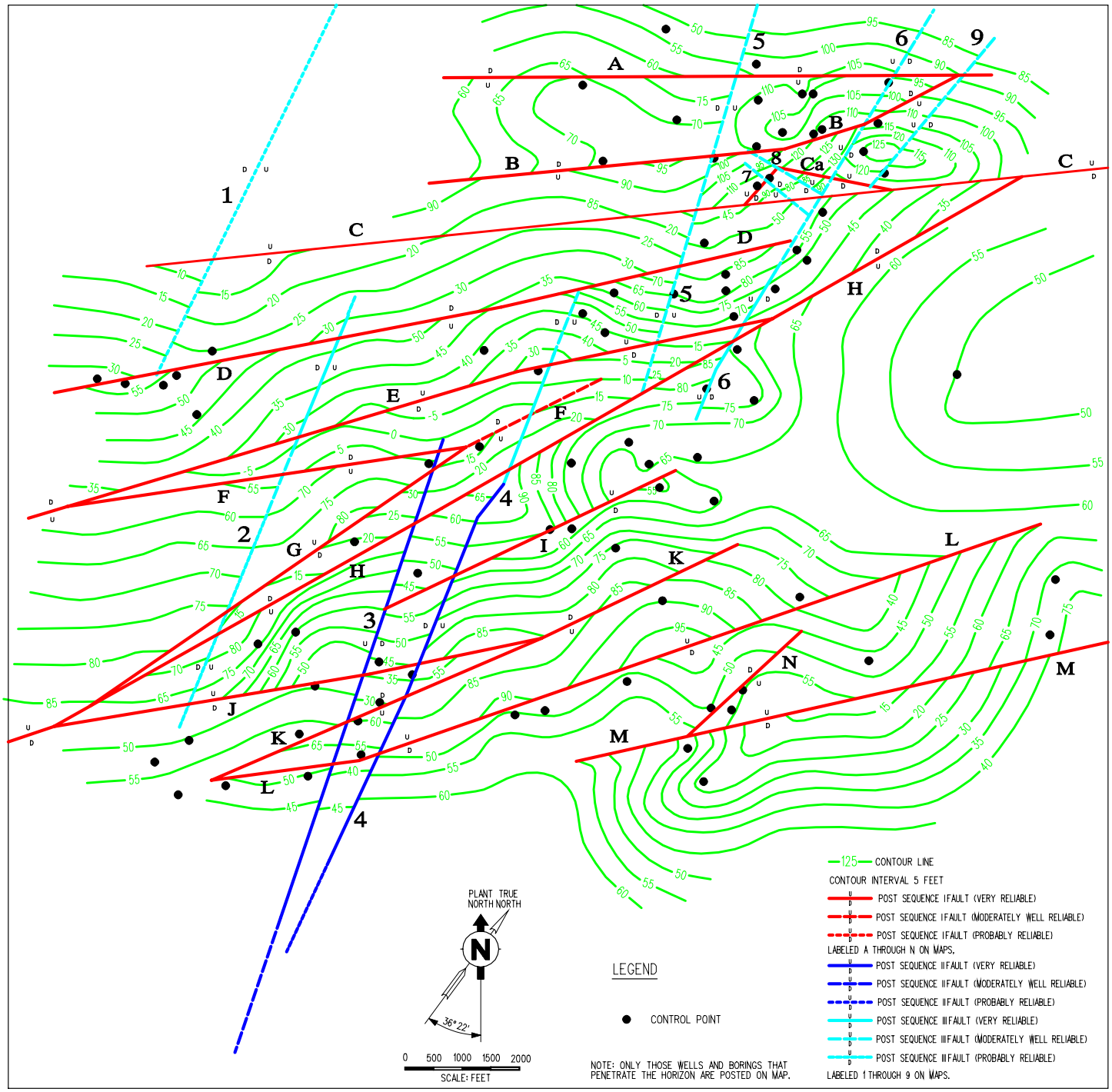

Figure 6. "C" Sand horizon structure map. Stratigraphic position of "C" Sand shown in Figures 2 and 3. "C" Sand horizon mapped from mean sea level. Contours in feet above mean sea level.

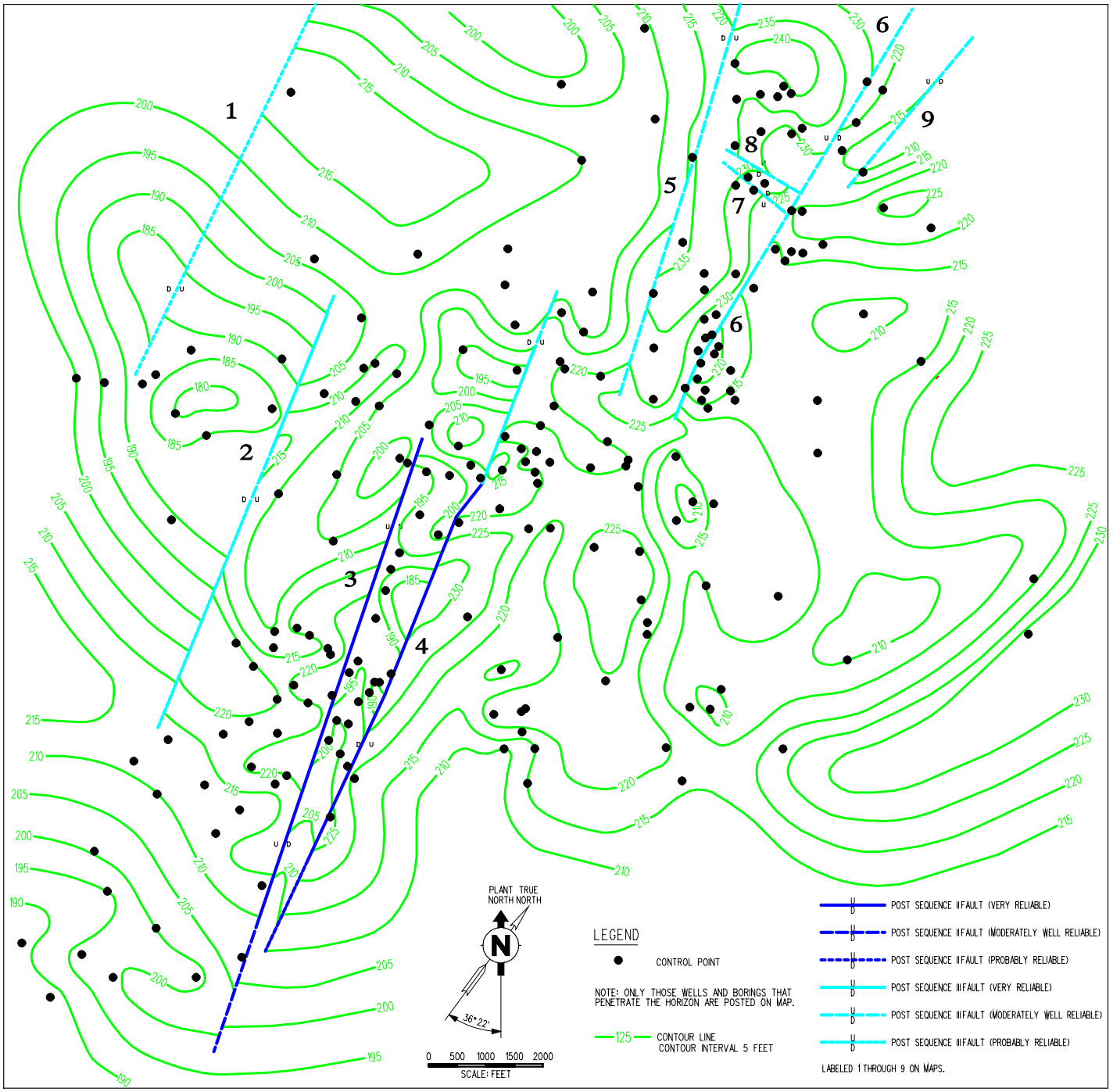

Figure 7. Top of Warley Hill structure Map Contours in feet above mean sea level.

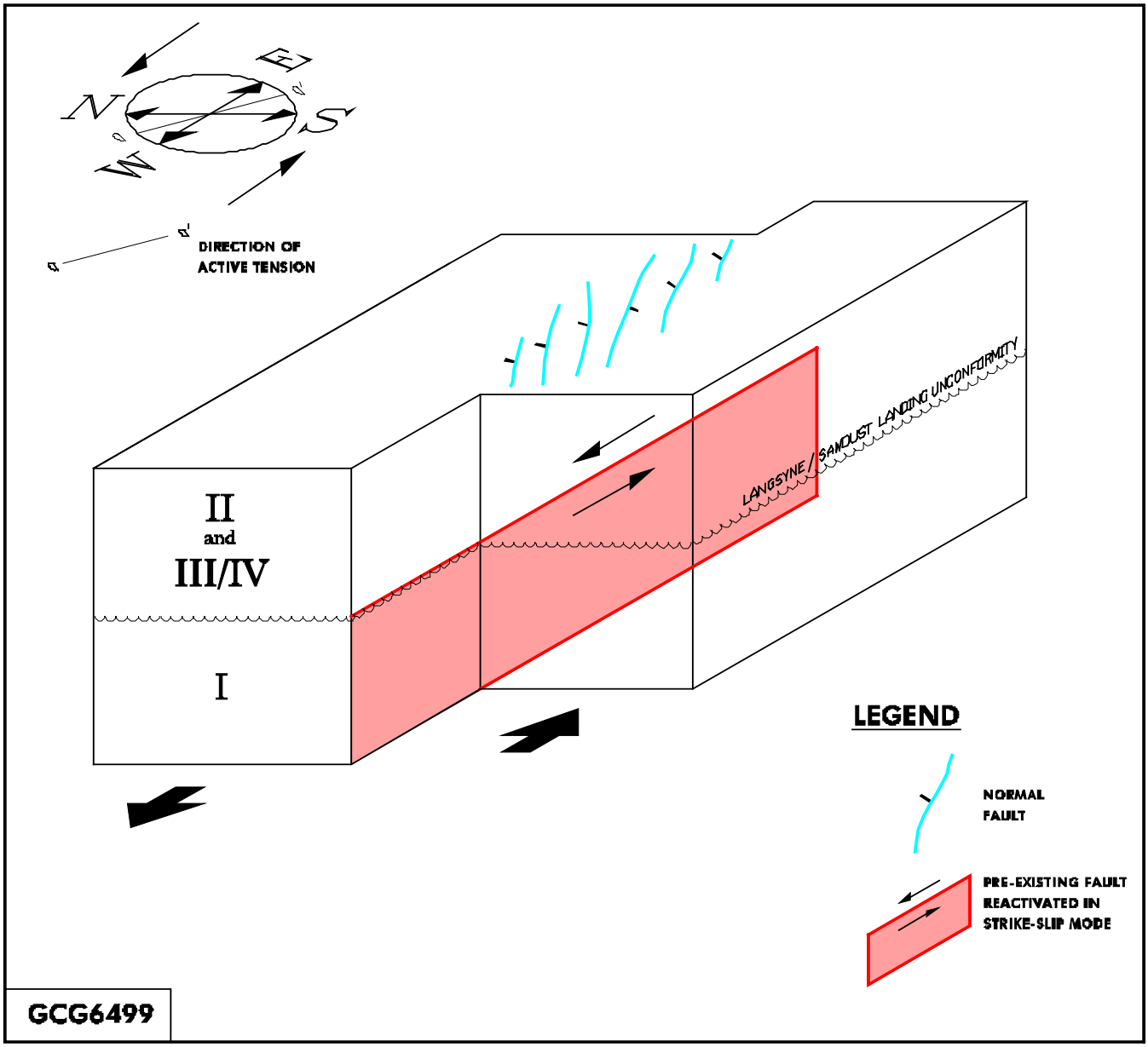

Figure 8. En echelon pattern of normal faults in the sediments formed above a 90° basement fault reactivated in a pure strike-slip mode. (Modified from Billings, 1972 and Pascal and Kranz, 1991).

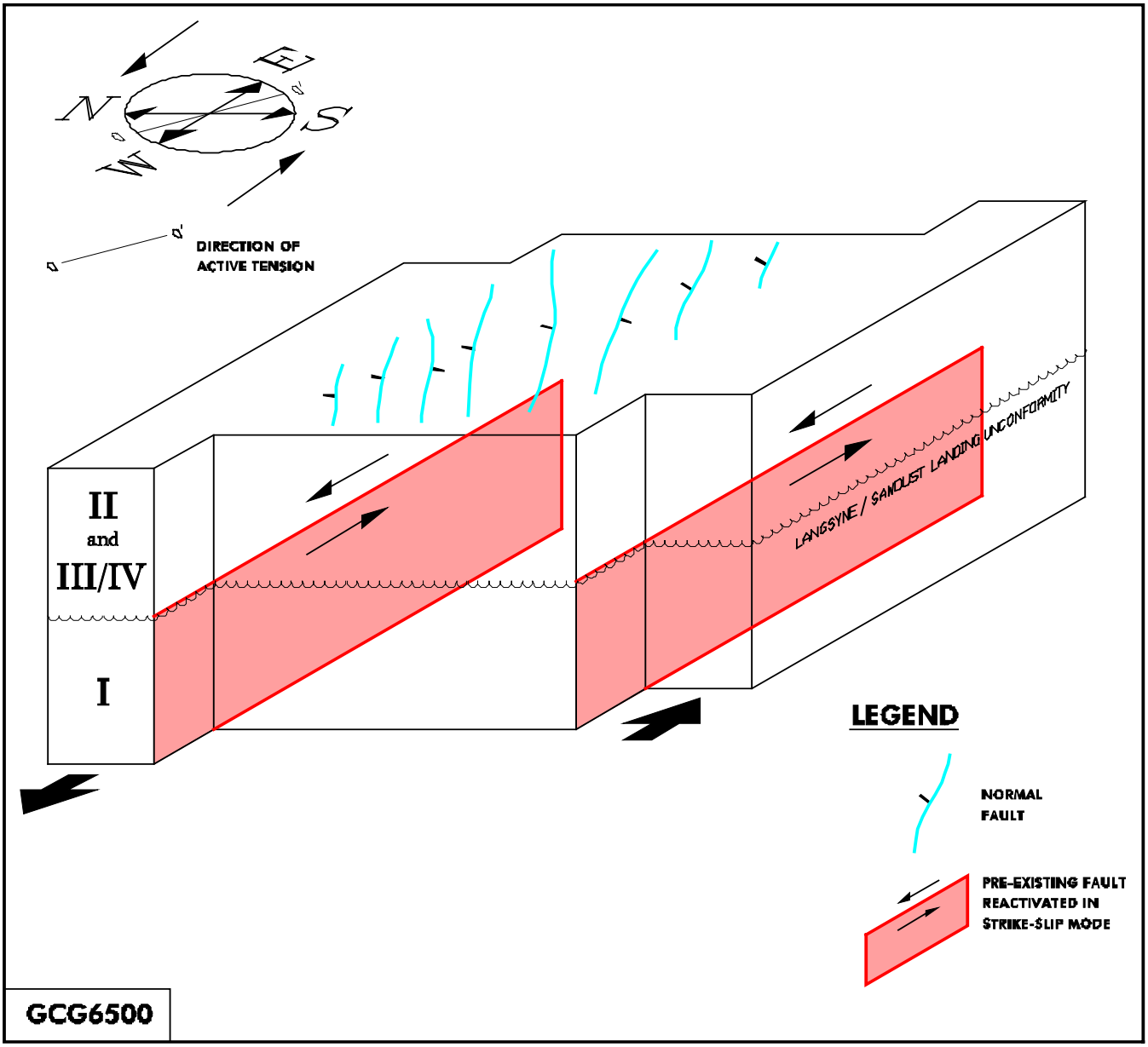

Figure 9. En echelon pattern of normal faults in the sediments formed above a 90° basement fault couple reactivated in a pure strike-slip mode, where a northerly block moved toward the west relative to a southerly block, resulting in the en echelon normal faulting in the passive sediments of the intervening block. (Modified from Billings, 1972 and Pascal and Krantz, 1991).

Notes

Geological Interpretation of the Pre-Eocene Structure and Lithostratigraphy of the A/M Area, Savannah River Site, South Carolina

D. E. Wyatt, R. K. Aadland and R. J. Cumbest, WSRC, Aiken, SC 29808

ABSTRACT

The geological interpretation of the structure and stratigraphy of the A/M Area was undertaken in order to evaluate the effects of deeper Cretaceous aged geological strata and structure on shallower Tertiary horizons. The shallow horizons are often involved in environmental issues. Additionally, this study attempted to evaluate the nature, extent, affects and timing of regional faults that have affected the area.

This interpretation was completed by combining 87 existing cone penetrometer tests, 10 new cone penetrometer tests, 234 existing boring and geophysical log locations and 21 new geophysical log locations with 22 km of new high resolution seismic data, 27 km of existing data and a 275 m by 350 m 3-D seismic grid. Horizon information and fault intervals were interpreted from the seismic data and combined into a database with stratigraphic picks from the geophysical logs and cone penetrometers. Regional deep boring correlations were made using the geophysical logs to constrain the seismic horizon identification. Seismic horizon to stratigraphic interval correlations were made from sonic information derived from geophysical logging.

This study interpreted four major, crystalline basement involved faults. The apparent oldest regional fault trends NNE and is identified as the Crackerneck Fault. Three parallel (younger?) faults trend north. The westernmost fault is identified as the MWESTA Fault and the easternmost fault as the Steed Pond Fault. The central fault intersects the Crackerneck Fault and is identified as the Lost Lake Fault. These faults are not thought to be single breaks in all areas but linear zones of disruption. These faults are thought to be predominantly reverse faults with possible dip-slip, or minor strike slip motion.

At least three episodes (and possibly more) of faulting are observed in the data, 1) Mesozoic, probably Jurassic to Triassic in age, faulting in the crystalline basement rocks, 2) post-Cretaceous aged faulting that disrupted the entire Cretaceous sediment column and 3) Paleocene or later faulting that disrupted younger sediments. These younger structures trend to the NW and occur in an en-echelon pattern. This pattern may affect strata to near surface or surface horizons.

The stratigraphic information for the deeper horizons is limited due to the limited number of deep geophysical logs tied to the seismic information. However, a comparison of regional deep logs and seismic data confirm the near shore, fluvial to deltaic, transitional to near shore marine, depositional character of the deeper A/M Area sediments.

INTRODUCTION

The A/M Combined Geological and Geophysical Program was organized to provide a comprehensive correlation capability between existing geological information, newly acquired geological core, advanced borehole geophysical data, surface high resolution reflection seismic information and ground penetrating radar data within the greater A and M Areas of the Savannah River Site. Specifically, the locations for all borings, seismic, cone penetrometer and ground penetrating radar data were chosen to maximize correlation to existing or newly acquired data and to compliment existing or ongoing environmental programs. This report presents an integration of new and advanced

data with existing information combined into a comprehensive picture of the deep subsurface geology of the A/M Area. The area of investigation is defined on Figure 1. The location of the seismic lines and deep borings is shown on Figure 2.

The A/M Advanced Geological Study was a joint effort supported by several organizations and agencies. Funding for the program was provided through the WSRC Environmental Restoration Department and administered by WSRC Site Geotechnical Services. Drilling and field oversight was provided by the US Geological Survey through an inter-agency agreement administered through DOE-SRS Environmental Division. All field work was coordinated through WSRC Site Geotechnical Services. Additional subcontract services were provided as follows: drilling by EM&TC, Inc., core descriptions by SAIC, field support and coordination by Bechtel Savannah River, Inc., and Raytheon. Core geochemical sampling was provided by Microseeps, Inc. Core from the upper 150 feet of each boring was split with half sent to Rutgers University for detailed soils and transport analysis as part of the DOE-HQ FERC program. Borehole geophysical data were acquired by Schlumberger Wireline Services, Inc, and Western-Atlas Wireline, Inc. Additional well logging was provided by Graves Logging Services. Downhole acoustic suspension logging was acquired in GCB-1 and GCB-2 by Agbabian and Associates. Surface seismic information was obtained and processed by the Earth Sciences and Resources Institute of the University of South Carolina. Palynological data and additional core analysis were provided by the Department of Geological Science of Clemson University. Ground Penetrating Radar data for the GCB program were acquired and processed by Microseeps, Inc. All data analysis, interpretation and correlation are provided by WSRC, Site Geotechnical Services and the authors.

This report utilizes seismic and deep borehole geophysical data to characterize the pre-Tertiary strata. Tertiary maps are made as a comparison to Aadland's (1997) work and as a tie to his interpretations. Aadland's (1997) work was completed using a manual interpretation and mapping approach.

APPROACH TO INTERPRETATION

The general process for geological correlation within the A/M Area follows a basement to surface "bottoms up" depositional and lithostratigraphic approach. For deeper strata, the interpretation of geophysical log well ties are made to seismic reflection events and are used to establish base correlation horizons. For shallower strata, older geophysical logs and core are correlated with advanced geophysical logs and core from the GCB-1,2,3 borings to establish type lithostratigraphic locations. Activities defining the general approach are described in order:

- Install borings, obtain and analyze core, and geophysically log GCB-1, GCB-2 and GCB-3. Obtain spectral gamma logs in additional A/M deep cased wells P8R, P6R, P9R and from deep boring MMP-4SB.

- Acquire and process A/M seismic data.

- Correlate GCB's to existing basement boreholes using geophysical logs, core data, field description of core, Type Well picks and Aadland (1997) picks.

- Establish synthetic seismic data from GCB wells correlated to lithologic picks from core and geophysical log horizons.

- Correlate seismic horizons to GCB lithologic picks. Establish fault and structure trends through the area based on seismic offsets in the basement. Establish principal lithostratigraphic horizons on seismic and geophysical logs.

- Correlate existing A/M well data picks to lithostratigraphic picks in the GCB borings.

- Incorporate CPT data into well grid. Correlate shallowest interpretable horizon to well picks.

- Incorporate geophysical data from new shallow environmental borings to fill data gaps

- Generate combined correlation maps based on interpretable seismic horizons and geophysical logs. Establish basement structural trends based on seismic offsets.

- Combine maps with structure into a three dimensional A/M data volume.

- Develop and present cross-sections through the data volume.

- Interpret data.

SOURCES OF INFORMATION

Nine high resolution reflection seismic lines were obtained to support deep mapping. The location of these lines are shown on Figure 2. In addition to these lines, three existing regional seismic lines were also utilized. These location of these lines are also shown on Figure 2.

Field data were acquired using an OYO DAS-1 signal enhancement seismograph operating in 96 channel mode. 40 Hz OYO geophones were used in geophone strings having 3 phones per string. The energy source consisted of an IVI MiniVIBE® remotely triggered vibrator sweeping from 50 to 200 Hz. In general, an asymmetric split spread acquisition geometry (24-gap-72 spread) was utilized, with shot and geophone spacings of 1.5 and 3.1 meters depending on the seismic line.

The following processing sequence was applied to the data: reformat SEG-2 field files to SEG-Y format, apply vibroseis whitening, F-K filter, predictive deconvolution, bandpass filter, trace edit, crooked line sort, statics, bulk velocity shift, velocity analysis, residual statics, apply normal moveout, stack, bandpass filter, trace amplitude balance, apply AGC.

The dominant frequency from the high resolution survey is approximately 120 Hertz. The highest frequencies observed were approximately 200 Hertz. Based on the frequencies available, it was possible to discern horizons approximately 4 meters in thickness. Features that were thin, or sporadic, may have been imaged in some cases, but were not interpreted in this study.

Velocity logs from GCB-1 and 2, and from P8R and P9R, were used to construct synthetic seismic sections tied to stratigraphic horizons. The synthetic seismic section from GCB-1 tied to seismic line A-5 is shown in figure 3. Using the synthetic seismic ties, it was possible to identify specific reflection horizons on the seismic lines as specific defined stratigraphic horizons. The crystalline basement reflector, Top of Cape Fear Formation, Top of Middendorf equivalent zone, and in some cases, the McQueen Branch Confining Unit were interpretable. These surfaces represent regional unconformities or eustasy related sequence boundaries and generally represent an acoustic impedance zone detectable by the seismic technique. In only a few cases were shallower horizons interpretable.

BACKGROUND GEOLOGY

Figure 3 is the generalized stratigraphic column for the Savannah River Site region. The depositional environments and sediment character for GCB-1, located in the center of the study area and thought to be representative, are shown on Figure 4a. Figure 4b shows the tie between key borngs GCB-1, 2, and 3. A detailed discussion of the

stratigraphy and deposition is found in Fallow and Price (1995) and Aadland et al., (1995). Parts 1 and 2 of the Advanced A/M Geology Study (Wyatt et al., 1997 a and b) discuss the data derived from the ground penetrating radar, cone penetrometers and the geophysical characterization of borings GCB-1, 2 and 3.

A conceptual model of the anticipated geology in the region of the A/M Area provides an intellectual framework to interpret the borehole geophysical and seismic data. The basic model should be consistent with known regional geology as described in established scientific literature. As data are evaluated against the model, an iterative thought process will allow features to be interpreted within the framework, or will suggest that modifications need to be made in the model. If there are highly unusual features that violate the character of the anticipated geology within the model, then a data "bust" may be indicated, or new information may be present to advance the known geology within the area.

The conceptual model of the anticipated deposition environment within the A/M Area is a near shore to delta plain environment. Therefore, sediments associated with a near shore deltaic, fluvial and near shore marine are anticipated. Variations in facies architecture associated with depositional processes in these environments are also anticipated. Facies architecture variations include "fining upwards" or "coarsening upwards" sedimentary sequences in a transgressive-regressive system. Sediments associated with near shore, littoral zone and beach environments may be highly variable both laterally and vertically. The model assumes that depositional sequences within the area are consistent with those published by Fallaw and Price (1995) and anticipates the regional unconformities present in these sequences to also be present in the area.

Structural features within the area are assumed to be consistent with the known post depositional regional stress fields. The presence of the Crackerneck Fault as defined in Stephenson and Stieve (1992) is also assumed. Any subsequent faulting within the area is assumed to be consistent with the Crackerneck Fault or associated with the post depositional stress fields. The conceptual model assumes no preferred age restrictions on structural features. The presence of faults, fractures and folds are anticipated.

The description of the sediments encountered in GCB-1 and described on Figure 5 verifies the basic conceptual model.

STRATIGRAPHIC INTERPRETATION

Geophysical logs and core data from shallow borings and wells are the dominant source of data within the A/M Area. Few borings penetrate depths greater than 100m (330 feet) and most logs terminate within the Lang Syne/Sawdust Landing Formation (near the Paleocene-Eocene contact) and are too shallow for direct correlation with the seismic information. To allow for direct correlation with the higher quality information from the deep borings, the geophysical logs and core data from the shallow wells were tied to the stratigraphy determined from the deeper borings. The correlation of the shallow borings is discussed in Aadland (1997) and elsewhere in this guidebook.

Cone penetrometer soundings generally extend to depths of approximately 50m (150 feet) or approximately to the top of the Warley Hill Formation and occasionally reach the "green clay" bed within the formation. The Friction Ratio's from the cone penetrometer data were correlated with the geophysical logs from the shallow borings. See Syms et al., in this guidebook for a further discussion of the CPT.

INTERPRETATION OF DEEP COR-RELATION BORINGS

Lithostratigraphy

The interpretation of the GCB borings was guided by the need to establish relationships

between core derived and geophysically derived geology. Additionally, the correlation between the geophysical log interpretation and surface derived seismic data is important to understanding the overall A/M, and SRS, geological setting. The GCB-1,2,3 interpretation will be presented as a unit by unit correlation comparing core geology and log derived depositional signatures. Hydrostratigraphic nomenclature follows that of Aadland et al. (1995). Stratigraphic nomenclature and environmental comparisons are from Fallaw and Price (1995) and Reineck and Singh (1980). Log interpretations follow suggestions from Schlumberger (1989) and Serra (1985).

Saprolite and Basement (Pzm/Sap and Acoustic Basement)

Crystalline basement lithologies are similar across the GCB-1,2,3 area. In GCB-1, an olive to gray/green weathered chlorite schist overlies a highly fractured bluish gray gneiss. The thickness of the schist is approximately 47 feet (14.3 m) and a distinct contact is present between the schist and gneiss. In GCB-2 and 3, only the chlorite schist interval was sampled which had a similar appearance to the schist of GCB-1. Fractures within the schist of GCB-1 have an approximate northwest strike orientation with a dip varying between 13 and 27 degrees. Fractures and quartz veins within the gneiss appear to have a northeast strike orientation and gentle dips, however, only the upper few feet of the gneiss were sampled for dip information. No oriented dip or strike information is available for GCB-2 and 3. All of the crystalline basement lithologies encountered in GCB-1,2 and 3 were expected as referenced in Cumbest and Price (1989).

The top of basement contact is the first contact with the highly weathered and fractured saprolite. Generally, the saprolite increases in thickness from GCB-2 and 3 to GCB-1 from approximately 13 feet (4 m) in GCB-3 and 15 feet in GCB-2 to approximately 32 feet (9.8 m) in GCB-1. The character of the saprolite varies in each boring. In GCB-1 the saprolite contact is defined by a sharp change between a well indurated sandy/silty clay to gray-green clay with numerous iron oxide stains. The color varies from gray-green to brown-red. In GCB-2 the saprolite is a brown to red mottled clay grading into a dense, massively foliated olive green clay while in GCB-3 the saprolite is a bluish gray to off white, well indurated clay.

Cape Fear Formation (Top CF)

The Cape Fear Formation generally thickens towards the southeast from GCB-3 to GCB-1. The overall lithology of the formation consists of interbedded gravel, sands and clays of varying colors and sizes. Rock fragments and angular sands suggest that the Cape Fear Formation was deposited near its source. There are generally three member sequences, alternating coarsening and fining upwards, that define the formation and that are most developed in GCB-1. The overall geophysical log pattern of the sequences, which matches the field core descriptions, suggests that each unit within the formation is a lag channel, shoaling deposit fill with pebbles and heavy sands grading into finer sands with interspersed clays. This interpretation is consistent with the description in Aadland et al., (1995) and Fallaw and Price, (1995).

Within the Cape Fear and at the basal Middendorf, rock resistivity values and deep versus shallow curve separation (an indicator of relative permeability) decrease rapidly. The overall neutron porosity drops from an average of approximately 35% to approximately 20%. The low relative permeability and porosity suggests tighter formations. The lower resistivity values are associated with higher concentrations of heavy minerals and interstitial waters are more mineralized than shallower aquifers. Overall, the Cape Fear and saprolite are indurated with lower permeability, forming the Appleton Confining Unit.

Middendorf Zone (Top Mid)

The Middendorf Zone (formerly Formation) gradually thickens towards the southeast from GCB-3 to GCB-1. There are correlatable packages of sediments across the formation but it is difficult to correlate specific sand or clay units across the area defined by GCB-1, 2 and 3. Channel and sheet type sands are interbedded with indurated clays suggesting a lower delta plain depositional environment. Many of the sand units in GCB-1,2,3 appear to alternate between fining and coarsening upwards suggesting that they are marine influenced channels or bars. Spectral gamma data, when combined with field core descriptions and lab core analysis, suggests that there are few clays of significant thickness within the formation. Generally, the clays are thin and less than one meter thick. Numerous heavy minerals and micas, as well as fine grained sands with clay balls, generate a spiked appearance of the gamma curve which may be interpreted as numerous interspersed clays. Focused or Induction Resistivity data suggests that there are numerous high permeability zones separated by numerous 'tight' streaks of clay or silt to silty-sand. These zones also suggest that there are non-correlatable sand bodies within the formation with variable permeability, therefore, tracking groundwater movement within the Middendorf within the A/M Area would be extremely difficult.

Black Creek Formation (Top BC)

The Black Creek Formation in borings GCB-1,2,3 may be described in terms of an upper and lower member, possibly two sequences, separated by the McQueen Branch Confining Unit (MqBCU) regional aquitard. Both upper and lower zones have geophysical log and core characteristics that define them as primary regional aquifers.

The lower zone lies unconformably over the Middendorf and consists of interbedded thin clays and sands occurring, more or less, randomly distributed and uniformly spaced throughout the interval. Spectral gamma peak to peak correlation, indicating regional clay units, are possible to track across the borings. These clays are probably localized maximum flooding surfaces, while the basal clays, similar across the area, were deposited in a near shore marine environment. The interbedded sands and clays, often with interspersed iron staining and heavy minerals, is suggestive of a fluvial to upper delta depositional environment.

The MqBCU is a sequence of three principal clays and silty clays occurring in a 40 foot (12.2 m) interval separated by clayey to silty sands. Each of the three units is approximately 10 to 15 feet (3.0 to 4.6 m) thick with the lower unit having the most consistent clay content and thickness. Many of the sands within the MqBCU are moderately sorted and sub-angular with a consistent presence of micas suggesting that these sands are fluvial and deposited near their source. The clays also consistently have micas presence, suggesting that the clays and the sands are both fluvial deltaic to near shore sub-tidal.

The upper zone of the Black Creek is variable across the region of the GCB borings. In GCB-2, the interval consists principally of interbedded clays and sands in beds averaging 5 to 7 feet (1.7 to 2.1 m) thick. This 'serrated' depositional style is common along the margins of bar-finger sands (Busch and Link, 1985). In GCB-1 and 3, the dominant lithology in the upper zone is sand with thin interspersed silt and clay intervals. The sands are dominantly moderately to well sorted, tan to cream in color, and sub-angular to sub-rounded. Micas are present and sometimes abundant with rare heavy minerals. The sand is 75 feet (22.9 m) thick in GCB-3 and 37 feet (11.4 m) thick in GCB-1. These sands are not massive but consist of stacked bar finger, bar-axis and barrier sequences with dips (in GCB-1) of 2^o to 12^o to the northwest in the upper units, to 14^o to 21^o to the south-southwest in the middle sands followed by 15^o to 29^o dips to the northeast in the lower sand units. The average dip direction is to the south. The

alternating dip directions are indicative of near shore influence and the measured dips are probably alternating barrier or dune foreset beds.

Samples for palynological analysis were obtained from the GCB-1 boring in a dark, organic rich clay from a depth of 439.5 feet (134 m, Figure 4a) at the base of the upper sand unit and top of the MqBCU. Palynomorphs were present indicating a late Campanian to early Maestrichtian age. The spores, pollen, plant cuticle, wood fibers and inertinite, plus a lack of marine algae, indicates that this interval is non-marine (Christopher, personnel communication, 1996).

Steel Creek Formation (Base of CBCU to Top BC)

The Steel Creek Formation is defined from the base of the Crouch Branch Confining Unit (CBCU) to the top of the Black Creek Formation. Dominant lithologies consist of micaceous clays interbedded with sands, sands and silty sands interbedded with thin clays and pebble zones. Micas, including angular grains, are present throughout the interval and iron staining is common. In the basal 50 feet (15.2 m) of each boring, clay content increases and alternates with fine grained silty sands. The overall dip direction is generally random. Sands appear to be more prevalent in the upper portions of the Steel Creek and exhibit morphologies similar to distributary barrier and bar sequences. In GCB-1, these sands generally fine upwards, and exhibit varying dip angles from up to 20^{o} northwest to 12^{o} southeast and 18^{o} northeast. The ‘C” sand of Aadland et al., (1995) is present in all wells and gradually varies from a coarsening upwards distributary bar finger and delta lobe sands (Busch and Link, 1985) in GCB-1 and 2 to a more marginal bar finger sand or delta lobe in GCB-3. The remaining sands in the upper portion of the Steel Creek are depositionally similar to the ‘C’ sand but tend to be more tidal in GCB-3. In general, the sands of the Steel Creek appear to be more landward in GCB-3 and more seaward in GCB-1. It is possible that the Cretaceous/Tertiary boundary (K/T), and contact with the Paleocene, is present at the basal contact of the clay unit immediately overlying the ‘C’ sand. The presence of pebble lag layers and heavy minerals may define this time sequence marker.

Crouch Branch Confining Unit (Top CBCU to Base CBCU)

The Crouch Branch Confining Unit varies in thickness and clay content from approximately 17 feet (5.2 m) of thin and sparse clays in GCB-3 to 44 feet (13.4 m) of thick silts and clays in GCB-2 to 50 feet (15.2 m) of silty clays and clays in GCB-1. The clays tend to be a white to light gray, plastic kaolinite with thinly laminated purple mineral horizons. The CBCU in GCB-1 is predominantly kaolinitic clay with only minor interspersed laminae of silty clay. In GCB-2, thin lamina of heavy minerals and silts are interspersed within the clays. Thin sands within the unit often have heavy minerals and abundant micas. Thin zones of cemented iron laminae are also present. In GCB-3, only thin clay units are present interspersed with silty clays, sandy silts and sands. Numerous lamina with iron staining and heavy minerals are present. The thin sands tend to grade into pebbles and clay balls. The thin clays, clay balls and shoaling sands units in GCB-3 suggest that GCB-3 CBCU sediments were deposited in a fairly high energy, near shore, possibly intertidal zone, transitioning into a subtidal to delta distributary depositional environment in GCB-1.

This unit, which consists of parts of various formations, forms the principal confining unit across the SRS; therefore is discussed in detail as it controls downward contaminant movement. Permeability variations in the CBCU, determined from magnetic resonance geophysical logs, are observable in GCB-1. The interval from 240 feet (73.2 m) to 250 feet (76.2 m) is a well indurated and mottled clay. Permeability average less than 200

millidarcies. From 240 feet (73.2 m) to 265 feet (80.8 m), subsurface, the measured permeabilites increase to greater than 1 darcy. All clay within this interval is well indurated and without other noticeable features. Various color changes, suggesting changes in the geochemical makeup of the clays, form numerous lamina throughout the section. The magnetic resonance tool is probably imaging the horizontal permeability associated with these lamina. In the base of the CBCU, from approximately 265 feet (80.8 m) to the top of the Steel Creek Formation at 290 feet (88.4 m) subsurface, the permeability decreases from approximately 500 millidarcies to zero. This interval is also a well indurated clay with fewer lamina, grading into a silty, micaceous clay. At 290 feet (88.4 m) subsurface, the magnetic resonance permeability increase dramatically in the sands of the Steel Creek Formation.

Lang Syne/Sawdust Landing Members (Top LS/SL to Top CBCU)

The Lang Syne and Sawdust Landing Formations (refer to Aadland et al., 1995 and Fallaw and Price, 1995 for nomenclature discussions) are not lithologically differentiated within the A/M Area of the Savannah River Site. Within the area of GCB-1,2,3, these formations vary in thickness between 28 feet (8.5 m) in GCB-3 to 46 feet (14 m) in GCB-2 and 12 feet (3.6 m) in GCB-1. Two distinct, lithologically different and correlatable, members are seen in each boring. The basal member of the Lang Syne/Sawdust landing is a lower bar to delta sheet sand that thins downdip to the southeast. The upper member is a silty clay to clay coarsening upwards into a delta front sheet sand that has the greatest thickness in GCB-2. The silty-sand interval in the upper member in GCB-1 appears to be the distal edge of the delta front. Overall, the general dip of the LS/SL sediments is south-southeast. The sand interval in the upper member appears to be a bar sand that is probably regressive, intertidal and defines the Lang Syne/Sawdust Landing regional unconformity.

The lower 10 feet (3 m) (230 feet (70.1 m) to 240 feet (73.2 m) subsurface) of the LS/SL has an average permeability that exceeds 1 darcy. This interval is a well indurated clay with iron oxide staining and containing some pyrite. The measured permeability in this interval is probably due to microfracturing and the horizontal character of the iron oxide lamina. This interval is capped by a low permeability (less than 10 millidarcies) thinly bedded clay and silty clay. Overlying this clay, is a zone that transitions into a high permeability (greater than 1 darcy) that probably corresponds with the Lang Syne/Sawdust Landing unconformity. In GCB-1, the combination of the underlying CBCU and the high permeability associated with the LS/SL unconformity create the zone with the highest TCE concentrations. The ability to track and map the Lang Syne/Sawdust Landing Formations and the unconformity zone suggests a way to possibly track halogenated solvents.

The following stratigraphic units, although Eocene in age, are discussed for continuity with the work of Aadland in this guidebook.

Congaree Formation (Top Congaree)

Unconformably overlying the Lang Syne/Sawdust Landing Formations are the assemblages of Early Eocene sediments that comprise the Fourmile Formation. It is lithologically difficult to distinguish these specific formations from the overlying lower middle Eocene Congaree Formation and the entire interval is generally referred to as the Congaree Formation (Aadland et al., 1995). Generally, the lower sands within the interval, when present, are considered equivalent to the Fourmile Formation while the upper sands, when present, are a portion of the Congaree Formation.

Generally, the depositional character of the Congaree in GCB-1,2,3 is similar. There is a slight increase in formation thickness from

GCB-3 towards GCB-1 and 2 suggesting a seaward dip. The lithology of GCB-2 and 3 consists of sands, medium to coarse grained, interspersed with thin indurated clays. GCB-2 is dominantly sands with thin silts and a few clay lamina and GCB-3 is dominantly sand with thin clay and iron stained lamina. In GCB-1, there are lithified sand intervals 1.2 to 1.6 inches (30 to 40 mm) thick and siliceous sandstones up to 2 inches (50 mm) thick. Well indurated clays are present as a central unit within the formation and are approximately 10 to 15 feet (3 to 4.6 m) thick associated with silty clays and clayey silts.

Permeability zones are variable within the Congaree. In GCB-1, generally, within the formation, cleaner sand zones have higher permeability, approaching 500 millidarcies, and silty to clayey sands have permeability less that 5 millidarcies. Traces of PCE and TCE are generally seen in the thin sands that are immediately above the well indurated clays.

A shallow shelf to shoreline environments of deposition for the Congaree is evidenced by the dip directions in GCB-1. Basal Congaree sands (possible Fourmile or Fishburne Formation equivalents) generally rotate from a low angle south-southwest dip through a westward to north-northwest dip direction with an angle of 6^o to 8^o to a low angle northeasterly dip. The upper sand unit (probable Congaree Formation equivalent) has very high, up to 24^o dips generally striking to the northeast. The upper sand interval is most indicative of a possible dune sand with the high angle dips suggesting foreset bedding. The basal sands are most indicative of deltaic to near shore barriers and bars.

Warley Hill Formation (Top WH)

The Warley Hill Formation is present in GCB-1, 2 and 3. In GCB-3, the formation is generally geophysically indistinguishable from the over and underlying units, however, a subdued gamma pattern is similar to the patterns from GCB-1 and 2. In GCB-1, the Warley Hill consists of a sand with interspersed iron oxide modules overlying a silty sand to thinly laminated silty clay. The silty clay, and to some extent the silty sand, form the Gordon Confining Unit with measured log permeability of less than 50 millidarcies. This clay interval is regionally extent and is thought to represent a maximum flooding surface. Sands within the upper portion of the formation generally have permeability on the order of 100 to 200 md. In GCB-1, the dip directions within the Warley Hill are varied.

In GCB-2, the Warley Hill sediment character is similar to GCB-1 but the formation is locally exposed on the surface and has been affected by near surface processes. In GCB-3, the formation is generally sandier than GCB-1, and lacks the thin clay lamina and silty sands that constitute the confining unit.

Correlation With Other Deep Borings

The deep correlation borings used to calibrate the seismic data are GCB-1, 2, 3 and P8R, P9R, MMP-4-SB and MBC08ASB. The locations for these boring are shown on Figure 2. The stratigraphic horizons from GCB-1, 2, 3 were used to correlate the horizons from P8R, P9R, MMP-4-SB and MBC08ASB. The geophysical data from all of these borings (except MCB08ASB) are calibrated to international standards and were used to correlate and verify all geophysical logs within the A/M Area. Data were correlated using LandMark® and TerraSciences® geological software. Figure 6 is a structural correlation panel showing the stratigraphic horizons for these deep correlation wells. This panel is flattened on an elevation of 97m (300 feet) relative to mean sea level. The stratigraphic horizons are those utilized to map specific intervals within the study area. In general, only the Late Cretaceous horizons are visible on the seismic data.

The figure 6 correlation panel follows no particular strike or trend except that P8R, GCB-1 and P9R are in the central portion of

the A/M Area with P8R being more westerly, GCB-2 is in the southeastern area, MMP-4SB and GCB-3 are in the eastern area and MCB08ASB is in the northern area. Therefore, the correlation panel proceeds from the west central portion of the study area southeastward, westward and then to the north. These logs are used only to evaluate the relationship of the stratigraphic units across the study area and, along with their velocity and other data, provide a framework for interpreting the seismic data. Also, "flattening" on stratigraphic horizons allows for the relative interpretation of depositional character and relative fault motions to be made.

This panel demonstrates several interesting features. All horizons, except the McQueen Branch Confining Unit, from MCB08ASB in the north to P8R in the southwest, show the southerly basinal dip. There are offsets in crystalline basement, particularly associated with GCB-3,P9R and GCB-1, that are continuous through to the Lang Syne/Sawdust Landing unconformity. In GCB-3 and MCB08ASB the regional structure does not track as well as in the wells to the south and west and it is possible that there is another erosion event beveling the structure prior to the Lang Syne/Sawdust Landing event, and probably occurring at the Cretaceous/Tertiary boundary. In well P8R, the structure reverses from a general downward sense of motion to an upward sense of motion in the lower Black Creek Formation. It is possible that well P8R cuts a reverse fault in the Middendorf/Black Creek intervals. This is supported from historic anecdotal evidence that the lower intervals of well P8R are deviated along a fault plane.

The Middendorf, Black Creek (including McQueen Branch Confining Unit) and Steel Creek Formations (generally, the entire Cretaceous section) are fairly uniform in thickness across the area. The Middendorf thins (or the Cape Fear may be missing) in P9R suggesting that the upwards motion noted in basement was present and either erosion or non-deposition occurred during Middendorf time. The upper Black Creek also thins suggesting reactivation of the upward sense of motion during Black Creek time.

The Steel Creek thins in GCB-3 suggesting erosion or non-deposition at this location during or in post Steel Creek time. The overall thickness of the Steel Creek to Lang Syne/Sawdust Landing interval including the clays of the early Paleocene, may be described as a transitional strata. The Lang Syne/Sawdust Landing shows only minimal effects from the underlying structure (on the order of 3 to 4 meters). The basement related structures show approximately 30 to 40 meters of relief.

The Congaree and Warley Hill Formations are fairly uniform in thickness. The sag seen in the Warley Hill in GCB-3 is contrary to regional dip and is probably associated with the basement structure. The sag seen in GCB-1 may also be associated with a basement related structure. The interval from the Santee unconformity to the Warley Hill unconformity is generally uniform but thickens in GCB-1. The Santee surface is also a cut and fill surface and suggests that the motion documented in GCB-1 was not active in post-Santee time.

Interpretation of Seismic Data

The seismic data were interpreted using the LandMark® software system according to the following approach. Each processed seismic line was plotted on the regional map with associated deep correlation borings. Available borehole sonic data from the deep borings, (from GCB-1, 2, 3, P8R, P9R and MMP-4-SB), were utilized to generate a synthetic seismic image, using the GMA® seismic software, for the area adjacent to the borehole. The synthetic seismogram ties well derived stratigraphic horizons to specific seismic horizons and allows for the interpretation and tracking of stratigraphy and structure across a seismic profile. Figure 5 is the synthetic seismogram from GCB-1.

The synthetic seismogram for each well was correlated with the adjacent seismic profiles. Horizons on the seismic profile that were correlative with the synthetic well tie were traced across the profile. In general the crystalline basement reflector (rock), the Cape Fear/Middendorf contact (top Cape Fear), the basal Black Creek/Middendorf contact (top Middendorf), and McQueen Branch Confining Unit horizons were interpretable stratigraphic events. The Lang Syne/Sawdust Landing intervals were not consistently discernible across the seismic data. In a few areas, the Warley Hill interval appeared to be interpretable, however this occurred too sporadically to map. In general, no shallower horizons were obviously interpretable on the seismic data. Figures 7 and 8 show representative seismic data with stratigraphic horizons and faults interpreted.

Stratigraphic horizons were traced from well tie points following dominant seismic amplitude events. In areas where the horizons were difficult to track, no interpretations were made. In many cases, one stratigraphic horizon may be interpretable while others were not. The two way travel time values for each seismic shotpoint with an interpreted horizon were tracked, converted to depth based on the synthetic seismograms, and transferred to EarthVision 4.0® for mapping.

Faulted intervals were determined using the criteria of Sheriff (1982) and Campbell (1965) and include: 1) abrupt reflector terminations, 2) direct fault plane reflections, 3) presence of diffractions especially at a termination, 4) visible drag and rollover, 5) correlations of reflectors across a fault plane and possibly 6) loss of coherency beneath a fault plane or distorted dips seen through the fault plane (fault shadow). Using these criteria, faults were defined on the seismic profiles in LandMark® and transferred into EarthVision® for mapping.

It is probable that channels and other depositional features exist within the A/M Area and are imaged on the seismic data. However, the channels or other feautures are not highlighted on the seismic data and are not discussed in detail in this document because they will require a more intense interpretive effort using seismic signal attribute data (such as instantaneous frequency and phase). If obvious channels are observed in the data, then they are mentioned. The criteria used to define a channel are discussed in Reineck and Singh (1980) and include: 1) an obvious, incised erosional surface, 2) the presence of cross-bedding, 3) presence of point bar sequences, 4) an apparent thalweg, and 5) alternating sand/clay/gravel bars.

Individual 2-D Seismic Line Interpretations

Representative seismic data are shown on figures 7 and 8 and the overall pattern and distribution of seismic coverage is shown on figure 9. Figure 9 also shows the relative seismic depths in time and the trend of the major faults in the area.

All seismic data are interpreted for faulting and stratigraphic horizon markers, as determined from the synthetic seismic data shown on figure 5. For all lines, the yellow horizon represents the top of “rock” or the surface of the unweathered Paleozoic crystalline basement. The dark red horizon marker is the contact of the Cape Fear Formation (Coniacian/Turonian, 90 mybp) with the overlying Middendorf Formation. The pink horizon is top of the Middendorf Formation (Campanian/Santonian, 82 mybp) or contact with the overlying Black Creek Formation, a regional unconformity. The orange horizon is the top of the confining unit or clay package that has been designated as the McQueen Branch Confining Unit (Aadland et al., 1995). This horizon lies within the Black Creek Formation and may represent the Campanian/Maestrichtian contact, another major unconformity. These four Cretaceous aged horizons appear consistently on all of the data and are used as the principal subsurface horizons for seismic mapping.

On all seismic lines, only five possible faults are shown (reference Figure 9). Faults, and projection lines, designated in red refer to the Crackerneck Fault (CNF). Faults in green refer to the MWESTA Fault and faults in pink refer to the Lost Lake Fault. Fault segments in orange refer to the Steed Pond Fault. Yellow fault segments are faults with no assigned orientation or name. These faults may have limited extent, may be associated with a named fault, or their extent may not be determined from our seismic coverage. The angle of the fault segments posted on each seismic line is somewhat arbitrary since our data were not designed to image structure below the crystalline surface.

Line SRS-1 is shown on figure 7 and is discussed as a representation of the remaining seismic data.. This approximate north-south line is the definitive data for the existence of the CNF, shown as a red line. Regional dip from this data is southerly at approximately 1.5%. The vertical offset in the CNF is approximately 12 ms two way time (TWT), or 30 to 35 meters, on the basement horizon. The horizontal extent of the offset is across two shotpoints or approximately 35 meters. Compensating faults, or more recent faults, associated with the CNF, are shown in yellow. These faults may accommodate the stresses associated with the CNF. The northwestern fault (in yellow) is associated with the green dashed line which is the projection of the AMWESTA fault, therefore, these two faults are probably the same. The fault noted in pink to the southeast of the CNF is the Lost Lake Fault and the dashed pink lines are the projections of this fault through the area from other seismic data. The basement reflector, in yellow is consistently tracked by the dark red Cape Fear marker horizon except immediately northwest of the CNF where there is an apparent increase in thickness of the Cape Fear, or where there may be remnant Triassic trough sediments. The pink horizon is the Middendorf Formation contact with the Black Creek Formation. Over the faulted intervals, it is difficult to track a consistent horizon and disturbed or eroded sediments are seen. The orange McQueen Branch horizon demonstrates a fault propagation fold geometry. Folded and flexed sediments are apparent from the McQueen Branch to approximately 100 ms, although these events are not traceable across the data. The overall sediment wedge thickness appears to increase to the southeast as expected. Changes in amplitude laterally along horizons to the southeast, particularly in the lower Black Creek, may indicate the stratigraphic or facies changes associated with shallow channeling, other near shore or fluvial processes. This line intersects five of the A/M lines CNF-1, A-3, A-1A, A-2 and SRS-7. In all cases, the interpreted horizons match those from the other lines and the data are consistently tied.

3-Dimensional Seismic Data

A three dimensional seismic survey was obtained immediately southeast of line MCB-1. Results are shown in figure 10. The rectangular cube was obtained over a surface area of approximately 275 meters by 352 meters using 120 cross-lines and 154 inlines with a 2.2 meter spacing (a 2.2 meter bin size). An IVI MiniVibe vibratory source was used. In general, best results were obtained from 200 ms and deeper. Little to no data were interpretable above 200 ms.

Figure 10 shows time slices, in relative amplitude, through the data cube. Each time slice has the time and stratigraphic interval noted. The projection and strike of the Lost Lake Fault, with relative sense of motion, which is projected through the area from the 2-D seismic lines, is included for reference. The 325 ms time slice corresponds to the approximate top of “rock” or crystalline basement. A pronounced negative amplitude (purple) feature is seen in the southeastern portion of the cube, surrounded by a higher amplitude event. This low amplitude feature is the same low amplitude feature seen surrounding the heart shaped high amplitude feature seen in the 320 ms time slice (approximately 20 meters shallower). Therefore, the low amplitude event is higher

by 5 ms and has the same approximate sense of motion as the Lost Lake Fault predicts. At 340 ms, approximately 40 meters below the top of "rock", the trend of the Lost Lake Fault bisects a phase change (of about 180^{o}) event presumed to be the same for the shallower horizons. It is not evident that this relationship exists upwards through the cube, although there are notable changes across the projected strike of the Lost Lake Fault. The features that trend northwest to southeast in the 260 ad 270 ms time slices may be faults at oblique angles to the main basement trend. This is supported in the time slices at 256 and 260 ms. The NW-SE trending high amplitude reflector in the eastern central portion of the cube in slice 260 ms is the same high, but weak, reflector in the central west portion of the cube, between inlines 40 and 60 of time slice 256 ms. This implies a general up to the west sense of motion, however, the trend of the features is oblique to the trend of the Lost Lake Fault. It is interesting to note that the trend of these features parallel the NW to SE trending sides of the high amplitude basement feature seen in the 320 and 325 ms time slices. This suggests that the basement trend of the Lost Lake Fault zone is NE to SW but individual faults within the zone may be parallel or synthetic/antithetic to the basement trend. This also suggests that individual basement fault blocks may be small in size along the fault zone (approximately 150 by 150 meters in the case of the high amplitude feature in the basement). It is not evident how far the fault extends into basement on the 500 ms time slice. These data are basically random and out of the range of the seismic investigation.

It should also be noted that there are linear, amplitude coherency events in the 3-D data. These features are often associated with structural features such as fault cuts, and are also associated with sedimentary features such as channel boundaries. Within the useable 3-D data, there are no obvious channel features or unique facies changes, although it is possible that there are facies changes associated with the slopes of the faulted blocks. The trend of the low amplitude events in time slice 256 ms, for example, may be interpreted as a channel meander, however, inline evaluation suggests that the reflection event is structurally controlled. The lack of channels and definitive structures is probably a function of the small size of the 3-D cube and the representative subsurface sampled.

DISCUSSION

Mapping

Seismic horizon picks, converted from time to depth using the synthetic information from GCB-1, GCB-3, P8R and P9R were combined with the stratigraphic picks from the geophysical logs and CPT's (where applicable) to create the database for mapping. Mappable horizons from the seismic data include the acoustic crystalline basement ("rock"), Cape Fear, Middendorf and McQueen Branch surfaces. In a few cases the Black Creek horizon was observable but these were too sporadic to adequately map. Data were forced, using a static shift and velocity/depth corrections, to match actual depths from the deep correlation borings. The data from each horizon were then mapped. For the seismically derived horizons, the projected major fault planes (MWESTA, CNF, Lost Lake and Steed Pond) were included in the mapping database and used to constrain contours adjacent to the faults. Each mapped surface is discussed.

Stratigraphic intervals from shallower horizons are discussed in Aadland (this guidebook). The previous intervals from the work of Aadland (1997) were reviewed and modified according to the regional deep boring correlations. Stratigraphic picks from available cone penetrometer data were combined with new and existing information. These stratigraphic "picks" were incorporated into Earth Vision® 4.0 for mapping. Shallow mapped horizons include the top of Black Creek Fm., top of Steel Creek Fm., Lang Syne/Sawdust Landing unconformity, and

Warley Hill unconformity. A surface elevation map is included for discussion.

Top of Crystalline Basement ("rock")

Figure 11 is the surface of the crystalline basement. The dominant faults projected through the area and seen on figure 9 are shown. It is obvious that the area in the center of the map is complexly disturbed. The area between the Steed Pond Fault (most eastern fault) and the Crackerneck Fault is structurally higher than areas east and west. Deeper basement is to the southwest and westward of the CNF and MWESTA faults. The overall maximum structural elevation change across the area is approximately 70 meters. Regional dip is to the southeast. Structure and dip on the northwest, northern, northeast and southeast, and possibly the southwest edges of the map are influenced by map edge gridding affects and are extrapolations of data.

Top of Cape Fear Formation

The surface of the Cape Fear Formation is shown on Figure 12. Although the same map edge affects are present as in the basement map, the general trend of the data are similar. The deeper basin is to the west southwest in these data and the structural high through the center of the study area associated with the CNF and Lost Lake Fault is present. The Cape Fear is basically draped over the basement structure and has smoothed many of the minor structural perturbations found on the basement map by infilling. However, the formation is offset by faulting. The structural change across the area on the Cape Fear is also approximately 70 meters, suggesting that much of the structure is post Cape Fear in age. Basinward dip is to the west southwest. The depositional character is not obvious on this map, although sediments primarily associated with structurally lower areas east of the central high are present. It is probable that this area has been lowered structurally, but it is also possible that there was a trough or flow passage through the area as well.

Top of Middendorf Inteval

The structural top of the Middendorf interval is shown on figure 13. The central structure is present with an overall elevation change across the area of approximately 50 meters. Generally the formation dips to the south. The structural affects of the Crackerneck and Steed Pond Faults are immediately obvious. Map edge effects are great, particularly the steep structural change to the north between the Crackerneck and Steed Pond Faults. A ramp like structure may be present from the central high eastward to the Steed Pond Fault. Structure is more complex west of the Crackerneck/Lost Lake Faults.

Top of McQueen Branch Unit

The top of the McQueen Branch unit is shown on figure 14. This map is different than the underlying Middendorf in that the regional dip appears to be dominantly to the southeast. Structural elevation change across the area is approximately 20 meters and is represented by a monocline or dip reversal flexure across the regional faults. Minimal effects are seen from the MWESTA and Steed Pond Faults. More convoluted structure is seen associated with the CNF and Lost Lake Faults, particularly in the area of the greatest seismic data density in the center of the map. The gridding edge effects are great in the northern portion of this map.

Top of Steel Creek Formation

The top of the Steel Creek Formation is shown on figure 15 and is generated from borehole geophysical data. These values are the same as those used in the manually contoured maps of Aadland (1997). The shallower faulting on the surface of the Cretaceous from Aadland (1997) is shown on the maps for reference and may be affecting the depositional pattern. Few borings penetrated the Steel Creek horizon within the area and most are centrally located, therefore the edge effects on this map are

large. There are few regional faulting effects seen in the map except for the convoluted structure adjacent to the CNF and Lost Lake Faults. Between the time of deposition of the McQueen Branch unit and Steel Creek Formation, there was a large near shore marine depositional influence across the area. Thick marine sands were deposited in the upper Black Creek Formation, and a regional unconformity or disconformity at the top of the Black Creek-contact with basal Steel Creek has smoothed the surface. A regional unconformity, the possible Cretaceous/Tertiary boundary global erosion event has further planed the Steel Creek surface.

Surface of the Lang Syne/ Sawdust Landing Unconformity

The top of the Lang Syne/Sawdust Landing Formation is shown on figure 16. This map was also created using the same data as Aadland (1997). The northwest to southeast trending structures may be associated with shear reactivation along the CNF and Lost Lake Faults (shown on this and subsequent maps for trend information). There are thickness variation in the Lang Syne/Sawdust Landing sediments across the area that appear to be related to older structure on the surface of the Steel Creek Formation. The trend of the structural features is oblique to the strike of the regional faulting. Deformation extent may be restricted by the bounding AMWESTA and Steed Pond Faults. The initial timing of this oblique faulting/folding is observed in the structural map of the Steel Creek Formation, therefore it is assumed that the timing of the reactivation is post-Ypresian. The change in structural elevation across the features is approximately 12 meters as compared with approximately 14 to 16 meters at Steel Creek time. It is not known whether the structure is accomodated by folding or faulting but the abrupt elevation change in some areas may suggest faulting while the less abrupt changes may suggest folding. The en-echelon, periodic character of the structural events (high, low, high. low, high) occurring approximately every 1000 meters, is strong evidence for structural control. A current dominated near shore sand depositional character is not thought be the cause of the en-echelon pattern because the features are along dip into the basin and not along margin strike.

Faulting and Structure

The four major faults, interpreted from the seismic data, are accompanied by several smaller, unassigned faults. It is possible that many of the unassigned faults may be correlated together and form additional fault systems, possibly those of Aadland (1997). It is also probable that many of the smaller fault are basement splays from the regional faults and that the larger faults are the primary offsets in a complex fault system. However, it is not possible, without additional data, to confirm these alignments. Many of the unassigned faults have significant offsets, or have complex structures, and may be important to shallower horizons, however, additional data are required to examine this possibility in detail.

The oldest fault thought to affect the A/M Area is the CNF. This fault trends approximately N35E across the study area and may extend an indeterminate distance to the SSW and NNE. This fault shows reverse motion and is generally up on the SE and down on the NW. The amount of throw on crystalline basement varies from approximately 30 to 35 meters maximum to approximately 10 meters minimum within the study area. The angle of the fault is generally greater than 60^{o} from horizontal. The CNF follows a propagation fold model (Cumbest and Wyatt, 1997) and disturbs sediments through the Warley Hill Formation. It is possible that horizons shallower than the Warley Hill are influenced but this is difficult to determine from the seismic data or borehole mapping. The correlation of CPT, GPR and high resolution seismic data from Wyatt, et al., (1997) suggests that there are near surface structural influences, however, it is not clear

that the shallow effects are from the CNF. They may possibly be from later faulting.

On seismic lines SRS-1 and A-5 (figures 7 and 8 respectively), which cross the fault perpendicularly, a synclinal trough is noted in the footwall block. An additional sediment fill is seen in the trough suggesting that either syndeposition was occurring during pre-Cape Fear compressional faulting (Coniacian/Turonian?, 90 mybp) or that the CNF is a re-activated Mesozoic normal fault with a depositional remnant in the down warped interval associated with the extensional event (Triassic/Jurassic/early Cretaceous, > 90 mybp?).

A schematic of the fault propagation model similar to the CNF is shown on Figure 17 along with an actual seismic schematic of the CNF from line SRS-1. The comparison between these two figures is obvious although the seismic schematic does not demonstrate any fore limb thickening of sediments except possibly in the Lang Syne or Warley Hill intervals. The lack of sediment thickening may be from the high angle of the CNF and unconsolidated nature of the sediments above the axis.

The Lost Lake Fault is thought to be younger than the CNF because it apparently intersects and disturbs the CNF near the northern end of seismic line A-3 (refer to figure 9). Because of the conjugate nature of the Steed Pond and MWESTA faults to the Lost Lake Fault, they are thought to also be younger than the CNF, and approximately the same age as the Lost Lake. These faults trend approximately N10E, and within the study area, only the Lost Lake Fault intersects the CNF. To the southwest, and beyond the study area, the MWESTA Fault may also intersect the CNF.

The MWESTA, Lost Lake and Steed Pond Faults were grouped because they generally exhibited the same relative sense of motion, along linear trends, throughout the study area. However, the relative sense of motion may vary along these faults because of shear displacement. On many of the mapped horizons, the sense of offset varies along these faults and between faults. At the McQueen Branch Confining Unit (Figure 14) for example, the Steed Pond and MWESTA Faults appear to have a left lateral offset while the Lost Lake may have more of a right lateral motion. On this figure, it is possible that offset exists in the shallow horizons (up on the NE) and that the fault splays into a positive flower structure, indicative of a shear motion.

On figure 16 the Lang Syne/Sawdust Landing NW/SE trending highs appear to truncate at the MWESTA and Steed Pond Faults. These highs may be flexural folds associated with the differential shear motion between the MWESTA and Steed Pond Faults. The overall sense of motions for the fault zone bounded by the MWESTA and Steed Pond faults would be right lateral. The axial crests of the structural highs appear to be offset by approximately 3000 meters from crest axis to crest axis, which may be a predictive tool for location of additional highs.

Of the MWESTA, Steed Pond and Lost Lake Faults, only the Lost Lake appears to influence shallow sediments. In general, the structural influence from these faults, as derived from the seismic data, appears to diminish above the Middendorf horizon., however, the resolution of the data do not preclude the possibility of shallow deformation.

Assuming that structural influences have affected the topography of various stratigraphic horizons through time, then it should be possible to estimate timing and total displacement of sediments. The effects of erosion are difficult to estimate. Figure 18 is a graph of approximate maximum elevation relief, average, minimum and maximum interval thickness for the stratigraphic horizons. Data were extracted from map figures 11 through 16 and values from the stratigraphic picks

Several observations may be made from this graph. The amount of structural relief on the surface of the crystalline basement is the greatest observed. The structural relief on the Cape Fear and Middendorf exceeds the average and maximum sediment thickness, suggesting post or syndepositional structure dominated during the Mesozoic through Santonian time. The minimum (and average) sediment thickness from the McQueen Branch Confining Unit to the Middendorf (lower Black Creek), and Steel Creek to McQueen Branch (Steel Creek and upper Black Creek), exceeds the overall amount of structural relief on these horizons. This suggests that depositional events predominated over structural events during the Campanian through Maestrichtian time. For the Lang Syne/Sawdust Landing to Steel Creek interval, the structural relief is greater than the minimum sediment thickness and less than the average thickness. This suggests that a combination of structural and depositional events have occurred during the Paleocene. From the Warley Hill to Lang Syne/Sawdust Landing (Lutetian to Ypresian), the sediment thickness exceeds the overall amount of structural relief available suggesting a dominantly depositional environment. From the present day land surface to the Warley Hill (Bartonian and younger), the average sediment thickness is exceeded by the structural relief but the maximum sediment thickness exceeds the relief. Therefore, this suggests a combination of depositional and structural events.

Based on the data from this graph, it is possible to establish the following series of events: 1) Paleozoic to Coniacian/Turonian: structural events dominant (assumed), 2) Coniacian/Turonian to Santonian: structural events dominant, 3) Campanian to Maestrichtian: depositional events dominant, 4) Paleocene: depositional and structural events, 5) Lutetian to Ypresian depositional events dominant, 6) Bartonian and younger, depositional and structural events.

Stratigraphy

A variety of depositional environments and structural influences have affected the strata within the A/M Area. In general, all sediments within the area may be characterized as near shore marine to fluvial punctuated by submarine or subaerial erosional events. Within formations, the depositional character may change across the area as the environment of deposition changed along slope. Adjacent to faults, the sediment character may vary due to tectonic influences. The regional stratigraphy is discussed in Fallaw and Price (1995), Aadland et al., (1995) and Aadland (1997).

The deep borings and seismic data may be combined to define the lateral variability and character of sediments within a specific formation. The log signatures of the geophysical curves may be used to interpret the depositional sequence or environment relative to formation and depth, particularly for the sand sequences (Busch and Link, 1985, and Serra, 1985). This, in turn, may be associated with an area along a seismic line and further associated over a larger area. Each deep Cretaceous stratigraphic horizon will be discussed. Tertiary strata are discussed in Aadland (1997) and this guidebook.

Cape Fear Formation

The Cape Fear Formation varies in thickness across the A/M Area from approximately 6 meters eastward to 12 meters westward. The geophysical log signature is similar in all penetrating borings, therefore the depositional environments are thought to be similar, although no definitive environment may be interpreted from the geophysical data. In general, and referencing the core descriptions in Wyatt et al., (1997), the formation appears to be a fluvial or shoaling lag deposit with interspersed sands, cobbles, pebbles, silts and heavy minerals. Aadland (1997) contends that the Cape Fear may be missing in well P9R.

The geophysical logs from GCB-1, GCB-3, P8R and MMP-4-SB suggest that the formation may consist of at least two and possibly three shoaling events. Three distinctive lower energy intervals, punctuated by sandy/silty higher energy events are noted in the GCB-1 log. In MMP-4-SB, three events are also noted but have a different character, suggesting a low energy or shoaling (possible heavy mineral) lag, then a higher energy environment, followed by another low energy environment. Since structural relief exceeds depositional thickness, it is possible that the stratigraphic and depositional character of the Cape Fear is dominated by episodic structural events causing periodic shoaling.

The seismic data provide little information on the depositional or stratigraphic character of the Cape Fear. The seismic data does support a thickening of the interval westward but in general, the thickness of the Cape Fear is less than the resolution of the data. Overall, the near source, shoaling environments interpreted for the Cape Fear are consistent with the initial rising sea levels during the Late Cretaceous and suggests that the A/M Area was near shore during this eustatic event.

Middendorf Interval

The Middendorf interval varies in thickness across the area from approximately 25 meters along a central axis to 35 meters eastward and westward in the area. It is possible to track consistent members through the formation, therefore the thinned areas are apparently caused by erosion. Individual members or beds within the formation alternate between thinly bedded, high frequency, dominantly sands with interspersed clays to thinly bedded, high frequency, dominantly clays with interspersed sands. The varying pattern of sand units from “spikey” to “bell”, “funnel” and “serrate” shapes all suggest a bar, bar-finger, delta front sheet sand, depositional environment. The best developed sand units are in GCB-3, PW-113, MMP-4-SB and MBC08ASB, suggesting that the north and west portions of the study area were shoreward during the Middendorf deposition. Neither the sand or clays are well developed in GCB-1, P8R or GCB-2 suggesting an environment with more of a marine influence.

The seismic data suggest that the Middendorf develops a more variable character to the south-southeast. Line SRS-7, an approximate dip line for Middendorf depositional time, shows a more variable character seaward, while having a relatively stable “railroad tracks” character landward or up dip. Seismic line CNF-2, an updip strike line for Middendorf deposition also displays a “railroad track” appearance while line CNF-1, further down dip, has a more variable character.

Black Creek Formation (including the McQueen Branch Confining Unit)

The Black Creek Formation’s depositional character and environment is similar to the Middendorf Formation except that an increase in silts and clays throughout the formation is suggestive of a lagoonal to back bay shallow water and lower delta plain environments. Distinctive sand and clay units are mappable across the area and are generally well developed to the north and east and less developed to the south and southwest.

The McQueen Branch Confining Unit (MqBCU) is a member of the Black Creek Formation, consisting of thick clays intercalated with thin sand/silt layers. The MqBCU approximately divides the Black Creek into upper and lower units. In GCB-1, 2 and 3, the MqBCU contains rich organic clays interspersed with heavy minerals and iron staining. A greater abundance of heavy minerals and staining is present in GCB-3 suggesting deposition further up slope. Across the structural high associated with GCB-1 and P9R, the MqBCU thins suggesting a structural influence affecting deposition. In general, the MqBCU appears to be distributed in a near shore, back barrier bay environment and may represent a sequence time line or surface

erosional interval between depositional cycles of the over and underlying Black Creek.

The lower Black Creek zone is generally more clay dominated than the upper zone. Several (generally three) clay units may be tracked across the lower portion of the Black Creek but are missing or thin above the GCB-1 and P9R high. The sand units within the lower zone have log characteristics of bar-finger sands or delta sheet sands combined with bar sands. Since the sand signatures are difficult to track across the data, they are probably more associated with discontinuous bars rather than delta type sheet sands.

The upper Black Creek zone is sand dominated and was probably deposited in a higher energy environment. Individual sand units are difficult to map across the area and the overall log signatures suggest bar-finger sands and bar pinchouts. In some logs, MBC08ASB for example, there may be a tidal inlet fill log signature.

Across the A/M Area, the overall character and variation of the lower Black Creek and MqBCU remains fairly constant. Further down dip to the south and southeast (south and east of the Crackerneck Fault), the depositional character appears to change and a more varied depositional pattern is seen. This may be the transition from upper delta, tidally influenced deposition to a lower delta marine influenced environment.

The seismic character of the upper Black Creek is less distinct than the lower Black Creek and the overall depositional pattern is more difficult to discern. In lines CNF-2 and SRS-7, the character is more consistent in the down dip areas to the south and southeast. This may indicate a more stable, marine influenced environment, while a higher energy, more discontinuous environment existed to the north and northwest.

Steel Creek Formation

The stratigraphic character of the Steel Creek Formation is not discernible from the seismic data. From the deep borings, the formation is fairly uniform in thickness across most of the study area but thins in GCB-3. The GCB-3 log suggests that the upper portions of the Steel Creek have been eroded. There are distinctive sand units within the formation that may be locally tracked, however, they are not traceable through all of the deep borings. The overall log character of the sand units suggests a near shore bar-finger environment.
Figure 11 shows the suggested depositional environments by formation.

SUMMARY

This study identified four principal crystalline basement involved faults. The oldest regional fault trends NNE and is identified as the Crackerneck Fault. Three younger faults trend north. The westernmost fault is identified as the MWESTA Fault and the easternmost fault as the Steed Pond Fault. The central fault intersects the Crackerneck Fault and is identified as the Lost Lake Fault. These faults are not thought to be single breaks in all areas but linear zones of disruption. The intersection of the Lost Lake and Crackerneck Faults is a highly complex area. These faults are thought to be predominantly reverse faults with possible dip-slip, or minor strike slip motion. The overall pattern of the Crackerneck Fault and possibly the Lost lake Fault follows a fault propagation fold model. The Crackerneck may be a re-activated Mesozoic normal fault. The overall subsurface structural relief within the A/M Area is thought to be controlled by these faults for strata older than the Middendorf and by a combination of sedimentation and structure for more recent sediments.

At least three ages of faulting are observed in the data. The oldest faulting is probably pre-Cretaceous and affected deposition of the Cape Fear Formation. There may be sediments

pre-Cape Fear in the synclinal troughs associated with these older faults. The majority of faults are post-Cretaceous in age and disrupt the entire Cretaceous sediment column. At least two pulses of post-Cretaceous movement are noted. A more recent structural event is seen in the Paleocene and younger sediments. This event may be a re-activation of the deeper faulting in a strike slip mode. These younger structures trend to the NW and occur in an en-echelon pattern. This pattern may affect strata to near surface or surface horizons.

The stratigraphic information for the deeper horizons is limited due to the limited number of deep geophysical logs tied to the seismic information. However, a comparison of regional deep logs allows for a discussion of possible deep stratigraphy. In general, all sediments were deposited in a near shore, marine to fluvial environment and vary from a tidally dominated to a wave dominated depositional character. For all Cretaceous strata, there is a noticeable change in depositional character south and southeast of the Crackerneck Fault from a near shore to more distal environment. Overall, there is a general thickening of Cretaceous strata to the southeast and south. Figure 19 provides a depositional relationship of the various stratigraphic units underlying the A/M Area to a deltaic, near shore model.

REFERENCES

Aadland, R. K., 1997. Tertiary Geology of A/M Area Savannah River Site, South Carolina (U), WSRC-RP-97-0505, Rev 1., 62 p.

Aadland, R.K., J. A. Gellici, and P.A. Thayer, 1995. Hydrogeologic Framework of West-Central South Carolina. State of South Carolina Department of Natural Resources, Water Resources Division. Report 5.

Busch, D. A. and D. A. Link, 1985. Exploration Methods for Sandstone Reservoirs, OGCI Publications, Tulsa, 327 p.

Campbell, F. F., 1965. Fault criteria. Geophysics, Vol. 30, No. 6, pp. 976-997.

Cumbest, R. J. and D. E. Wyatt, 1997. Fault-bend folding in unconsolidated Coastal Plain sediments and possible effects on hydrologic and contaminant transport properties. Geological Society of America Abstracts with Programs, Southeastern Section, V. 29(3), p. 44.

Fallaw, W.C., and V. Price, 1995. Stratigraphy of the Savannah River Site and Vicinity, Southeastern Geology. Vol. 35, No. 1, p. 21-58.

Faye, R. E., and D. C. Prowell, 1982. Effects of Late Cretaceous and Cenozoic Faulting on the Geology and Hydrology of the Coastal Plain Near the Savannah River, Georgia, and South Carolina. U.S. Geological Survey. Open File Report 82-156.

Pascal, R., and R.W. Krantz, 1991. Experiments on Fault Reactivation in Strike-Slip Mode, Tectonophysics. 188:117-131.

Prowell, D. C, 1994. Preliminary geologic map of the Savannah River Site, Aiken, Allendale, and Barnwell counties, South Carolina. USGS OFR 94-181. 11 p.

Reineck, H. E. and I. B. Singh, 1980. Depositional sedimentary environments, 2nd ed. Springer-Verlag, New York, 549 p.

Serra, O., 1985. Sedimentary Environments from Wireline Logs, Schlumberger Educational Services, Houston, 211 p.

Sheriff, R. E., 1982. Structural interpretation of seismic data, Education Course Series #23, AAPG, Tulsa, 73 p.

Stephenson, D. and A. Stieve, 1992. Structural model of the basement in the Central Savannah River Area, South Carolina and Georgia (U), WSRC-TR-92-120, 43 p.

Wyatt, D. E., R. J. Cumbest, R. K. Aadland, F. H. Syms, D. E. Stephenson, J. C. Sherrill, 1997. Investigation on the Combined Use of Ground Penetrating Radar, Cone Penetrometer and High Resolution Seismic Data for Near Surface and Vadose Zone Characterization in the A/M Area of the Savannah River Site, WSRC-RP-97-0184

Wyatt, D. E., R. J. Cumbest, R. K. Aadland, F. H. Syms, D. E. Stephenson, J. C. Sherrill, 1997. Interpretation of Geological Correlation Borings 1, 2, 3 in the A/M Area of the Savannah River Site WSRC-RP-97-0185

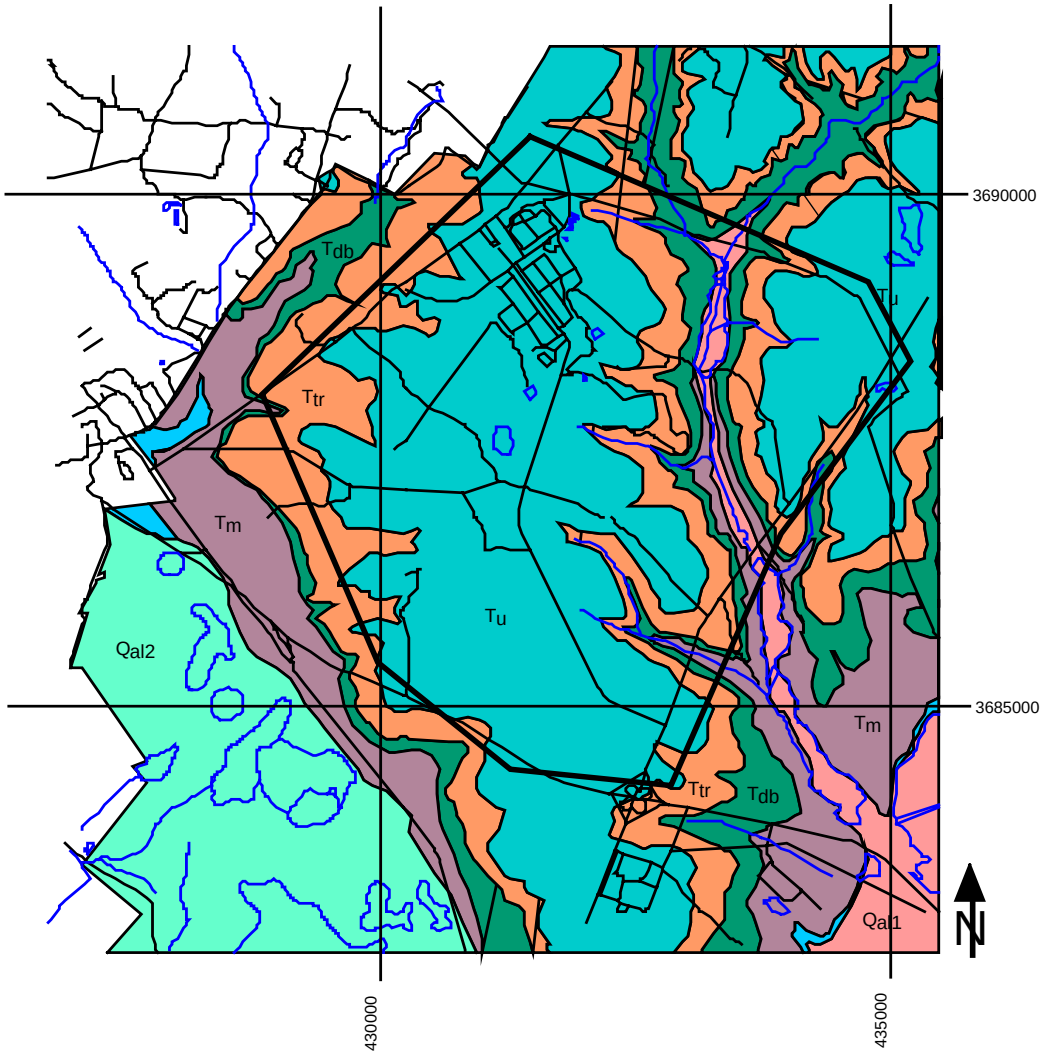

Figure 1. General study area. Colors represent the surface exposure of various geological formations. 'Tu' is the Upland unit, 'Ttr' is the Tobacco Road Formation. 'Tdb' is the Dry Branch Formation. 'Tm' is the McBean Formation. 'Qal1' and 'Qal2' represent Quaternary alluvial fill material, with the numbers representing relative ages of deposition. Grid coordinates are in UTM. Roads are noted as thin black lines. The heavy black line defines the area of data used for this study. Geology is from Prowell (1994).

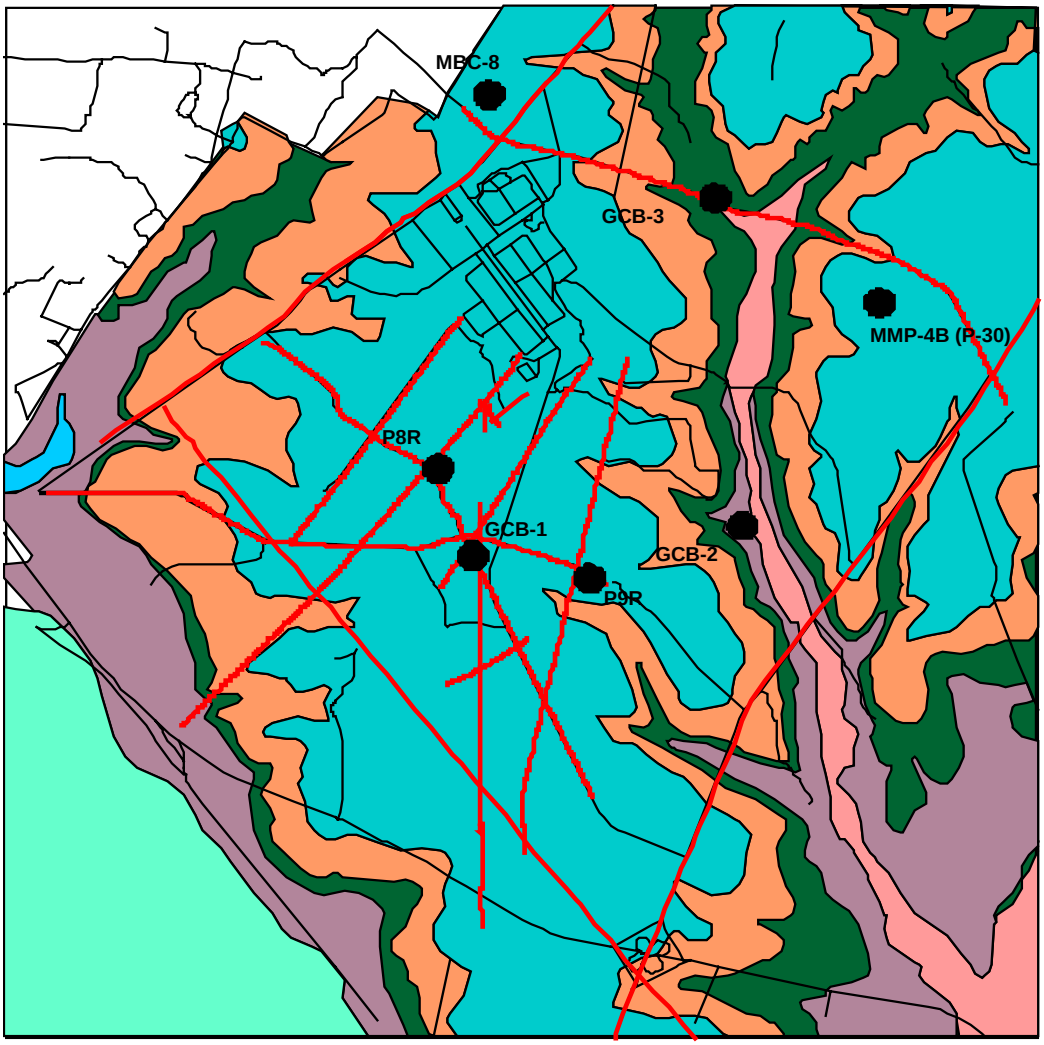

Figure 2. Location of seismic lines and deep correlation wells and borings used in the study. Red lines are the seismic lines and the well or boring locations are labeled. Data are superimposed on surface geology (from Figure 1).

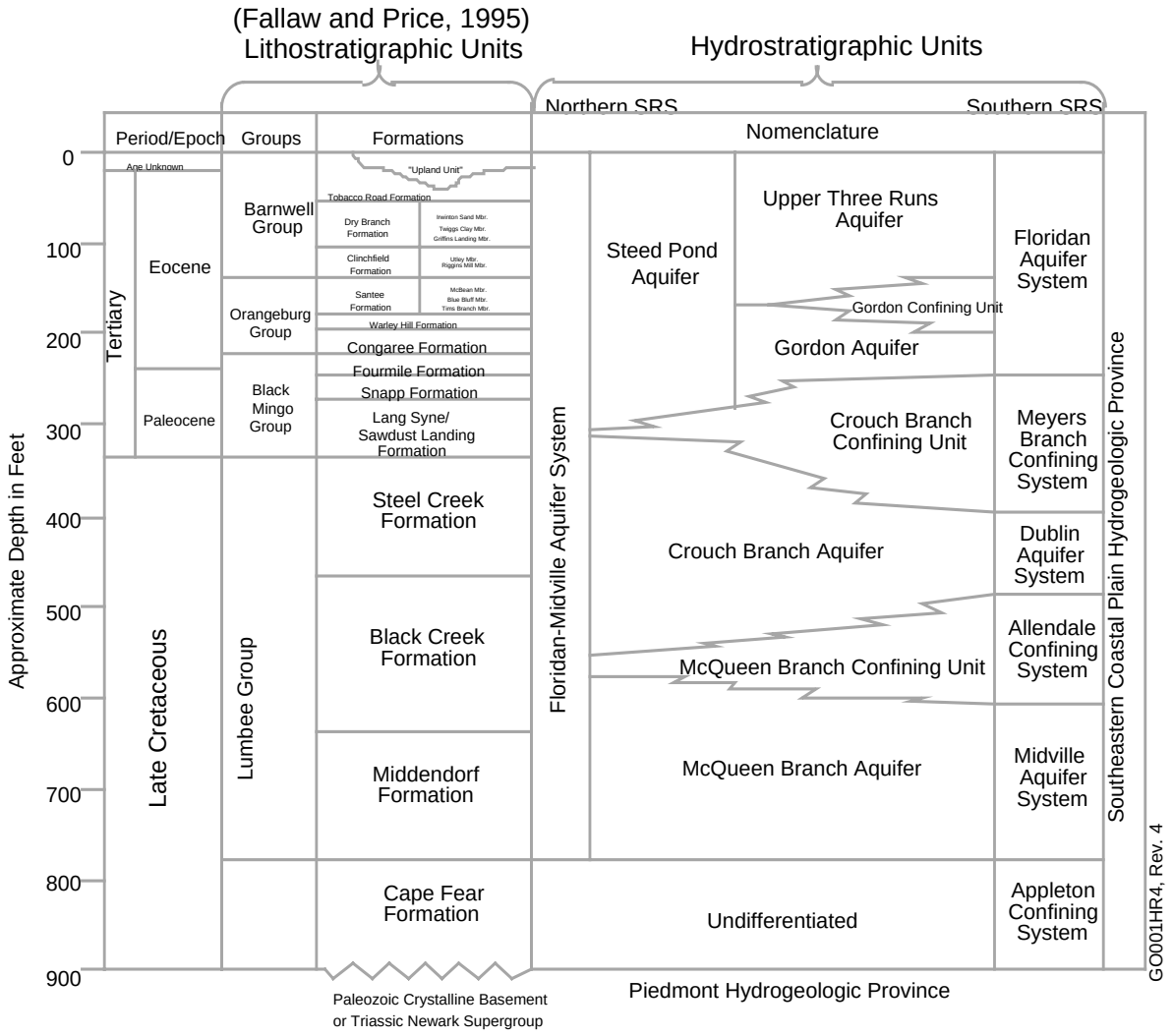

Figure 3. Stratigraphic chart representing the sediments within the A/M Study Area. Data are from Aadland et al., (1995).

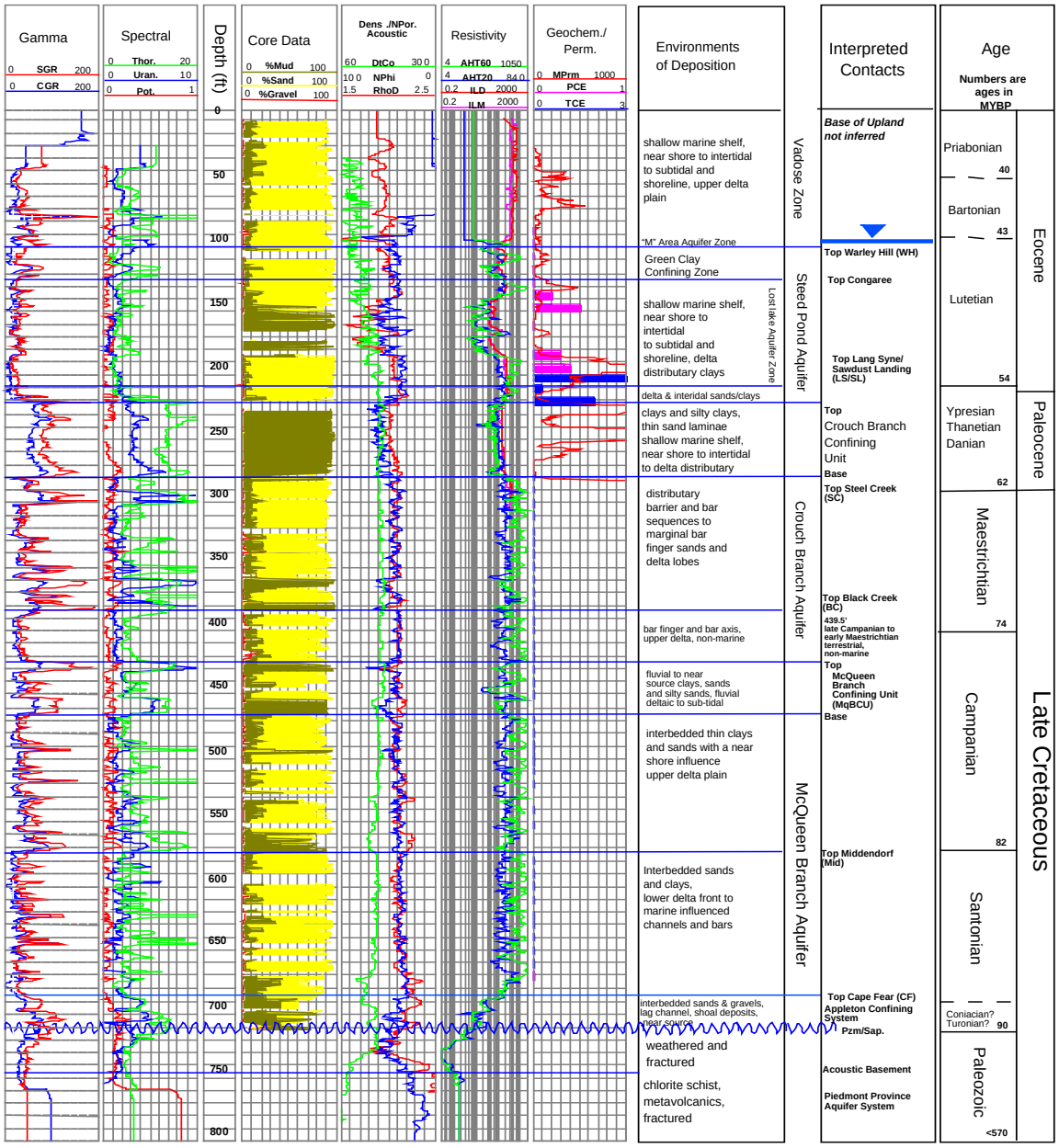

GCB-1

Figure 4a. Combined interpretation of GCB-1. Stratigraphic picks are from the correlation of GCB-1,2 and 3 to regional horizons. Depositional environments are interpreted from the geophysical log signatures, field core descriptions and core laboratory data. Hydrostratigraphy is from Aadland et al., (1995). Stratigraphy and chronostratigraphy are from Aadland et al. (1995), Fallaw and Price, (1995) and DNAG, 1983. Palynology is from Christopher (personal communication).

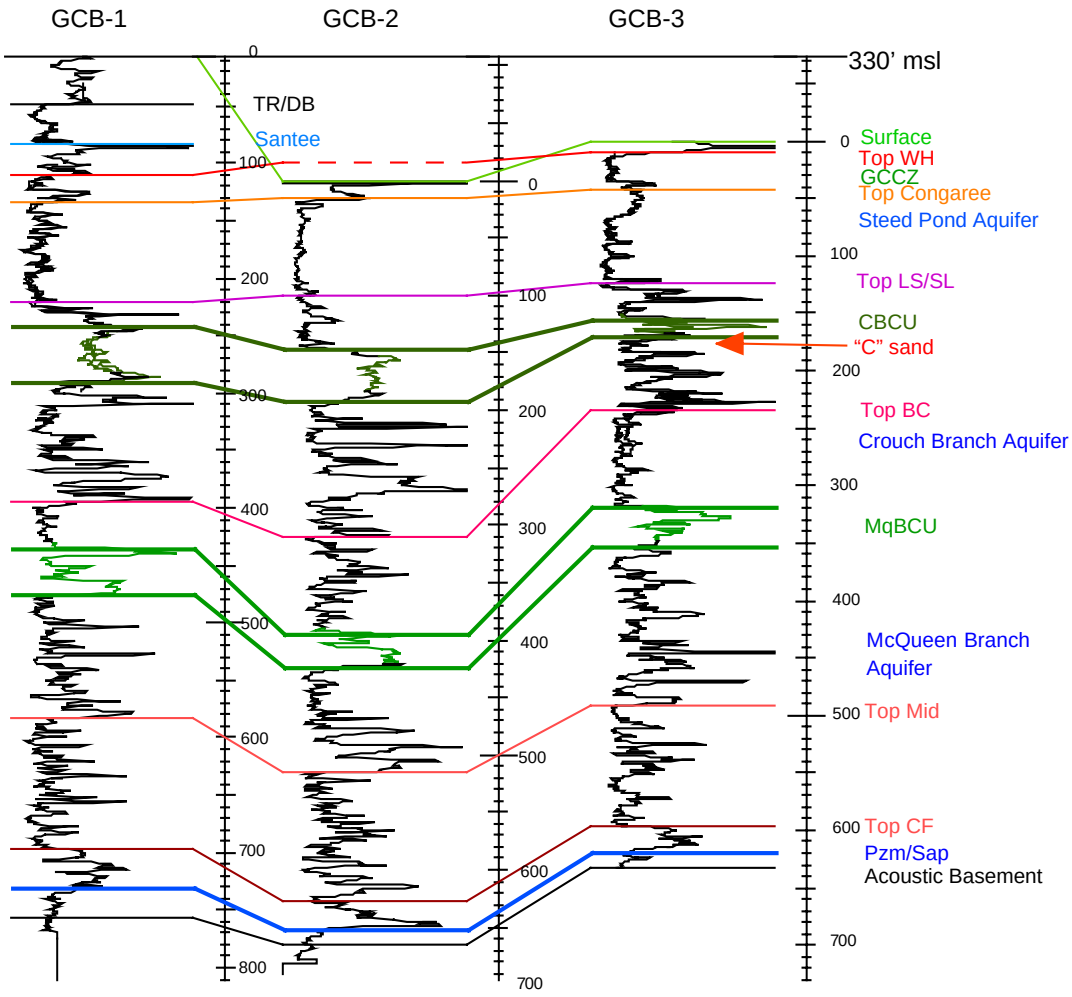

Figure 4b. GCB-1, 2 and 3 correlation panel. Datum is set to 330' (110 m) msl. Depths are in feet. Color of correlation lines correspond to color of horizon name. "Top WH" is the top of the Warley Hill Formation. "GCCZ" is the Green Clay Confining Zone. "Top LS/SL" if the top of the Lang Syne/Sawdust Landing Formations. "CBCU" is the Crouch Branch Confining Unit. "Top BC" is the top of the Black Creek Formation. "MqBCU" is the McQueen Branch Confining Unit. "Top Mid" is the top of the Middendorf Formation. "Top CF" is the top of the Cape Fear Formation. "Pzm/Sap" is the contact with the weathered basement rocks or saprolite. Acoustic Basement is the velocity crossover from coastal plain seismic velocities to those more typical of crystalline rocks.

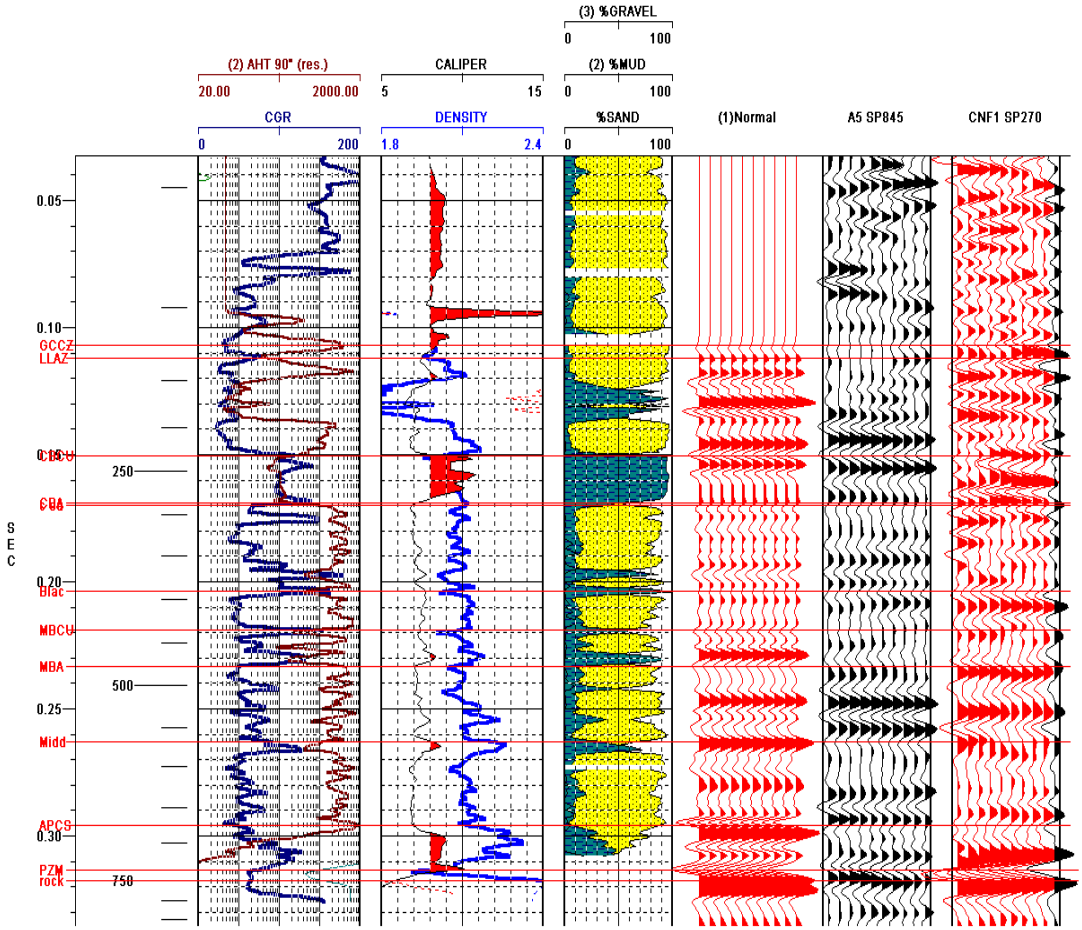

Figure 5. Synthetic seismogram and tie to seismic data. Sonic and density data from GCB-1 were used to calculate the synthetic seismogram. Traces from seismic lines A-5 and CNF-1, adjacent to GCB-1, were used for correlation. The synthetic data have been phase shifted by 300^{o}. Key stratigraphic horizons, identifiable on the seismic data, have been defined.

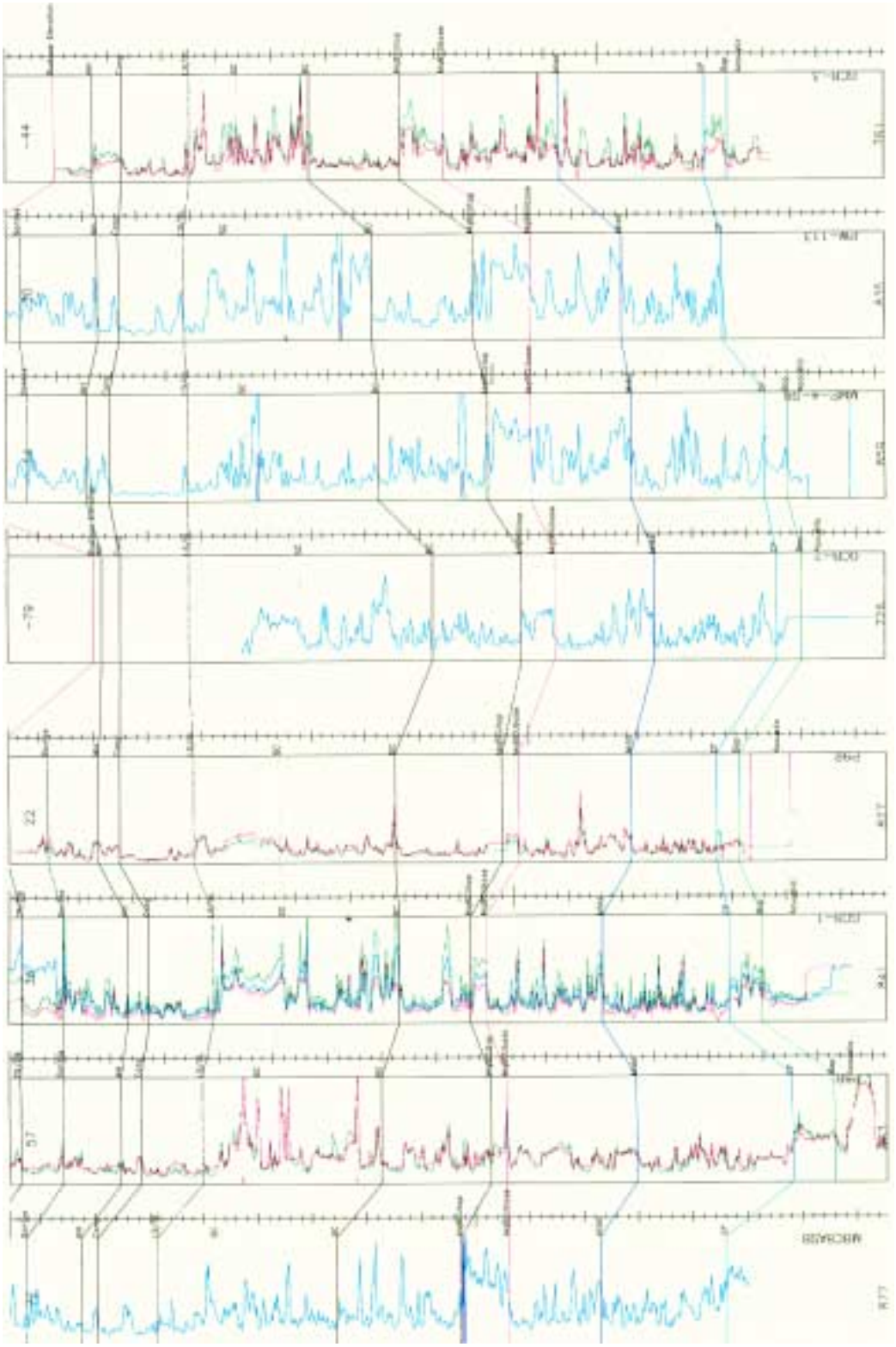

Figure 6. Deep borehole correlation panel flattened on a 30 foot datum relative to mean sea level. Key stratigraphic horizons are labeled. Natural gamma, spectral gamma and/or calculated gamma ray curves are shown.

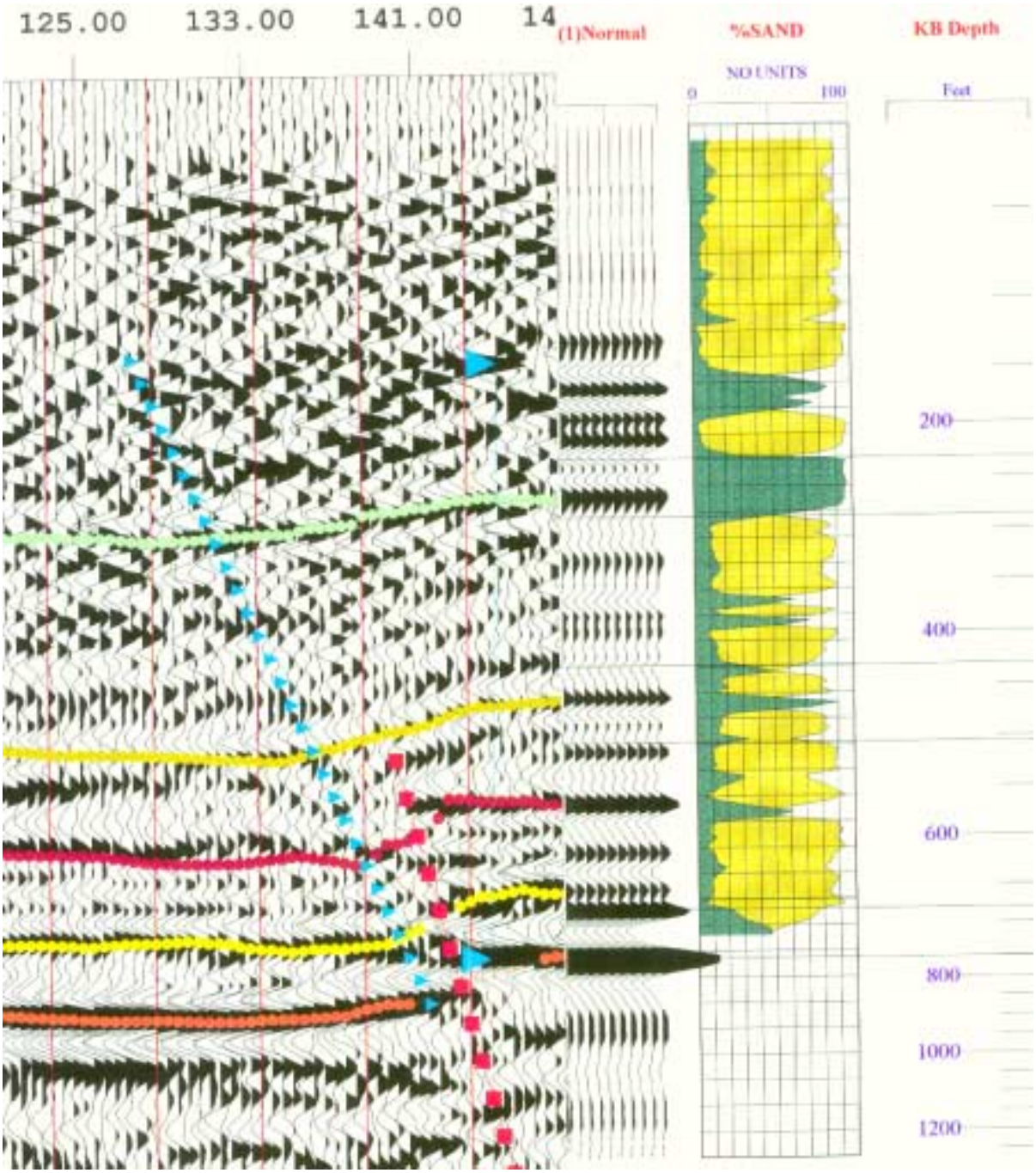

Figure 7. Synthetic seismogram from GCB-1 plotted against seismic line SRS-1 and core data adjacent to the Crackerneck Fault.

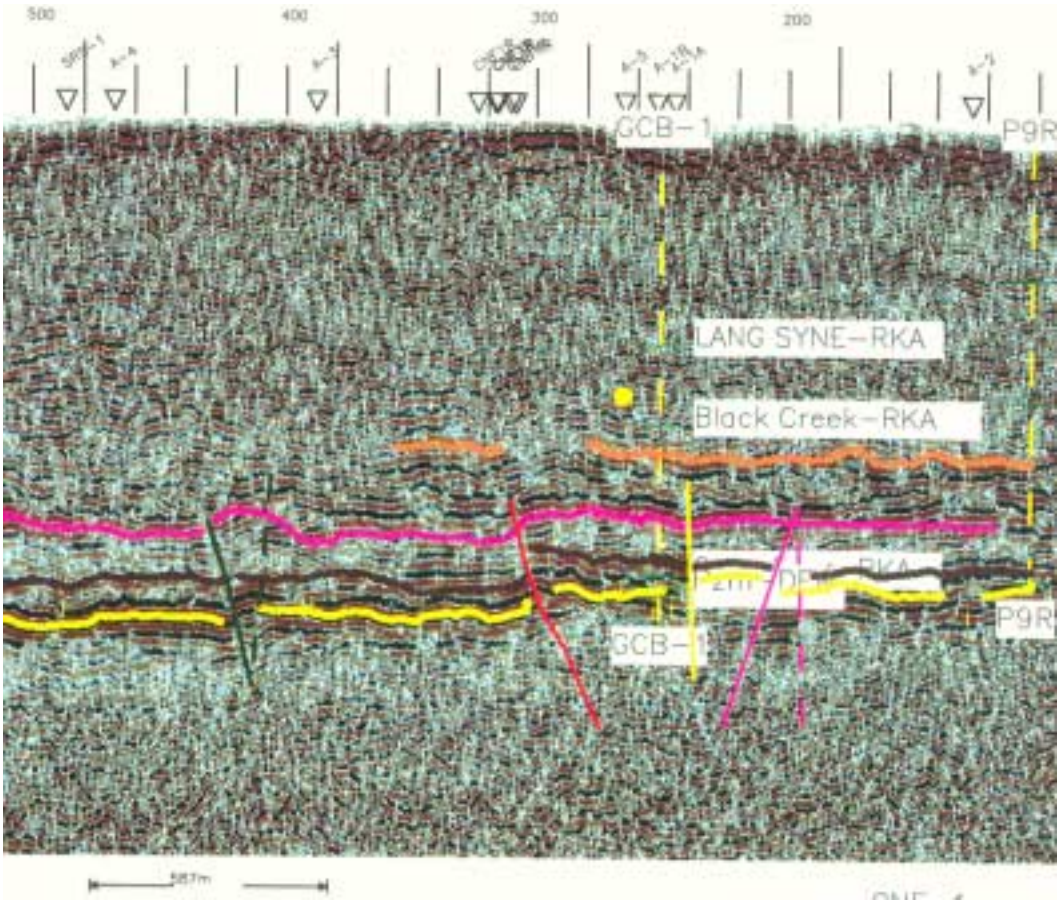

Figure 8. A portion of seismic line A-5, shown as representative of the seismic data distribution shown in Figure 9.

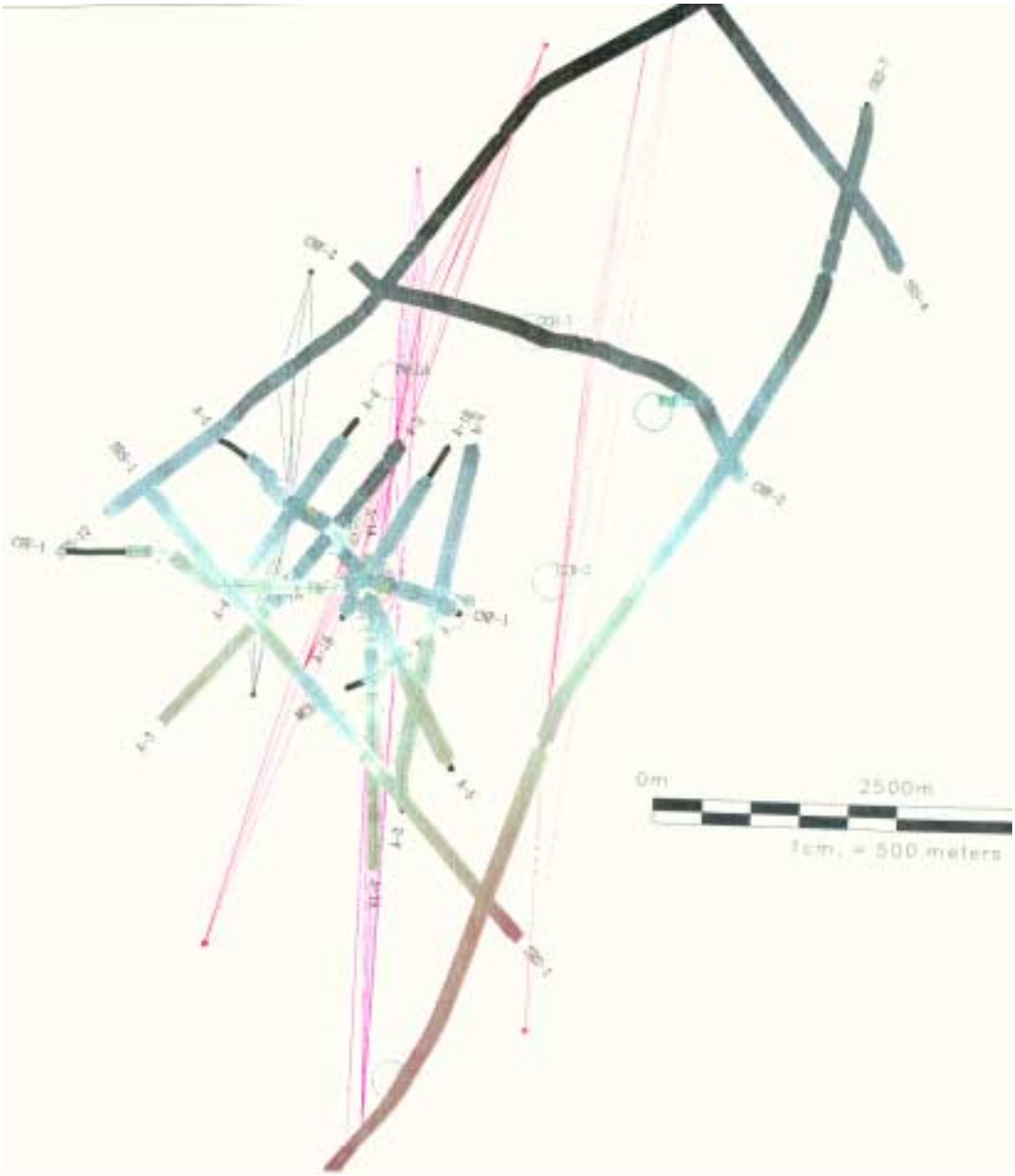

Figure 9. Distribution of seismic data interpreted for this paper. Seismic lines SRS-1, SRS-7, and SRS-12 are regional lines acquired in 1987. Lines CNF-1 and CNF-2 were obtained to help map the Crackerneck Fault system for regional implications and are high resolution data. Lines A-1 through A-5 were obtained to aid in mapping the subsurface associated with the M-Area plume remediation efforts and are also high resolution data. Line MCB-1 was acquired to evaluate the shallow structure and stratigraphy associated with the Miscellaneous Chemical Basin waste unit and to evaluate the use of very high resolution acquisition with a vibroseis source. The shaded colors correspond with calculated depth to crystalline basement, darker colors (blues) are shallower and lighter colors (reds) are deeper. The pink lines crossing the seismic data are the projections of the faults.

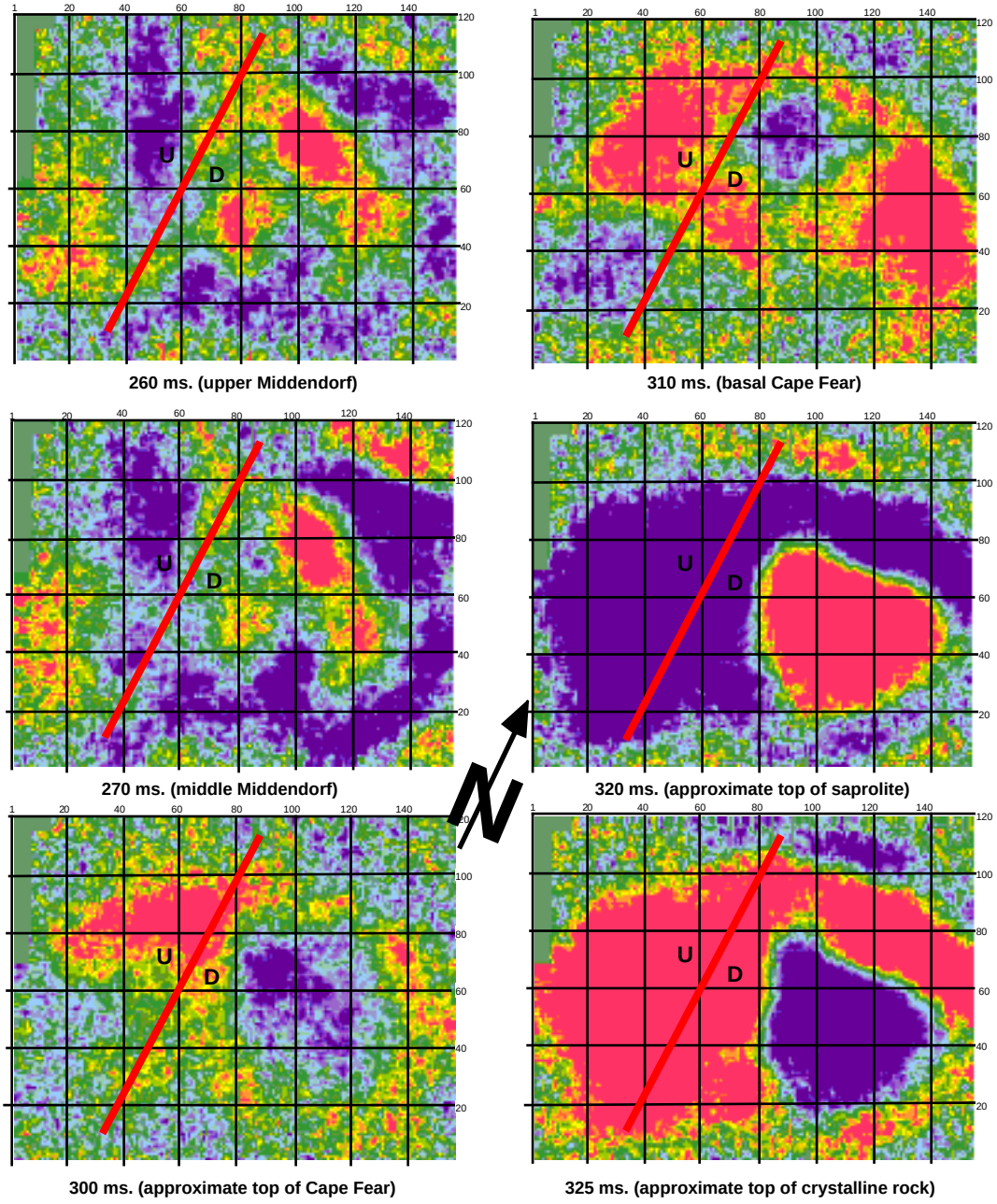

Figure 10. Three dimensional seismic data. Time slices are shown as labeled. Red colors are area of higher amplitude, and blues are lower amplitude. Amplitude changes across the figure suggest either structural or stratigraphic variations.

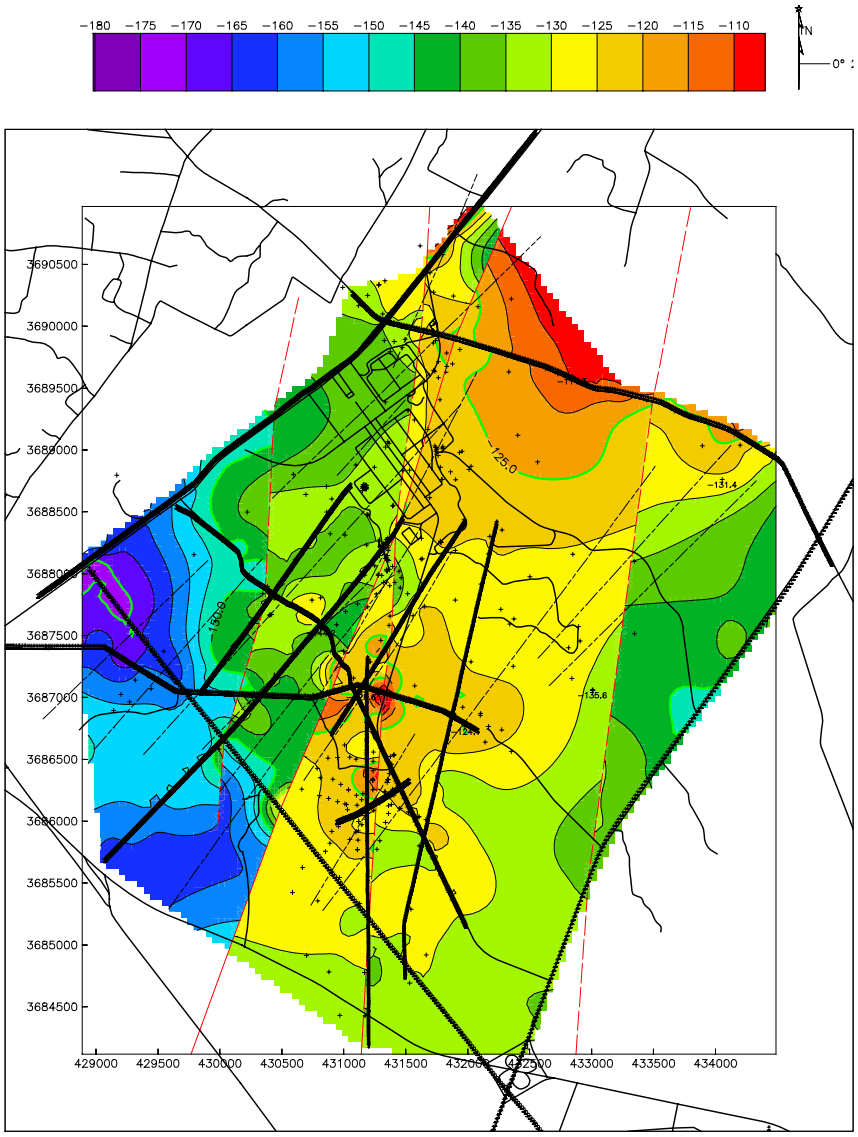

Figure 11. Subsurface map on top of the crystalline basement "rock" as determined from the seismic data and the deep borings. Elevation are in meters relative to mean sea level. The grid is in UTM coordinates. SRS roads are shown for location. The pattern of seismic data is shown by thick black lines (numbered with shotpoints where data has been interpreted). The Crackerneck Fault is shown as a north trending solid thin black line, the MWESTA, Lost Lake and Steed Pond Faults are shown as NNE trending dashed lines. Faults interpreted from the deepest stratigraphic investigation of Aadland (1997) are shown as dotted lines.

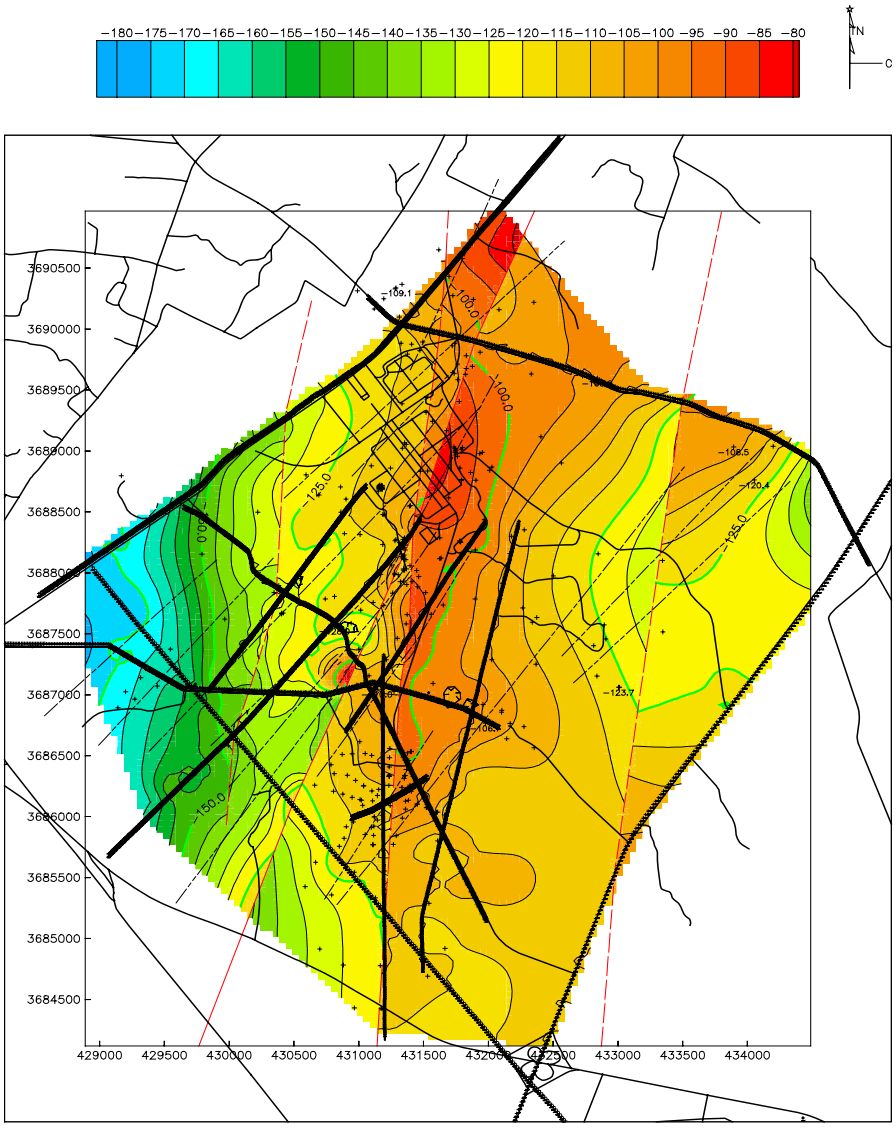

Figure 12. Subsurface map on top of the Cape Fear Formation as determined from the seismic data and the deep borings.

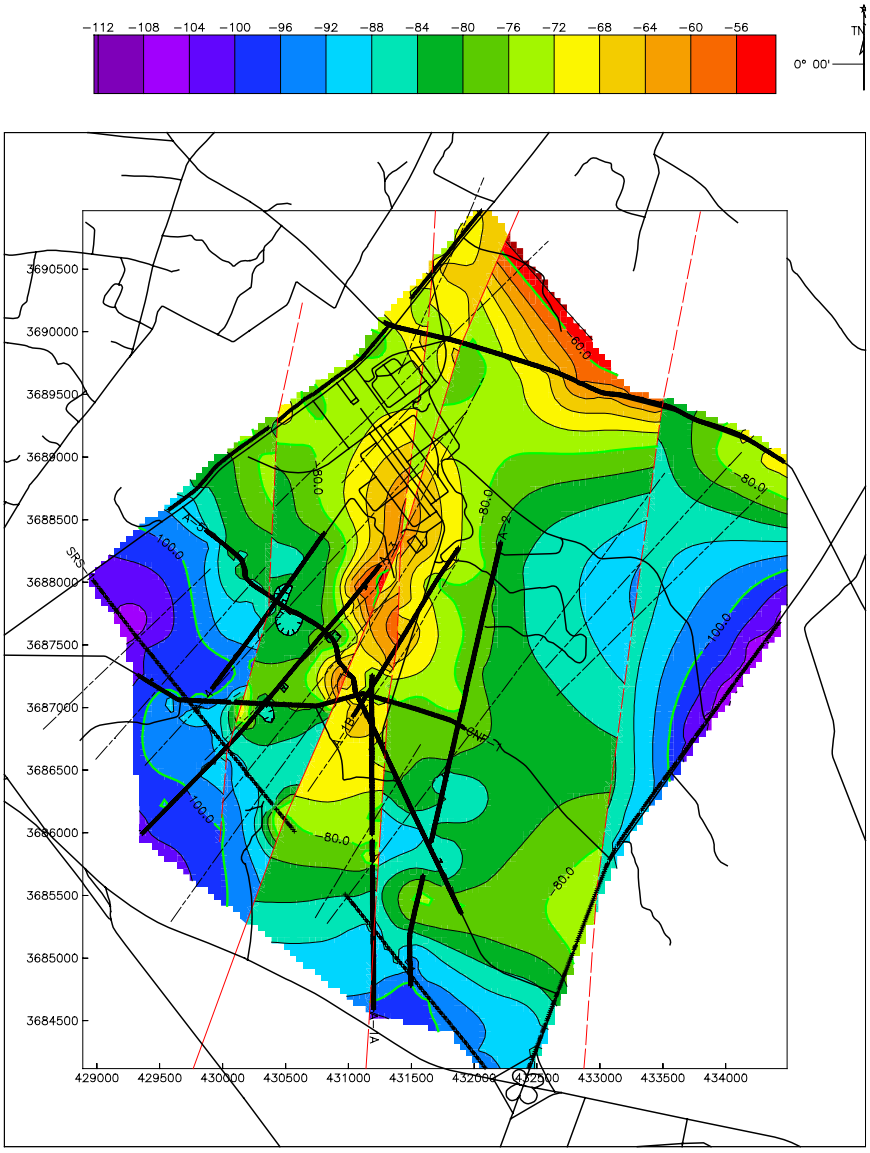

Figure 13. Subsurface map on top of the Middendorf horizon as determined from the seismic data and the deep borings.

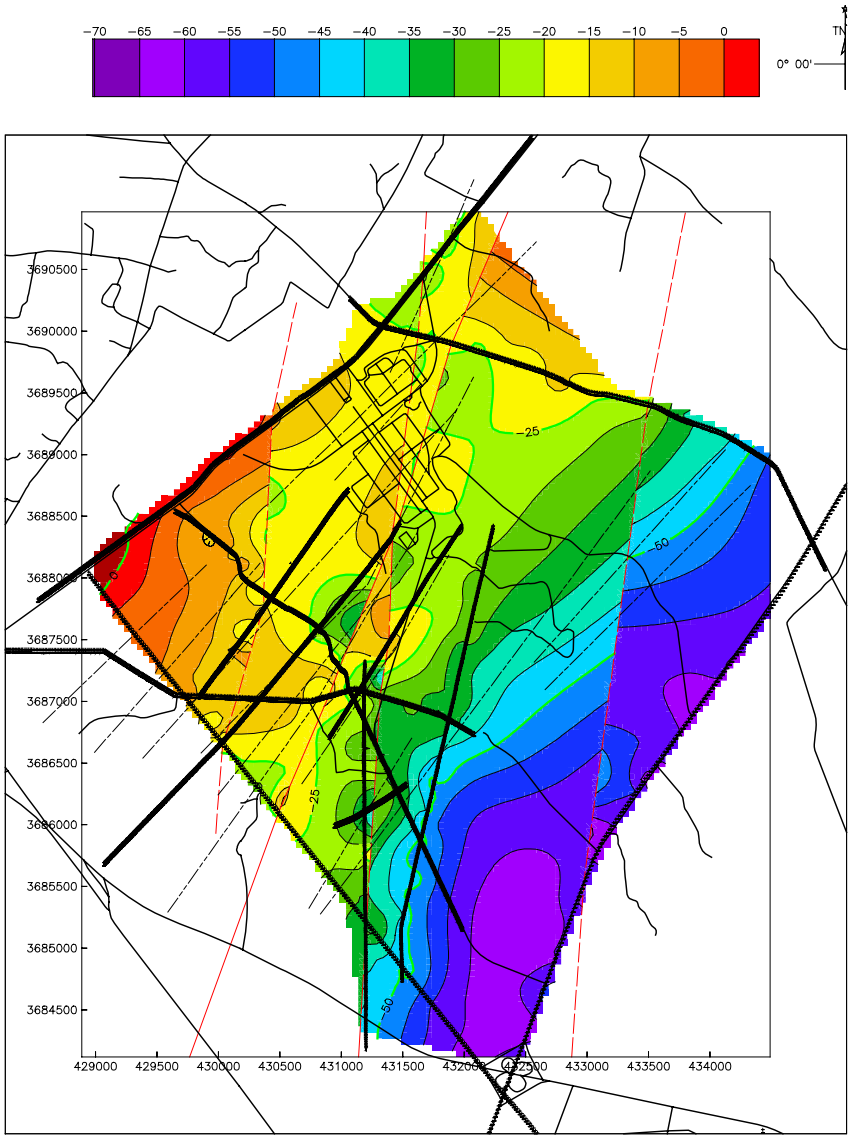

Figure 14. Subsurface map on top of the McQueen Branch Confining Unit as determined from the seismic data and unit penetrating borings.

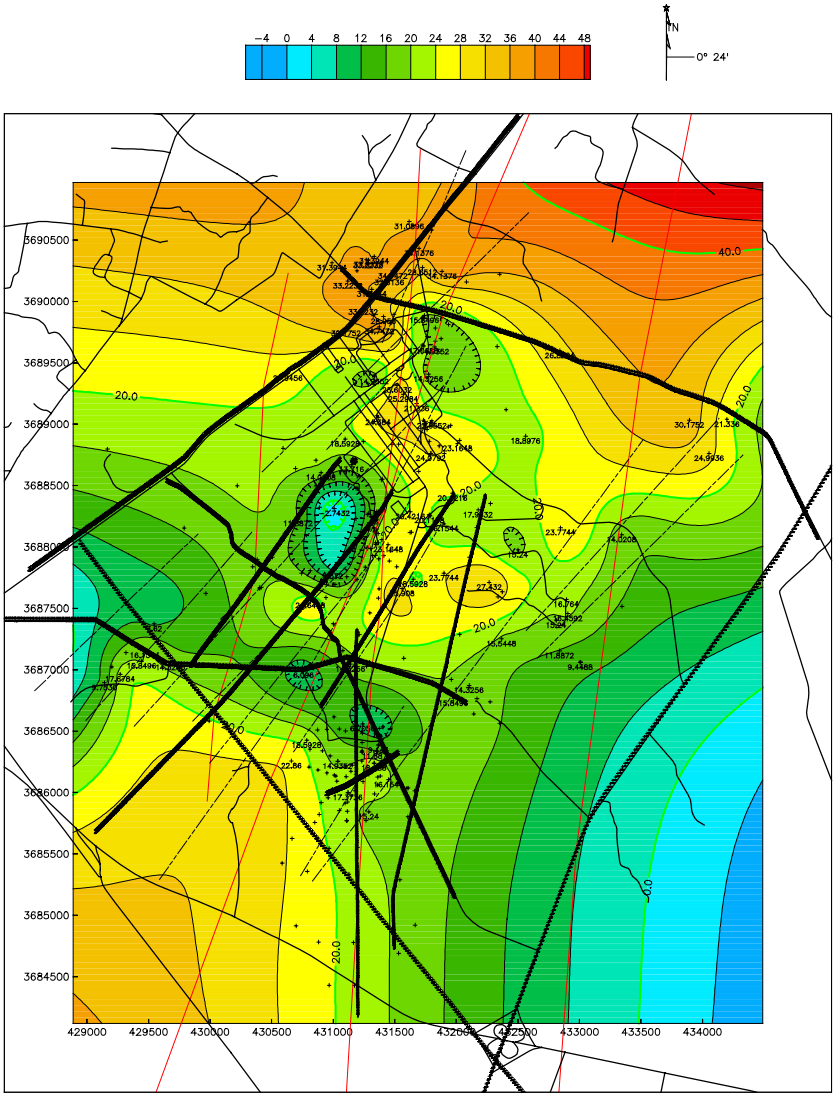

Figure 15. Subsurface map on top of the Steel Creek Formation as determined from the seismic data and unit penetrating borings.

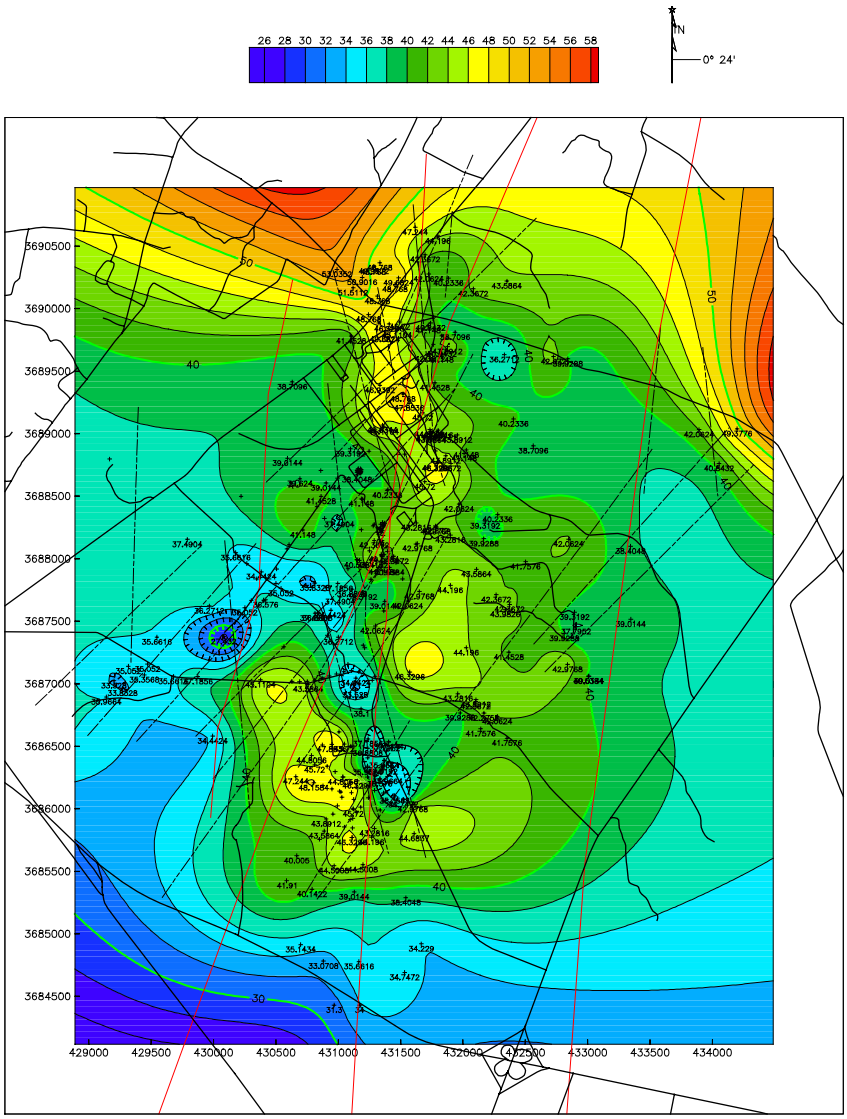

Figure 16. Subsurface map on top of the Lang Syne/Sawdust Landing unconformity as determined from the seismic data and unit penetrating borings.

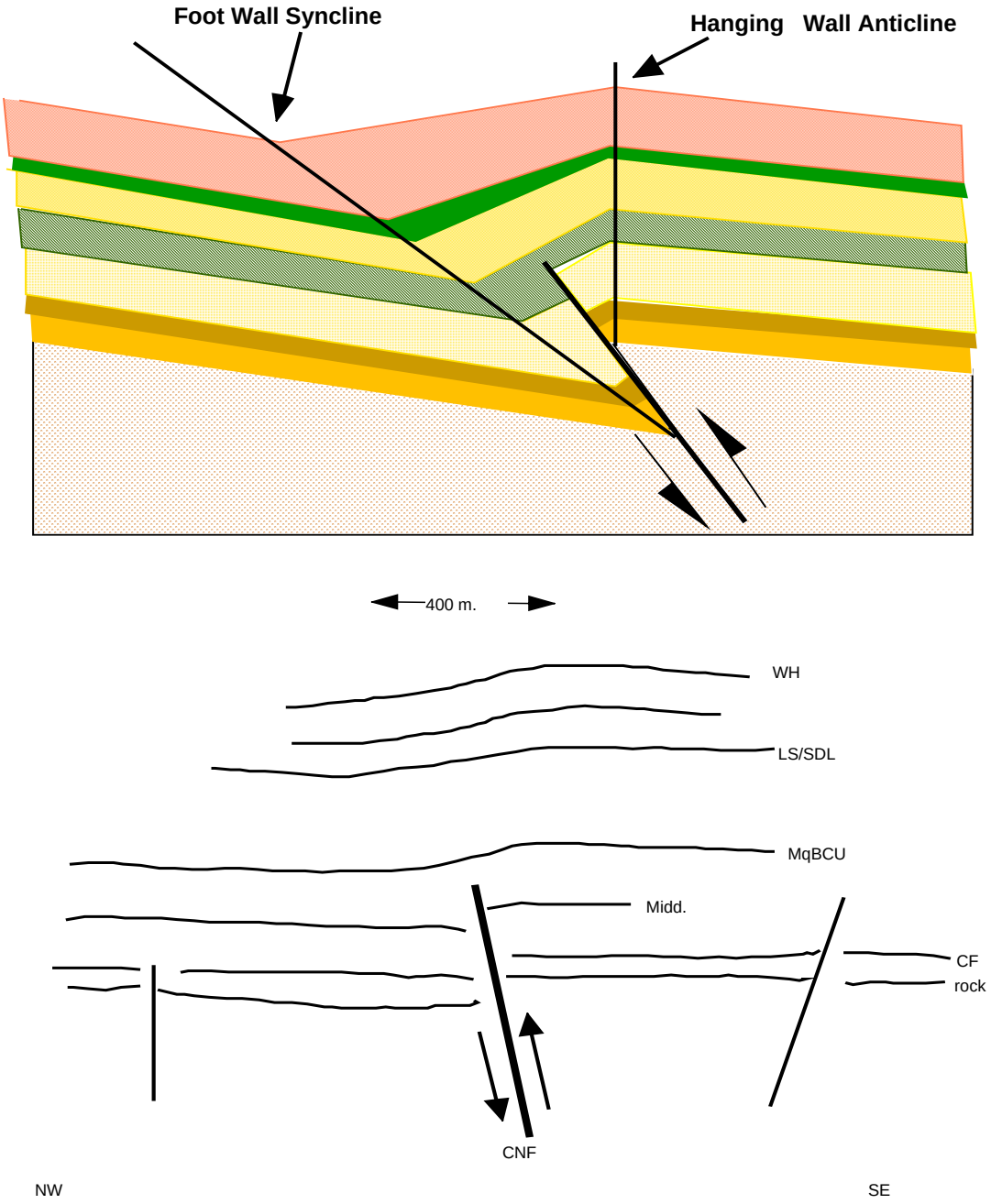

Figure 17. Top figure is fault propagation folding over a reverse fault. (Modified after Cumbest and Wyatt, 1997). The lower figure is the actual seismic horizon schematic from line SRS-1 over the CNF. The horizons are labeled as; "rock" is crystalline basement, "CF" is the Cape Fear Fm., "Midd." is the Middendorf Fm., "MqBCU" is the McQueen Branch Confining Unit, "LS/SL" is the Lang Syne/Sawdust Landing Fm., and "WH" is the Warley Hill Fm. The offset in basement rock is approximately 30-35 m. The distance from the anticline axis to the syncline axis is approximately 400 meters.

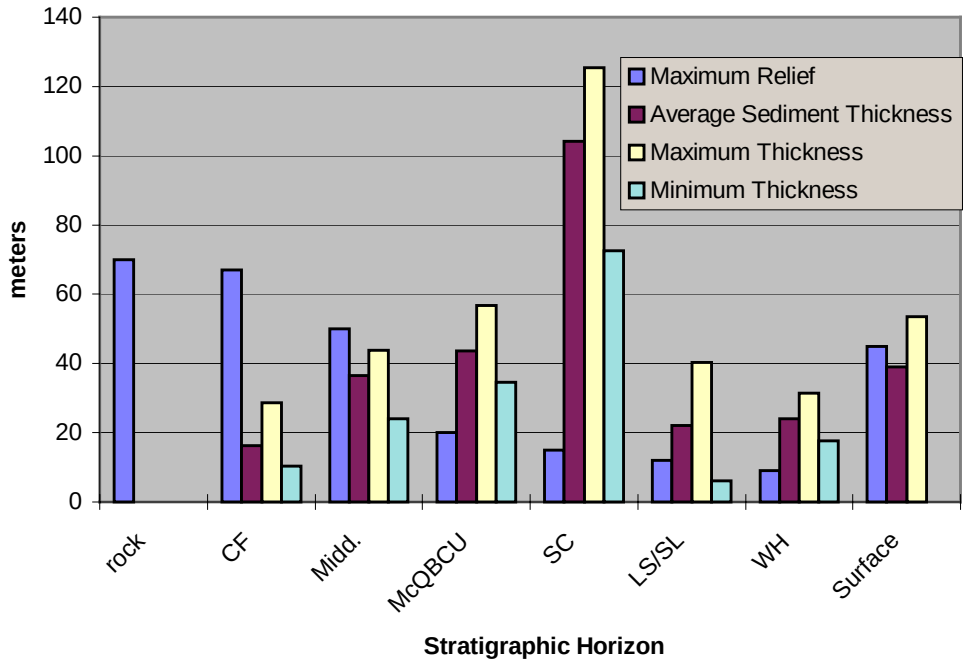

Figure 18. Graph of structural relief, average, maximum and minimum sediment thickness for the mapped stratigraphic horizons. "CF' is Cape Fear, "Midd" is Middendorf, "McQBCU" is McQueen Branch Confining Unit, "SC" is Steel Creek, "LS/SL" is Lang Syne/Sawdust Landing, "WH" is Warley Hill.

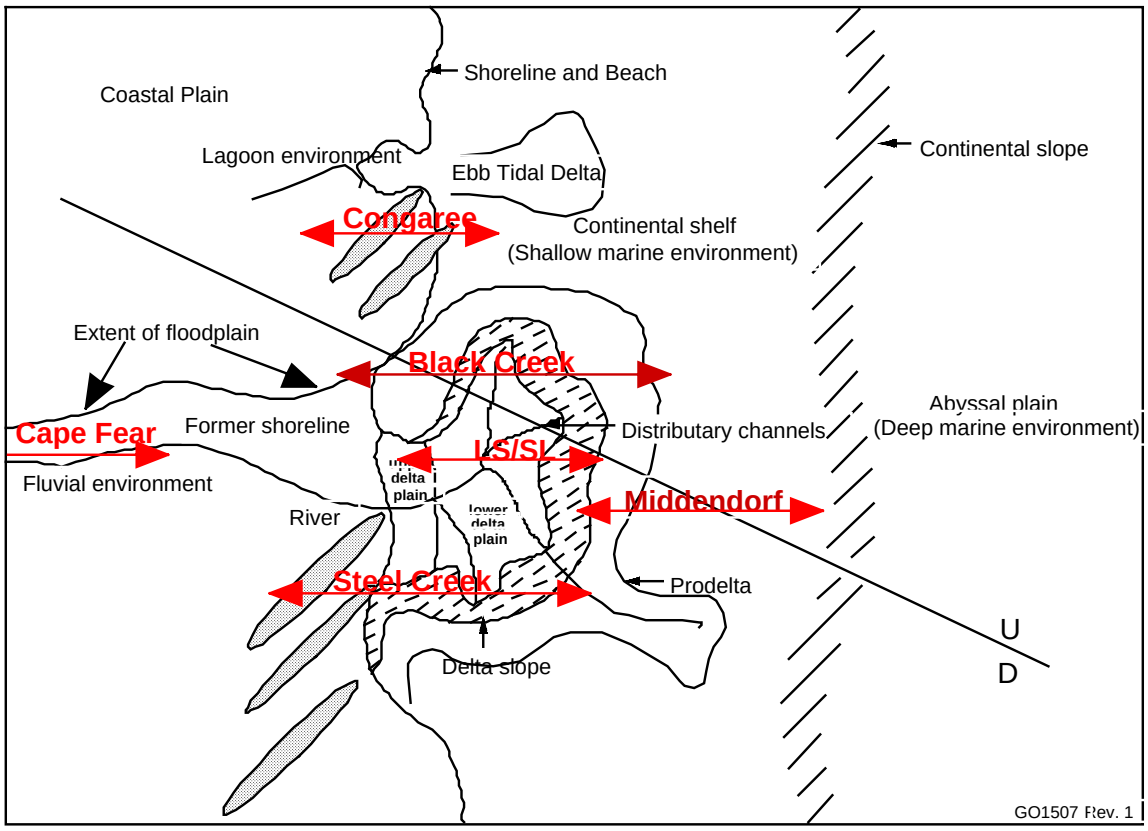

Figure 19. Environments of deposition anticipated within the A/M Area. Figure is modified from Aadland (1997). Stratigraphic units, with the anticipated environments of deposition within the A/M Area are shown in red.

Notes

Use of Seismic Reflection Amplitude Versus Offset (AVO) Techniques to Image Dense Nonaqueous Phase Liquids (DNAPL) at the M-Area Seepage Basin, Savannah River Site, South Carolina

M. G. Waddell, W. J. Domoracki, T. J. Temples, Earth Sciences and Resources Institute, University of South Carolina, Columbia, SC 29208

ABSTRACT

One of the most difficult problems in designing a remediation plan for cleaning up DNAPL contamination is locating the pools of free-phase DNAPL. The seismic modeling of a DNAPL saturated sand versus a water saturated sand suggests that with frequencies of 120 Hz or higher there would be an amplitude versus offset (AVO) anomaly. Seismic survey acquisition parameters for imaging the DNAPL were derived from an AVO model, which was based upon previously acquired seismic and well data. The seismic line was located in such a manner that it started in an area where the unconsolidated sand was water saturated and crossed a known pool of free-phase DNAPL saturated sand and continued back into a water saturated sand. Using a weighted stack processing technique (Smith and Gidlow, 1987) a "fluid factor" stack indicated an anomaly at the depth and location of the known free-phase DNAPL plume. The initial results suggest that under certain conditions free-phase DNAPL can be imaged using high-resolution seismic reflection techniques.

INTRODUCTION

Imperative to any DNAPL remediation effort is the ability to locate high concentrations of contaminants. Traditional techniques such as borehole sampling run the risk of cross-contamination of aquifers. In addition, high concentrations of DNAPL can be missed because of inadequate spatial sampling. Seismic reflection profiling is a geophysical technique that can be conducted to yield horizontal measurements every foot and vertical measurements every 3-5 feet depending on the survey design. The principal data collected from a seismic reflection survey are the arrival time and amplitude of acoustic waves reflected from subsurface. The section can reveal faults, burial channels, and subsurface lows that might influence the migration of DNAPL in the subsurface.

The amplitude and arrival time of seismic waves is dependent on the elastic parameters of the subsurface including bulk modulus, shear modulus, density, Poisson ration, and angle of the incidence of the impinging energy. The last two parameters can, in certain instances, be used to infer the fluid content within the pore spaces. In the Petroleum industry seismic amplitude versus offset (AVO) methods are used to directly detect hydrocarbon bearing strata. In this study we adapt some of these techniques to directly detect the presence of DNAPLs at the United States of Department of Energy Savannah River Site (Waddell and Domoracki, 1997). If these techniques can be found to be applicable to other sites, remediation of DNAPLs can be facilitated and be achieved at lower cost.

Savannah River Site

The Savannah River Site (SRS) is located in South Carolina on the South Carolina- Georgia border. During the Cold War SRS was a major production facility of nuclear materials for defense purposes. Since the late 1980's an emphasis on environmental restoration has led to the development of programs and strategies to remediate DNAPL spill at the site. One area of SRS targeted for remediation is the M-Area seepage basin.

The M-Area seepage basin was constructed in 1958 to contain uranium wastes and residual solvents produced from reactor fuel and target degreasing operations (Fig. 1). An estimated two million pounds of residual solvents were

released into the eight million gallon unlined surface impoundment over a period of nearly thirty years. In 1988 the basin was closed, backfilled, and covered with an impermeable cap. Chlorinated solvents, including free-phase constituents, have been detected in the groundwater near the seepage basin since 1981. The majority of the DNAPL found in the subsurface is composed of Trichloroethylene (TCE), Tetrachloroethylene (PCE), and Trichloroethane (TCA) (Looney, 1992). Environmental remediation strategies have included groundwater pump and treat, soil vapor extraction, in situ air stripping, and in situ biomediation.

The near-surface geology at the M-Area seepage basin is comprised of Eocene age Upper Coastal Plain sedimentary units. On the surface is the "Upland unit" which consists of cobbles and coarse sand ranging in thickness from zero to fifty feet. Underlying the "Upland unit" are the Tobacco Road and Dry Branch formations which are composed of fine to medium grain sand, clayey sand, and discontinuous layers of clay. The amount of clay in the formations decreases with depth. Directly below the Dry Branch Formation is the Warley Hill Formation ranges in thickness from 0 to 10 feet and occurs at a depth of approximately 155 feet below the surface. This clay, when present, is considered the confining unit which separates the overlying surficial aquifer from the semi- to confined aquifer below. The DNAPL in the M-Area pools on top of the "green clay".

OBJECTIVES

The primary objective of this study was to test the feasibility of using high-resolution seismic techniques and direct hydrocarbon indicator analyses to image free-phase and dissolved phase DNAPLs at the M-Area seepage basin. Other objectives were to use the seismic data to map the subsurface geology and to determine the geologic controls on the distribution of the DNAPL.

METHODOLOGY

The approach taken was thee fold consisting of 1) evaluation of existing geological and geophysical data concerning the amount and distribution of DNAPL, 2) seismic modeling to determine whether or not an AVO anomaly would be expected from DNAPL saturated sediments, 3) acquisition and processing of a seismic line designed specially to image the DNAPL.

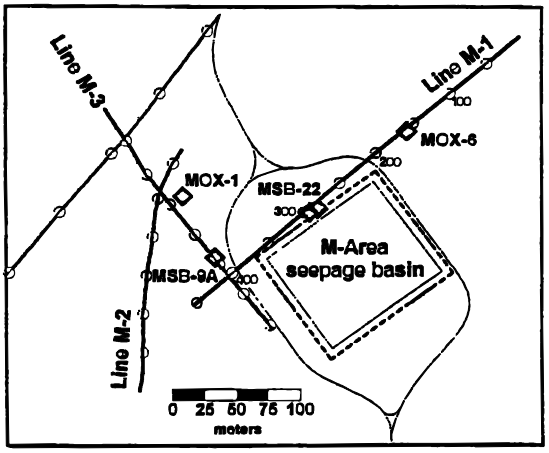

Figure 1. Location map of all the 2-D seismic lines acquired for AVO analysis. Well MSB-3 is adjacent to well MSB-22.

Seismic Amplitude Techniques

In the 1960's petroleum companies recognized that in young sediments (Tertiary age) large seismic amplitudes were associated with gas saturated sands. However, it was soon realized that not all large seismic amplitudes represented hydrocarbon saturated sands. The normal incidence (NI) reflectivity (bright spot) techniques involved three different scenarios based upon a water saturated state and a hydrocarbon saturated state (for this discussion a sand/shale or sand/clay interface). The scenarios are classified by changes in NI reflectivity from a water saturated sand to a gas or hydrocarbon bearing sand.

The three scenarios are:

- Dim-spot- a large positive amplitude that

is reduced to a smaller positive amplitude,

- Phase reversal- a small positive amplitude that changes to small negative amplitude and

- Bright spot- a negative amplitude increasing to a large negative amplitude.

The dim-spot is generally associated with a large acoustic impedance contrast and is a technique for inferring lithology. Bright spot anomalies are generally used for interpreting lithology and estimating sand thickness. Phase reversal reflections are not generally reliable because geologic features (e.g. faults) can cause the reflections to appear to reverse phase. Thus, a reflection phase reversal does not necessarily indicate a change in lithology (Verm and Hilterman, 1995). The bright spot technique was the first direct hydrocarbon indicator.

In 1984 Ostrander published a article entitled "Plane-wave reflection coefficients for gas sands at non-normal angles of incidence." Ostrander observed that the P wave reflection coefficient at the interface between two media varies with the angle of incidence of the impinging energy. Ostrander also investigated the phenomenon of compressional wave reflection amplitude variation with angle of incidence and changes in Poisson's ratio. Poisson's ratio is defined as the ratio of transverse strain to longitudinal strain and can be expressed in terms of P wave and S wave velocity (Sheriff, 1991):

$$\sigma = \frac{\frac{V_p^2}{V_s} - 2}{2\left(\left[\frac{V_p}{V_s}\right]^2 - 1\right)} \qquad (1)$$

σ = Poisson's ratio
V_p= compressional wave velocity
V_s= shear wave velocity

Much of Ostrander's work was based upon Koefoed's 1955 work on determining the reflection coefficients of plane longitudinal waves reflected at a boundary between two elastic media. Koefoed observed that if there were two elastic media with the top medium having a smaller Poisson's ratio than the underlying medium there would be an increase in the reflection coefficient with increasing angle of incidence. He also observed that if Poisson's ratio of the lower medium was lower than the overlying medium, the opposite would occur with a decrease in the reflection coefficient with an increase in the angle of incidence. Another observation showed that the relative change in reflection coefficient increases as the velocity contrast between two media decreases. Koefoed also observed that if Poisson's ratio for two media was increased, but kept equal, the reflection coefficient at the larger angles of incidence would also increase. Ostrander (1984) observed that changes in Poisson's ratio caused by the presence of hydrocarbons in the pore space has dramatic effect on the P wave reflection coefficients and that these effects can be related to seismic amplitude anomalies.

In order to understand amplitude versus offset (AVO) analysis, one has to understand offset dependent reflectivity. Offset dependent reflectivity is defined as the variation of the reflection and transmission coefficients with changing of the incident angle (Castagna and Backus, 1993). The offset refers to source to receiver separation. Increasing source to receiver separation results in increasing angle of incidence for raypaths as measured from the normal to a horizontal interface. Coincident source and receiver locations results in what is termed normal incidence, i.e. vertical transmission and reflection from a horizontal interface. The amplitude of the reflected and transmitted waves are described by the reflection and transmission coefficients. The following discussion describes the equations and theory used to determine amplitude for both the reflected and transmitted waves at an acoustic boundary for normal incident energy and non-normal incident energy, i.e. offset dependent reflectivity. Note that this discussion is for a simplistic model of a single interface. The majority of reflections observed on a seismic profile are the superposition of events from

multiple layers and has a more complex AVO response.

As implemented in the Petroleum industry, AVO analysis involves comparing modeled AVO responses with field data to find a deviation from an expected background response. The expected background response is usually taken to be a water saturated reservoir; hence, the deviation from the expected response is an indication of hydrocarbon presence but does not indicate quantity. DNAPLs have the same acoustic characteristics as liquid hydrocarbons; therefore, if DNAPL is present in free-phase and in large enough quantities, similar types of analyzes as those performed for the petroleum industry can be applied to directly detect the presence of DNAPL.

An understanding of reflection AVO techniques can be obtained by a review of elastic wave propagation. A P wave incident on a boundary between two linear elastic homogeneous isotropic (LEHI) media generates four types of waves: 1) transmitted P wave, 2) reflected P wave, 3) reflected S wave, 4) a transmitted S wave (Figure 3). The amplitudes of the reflected and transmitted waves at the boundary depend upon the P wave and S wave velocities. The density of the two media and the angles of incidence and refraction, are determined from Snell's Law.

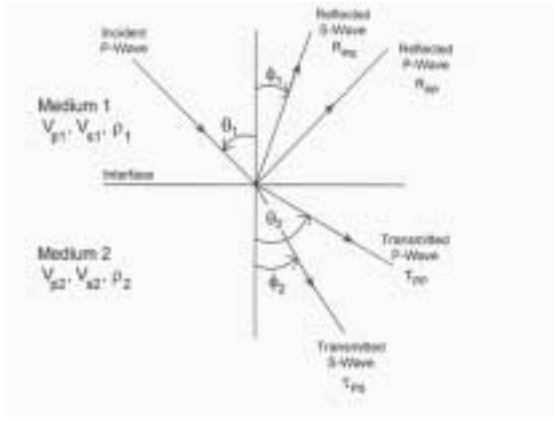

Figure 2. Elastic waves generated at a boundary. A P wave incident at an angle θ on a boundary between two liner elastic homogenous isotopic (LEHI) materials generates four wave types: reflected P, reflected S, transmitted P, and transmitted S. Snell's law from optics governs the angles of reflection and refraction. The P wave velocity, density, and Poisson's ratio describe the material properties of the media. The S wave velocity can be found from the P wave velocity and Poisson's ratio.

Snell's Law,

$$p = \frac{\sin\Theta_1}{V_{P_1}} = \frac{\sin\Theta_2}{V_{P_2}} = \frac{\sin\phi_1}{V_{S_1}} = \frac{\sin\phi_2}{V_{S_2}} \qquad (2)$$

V_{p1} = P wave velocity in medium 1,
V_{p2} = P wave velocity in medium 2,
V_{s1} = S wave velocity in medium 1,
V_{s2} = S wave velocity in medium 2,
Θ_1 = incident P wave angle,
Θ_2 = transmitted P wave angle,
φ_1 = reflected S wave angle,
φ_2 = transmitted S wave angle, and
p is the ray parameter.

The reflection coefficient of the P wave as a function of the incident angle, $R_p(\Theta)$, is defined as the ratio of the amplitude of the reflected P wave to that of the incident P wave (Castagna and Backus, 1993). The P wave transmission coefficient, $T_p(\Theta)$, is the ratio of the amplitude of the transmitted P wave to that of the incident P wave (Castagna and Backus, 1993). The P wave reflection coefficient, R_p ,at normal incidence is given by the following equation:

$$R_p = \frac{I_{p_2} - I_{p_1}}{I_{p_2} + I_{p_1}} = \frac{1}{2} * \frac{\Delta I_p}{I_{pa}} \approx \frac{1}{2} * \ln * \frac{I_{p_2}}{I_{p_1}} \qquad (3)$$

I_{p2} = acoustic impedance of medium 2 = $\rho_2 V_{p2}$
ρ_2 = density of medium 2
I_{p1} = acoustic impedance of medium 1 = $\rho_1 V_{p1}$
ρ_1 = density of medium 1
I_{pa} = average acoustic impedance across the interface = $(I_{p2}+I_{p1})/2$, and
$\Delta I_p = I_{p2}-I_{p1}$.

The P-wave transmission coefficient at normal incidence T_p is given by:

$$T_p = 1-R_p. \qquad (4)$$

The variation of the reflection and transmission

coefficients with incident angle and source to receiver offset is referred to as offset dependent reflectivity (Castagna and Backus, 1993). The values of the reflection and transmission coefficients for non-normal angles of incidence are given by the Zoeppritz (1919) equations. The complexity of the Zoeppritz equations has led to numerous approximations to simplify the calculations. Some of the approximations are Bortfield (1961), Aki and Richards (1980), and Shuey 1985. The Aki and Richards (1980) approximation to the Zoeppritz equations is given below:

$$R(\theta)\_a\ (\frac{\Delta V_P}{V_P}) + b\ (\frac{\Delta \rho}{\rho}) + c\ (\frac{\Delta V_S}{V_S}) \qquad (5)$$

θ = arcsin [(V_{P2} / V_{P1}) $\sin\theta_{incident}$]
a = ½ + $\tan^2\theta$
b= 0.5-[$(2V_S^2 / V_P^2)$ $\sin^2\theta$]
c = -($4V_S^2 / V_P^2$) $\sin^2\theta$
$V_P = (V_{p1} + V_{p2}) / 2$; V_p is P wave velocity
$V_S = (V_{s1} + V_{s2}) / 2$; V_s is S wave velocity
$\rho = (\rho_1 + \rho_1) / 2$; ρ is bulk density
$\Delta V_P = V_{P2} - V_{P1}$
$\Delta V_S = V_{S2} - V_{S1}$
$\Delta\rho = \rho_2 - \rho_1$

In this equation the reflection amplitude is expressed in three terms containing P wave velocity, S wave velocity, and bulk density.

The Aki and Richards approximation (Equation 5) was rearranged by Shuey (1995) to obtain a more convenient form. The Shuey approximation of the Zoeppritz equations stresses the importance of Poisson's ratio as the primary determinant of the AVO response of a reflection (Allen and Peddy, 1993). In this study we used the Shuey approximation, which expresses angle dependent reflectivity in terms of P wave velocity, bulk density, and Poisson's ratio to compute the AVO models.

The Shuey (1985) formula for the reflection coefficient (amplitude) is:

$$R(\theta) \approx R_0 + (A_0 * R_0 + \frac{\Delta\sigma}{1-\sigma^2}) * \sin^2\theta + \frac{1}{2} * \frac{\Delta V_p}{V_p} * \tan^2\theta - \sin^2\theta \qquad (6)$$

$\Delta V_p = (V_{p2} - V_{p1})$ $\theta = (\theta_2 + \theta_1) / 2$

$V_p = (V_{p2} + V_{p1}) / 2$ $\Delta\sigma = (\sigma_2 + \sigma_1)$

$\Delta V_s = (V_{s2} - V_{s1})$ $\sigma = (\sigma_2 + \sigma_1) / 2$

$V_s = (V_{s2} + V_{s1}) / 2$

$\Delta\rho = (\rho_2 - \rho_1)$ $\rho = (\rho_2 + \rho_1) / 2$

$$R_o \approx \frac{1}{2} (\frac{\Delta V_p}{V_p} + \frac{\Delta_\rho}{\rho}) \qquad A = A_0 + (\frac{1}{(1-\sigma)^2}) \frac{\Delta\sigma}{R_0}$$

$$A_0 = B - 2\ (1 + B)\ (\frac{1-2\sigma}{1-\sigma}) \qquad B = \frac{\frac{\Delta V_P}{V_p}}{\frac{\Delta V_p}{V_p} + \frac{\Delta_\rho}{\rho}}$$

V_{p1}= P wave velocity of layer one
V_{p2}= P wave velocity of layer two
V_{s1}= S wave velocity of layer one
V_{s2}= S wave velocity of layer two
ρ_1 = density of layer one
ρ_2 = density of layer two
σ_1 = Poisson ratio of layer one
σ_2 = Poisson ratio of layer two
θ_1 = incidence and transmission angle layer one.
θ_2 = incidence and transmission angle layer two.
R_0 = Normal incidence (NI), i.e. reflection coefficient for zero-offset.
B = is the AVO gradient.
A_0= is the normal incidence amplitude.

The approximation above can be simplified further. If the average Poisson's ratio is assumed to be 1/3 and higher order terms that are insignificant above 30° are dropped, the formula for the angle dependent reflection coefficient becomes:

$$R(\theta) \approx NI + (\frac{9}{4}\Delta\sigma - NI)\sin^2\theta \qquad (7)$$

$$\approx NI + B\sin^2\theta \qquad (8)$$

$$R(\theta) \approx NI\cos^2\theta + PR\sin^2\theta \qquad (9)$$

NI and PR are defined as

$NI = \frac{(V_{p_2}\rho_2)-(V_{p_1}\rho_1)}{(V_{p_2}\rho_2)+(V_{p_1}\rho_1)} = \frac{(z_2 - zSUB1)}{(z_2 + z_1)}$ z is the acoustic impedance: (10)

$$PR = \frac{\Delta\sigma}{(1-\sigma_{avg})^2} \quad (11)$$

(Verm and Hilterman, 1995). Reflection AVO can be thought of a combination of normal incidence reflectivity and a far offset reflectivity, or "Poisson reflectivity," that arises primarily as a result of changes in the Poisson's ratio between media.

To implement AVO analysis, the NI and PR coefficients are extracted from a common depth point (CDP) gather. Initially the CDP gather is transformed from a function of offset to incident angle. This transformation requires knowledge of the root mean square (RMS) velocity, which is ideally obtained from borehole sonic logs. In the absence of sonic logs a rough estimate of the RMS velocity can be obtained from the normal moveout (NMO) stacking velocities. Next, the NI and PR coefficients are found by fitting either Equation (8) or (9) to the amplitudes.

Modeling

The most important aspect to this study is the AVO modeling, which was used to design the field acquisition parameters for seismic profiles M-1, M-2, and M-3. The first type of model was generated using the Aki-Richards (1980) and Smith and Gidlow (1987) approximations to the Zoeppritz equations. The model is a sand wedge saturated with either water or TCE overlying either a clay layer or a water saturated sand (Table 1).

Using the parameters in Table 1, the results of the modeling suggested that there would be an AVO effect caused by the presence of DNAPL (Figures 3,4, 5). Furthermore, these results indicated that changes in the reflection coefficient would begin to occur at approximately 22^0 angle of incidence. Using this information the seismic lines were designed such that half the receivers would be under this incident angle and half would be over.

The second type of model was generated using the P wave, S wave, and density from an existing well. For this type of modeling a synthetic CDP gather was generating using the velocity and density data from the well is shown in Figure 6 (left). To investigate the AVO response caused by the presence of DNAPL a ten foot interval of the logs corresponding to the depth where the DNAPL is accumulating was replaced with the same velocity and density parameters for TCE used to generate the models shown in Figure 3, 4, and 5. Also, the model was convolved with a 120 Hz Ricker wavelet to simulate typical high-resolution seismic data. Figure 6 (right) is the modeled CDP gather for a TCE contaminated sand layer.

Comparison between the synthetic CDP gather models demonstrates that, in this case, an AVO effect can be expected due to the presence of TCE. This AVO effect is manifested as a large increase in amplitude with increasing shot to receiver offset. The increase in amplitude is much larger than if no TCE were present

TABLE 1. Parameters Used to Generate AVO Models

Lithology	V_p	V_s	Density
	ft/s	ft/s	g/cc
Wedge			
Water Sand	5800	1450	1.9
TCE Sand	4968	1634	2.07
Substrate			
Clay	5600	1300	1.85
Water Sand	5600	1460	1.89

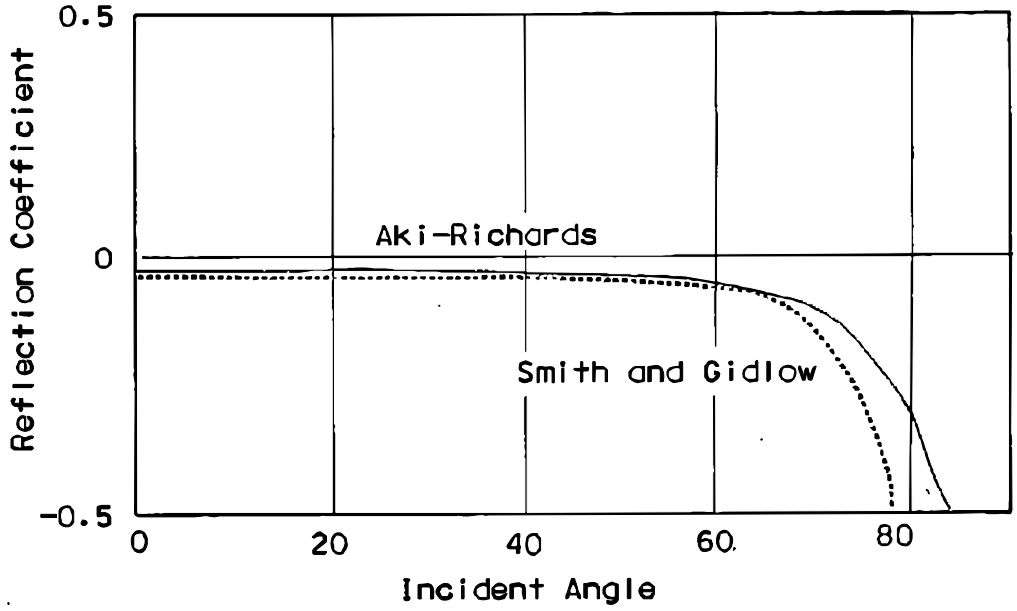

Figure 3. Graph of reflection coefficient versus angle of incidence using the Aki-Richards (solid line) and Smith and Gidlow (dashed line) approximations to the Zoeppritz equations for water saturated sand overlying the "green clay". At the sand/clay interface the reflection coefficient is slightly negative and becomes more negative with increasing angle of incidence. At large angles of incidence (greater than 50°) this effect is pronounced.

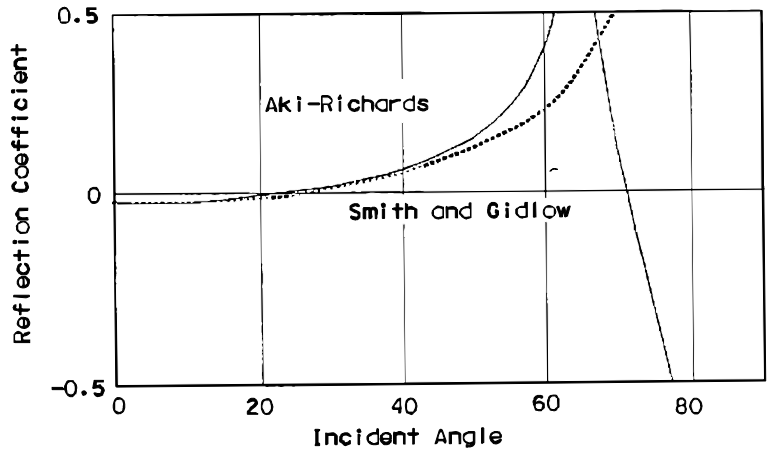

Figure 4. Graph of reflection coefficient versus angle of incidence using the Aki-Richards (solid line) and Smith and Gidlow (dashed line) approximations to the Zoeppritz equations for TCE saturated sand overlying the "green clay". In this scenario, the amplitude is slightly negative, but at 22° the reflection coefficient goes from slightly negative to positive and increases with angle of incidence.

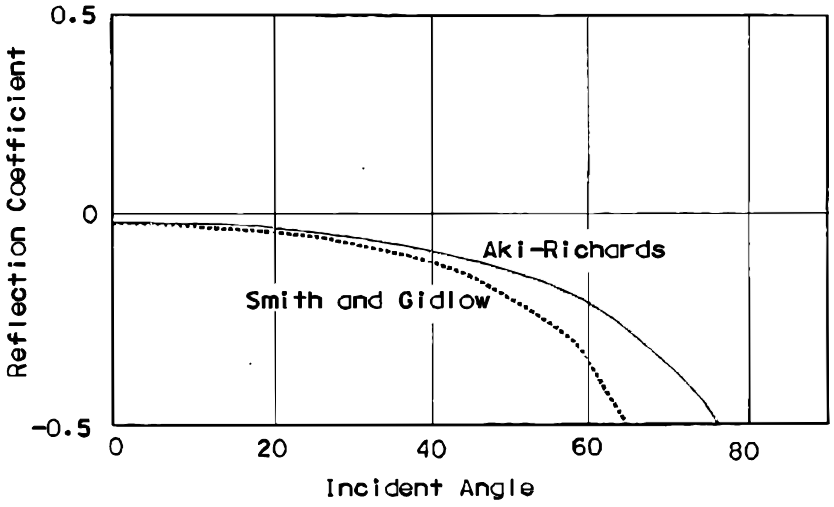

Figure 5. Graph of reflection coefficient versus angle of incidence using the Aki-Richards (solid line) and Smith and Gidlow (dashed line) approximations to the Zoeppritz equations for water saturated sand overlying TCE saturated sand. The reflection coefficient at 0 angle of incidence is near 0º, or is slightly negative, and at 22º becomes increasingly negative.

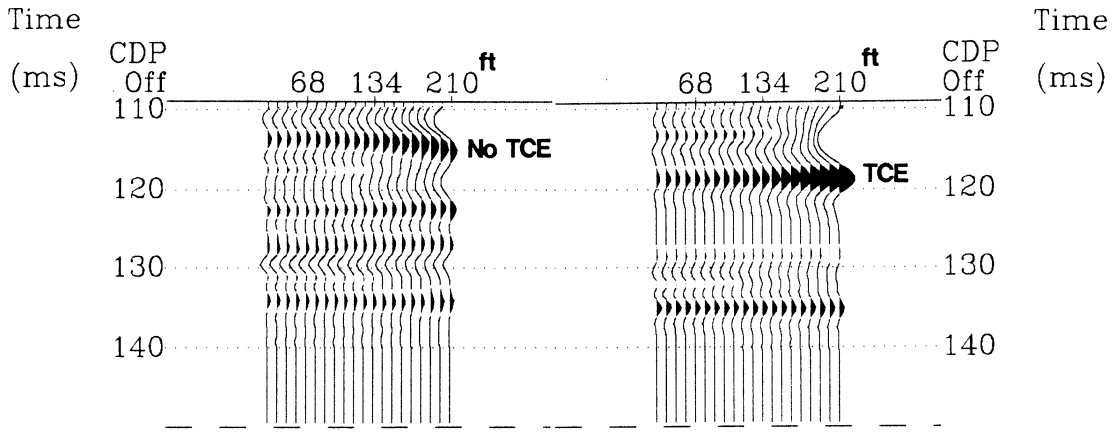

Figure 6. Synthetic CDP gather generated using P wave and S wave velocity logs from well MHM-21 and a density log from nearby well MHT-1. Notice that the reflection at 120 ms has a slight increase in amplitude with increasing offset. The synthetic seismogram on the right is the same as on the left, but the P wave, S wave, and density values have been replaced using the parameters as in Figures 4-5 to simulate a 10 foot section of TCE saturated sediment. Notice that the reflection at 120 ms has a much greater increase in amplitude with offset as a consequence of the presence of TCE.

Seismic Data Acquisition

The original project consisted of recording one seismic profile, line M-1, across a known DNAPL plume that has a free-phase component (Fig. 1). However, after processing M-1 and preliminary AVO analysis (fluid factor stack) was preformed, an AVO anomaly was detected at the location and depth of the known DNAPL plume. As a result, it was decided to acquire two additional lines M-2, and M-3 and a vertical seismic profile (VSP) at well MSB-9A (Fig. 1).

All of the data were collected with a 24 bit OYO DAS-1 seismograph recording either 48 channels (M-1) or 96 channels (M-2 and M-3). The M-Area is a notorious low signal-to-noise seismic data area. Two test lines were shot prior to the acquisition of the M-series lines using mini-vibrator, downhole Seisgun$_{tm}$, and EWG-1 weight drop sources. None of these sources were able to combine the requirements of adequate signal penetration, high frequency content, and minimal source generated noise. Lastly, a 10 lb. Sledgehammer was tested. The sledgehammer was found to be a repeatable high frequency source that generated a relatively small surface wave.

The acquisition parameters for seismic line M-1 appear in Table 2. The parameters such as group spacing , near offset, and far offset, were based upon the modeling results. The target interval was the "green clay" aquitard at approximately 155 feet depth. The recording offsets were chosen in such a way as to have at least 15 to 20 geophone groups under 22^0 angle of incidence so that the AVO analysis described above could be preformed on the seismic lines.

TABLE 2. Acquisition Parameters for Seismic Line M-1

Number of Channels	48
Group interval	2ft.
Shot interval	2 ft.
Near offset	20 ft.
Far offset	114 ft.
Nominal CDP fold	24
Geophone frequency	40 Hz
Energy source	Hammer /8 hits
Sample rate	0.25ms
Record length	500 ms

After line M-1 was processed, modifications were made to the basic recording parameters for acquisition of lines M-2 and M-3. For those lines, a 96 channel recording system was used which allowed a greater range of offsets to be recorded. For lines M-2 and M-3 the minimum and maximum offsets were 29 and 219 feet respectively.

Seismic Data Processing

The seismic data were processed with standard CDP data processing sequence (Yilmaz, 1987) that included frequency-wave number filtering (F-K or pie slice filtering) to eliminate linear noise trains, spiking deconvolution, and iterative velocity analysis and residual statics application. For display, the data were filtered to a 90-275 Hz passband and five point running mean was

applied to enhance the lateral continuity of reflections. To analyze AVO variations, near and far offset stacks were generated as well as Smith and Gidlow (1997) fluid factor stack.

DIRECT DETECTION OF DNAPL

At the M-Area seepage basin two primary types of DNAPL are present below the water table, trichloroethylene (TCE) and tetrachloroethylene (PCE). The latter being the predominate type of solvent. Water samples taken from well MSB-3D (Fig. 1) consisted of a separate phase liquid composed of PCE with a subordinate amount of TCE (Looney, 1992).

In this project two methods were used to investigate any AVO effects caused by the presence of DNAPL. As previously mentioned, the recording geometry was such that 15 to 20 geophone groups were under 22^0 angle of incidence. If the models were correct, there would not be any significant change in amplitude under 22^0 . Method one was ranged limited stacking. In this method data were gathered and stacked using subsets of the range of offsets to produce a near offset section (Fig. 7 top) and far offset section (Fig. 7 middle). AVO anomalies produce by the presence of DNAPL should show as high amplitudes present on the far offset section , but not on the near offset section. The second AVO analysis technique used was the Smith and Gidlow "fluid factor" stack (Smith and Gidlow, 1987) (Fig. 7 bottom).

The "fluid factor" stack is derived from the Aki and Richards (1980) approximation of Zoeppritz equations and the Castagna, Batzle and Eastwood (1985) "mudrock line" for 100% water saturated clastic silicate rocks. In this method a series of time and space variant weighting factors are applied to the CDP gather after NMO (normal moveout) corrections. If the model is valid, the CDP stack will be zero for 100% water saturated clastic sediments. Any residual reflections should denote sediments saturated with fluids other than water. In this project, DNAPL would be the only fluid other than water to saturate or partially saturate the sediments.

Profile M-1 Offset Range Limited Stack

In Figure 7 the upper profile is a near offset stack and the middle profile is a far offset stack. If there are any AVO anomalies, they should be present on the far offset stack and absent on the near offset stack. At shot point (SP) 79 at about 89 ms is an anomaly that was drilled (well MOX-6) and TCE was found to be present. On the near offset stack the anomaly is absent. Another anomaly is shot point 297 at about 109 ms. This anomaly is adjacent to well MSB-3 which had free phase DNAPL. Another anomaly is at shot point 430 at about 110 ms which is believed to be DNAPL, but is as yet untested.

Profile M-1 Smith-Gidlow (Fluid Factor) Stack

Contained in Figure 7 (bottom) is a fluid factor stack based upon the Smith and Gidlow (1987) weighted stack technique. The amplitude anomalies observed on the far offset stack are present. The anomaly observed on the far offset range limited stack at shot point 79 at 89 ms is present as is the other anomalies at shot points 297 at 109 ms and shot point 430 at 110 ms. However, it must be pointed out that any anomaly above 100 ms must be treated with caution, because the fluid factor analysis assumes 100% water saturation. The water table at the M-Area seepage basin occurs at approximately 100 ms; therefore, any anomaly above 100 ms in not at 100% water saturation unless it is perch water.

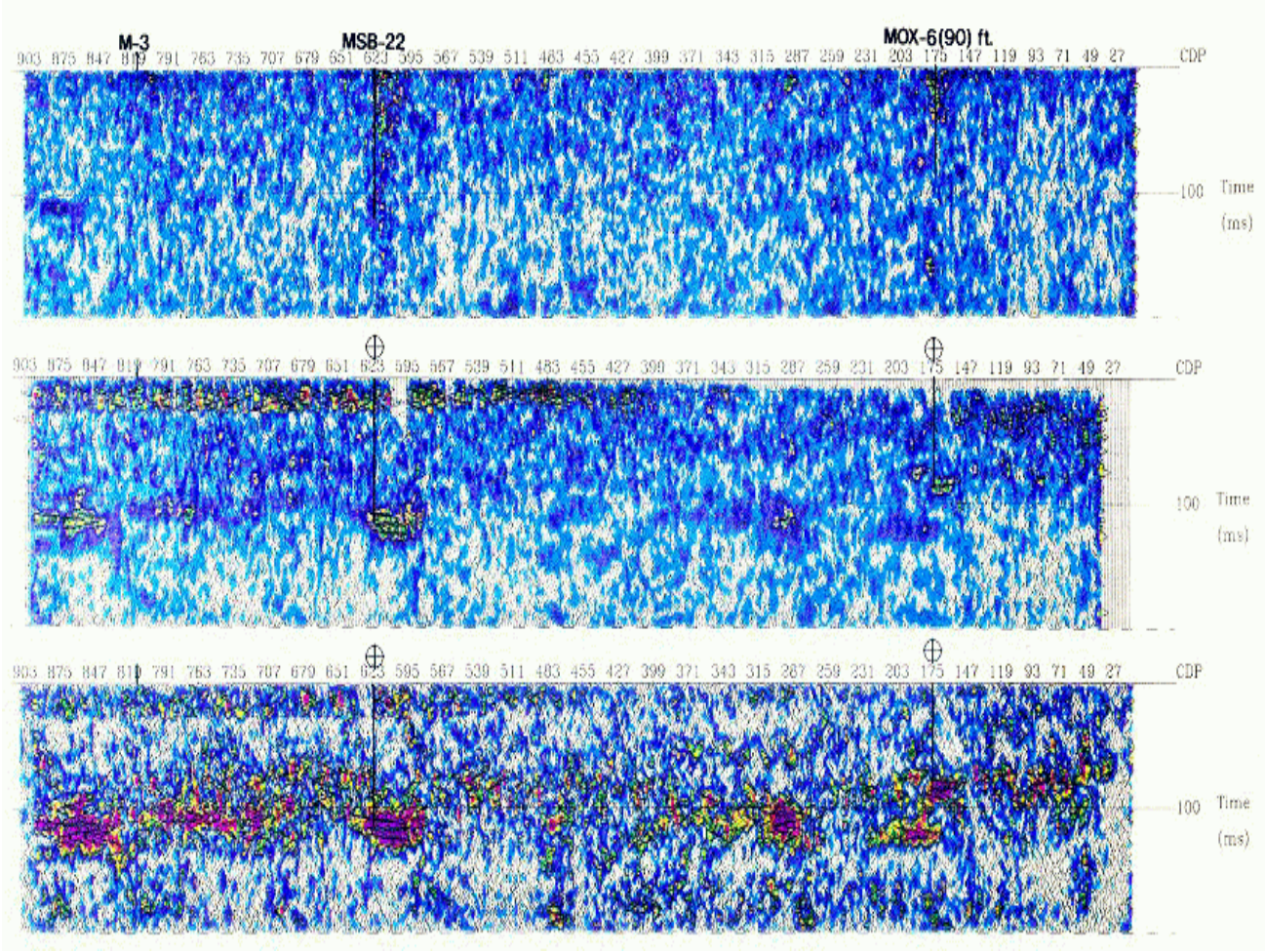

Figure 7. Offset range limited stacks and fluid factor stack for profile M-1. Near offset section (top), far offset (middle), and fluid factor (bottom). The middle section was generated by stacking offsets greater than 58 feet. High amplitudes that occur only at far offsets should denote presence of DNAPL. Every second trace is plotted. CDP spacing is one foot. The bottom section is a fluid factor stack of M-1. The water table occurs at a depth corresponding to approximately 100 ms time. The amplitude envelope (magnitude of Hilbert transform) is displayed.

CONCLUSIONS

At the M-Area seepage basin, Savannah River Site it appears that DNAPLs can be imaged in the subsurface using high-resolution seismic data. Two wells were drilled on anomalies recognized by the seismic data and DNAPLs were found at the predicted depth in parts per million (head space data).

Caution must be exercised in applying this technique to other areas. Before any seismic data are acquired some basic modeling has to be done. The modeling will determine what is the minimum amount of DNAPL that can be imaged given the geologic conditions for a particular site and provide the necessary data for designing seismic acquisition parameters.

ACKNOWLEDGMENTS

Funding for this project was provided by U.S. Department of Energy, Savannah River Site. We would also like to thank Mike Graul at Texseis, Inc. of providing the initial modeling data. We

also thank Landmark Graphics Corporation for donating the ProMAX software, Hampson-Russel Software Services Ltd. for donating their AVO software, and Seismic Micro Technology for donating their KINGDOM software.

REFERENCES

Aki, K. and Richards, P.G., 1980, Quantitative Seismology: W.H. Freeman and Co., San Francisco, 932 p.

Bortfield, R., 1961, Approximation to the reflection and transmission coefficients of plane longitudinal and transverse waves: Geophysical Prospecting, v. 9, p. 485-502.

Castagna, J.P. and Backus, M. M., eds., 1993, Offset-dependent reflectivity - Theory and practice: SEG Investigations in Geophysics No. 8, Society of Exploration Geophysicists, Tulsa, OK, 345 p.

Castagna, J.P., Batzle, M.L., and Eastwood, R.L., 1985, Relationships between compressional-wave and shear-wave velocities in clastic silicate rocks: Geophysics, v. 50, p. 571-581.

Gardner, G.H.F., Gardner, L.W., and Gregory, A.R., 1974, Formation velocity and density-the diagnostic basics for stratigraphic traps: Geophysics, v. 39, p. 770-780.

Koefoed, O., 1955, On the effect of Poisson's ratios of rock strata on the reflection coefficients of plane waves: Geophysical Prospecting, p. 381-387.

Looney, B.B., 1992 "Assessing DNAPL Contamination in A/M Area, SRS: Phase 1," WSRC-RP-92_1302, Prepared for the U.S. Department of Energy under Contract No. DE-AC09-89SR18035, p 1-85.

Mavko, G., Mukerji, T. and Dvorkin, J., 1998: The Rock Physics Handbook: Cambridge University Press, p 1-220.

Ostrander, W.J., 1984, Plane-wave reflection coefficients for gas sands at non-normal angles of incidence: Geophysics, v. 49, p. 1637-1648.

Rutherford, S.S. and Williams, R.H., 1989, Amplitude-versus-offset variations in gas sands: Geophysics, v. 54, p. 680-688.

Sheriff, R, 1991, Encyclopedic Dictionary of Exploration Geophysics: SEG Geophysical Reference Series No. 1, Society of Exploration Geophysicists, Tulsa, OK, 376 p.

Shuey, R.T., 1985, A simplification of the Zoeppritz equations: Geophysics, v. 50, p. 609-614.

Smith, G.C. and Gidlow, P.M., 1987, Weighted stacking for rock property estimation and detection of gas: Geophysical Prospecting, v. 35, p. 993-1014.

Verm, R. and Hilterman, F., 1995, Lithology color-coded seismic sections: The calibration of AVO crossplotting to rock properties: The Leading Edge, v. 14, n. 8, p. 847-853.

Waddell, M.G, Temples, T.J., and Domoracki, W.J., 1997, Using high-resolution reflection seismic to image free-phase DNAPLs at the M-area, Savannah River Site (Abstract): Ann. Mtg. Am. Assoc. Petroleum Geologists, Dallas, TX.

Waters, K.H., 1981, Reflection seismology: A tool for energy resource exploration: John Wiley and Sons, New York, 453 p.

Zoeppritz, K., 1919, Uber reflexion und durchgang seismischer wellen durch Unstetigkerlsflaschen: Berlin, Uber Erdbebenwellen VII B, Nachrichten der Koniglichen Gesellschaft der Wissenschaften zu Gottingen, math-phys. K1., p. 57-84.

Geology: Improving Environmental Cleanup of the A/M Area, Savannah River Site

Mary K. Harris[1], D. G. Jackson[1], Brian B. Looney[1], Andrew D. Smits[2], and R. S. VanPelt[3]

[1]Savannah River Technology Center, Aiken SC
[2]Science Applications International Corporation, Augusta GA
[3]Environmental Restoration Division, Savannah River Site, Aiken SC

Introduction

Successful environmental cleanup programs rely on an interdisciplinary team of scientists – geologists, engineers, chemists, mathematicians, and others. The solutions developed by the team are based on focused environmental characterization followed by selecting and deploying clean-up technologies that are matched to the problem. Each technological advance is grounded in a clearly stated conceptual model that is continually developed and refined using the scientific method. Successful technologies always obey natural laws, and often rely on natural processes or capabilities. In the work, geology plays a particularly important role. Stratigraphy and hydrostratigraphy control both the migration of contaminant plumes and the performance of cleanup technologies. Understanding depositional processes and post-depositional alterations – erosional features and the like – are critical to proper selection and optimization and ultimate success of cleanup. Cleanup of the A/M Area of the Savannah River Site exemplifies both the interdisciplinary nature of the work, as well as the pivotal role of geology.

Objective

The primary goal of geological support in the A/M Area is to assist in safe and effective operations and in environmental stewardship. This overall objective requires comprehensive geological activities including both basic and applied studies. These include a wide variety of invasive, noninvasive and data interpretation tools. In the sections, below, we introduce the general philosophy for the A/M Area environmental clean-up program, present a brief background of A/M Area, provide a summary of the local geologic conditions, and provide detail from a few specific A/M area geology studies. In the conclusions, we relate the various geological findings to specific clean-up technology and implementation decisions within the program.

Anatomy of a Contaminated Site

Figure 1 depicts a conceptual diagram of a contaminated site that has impacted its surroundings – in this case, the underlying soil and groundwater. The three ovals – the source zone, the primary contaminant plume, and the dilute fringe – represent different portions of the impacted environment that each have a different character. The source zone contains significant contamination in concentrated and hazardous forms. The source zone can contain materials such as undissolved organic liquids (oils, fuels or solvent), strong acids or bases, high levels of radiation, and/or toxic chemicals or elements. The second oval, the primary contaminant plume, is comprised of contaminated groundwater or vapor that carries pollutants at lower levels, but levels that still represent a potentially significant present or future hazard. The third oval, the dilute fringe, contains contamination at relatively low concentrations, but in large volumes of water.

Efficient and effective environmental clean up requires matching the character of the clean-up and stabilization methods to the character of the target zone of contamination. Thus, aggressive and relatively expensive methods are often appropriate for the source zone,

classical pump-and-treat methods are often good for the primary contamination zone, and various methods based on natural processes are often best for the dilute fringe. Figure 1 identifies several example technologies that are appropriate for each of the zones.

Figure 2 extends this conceptual model by identifying the cost basis for the typical clean up technologies. In the source zone, stabilization and removal methods are normally priced in terms of volume of soil or amount of contaminant in the treatment zone ($ per cubic yard treated, $ per pound and the like). The reference source zone technologies require aggressive access and subsequent use of targeted energy or chemical reagents. It is clear that in the source zone it is important to characterize the site in such a way that the precise location of the source zone is delineated as carefully as possible as increases in treatment volume result in additional remediation costs. Detailed source characterization reduces costs by focusing energy or reagent to areas where they are needed. Equally important, however, is a desire to minimize any undesired negative impacts (wasting energy, harming microbiological populations, etc.) associated with using aggressive remedies on regions without source level contamination.

In the primary contaminant plume, treatment technologies are normally priced in terms of the amount of water (or vapor) treated ($ per gallon and the like). Thus, the goal of characterization in this portion of the plume is to define the flow directions and general plume structure to allow the most contaminant to be treated in the fewest “gallons”. Figure 3 illustrates an important-final extension to our simplified conceptual model. This diagram of the primary contaminant plume in A/M Area shows that contamination moves in response to many factors – contaminant release location and type, geology, sources and discharges of water, and others. The resulting contaminated soil and groundwater zone occupies a complicated three-dimensional shape rather than the simple ovals that we began with. This complexity must be recognized when developing and implementing technologies for both characterization and clean up of the primary contaminant plume.

The dilute fringe contains low concentrations of contamination in large volumes of water. Thus, the best technologies for this zone are those that are priced in terms of time ($ / year and the like). To be successful, these technologies must rely on natural-sustainable-measurable processes. This class of technology has gained recent regulatory support under the terminology “monitored natural attenuation”. For the dilute fringe, technology selection is biased toward understanding the contaminant destruction and stabilization capabilities of native species and natural populations. A second step is identifying engineering interventions, if needed, to maximize the performance and to assure that the attenuation process will operate for extended periods. As a consequence, logical and cost-effective monitoring strategies are critical to the success of “natural attenuation” technologies.

The three zones depicted in Figure 1 are present at contaminated sites of all sizes. At a “mom-and-pop” gas station, the entire contaminated zone – all three ovals – might occupy a portion of a city block. At a large industrial facility like the A/M Area at SRS, the contaminated zone can extend over a few square miles. The size of a problem impacts how distinct the actions to address the different zones need to be. Time is also a factor. Concentrations change, as cleanup progresses, so that dilute fringe technologies become appropriate for polishing areas that were formerly at higher concentrations.

General Background on A/M Area

The Savannah River Site (SRS) is a U.S. Department of Energy (DOE) facility that was set aside in 1950 as a controlled area for production of nuclear materials for national defense. This report focuses on the A/M Area at the north boundary of the SRS (Figure 4).

This area includes the facilities which were used for fabrication of reactor fuel and target assemblies (M Area), laboratory facilities (SRTC), and administrative support facilities (A Area). Operations within the A/M Area resulted in the release of chlorinated solvents to the subsurface (Marine and Bledsoe, 1984). Released solvents include trichlorethylene (TCE), tetrachloroethylene (PCE) and 1,1,1-trichloroethane (TCA) which have contaminated the soil and groundwater within the area. Since the detection of these volatile organic compounds (VOCs), the SRS has pursued a program of soil and groundwater remediation.

The SRS remediation program integrates technologies to address various portions of the contaminant plume conceptually presented earlier. Within the immediate source zone a series of soil-vapor extraction units are combined with enhanced source removal/destruction methods, and an extensive network of groundwater recovery wells. This combination provides for the removal of contaminants in the vadose zone and reduces additional migration in the groundwater. The extensive groundwater pump & treat system also provides for the extraction and treatment of contaminated groundwater in the primary contaminant zone. A series of vertical recirculation wells treats groundwater before it enters the dilute fringe. SRS maintains an on-site research and demonstration program for developing innovative remediation techniques and maximizing the efficiency and effectiveness of the SRS remediation strategy. The SRS remediation strategy includes on-going characterization of subsurface features and conditions that may have a significant influence on groundwater flow and contaminant transport.

Recent characterization efforts emphasize locating dense non-aqueous phase liquid (DNAPL) in the subsurface beneath A/M Area (Looney and others, 1992). Upon release at the surface, DNAPL migrates down through the vadose zone into the saturated zone. The relatively high density of the DNAPL causes it to move in an overall vertical direction, following a “path of least resistance” through zones of highly permeable gravel and coarse-grained sand. The DNAPLs tend to slow and spread laterally upon encountering strata composed of less-permeable silty sand and clay (Jackson and others, 1996). Potential migration paths and distribution of DNAPL are therefore related to the distribution and configuration of less-permeable, fine-grained sediment.

Once emplaced within the saturated zone, DNAPLs serve as a source for the release of dissolved VOCs to the groundwater. The groundwater carries dissolved VOCs as plumes, which emanate from the DNAPL source and extend in a direction corresponding to the local hydraulic gradient. Movement of VOC-contaminated groundwater is largely controlled by the geometry and distribution of more permeable strata, the nature and extent of the DNAPL source, and the overall dynamics of water recharge and discharge from the subsurface system.

The distribution of fine-grained sediment layers and variations in the quantity of clay and silt within the sediment is extremely important in order to fully characterize the extent of DNAPL layers beneath the A/M Area and determine the geometry of the contaminant plumes emanating from them. Indirect assessment techniques have been applied to historical groundwater concentrations in the A/M Area and indicate that the distribution of DNAPL beneath A/M Area may be laterally extensive (Jackson and others, 1996). The delineation of layers of less-permeable sediment is therefore critical to aid remediation efforts. Detailed mapping of these geologic features can aid in locating areas where contamination is most likely to have migrated into the saturated zone. These data are valuable aids for accurate modeling of groundwater flow and contaminant transport. In addition, this information can be used to refine the current remediation systems

or assist in designing new ones. The results of a recent geospatial mapping study are presented below to exemplify the work in A/M Area.

A/M Area Geological Setting

The SRS comprises approximately 300 square miles within Aiken, Barnwell, and Allendale counties in southwestern South Carolina. The center of the SRS is 22.5 miles southeast of Augusta, Georgia, approximately 100 miles from the Atlantic Coast within the Upper Atlantic Coastal Plain Physiographic Province (Figure 4). The Savannah River forms the southwest boundary of the SRS. The SRS lies on the Aiken Plateau of the Atlantic Coastal Plain at an average elevation of 300 feet above mean sea level (ft msl). The Aiken Plateau is well drained, although many poorly drained sinks and depressions exist, especially in upland areas. Overall, the Aiken Plateau displays highly dissected topography, characterized by broad inter-fluvial areas separated by narrow, steep-sided valleys. Local relief can attain 280 feet (Siple, 1967).
The A/M Area comprises approximately eight square miles near the northern boundary of the SRS (Figures 4 & 5).

Lithostratigraphy
The SRS is underlain by sediment of the Atlantic Coastal Plain. The Atlantic Coastal Plain consists of a southeast-dipping wedge of unconsolidated and semi-consolidated sediment that extends from its contact with the Piedmont Province at the Fall Line to the edge of the continental shelf. These deposits consist of sediment that is deltaic and near-shore marine in origin, with evidence of considerable fluvial influence (Fallaw and Price, 1995). The sediment consists of interbedded sand, muddy sand, and mud (clay and silt), with a subordinate amount of calcareous sediment. Strata range from Late Cretaceous to Miocene in age and rest unconformably on crystalline and sedimentary basement rock (Figure 6). The A/M Area lies within the up-dip area of the coastal plain deposits, approximately 20 miles from the Fall Line. Beneath the A/M Area, Cretaceous-aged strata rest on crystalline basement rock at a depth of 500 to 700 feet below the land surface (ft bls). For a detailed discussion of the lithostratigraphy the reader is referred to Wyatt, 2000 (this volume). This paper will concentrate on the hydrostratigraphy of the A/M Area.

Hydrostratigraphy
The hydrostratigraphy of the SRS has been the subject of several different systems of hydrostratigraphic classification. This report incorporates the hydrostratigraphic nomenclature currently established for the SRS region and A/M Area by Aadland and others (1995a, 1995b). This study focuses on the up-dip part of the Floridan-Midville aquifer system as defined for A/M Area by Aadland and others (1995b). Strata within units of the Floridan-Midville aquifer system that exhibit internally consistent hydraulic characteristics and which, on a local scale, behave as distinct hydrostratigraphic units, are delineated as informal aquifer and confining zones (Aadland and others, 1995b). Figure 6 correlates the nomenclature of Aadland and others (1995b) with the lithostratigraphy of Fallaw and Price (1995).

The hydrostratigraphy of the A/M Area consists of three aquifers within the Floridan-Midville aquifer system divided by one confining unit and one confining system. In the vicinity of SRS, this aquifer system includes, the McQueen Branch aquifer, overlain by the Crouch Branch aquifer, and the Steed Pond aquifer. The Crouch Branch aquifer is the principal water-producing aquifer at SRS and is the deepest unit that is routinely sampled by the current monitoring well system. Since the principle components of large scale contaminant migration in the A/M Area are dissolution of source (DNAPL) solvents followed by dissolved transport within the shallow aquifers overlying the Crouch Branch aquifer, the information selected for presentation below addresses critical features of the Steed Pond aquifer and

the nature of the aquitard between the Steed Pond aquifer and Crouch Branch aquifer.

Within the A/M Area, the flow of shallow groundwater is controlled by numerous local and regional parameters. These parameters include the influence of the Savannah River to the west of the A/M Area, the facies changes within the Crouch Branch confining zone in the northeast portion of the study area, the topographic relief that creates a strong downward gradient through out the entire A/M Area, and the incision of locally important confining zones due to erosion in the southern portion of the study area.

The majority of the groundwater contamination in the A/M Area is located in the Steed Pond aquifer and is the target of current remediation activities. This aquifer contains the water-table unit. In the Central A/M Area the Steed Pond aquifer is divided into the M-Area and the Lost Lake aquifer zones, which are separated by the Green Clay confining zone. Towards the north, in the vicinity of the SRTC complex, these units are not well distinguished and the unit is treated as one aquifer unit. The elevated topography, location of drainage features, and the numerous interbedded layers of sands, silts and clays combine to create a predominately downward flow direction within the aquifer. In the southern region of the study area the M-Area and Lost Lake aquifer zones become distinct hydrologic units due to increased thickness of clays within the Green Clay confining zone. The groundwater flow is strongly downward in the M-Area aquifer zone in this region. Upon entering the Lost Lake aquifer zone the flow transitions to the lateral direction and is controlled by regional discharges to surface streams towards both the south and the southeast. At the extreme southeastern portion of the study area, erosion of the Green Clay confining unit has resulted in the outcropping of the contaminant plume contained in the Lost Lake aquifer zone.

Lithofacies Mud Mapping of Critical Intervals in A/M Area

Geologic drill core descriptions and geophysical logs (caliper, gamma-ray and resistivity) for 42 cores were utilized in this study to delineate hydrostratigraphic boundaries beneath the study area (Figure 5). The drill core descriptions are detailed and provide a foot-by-foot microscopic description which includes percent mud, gravel, and sand along with estimated porosity and sorting characteristics. Altitude contour maps, isopach maps, and lithofacies maps were produced for each hydrostratigraphic unit using EarthVision® software (Dynamic Graphics Inc., Alameda CA, www.dgi.com). Lithofacies maps were created to depict the lateral distribution of mud and the internal variation of the mud content within the unit using the geometric mean and standard deviation of the parameter. The maps of the geometric mean are interpreted as an average expression the overall mud content within the unit while the standard deviation provides an indication of the degree of vertical lithologic variation, such as interbedding of sediment types within the unit. Both of these lithofacies parameters are functions of the thickness of the unit. Isopach maps and geometric mean mud content maps for selected hydrostratigraphic units are presented in this paper. The Crouch Branch confining unit and the Green Clay confining zone will be discussed in detail. For discussion of the other hydrostratigraphic units the reader is referred to Smits and others, 1998, and Parker and others, 1999.

Crouch Branch Confining Unit

The Crouch Branch confining unit separates the Crouch Branch aquifer from the Steed Pond aquifer (Figure 6). The Crouch Branch confining unit may be divided into three hydrogeologic zones beneath the A/M Area (Aadland and others, 1995b). These zones, in ascending order, are the “lower clay” confining zone, the “middle sand” aquifer zone, and the “upper clay” confining zone. As

described below, the "upper clay" confining zone thins and disappears toward the northern edge of A/M Area. In this region, the "middle sand" aquifer zone coalesces with the overlying "Lost Lake" aquifer zone of the Steed Pond aquifer. In the western part of the A/M Area, these zones are not delineated due to the absence of the sand beds referred to as the "middle sand" aquifer zone. In the northeastern portion of the area the clay beds of the "upper clay" and "lower clay" zone of the unit are thin or absent. It is in this region where groundwater flow occurs between the overlying Steed Pond aquifer and the underlying Crouch Branch aquifer (Aadland and others, 1995b). The interpretation outlined below is supported by a recent geophysical study that creatively combined the results of time domain electromagnetic (TDEM) soundings and shallow seismic reflection surveys to characterize the Crouch Branch confining unit (Eddy-Dilek and others, 1997). The geophysical study was particularly successful in noninvasively corroborating both the position and lithological character of the Crouch Branch confining unit (e.g., areas where the Crouch Branch confining unit is dominated by sand).

"Lower" Interval of the Crouch Branch confining unit

The surface of the "lower" interval of the Crouch Branch confining unit ranges from 119 to 75 ft msl and dips to the south-southeast. The isopach map of this interval indicates a variation from 17 to 60 ft in thickness (Figure 7). The "lower" interval of the Crouch Branch confining unit is generally thicker in areas that correspond with channel-like features on the top of the Crouch Branch aquifer. These variations are attributed to depositional fluvial facies changes such as channel and point bar deposits.

Figure 8 illustrates the geometric mean of the mud percentage within the "lower" interval of the Crouch Branch confining unit. The geometric mean of the mud percentage is generally high which corresponds to thick intervals, ranging from 75% in the center of the study area to 90-95% in the southern part. In contrast, this interval of the Crouch Branch confining unit contains relatively low quantities of mud beneath the northeast corner of the study area, corresponding to the channel-like feature beneath A Area. This interpretation is further supported by small standard deviations in this area which represent clean well-sorted sands indicative of fluvial deposition. In contrast, the areas of low mud percentages with higher standard deviations are interpreted to represent interbedded sands and clays of fluvio-deltaic origin.

"Middle" Interval of the Crouch Branch confining unit

The surface of the "middle" interval of the Crouch Branch confining unit ranges from 105 to 140 ft msl and varies in thickness from 46 ft to 3 ft (Figure 9). The isopach map indicates that thick parts of this interval generally correspond with channel-like features on the top of the "lower" interval. The mean mud fraction varies from less than 5% to greater than 60%. The larger mud percentages generally correlate with the thinner parts of the interval, especially in the southern sector of the A/M Area and in the western part of the study area (Figures 9 and 10). The standard deviation of the mud fraction within the "middle" interval is higher in areas where the mean mud fraction is higher. These fine-grained muddy sediments of the "middle" interval of the Crouch Branch confining unit are interpreted to represent interbedded layers of sand and mud that are not laterally extensive.

"Upper" Interval of the Crouch Branch confining unit

The surface of the "upper" interval ranges from 117 to 158 ft msl and varies in thickness from 5 to 46 ft (Figure 11). Two channel-like features were recognized in this interval, one that trends northwest to southeast beneath A and M Areas and the other in the western portion of the study area. The mean mud fraction ranges from less than 5% to greater than 80%. Areas with high mean mud values

correspond with thin parts of the interval (Figures 11 and 12). Standard deviation of this interval indicates high internal variability of the mud content. Where significant amounts of clay do exist, they are highly interbedded with sand. As with the "lower" and "middle" interval the northeastern portion of the study area has a sporadic distribution of mud. The areas of mean mud values greater than 50% within the "upper" interval probably define the areal extent of the "upper clay" confining zone of the Crouch Branch confining unit (Figure 12). The absence of significant quantities of mud from all three intervals in the northern sector of the A/M Area indicates that the Steed Pond aquifer is probably in hydraulic communication with the Crouch Branch aquifer in this part of the study area.

Steed Pond Aquifer

The Steed Pond aquifer is composed primarily of sand and clayey sands interbeds (Aadland and others, 1995b). The Steed Pond aquifer is divided into the M Area aquifer zone, Green Clay confining zone, and Lost Lake aquifer zone (Figure 6). The Lost Lake aquifer zone consists of yellow, tan, orange, and brown , loose to slightly indurated, fine to coarse, moderately to well-sorted, occasionally pebbly sand and minor clayey sand. The Green Clay confining zone overlies the Lost Lake aquifer zone. This zone is considered correlative with the clay and silty clay beds of the Gordon confining unit of the Floridan aquifer system south of Upper Three Runs (Aadland and others, 1995b). In the A/M Area the Green Clay confining zone consists of primarily orange and yellow, fine to coarse, poorly to well-sorted, often pebbly sand and clayey sand interbedded with gray, green, and tan clay to silty clay beds (Fallaw and Price, 1992). Aadland and others (1995b) consider these clay and silty clay beds the Green Clay confining zone when they are sufficiently thick and continuous. The M Area aquifer zone extends from the water table to the top of the Green Clay confining zone (Aadland and others, 1995b). In A/M Area the M Area aquifer zone consists of orange to tan and yellow, fine to coarse, poorly to well-sorted sand of the Tobacco Road and Dry Branch formations (Fallaw and Price, 1992). Pebbly layers, interbedded clay laminae, and clay interbeds (up to 8 ft thick) are common. Only the Green Clay confining zone will be discussed in detail. The Green Clay confining zone was theorized to be a principle control on the accumulation and migration of DNAPL below the water table in A/M Area (Looney and others, 1992). This hypothesis was further supported using indirect DNAPL characterization techniques along with heuristic DNAPL modeling (Jackson and others, 1996).

Green Clay confining zone

The surface of the Green Clay confining zone varies from 197 to 223 ft msl with thickness varying from 9 to 32 ft (Figure 13). The Green Clay confining zone is generally thicker in the southern part of the study area. The thicker areas are related to the channel-like features in the Lost Lake aquifer zone. The Green Clay confining zone is interpreted to represent a fluvio-deltaic environment with varying amounts of nearshore marine influence.

The mean mud content within the Green Clay confining zone varies from less than 5% to greater than 50% and is significantly higher in the southeast corner and southern edge of the study area (Figure 14). The isolated thick area northeast of A Area is characterized by relatively small mud percentages. The Green Clay confining zone contains very little mud at the western end of the study area. The standard deviation of the mean mud percentages is generally greater in the areas with larger mud fractions. The parts of the Green Clay confining zone that lack mud tend to be thicker, and show smaller standard deviation values. This indicates that the Green Clay confining zone consists primarily of sand, with moderate amounts of interbedded clay present in the southeastern part of the study area where the unit is relatively thin. The maps of mud distribution

indicate that the zone is probably a competent confining zone southeast of the M Area Basin. The low mud percentages and low standard deviation values west of the M Area Basin suggest that the Green Clay confining zone is relatively permeable in this area.

Summary and Conclusions

The distribution of mud layers and variations in the percentage of fine-grained sediments in the subsurface is essential in characterizing and understanding the DNAPL accumulation, movement, and geometry of the resulting contaminant plumes beneath the A/M Area. In general, characterizing the nature and distribution of confining zones in Coastal Plain sediments is challenging. These sediments were deposited by fluvial, deltaic, and/or coastal processes and are often altered by post depositional erosion and weathering. As a result, they exhibit significant lateral and vertical variations typical of ephemeral depositional settings. Variations in lithology and stratigraphy can occur abruptly or gradually. Abrupt changes can occur due to local depositional environment (e.g., meanders), structural modification, (e.g., faults), and erosional events (e.g., unconformities). Gradual changes are often more difficult to evaluate and are often manifested in coarsening or fining of sediments vertically or along the dip of a bed. Precision mapping of critical sediment layers can aid in locating areas where contamination is most likely to have migrated. Additionally, this information can be used to refine remediation systems or assist in designing new systems.

The mud distribution for the “lower”, “middle”, and “upper” intervals of the Crouch Branch confining unit indicates a series of facies changes beneath the study area. The distribution of mud in the northern sector of the study area indicates all three intervals consist primarily of sand. In the remainder of the study area, the “middle” and “upper” intervals both consist primarily of sand, with a relatively sporadic distribution of mud in comparison to the “lower” interval. The “lower interval” consists primarily of thick clay layers with high mud percentages in the central and southern sectors of the study area and represents the most competent and extensive portion of the Crouch Branch confining unit. The absence of significant quantities of mud from all three intervals in the northern sector of the A/M Area indicates that the overlying Steed Pond aquifer is in hydraulic communication with the Crouch Branch aquifer in this region. This facies change is probably a significant contributor to the migration of dissolved contamination from the Steed Pond aquifer into the Crouch Branch aquifer (Jackson and other, 1997).

The Green Clay confining zone is within the Steed Pond aquifer and has a mean mud content ranging from approximately 5% to 50%. While this zone is relatively thin and sandy it contains enough fine-grained sediment to control the accumulation and migration of DNAPL below the water table near known sources (e.g., the M-Area Settling Basin). This is illustrated in Figure 15 that presents the results of a DNAPL screening analysis where the pure-phase solubility was compared to historically reported groundwater. Screening of historical concentrations against 1% of pure-phase solubility identified 43 monitoring wells and 10 recovery wells that likely contained DNAPL within the A/M Area.

The geological characterization has had specific impacts on the design and operation of the A/M Area environmental clean-up. Near the original DNAPL sources, delineation of confining layers above and below the water table is the basis for design of sampling strategies and for targeting aggressive treatment technologies. Below the water table, these structures impede downward migration and serve to control accumulation of solvent into thin-laterally-extensive layers of contaminant rich fluid within overlying sand and ultimately into “pools” occupying structural lows. One such area, southwest of the M-Area Settling Basin, was identified

using geophysics and sampling and was treated using injection of Fenton's reagent (Jerome and others, 1997). Above the water table, our data indicate that residual DNAPL solvents are trapped within fine-grained sediment layers. As a result, we performed geological investigations of these shallow intervals (Parker and others, 1999) and have identified and implemented source treatments that have specific abilities to overcome the mass transfer limited clean-up rates. The three enhanced remediation technologies tested to date are heating technologies – steam heating (Dynamic Underground Stripping, DUS), radio frequency heating (Jarosch and others, 1994), and six phase joule heating (Gauglitz and others, 1994). The differences in technology selection for the different source scenarios is a direct result of controlling geological conditions and the observed interaction of contaminant with the subsurface materials.

Once the contaminant dissolves from the source zone, the resulting plume migrates with the groundwater toward the discharge along Tim's Branch and Upper Three Runs. The focus for geology contribution to remedial design shifts to understanding the precise trajectory of the contaminant plume. We optimize the performance of "pump and treat" remediation using knowledge of the plume centerline and by careful placement of recovery well screens. Geological information and depth discrete sampling performed during recovery well installation allow maximum efficiency because design can be customized to extract the maximum amount of contaminant in the minimum volume of water. Similarly, the in well vapor stripping systems installed in A/M Area were designed with the intake screen centered in a carefully identified discrete layer of contamination that occupied only a portion of the Lost Lake aquifer – maximizing system efficiency.

A particularly significant example of the importance of geology in the A/M Area clean up is the change made to the groundwater corrective action system based on knowledge about the Crouch Branch confining unit. The observed facies changes – the thinning and more sandy character of this major hydrostratigraphic "confining unit" near A Area – was the basis of modification of the pump and treat operation. To minimize future downward migration and contamination of the Crouch Branch aquifer, increased water treatment capacity was installed and the number of recovery wells and pumping rate in shallow groundwater in A Area was aggressively expanded. These modifications represent a significant improvement in long term protection of the important Crouch Branch aquifer for a relatively low cost.

Finally, the geological and chemical data indicated that the bulk of the plume is migrating toward Tim's Branch and Upper Three Runs and suggested likely areas of future plume discharge. Recently, passive samplers placed in active flow lines near the projected groundwater-surface water discharge area have confirmed this conceptual model. Geological considerations, particularly knowledge of the area where the stream channel has eroded below the green clay, were critical in successfully determining the location of the future contaminated groundwater discharges (since the plume is in the middle of the Lost Lake aquifer in the southern portion of A/M Area). The flow path knowledge is now available for design and implementation of effective long term remediation concepts. Two examples of such concepts are phytoremediation and microbial degradation in the wetland sediments adjacent to the stream.

Delineation of the hydrogeologic framework of a contaminated site is a critical component of effective environmental characterization and remediation. A/M Area demonstrates that development and refinement of a conceptual model using a variety of approaches, including drilling, coring, geophysical logging, aquifer testing, surface geophysics, modeling and data interpretation, enhances decision making and technical performance.

References

Aadland, R. K., Gellici, J. A, and Thayer, P. A., 1995a. *Hydrogeologic Framework of West-Central South Carolina*, Report 5, Water Resources Division, South Carolina Department of Natural Resources, Columbia, SC.

Aadland, R. K., Lewis, S. E., and McAdams, T. D. 1995b. *Hydrogeological Characterization Report for the A/M Area (U)*. WSRC-RP-95-0052, Westinghouse Savannah River Company, Aiken, SC 29808.

Eddy-Dilek, C. A., Looney, B. B., Hoekstra, P., Harthill, N., Blohm, M., and Phillips, D. R., 1997. "Definition of a Critical Confining Zone Using Surface Geophysical Methods", *Ground Water*, v. 35(3): 451-462.

Fallaw, W. C. and Price, V., 1992. "Outline of Stratigraphy at the Savannah River Site", *Geological Investigations of the Central Savannah River Area, South Carolina and Georgia*, Fallaw, W. C., and Price, V., eds., Carolina Geological Society Field Trip Guide Book, November 13-15, 1992, CGS-92-B-11-1-33, U.S. Department of Energy and S.C. Geological Survey.

Fallaw, W. C. and Price, V., 1995. "Stratigraphy of the Savannah River Site and Vicinity", *Southeastern Geology, 35: 21-58*.

Gauglitz, P. A., Bergsman, T. M., Caley, S. M., Heath, W. O., Miller, M. C., Moss, R. W., Roberts, J. S., Schalla, R., Schlender, M. H., Jarosch, T. R., Eddy-Dilek, C. A., andLooney, B. B., *Six Phase Soil Heating for Enhance Removal of Contaminants: Volatile Organic Compounds in Non-Arid Soils Integrated Demonstration, Savannah River Site*, PNL-10184, Pacific Northwest National Laboratory, Richland WA.

Jackson, D. G., Payne, T. H., Looney, B. B., and Rossabi, J. R., 1996, *Estimating the Extent and Thickness of DNAPL within the A/M Area of the Savannah River Site* (U), WSRC-RP-06-0574, Westinghouse Savannah River Company, Aiken, SC 29808.

Jackson, D. G., B. B. Looney, and H. W. Campbell. 1997, *Assessment of Chlorinated Solvent Contamination in the Crouch Branch Aquifer of the A/M Area (U).* WSRC-RP-97-0247: September 30, 1997. Westinghouse Savannah River Company, Aiken, SC 29808.

Jarosch, T. R., Beleski, R. J., and Faust, D., 1994, *Final Report: In Situ Radio Frequency Heating Demonstration*, WSRC-TR-93-673, Westinghouse Savannah River Company, Aiken, SC 29808.

Jerome, K. M., Riha, B. D., and Looney, B. B., 1997, *Final Report for Demonstration of In Situ Oxidation of DNAPL Using the Geo-Cleanse® Technology*, WSRC-TR-97-00283, Westinghouse Savannah River Company, Aiken, SC 29808.

Looney, B. B., Rossabi, J. R., and Tuck, D. M., 1992. *Assessing DNAPL contamination, A/M-Area, Savannah River Site: Phase I Results (U)*, WSRC-RP-92-1302, Westinghouse Savannah River Company, Aiken, SC 29808.

Marine, I. W. and Bledsoe, H. W. 1984. *Supplemental Technical Summary M-Area Groundwater Investigation*, DPSTD-84-0112, E. I. du Pont de Nemours & Co., Savannah River Laboratory, Aiken, SC 29808.

Siple, G. E., 1967. *Geology and Ground Water of the Savannah River Plant and Vicinity, South Carolina*, U.S. Geological Survey Water Supply Paper 1841.

Smits, A. D., Harris, M. K., Jackson, D. G., and Hawkins, K. L., 1998, *Baseline Mapping Study of the Steed Pond Aquifer and Crouch Branch Confining Unit Beneath A/M Area, Savannah River Site, Aiken, South Carolina (U)*, WSRC-RP-98-00357, Westinghouse Savannah River Company, Aiken, SC 29808.

Parker, W. H., Smits, A. D., Harris, M. K., Jackson, D.G., and Hawkins, K.L, 1999, *Baseline Mapping Study of the Steed Pond Aquifer and Vadose Zone beneath A/M Area, Savannah River Site, Aiken, South Carolina (U),* WSRC-RP-99-00295, Westinghouse Savannah River Company, Aiken, SC 29808.

Wyatt, D. E., Aadland, R. K., and Syms, F. H., 2000, *Overview of the Savannah River Site Stratigraphy, Hydrostratigraphy, and Structure* (This volume).

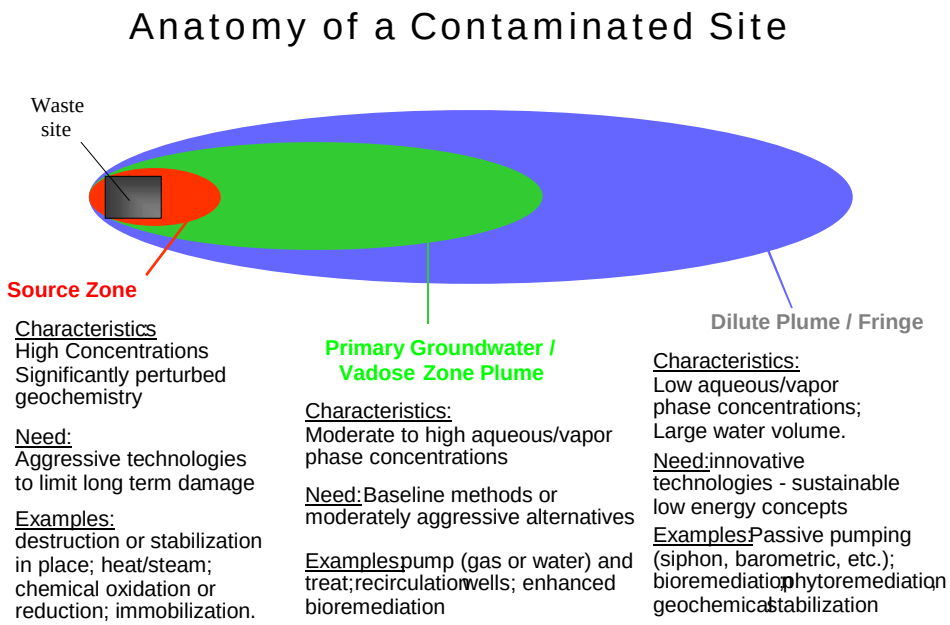

Figure 1: Conceptual Diagram of a Contaminated Site

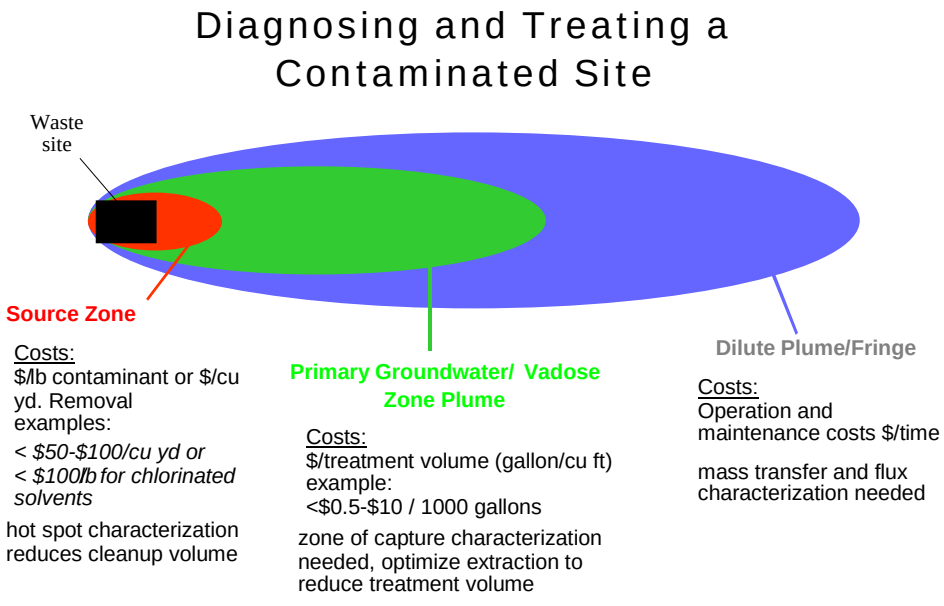

Figure 2: Conceptual Diagram of a Contaminated Site with cost considerations for clean-up technologies

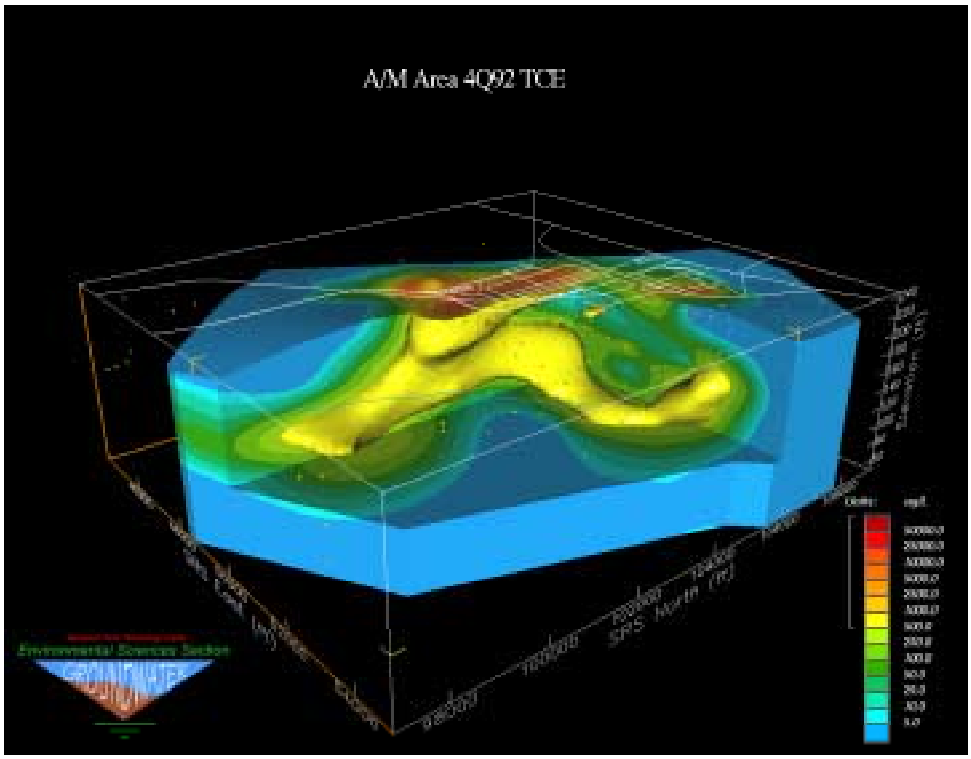

Figure 3. Cut-away diagram showing the 3D structure of a real groundwater plume

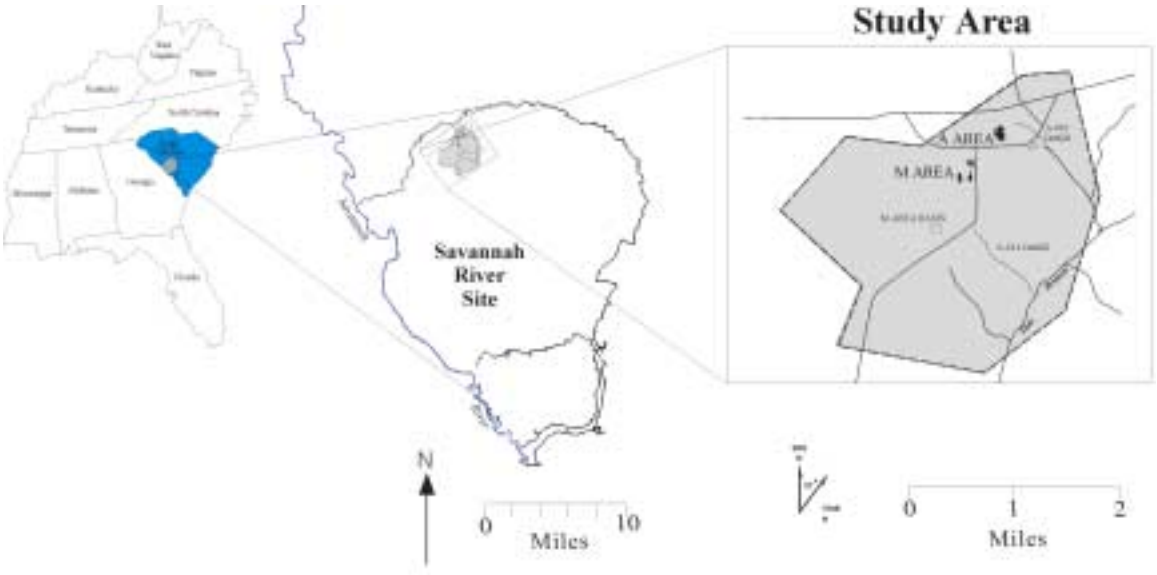

Figure 4: Location of the Savannah River Site and the A/M Area

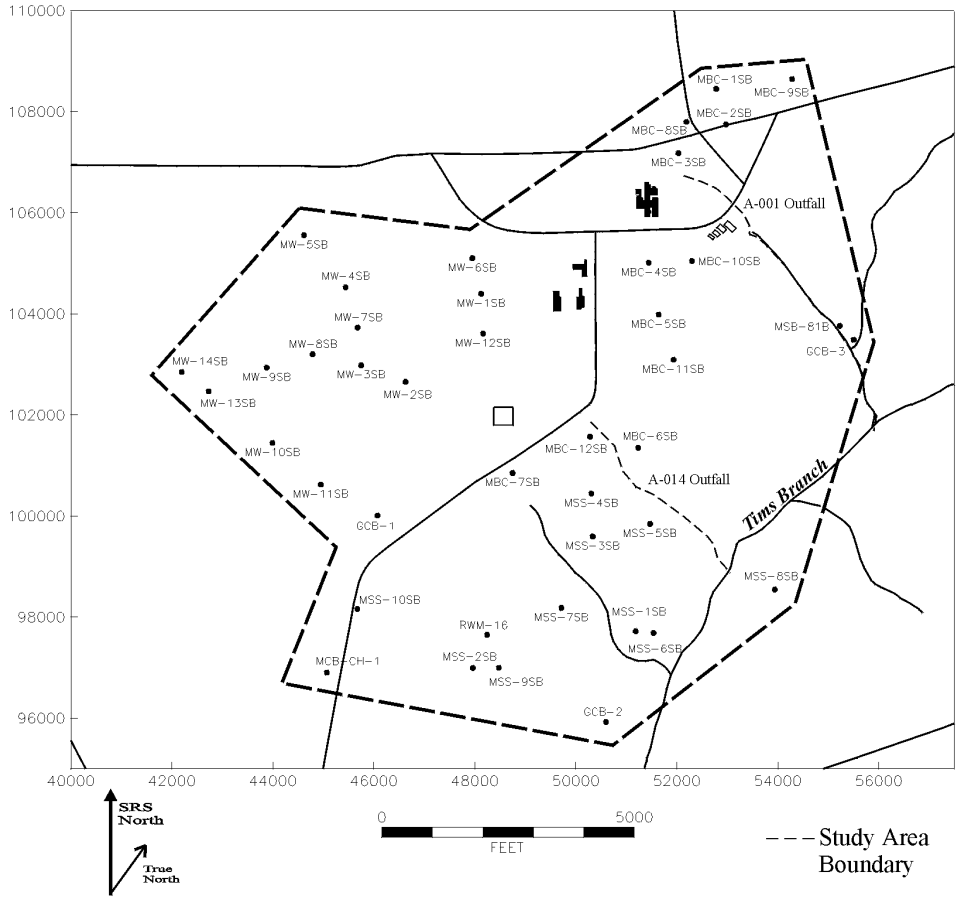

Figure 5: Detailed map of A/M Area illustrating core locations

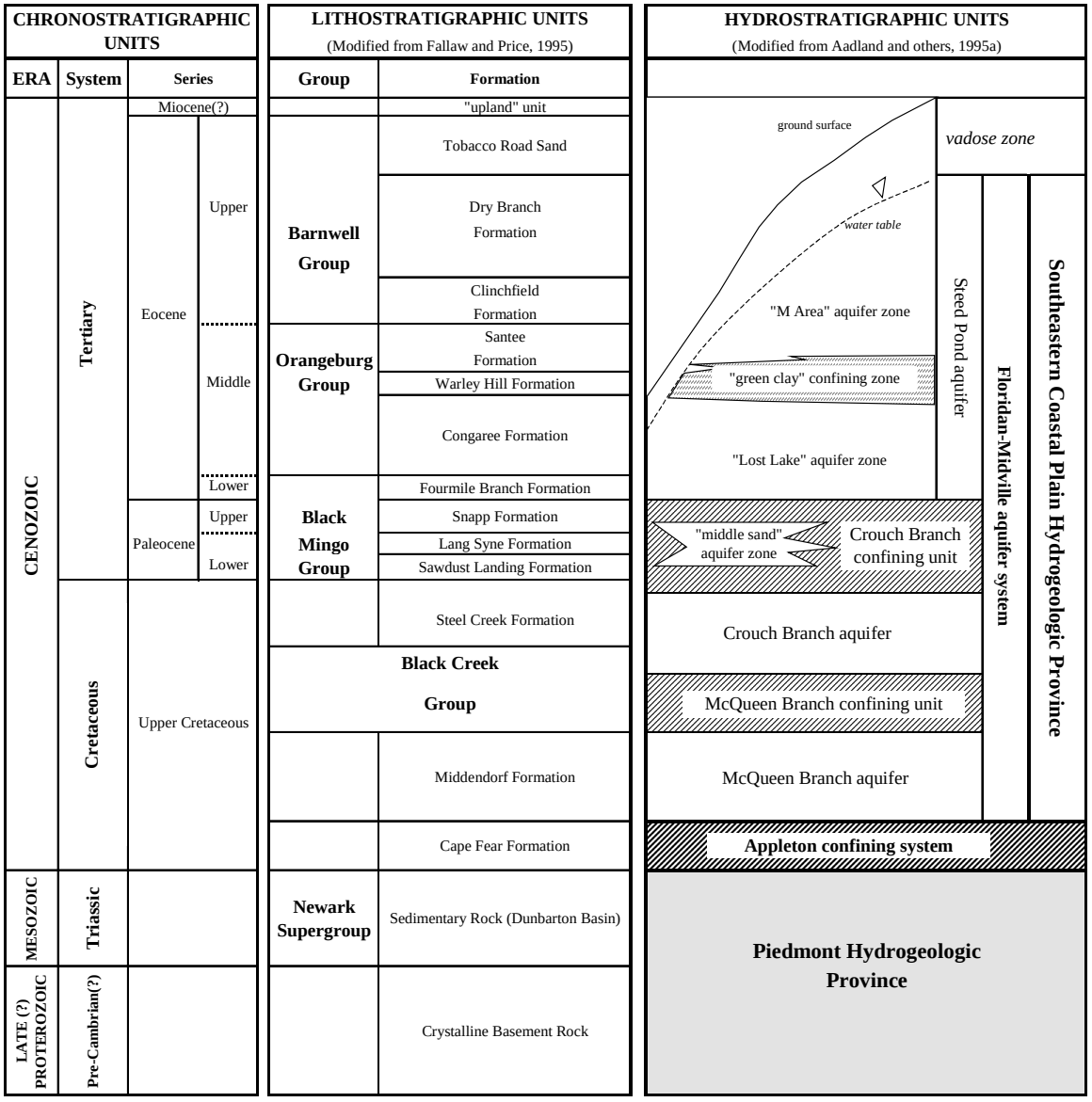

Figure 6: Comparison of Chronostratigraphic, Lithostratigraphic, and Hydrostratigraphic Units

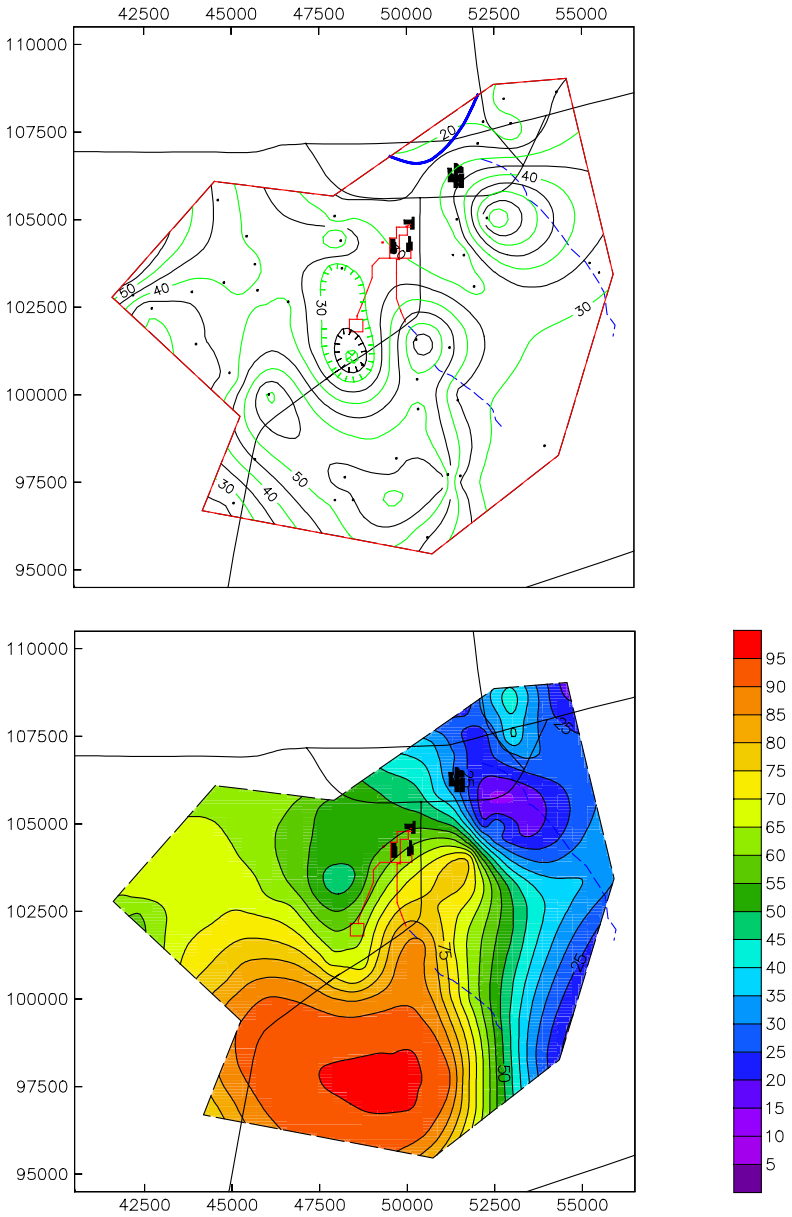

Figures 7 & 8: Isopach and Geometric Mean Mud percentage in the "Lower" interval of the Crouch Branch Confining Unit

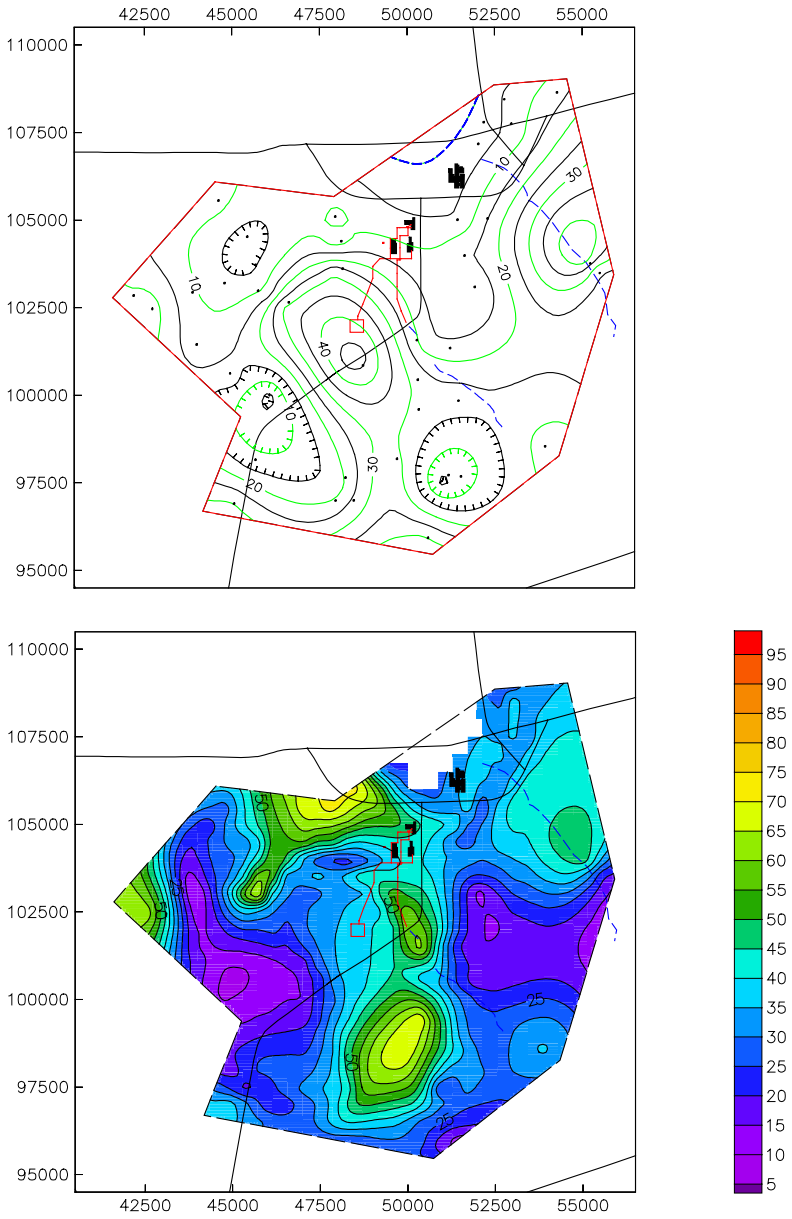

Figures 9 & 10: Isopach and Geometric Mean Mud percentage in the "Lower" interval of the Crouch Branch Confining Unit

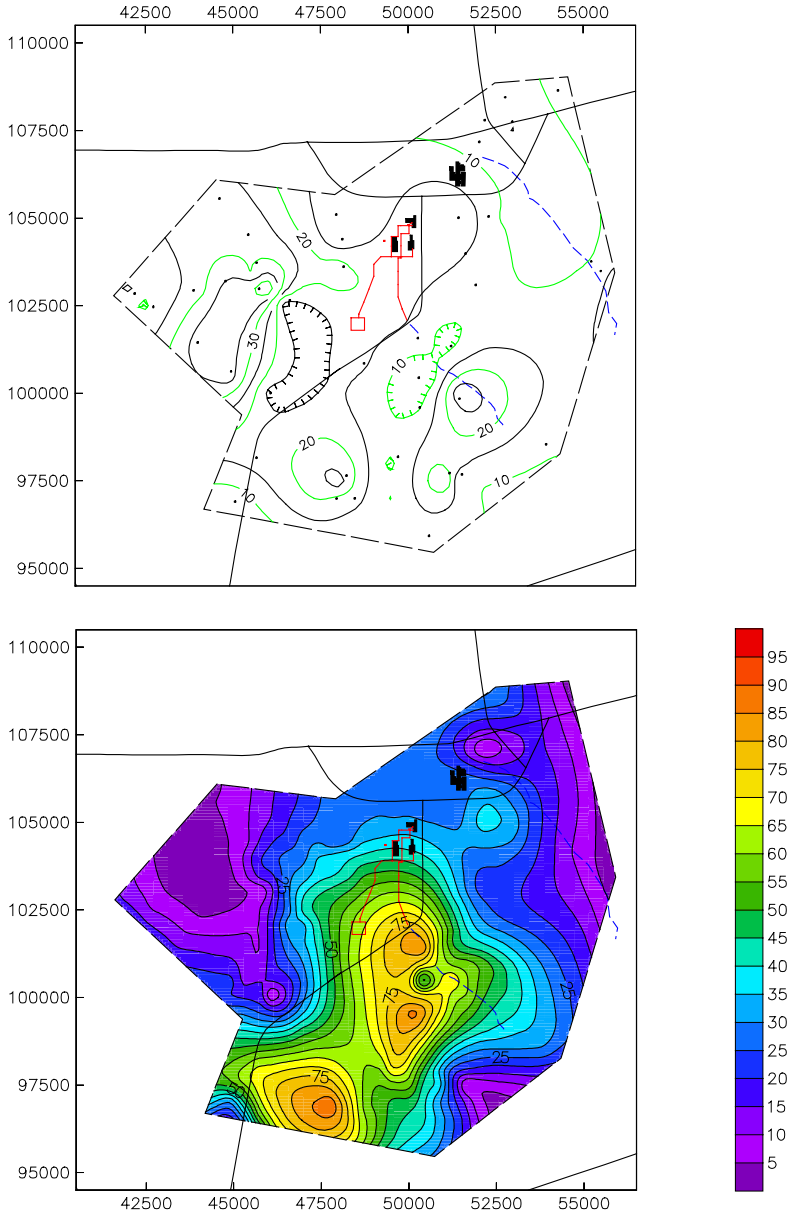

Figures 11 & 12: Isopach and Geometric Mean Mud percentage in the "Lower" interval of the Crouch Branch Confining Unit

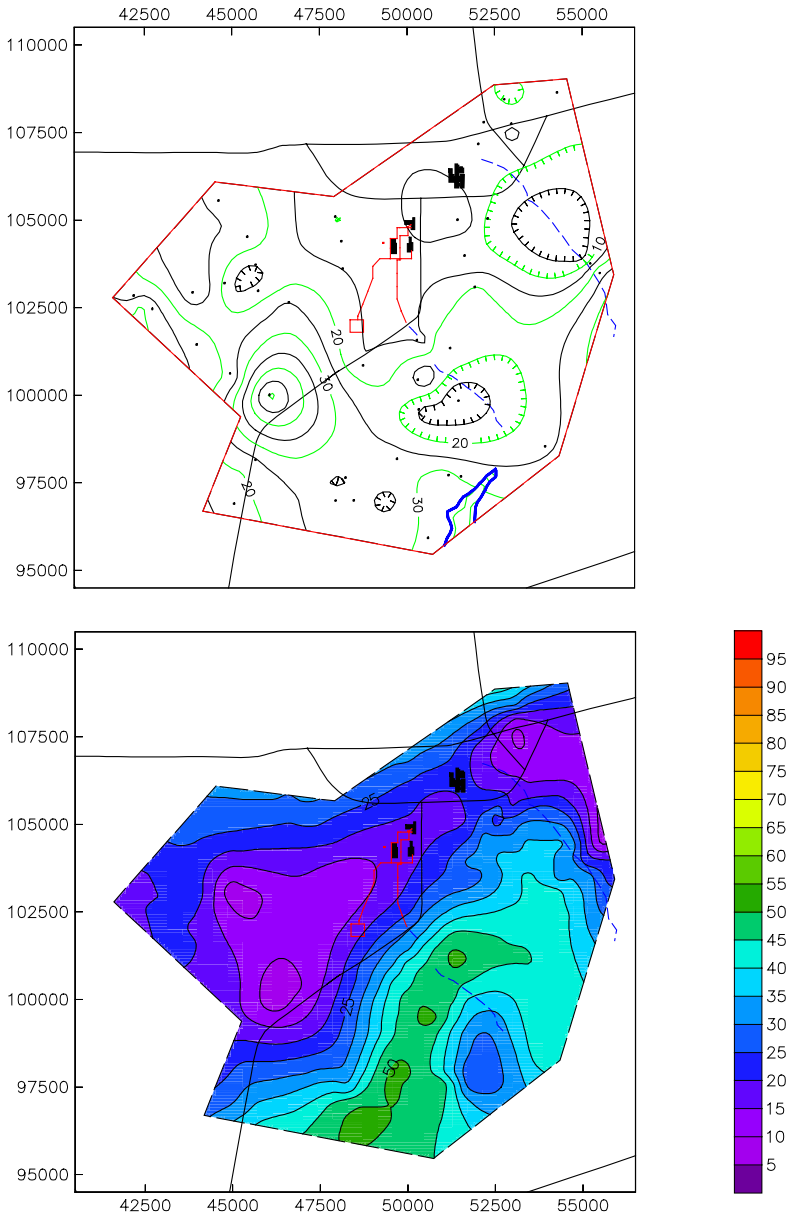

Figures 13 & 14: Isopach and Geometric Mean Mud percentage in the Green Clay Confining Zone

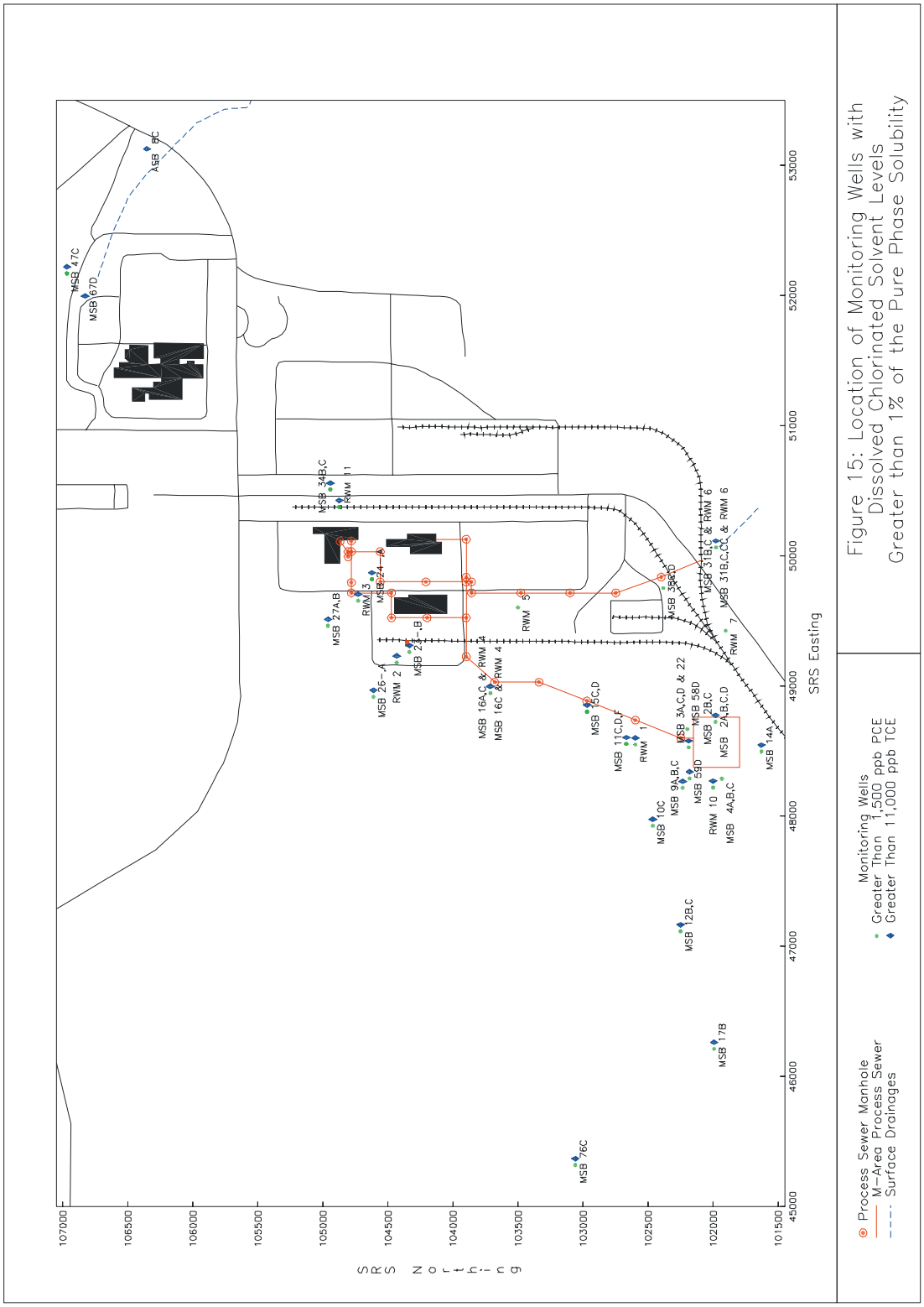

Figure 15: Monitoring Wells considered to have DNAPL contamination based on screening analysis comparing the pure-phase solubility to historically reported groundwater concentrations (Jackson and others, 1996).

Short Note: Seismic Monitoring at SRS

D. Stevenson, WSRC, Aiken, SC 29808

INTRODUCTION

The Savannah River Site (SRS) has been operating and maintaining a continuous recording seismic network on Site since the mid-seventies. The network was developed to monitor Site and regional seismic activity that may potentially impact the safety of existing or planned structures and systems at SRS. Operation and maintenance of the network is an important ongoing task contributing to Site seismic hazards analyses. It provides SRS with earthquake data collection and analysis capability to insure accurate reliable information on current earthquake activity that may occur within the immediate Site vicinity. Additionally, network seismic data directly addresses seismic safety considerations by providing an historical background database documenting levels of seismic activity impacting the Site through the years.

Current station configuration includes nine short-period seismic recording stations, six are confined within the plant boundary with an additional three off-Site (Figure 1). The off-site station locations are within a 10 to 50 km radius from the center of the SRS. Currently, we have a mix of digital and analog stations depending on quality of communication link between the field and the central recording laboratory. One station, Hawthorne Firetower, has a unique configuration consisting of both a short-period and long period instrument housed in a borehole package. This instrumentation package is presently installed in a relatively shallow borehole (100ft). However, through a cooperative effort with the USGS, drilling of a deeper bedrock hole (~1000 ft) at the same location is planned for January 2001. Upon completion of a deeper hole the existing sensor package will be re-deployed. It is hoped that the station will then become a part of the USGS National Seismic Network.

In addition to local events, regional earthquake activity occurring outside the relatively small area covered by the SRS monitoring network also has the potential for significantly impacting seismic safety considerations of the Site. Good quality regional seismic data are required when defining the range of seismogenic sources that may influence estimates of Site vibratory ground motion as well as identification of possible seismically active tectonic features. Regional coverage is currently provided cooperatively with the University of South Carolina through data from the SCSN (South Carolina Seismic Network). The University of South Carolina seismic network stations serve to compliment the SRS network contributing greatly to the regional and Site area seismic monitoring effort.

On-Site Earthquake Activity

Three earthquakes of MMI III or less have occurred with epicentral locations within the boundaries of SRS (Figure 2). On June 9, 1985, an intensity III earthquake with a local duration magnitude of 2.6 occurred at SRS. Felt reports were more common at the western edge of the central portion of the plant site. Figure 3 shows the resulting isoseismal intensity map. Another event occurred at SRS August 5,1988, with an MMI I-II and a local duration magnitude of 2.0. A survey of SRS personnel who were at the plant during the 1988 earthquake indicated that it was not felt at SRS. Neither of these earthquakes triggered the seismic alarms (set point 0.002g) at SRS facilities. These earthquakes were of similar magnitude and intensity as several recent events within the region.

On the evening of May 17, 1997, at 23:38:38.6 UTC (7:38 pm EDST) an MD ~ 2.3 (Duration Magnitude) earthquake occurred within the boundary of the Savannah River Site. It was reported felt by workers in K-Area and by

Wackenhut guards at a nearby barricade. An SMA (strong motion accelerograph) located 3 miles southeast of the epicenter at GunSite 51 was **not** triggered by the event. The SMA located approximately 10 miles (16 km) north of the event in the seismic lab building 735-11A was **not** triggered. The closest instrument to the epicenter (GunSite 51) is set at a trigger threshold of 0.3% of full scale where full scale is 2.0g (0.006g). The more distant lab SMA is set to trigger at a threshold of 0.1% of full scale where full scale is 1.0g (0.001g).

Other Seismic Monitoring Efforts at SRS

Monitoring of structural response to earthquake motions is being done through deployment and operation of accelerographs (strong ground motion recorder) in ten selected mission-critical structures. Instrument placement ranges from foundation level, selected elevations and in the free-field depending on the structure being studied. Free-field instrumentation data will be used to compare measured response to the design input motion for the structures and to determine whether the OBE has been exceeded. The instruments located at the foundation level and at elevation in the structures will be used to compare measured response to the design input motion for equipment and piping, and will be used in long-term evaluations. In addition, foundation-level instrumentation will provide data on the actual seismic input to the mission critical structures and will be used to quantify differences between the vibratory ground motion at the free-field and at the foundation level. All instruments are Kinemetrics Etna Strong Motion Accelerographs with dial-up modem data download capability. All SMA instrumentation is set to trigger at 2.0% full scale with full scale being 1g (i.e. trigger set at 0.02g).

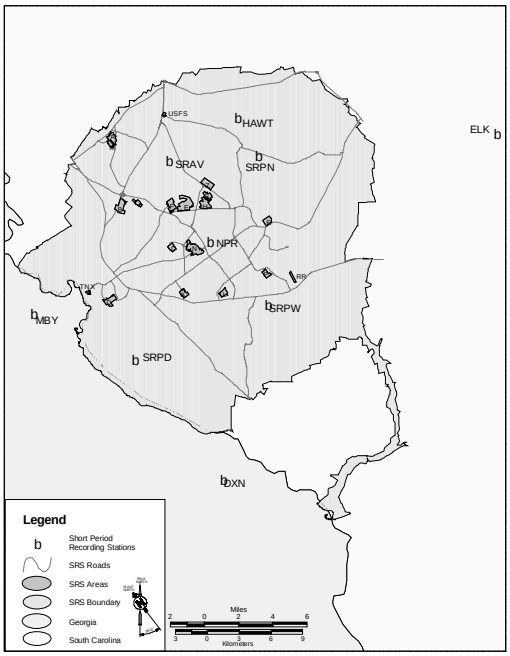

Figure 1. SRS short period recording stations.

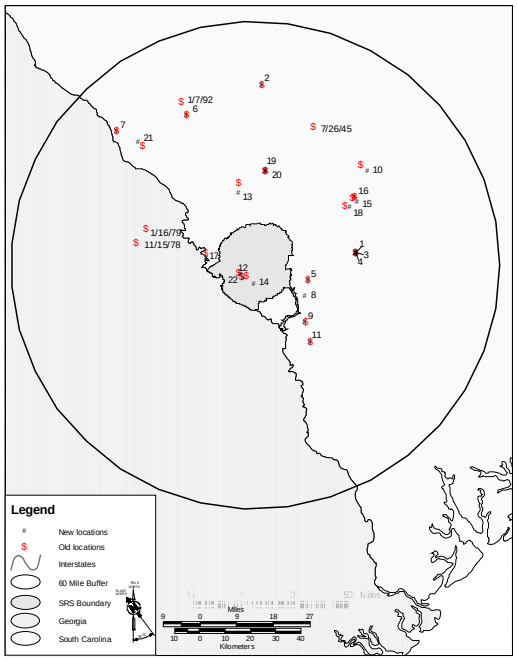

Figure 2. Historical earthquake epicenters located on the SRS. Triangles with date are historically mis-located.

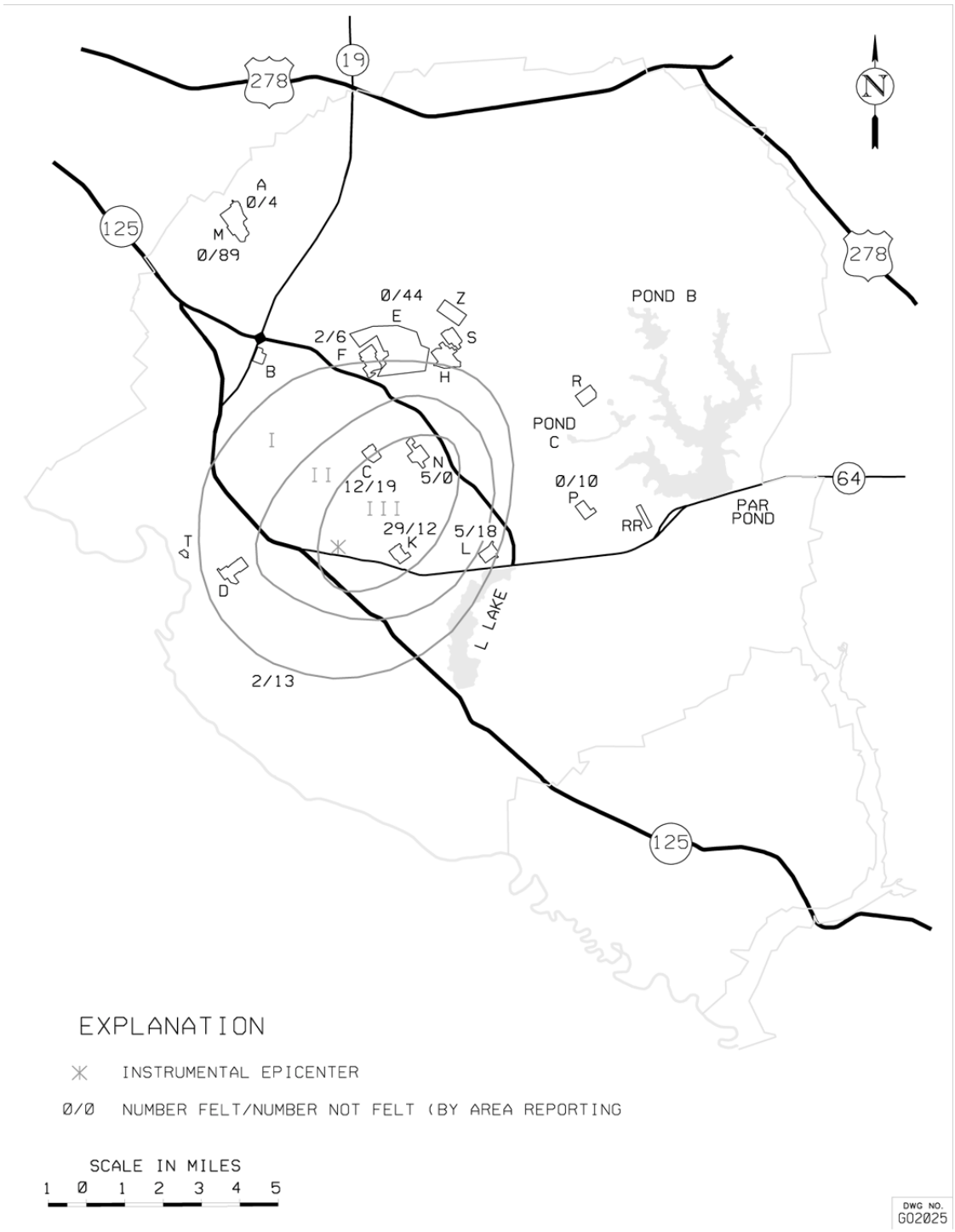

Figure 3. Isoseismal Intensity map from the June 9, 1985, intensity III earthquake.

Notes

Short Note:
Formation Damage Caused by Excessive Borehole Fluid Pressures in Coastal Plain Sediments

D. E. Wyatt, WSRC, Aiken, SC 29808

Introduction

During the initial characterization and engineering studies of the SRS, performed by the Corps of Engineers, numerous zones of lost circulation, "grout take" and rod drop were noted. Large foundation grouting programs discovered that intervals of "micro-channeling" and fracturing occurred during pumped grout programs. Ongoing drilling activities often report zones of lost circulation and rod drop, generally thought to be "soft zones" (see Aadland et al. in this guidebook). In many cases rod drops and lost circulation are due to soft zones, however an abundance of cone penetrometer (CPT) data suggests that many coastal plain sediments may be subject to hydraulic fracturing during drilling operations. Hydraulic fracturing may be the cause of some of the lost circulation problems and may cause problems if key aquitards are damaged.

An Example of the Problem

State regulations and SRS Drilling Procedures require that surface casing be set in monitoring wells penetrating deeper aquifers in 1) areas where known contamination exists in overlying aquifers, and 2) areas downgradient from facilities or areas with known contamination. Typical casing set points are within the "Green Clay" interval (Gordon Confining Unit) of the Warley Hill Formation and occasionally within the "Tan Clay" interval of the Dry Branch Formation (Tan Clay Confining Zone of the Upper Three Runs Aquifer). These two units are clayey aquitards that are generally less than ten feet thick for the "Tan Clay" and less than six feet thick for the "Green Clay". Neither of these units are massively bedded clays but generally consist of thin to thick (<1" to <2') lamina interspersed within clayey silts and fine grained sands. However, few studies have been completed on the potential formation damage effects caused by hydraulic fracturing during casing and cementing activities within these sediments. Exploration conducted to investigate the effects of foundation grouting programs showed that large volumes of injected grout traveled radially, in thin layers, considerable distances from the borehole. Intuitive experience from the petroleum industry suggests that formation damage is likely when the hydraulic pressure gradient from the drilling or grouting exceeds the fracture gradient of the formation. Formation damage may lead to "leaking" of downward moving contaminants or upward moving groundwater through fractures and micro-fractures adjacent to the borehole. Hydraulic over-pressuring may be caused by excessive mud weight, grout weight or pump over-pressuring.

Approach

Since few measurements of formation damage have been made at the SRS, a theoretical approach is made based on data collected at the Hydrogeological Field Test Site in well MWD-12. This well is centrally located at the SRS and is representative of the majority of monitoring wells in the area. MWD-12 was completed to provide core information for a comparison study between core property measurements and data obtained from geophysical tools, principally the magnetic resonance and formation fluid/pressure tester (the MRIL and Formation Multi-Tester (FMT) tools). In addition to core and geophysical measurements, Cone Penetrometer Test (CPT) information was also obtained immediately adjacent to the boring location. CPT data are available to a depth of 153' and geophysical data to a depth of 342'.

Formation damage is probable once the fluid pressures in a borehole exceed the fracture stress pressure of the formation. When this happens, borehole fluids will tend to flow under gravity and/or pumped pressure into the formation along preferentially oriented planes of weakness. In most sediments, these planes of weakness are lateral or horizontal (along the shear plane) rather than vertical (along the compressive plane) (Adams and Charrier, 1985). However, vertical fractures are known in soft sediments in outcrop Formation damage is caused by flowing borehole fluids displacing formation fluids and sediments.

Two key values are required to estimate whether formation damage is likely, the pressure of the borehole fluids at a given depth, and the fracture stress gradient of the sediments. For this study, it is assumed that sediments at the SRS are not over-pressured (for example, due to hydraulic charging from oil or gas) and are in iso-static equilibrium. If the density or composition of the borehole fluids is known, or the weight of the fluids per unit volume, then the hydrostatic pressure of the fluid per depth may be calculated, or read from prepared tables. The formation fracture gradient, by rule of thumb in Gulf Coastal Plain type sediments is approximately 1.0 psi/ft (Adams and Charrier, 1985). However, in the shallow sediments of the SRS, which are relatively less consolidated than deeper Gulf Coastal Plain sediments, (although they are of the same relative type and age) it is possible to calculate and extrapolate a stress gradient based on data from the CPT and FMT information.

Figure 1 is a graph showing the calculated pressure at depth for typical drilling mud and grout as defined in the Halliburton Cementing Tables. Overburden pressures, from the CPT tool from MWD-12 and hydrostatic pressures from the FMT tool are also shown. The FMT is a direct measure of total formation fluid pressure. CPT overburden pressure are calculated as “total” which is a function of depth, while “effective” overburden pressures consider the effects of saturated sediments below the water table. The CPT data (measured to a depth of 153’) are extrapolated to approximately 300’.

If the pore pressure is known, then it is possible to calculate the formation fracture stress gradient using the equation of Hubbert and Willis (in Adams and Charrier, 1985) as follows:

$$P/Z\ (\text{min, max}) = (1/3\ \text{min}, \tfrac{1}{2}\ \text{max})\ (S_z/Z + 2p/Z)$$

Where:

P = fracture pressure, psi
Z = depth, feet
S_z = overburden at depth Z, psi
p = pore pressure, psi

Example:

for p = 43 psi, S_z = 68 psi, Z=100 ft., then P = 78 psi minimum and 118 psi maximum

The maximum and minimum calculated fracture pressures from this equation are also shown on Figure 1. It should be understood that this equation is generally used for much deeper strata, however, the match between the CPT derived Effective Overburden pressure and the minimum fracture pressure, is interesting (the pore pressure, p, used in the Hubbert and Willis equation is utilized from the CPT data).

The FMT tool measures formation fluid pressure directly at discrete depths. These data are also shown on Figure 1. Compared to the normal hydrostatic curve (assuming freshwater) demonstrates that the measured FMT pressures are higher and tend to parallel the normal hydrostatic curve.

An assumption that the CPT Effective Overburden pressure, measured FMT MWD-12 hydrostatic pressure and the minimum Formation Fracture pressures are equivalent is valid because the curves are similar on Figure 1 (the CPT Effective Overburden pressure and the minimum Fracture Pressure curves are

measured to 153' and extrapolated to approximately 300'). This assumption is intuitive for saturated sediments if the total pressure at a given depth is a sum of the lithologic and hydrostatic pressure at that depth. Since the sediments are not over-pressured, the measured formation pressure from the FMT and measured Effective Overburden Pressure from the CPT will be equivalent to the hydrostatic pressure of the formation at a given depth.

Results and Conclusions

A review of the graph demonstrates that:

- calculated overburden pressures from the CPT and the minimum fracture pressures from the Hubbert and Willis equation generally agree, and are equivalent with the FMT derived pressures,
- the CPT Total Overburden and Effective Overburden curves diverge at the water table,
- the hydrostatic pressure from the 13.2 lb./gal. grout exceeds the Total Effective Overburden curve the at approximately 90 feet (Area A) suggesting the possibility of hydraulic fracturing in sediments at this depth,
- the 10 lb./gal. mud weight exceeds the CPT Effective Overburden and minimum Fracture Pressure a approximately 240 feet, suggesting the possibility of hydraulic fracturing at this depth (Area B),
- the FMT pressures are essentially equivalent to the extrapolated minimum Fracture Pressure and CPT Effective Overburden, but demonstrate a divergence in Area C suggesting that measured formation pressures and calculated formation pressures also diverge at these depths.
- the maximum Formation and Total Overburden Pressures are generally greater than pressures anticipated in the depth ranges evaluated,
- any pumping pressures from the surface must be added to the hydraulic pressures to estimate subsurface pressure effects.

Based on these observation, it is possible for drilling operation to hydraulically fracture typical unconsolidated sediments when grout and mud weights exceed the CPT measured Effective Overburden Pressure or the calculated Minimum Formation Fracture Pressure. It may be worthwhile, in areas to be evaluated using monitoring wells requiring casing, to obtain CPT derived data formation pressure data, and perform a hydraulic fracture potential analysis. Key formations, such as those mentioned earlier, may be damaged by excessive mud and/or grout weight induced hydraulic fracturing.

References

Adams, N. J. and Charrier, T., 1985, Drilling Engineering, PennWell Books, Tulsa, 960 p.

Field Data Handbook, Dowell-Schlumberger, Houston, TX

Halliburton Cementing Tables, 1981, Haliburton Services Co., Duncan, OK

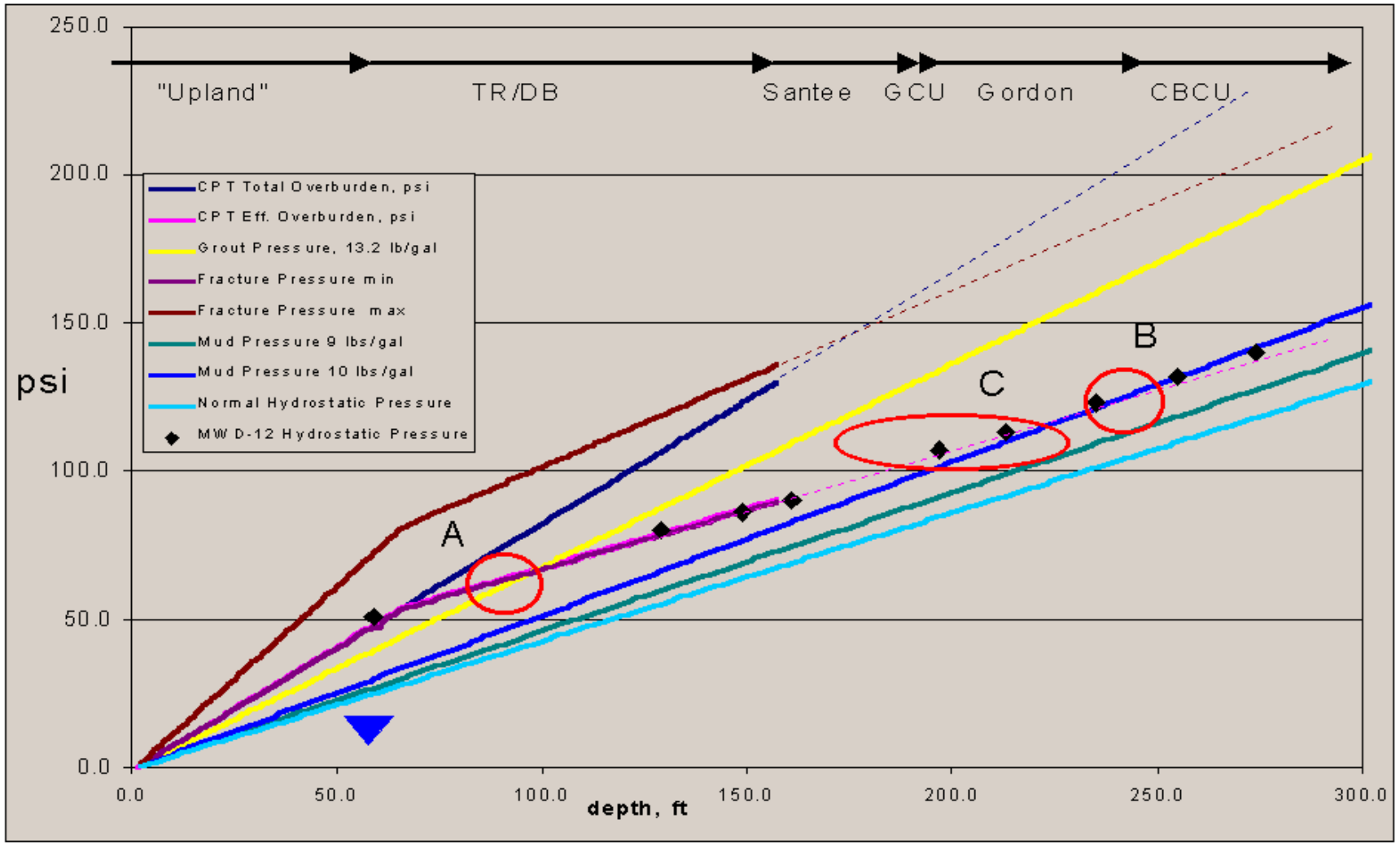

Figure 1. This graph presents the calculated maximum and minimum fracture pressures, measured hydrostatic pressures from the FMT tool, total and effective overburden pressures measured from the CPT tool, pressure weights of typical grout and drilling mud versus depth, from well MWD-12. A normal freshwater hydrostatic curve is also shown for comparison. The interpreted formation horizons are shown across the top of the graph associated with the depth. "Upland" is the Upland Unit, "TR/DB" is the Tobacco Road Fm. – Dry Branch Fm. contact, "Santee" is the Tinker/Santee Fms. interval, "GC" is the Green Clay or Gordon Confining unit of the Warley Hill Fm., ""Gordon"" is the Gordon Aquifer Unit and "CBCU" is the Crouch Branch Confining Unit. Several lines are extrapolated (dashed lines) to depths beyond the available CPT data. The water table depth is shown as a blue triangle. These data do not include surface pump pressures the inclusion of which would shift the intersection areas "A" and "B" to shallower depths.

Bibliography

Selected references from the SRS Generic Safety Analysis Report

Aadland R. K., and Bledsoe, H. W., 1990b, "Hydrostratigraphy of the Coastal Plain sequence, Savannah River Site (SRS), South Carolina": GSA Abstracts with Programs, v. 22, no. 7.

Aadland, R. K., 1997, Tertiary Geology of A/M Area Savannah River Site, South Carolina, WSRC-RP-97-0505, Rev 1. Westinghouse Savannah River Company, Aiken SC 298098, 60 p.

Aadland, R. K., and Bledsoe, H. W., 1990a, *Classification of hydrostratigraphic units at the Savannah River Site, South Carolina*: USDOE Report, WSRC-RP-90-987, Westinghouse Savannah River Co., Westinghouse Savannah River Laboratory, Aiken, SC 29808, 15 p.

Aadland, R. K., et al. Significance of Soft Zone Sediments at the Savannah River Site (U), Historical Review of Significant Investigations and Current Understanding of Soft Zone Origin, Extent and Stability. WSRC-TR-99-4083, Rev. 0, Westinghouse Savannah River Company, September 1999.

Aadland, R. K., Smits, A. D., and Thayer, P. A., 1992a, *Geology and hydrostratigraphy of the A/M Area, Savannah River Site (SRS), South Carolina (U)*: USDOE Report WSRC-RP-92-440, Westinghouse Savannah River Company, Savannah River Site, Aiken, SC 29808, 104 p.

Aadland, R. K., WSRC-RP-97-0505, Rev. 1, Tertiary Geology of A/M Area Savannah River Site, South Carolina (U).

Aadland, R.K. Geology of A/M Area, Savannah River Site South Carolina. WSRC-RP-96-0505, Rev. 0, Westinghouse Savannah River Company, Aiken, SC, 1996.

Aadland, R.K., Gellici, J. A. and P. A. Thayer, 1995, Hydrogeologic Framework of West-Central South Carolina, South Carolina Department of Natural Resources, Water Resources Division, Report 5, Columbia, South Carolina, 200 p.

Amick, D. and Gelinas, R. "The Search for Evidence of Large Prehistoric Earthquakes along the Atlantic Seaboard." American Association for the Advancement of Science, February 1991. Vol. 251, 1991.

Amick, D.R., et.al. Paleoliquefaction Features Along the Atlantic Seaboard. NUREG/CR-5613, U.S. Nuclear Regulatory Commission, Washington, DC, 1990.

Anderson, E. E. "The Seismotectonics of the Savannah River Site: The Results of a Detailed Gravity Survey". M.Sc. Thesis, University of South Carolina, Columbia, SC, 246p. 1990.

ASCE. Technical Engineering and Design Guides Adapted from the US Army Corps of Engineers, No. 9, Settlement Analysis, American Society of Civil Engineers Press, New York, New York, 1994.

ASTM. Laboratory Compaction Characteristics of Soil Using Modified Effort. ASTM D1557-91, American Society for Testing and Materials, Conshohocken, PA, 1999.

Aucott, W. R., and Speiran, G. K., 1985a, "Ground water flow in the Coastal Plain aquifers of South Carolina": *Journal of Ground Water*, v. 23, no. 6, p. 736-745.

Aucott, W. R., Davis, M. E., and Speiran, G. K., 1987, *Geohydrologic framework of the Coastal Plain aquifers of South Carolina*: U.S. Geological Survey Water-Resources Investigations Report 85-4271.

Barstow, N.L., et.al. An Approach to Seismic Zonation for Siting Nuclear Electric Power Generation Facilities in the Eastern United States: NUREG/CR-1577. U.S. Nuclear Regulatory Commission, 1981.

Bates, R. L., and Jackson, J. A., 1980, eds. *Glossary of Geology*: American Geological Institute, Falls Church, Va., 857 p.

Baum, G.R., et.al. "Structural and Stratigraphic Framework for the Coastal Plain of North Carolina." Field Trip Guidebook for Carolina Geological Society and Atlantic Coastal Plain Geological Society. North Carolina Department of Natural Resources and Development, 1979.

Beard, D. C., and Weyl, P. K., 1973, "Influence of texture on porosity and permeability of unconsolidated sand": *American Association of Petroleum Geologists Bulletin, 57*, p. 349-369.

Bechtel Corporation, 1982, *Studies of postulated Millett Fault*: Report prepared for Georgia Power Company with Southern Company Services.

Benedict, M., Cooke, J. B., Deere, D. U., Garrels, R. M., Graham, R. M., and Wolman, A., 1969, *Permanent storage of radioactive separations process wastes in bedrock on the Savannah River Plant Site*: E. I. du Pont de Nemours and Co., Savannah River Laboratory, Aiken, SC 29801, 57 p.

Berkman, E. High Resolution Seismic Survey, Pen Branch Fault, Savannah River Site, South Carolina. WSRC-TR-91-38, Westinghouse Savannah River Company, Aiken, SC, 1991.

Bledsoe, H.W., Aadland, R. K., and Sargent, K. A., 1990, Baseline Hydrogeologic Investigation - Summary Report. WSRC-RP-90-1010, Westinghouse Savannah River Company, Aiken, SC, 1990.

Bobyarchick, A.R. "The Eastern Piedmont Fault System and Its Relationship to Alleghanian Tectonics in the Southern Appalachians." Journal of Geology. Vol. 89, 1981.

Bollinger, G.A. "Reinterpretation of the Intensity Data for the 1886 Charleston, South Carolina Earthquake." Studies Related to the Charleston, South Carolina, Earthquake of 1886--A Preliminary Report. U.S. Geological Society Professional Paper 1028, 1977.

Bollinger, G.A. "Seismicity of the Southeastern United States." Bulletin of the Seismological Society of America. Vol. 63, No. 5, 1973.

Bollinger, G.A. "Specification of Source Zones, Recurrence Rates, Focal Depths, and Maximum Magnitudes for Earthquakes Affecting the Savannah River Site in South Carolina." U.S. Geological Survey Bulletin. No. 2017, 1992.

Bollinger, G.A. "Specification of Source Zones, Recurrence Rates, Focal Depths, and Maximum Magnitudes for Earthquakes Affecting the Savannah River Site in South Carolina." U.S. Geological Survey Bulletin. No. 2017, 1992

Bollinger, G.A., et.al. "An Analysis of Earthquake Focal Depths in the Southeastern United States." Geophysical Research Letters. Vol. 12, 1985.

Bollinger, G.A., et.al. "Seismicity of the Southeastern United States: 1698-1986." Neotectonics of North America. Geological Society of America DNAG Map Vol. 1, 1991

Bollinger, G.A., et.al. "Seismicity of the Southeastern United States -- 1968–1986." Decade of Geology. 1987.

Bramlett, K.W. Geology of the Johnston-Edgefield Area, South Carolina, and its Regional Implications. (M.S. Thesis). University of South Carolina, Columbia, SC, 1989.

Bramlett, K.W., et.al. "The Belair Fault: A Cenozoic Reactivation Structure in the Eastern Piedmont." Geological Society of America Bulletin. Vol. 93, 1982.

Brown, P.M., et.al. Structural and Stratigraphic Framework, and Spatial Distribution of Permeability of the Atlantic Coastal Plain, North Carolina to New York. U.S. Geological Survey Professional Paper 796, 1972.

Chapelle, S. H. and Lovley, D. R., 1991, Competitive exclusion of sulfate reduction by F(III) – reducing bacteria: A mechanism for producing discrete zones of high-iron groundwater, Groundwater, Vol. 30 No. 1, p. 29-36.

Chapman, W.L. and DiStefano, M.P. Savannah River Plant Seismic Survey, 1987-88. Research Report 1809-005-006-1-89, Conoco, Inc., Seismic Acquisition Section, 1989.

Chowns, T.M., Fritz, W.J., Latour, T.E., 1996, "Investigation of Triassic Basin Sediments – Savannah River Site. Final Report Prepared for Westinghouse Savannah River Co. Prime Contract No. :DE-AC09-89SR18035 ERDA Task #52.

Christopher, R. A., 1978, "Quantitative palynologic correlation of three Campanian and Maestrichtian sections (Upper Cretaceous) from the Atlantic Coastal Plain": *Palynology*, v.2, p. 1-27.

Clarke, J. S., Brooks, R., and Faye, R. E., 1985, *Hydrogeology of the Dublin and Midville aquifer systems of east-central Georgia*: Georgia Geological Survey Information Circular 74.

Clarke, J. S., Hacke, C. M., and Peck, M. F., 1990, *Geology and ground-water resources of the coastal area of Georgia*: Georgia Geological Survey Bulletin 113, 106 p.

Colquhoun, D. J., J. M. Rine, M. P. Segall, M. P. Katuna, A. D. Cohen, and D. L. Siron, 1994, Sedimentology and Stratigraphy of the Upland Unit, Final. Prepared under SCUREF cooperation Agreement with DOE, Task 119 AA00900T.Columbia, South Carolina: University of South Carolina, Geological Sciences Department, Earth Science and Resources Institute.

Colquhoun, D. J., Oldham, R. W., Bishop, J. W., and Howell, P. D., 1982, *Up-dip delineation of the Tertiary limestone aquifer*: South Carolina Department of Geology, University of South Carolina, Columbia, SC, 29201

Colquhoun, D.J. and Steele, K.B. Chronostratigraphy and Hydrostatigraphy of the Northwestern South Carolina Coastal Plain. Annual Cooperative Grant Agreement No. 13040 R-83-591, Project No. G868-05, Interim Technical Report to Water Resources Research Institute, Clemson University, Clemson, South Carolina, 1985.

Colquhoun, D.J., et.al. "Surface and Subsurface Stratigraphy, Structure and Aquifers of the South Carolina Coastal Plain." SCDHEC Report ISBN 0-9613154-0-7, 1983.

Cook, F.A., et.al. "COCORP Seismic Profiling of the Appalachian Orogen Beneath the Coastal Plain of Georgia." Geological Society of America Bulletin. Vol. 92, No. 10, 1981.

Cook, F.A., et.al. "Thin-skinned Tectonics in the Crystalline Southern Appalachians: COCORP Seismic Reflection Profiling of the Blue Ridge and Piedmont." Geology. Vol. 7, 1979.

Cooke, C.W. "Geology of the Coastal Plain of South Carolina." U.S. Geological Survey Bulletin. No. 867, 1936.

Coruh, C., et.al. "Results from Regional Vibroseis Profiling: Appalachian Ultradeep Core Hole Site Study." Geophysical Journal of the Royal Astronomical Society. Vol. 89, 1987.

Coruh, C., et.al. "Seismogenic Structures in the Central Virginia Seismic Zone." Geology. Vol. 16, 1988.

Cox, J. and Talwani, P. "Paleoseismic Studies in the 1886 Charleston Earthquake Meizoseismal Area." Geological Society of America, Abstracts with Programs. No. 16, 1983.

Cumbest, R.J., et.al. "Gravity and Magnetic Modeling of the Dunbarton Triassic Basin, South Carolina." Southeastern Geology. Vol. 33, No. 1, 1992.

Cumbest, R.J., Stephenson, D.E., Wyatt, D.E., Maryak, M. "Basement Surface Faulting for Savannah River Site and Vicinity" WSRC-TR-98-00346. 1998.

Dallmeyer, R.D., et.al. "Character of the Alleghanian Orogeny in the Southern Appalachians: Part II, Geochronological Constraints on the Tectonothermal Evolutions of the Eastern Piedmont in South Carolina." Geological Society of America Bulletin. Vol. 97, 1986.

Daniels, D.L. "Geologic Interpretation of Geophysical Maps, Central Savannah River Area, South Carolina and Georgia." Geophysical Investigation Map GP-893, U.S. Geological Survey, 1974.

Davis, G.J. The Southwestern extension of the Middleton-Lowndesville Cataclastic Zone in the Greensboro, Georgia, Area and its Regional Implications (M. S. Thesis). University of Georgia, Athens, Georgia, 1980.

Dennehy, K.F., et.al. "Geohydrology of the Defense Waste Processing Facility and Vicinity, Savannah River Plant, South Carolina." U.S. Geological Survey Water Resources Investigation, WRI 88-4221, 1988.

Dennis, A.J. "Is the Central Piedmont Suture a Low-Angle Normal Fault?" Geology. Vol. 19, 1991

Dennis, A.J., Maher Jr., H. D., Mauldin, J.C., Shervais, J.W., 1996, "Repeated Phanerozoic Reactivation of a Southern Appalachian Fault Zone Beneath the Up-Dip Coastal Plain of South Carolina. Report submitted for SCURF Task 170.

Dept. of the Navy. Soil Mechanics, NAVFAC DM-7.01, Washington D. C., September 1986.

Dewy, J. W., "Relocation of instrumentally recorded pre-1974 earthquakes in the South Carolina region". In Gohn, G.S. (ed.), Studies Related to the Charleston, South Carolina Earthquake of 1886 – Techtonics and Seismicity, U.S. Geological Survey Professional Paper 1313, q1-q9, 1983.

Dillon, W.P. and Popenoe, P. "The Blake Plateau Basin and Carolina Trough." The Geology of North America. V I-2, The Atlantic Continental Margin. DNAG Publication, Geological Society of America, Boulder, CO, 1988.

Dobry, R., et.al. Predication of Pore Water Pressure Buildup and Liquefaction of Sands During Earthquakes by the Cyclic Strain Method. National Bureau of Standards Building Science Series 138, 1982.

Domoracki, W.J. A "Geophysical Investigation of Geologic Structure and Regional Tectonic Setting at the Savannah River Site, South Carolina". PhD Dissertation, Virginia Polytechnic Institute, Blacksburg VA. 1995.

Domoracki, W.J., et.al. "Seismotectonic Structures Along the Savannah River Corridor, South Carolina, USA." Journal of Geodynamics. 1997.

Dutton, C. E. The Charleston Earthquake of August 31, 1886. U.S. Geological Survey, 1890.

Dutton, C.E. "The Charleston Earthquake of August 31, 1886." U.S. Geological Survey Annual Report 1887-1888. Government Printing Office, Washington, DC, 1889.

Evans, E. K. and Parizek, R. R., 1991, *Characterization of hydraulic conductivity heterogeneity in Tertiary sediments within the General Separations Area, Savannah River Site, South Carolina*: Department of Geosciences, Pennsylvania State University, Pa., 157 p.

Facility Safety. DOE Order 420.1, U.S. Department of Energy, Washington, DC, 1995.

Fallaw, W. C. and Price, V., 1992, Outline of Stratigraphy at the Savannah River Site: In Fallaw, W. C., and Price, Van, eds., 1992, Carolina Geological Society Field Trip Guidebook, Nov. 13-15, 1992, Geological Investigation of the Central Savannah River Area, South Carolina and Georgia: US Dept of Energy and SC Geological Survey, P. CGS-92-B-11-1-33.

Fallaw, W.C. and Price, Van. "Stratigraphy of the Savannah River Site and Vicinity." Southeastern Geology. Vol. 35, No. 1, 1995.

Fallaw, W.C., et.al. "Effects of Varying Degrees of Marine Influence on Tertiary Sediments in Southwestern South Carolina." Geological Society of America Abstracts with Programs. Vol. 22, No 7, 1990.

Farrar, S.S. "Tectonic Evolution of the Eastern-Most Piedmont, North Carolina." Geological Society of America Bulletin. Vol. 96, 1985.

Faye, R.E. and Prowell, D.C. Effects of Late Cretaceous and Cenozoic Faulting on the Geology and Hydrology of the Coastal Plain Near the Savannah River, Georgia and South Carolina. U.S. Geological Survey Open File Report 82-156, 1982.

Fetter, C. W., 1986, *Applied Hydrogeology (2nd Edition)* Merrill Publishing Company, Columbus, Oh.

Fullagar, P.D. and Bartholomew, M.J. "Rubidium-Strontium Ages of the Watauga River Cranberry, and Crossing Knob Gneisses, Northwestern North Carolina." Geological Investigations in the Blue Ridge of Northwestern North Carolina: 1983 Guidebook for the Carolinas. Geological Society, North Carolina Division of Land Resources, Article 11, 1983.

Fullagar, P.D. and Odom, A.L. "Geochronology of Precambrian Gneisses in the Blue Ridge Province of Northwestern North Carolina and Adjacent Parts of Virginia and Tennessee." Geological Society of America Bulletin. Vol. 84, 1973.

Fullagar, P.D., et.al. "1200 m.y.-Old Gneisses in the Blue Ridge Province of North and South Carolina." Southeastern Geology. Vol. 20, 1979.

General Design Criteria. DOE Order 6430.1A, U.S. Department of Energy, Washington, DC, 1989.

GeoTrans, Inc., 1988, *Characterization of ground water flow and transport in the General Separations Area, Savannah River Plant*: Effects of closure options on groundwater flow at the F-Area seepage basins.

Glover, L., III, et.al. "Diachronous Paleozoic Mylonites and Structural Heredity of Triassic-Jurassic Basins in Virginia." Geological Society of America Abstracts with Programs. Vol. 12, 1980.

Gohn, G.S. "Late Mesozoic and Early Cretaceous Geology of the Atlantic Coastal Plain: North Carolina to Florida." The Geology of North America. Vol. I-2, The Atlantic Continental Margin, pp. 107-130, DNAG Publication, Geological Society of America, Boulder, CO., 1988

Gohn, G.S. Studies Related to the Charleston Earthquake of 1886: Tectonics and Seismicity. U.S. Geological Survey Professional Paper 1313, 1983.

Gohn, G.S., et.al. "Field Studies of Earthquakes Induced Liquefaction-Flowage Features in the Charleston, South Carolina, Area Preliminary Report". U.S. Geological Survey Open-File Report 84-670, 1984.

Goldsmith, R., et.al. "Geologic Map of the Charlotte 1x2 Quadrangle, North Carolina and South Carolina." U.S. Geological Survey Miscellaneous Investigations Series Map I-1251-E, Scale 1:250,000, 1988.

Gore, P.J.W. "Depositional Framework of a Triassic Rift Basin: The Durham and Sanford Sub-basins of the Deep River Basin, North Carolina." Society of Economic Paleontologists and Mineralogists Field Guidebook. Third Annual Midyear Meeting, Raleigh, NC, 1986.

Griffin, V.S., Jr. "Geology of the Abbeville East, Abbeville West, Latimer and Lowndesville Quadrangles, South Carolina." South Carolina Geological Survey MS-24. 1979.

Grow, J.A., et.al. "Structure and Evolution of Baltimore Canyon Trough." The Geology of North America. Vol. I-1, *The Atlantic Continental Margin*. DNAG Publication, Geological Society of America, Boulder, CO, 1988.

Grubb, H. F., 1986, *Gulf Coast regional aquifer-system analysis - A Mississippi perspective*: U. S. Geological Survey Water-Resources Investigations Report 86-4162, 22 p.

Guidelines for Use of Probabilistic Seismic Hazard Curves at Department of Energy Sites. DOE-STD-1024, U.S. Department of Energy, Washington, DC, December 1992.

Gutierrez, B.J. (1999). Letter from the DOE to to L.A. Salomone and F. Loceff, on "Revised Envelope of the Site Specific PC-3 Surface Ground Motion", September 9, 1999.

Hall, M.H. "Heavy Mineral Provinence of Triassic Dunbarton Basin Deposits, South Carolina". MSc. Thesis, University of North Carolina Wilmington, Wilmington, NC. 1997.

Hanson, K.L., et.al. "Applications of Quaternary Stratigraphic, Soil-Geomorphic, and Quantitative Geomorphic Analyses to the Evaluation of Tectonic Activity and Landscape Evolution in the Upper Coastal Plain, South Carolina." Proceedings, 4th DOE Natural Phenomena Hazards Mitigation Conference. Vol. 2, Atlanta, Georgia, 1993.

Hasek, M. J. Settlement of H-Area Waste Storage Tanks and Structures (U), K-ESR-H-00011, Rev. 0.0, October 1999.

Hatcher, R.D., et.al. "The Smokies Foothills Duplex and Possible Significance of the Guess Creek Fault, A Corollary to the Mapping of King and Neuman." Geological Society of America Abstracts with Programs. Vol. 18, 1986a.

Hatcher, R.D., et.al. Continent-Ocean Transect E5 Cumberland Plateau (North American Craton) to Blake Plateau Basin. The Decade of North American Geology Project, Geological Society of America, Boulder, CO, 1994

Hatcher, R.D., Jr. "Developmental Model for the Southern Appalachians." Geological Society of America Bulletin. Vol. 83, 1972.

Hatcher, R.D., Jr. "Tectonics of the Western Piedmont and Blue Ridge, Southern Appalachians: Review and Speculation." American Journal of Science. Vol. 278, 1978.

Hatcher, R.D., Jr. and Butler, J.R. Guidebook for Southern Appalachian Field Trip in the Carolinas, Tennessee, and Northeastern Georgia. International Geologic Correlation Program Project 27, University of North Carolina, Chapel Hill, NC, 1979.

Hatcher, R.D., Jr. and Edelman, S.H. "Macro-Scale Partitioning in the Southern and Central Appalachians: Thrusting and Strike-Slip as Products of Alleghanian Collision." Geological Society of America Abstracts with Programs. Vol. 19, 1987.

Hatcher, R.D., Jr. and Goldberg, S.A. "The Blue Ridge Geologic Province." The Geology of the Carolinas. Carolina Geological Society 50th Anniversary Volume, 1991.

Hatcher, R.D., Jr., et.al. "Eastern Piedmont Fault System: Speculations on its Extent." Geology. Vol. 5, 1977.

Hatcher, R.D., Jr., et.al. "Geometric and Time Relations of Thrusts in the Crystalline Southern Appalachians." Geometry and Mechanisms of Appalachian Thrusting, with Special Reference to the Appalachians. Geological Society of America Special Paper 222, 1988.

Hatcher, R.D., Jr., et.al. "Tectonic Map of the U.S. Appalachian, Plate 1, the Applachian-Ouachita Orogen in the United States." The Geology of North America. Vol. F-2. Geological Society of America, Boulder, CO, 1990**.**

Heller, P.L., et.al. "Episodic Post-Rift Subsidence of the United States Atlantic Margin." Geological Society of America Bulletin. Vol. 93, No. 5, 1982.

Herrick, S. M., and Vorhis, R. C., 1963, *Subsurface geology of the Georgia Coastal Plain*: Georgia Department of Natural Resources, Division of Mines, Mining, and Geology Information Circular 25, 80 p.

Herrmann, R.B. "Surface-Wave Studies of Some South Carolina Earthquakes." Bulletin of the Seismological Society of America. Vol. 76, No. 1, 1986.

Heyn, T. "Geology of the Hinge Zone of the Sauratown Mountains Anticlinorium, North Carolina: Structure of the Sauratown Mountains Window, North Carolina." Carolina Geological Society Guidebook. 1988.

Hooper, R.J. and Hatcher, R.D., Jr. "The Pine Mountain Terrane, a Complex Window in the Georgia and Alabama Piedmont-Evidence from the Eastern Termination." Geology. Vol. 16, 1988.

Hopson, J.L., et.al. "Geology of the Eastern Blue Ridge of Northeast Georgia and the Adjacent Carolinas." Georgia Geological Society Guidebook. Vol. 9, 1989.

Hopson, J.R. "Structure, Stratigraphy, and Petrogenesis of the Lake Burton Mafic-Ultramafic Complex." Georgia Geological Society Guidebook. Vol. 9, 1989.

Horton, J.W., Jr. "Shear Zone Between the Inner Piedmont and Kings Mountain Belts in the Carolinas." Geology. Vol. 9, 1981.

Horton, J.W., Jr. and McConnell, K.I. "The Western Piedmont." The Geology of the Carolinas. Carolina Geological Society 50th Anniversary Volume, 1991.

Housner, G.W. Earthquake Criteria for the Savannah River Plant. DPE-2383, E.I. du Pont de Nemours and Company, Savannah River Plant, Aiken, SC, 1968.

Huddlestun, P.F. and Hetrick, J.H. "Stratigraphy of the Tobacco Road Sand - A New Formation." Georgia Geologic Survey. Bulletin 93, 1978.

Hutchinson, D.R. and Klitgord, K.D. "Evolution of Rift Basins on the Continental Margin Off Southern New England: Triassic-Jurassic Rifting: North America and Africa." American Association of Petroleum Geologists Memoir, 1986.

Hydrogeologic Characterization of the MWMF (Mixed Waste Management Facility), SRS. WSRC-RP-92-837, Westinghouse Savannah River Company, Aiken, SC, 1992

Kanter, L.R. Tectonic Interpretation of Stable Continental Crust in: The Earthquakes of Stable Continental Regions. Electric Power Research Institute, Palo Alto, CA, 1994.

Keen, C.E. and Haworth, R.T. "DNAG Transect D-3: Rifted Continental Margin Off Nova Scotia: Offshore Eastern Canada." Geological Society of America, Centennial Continent/Ocean Transect #4. Boulder, CO, 1985.

Kimball, J.K. "The Use of Site Dependent Spectra." Proceedings of the U.S. Geological Survey Workshop on Site Specific Effects of Soil and Rock on Ground Motions and the Implications for Earthquake-Resistant Design. U.S. Geological Survey Open File Report 83-845, 1983.

King, P.B. "A Geologic Cross Section Across the Southern Appalachians, An Outline of the Geology in the Segment in Tennessee, North Carolina, and South Carolina." Guides to Southeastern Geology. Geological Society of America Annual Meeting, 1955.

King, P.B. Systematic Pattern of Triassic Dikes in the Appalachian Region, Second Report. U.S. Geological Survey Professional Paper 759-D, 1971

King, P.B., et.al. 1968, Geology of the Great Smoky Mountains National Park, Tennessee and North Carolina. U.S. Geological Survey Professional Paper 587.

Klitgord, K.D. and Schouten, H. "Plate Kinematics of the Central Atlantic." The Geology of North America. Vol. M, The Western North Atlantic Region. DNAG Publication, Geological Society of America, Boulder, CO, 1986.

Klitgord, K.D., et.al. "US Atlantic Continental Margin: Structural and Tectonic Framework." The Geology of North America. V I-2, The Atlantic Continental Margin. DNAG Publication, Geological Society of America, Boulder, CO, 1988.

Koester, J.P. and Franklin, A.G. Current Methodologies for Assessing the Potential for Earthquake-Induced Liquefaction in Soils. NUREG/CR-430, U.S. Nuclear Regulatory Commission, Washington, DC, 1985.

Krause, R. E. and Randolph, R. B., 1989, *Hydrology of the Floridan aquifer system in southeast Georgia and adjacent parts of Florida and South Carolina*: U. S. Geological Survey Professional Paper 1403-D, 64 p.

Krause, R. E., 1982, *Digital model evaluation of the predevelopment flow system of the Tertiary limestone aquifer, southeast Georgia, northeast Florida, and southern South Carolina*: U. S. Geological Survey Water-Resources Investigations Report 82-173, 27 p.

Lahr, J.C., "HYPOELLIPSE: a computer program for determining local earthquake hypocentral parameters, magnitude, and first motion pattern." U.S. Geological Survey Open-File report 84-519, 35p., 1984.

Latour, T.E., Roden, M.F., Vanko, D.A., Whitney, J.A. "Crystalline Basement Core – Savannah River Site. Final Report". ERDA Task 53, 303p, 1995.

Lee, R.C. Investigations of Nonlinear Dynamic Soil Properties at the Savannah River Site.

WSRC-TR-96-0062, Rev. 0, Westinghouse Savannah River Company, Aiken, SC, March 1996

Leutgert et.al. "Crystal Structure Beneath the Atlantic Coast Plain of South Carolina." Seismological Research Letters. Vol. 65, No. 2, 1994.

Lewis, M. R., Arango, I., Kimball, J. K. and T. E. Ross. "Liquefaction Resistance of Old Sand Deposits," Proceedings of the XI Panamerican Conference on Soil Mechanics and Geotechnical Engineering. Foz do Iguassu, Brazil, August 1999.

Li, W. T. Settlement of Defense Waste Processing Facility (U), K-ESR-S-00003, Rev. 0, September 1999.

Lindholm, R.C. "Triassic-Jurassic Faulting in Eastern Northern America - A Model Based on Pre-Triassic Structures." Geology. Vol. 6, 1978.

Logan, W. R. and Euler, G. M., 1989, Geology and ground-water resources of Allendale, Bamberg, and Barnwell Counties and part of Aiken County, South Carolina: Water Resources Commission Report 155, 113 p.

Lohman, S. W., et al, 1972, *Definitions of selected groundwater terms - revisions and conceptual refinements*: U. S. Geological Survey Water-Supply Paper 1988, 21 p.

Long, L.T. "The Carolina Slate Belt-Evidence of a Continental Rift Zone." Geology. Vol. 7, 1979.

Long, L.T. and Chapman, J.W., Jr. "Bouguer Gravity Map of the Summerville-Charleston, South Carolina Epicentral Zone and Tectonic Implications." Studies Related to the Charleston, South Carolina Earthquake of 1886--A Preliminary Report. U.S. Geological Survey Professional Paper 1028, 1977.

Luetgert, J.H., H.M. Benz, and S. Madabhushi, "Crustal Structure beneath the Atlantic coastal plain of South Carolina." Seismological Research Letters, vol 30, no. 7, 180-191, 1994

Madabhushi, S. and Talwani, P. "Fault Plane Solution and Relocations of Recent Earthquakes in Middleton Place Summerville Seismic Zone Near Charleston South Carolina." Bulletin of the Seismological Society of America. Vol. 83, No. 5, 1993.

Maher, H.D. "Stratigraphy and Structure of the Belair and Kiokee Belts near Augusta, Georgia, Geological Investigations of the Eastern Piedmont, Southern Appalachians." Carolina Geological Society Field Trip Guidebook. South Carolina Geological Survey, 1978.

Maher, H.D., et.al. "40Ar/39Ar Constraints on Chronology of Augusta Fault Zone Movement and Late Alleghanian Extension, Southern Appalachian Piedmont, South Carolina and Georgia." American Journal of Science. Vol. 294, 1994.

Maher, H.D., et.al. "The Eastern Piedmont of South Carolina." The Geology of the Carolinas. University of Tennessee Press, Knoxville, 1991.

Maher, H.D., Jr. "Kinematic History of Mylonitic Rocks from the Augusta Fault Zone, South Carolina and Georgia." American Journal of Science. Vol. 287, 1987.

Maher, H.D., Jr. Stratigraphy, Metamorphism, and Structure of the Kiokee and Belair Belts Near Augusta, Georgia (MS Thesis). University of South Carolina, Columbia, SC, 1979.

Maher, H.D., Jr., et.al. "Magmatic Softening in the Orogenic Hinterlands Southern Appalachian Piedmont, Georgia." Geological Society of America Abstracts with Programs. Vol. 24, No. 2, 1992.

Manspeizer, W., et.al. "Separation of Morrocco and Eastern North America: A Triassic-Liassic Stratigraphic Record." Geological Society of America Bulletin. Vol. 89, 1978.

Marine, I. Geohydrology of the Buried Triassic Basin at the Savannah River Plant Groundwater. Vol. 2, 1974a.

Marine, I. W., 1966, "Hydraulic correlation of fracture zones in buried crystalline rock at the Savannah River Plant near Aiken, South Carolina": *Geological Survey Research 1966*, Chapter D, U.S. Geological Survey Professional Paper 550-D, p. D223-D227.

Marine, I. W., 1967a, "The permeability of fractured crystalline rock at the Savannah River Plant near Aiken, South Carolina": *Geological Survey Research 1967*, Chapter B, U.S. Geological Survey Professional Paper 575-B, p. B203-B211.

Marine, I. W.,1967b, "The use of tracer test to verify an estimate of groundwater velocity in fractured crystalline rock at the Savannah River Plant near Aiken, South Carolina": in *Isotope Techniques in the Hydrologic Cycle: Geophysical Monograph Series*, v. 11, ed., G. E. Stout, Washington, DC, American Geophysical Union, p. 171-178.

Marine, I.W. "Geohydrology of Buried Triassic Basin at Savannah River Plant, South Carolina." American Association of Petroleum Geologists Bulletin. Vol. 58, 1974b.

Marine, I.W. and Siple, G.E. "Buried Triassic Basin in the Central Savannah River Area, South Carolina and Georgia." Geological Society of America Bulletin. Vol. 85, 1974.

Martin, G.R., et.al. "Fundamentals of Liquefaction Under Cyclic Loading." Journal of the Geotechnical Engineering Division. Proceedings Paper 11284, ASCE, Vol. 101, No. 5, May 1975.

Mauldin, J., Shervais, J.W., Dennis, A.J., 1996, "Petrology and Geochemistry of Metavolcanic Rocks from a Neoproterozoic Volcanic Arc, Savannah River Site, South Carolina". Report submitted for SCURF Task 170.

McBride, J.H. "Constraints on the Structure and Tectonic Development of the Early Mesozoic South Georgia Rift, Southeastern United States; Seismic Reflection Data Processing and Interpretation." Tectonics. Vol. 10, No. 5, 1991.

McConnell, K.I. "Geology of the Sauratown Mountains Anticlinorium; Vienna and Pinnacle 7.5 Minute Quadrangles: Structure of the Sauratown Mountains Window, North Carolina." Carolina Geological Society Guidebook. 1988.

Meisler, H., 1980, *Plan of study for the northern Atlantic Coastal Plain regional aquifer system analysis*: U.S. Geological Survey Water-Resources Investigations Report 80-16, 27 p.

Miller, J. A, and Renken, R. A., 1988, *Nomenclature of regional hydrogeologic units of the Southeastern Coastal Plain aquifer system*: U. S. Geological Survey, Water Resources Investigations Report 87-4202, 21 p.

Miller, J. A., 1986, *Hydrogeologic framework of the Floridan aquifer system in Florida and in parts of Georgia, Alabama, and South Carolina*: U.S. Geological Survey Professional Paper 1403-B, 91 p.

Mitchell, J. K. "Practical Problems from Surprising Soil Behavior," The 20th Terzaghi Lecture, Journal of Geotechnical Engineering, Vol. 112, No. 3, American Society of Civil Engineers, March 1986.

Mitchell, J. K. and Solymar, Z. V. "Time Dependent Strength Gain in Freshly Deposited or Densified Sand," Journal of Geotehcnical Engineering Division. Vol. 110, No. 11, American Society of Civil Engineers, November 1984.

Mitwede, S.K., et.al. "Major Chemical Characteristics of the Hammett Grove Meta-Igneous Suite, Northeastern South Carolina." Southeastern Geology. Vol. 28, No. 1, 1987.

Moos, D. and Zoback, M.D. In Situ Stress Measurements in the NPR Hole, Savannah River Site, South Carolina: Final Report to Westinghouse Savannah River Co., Vol. 1, Results and Interpretations. Subcontract AA00925P, Science Applications International Corporation, Augusta, GA, 1992.

National Center for Earthquake Engineering Research. Proceeding of the NCEER Workshop on Evaluation of Liquefaction Resistance of Soils. Technical Reprot NCEER-97-0022, Buffalo, NY, December 31, 1997.

National Earthquake Hazards Reduction Program (NEHRP) Recommended Provisions for Seismic Regulations for New Buildings and Other Structures. Building Seismic Safety Council, part 1 Provisions (FEMA 302).

Natural Phenomena Hazards Assessment Criteria. DOE-STD-1023-95, U.S. Department of Energy, Washington DC, 1995.

Natural Phenomena Hazards Design and Evaluation Criteria for Department of Energy Facilities. DOE-STD-1020-94, U.S. Department of Energy, Washington, DC, April 1994.

Natural Phenomena Hazards Performance Categorization Criteria for Structures, Systems, and Components. DOE-STD-1021-93, U.S. Department of Energy Washington, DC, 1993.

NCEER, Youd, T. L. and I. M. Idriss. Proceeding of the NCEER Workshop on Evaluation of Liquefaction Resistance of Soils. Technical Reprot NCEER-97-0022, Buffalo, NY, December 31, 1997.

Nelson, A.E., et.al. "Generalized Tectonic Map of the Greenville 1x2 Quadrangle, Georgia, South Carolina, and North Carolina." U.S. Geological Survey Miscellaneous Field Studies Map MF-1898, Scale 1:250,000, 1987.

Nelson, K.D., et.al. "New COCORP Profiling in the Southeastern United States: Part I: Late Paleozoic Suture and Mesozoic Rift Basin." Geology. Vol. 13, 1985.

Neuman, R.B. and Nelson, W.H. Geology of the Western Great Smoky Mountains, Tennessee. U.S. Geological Survey Professional Paper 349-D, 1965.

Noel, J.R., et.al. "Paleomagnetism and 40 Ar/39 Ar Ages from the Carolina Slate Belt, North Carolina: Implications for Terrane Amalgamation." Geology. Vol. 16, 1988.

Nystrom, P. G., and Willoughby, R. H., 1982, "Geological investigations related to the stratigraphy in the kaolin mining district, Aiken County, South Carolina": in, *South Carolina Geological Survey, 1982 Carolina Geological Society Field Trip Guidebook*, 183 p.

Nystrom, P. G., Jr., Willoughby, R. H. and Kite, L. E., 1986, "Cretaceous-Tertiary stratigraphy of the upper edge of the Coastal Plain between North Augusta and Lexington South Carolina": in, *Carolina Geological Society Field Trip Guidebook*, South Carolina Geological Survey.

Nystrom, P.G., et.al. "Claibornian Stratigraphy of the Savannah River Site and Surrounding Area, 1990, Savannah River Region: Transition Between the Gulf and Atlantic Coastal Plains." Proceedings of the Second Bald Head Island Conference on Coastal Plains Geology. Hilton Head Island, November 6-11, 1990.

O'Connor, B.J. and Prowell, D.C. "The Geology of the Belair Fault Zone and Basement Rocks of the Augusta, Georgia Area." Georgia Geological Society Guidebook 16. 1976.

O'Connor, B.J. and Prowell, D.C. "The Geology of the Belair Fault Zone and Basement Rocks of the Augusta, Georgia Area." Georgia Geological Society Guidebook 16. 1976.

O'Connor, et.al. "Recently Discovered Faults in the Central Savannah River Area." abstract, Georgia Academy of Science Bulletin. Vol. 32, 1974.

Obermeier, S.F., et.al. "Geologic Evidence for Recurrent Moderate to Large Earthquakes near Charleston, South Carolina." Science. Vol. 227, 1985.

Obermeier, S.F., et.al. Earthquake-Induced Liquefaction Features in the Coastal Setting of South Carolina and in the Fluvial Setting of the New Madrid Seismic Zone. U.S. Geological Survey Professional Paper No. 1504, 1990.

Olsen, P.E. "On the Use of the Term Newark for Triassic and Early Jurassic Rocks of Eastern North America." Newsletters on Stratigraphy. Vol. 7, 1978.

Olsen, P.E. and Schlische, R.W. "Unraveling the Rules of Rift Basins." Geological Society of America Abstracts with Programs. Vol. 20, 1988.

Olsen, P.E., et.al. "Rift Basins of Early Mesozoic Age." The Geology of the Carolinas. University of Tennessee Press, Knoxville, 1991.

Ou, G.B. and Herrmann, R.B. "A Statistical Model for Ground Motion Produced by Earthquakes at Local and Regional Distances." Bulletin of the Seismological Society of America. Vol. 80, No. 6, 1990.

Parsons, et.al. Bedrock Waste Storage Project, Triassic Basin Fault Probing Program Report. E. I. du Pont de Nemours and Co., Savannah River Plant, Aiken, SC, 1973.

Pen Branch Fault Basement Drilling. Westinghouse Environmental and Geotechnical Services, 1991.

Petersen, T.A., et.al. "Structure of the Riddleville Basin from COCORP Seismic Data and Implications for Reactivation Tectonics." Journal of Geology. Vol. 92. 1984.

Phinney, R.A. and Roy-Chowdhury, K. Reflection Seismic Studies of Crustal Structure in the Eastern United States: Geophysical Framework of the Continental United States. Geological Society of America Mem. 172, 1989.

Poag, C.W. and Valentine, P.C. "Mesozoic and Cenozoic Stratigraphy of the US Atlantic Continental Shelf and Slope." The Geology of North America. V I-3, The Atlantic Continental Margin. DNAG Publication, Geological Society of America, Boulder, CO, 1988.

Poland, J. F., Lofgren, B. E., and Riley, F. S., 1972, *Glossary of selected terms useful in studies of the mechanics of aquifer systems and land subsidence due to fluid withdrawal*: U. S. Geological Survey Water Supply Paper 2025, 9 p.

Preliminary Report on Belair Exploratory Trench No. 10-76 Near Augusta, Georgia. Open File Report No. 77-411, U.S. Geological Survey, Atlanta, GA, 1977.

Price, V., et.al. Pen Branch Fault Investigation Program Plan. ESS-SRL-89-395, 1989.

Prowell, D. C., Christopher, R. A., Edwards, L. E., Bybell, L. M., and Gill, H. E., 1985a, "Geologic section of the updip Coastal Plain from central Georgia to western South Carolina": *USGS Miscellaneous Field Studies*, Map MF-1737.

Prowell, D.C. "Cretaceous and Cenozoic Tectonism on the Atlantic Coastal Margin, the Geology of North America, the Atlantic

Continental Margin." Geological Society of America. Vol. I-2, 1988.

Prowell, D.C. Index of Faults of Cretaceous and Cenozoic Age in the Eastern United States. U.S. Geological Survey Miscellaneous Field Studies Map MF-1269, 1983.

Prowell, D.C. Preliminary Geologic Map of the Barnwell 30' x 60' Quadrangle, South Carolina and Georgia. Open File Report 94-673, U.S. Geological Survey, Atlanta, GA, 1994.

Prowell, D.C. and O'Connor, B.J. "Belair Fault Zone: Evidence of Tertiary Fault Displacement in Eastern Georgia." Geology. Vol. 6, 1978.

Prowell, D.C. and Obermeier, S.F. "Evidence of Cenozoic Tectonism." The Geology of the Carolinas. University of Tennessee Press, Knoxville, TN, 1991.

Prowell, D.C., et.al. "The Ellenton Formation in South Carolina: A Revised Age Designation from Cretaceous to Paleocene." U.S. Geological Survey Bulletin. No. 1605-A, 1985.

Prowell, D.C., et.al. Preliminary Evidence for Holocene Movement Along the Belair Fault Zone Near Augusta, Georgia. Open File Report 75-680, U.S. Geological Survey, Atlanta, GA, 1976.

Rast, N. and Kohles, K.M. "The Origin of the Ocoee Supergroup." American Journal of Science. V. 286, 1986.

Ratcliffe, N.E. "The Ramapo Fault System in New York and Adjacent Northern New Jersey: A Case of Tectonic Heredity." Geological Society of America Bulletin. Vol. 82, 1971.

Reactor Site Criteria. 10 CFR 100, Washington, DC, November 15, 1983.

Reactor Site Criteria. 10 CFR 100, Washington, DC, November 15, 1983

Rozen, R.W. "The Middleton-Lowndesville Cataclastic Zone in the Elberton East Quadrangle, Georgia." Geological Investigations of the Kings Mountain Belt and Adjacent Areas in the Carolinas. Carolina Geological Society Guidebook, 1981.

Sacks, P.E. and Dennis, A.J. "The Modoc Zone-D_2 (Early Alleghanian) in the Eastern Appalachian Piedmont, South Carolina and Georgia, Anatomy of the Alleghanian Orogeny as Seen from the Piedmont of South Carolina and Georgia." Carolina Geological Society Field Trip Guidebook. South Carolina Geological Survey, 1987

Samson, S., et.al. "Biogeographical Significance of Cambrian Trilobites from the Carolina Slate Belt." Geological Society of America Bulletin. Vol. 102, 1990.

Sawyer, D.S. "Thermal Evolution." The Geology of North America. Vol. I-2, The Atlantic Continental Margin. DNAG Publication, Geological Society of America, Boulder, CO, 1988.

Schlische, R.W. and Olsen, P.E. "Quantitative Filling Model for Continental Extensional Basins with Application to the Early Mesozoic Rifts of Eastern North America." Journal of Geology. 1992.

Schmertmann, J. H. "The Mechanical Aging of Soils," The 25th Terzaghi Lecture, Journal of Geotechnical Engineering, Vol. 117, No. 9, , American Society of Civil Engineers, September 1991.

Schmertmann, J. H. "Update on the Mechanical Aging of Soils," for the symposium "Sobre Envejecimiento de Suelos," The Mexican Society of Soil Mechanics, Mexico City, August 1993.

Scholz, C.H. The Mechanics of Earthquakes and Faulting. Cambridge University Press, 1990.

Secor, D.T., Jr. "Regional Overview, Anatomy of the Alleghanian Orogeny as Seen from the Piedmont of South Carolina and Georgia." Carolina Geological Society Field Trip Guidebook. South Carolina Geological Survey, 1987.

Secor, D.T., Jr. et.al. "Character of the Alleghanian Orogeny in the Southern Appalachians, Part I: Alleghanian Deformation in the Eastern Piedmont of South Carolina." Geological Society of America Bulletin. Vol. 97, 1986a.

Secor, D.T., Jr., et.al. "Character of the Alleghanian Orogeny in the Southern Appalachians: Part III, Regional Tectonic Relations." Geological Society of America Bulletin. Vol. 97, 1986b.

Secor, D.T., Jr., et.al. "Confirmation of Carolina Slate Belt as an Exotic Terrane." Science. Vol. 221. 1983.

Seed, H.B. "Soil Liquefaction and Cyclic Mobility Evaluation for Level Ground During Earthquakes." Journal of Geotechnical Engineering Division.

Vol. 105, No. 2, American Society of Civil Engineers, February 1979.

Seed, R.B., Idriss, I. M. and I. Arango. "Evaluation of Liquefaction Potential Using Field Performance Data." Journal of Geotechnical Engineering Division. Volume 109, No. 3, American Society of Civil Engineers, 1983.

Seismograph Services Corporation. Gravity and Magnetic Survey, Savannah River Plant, South Carolina. Unpublished report prepared for E.I. du Pont de Nemours and Co., Inc., Engineering Department, Wilmington, DE, 1972.

Sen, A.K. and Coruh, C. Removing Near-Surface Effects in Seismic Data: Application for Determination of Faults in the Coastal Plain Sediments. WSRC-TR-92-169, Westinghouse Savannah River Company, Aiken, SC, 1992.

Sheridan, R.E. and Grow, J.A. "The Geology of North America." The Atlantic Continental Margin. Vol. I-1 and I-2, DNAG Publication, Geological Society of America, Boulder, CO, 1988.

Shervais, J.W., Mauldin, J., Dennis, A.J., 1996, "Petrology and Geochemistry of Neo- Proterzoic Arc Plutons beneath the Atlantic Coastal Plain: Savannah River Site, South Carolina". Report Submitted for SCURF Task 170.

Sibol, M.S. and Bollinger, G.A. Earthquake Catalog for the Southeastern United States, 1698-1989. Virginia Polytechnic Institute and State University Seismological Observatory Computer File, Blacksburg, VA, 1990.

Sibol, M.S. and Bollinger, G.A. Earthquake Catalog for the Southeastern United States, 1698-1989. Virginia Polytechnic Institute and State University Seismological Observatory Computer File, Blacksburg, VA, 1990.

Sibson, R.H. "Earthquakes and Rock Deformation in Crustal Fault Zones." Annual Review of Earth Planet Sciences. Vol. 14, 1986.

Sibson, R.H. "Frictional Constraints to Thrust, Wrench, and Normal Faults." Nature. Vol. 249, 1984.

Siple, G.E. "Geology and Ground Water of the Savannah River Plant and Vicinity, South Carolina." Paper No. 1841, United States Geological Survey Water Supply. 1967.

Skempton, A. W. "Standard Penetration Test Procedures and the Effects in Sands of Overburden Pressure, Relative Density, Partical Size, Aging and Overconsolidation," Geotechnique, Vol. 36, No. 3, 1986.

Smoot, J.P. "The Closed-Basin Hypothesis and Its Use in Facies Analysis of the Newark Supergroup." Proceedings of the Second U.S. Geological Survey Workshop on the Early Mesozoic Basins of the Eastern United States. U.S. Geological Survey Circular 946, 1985.

Snipes, D. S., et.al. "The Pen Branch Fault: Documentation of Late Cretaceous-Tertiary Faulting in the Coastal Plain of South Carolina." Southeastern Geology. Vol. 33, No. 4, 1993.

Snoke, A.W. and Frost, B.R. "Exhumation of High Pressure Pelitic Schist, Lake Murray Spillway, South Carolina: Evidence for Crustal Extension During Alleghanian Strike-Slip Faulting." American Journal of Science. Vol. 280, 1990.

Snoke, A.W., et.al. "Deformed Hercynian Granitic Rocks from the Piedmont of South Carolina." American Journal of Science. Vol. 280, 1980.

Sohl, N. F., and Christopher, R. A., 1983, *The Black Creek-Peedee formational contact (Upper Cretaceous) in the Cape Fear River region of North Carolina*: U. S. Geological Survey Professional Paper 1285, 37 p.

Somerville, P.G., et.al. Comparison of Source Scaling Relation of Eastern and Western North American Earthquakes. BSSA, 77, #2, 322-346. 1987.

Somerville, P.G., et.al. Comparison of Source Scaling Relation of Eastern and Western North American Earthquakes. BSSA, 77, #2, 322-346. 1987.

Steckler, M.S., et.al. "Subsidence and Basin Modeling at the U.S. Atlantic Passive Margin." The Geology of North America. Vol. I-2, The Atlantic Continental Margin. DNAG Publication, Geological Society of America, Boulder, CO, 1988.

Steltenpohl, M.G. "Kinematics of the Towaliga, Bartletts Ferry, and Goat Rock Fault Zones, Alabama: The Late Paleozoic Dextral Shear System in the Southernmost Appalachians." Geology. Vol. 16, 1988.

Stephenson, D.E. Savannah River Plant Earthquake. DPST-88-841, E.I. du Pont de Nemours and Co., Savannah River Laboratory, Aiken, SC, August 1988.

Stephenson, D.E. and Stieve, A. Structural Model of the Basement Based on Geophysical Data in the

Central Savannah River Area, South Carolina and Georgia. WSRC-TR-92-120, Westinghouse Savannah River Company, Aiken, SC, 1992.

Stephenson, D.E., et.al. "Savannah River Site Disaggregated Seismic Spectra." Fourth DOE Natural Phenomena Hazards Mitigation Conference. U.S. Department of Energy, Washington, DC, 1993.

Stephenson, D.E., P. Talwani, J. Rawlins, Savannah River Plant Earthquake of June 1985. DPST-85-583, E.I. du Pont de Nemours & Co., Savannah River Laboratory, Aiken, SC, 1985.

Stephenson, D.S. and Chapman, W.L. "Structure Associated with the Buried Dunbarton Basin, South Carolina from Recent Seismic Data." Geological Society of America, Southeastern Section Abstracts with Programs. Vol. 20, 1988.

Stieve, A.L. Pen Branch Fault Program: Interim Report on the High Resolution, Shallow Seismic Reflection Surveys. WSRC-TR-91-30, Westinghouse Savannah River Company, Aiken, SC, 1991b.

Stieve, A.L. and Stephenson, D.E. "Geophysical Evidence for Post Late Cretaceous Reactivation of Basement Structures in the Central Savannah River Area." Southeastern Geology. Vol. 35, No. 1, 1995.

Stieve, A.L. et.al. Confirmatory Drilling Project Final Report. WSRC-RP-94-0136, Westinghouse Savannah River Company, Aiken, SC, 1994.

Stieve, A.L. et.al. Confirmatory Drilling Project Final Report. WSRC-RP-94-0136, Westinghouse Savannah River Company, Aiken, SC, 1994.

Stieve, A.L., et.al. Pen Branch Fault Program: Consolidated Report on the Seismic Reflection Surveys and the Shallow Drilling. WSRC-TR-91-87, Westinghouse Savannah River Company, Aiken, SC, 1991a.

Stokoe, K.H., et.al. Correlation Study of Nonlinear Dynamic Soil Properties: Savannah River Site, Aiken, South Carolina. Rev. 0, File No. SRS-RF-CDP-95, University of Texas at Austin, Department Civil Engineering, September 13, 1995.

Stringfield, V. T., 1966, *Artesian water in Tertiary limestone in the Southeastern States*: U.S. Geological Survey Professional Paper 517, 226 p.

Strom, R. N., and Kaback, D. S., 1992, *SRP baseline hydrogeologic investigation: aquifer characterization, groundwater geochemistry of the Savannah River Site and vicinity*: WSRC-RP-92-450, Westinghouse Savannah River Company, Aiken, SC 29808, 96 p.

Talwani, P. "Current Thoughts on the Cause of the Charleston, South Carolina Earthquakes." South Carolina Geology. Vol. 29, 1985.

Talwani, P. "Seismotectonics of the Charleston Region." Proceedings, National Conference on Earthquake Engineering, 3rd. Earthquake Engineering Research Inst., Vol. 1, 1986.

Talwani, P. The Woodstock Fault is Alive and Ticking Near Charleston, South Carolina. Submitted to the Bulletin of the Seismological Society of America, 1982.

Talwani, P. and Cox, S. "An Internally Consistent Pattern of Seismicity Near Charleston, South Carolina." Geology. Vol. 10, 1985.

Talwani, P. and Cox, S. "Paleoseismic Evidence for Recurrence of Earthquakes near Charleston, South Carolina." American Association for the Advancement of Science. Vol. 229, July 1985.

Talwani, P., "Crustal Structure of South Carolina." Second Technical Report to the U.S. Geological Survey, contract #14-08-0001-14553, 1975.

Talwani, P., B.K. Rastogi, and D.A. Stevenson, "Induced seismicity and earthquake prediction studies in South Carolina." Tenth Technical Report to the U.S. Geological Survey, contract #14-08-0001-17670, 1980.

Talwani, P., et.al. Induced Seismicity and Earthquake Prediction Studies in South Carolina. Tenth Technical Report to the USGS, Contract 14-08-001-17670.1980.

Talwani, P., J. Rawlins, D. E. Stephenson. "The Savannah River Plant, South Carolina, Earthquake of June 9, 1985 and its Tectonic Setting." Earthquake Notes. Vol. 56, No. 4, 1985.

Talwani, P.J., et.al. "The Savannah River Plant, South Carolina, Earthquake of June 9, 1985 and its Tectonic Setting." Earthquake Notes. Vol. 56, No. 4, 1985.

Tarr, A., P. Talwani, S. Rhea, D. Carver, and D. Amick. "Results of Recent South Carolina Seismological Studies." Bulletin of the Seismological Society of America. Vol. 71, 1981.

Tarr, A.C., et.al. "Results of Recent South Carolina Seismological Studies." Bulletin of the Seismological Society of America. Vol. 71, 1981.

URS/John A. Blume and Associates, Engineers. Update of Seismic Criteria for the Savannah River Plant, Vol. 1 of 2, *Geotechnical.* USR/JAB8144, San Francisco, CA. Prepared for E.I. du Pont de Nemours and Company as DPE-3699, Savannah River Plant, Aiken, SC, 1982.

US Army Corps of Engineers (COE), Charleston District. "Geologic Engineering Investigations, Savannah River Plant", Volumes 1 and 2, Waterways Experimental Station, Vicksburg, MS, 1952.

Vick, H.K., et.al. "Ordovician Docking of the Carolina Slate Belt." Paleomagnetic Data: Tectonics. Vol. 6, 1987.

Visvanathan, T.R., "Earthquakes in South Carolina, 1698-1975." South Carolina Geol. Surv. Bull. , vol. 40, 61p., 1980.

Wait, R. L., and Davis, M. E., 1986, *Configuration and hydrology of the pre-Cretaceous rocks underlying the Southeastern Coastal Plain aquifer system*: U.S. Geological Survey Water-Resources Investigations Report 86-4010, 1 sheet.

Walton, W. C., 1970, Ground Water Resource Evaluation, McGraw-Hill Book Co., New York, N. Y., 664 p.

Wang, W. Some Findings in Liquefaction. Water Conservancy and Hydroelectric Power Scientific Research Institute, Beijing, China, August 1979.

Webster, D. S., Proctor, J. R., and Marine, I. W., 1970, *Two-well tracer test in fractured crystalline rock*: U.S. Geological Survey Water-Supply Paper 1544-I.

Wehr, F. and Glover, L., III. "Stratigraphy and Tectonics of the Virginia-North Carolina Blue Ridge: Evolution of a Late Proterozoic-Early Paleozoic Hinge Zone." Geological Society of America Bulletin. Vol. 96, 1985.

Wentworth, C.M. and Mergener, K.M. "Regenerate Faults of the Southeastern United States." Studies Related to the Charleston, South Carolina, Earthquake of 1886, Tectonics and Seismicity. U.S. Geological Survey Professional Paper 1313, 1983.

Winkler, C.D. and Howard, J.D. "Correlation of Tectonically Deformed Shorelines on the Southern Atlantic Coastal Plain." Geology. Vol. 5, 1977.

Wyatt. D. E., Aadland, R. K., Cumbest, R. J., Stephenson, D. E., Syms, F. H., 1997 A/M Area Advanced Geological Study, Part 3 of 3, Geological Interpretation of the Structure and Stratigraphy of the A/M Area, Savannah River Site, South Carolina (U), WSRC-RP-97-0186, Rev. 0, 46 p.

Youd, T.L. "Liquefaction, Flow and Associated Ground Failure." U.S. Geological Survey Circular. No. 688, 1973.

Youd, T.L. and Hoose, S.N. "Liquefaction Susceptibility and Geologic Setting." Proceedings, 6th World Conference on Earthquake Engineering. New Delhi, India, Vol. III, 1977.

Zoback, M.D. and Zoback, M.L. Tectonic Stress Field of North America and Relative Plate Motions in Neotectonics of North America. Vol. I, Decade Map, Geological Society of America, Boulder, CO, 1991.

Zoback, M.L. and Zoback, M.D. "State of Stress in the Conterminous United States." Journal of Geophysical Research. Vol. 85, 1980.

Notes